Pr 260 C1 Magasins

Peri-Tethys Memoir 5

New Data on Peri-Tethyan Sedimentary Basins

Edited by
Sylvie CRASQUIN-SOLEAU
& Éric BARRIER

MÉMOIRES DU MUSÉUM NATIONAL D'HISTOIRE NATURELLE
TOME 182
2000

COM

Source : MNHN, Paris

MÉMOIRES DU MUSÉUM NATIONAL D'HISTOIRE NATURELLE

Rédacteur en chef *(Editor-in-Chief)* : Philippe GRANDCOLAS
Rédacteurs (*Editors*) : Jean-Marie BETSCH, Philippe BOUCHET, Christian ÉRARD & Jean-Lou JUSTINE
Assistantes de rédaction (*Copy editors*) : Bernadette GOTTINI-CHARLES & Laurence BÉNICHOU

Adresse (*Address*)
Mémoires du Muséum national d'Histoire naturelle
57, rue Cuvier
F-75005 Paris
Tél. : [33] 01 40 79 34 37
Fax. : [33] 01 40 79 38 08
e-mail : memoires@mnhn.fr

Les *Mémoires du Muséum national d'Histoire naturelle* publient des travaux originaux majeurs, tels que des monographies ou des volumes à auteurs multiples. Les auteurs sont invités, pour toutes les questions éditoriales, à prendre contact avec le directeur de la publication. Les manuscrits peuvent être en français ou en anglais.

Parution et prix irréguliers. Les ordres permanents d'achat et les commandes de volumes séparés sont reçus par le **Service des Publications Scientifiques, Diffusion**. Catalogue sur demande. Une liste des derniers titres parus figure en page 3 de couverture.

The Mémoires du Muséum national d'Histoire naturelle *publishes major original contributions, such as monographs or multi-authored volumes. Prospective authors should contact the Editor-in-Chief. Manuscripts in French or English will be considered.*

Volumes are published at irregular intervals, and at irregular prices. Standing orders and orders for single volumes should be directed to the ***Service des Publications Scientifiques du Muséum****. Price list and catalogues are available on request. Recently published memoirs are listed on page 3 of the cover.*

MUSÉUM NATIONAL D'HISTOIRE NATURELLE
SERVICE DES PUBLICATIONS SCIENTIFIQUES
Diffusion : Delphine HENRY
57, rue Cuvier
F-75005 Paris
Tél. : [33] 01 40 79 37 00
Fax : [33] 01 40 79 38 40
e-mail : dhenry@mnhn.fr

Printed on acid-free paper
Imprimé sur papier non acide

Source : MNHN, Paris

Bibliothèque Centrale Muséum
3 3001 00099870 7

Source : MNHN, Paris

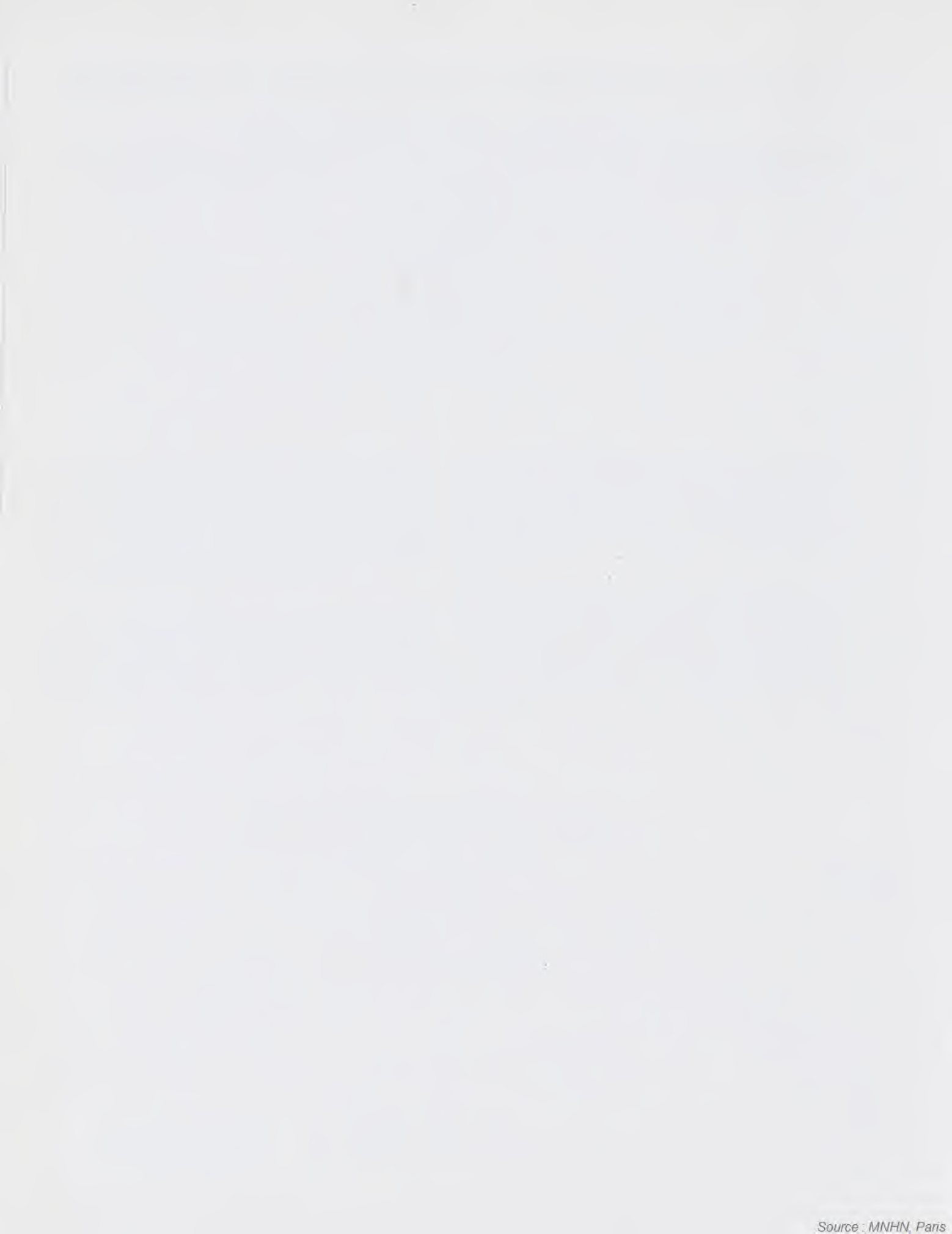

Source : MNHN, Paris

Source : MNHN, Paris

Cover photograph / *Photographie de couverture :*

Aggradational internal platform beds (marls and limestones, mudstone and floatstone) in the Bathonian infilling of the Atlas Trough (Tana Plateau, Central High Atlas, Morocco) photograph Ch. DURLET.

Agradation des dépôts de plate-forme interne (marnes et calcaires, mudstone à floatstone) dans le remplissage bathonien du Sillon Atlasique (Plateau de Tana, Haut Atlas Central, Maroc) cliché *Ch. DURLET.*

The Peri-Tethys Program, sponsored by international industries (AGIP, ARCO, BRGM, CHEVRON, CONOCO, EAP(ELF), EXXON, SHELL, SONATRACH, TOTAL), research centres (CNRS, IFP), and a university (UPMC), started in 1993. It examines the influence of Tethyan evolution on the bordering cratons since its birth (through the break-up of Pangea), its life (by the extension and formation of oceanic seaways) and finally its death (by collision between the main bordering plates which led to inversion within the epicratonic basins).

Volumes déjà parus/*Previously published volumes:*

Peri-Tethys Memoir 1 (1994): *Peri-Tethyan platforms. Proceedings of the IFP/Peri-Tethys Research Conference.* Technip, Paris: 1-275. ISBN: 2-7108-0679-7.

Peri-Tethys Memoir 2 (1996): Structure and Prospects of Alpine Basins and Forelands. *Mém. Mus. natn. Hist. nat.*, **170**: 1-550 (+ Atlas). ISBN: 2-85653-507-0.

Peri-Tethys Memoir 3 (1998): Stratigraphy and Evolution of Peri-Tethyan Platforms. *Mém. Mus. natn. Hist. nat.*, **177**: 1-262. ISBN: 2-85653-512-7.

Peri-Tethys Memoir 4 (1998): Epicratonic Basins of Peri-Tethyan Platforms. *Mém. Mus. natn. Hist. nat.*, **179**: 1-294. ISBN: 2-85653-518-4.

Peri-Tethys Memoir 5 (2000): New Data on Peri-Tethyan Sedimentary Basins. *Mém. Mus. natn. Hist. nat.*, **182**: 1-266. ISBN: 2-85653-524-0.

Aussi/*Also:*

Peri-Tethys: stratigraphic correlations 1 (1997). 330 pp. *Geodiversitas*, **19** (2): 169-499. ISSN: 1280-9659.

Peri-Tethys: stratigraphic correlations 2 (1998). 224 pp. *Geodiversitas*, **20** (4): 515-738. ISSN: 1280-9659.

Peri-Tethys: stratigraphic correlations 3 (1999). 211 pp. *Geodiversitas*, **21** (3): 285-496. ISSN: 1280-9659.

Source : MNHN, Paris

Peri-Tethys Memoir 5

New Data on Peri-Tethyan Sedimentary Basins

BIBL. DU MUSÉUM PARIS

Source : MNHN, Paris

ISBN : 2-85653-524-0
ISSN : 1243-4442
© Publications Scientifiques du Muséum, Paris, 2000

PHOTOCOPIES :

Les *Publications Scientifiques du Muséum* adhèrent au Centre Français d'Exploitation du Droit de Copie (CFC), 20, rue des Grands Augustins, 75006 Paris. Le CFC est membre de l'International Federation of Reproduction Rights Organisations (IFRRO). Aux États-Unis d'Amérique, contacter le Copyright Clearance Center, 27, Congress Street, Salem, Massachusetts 01970.

PHOTOCOPIES:

The Scientific Publications of the Muséum *adhere to the Centre Français d'Exploitation du Droit de Copie (CFC), 20, rue des Grands Augustins, 75006 Paris. The CFC is a member of International Federation of Reproduction Rights Organisations (IFRRO). In USA, contact the Copyright Clearance Center, 27, Congress Street, Salem, Massachusetts 01970.*

Source : MNHN, Paris

MÉMOIRES DU MUSÉUM NATIONAL D'HISTOIRE NATURELLE

TOME 182
GÉOLOGIE

Peri-Tethys Memoir 5

New Data on Peri-Tethyan Sedimentary Basins

edited by

Sylvie CRASQUIN-SOLEAU [1] & Éric BARRIER [2]

[1] Université Pierre et Marie Curie / CNRS
Département de Géologie Sédimentaire
T15-25, E.4, case 104
4, Place Jussieu
F-75252 Paris Cedex 05

[2] Université Pierre et Marie Curie / CNRS
Département de Géotectonique
T25-26, E.1, case 129
4, Place Jussieu
F-75252 Paris Cedex 05

PUBLICATIONS SCIENTIFIQUES
DU MUSÉUM
PARIS

2000

Source : MNHN, Paris

Source : MNHN, Paris

Nous dédions ce volume à la mémoire de A. BOUDJEMA (SONATRAC) assassiné à Alger en 1994 et du Professeur P. HANCOCK (Bristol University) décédé en 1998.

This volume is dedicated in the memory of A. BOUDJEMA (SONATRAC) murdered in Alger in 1994 and Professor P. HANCOCK (Bristol University) died in 1998.

Source : MNHN, Paris

Source : MNHN, Paris

CONTENTS
SOMMAIRE

Pages

1. **The Westphalian Basin of Sidi-Kassem (Central Massif, Morocco). Continental sedimentation and Late Variscian deformations** 11
Christian HOEPFFNER, Mohamed EL WARTITI, Abdesslam BENSAHAL & Karima GHAZALI

2. **Triassic series of Morocco: stratigraphy, palaeogeography and structuring of the Southwestern Peri-Tethyan Platform. An overview.** 23
Mostafa OUJIDI, Louis COUREL, Naïma BENAOUISS, Mohamed EL MOSTAINE, Mohamed EL YOUSSI, Mohamed ET TOUHAMI, Driss OUARHACHE, Abdellah SABAOUI & Abdel-Illah TOURANI

3. **The Liassic carbonate platform on the western part of the Central High Atlas (Morocco): stratigraphic and palaeogeographic patterns** 39
Abdellatif SOUHEL, Joseph CANÉROT, Fatma EL BCHARI, Driss CHAFIKI, Abdelhak GHARIB, Khadija EL HARIRI & Aziz BOUCHOUATA

4. **The Jurassic events and their sedimentary and stratigraphic records on the Southern Tethyan margin in Central Tunisia** 57
Mohamed SOUSSI, Raymond ENAY, Charles MANGOLD & Moncef TURKI

5. **The Tethys southern margin in Morocco; Mesozoic and Cainozoic evolution of the Atlas domain** 93
Alain PIQUÉ, Mohamed CHARROUD, Edgard LAVILLE, Lahcen AÏT BRAHIM & Mustafa AMRHAR

6. **The Southern Tethyan margin in Northeastern Morocco; sedimentary characteristics and tectonic control** 107
Pierre CHOTIN, Lahcen AÏT BRAHIM & Hassan TABYAOUI

7. **Subsidence history of the Essaouira Basin (Morocco)** 129
Kamal LABBASSI, Fida MEDINA, Abdelkrim RIMI, Hosna MUSTAPHI & Rkia BOUATMANI

Source : MNHN, Paris

8. **Hydrocarbon systems of Morocco** 143
Haddou JABOUR, Al Moundir MORABET & Rabah BOUCHTA

9. **The Jurassic in Syria: an overview. Lithostratigraphic and biostratigraphic correlations with adjacent areas** 159
Mikhail MOUTY

10. **Basin development and tectonic history of the Euphrates graben (Eastern Syria): a stratigraphic and seismic approach** 169
Cécile CARON, Maher JAMAL, Hassan ZEINAB & Francis CERDA

11. **Palaeogeography and palaeotectonic of the jointing area between the Eastern European Basin and the Tethys Basin during Late Carboniferous (Moscovian) and Early Permian (Asselian and Artinskian)** 203
Boris I. CHUVASHOV & Sylvie CRASQUIN-SOLEAU

12. **Palaeotectonic conditions of Cretaceous basin development in the southeastern segment of the Mid-Polish Trough** 239
Jolanta SWIDROWSKA & Maciej HAKENBERG

INDEX 257

Source : MNHN, Paris

The Westphalian Basin of Sidi-Kassem (Central Massif, Morocco). Continental sedimentation and Late Variscan deformations

Christian HOEPFFNER, Mohamed EL WARTITI, Abdesslam BENSAHAL & Karima GHAZALI

Département des Sciences de la Terre, Faculté des Sciences, Avenue Ibn Batouta, Rabat, Maroc

ABSTRACT

The Sidi-Kassem Carboniferous basin is located in the northwestern Meseta. It unconformably overlies a basement of Ordovician to Devonian age, strongly deformed by the major Variscan phase. The basin is filled by continental red rocks, flora indicates a late Westphalian age. The sedimentological study shows that the basin is of intramontane type, feeded by braided fluvial networks. Lacustrine and flood plain deposits are periodically interrupted by high energy currents related to floods and tectonic activity of the basin margins. Cartography and structural analysis show that deformations are represented by open kilometric NE-SW trending folds. A rough cleavage appears occasionally. The main structures are NE-SW striking reverse or thrust faults verging to the NW or to the SE. The kinematic analysis of microfaults systems indicates a compressionnal phase with a N-S to NNW-SSE shortening. All these Late Variscan events are not precisely dated, but a Latest Permian to Earliest Triassic age is probable.

RÉSUMÉ

Le bassin westphalien de Sidi-Kassem (Massif Central, Maroc). Sédimentation continentale et déformation tardi-varisque.

Le bassin carbonifère de Sidi-Kassem est situé dans la Méséta marocaine nord-occidentale. Il est discordant sur un socle d'âge ordovicien à dévonien, fortement déformé par la phase majeure varisque. Le bassin est rempli de couches rouges continentales, des flores indiquent un âge westphalien terminal. L'étude sédimentologique montre que bassin est de type intramontagneux, parcouru par un réseau fluviatile en tresses. Des dépôts lacustres et de plaine d'inondation sont périodiquement interrompus par des courants de haute énergie en relation avec des évènements pluviaux et une activité tectonique des marges du bassin. La cartographie et l'analyse structurale montrent que les déformations sont représentées par des plis kilométriques ouverts, orientés NE-SW. Une schistosité grossière se développe localement. Les principales structures sont des failles inverses NE-SW et des chevauvements à vergence NW ou SE. L'étude microtectonique de la fracturation

HOEPFFNER, C., EL WARTITI, M., BENSAHAL, A. & GHAZALI, K., 2000.— The Westphalian Basin of Sidi-Kassem (Central Massif, Morocco). Continental sedimentation and Late Variscan deformations. *In* : S. CRASQUIN-SOLEAU & É. BARRIER (eds), Peri-Tethys Memoir 5: new data on Peri-Tethyan sedimentary basins, *Mém. Mus. natn. Hist. nat.*, **182** : 11-22 Paris ISBN : 2-85653-524-0.

Source : MNHN, Paris

indique une phase compressive avec une direction de raccourcissement N-S à NNW-SSE. Tous ces évènements tardi-varisques ne sont pas datés avec précision, mais un âge Permien terminal-Trias basal est probable.

INTRODUCTION

The Late Carboniferous of Northern Africa was represented, during Westphalian time, by detritic deposits which are interpreted as the erosional products of the Variscan belt. These deposits, exclusively continental, indicate the eastward regression of the Palaeo-Tethys sea. We can distinguish: on one hand, in the northern margin of the African shield, the weakly deformed deposits of the Tindouf and Bechar basins; on the other hand, small basins included in the Hercynian chain, especially in Morocco. Here, the Westphalian is represented in two areas: the paralic basin of Jerada to the east and the limnic basin of Sidi-Kassem to the west (Fig. 1).

FIG. 1.— Palaeozoic outcrops in North Africa. **1**: Variscan allochtonous terranes included in the rifo-tellian Alpine nappes; **2**: Variscan belt of Northern Africa, Palaeozoic terranes strongly deformed; **3**: West African craton margin, Palaeozoic terranes weakly deformed; **4**: Undeformed Palaeozoic terranes; **5**: Panafrican belt (Hoggar); **6**: Lower Proterozoic and Archeozoic (Reguibat shield). S.K.: Sidi-Kassem; Je: Jerada.

*FIG. 1.— Affleurements paléozoïques en Afrique du Nord. **1** : terrains varisques allochtones inclus dans les nappes alpines rifo-telliennes ; **2** : chaîne varisque d'Afrique du Nord, terrains paléozoïques fortement déformés ; **3** : marge du craton Ouest-Africain, terrains paléozoïques peu déformés ; **4** : terrains paléozoïques non déformés ; **5** : chaîne panafricaine (Hoggar) ; **6** : Protérozoïque inférieur et Archéen (bouclier Reguibat). S.K. : Sidi-Kassem, Je : Jerada.*

The Sidi-Kassem basin, subject of this paper, is located in the northwestern Moroccan Meseta, in the center of the Khouribga-Oulmes anticline (Fig. 2). It is an elongated, rectangular basin trending ENE-WSW (6 x 30 km).

The Sidi-Kassem basin has been discovered by TERMIER (1936) and described as limnic basin type. Piedmont plain and fluvio-lacustrine basin continental deposits unconformably overlie a strongly deformed basement of Ordovician to Devonian age. They are conglomerates, red sandstones, shales with thin coal levels and lacustrine limestones. Flora found in pelitic beds indicate a late Westphalian age for the whole of the formation (PRUVOST & TERMIER, 1949). Lithostratigraphic descriptions are old (ROCH, 1950) or very localised (EL WARTITI, 1990; CHAKIRI, 1991).

Informations about the structure are very scarce: the geological map of TERMIER (1936), and the unpublished data which have been used to draw the geological maps of Morocco at 1/500 000

Source : MNHN, Paris

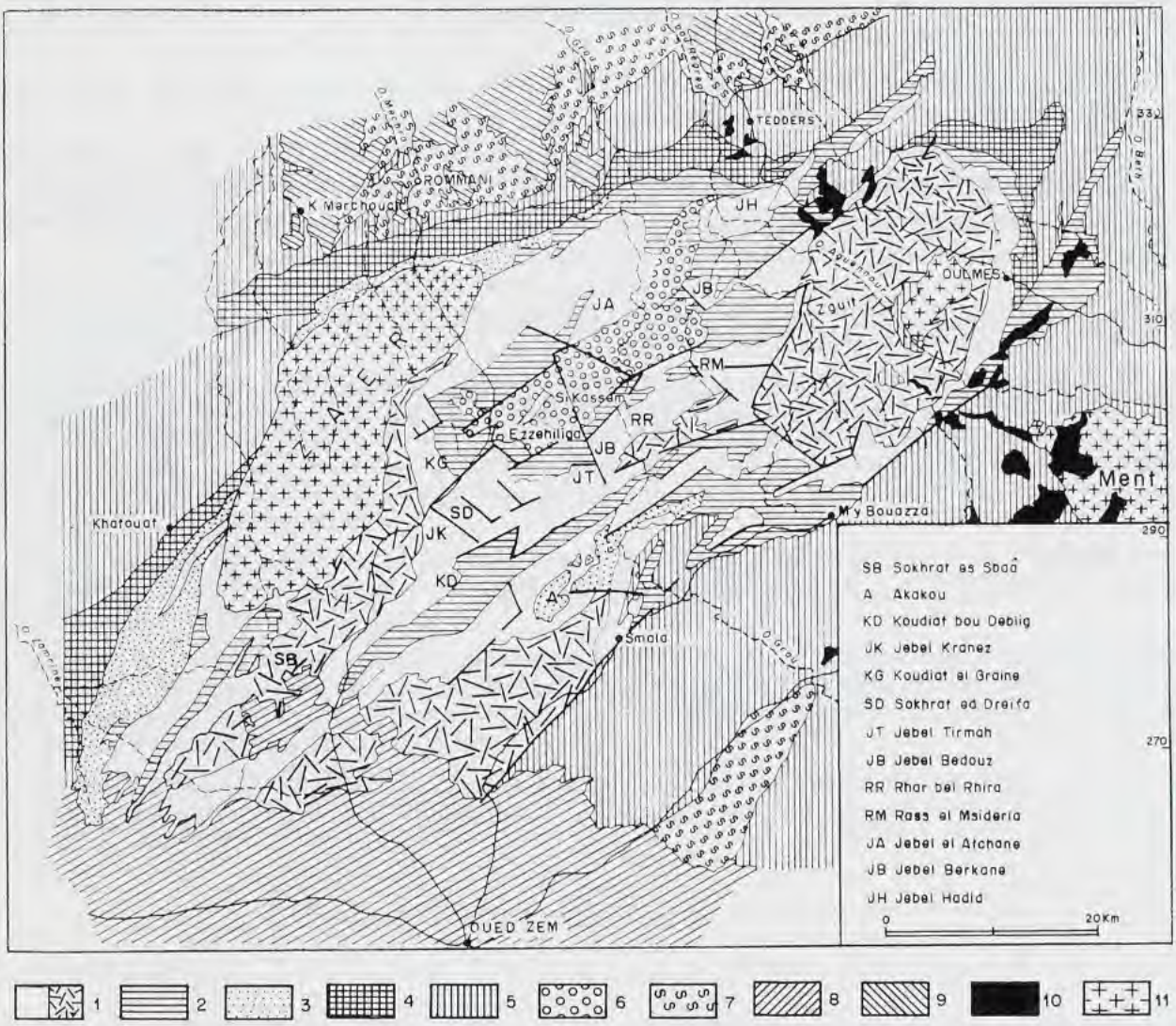

FIG. 2.— Geological map of the Moroccan Central Hercynian Massif, area of the NE-SW trending Khouribga-Oulmès anticline (from the geological map of Morocco, 1/500 000). **1**: Ordovician; **2**: Silurian; **3**: Lower Devonian; **4**: Lower and Middle Devonian; **5**: Lower Carboniferous; **6**: Westphalian; **7**: Permian and Triassic; **8**: Cretaceous; **9**: Miocene; **10**: Recent lavas; **11**: Hercynian granites.

*FIG. 2.— Carte géologique du Massif Hercynien central marocain, secteur de l'anticlinal de Khouribga-Oulmès orienté NE-SW (d'après la carte géologique du Maroc à 1/500 000). **1** : Ordovicien ; **2** : Silurien ; **3** : Dévonien inférieur ; **4** : Dévonien inférieur et moyen ; **5** : Carbonifère inférieur ; **6** : Westphalien ; **7** : Permien et Trias ; **8** : Crétacé ; **9** : Miocène ; **10** : Laves récentes ; **11** : Granites hercyniens.*

(CHOUBERT, 1956) and 1/1 000 000 (HOLLARD, 1985). Main structures are open or tight folds and fault systems trending NE-SW and NW-SE. An overthrust involving the Westphalian beds was mentioned in a borehole by TERMIER & TERMIER (1951); at last, CHAKIRI (1991) and GHAZALI (1995) described a spaced cleavage in conglomerates of the northern part of the basin.

This review demonstrates the lack of modern and detailed studies in the basin, although it is always described as a very important reference for dating the major Hercynian phase in the western Moroccan Meseta (PIQUÉ & MICHARD, 1989).

Source : MNHN, Paris

SEDIMENTOLOGY

Following TERMIER (1936), PRUVOST *in* ROCH (1950) and CHOUBERT (1951), the Sidi-Kassem formation could be divided into two members:

— the lower member is constituted by conglomerates in the NW area (600 m) grading into shales and sandstones with intercalations of coal veins and lacustrine limestones toward the SE (1200 m).

— the upper member is formed by shales, red sandstones and the "Sidi-Kassem conglomerate" (300-400 m).

Flora indicates a Westphalian C (and D?) age for the formation (*Cordaites, Cardiocarpus, Calamites, Odontoperis* and *Mixoneura,* after ROCH, 1950).

With the aim at doing a sedimentological study of the basin, several sections have been made in the lower member. Two sections are described here: the first is situated in the northern part, between the Grou and Bou-Regreg rivers, the second, in the SW part is located near Sidi Mohammed ben Hammou (Fig. 3).

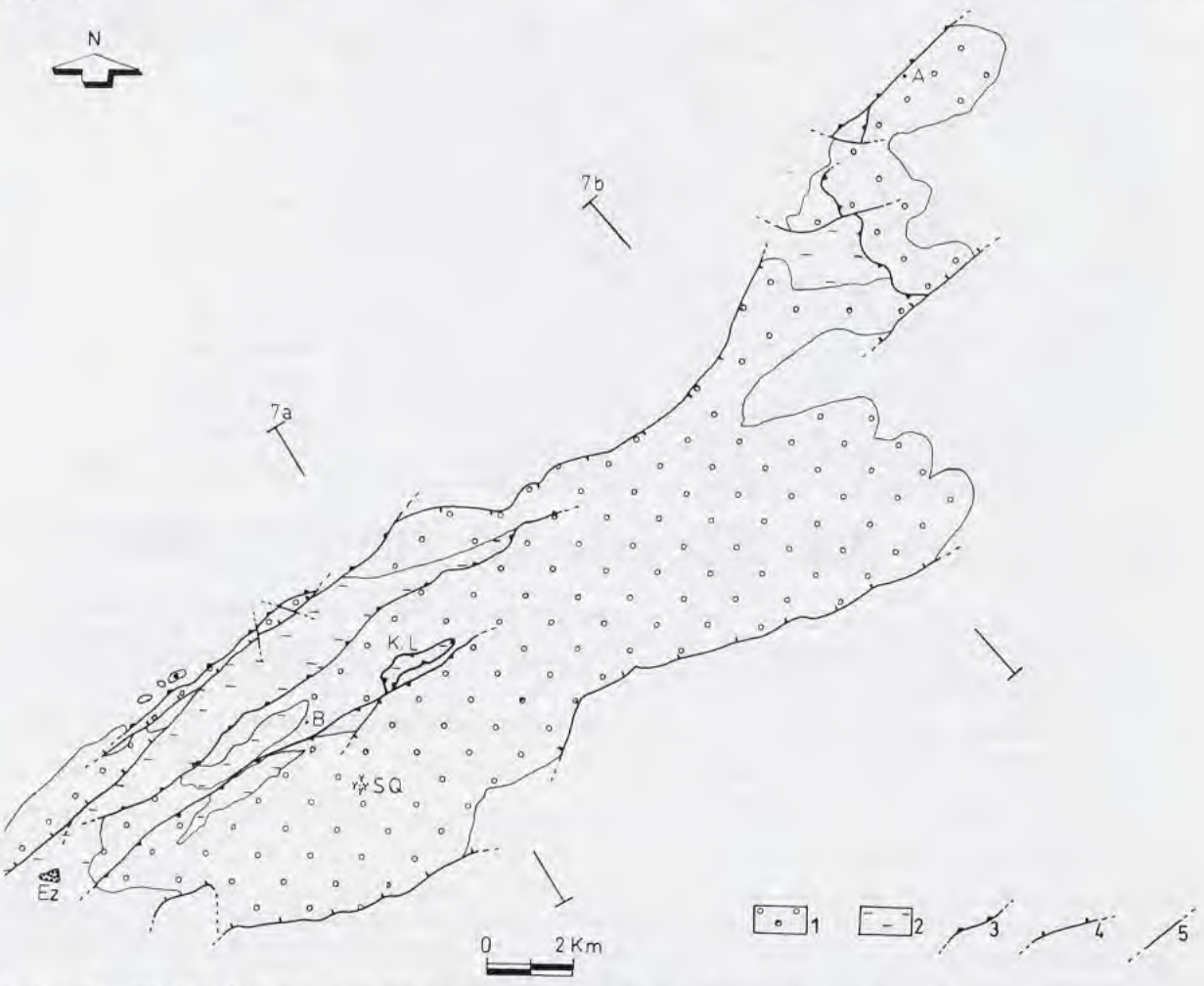

FIG. 3.— Simplified geological map of the Sidi-Kassem basin. **1**: late Westphalian red-beds; **2**: Ordovician to Devonian basement; **3**: reverse faults; **4**: normal faults; **5**: strike slip faults. EZ: Ez-Zehiliga village; SQ: Sidi-Kassem sanctuary; KL: Ktab Lahmar hill. a, b: location of the sedimentological sections.

*FIG. 3.— Carte géologique simplifiée du bassin de Sidi-Kassem. **1** : couches rouges du Westphalien supérieur ; **2** : socle d'âge ordovicien à dévonien ; **3** : failles inverses ; **4** : failles normales ; **5** : décrochements. EZ : village de Ez-Zehiliga ; SQ : sanctuaire de Sidi-Kassem ; KL : colline de Ktab Lahmar. a, b : situation des coupes sédimentologiques.*

Source : MNHN, Paris

Our sedimentological study involves determination and classification of the facies, according to MIALL (1978), sequential analysis, and determination of the depositional environment.

MAIN FACIES OF THE WESTPHALIAN DEPOSITS

According to the MIALL's classification (1978), five facies can be distinguished in the lower member of the Sidi-Kassem formation.

K1: this facies is characterised by lenticular beds of immature conglomerates. The pebbles, sometimes imbricated, are principally sandstones and quartzites.

K'1: this facies is organised in conglomeratic lenses poorly stratified, with erosional base level and slumpings. Pebbles are small.

These facies are similar to the Gm facies of MIALL (1978) and they characterise a proximal deposit in a braided fluviatile network or more accurately a deposit in a longitudinal bar.

K2: this facies is characterised by continous beds of thin to medium tickness (10-15 cm). They show massive structures or horizontal laminations. It is analogous to the Sh facies of MIALL (1978) and indicates sheet flood distal deposits.

K3: red mudstones are organised in metric beds with horizontal bedding. This facies alternates with sandstones or overlies the conglomerates. It is similar to the F1 facies of MIALL (1978) and is related to decreasing energy of the current transport.

K'3: green mudstones with horizontal bedding and vegetal remains. Very thin coal levels appear near the bottom of the beds. Spore and pollen have been recently discovered in these coal levels (EL WARTITI *et al.*, in progress). This facies is similar to the Fh facies of MIALL (1978) and characterises a lacustrine or a palustrine environment in a flood plain.

K4: this facies corresponds to thin (50 cm), lenticular, massive limestones interstratified in the green mudstones. Identical with the P facies of MIALL (1978), they are palustrine or lacustrine deposits in a quiet and shallow environment.

EXAMPLES OF SECTIONS AND SEQUENTIAL ANALYSIS

SECTION A (FIG. 4)

This section is located on the left side of the Bou-Regreg river (x= 143; y=321; Sidi Matla ech Chems map at 1/50 000) near the Feddane Lebtam hills. This section shows four parts, two megasequences can be distinguished.

MEGASEQUENCE 1.— The bottom is formed by an alternation of the K1 and K3 facies. The sequences characterise braided fluvial network, in proximal position.

The lower part is essentially formed by mudstones or siltstones with intercalations of conglomerates and sandstones (K'1). The main sequence indicates quiet environment like a sheet flood plain.

This megasequence shows a upward fining grain size evolution. The very coarse early deposits indicate a strong erosion of high reliefs, and a transport by fluvial currents in a proximal position. Later, near the top of the megasequence, finer deposits indicate a sheet-flood environment in distal position with temporary irruption of fluviatile high-energy currents.

MEGASEQUENCE 2.— The medium part of the section is a conglomerate stacking with intercalations of thin and lenticular pelitic beds. The sequences are formed by associations of the K'1 and K3 facies, which characterise a braided fluviatile network in proximal position.

The upper part is formed by repetitions of rythmic sequences with upward fining grain size. Each sequence, from 4 m up to 6 m thick, contains alternations of sandstones, mudstones and centimetric beds of conglomerates. The predominance of thin deposits indicates a fluviatile braided network in distal position, probably located in the downstream part of an alluvial fan.

Source : MNHN, Paris

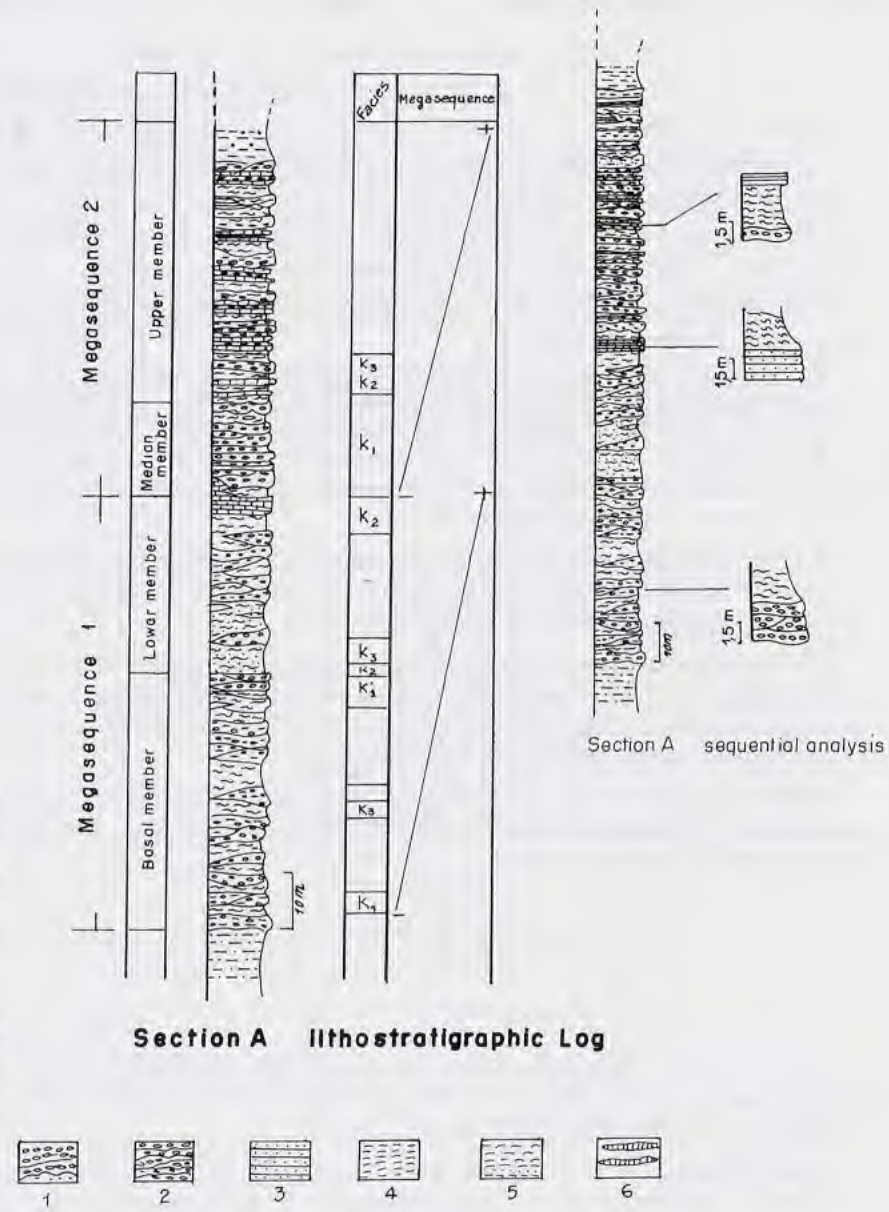

FIG. 4.— Lithostratigraphical column and sequential analysis of the section A. **1**: massive conglomerates; **2**: conglomerates weakly stratified; **3**: sandstones; **4**: pelites; **5**: pelites and sandstones; **6**: limestone lenses.

*FIG. 4.— Colonne lithostratigraphique et analyse séquentielle de la coupe A. **1** : conglomérats massifs ; **2** : conglomérats mal stratifiés ; **3** : grès ; **4** : pélites ; **5** : pélites et grès ; **6** : lentilles de calcaires.*

In this megasequence, the conglomerates are well organised as in the first one. Their occurrence probably indicates a new tectonic activity with rejuvenation of the marginal reliefs, followed by their aplanation, as indicated by decreasing grain size in the upper part of the megasequence.

SECTION B (FIG. 5).

This section is located in the SW part of the basin near Sidi Mohammed Ben Hammou (x=398.7; y=304.8; Sidi Matla ech Chems map, 1/50 000). The sedimentation is chiefly pelitic, with rare occurrences of limestones.

Sequential analysis shows only one megasequence where four facies can be distinguished. Red siltstones and mudstones with rare lenticular beds of conglomerates (K3), lenticular conglomerates with

Source : MNHN, Paris

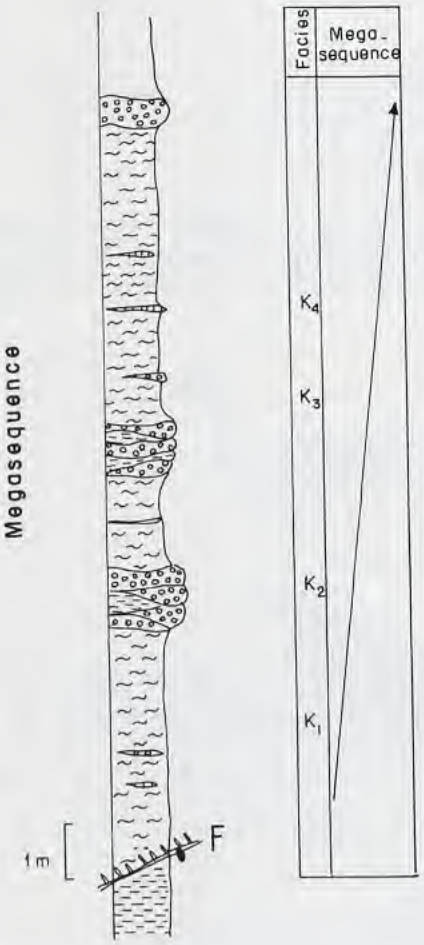

Section B

FIG. 5.— Lithostratigraphical column of the section B (legend: see Fig. 4).

FIG. 5.— Colonne lithostratigraphique de la coupe B (légende : voir Fig. 4).

siltstones and mudstones with rare lenticular beds of conglomerates (K3), lenticular conglomerates with small pebbles (K'1), green mudstones with plant debris and coal levels (K'3), massive and discontinous limestones (K4).

All these facies are organised in small sequences that indicate a quiet environment, a weakly dipping hydrographic network and low energy currents. Limestones and plants indicate palustrine or lacustrine environments temporarily invaded by high energy currents.

Therefore these observations concern only the lower member of the Sidi-Kassem formation, they allow us to display the main characteristics of the sedimentary palaeoenvironment during part of the late Westphalian in the western Moroccan Meseta. The Sidi-Kassem basin is an intramountain type; it is feeded by braided hydrographic networks whose direction of transport and current energy are very variable.

Erosional periods are probably related with raining seasons under warm and wet climate. Sediments become finer toward the top of the formation, in relation with the peneplanation of the reliefs. The tectonic control of the sedimentation is certainly important, but the synsedimentary displacements along the main faults in the basin are not yet well known.

Source : MNHN, Paris

TECTONIC SETTING

SOUTHWESTERN PART OF THE BASIN

The structural analysis is based on the mapping of the whole basin and some detailed studies, which are carried out in the southwestern part. Map (Fig. 6) and cross-sections (Fig. 7) clearly show the major unconformity of the Westphalian beds upon the Silurian-Devonian which is represented by shales, sandstones and limestones.

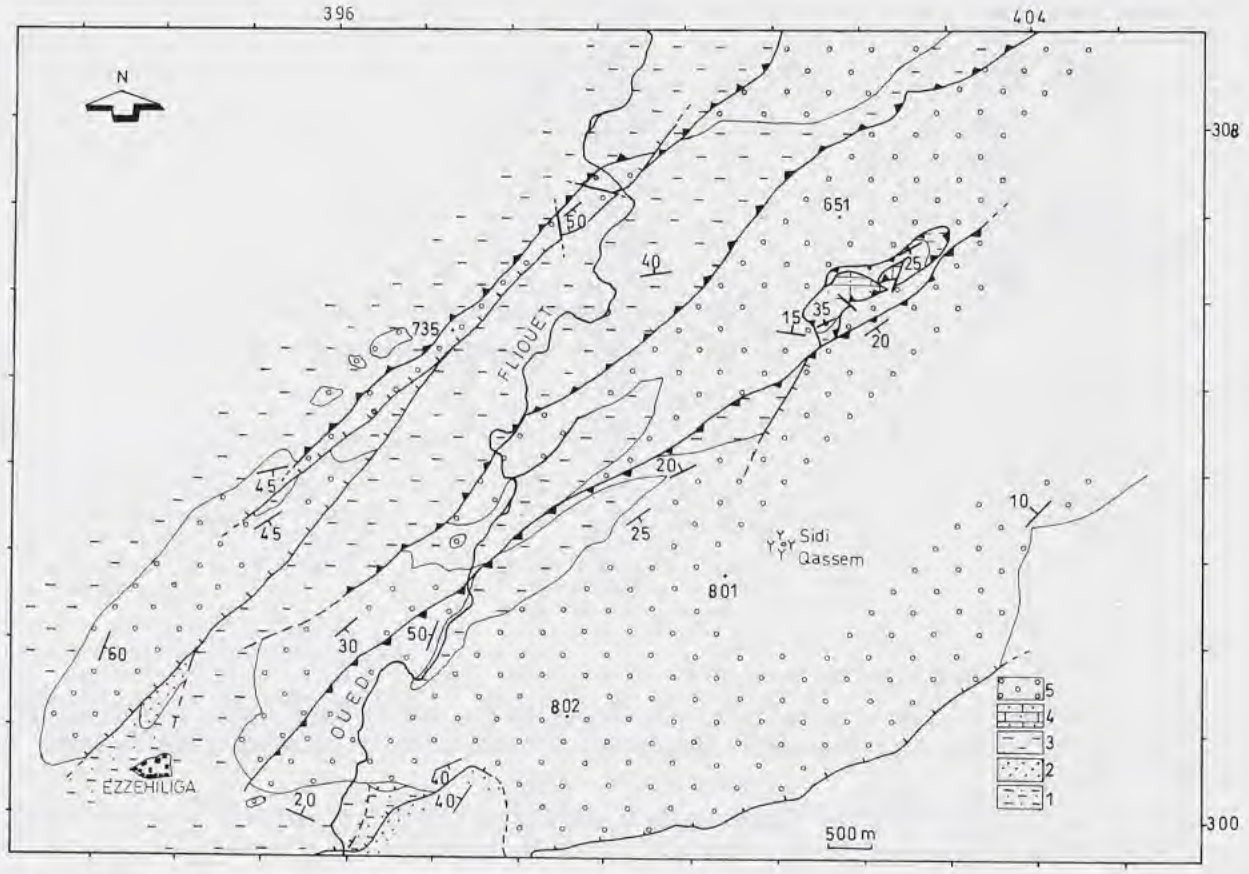

FIG. 6.— Geological map of the southwestern part of the Sidi-Kassem basin. **1**: Ordovician slates; **2**: Ordovician quartzites (Ashgillian); **3**: Silurian-Devonian mudstones and sandstones; **4**: Devonian limestones and greywackes (Ktab Lahmar hill); **5**: Westphalian conglomerates.

*FIG. 6.— Carte géologique de la partie SW du bassin de Sidi-Kassem. **1** : schistes ordoviciens ; **2** : quartzites ordoviciens (Ashgill) ; **3** : pélites et grès du Siluro-Dévonien ; **4** : calcaires et grauwackes du Dévonien (colline de Ktab Lahmar) ; **5** : conglomérats westphaliens.*

The whole structure results from Late Variscan tectonic events. Westphalian beds are organised in NE-SW trending belts. Thus, the limits between the Late Carboniferous and the basement appear as reverse faults verging to the NW or to the SE, or sometimes, as normal faults.

Regional structures of Late Variscan age are kilometric, open folds like the Sidi-Kassem syncline (Fig. 7a). Dips of bedding planes are moderate except near the faulted zones where they reach 50-60°. Flexural folding is accomodated by layer-parallel-slip.

Source : MNHN, Paris

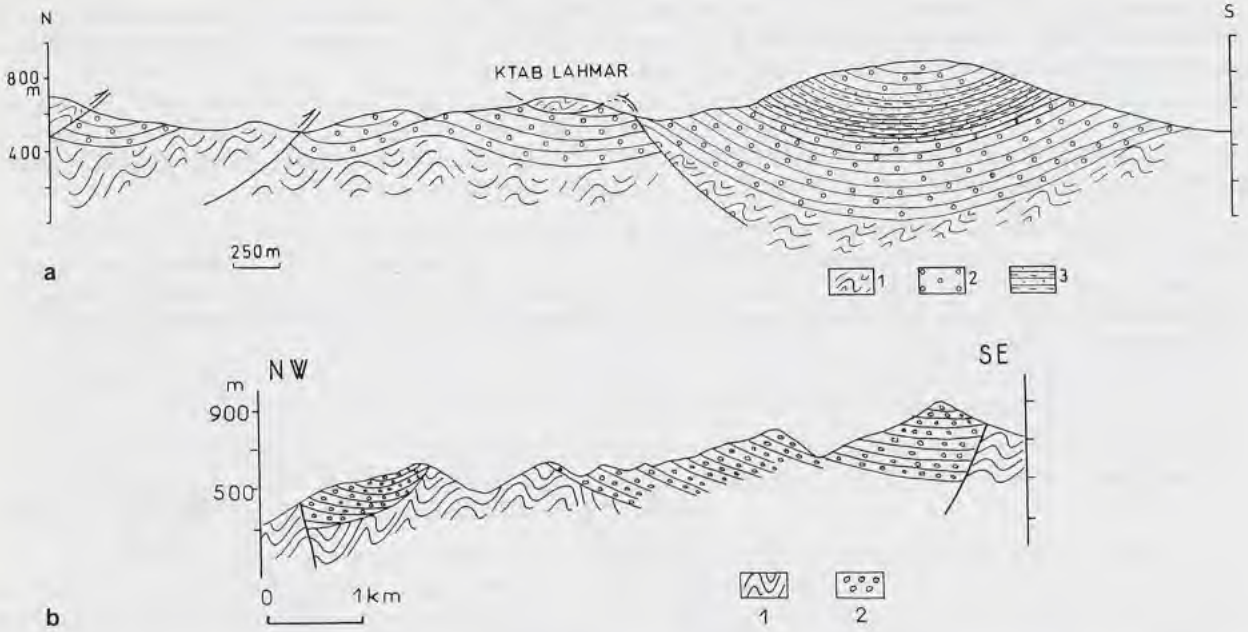

FIG. 7.— Cross-sections in the Sidi-Kassem basin. **7a**.— Cross-section in the southwestern part of the Sidi-Kassem basin showing the Ktab Lahmar tectonic klippe. **1**: Silurian-Devonian basement; **2**: Westphalian conglomerates; **3**: Westphalian mudstones and sandstones (for location see Fig. 3). **7b**.— Cross-section in the northern part of the basin. **1**: basement (Ordovician to Devonian); **2**: late Westphalian sandstones and conglomerates (for location, see Fig. 3).

*FIG. 7.— Coupes dans le bassin de Sidi-Kassem. **7a**.— Coupe dans la partie SW du bassin de Sidi-Kassem montrant la klippe tectonique de Ktab Lahmar. **1** : socle siluro-dévonien ; **2** : conglomérats westphaliens ; **3** : grès et pélites du Westphalien (situation, voir Fig. 3). **7b**.— Coupe dans la partie nord du bassin. **1** : socle (Ordovicien à Dévonien) ; **2** : grès et conglomérats du Westphalien supérieur (situation, voir Fig. 3).*

In the southwestern part of the basin, a major thrust fault outcrops from Ez-Zehiliga up to the Ktab Lahmar hill, with an average dip of 50° SE. The displacement toward the NW along this fault is locally important, as clearly illustrated by the Devonian tectonic klippe of Ktab Lahmar.

The Ktab Lahmar hill is very interesting. Devonian limestones and sandstones constitute a crest NE-SW trending (spots height 767m and 732m) which rises above the Westphalian red beds. Since TERMIER's thesis (1936), this area was interpreted as a Devonian horst or an extrusive anticline. However, recent detailed mapping and structural analysis show that the Ktab Lahmar hill is a tectonic klippe overthrusting the Carboniferous (Figs 6 and 7):

— the abnormal contact which encompasses the hill is clearly a subhorizontal surface;

— Westphalian deposits are very coarse red conglomerates, where there is no Devonian pebble. Bedding planes seem subhorizontal;

— structures in the Devonian are metric upright or overturned folds, EW trending.

Following these data it is not possible to root the Devonian basement below the conglomerates. The only geometrical solution is a tectonic klippe.

South of the Ktab Lahmar hill, along the Ez-Zehiliga track, the Devonian outcrops in a ENE trending belt. Its northern limit is the major SE dipping thrust-fault, many microfault zones show quartzose slickensides where striae have a strong pitch (70-80°). Its southern limit is not clear on the field, but it can be interpreted as the unconformity of the Westphalian on the Devonian.

Source : MNHN, Paris

Southwards, the deformations of the Westphalian conglomerates outcropping between Ktab Lahmar and the Sidi-Kassem sanctuary correspond to layer parallel slip with striated slickensides, small metric box-folds with a forelimb truncated by shear planes.

An important microfracturation characterises the internal deformation of the Westphalian. A fault-slip data analysis has been made on several sites in the SW part of the basin (Fig. 8).

The "dièdres droits" method has been used to determine the palaeostress field (ANGELIER & MECHLER, 1977). The results indicate two phases. 1) A compressional phase with strike-slip and reverse microfaults and a N-S to NNW-SSE trending shortening axis. It is compatible with the motion along the major reverse faults. 2) An extensional phase with normal microfaults and a NE-SW trending elongation axis.

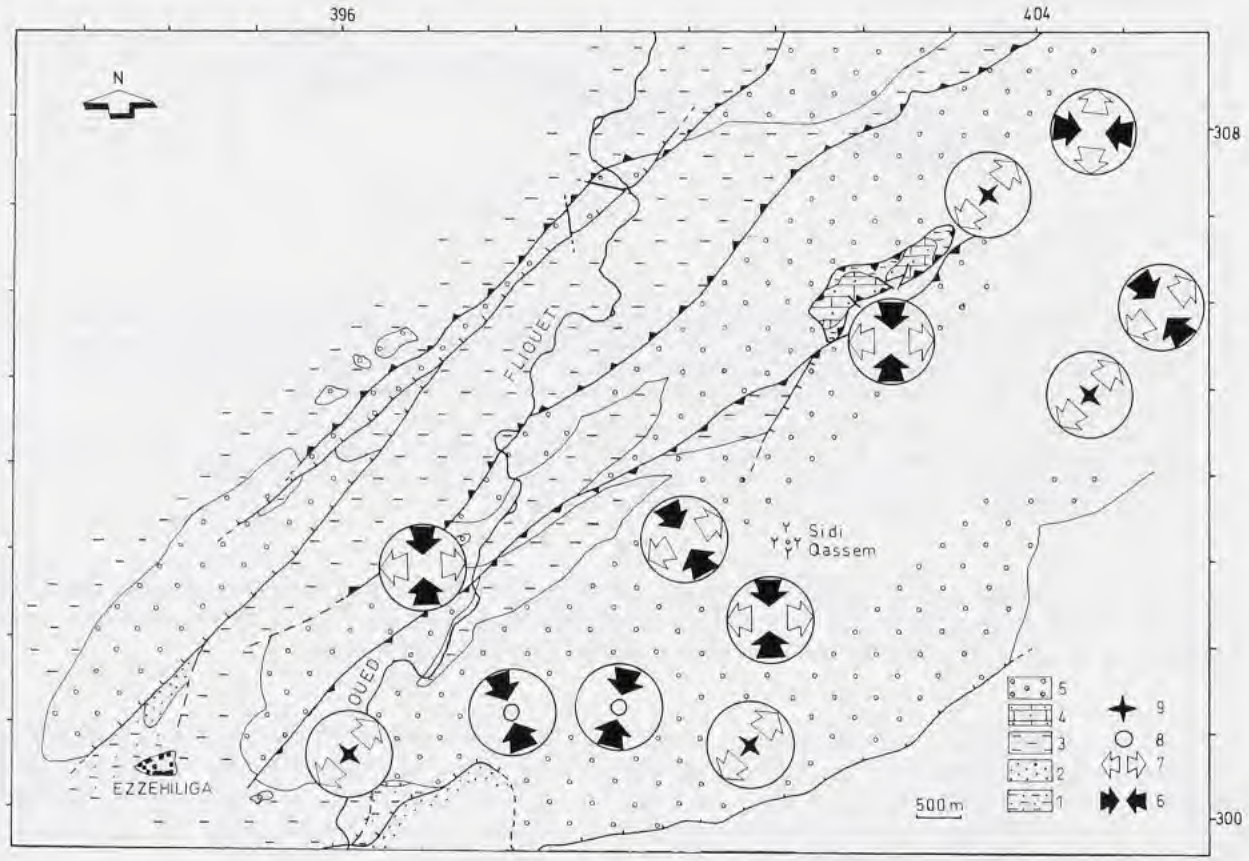

FIG. 8.— Simplified representation of the deformation fields according to the fault-slip data analysis ("dièdres droits" method, ANGELIER & MECHLER, 1977). **1** to **5**, see Fig. 6; **6**: shortening direction; **7**: stretching direction; **8**: vertical extension; **9**: vertical shortening.

*FIG. 8.— Représentation simplifiée des champs de déformation obtenus par l'analyse microtectonique de la fracturation (méthode des dièdres droits, ANGELIER & MECHLER, 1977). **1** à **5**, voir Fig. 6 ; **6** : direction de raccourcissement ; **7** : direction d'allongement ; **8** : extension verticale ; **9** : raccourcissement vertical.*

NORTHERN PART OF THE BASIN

This area extends between the Grou and Bou Regreg rivers. Our observations are not as detailed as in the southwestern zone. Cross-section (Fig. 7b) shows, like elsewhere, that the Westphalian overlies unconformably the Silurian-Devonian basement. The detrital red beds are deformed by large open folds NE-SW trending.

Source : MNHN, Paris

In addition to folding and fracturing, the Late Hercynian deformation is characterised in this area and especially near the northwestern border of the basin (Feddane Lebtam, northern flank of the Jebel Hadid) by the development of a subvertical cleavage, NE-SW trending. Closely spaced in the red sandstones and mudstones, the cleavage also cuts the conglomerates where it appears irregular and spaced. Following microscopical observations, the flattening is accomodated by both mechanical rotation and pressure-solution.

CONCLUSIONS

The main deformation of the late Westphalian Sidi-Kassem formation was controlled by motion along NE-SW trending reverse faults. Displacements can be locally important, especially toward the NW, with thrusting of the Devonian upon the Westphalian. The whole structure could be interpreted like flat-ramp systems with the decollement level localised in the Silurian-Devonian mudstones.

Physical conditions have permitted the development of a spaced cleavage on the northern basin border. But on the whole, the internal deformation corresponds to a pervasive microfracturation indicating a N-S to NNW-SSE directed compressional phase.

The deformation age is not accurately determined. Indeed the Sidi-Kassem formation is the only late Westphalian deposit in western Morocco, where erosional products of the Variscan belt are principally represented by the Stephanian (western High Atlas: KONING, 1957; SABER, 1994) and the Early Permian (Moroccan Meseta: EL WARTITI, 1990; EL WARTITI *et al.*, 1990). Structural relationships (conformity or unconformity) between Westphalian and Stephanian-Permian are not known. However, the post-Permian/pre-Triassic tectonic events are well documented in the Meseta and we recognise an important similarity between both style and direction of the deformations described in the Westphalian and those described in the Permian. For instance: thrusting and reverse-faults in the Rehamna massif (MULLER *et al.*, 1991), fault-slip-data analysis in the Central Massif (AÏT BRAHIM & TAHIRI, 1996). Thus, the compressional late Variscan phase described here in the Sidi-Kassem basin could probably be of Latest Permian-Earliest Triassic.

REFERENCES

AÏT BRAHIM, L. & TAHIRI, A., 1996.— Rotation horaire des contraintes et mécanismes d'ouverture et de fermeture des bassins permiens du Maroc central. *In*: F. MEDINA (ed.), *Le Permien et le Trias du Maroc: état des connaissances*. Pumag, Marrakech: 87-98.

ANGELIER, J. & MECHLER, P., 1977. — Sur une méthode graphique de recherche des contraintes principales également utilisables en tectonique et en séismologie: la méthode des dièdres droits. *Bulletin de la Société géologique de France*, **6**: 1309-1318.

CHAKIRI, S., 1991. — *Le Paléozoïque de la région de Tsili-Tiddas (Maroc central occidental). Stratigraphie, sédimentologie et évolution structurale hercynienne.* Thèse de 3ème cycle, Université Mohammed V, Rabat, Maroc: 1-227.

CHOUBERT, G., 1951.— Essai de chronologie hercynienne. *Notes et Mémoires du Service géologique du Maroc, Rabat*, **83**: 9-78.

CHOUBERT, G., 1956 (ed.).— Carte géologique du Maroc à 1/500 000ème, feuille Rabat. *Notes et Mémoires du Service géologique du Maroc, Rabat*, **70**.

EL WARTITI, M., 1990.— *Le Permien du Maroc mésétien. Étude géologique et implications paléogéographiques.* Thèse d'État, Université Mohammed V, Rabat, Maroc: 1-501.

EL WARTITI, M., BROUTIN, J., FREYTET, P., LAHRIB, M. & TOUTIN-MORIN, N., 1990.— Continental deposits in Permian basins of the Mesetian Morocco. Geodynamic history. *Journal of African Earth-Sciences*, **10** (1/2): 361-368.

GHAZALI, K., 1995.— *Contribution à l'étude géologique du bassin de Sidi-Kassem (Formation de Feddane Lebtam). Maroc hercynien central.* Mémoire de DEA, Université Mohammed V, Rabat, Maroc: 1-43.

HOLLARD, H., 1985 (ed.).— Carte géologique du Maroc à 1/1 000 000ème. *Notes et Mémoires du Service géologique du Maroc, Rabat*, **260**.

KONING, G. DE, 1957.— *Géologie des Ida-ou-Zal (Maroc). Stratigraphie, pétrographie et tectonique de la partie SW du Bloc occidental du Massif ancien du Haut Atlas.* Edvard Ijdo N.V., Leyde: 1-210.

MIALL, A.D., 1978.— Lithofacies types and vertical profile models in braided river deposits. *In:* A.D. MIALL (ed.), Fluvial sedimentology. *Memoir- Canadian Society of Petroleum Geologists*, **5**: 597-604.

Source : MNHN, Paris

MULLER, J., CORNÉE, J.J. & EL KAMEL, F., 1991.— Évolution tectono-sédimentaire d'un bassin molassique post-orogénique: l'exemple des séries conglomératiques stéphano-triasiques de Mechra-ben-Abbou, Rehamna, Maroc. *Géologie méditerranéenne*, **1-2**: 109-120.

PIQUÉ, A. & MICHARD, A., 1989.— Moroccan Hercynides: a synopsis. The paleozoic sedimentary and tectonic evolution at the northern margin of the West Africa. *American Journal of Science*, **289**: 286-330.

PRUVOST, P. & TERMIER, H., 1949.— Sur l'âge de la formation houillère de Sidi-Kassem (Bled Zaer, Maroc). *Comptes Rendus de l'Académie des Sciences, Paris*, **229**: 7-9.

ROCH, E., 1950.— Histoire stratigraphique du Maroc. *Notes et Mémoires du Service géologique du Maroc, Rabat*, **80**: 1-435, 77 figs, 22 pls.

SABER, H., 1994.— Sédimentologie et évidence d'une tectonique tardi-hercynienne d'âge permien inférieur dans le bassin des Ida ou Ziki, SW du massif ancien du Haut Atlas (région d'Argana, Maroc). *Journal of African Earth-Sciences*, **19**: 99-108.

TERMIER, H., 1936.— Études géologiques sur le Maroc central et le Moyen Atlas septentrional. 1: Les Terrains primaires et le Permo-Trias. 2: Les Terrains post-triasiques. 3: Paléontologie, pétrographie. 4: Atlas. *Notes et Mémoires du Service des Mines et de la Carte géologique du Maroc*, **33**: 1-1566.

TERMIER, H. & TERMIER, G., 1951.— Présence de Viséen dans le bassin houiller de Sidi-Kassem. *Comptes Rendus de l'Académie des Sciences, Paris*, **232**: 1310-1312.

Source : MNHN, Paris

2

Triassic series of Morocco: stratigraphy, palaeogeography and structuring of the Southwestern Peri-Tethyan Platform. An overview

Mostafa OUJIDI [1], *Louis COUREL* [2], *Naïma BENAOUISS* [3], *Mohamed EL MOSTAINE* [4], *Mohamed EL YOUSSI* [5], *Mohamed ET TOUHAMI* [1], *Driss OUARHACHE* [6], *Abdellah SABAOUI* [6] & *Abdel-Illah TOURANI* [3]

[1] Université Mohamed I^er^, Laboratoire de Géodynamique, route de Sidi Maafa, 60 000 Oujda, Maroc

[2] Université de Bourgogne et UMR 5561 CNRS, 6, boulevard Gabriel, 21 000 Dijon, France

[3] Faculté des Sciences Semlalia, boulevard Prince Moulay Abdellah, BP S15, Marrakech, Maroc

[4] ONAREP, 34, avenue Al Fadila, Rabat, Maroc

[5] Université Mohamed V-Agdal, BP 1014, Rabat, Maroc

[6] Faculté des Sciences Dhar El Mahraz, BP 1796, Atlas Fès, Maroc

ABSTRACT

New biostratigraphic findings combined with earlier works allow us to establish a new stratigraphic framework for the epicratonic Triassic series of Morocco. The Tethyan transgression from the NE reached the Oujda area during the late Ladinian time before subsequently spreading extensively across the central High Atlas during the Carnian. The transgression from the Proto-Atlantic domain over SW Morocco developed at the end of the Triassic (late Carnian/Norian) and during the Early Jurassic. The structural-sedimentary history of the Triassic epicratonic platform can be divided into three major stages. Basalt flows and exceptional carbonate level deposition of the Oujda Mountains were related to reactivation of Hercynian and Late Hercynian ENE-WSW and EW faults. The Carnian episode was marked by active extension. Maximum subsidence and basalt flows in the High Atlas troughs were controlled by N45° conjugated with N70-90° normal synsedimentary faults. Normal or sinistral normal faulting guided the progressive transgression of the Tethys from the NE. Late Carnian/Norian eastward dipping normal faults generally post-date the ENE-WSW to EW faults bounding the Atlasic tectonic troughs. In the west of Morocco, from the late Norian up, grabens of the Proto-Atlantic domain were filled with clastic material mainly from SW tilted High Atlas rift compartments. Above the debatable boundary between the Triassic and Lower Jurassic series, basalt flows and thick evaporite depocentres developed over the Proto-Atlantic domains. At the scale of the whole Moroccan platform the homogeneity of the Late Triassic and early Liassic facies could be indicative of easier communication in coalescent basins during marine onlaps.

OUJIDI, M., COUREL, L., BENAOUISS, N., El MOSTAINE, M., El YOUSSI, M., ET TOUHAMI, M., OUARHACHE, D., SABAOUI, A. & TOURANI, A.-I., 2000.—Triassic series of Morocco: stratigraphy, palaeogeography and structuring of the southwestern Peri-Tethyan Platform. An overview. *In*: S. CRASQUIN-SOLEAU & E. BARRIER (eds), Peri-Tethys Memoir 5: new data on Peri-Tethyan sedimentary basins, *Mém. Mus. natn. Hist. nat.*, **182** : 23-38. Paris ISBN : 2-85653-524-0.

Source : MNHN, Paris

RÉSUMÉ

Séries triasiques du Maroc : stratigraphie, paléogéographie et structuration de la plate-forme péri-téthysienne du Sud-Ouest. Une revue.

Un nouveau cadre stratigraphique est proposé pour les séries triasiques du Maroc, basé sur des données biostratigraphiques anciennes et récentes. La transgression téthysienne venue du NE atteint la région d'Oujda au Ladinien supérieur/Carnien inférieur, avant de s'étendre plus largement jusqu'au Haut Atlas central pendant le Carnien. Une transgression venue du domaine proto-atlantique se développe plus tard sur l'Ouest du Maroc à la fin du Trias, au Norien et pendant le début du Jurassique. L'histoire sédimentaire de la structuration de la plate-forme épicratonique au Trias est divisée en trois stades principaux. Des coulées de basalte et le dépôt localisé de carbonates dans la région d'Oujda sont liés à la réactivation de failles hercyniennes et tardi-hercyniennes ENE-WSW et EW. Le stade carnien est marqué par une extension. Une subsidence maximum et des coulées de basalte dans le Haut Atlas sont contrôlées par des failles synsédimentaires N45° et N70-90° conjuguées. Une fracturation normale ou sénestre normale a guidé la transgression progressive de la Téthys venue du NE. Des failles normales d'âge carnien tardif/norien plongeant vers l'E reprennent les directions ENE-WSW des fractures limitant les gouttières atlasiques. Des grabens du domaine proto-atlantique, dans l'Ouest du Maroc, sont remplis à partir du Norien tardif par du matériel clastique venant principalement de blocs basculés du Haut Atlas. Au dessus de la limite discutable entre le Trias et la base du Lias, des coulées de basaltes et des dépôts-centres à évaporites se développent dans le domaine proto-atlantique. A l'échelle de l'ensemble de la plate-forme marocaine, l'homogénéité des faciès du Trias tardif et de la base du Lias témoignent de communications plus faciles dans des bassins coalescents pendant des onlaps marins.

INTRODUCTION

Work on the Triassic deposits of Morocco began in the 1930s (TERMIER, 1936; ROCH, 1939). The Marrakech symposium (1982) and the Rabat round-table (1995) presented compilations of the last thirty years work of local character. Palaeogeographic syntheses have attempted to situate the Triassic series of Morocco in a wider framework (VAN HOUTEN, 1977; MANSPEIZER *et al.*, 1978; SALVAN, 1984; BEAUCHAMP, 1985, 1988). Such efforts have been thwarted, though, by the paucity of chronological data. MANSPEIZER *et al.* (1978) and SALVAN (1984) concentrated particularly on the basalt-claystone sequences of Northeast Morocco and the Middle Atlas and on the High Atlas lava flows. It is suggested that at least four volcanic episodes occurred from Ladinian to Sinemurian times. Evidence for this hypothesis is the apparent difference in chemical composition of lava from these different provinces (MANSPEIZER *et al.*, 1978). In the absence of reliable chronological markers, VAN HOUTEN (1977) considered that except for basal deposits in the High Atlas (probably from the Lower Triassic), the Triassic deposits of Morocco do not pre-date the beginning of the Late Triassic. He further postulated that the more widespread uppermost strata (basalts, claystones and evaporite facies) date back to the Early Jurassic and may allow correlations to be made throughout Morocco.

This paper is one such attempt at correlating reference series from different Triassic basins in Morocco. Recent and mainly biostratigraphic data are compared with earlier findings for the purpose of proposing a new historical framework for the Moroccan domain during Triassic times. To this end, palaeogeographical reconstructions are proposed which lead to the hypothesis about the structuring of this Peri-Tethyan domain.

REGIONAL FRAMEWORK

The Triassic series lie unconformably over the deformed Palaeozoic basement or, locally, over coarse intra-mountane basin deposits dated to the Early Permian by plant fossils (CAILLEUX *et al.*, 1983; LARHRIB, 1996; SEBAN, 1996). The Triassic series is up to 2000 m. From outcrop and borehole data supplemented by seismic profiles, 15 separate basins have been identified for the transition from the Late Triassic to Early Jurassic, most of which are oriented NE or ENE (Fig. 1). Their boundaries are not clearly identified, however, and some may be simple depocentres in a largely coalescent complex. In the areas where subsidence was less intense, shallow series are made up of poorly dated evaporitic claystones. LORENZ (1988) distinguished three types of basin according to the dominant facies, including the evaporite levels of the lower Liassic whose thicknesses are quoted below:

Source : MNHN, Paris

— basins with thick sandstone and conglomerate series: Argana (>2500 m), Marrakech High Atlas (1500 m), Central High Atlas (1000 m) and Kerrouchen (600 m);

— basins with thick salt series: Essaouira (2300 m), Berrechid, Guercif, Ziz-Guir (500 m) and Hauts Plateaux (1200 m). Evaporite basins have also been detected along the present-day Atlantic coast and as far offshore as Tarfaya Basin;

— basins with detrital deposits overlain by thick halite series: Doukkala (1390 m), Rharb (1100 m), Khémisset (1095 m), Bou Fekrane (900 m) and Moyenne Moulouya (Tamdafet, 950 m).

Investigators agree that broad areas of non-deposition subsisted in the Meseta of Central Morocco.

The Rif domain to the north is composed of allochthonous sheets whose palinspastic position is uncertain. These units include red detrital facies (BAUDELOT *et al.*, 1984) or marine platform carbonates (WILDI, 1983). They are not discussed in this paper which only deals with the autochthonous epicratonic domain.

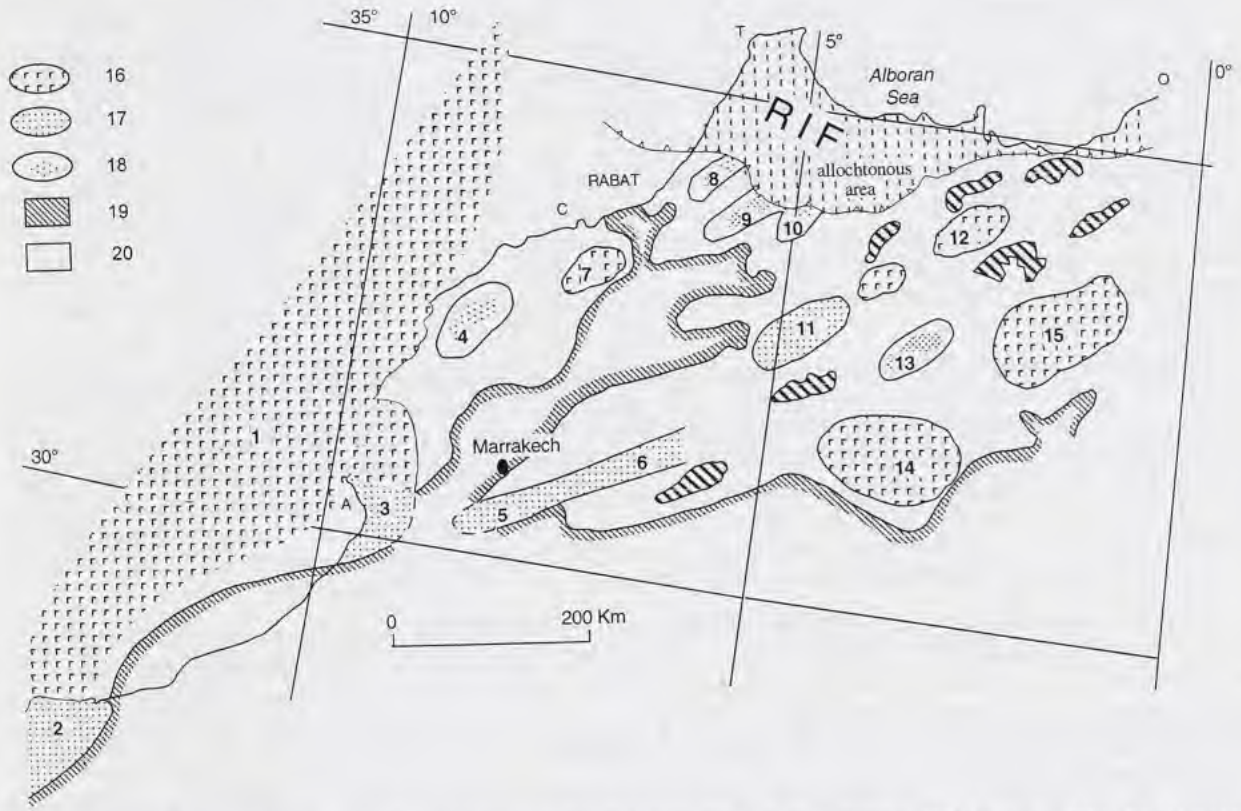

FIG. 1.— Location of the main Upper Triassic basins (after SALVAN, 1984; VAN HOUTEN, 1977; LORENZ, 1988; BEAUCHAMP *et al.*, 1995). **1**, Halitic and diapiric zone of the Atlantic margin; **2**, Tarfaya-Layoune; **3**, Essaouira; **4**, Doukkala; **5**, High Atlas of Marrakech; **6**, Central High Atlas; **7**, Berrechid; **8**, Rharb; **9**, Khémisset; **10**, Bou Fekrane; **11**, Kerrouchen; **12**, Guercif; **13**, Middle Moulouya; **14**, Ziz-Guir; **15**, High Plateaux; **16**, Basin containing predominantly halite; **17**, Basin containing predominantly clastics; **18**, Basin containing basal clastics and thick overlying halite; **19**, emerged during the Triassic time; **20**, Interbasin area covered mostly by evaporite mudstone.

*FIG. 1.— Principaux bassins marocains au Trias supérieur (d'après SALVAN, 1984 ; VAN HOUTEN, 1977 ; LORENZ, 1988 ; BEAUCHAMP et al., 1995). **1**, Zone salifère et diapirique de la marge atlantique ; **2**, Tarfaya-Layoune ; **3**, Essaouira ; **4**, Doukkala ; **5**, Haut Atlas de Marrakech ; **6**, Haut Atlas central ; **7**, Berrechid ; **8**, Rharb ; **9**, Khémisset ; **10**, Bou Fekrane ; **11**, Kerrouchen ; **12**, Guercif ; **13**, Moyenne Moulouya ; **14**, Ziz-Guir ; **15**, Hauts Plateaux ; **16**, Bassin contenant de la halite dominante ; **17**, Bassin contenant des clastiques dominants ; **18**, Bassin contenant des clastiques à la base recouverts par de la halite ; **19**, Emergé durant le Trias ; **20**, Domaine séparant les bassins principalement recouvert par des mudstones à évaporites.*

Source : MNHN, Paris

STRATIGRAPHIC FRAMEWORK

CHRONOLOGICAL DATA

The Triassic series of Morocco are poorly dated. Sedimentary strata have until recent years yielded almost exclusively imprints and plant remains. A handful of animal fossils, despite their palaeoecological value, were of little use in establishing a detailed stratigraphic scale. However, advances in palynology have recently made it possible to be more specific about many levels. Basalts have been weathered and radiochronological datings often lie outside the limits suggested by biostratigraphy. This tool must therefore be used with caution. All the ancient and recent data allow us significant datings for the main formations to attempt to make correlations between basins (Fig. 2).

The recent discovery of ostracod fauna in the Oujda Mountains (CRASQUIN-SOLEAU *et al.*, 1997) has allowed two beds to be dated. *Limnocythere keuperea* Will and *Speluncella* n. sp. Crasquin-Soleau *et al.* date to the late Norian while *Lutkevichinella kristanae* Crasquin-Soleau *et al.*, which is similar to *Lutkevichinella lata* Kozur, found in association with *Anoplophora lettica* Quenstedt, is ascribed to the late Ladinian / early Carnian boundary. These latest data corroborate and supplement those of OWODENKO (1946) in the same beds of that sector.

Recent studies have refined the biostratigraphic framework in the Middle Atlas south of Fès, between Central Morocco and the Tazekka Massif. Carnian spore and pollen associations (SABAOUI, 1996; BAUDELOT *et al.*, 1984, 1986) have been discovered in sedimentary levels beneath the first Triassic basalt flows. In addition, OUARHACHE (1987) and BAUDELOT *et al.* (1986) described early to mid Norian ostracods *Sulcocythere hajbensis* Colin associated with *Darwinula* in the El Hajeb inter lava flow bed.

EL YOUSSI (1986) subdivided the Oukaïmeden Sandstone formation in the High Atlas south of Midelt into three members (a, b, c) by facies and sedimentary environment. The top of the "a" member has proved to have high late Carnian spore and pollen content. In the Ourika region, COUSMINER & MANSPEIZER (1977) considered that the entire Oukaïmeden Sandstone formation is mid Carnian. In the Argana Basin, among the many vertebrate remains collected and described from 1962 to 1975 by DUTUIT (1976), JALIL & DUTUIT (1996) and JALIL (1996), the presence of large Metoposaurids (*Metoposaurus ouazzoui* Dutuit and *M. lyazidi* Dutuit) in T5 and of a Cyclotosaurus in T4, allows these units to be dated to the middle to late Carnian.

In the Essaouira Basin, SLIMANE & EL MOSTAINE (1997) reported ostracods *Darwinula* in borehole MKL-1 between 3027 and 3300 m and *Lymnocythere* at 2964 m in borehole MKL-104. The corresponding clay-siltstones have been ascribed to the Carnian-Norian. Furthermore, K/Ar dating of a fresh dolerite sample located at the base of the Triassic series between 2768 m and 3163 m in borehole JRP-1 yielded an absolute age of 210 Ma, making it Norian by ODIN's scale (1982).

In the Doukkala Basin, SLIMANE & EL MOSTAINE (1997) reported ostracods at the base of the fine clastic series located immediately below the lower salt formation of boreholes BHL-1 and DOT-1. The species recognised belong to *Gemmanella* in borehole BHL-1 at depths of 1654, 1680, 1812 and 1818 m and *Paracypris* and *Lutkevichinella* in the DOT-1 borehole at depths of 1758, 1867 and 1875 m. Those authors dated these formations to the Carnian-Norian. Foraminifers and ostracods have allowed the topmost clastic and salt formations to be dated to the Lower Jurassic (Sinemurian). Thus the age of the claystone and salt formations in association with the volcanic lava flows may range from Carnian-Norian to Sinemurian.

NEW STRATIGRAPHIC FRAMEWORK

We propose a new stratigraphic framework (Fig. 2) according to correlations based on the new biostratigraphic findings combined with earlier works.

Source : MNHN, Paris

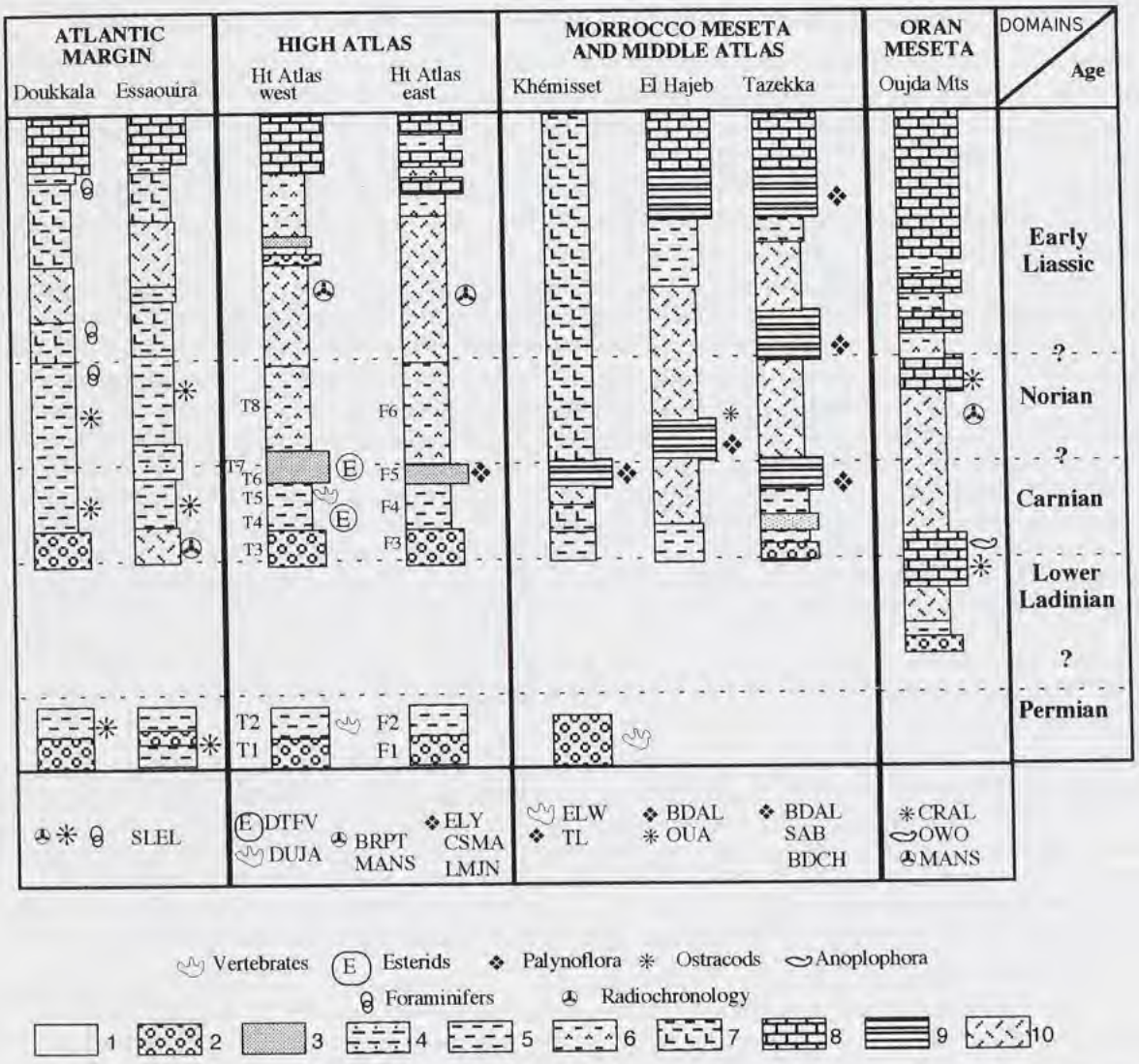

FIG. 2.— Permian to lower Liassic Moroccan series: correlations. **1**, gap; **2**, conglomerate; **3**, sandstones; **4**, clayey sandstones; **5**, silty claystones; **6**, gypsiferous claystones; **7**, halite and claystones; **8**, carbonates; **9**, grey claystones; **10**, doleritic basalts. DTFV-DEFRETIN & FAUVELET (1951); BRPT-BERTRAND (1991); DUJA-DUTUIT (1976); JALIL & DUTUIT (1996); ELY-EL YOUSSI (1986); CSMA-COUSMINER & MANSPEIZER (1977); LMJN-LE MARREC (1979); JENNY (1983); ELW-EL WARTITI (1990); TL-TAUGOURDEAU-LANZ (1978); MANS-MANSPEIZER *et al.* (1978); BDAL-BAUDELOT *et al.* (1990); OUA-OUARHACHE (1987); SAB-SABAOUI (1987); BDCH-BAUDELOT & CHARRIÈRE (1983); CRAL-CRASQUIN-SOLEAU *et al.* (1997); OWO-OWODENKO (1946); SLEL-SLIMANE & EL MOSTAINE (1997).

*FIG. 2.— Séries marocaines, du Permien au Lias inférieur : corrélations. **1**, lacune ; **2**, conglomérat ; **3**, grès ; **4**, grès argileux ; **5**, argilites silteuses ; **6**, argilites gypsifères ; **7**, halite et argilites ; **8**, carbonates ; **9**, argilites fétides ; **10**, basaltes doléritiques. DTFV-DEFRETIN & FAUVELET (1951) ; BRPT-BERTRAND (1991) ; DUJA-DUTUIT (1976), JALIL & DUTUIT (1996) ; ELY-EL YOUSSI (1986) ; CSMA-COUSMINER & MANSPEIZER (1976) ; LMJN-LE MARREC (1977), JENNY (1983) ; ELW-EL WARTITI (1990) ; TL-TAUGOURDEAU-LANZ (1978) ; MANS-MANSPEIZER* et al. *(1978) ; BDAL-BAUDELOT* et al. *(1990) ; OUA-OUARHACHE (1987) ; SAB-SABAOUI (1987) ; BDCH-BAUDELOT & CHARRIÈRE (1983) ; CRAL-CRASQUIN-SOLEAU* et al. *(1997) ; OWO-OWODENKO (1946) ; SLEL-SLIMANE & EL MOSTAINE (1997).*

Source : MNHN, Paris

No Permian deposits are recorded in Eastern Morocco. Permian intracontinental basins form in the Meseta, and the Middle and High Atlas Mountains. These coarse, post-orogenic deposits are lithologically distinct from those of the Triassic and have yielded Autunian and Stephano-Autunian flora (VAN HOUTEN, 1976, 1977; LORENZ, 1988; EL WARTITI, 1990; LARHIB, 1996; SEBBAN, 1996).

There is a large sedimentary gap between the Lower Permian and the upper Ladinian reflecting weathering and erosional processes in an arid climate (LUCAS, 1942; ROBINSON, 1973).

The oldest Triassic deposits in Morocco outside the Rif dated late Ladinian/early Carnian are found exclusively in the Oujda region (CRASQUIN-SOLEAU *et al.*, 1997). This first Tethyan onlap is materialised by a carbonate bar. The fauna is characteristic of brackish to marine conditions in an intertidal to subtidal environment (OUJIDI, 1994). This bar overlies clay-siltstones deposited as mud flats and the first basalt flow.

The Carnian deposits yield the earliest Triassic biostratigraphic assemblages in Morocco outside the Oujda Mountains. In the High Atlas, mainly continental fluvial or alluvial fan sedimentation (F3 or T3) overlies the Permian series (MATTIS, 1977; VAN HOUTEN, 1977; PETIT & BEAUCHAMP, 1986; EL YOUSSI, 1986). The silt and clay formation (F4 or T4/5) was interpreted as floodplain deposits by MATTIS (1977) on the evidence of dispersed channels and bioturbation of the clay and silt deposits. By contrast, PETIT & BEAUCHAMP (1986) interpreted it as a margin-littoral tidal-flat type environment because of the presence of symmetric ripples and marine bivalve tests. Formation F5 (or T6/7) or the Oukaïmeden Sandstones was interpreted by EL YOUSSI (1986) as a delta environment with the main SW-oriented flow. BENAOUISS (1996) and BENAOUISS *et al.* (1996) recognised in this F5 formation of the High Atlas intertidal structures which are indicative of brief marine incursions from the NE, the direction of the Peri-Tethyan marine domain (Fig. 5). They also discovered eolianites at the top of the formation. Contemporary series in Central Morocco reflect lagoonal clay sedimentation with a few evaporite levels to the Khemisset Basin. These claystones are associated with lignitic strata in the Tazekka Massif (SABAOUI, 1987, 1996). A new basalt outflow (the second phase) is recorded in the Carnian deposits of the Oujda Mountains. It is thought to correspond to the first phase of basalt outflow in the El Hajeb Causse.

It is currently difficult to make out separations between the upper Carnian and Rhaetian deposits. Assemblages of Norian ostracods are described in the Oujda Mountains, Middle Atlas, Essaouira Basin and Doukkala Basin which are characteristic of oligo- to mio-haline, limnic to brackish environments (CRASQUIN-SOLEAU *et al.*, 1997). They are said to correspond to permanent lacustrine or possibly lagoonal environments (BAUDELOT *et al.*, 1986). Their presence does not exclude upper Carnian and Rhaetian deposits in the same facies. At that time, salt claystones sometimes containing basalt flows largely dominated homogeneous sedimentation in coalescent basins (BEAUCHAMP, 1988).

It is difficult to locate the Triassic / Jurassic boundary. Carbonate beds are found above the Triassic series in the Oujda Mountains in Eastern Morocco and in the Argana corridor in Western Morocco. This suggests biostratigraphic dating should be possible, but new data are required yet. It seems that these carbonates are less developed, or even absent in the central part of Morocco where lagoonal, evaporite or stromatolite claystones are found. This is the case in the Khémisset Basin, for example, and ET TOUHAMI (1994) assumed that this basin was the site of mixing of Tethyan and Proto-Atlantic marine waters.

These correlations emphasise three main results:

— on the scale of Morocco, basalt flows occurred in succession from the Ladinian / Carnian boundary to the early Jurassic and are on the whole more and more younger toward the West;

— the Tethyan transgression from the NE reached the Oujda area during the late Ladinian before subsequently spreading extensively across the central High Atlas during the Carnian;

— the transgression from the Proto-Atlantic domain over SW Morocco developed at the end of the Triassic (late Carnian / Norian) and during the Early Jurassic.

Source : MNHN, Paris

STRUCTURING OF THE MOROCCAN EPICRATONIC DOMAIN

Most workers agree that the structuring of the Moroccan margin during the Triassic was mainly controlled by reactivation of Hercynian and late Hercynian faults (ENE-WSW to E-W) with, initially, a virtually homogeneous NW-SE direction of extension. However, different geodynamic models have been proposed to explain the formation of the Triassic basins of Morocco.

VAN HOUTEN (1977), MANSPEIZER *et al.* (1978), MANSPEIZER (1988), LAVILLE (1981), LAVILLE & PETIT (1984), LAVILLE & PIQUÉ (1991, 1992) and PIQUÉ & LAVILLE (1995) considered that the structuring of the basins is related to a fault field with a high normal component forming part of a megazone of sinistral shear faulting, corresponding to the reactivated "Atlas Palaeozoic transform zone" to the South and the "Gibraltar-Azores transform zone" to the north.

FAVRE & STAMPFLI (1992), STAMPFLI (1994) and MEDINA (1995, 1996) postulated that the Atlantic Rift probably developed in two major extensional stages. An initial Carnian, or slightly earlier stage, is related to NNW-SSE extension. This apparently induced shear faulting in the Atlas rift, partly by simple reactivation of inherited Hercynian and Late Hercynian structures. A late NW-SE extensional stage seems to have produced pure shear at the end of the rifting episode (SAWYER & HARRY, 1991). It is thought to be related to the emplacement of a thermal dome along the rift centerline together with the raising of the rift shoulders. However, LISTER *et al.* (1991) and MÉDINA *et al.* (1996) observed that the structural evolution of the Souss Basin in the Triassic was controlled by a deep detachment, probably an old, gently NNW sloping, Hercynian plane of weakness, from which the entire system of the Tizi n'Test fault zone arose.

EL KOCHRI & CHOROWICZ (1996), although dealing with the Jurassic rift, proposed an alternative hypothesis to the pure slip stress regime acting along the E-W faults. They assumed that at the beginning of the Jurassic, regional extension was oriented rather WNW-ESE, obliquely to the main rifting faults. These faults, which were largely divergent to the direction of maximum extension, worked like normal faults and were responsible for the tilting of the different tectonic blocks. The faults parallel to the direction of extension slipped and operated as transfer faults. The coexistence of single- or double-curve transfer faults defines a highly particular tectonic style to explain the kinematics of rift opening.

In the light of the new stratigraphic framework proposed and the review of the structural models that attempt to explain the opening of the basins on the Moroccan margin during the Triassic, we suggest that the structural-sedimentary history of the Triassic epicratonic platform can be divided into three major stages.

PRE-RIFT STAGE (BEFORE CARNIAN TIME)

Before the break-up of Pangea, the northwest edge of the African Craton was attached to North America between Nova Scotia and Newfoundland (BALLARD & UCHUPI, 1975; LORENZ, 1988). The nearest open marine domain was the Tethys, some 1000 to 1500 km to the east. During the start of the Triassic, Morocco was the site of erosion, with no deposits being conserved, and with an eastward palaeoslope (VAN HOUTEN *et al.*, 1974; VAN HOUTEN & BROWN, 1975, 1977). The oldest Triassic deposits on the Moroccan Craton are found in the Oujda Mountains and are dated to late Ladinian times (CRASQUIN-SOLEAU *et al.*, 1997) (Fig. 4). The deposits are a very condensed marine carbonate bed which was transgressive over tholeiitic basalt. The structural framework of the Oujda Mountains was characterised by small elongated depocenters several kilometers in length separated by shoals (Fig. 3). The direction of marine influences between the Tethys and the Moroccan platform was mainly controlled by WSW-ENE tectonic troughs. These synsedimentary extensional structures were related to reactivation of Hercynian and Late Hercynian faults (ENE-WSW and E-W) (OUJIDI, 1994, 1996). The exceptional carbonate beds of the Oujda Mountains replaced in their structural context suggest marine aggradation wedges from the Tethys to the northeast (CRASQUIN-SOLEAU *et al.*, 1997).

Source : MNHN, Paris

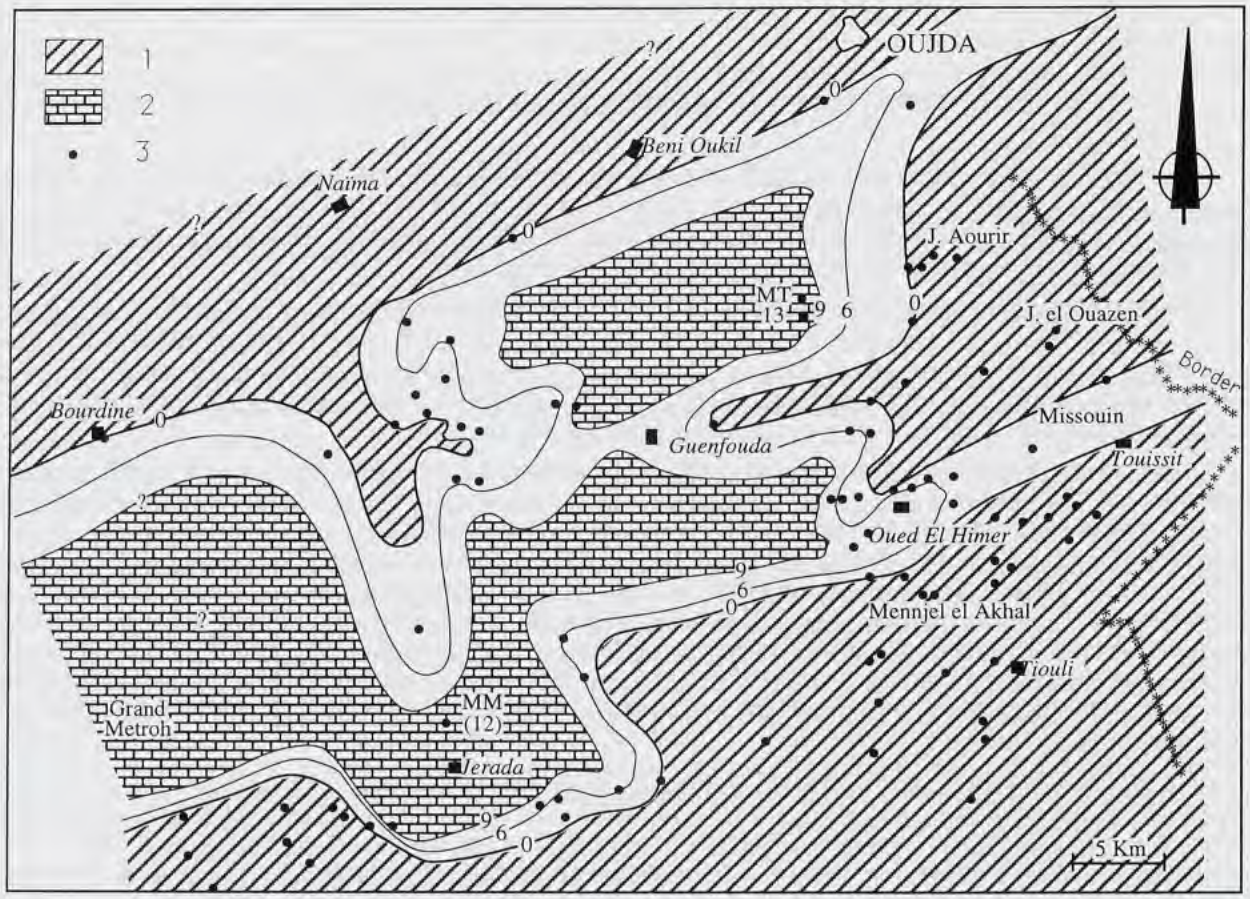

FIG. 3.— Isopach map of the "Barre carbonatée intercalaire" in the Oujda mountains (after OUJIDI, 1994). **1**, Area without "Barre carbonatée intercalaire"; **2**, Maximum thickness of the "Barre carbonatée intermédiaire": 11 to 13 m thick; **3**, data point location, MT-J. Metsila, MM-Moussa ou Mohammed, 12 et 13-maximum thickness of the "Barre carbonatée intercalaire" in metres.

*FIG. 3.— Carte des isopaques de la Barre carbonatée intercalaire dans les Monts d'Oujda. (d'après OUJIDI, 1994) **1**, domaine sans Barre carbonatée intercalaire ; **2**, Épaisseur maximum de la Barre carbonatée intermédiaire : 11 à 13 m ; **3**, localisation des points de données, MT-J. Metsila, MM-Moussa ou Mohammed, 12 et 13-épaisseur maximale de la Barre carbonatée intercalaire en mètres.*

SYN-RIFT STAGE

— Carnian: the climax of the Triassic rifting in Morocco is of Carnian age. Subsidence reached its maximum in the Triassic basins located in the High Atlas troughs and to a lesser extent in the Middle Atlas (Kerrouchen Basin) (Fig. 5). This episode is characterised by active extension in a strike slip system. N45° synsedimentary normal faults are highly developed and their movement is conjugated with N70-90° normal faults. Half-grabens are thus delineated that are up to several hundred metres thick, that link up to varying degrees and exhibit differential subsidence. This fracturation is responsible for the outpouring of basalts in relation with the onsetting of rifting over the whole of the Moroccan Margin. With the exception of the shallow marine carbonates of the Oujda Mountains, Carnian sedimentary environments were mainly continental: fluvial, fluvio-lacustrine or alluvial fans. However, reactivated normal or sinistral-normal faulting of the Hercynian and Late Hercynian structures (ENE-WSW to E-W) guided the progressive transgression of the Tethys from the northeast over the North African margin. Thus tidal marine interbeds appeared in the High Atlas (BEAUCHAMP *et al.*, 1995; BENAOUIS *et al.*, 1996).

Source : MNHN, Paris

FIG. 4.— Palaeogeographic map of the late Ladinian series in Morocco. **1**, Triassic erosion or non-deposition area; **2**, allochtonous domain; **3**, marine limestone and dolostone; **4**, marine incursion; **5**, volcanism. Ez-J. Ez Zidour. C-Casablanca, S-Safi, A-Agadir, O-Oran, T-Tanger.

*FIG. 4.— Carte paléogéographique du Maroc pendant le Ladinien supérieur. **1**, zone d'érosion triasique ou de non dépôt ; **2**, domaine allochtone ; **3**, calcaire et dolomie marines ; **4**, incursion marine ; **5** volcanisme. Ez-J. Ez Zidour. C-Casablanca, S-Safi, A-Agadir, O-Oran, T-Tanger.*

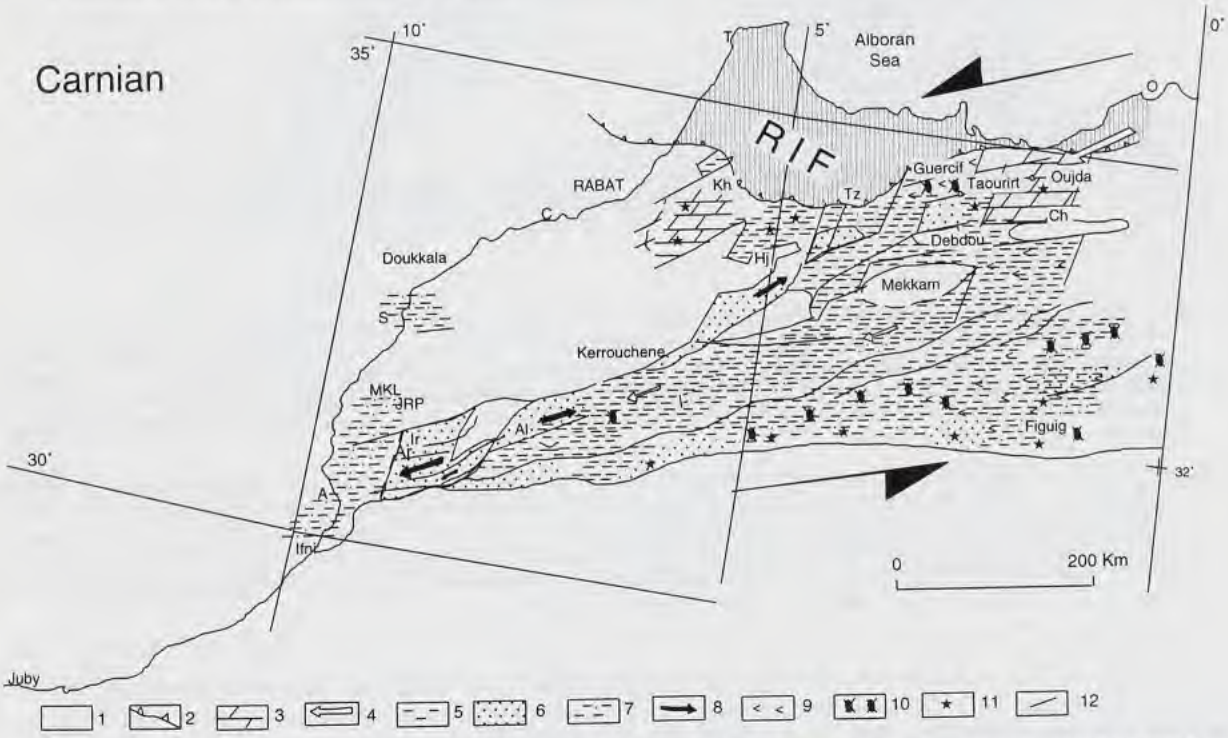

FIG. 5.— Palaeogeographic map of the Carnian series in Morocco. Lithologic and geographic captions, see the figure 6.

FIG. 5.— Carte paléogéographique du Maroc pendant le Carnien. Légendes lithologiques et géographiques, voir la figure 6.

Source : MNHN, Paris

— Late Carnian / Norian: in the Mesetian and the Atlasic domains, the N-S normal faults with medium to low eastward dipping generally postdate the ENE-WSW to E-W faults bounding the tectonic troughs initiated in the Carnian (Fig. 6). The direction of extension is NW-SE and the strike-slip component weak. This structuring is said to be controlled by a deep detachment plane, probably an old Hercynian plane of weakness, dipping slightly NNW (MEDINA *et al.*, 1996) according to the model of LISTER *et al.* (1991). It is related to the opening of the Proto-Atlantic domain, flooded by the epicontinental Tethys Ocean which supposedly crossed the Gibraltar fracture zone (E-W or NE-SW; RICOU, 1994) from the North. The NS faults occur mainly in the west of Morocco (Fig. 6) in the basins of Tarfaya-Laâyoun, Argana, Essaouira, Doukkala, Berrechid-El Gara and Khémisset. N30-40°E faults are interpreted (BIRON, 1982; BEAUCHAMP, 1988) as neo-breaks engendered by oblique extension of existing N70°E faults which operated as sinistral strike-slip / normal faults during the Triassic.

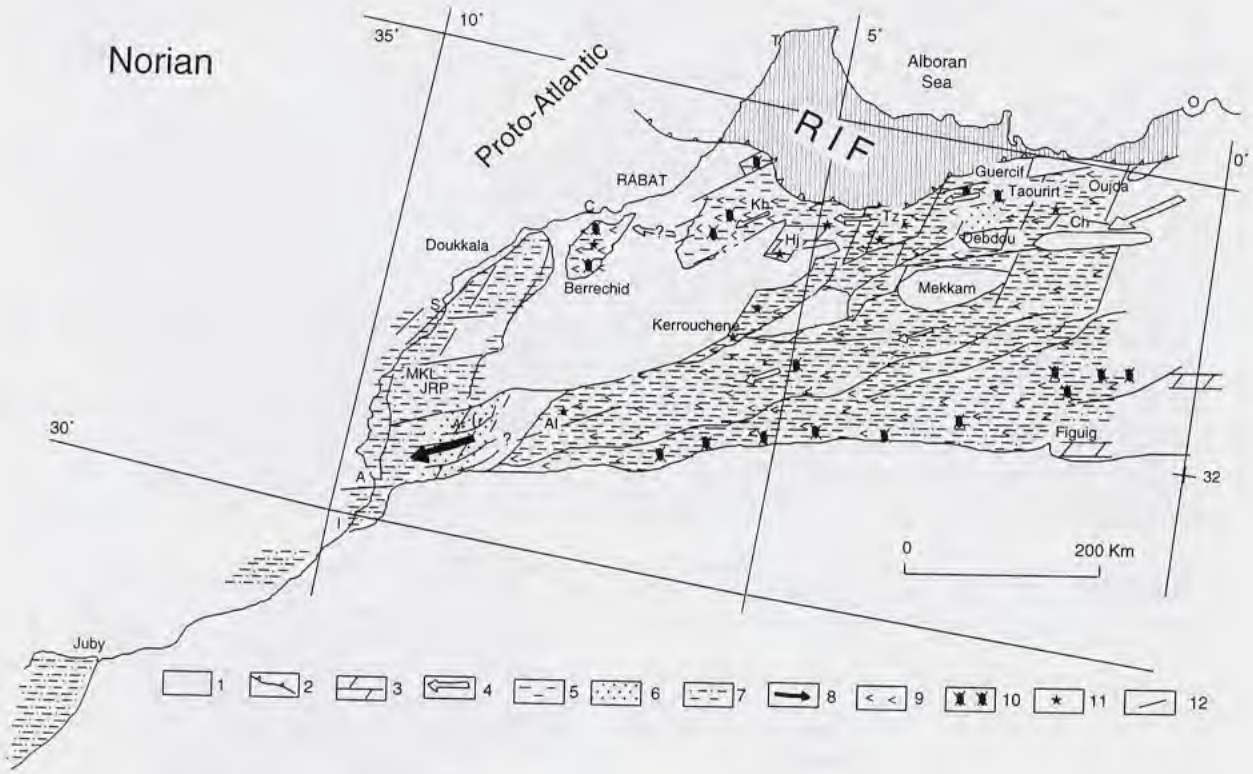

FIG. 6.— Palaeogeographic map of the Norian series in Morocco. **1**, Triassic erosion or non-deposition-area; **2**, allochtonous domain; **3**, shallow marine to lagoonal / lacustrine limestone and dolostone; **4**, marine incursion; **5**, mud flat type silty claystones; **6**, continental conglomerate; **7**, fluvial clayey sandstone; **8**, intra-basinal transit direction; **9**, gypsum and anhydrite; **10**, halite; **11**, volcanism; **12**, fault [Ch-J. Ech Chekhar, Tz-Massif de Tazekka, Hj-El Hajeb, Kh-Khémisset, MKL and JRP-ONAREP, borehales in Essaouira basin, Ir-Irohalène, Ar-Argana, Al-Ait Leqaq, C-Casablanca, S-Safi, A-Agadir, I-Ifni, O-Oran, T-Tanger].

*FIG. 6.— Carte paléogéographique du Maroc pendant le Norien. **1**, zone d'érosion triasique ou de non dépôt ; **2**, domaine allochtone ; **3**, calcaire et dolomie d'environnement marin peu profond à laguno-lacustre ; **4**, incursion marine ; **5**, argilites silteuses de type "mud flat" ; **6**,conglomérat continental ; **7**, grès argileux fluviatile ; **8**, sens de transport intra-basinal ; **9**, gypse et anhydrite ; **10**, halite ; **11**, volcanisme ; **12**, faille [Ch-J. Ech Chekhar, Tz-Massif de Tazekka, Hj-El Hajeb, Kh-Khémisset, MKL et JRP-sondages ONAREP, dans le bassin d'Essaouira, Ir-Irohalène, Ar-Argana, Al-Ait Leqaq, C-Casablanca, S-Safi, A-Agadir, I-Ifni, O-Oran, T-Tanger].*

A number of arguments led LAVILLE & PIQUÉ (1991) to distinguish between two rifting areas in Morocco separated by a NE-SW horst devoid of Triassic deposits: the Atlantic margin with its coastal basins to the west (diapiric zone, Essaouira Basin, Doukkala Basin) and the basins of the Atlas domains (High Atlas and Middle Atlas) to which the Eastern Meseta is added. This presumed horst is marked by an absence of Triassic deposits. This may be the result of subsequent erosion though. In the Oukaïmeden

Source : MNHN, Paris

Sandstones, west of the Argana region, there is only evidence of westward and eastward running currents (BENAOUISS *et al.*, 1996).

More generally on the Moroccan Margin, the late Carnian to Norian sedimentary environments are highly diverse. The grabens of the Proto-Atlantic domain were filled with alluvial materials from High Atlas rift compartments that were raised and tilted to the southwest (BEAUCHAMP *et al.*, 1995). Activity along the Zemmour Fault (N30) produced the Tarfaya Laâyoun Basin with southwesterly oriented alluvial piedmont sedimentation. The subsiding basins opened to the Tethys (Tiouli, Hauts Plateaux, Guercif, Ziz Guir and Khémisset) were the site of halite sedimentation in a shallow saline mud-flat type environment. These are known as the lower salt deposits.

LATE NORIAN / EARLY LIASSIC

The boundary between the Triassic series and those of the base of the Jurassic is difficult to localise. However, a clearly Jurassic stage of basalt flow is confirmed biostratigraphically in the Tazekka Massif (SABAOUI, 1996) and in the Doukkala and Essaouira Basins (SLIMANE & EL MOSTAINE, 1997) (Fig. 7). This episode is thought to be equivalent to the formation topping the Triassic series of Tarfaya, Argana, the Central High Atlas, Kerrouchen, El Hajeb and Tazekka.

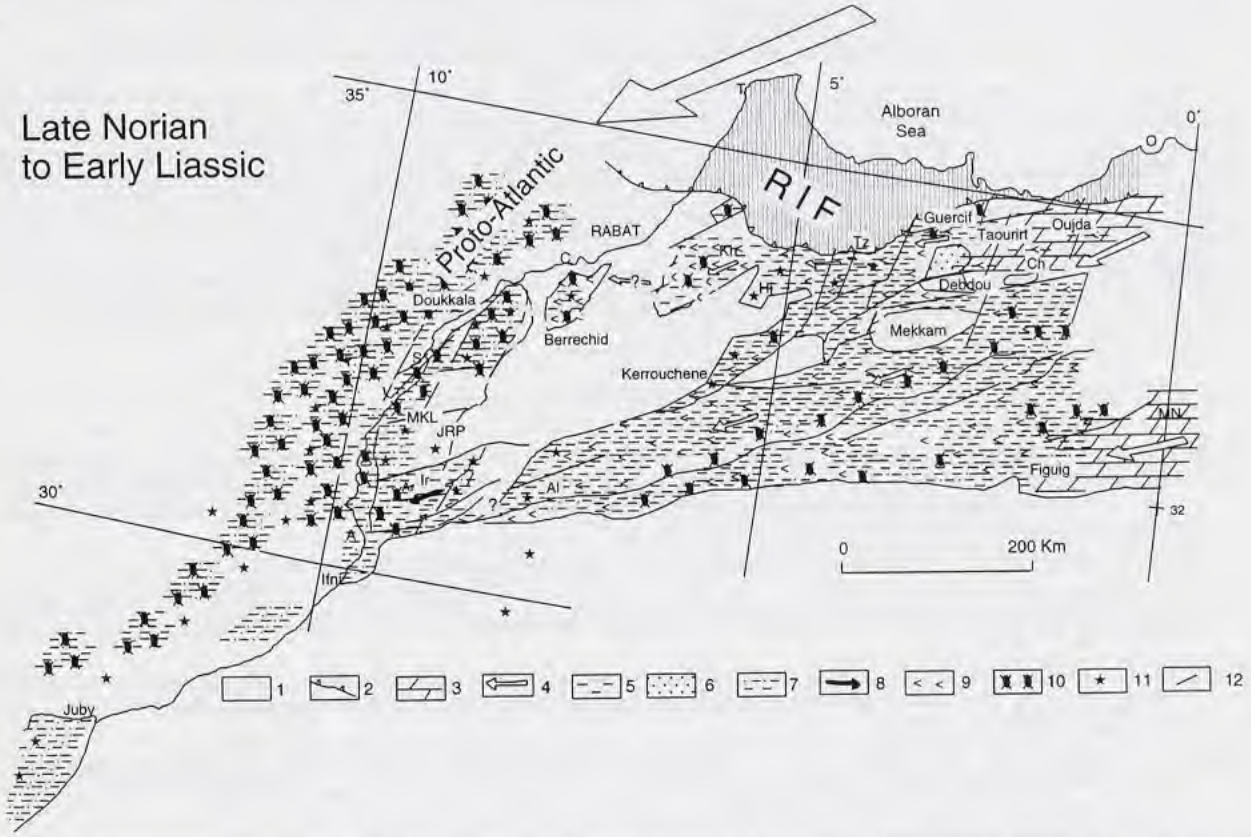

FIG. 7.— Palaeogeographic map of the Norian to early Liassic series in Morocco. Lithologic and geographic captions, see figure 6.

FIG. 7.— Carte paléogéographique du Maroc, du Norien au Lias inférieur. Légendes lithologiques et géographiques, voir figure 6.

While the Oujda Mountains in the northeast witnessed the progressive build-up of the Jurassic carbonate platform, all the subsiding basins were marked by the extension of mainly halitic evaporite deposits. This was the case for Tethyan basins (Hauts Plateaux, Guercif, Haute Moulouya) but also for

Source : MNHN, Paris

those which opened onto the Proto-Atlantic domains (Berrechid El Gara, Doukkala, Essaouira, Tarfaya-Laâyoun and the Atlantic Margin) or the intermediate basins (Boufekrane, Khémisset, Rharb). The bromine geochemistry in these deposits indicate an influx of sea water (PERETSMAN, 1985; HOLSER *et al.*, 1988; ET TOUHAMI, 1996). Despite the lack of evidence, it may be wondered whether the basal part of the evaporites known as the upper salt deposits capping what is recognised as the Triassic series are not of Late Triassic age in some locations. Sulphate and halite pseudomorphs are known in the uppermost Triassic beds of Argana. The onset of halite sedimentation may be diachronous, as shown in Algeria (AÏT SALEM *et al.*, 1998). The homogeneity of the Upper Triassic and lower Liassic facies could be also indicative of the fact that the basins were coalescent at the time of easier communication during Tethyan marine onlaps.

CONCLUSION

A new biostratigraphic division has made possible to propose palaeogeographic maps of three key periods in the history of the Triassic on the Moroccan epicratonic platform (Figs 4 to 6). Several major results can be summarised. At the scale of Morocco, sedimentation began only at the end of Ladinian times and the transgression over the Peri-Tethyan domain which was from the northeast both then and during the Carnian, occurred earlier in eastern Morocco. The transgression over the present-day west coast and Atlantic offshore area occurred later, from the late Carnian, from the Proto-Atlantic domain, even if there were link-ups with Tethyan waters, via a corridor between Africa and Iberia. At the scale of Morocco, the basalt flows occurred in succession from Ladinian / Carnian through to Jurassic times.

These results may be compared with structural data. The geological history of Morocco during the Triassic is of interest because the region was at the hinge-point between the Tethyan and Atlantic domains (RICOU, 1994). The Tethyan influence is seen in the direction of the marine advances over the Moroccan epicratonic platform from the northeast, where the open marine domain lay. Fault directions follow the Hercynian structures in part but the directions of extension and the major WSW-ENE structures such as those of the Atlasic trough were the same as in other parts of the Peri-Tethyan Maghreb until the late Carnian. The NS Atlantic fracturing was superimposed from late Carnian times in Western Morocco. It superseded the WSW-ENE fracturing over the entire Atlantic Margin of Morocco.

REFERENCES

AÏT SALEM, H., BOURQUIN, S., COUREL, L., FEKIRINE, B., HELLAL, C., MAMI, L. & TÉFIANI, M., 1998.— Triassic series on the Saharan Platform in Algeria; Peri-Tethyan onlaps and related structuration. *In*: S. CRASQUIN-SOLEAU & É. BARRIER (eds), Peri-Tethys Memoir 3: Stratigraphy and Evolution of Peri-Tethyan Platforms. *Mémoires du Muséum national d'Histoire naturelle*, **177**: 177-191.

BALLARD, R.D. & UCHUPI, E., 1975.— Triassic rift structures in Gulf of Maine. *AAPG Bulletin*, **59** (7): 1041-1072.

BAUDELOT, S., BOUHDADI, S. & DURAND-DELGA, M., 1984.— Datation palynologique du Trias moyen au sein des grès rouges "permo-triasiques" des environs de Tétouan (Rif septentrional, Maroc). *Comptes Rendus de l'Académie des Sciences, Paris*, **298** (II): 1061-1068.

BAUDELOT, S., COLIN, J.P. & OUARHACHE, D., 1986.— Le Niveau sédimentaire associé aux basaltes triasiques sur la bordure septentrionale du Causse d'El Hajeb (Maroc): données palynologiques et micropaléontologiques (Ostracodes). *Revue de Paléobiologie*, **5** (2): 281-286.

BAUDELOT, S. & CHARRIÈRE, A., 1983.— Définition et datation palynologique (Hettangien inférieur) de la Formation de Harira, niveau de décollement sous les formations dolomitiques du Causse moyen-atlasique (Maroc). *Comptes Rendus de l'Académie des Sciences, Paris*, **296** (II): 1806-1811.

BAUDELOT, S., CHARRIÈRE, A., OUARHACHE, D. & SABAOUI, A., 1990.— Données palynologiques nouvelles concernant l'Ordovicien et le Trias-Lias du Moyen Atlas (Maroc). *Géologie méditerranéenne*, **XVII** (3-4): 263-277.

BEAUCHAMP, J., 1983.— Le Permien et le Trias marocains. Quelques acquisitions récentes. *Bulletin de la Faculté des Sciences de Marrakech, section Sciences de la Terre*, numéro spécial **1**: 1-21.

BEAUCHAMP, J., 1985.— Modalités de la transgression triasique au Maroc. *In: Actes du 110ème Congrès national des Sociétés savantes, colloque Géologie africaine, Montpellier*. Tome 6. Comité des Travaux historiques et scientifiques, Paris: 247-256.

BEAUCHAMP, J., 1988.— Triassic sedimentation and rifting in the High Atlas (Morocco). *In*: W. MANSPEIZER (ed.), *Triassic-Jurassic Rifting: Continental Breakup and the Origin of the Atlantic Ocean and Passive Margins*. Elsevier, Amsterdam; Oxford; New-York: 477-497 (Developments in geotectonics; 22).

Source : MNHN, Paris

BEAUCHAMP, J., BENAOUISS, N. & COUREL, L., 1995.— Où était donc le domaine marin dans le Maroc africain au Trias supérieur? *Comptes Rendus de l'Académie des Sciences, Paris*, **321** (IIa): 1033-1040.

BENAOUISS, N., 1996.— Sédimentologie mixte: fluviatile, éolienne et tidale dans les couloirs tectoniques triasiques; Grès de l'Oukaïmeden du Haut Atlas de Marrakech. *In*: F. MEDINA (ed.), *Le Permien et le Trias du Maroc: état des connaissances*. Pumag, Marrakech: 251-268.

BENAOUISS, N., COUREL, L. & BEAUCHAMP, J., 1996.— Rift-controlled fluvial/tidal transitional series in the Oukaïmeden Sandstones, High Atlas of Marrakech (Morocco). *Sedimentary Geology*, **107**: 21-36.

BERTRAND, H., 1991.— The Mesozoic tholeitic province of Northwest Africa: a volcanotectonic record of the early opening of Central Atlantic. *In*: A.B. KAMPUNZU & R.T. LUBALA (eds), *Magmatism in Extensional Structural Settings*. Springer, Berlin: 147-188.

BIRON, P.E., 1982.— *Le Permo-Trias de la région de l'Ourika (Haut Atlas de Marrakech, Maroc). Lithostratigraphie, sédimentologie, tectonique et minéralisation*. Thèse de 3ème cycle, Université de Grenoble, Grenoble, France: 1-170.

CAILLEUX, Y., GONORD, H., LE GUERN, M. & SAUVAGE, M., 1983.— Taphrogenèse et magmatisme permiens dans le Maroc central. *Bulletin de la Faculté des Sciences de Marrakech*, section Sciences de la Terre, numéro spécial, **1**: 24-39.

COUSMINER, H.L. & MANSPEIZER, W., 1977.— Autunian and Carnian palynoflorules. Contribution to the chronology and tectonic history of the Moroccan pre-Atlantic borderland. *In*: F.M. SWAIN (ed.), *Stratigraphic micropaleontology of Atlantic Basin and Borderlands*. Elsevier, Amsterdam; London; New York: 185-201.

CRASQUIN-SOLEAU, S., RAKUS, M., OUJIDI, M., COUREL, L., ET TOUHAMI, M. & BENAOUISS, N., 1997.— Découverte d'une faune d'ostracodes dans le Trias des monts d'Oujda (Maroc): relations paléogéographiques entre les plates-formes nord et sud de la Téthys. *Comptes Rendus de l'Académie des Sciences, Paris*, **324** (IIa): 111-118.

DEFRETIN, S. & FAUVELET, J., 1951.— Présence de phyllopodes triasiques dans la région d'Argana-Bigoudine (Haut Atlas occidental). *Notes et Mémoires du Service géologique du Maroc, Rabat*, **85**: 129-135.

DUTUIT, J.M., 1976.— Introduction à l'étude paléontologique du Trias continental marocain. Description des premiers Stégocéphales recueillis dans le couloir d'Argana. *Mémoires du Muséum national Histoire naturelle, Paris*, **36** (C): 1-253.

EL KOCHRI, A. & CHOROWICZ, J., 1996.— Oblique extension in the Jurassic trough of the Central and Eastern High Atlas (Morocco). *Canadian Journal of Earth-Sciences*, **33**: 84-92.

EL WARTITI, M., 1990.— *Le Permien du Maroc mésétien. Étude géologique et implications paléogéographiques*. Thèse d'État, Université Mohammed V, Rabat, Maroc: 1-501.

EL YOUSSI, M., 1986.— *Sédimentologie et paléogéographie du Permo-Trias du Haut Atlas central (Maroc)*. Thèse de doctorat, Université de Grenoble, Grenoble, France: 1-195.

ET TOUHAMI, M., 1994.— Le Trias évaporitique du bassin de Khémisset (Maroc central). Géométrie des dépôts, évolution sédimentaire et géochimie. *Notes et Mémoires du Service géologique du Maroc, Rabat*, **373**: 1-211.

ET TOUHAMI, M., 1996.— L'Origine des accumulations salifères du Trias marocain: apport de la géochimie du brome du sel du bassin de Khémisset (Maroc central). *Comptes Rendus de l'Académie des Sciences, Paris*, **323** (IIa): 591-598.

FAVRE, P. & STAMPFLI, G.M., 1992.— From rifting to passive margin: the exemples of Red Sea. Central Atlantic and alpine Tethys as examples. *In*: P.A. ZIEGLER (ed.), Geodynamica of Rifting. *Tectonophysics*, **3** (215): 69-97.

HOLSER, W.T., CLÉMENT, G.P., JANSA, L.F. & WADE, J.A., 1988.— Evaporites deposits of the North Atlantic rift. *In*: W. MANSPEIZER (ed.), *Triassic-Jurassic Rifting: Continental Breakup and the Origin of the Atlantic Ocean and Passive Margins*. Elsevier, Amsterdam; Oxford; New-York: 525-556 (Developments in geotectonics; 22).

JALIL, N.E., 1996.— Les Vertébrés permiens et triasiques de la formation d'Argana (Haut Atlas occidental): liste faunique préliminaire et implications stratigraphiques. *In*: F. MEDINA (ed.), *Le Permien et le Trias du Maroc: état des connaissances*. Pumag, Marrakech: 227-250.

JALIL, N.E. & DUTUIT, J.M., 1996.— Permian Captorhinid reptiles from the Argana formation, Morocco. *Paleontology*, **39** (4): 907-918.

JENNY, J., 1983.— Lithostratigraphie des dépôts permo-triasiques du Haut Atlas central au sud d'Azilal (Maroc). *Bulletin de la Faculté des Sciences de Marrakech, section Sciences de la Terre*, numéro spécial, **1**: 1-50.

LARHIB, M., 1996.— Flore fossile et séquences des formations rouges fluviatiles du bassin autunien de Tiddas-Sebt Aït Ikkou (nord-ouest du Maroc central). *In*: F. MEDINA (ed.), *Le Permien et le Trias du Maroc: état des connaissances*. Pumag, Marrakech: 19-30.

LAVILLE, E., 1981.— Rôle des décrochements dans le mécanisme de formation des bassins d'effondrement du Haut Atlas marocain au cours des temps triasique et liasique. *Bulletin de la Société géologique de France*, **7, 23** (3): 303-312.

LAVILLE, E. & PETIT, J.P., 1984.— Role of synsedimentary strike-slip faults in the formation of Moroccan Triassic basins. *Geology*, **12**: 424-427.

LAVILLE, E. & PIQUÉ, A., 1991.— La Distension crustale atlantique et atlasique au Maroc au début du Mésozoique: le rejeu des structures hercyniennes. *Bulletin de la Société géologique France*, **162** (6): 1161-1171 also published as 1992.— *Notes et Mémoires du Service géologique du Maroc, Rabat*, **366**: 343-357

LE MARREC, A., 1979.— *Lithostratigraphie du Permo-Trias du haut Atlas de Demnat, Maroc: 7ème Réunion annuelle Sciences Terre, Lyon*. Laboratoire des Sciences de la Terre, Université Claude Bernard, Lyon: 1-291.

LISTER, G.S., ETHERIDGE, M.A. & SYMONDS, P.A., 1991.— Detachment models for the formation of passive continental margins. *Tectonics*, **10**: 1038-1064.

Source : MNHN, Paris

LORENZ, J.C., 1988.— Synthesis of Late Paleozoic and Triassic red bed sedimentation in Morocco. *In*: V.H. JACOBSHAGEN (ed.), The Atlas System of Morocco studies on its geodynamic evolution. *Lectures and Notes in Earth-Sciences*, **15**: 139-168.

LUCAS, G., 1942.— Description géologique et pétrographique des Monts du Ghar Roubane et de Sidi El Abed. *Bulletin du Service géologique de l'Algérie, Alger*, **2** (16): 1-539, 131 figs, 34 pl.

MANSPEIZER, W., 1988.— Triassic-Jurassic rifting and opening of Atlantic: an overview. *In*: W. MANSPEIZER (ed.), *Triassic-Jurassic Rifting: Continental Breakup and the Origin of the Atlantic Ocean and Passive Margins*. Elsevier, Amsterdam; Oxford; New-York: 41-79 (Developments in geotectonics ; 22).

MANSPEIZER, W., PUFFER, J.H. & COUSMINER, H.L., 1978.— Separation of Morocco and Eastern North America: a Triassic-Liassic stratigraphic record. *Geological Society of America Bulletin*, **89**: 901-920.

MATTIS, A.F., 1977.— Nonmarine Triassic sedimentation, Central High Atlas mountains, Morocco. *Journal of Sedimentary Petrology*, **47**: 107-119.

MEDINA, F., 1995.— Syn- and postrift evolution of the El Jadida-Agadir basin (Morocco): constraints for the rifting model of the central Atlantic. *Canadian Journal of Earth-Sciences*, **32**: 1273-1291.

MEDINA, F., 1996.— Le Trias du Maroc: introduction. *In*: F. MEDINA (ed.), *Le Permien et le Trias du Maroc: état des connaissances*. Pumag, Marrakech: 139-153.

MEDINA, F., MUSTAPHI, H., JABOUR, H., AHMAMOU, M., HOEPFNER, C., EL FARIATI, A. & ERRAMI, A., 1996.— Lithostratigraphie et structure des formations triasiques le long de la partie occidentale de la faille du Tizi n'Test (Haut Atlas occidental). *In*: F. MEDINA (ed.), *Le Permien et le Trias du Maroc: état des connaissances*. Pumag, Marrakech: 291-305.

ODIN, G.S., 1982.— The Phanerozoic time scale revisited. *Episodes*, **3**: 3-9.

OUARHACHE, D., 1987.— *Étude géologique dans le Paléozoïque et le Trias de la bordure NW du Causse Moyen Atlasique (S et SW de Fès, Maroc)*. Thèse de 3ème cycle, Université de Toulouse, Toulouse, France: 1-130.

OUJIDI, M., 1994.— *Le Complexe volcano-sédimentaire rouge du Trias et de la base du Lias du Pays des Horsts (Maroc Oriental). Géodynamique du bassin, dynamique sédimentaire et phénomène de silicification*. Thèse de doctorat ès-sciences, Université Mohamed I, Oujda, Maroc: 1-332.

OUJIDI, M., 1996.— Évolution tectono-sédimentaire des Monts d'Oujda au cours du Trias et de la base du Lias (Maroc Oriental). *In*: F. MEDINA (ed.), *Le Permien et le Trias du Maroc: état des connaissances*. Pumag, Marrakech: 201-212.

OWODENKO, B., 1946.— Mémoire explicatif de la carte géologique du bassin houiller de Djerada et de la région du Sud d'Oujda. *Mémoires de la Société géologique de Belgique, Liège*, **70**: 1-162.

PERETSMAN, G.S., 1985.— *Geochemical and Petrographic Analysis of Early Mesozoic Evaporites from Morocco: Implications of the History of the North Atlantic Rift*. M.S. thesis, University of Eugene, Oregon, USA: 1-82.

PETIT, J.P. & BEAUCHAMP, J., 1986.— Synsedimentary faulting and palaeocurrent patterns in the Triassic sandstones of the High Atlas (Morocco). *Sedimentology*, **33**: 817-829.

PIQUÉ, A. & LAVILLE, E., 1995.— L'Ouverture initiale de l'Atlantique central. *Bulletin de la Société géologique de France*, **166** (6): 725-738.

RICOU, L.E., 1994.— Tethys reconstructed: plates, continental fragments and their boundaries since 260 Ma from Central America to South-eastern Asia. *Geodinamica Acta*, **7** (4): 169-218.

ROBINSON, P.L., 1973.— Paleoclimatology and continental drift. *In*: D.H. TARLING & S.K. RUNCORN (eds), *Implications of Continental Drift to the Earth Sciences*. Academic Press, London: 451-476.

ROCH, E., 1939.— Description géologique des montagnes à l'Est de Marrakech. *Mémoires du Service géologique et de la Carte géologique du Maroc, Rabat*, **51**: 1-438.

SABAOUI, A., 1987.— *Structure et évolution alpine du Moyen Atlas septentrional sur la transversale Tleta des Zerarda-Meghroua (SW de Taza, Maroc)*. Thèse de 3ème cycle, Université de Toulouse, Toulouse, France: 1-162.

SABAOUI, A., 1996.— Les Formations rouges du Trias-Lias inférieur de la région de Tazekka (Moyen Atlas). *In*: F. MEDINA (ed.), *Le Permien et le Trias du Maroc: état des connaissances*. Pumag, Marrakech: 213-226.

SALVAN, H.M., 1984.— Les Formations évaporitiques du Trias marocain. Problèmes stratigraphiques, paléogéographiques et paléoclimatologiques. Quelques réflexions. *Revue de Géologie dynamique et de Géographie physique*, **25** (3): 187-203.

SAWYER, D.S. & HARRY, D.L., 1991.— Dynamic modeling for divergent margin formations: application to the U.S. Atlantic margin. *Journal of Geophysical Research*, **90**: 7751-7769.

SEBBAN, S., 1996.— Le Permien inférieur du bassin du Haouz oriental: données palynologiques et stratigraphiques. *In*: F. MEDINA (ed.), *Le Permien et le Trias du Maroc: état des connaissances*. Pumag, Marrakech: 31-42.

SLIMANE, A. & EL MOSTAINE, M., (1997).— Observations biostratigraphiques au niveau des formations rouges de la séquence synrift dans les bassins de Doukkala et Essaouira. *In*: *1ère Réunion du Groupe marocain du Permien et du Trias, Oujda, Maroc*. Faculté des Sciences, Université Mohammed I, Oujda: 54.

STAMPFLI, G.M., 1994.— Riftogenese in the Tethyan realm. *In*: *IGCP 369 Organizational Meeting, Bologna*. Università di Bologna, Bologna, Italy: 31-36.

TAUGOURDEAU-LANZ, J., 1978.— Pollens des niveaux sédimentaires associés aux basaltes du Trias sur la bordure septentrionale du Maroc central. Précisions stratigraphiques. *Notes et Mémoires du Service géologique du Maroc, Rabat*, **40** (275): 135-146.

Source : MNHN, Paris

TERMIER, H., 1936.— Études géologiques sur le Maroc central et le Moyen Atlas septentrional. 1: Les Terrains primaires et le Permo-Trias. 2: Les Terrains post-triasiques. 3: Paléontologie, pétrographie. 4: Atlas. *Notes et Mémoires du Service des Mines et de la Carte géologique du Maroc*, **33**: 1-1566.

VAN HOUTEN, F.B., 1976.— Late Variscan nonmarine deposits, NW Africa: implications for pre-rift North Atlantic reconstructions. *American Journal of Science*, **276**: 671-693.

VAN HOUTEN, F.B., 1977.— Triassic-Liassic Deposits of Morocco and Eastern North America: Comparison. *AAPG Bulletin*, **61** (1): 79-99.

VAN HOUTEN, F.B. & BROWN, R., 1975.— Triassic redbeds and evaporites, Northwest-Africa. *In*: Annual meeting, Salt Lake City, USA. *Proceedings- American Association of Petroleum Geologists*, **7** (7): 1306.

VAN HOUTEN, F.B. & BROWN, R.H., 1977.— Latest Paleozoic-Early Mesozoic paleogeography, Northwestern Africa. *Journal of Geology*, **85**: 143-156.

VAN HOUTEN, F.B., BROWN, R. & MATTIS, A.F., 1974.— Nonmarine Permo-Triassic sedimentary rocks, Morocco. *In*: Annual meeting, San Antonio, USA. *Proceedings- American Association of Petroleum Geologists*, **1**: 92.

WILDI, W., 1983.— La Chaîne tello-rifaine (Algérie, Maroc, Tunisie): structure, stratigraphie et évolution du Trias au Miocène. *Revue de Géologie dynamique et de Géographie physique, Paris*, **24** (3): 201-297.

Source : MNHN, Paris

Source : MNHN, Paris

3

The Liassic carbonate platform on the western part of the Central High Atlas (Morocco): stratigraphic and palaeogeographic patterns

Abdellatif SOUHEL[1], *Joseph CANÉROT*[2], *Fatma EL BCHARI*[1], *Driss CHAFIKI*[3], *Abdelhak GHARIB*[1], *Khadija EL HARIRI*[3] & *Aziz BOUCHOUATA*[2]

[1] Département de Géologie, Université Chouaib Doukkali, El Jadida, Maroc

[2] Laboratoire de Géologie des Bassins sédimentaires
URA CNRS 1405-ER 1746, Université Paul Sabatier
F-31400 Toulouse, France

[3] Département de Géologie, Université Cadi Ayyad, Faculté des Sciences et Techniques, Marrakech, Maroc

ABSTRACT

In the western part of the Central High Atlas, nine formations have been recognised within the Liassic (Hettangian-Pliensbachian) record. They are organised into eight third order sequences involved in two second order cycles. Five stages characterise the geodynamic evolution of the considered area. 1, Hettangian-early Sinemurian: wide dolomitic sabkhas; 2, late Sinemurian: huge NE dipping open marine carbonate platform; creation of the southern Telouet basin and central Tilougguit trough; 3, late Sinemurian-earliest Pliensbachian: marine regression and break down of the northern platform along the LPS ("Limite Plate-forme-Sillon"-boundary between platform and trough) fault zone; 4, middle Pliensbachian: transgression and drowning of the preceding troughs and platforms; 5, late Pliensbachian: tectonic activity leading to the infilling of the central Tilougguit trough and the emersion of the surrounding carbonate platforms.

RÉSUMÉ

La plate-forme liasique carbonatée dans la partie occidentale du Haut Atlas Central (Maroc) : stratigraphie et paléogéographie.

Dans la partie occidentale du Haut Atlas Central, la série liasique (Hettangien-Pliensbachien) a été subdivisée en neuf formations distinctes. Ces dernières s'organisent en huit séquences de troisième ordre, elles-mêmes comprises dans deux cycles

SOUHEL, A., CANÉROT, J., EL BCHARI, F., CHAFIKI, D., GHARIB, A., EL HARIRI, K. & BOUCHOUATA, A., 2000.— The Liassic carbonate platform on the western part of the Central High Atlas (Morocco): stratigraphic and palaeogeographic patterns. *In*: S. CRASQUIN-SOLEAU & É. BARRIER (eds), Peri-Tethys Memoir 5: new data on Peri-Tethyan sedimentary basins, *Mém. Mus. natn. Hist. nat.*, **182** : 39-56. Paris ISBN : 2-85653-524-0.

Source : MNHN, Paris

de deuxième ordre. L'évolution géodynamique régionale comporte cinq étapes successives. 1, Hettangien-Sinémurien inférieur: larges sabkhas dolomitiques ; 2, Sinémurien supérieur : vaste plate-forme marine carbontée, ouverte vers le NE ; création du bassin méridional de Telouet et du fossé central de Tilougguit ; 3, Sinémurien supérieur-Pliensbachien basal : régression marine et dislocation de la plate-forme septentrionale le long de la zone de fracture LPS ("limite plate-forme/sillon") ; 4, Pliensbachien moyen : transgression et ennoyage des plates-formes et des bassins précédents ; 5, Pliensbachien supérieur : activité tectonique intense conduisant au comblement du fossé central de Tilougguit et à l'émersion des plates-formes carbonatées avoisinantes.

INTRODUCTION

In the western part of the Central High Atlas (Béni-Mellal area, Fig. 1) the main outcropping formations are Jurassic (Sinemurian to Bathonian in age). These formations are folded into different narrow NE-SW, N-S or NW-SE oriented and faulted anticlines, involving sometimes injected Triassic materials, separated by wide synclines. So, the Mesozoic sedimentary cover shows a fan-shaped structural organisation with a northern vergency on the northern edge opposed to a southern vergency in the southern one. The compression rate related to Cainozoic structural inversion processes is rather low: 10 to 15% along the Béni-Mellal section (BREDE *et al.*, 1992).

DUBAR (1960-1962), CHOUBERT & FAURE-MURET (1960-1962), JOSSEN (1987) and ELMI (1996), provided the main palaeogeographic data for the Liassic period considered hereafter. These authors described more particularly the further end of a Tethyan eastward opened gulf, surrounded to the north, the west and the south, respectively by the emerged Mesetan, Atlasic and Saharian Highs.

Recent stratigraphic and sedimentologic works allow us to propose a detailed analysis of the Liassic sequence organisation and to present the different steps of the previously defined regional palaeogeographic evolution during this Lower Jurassic period.

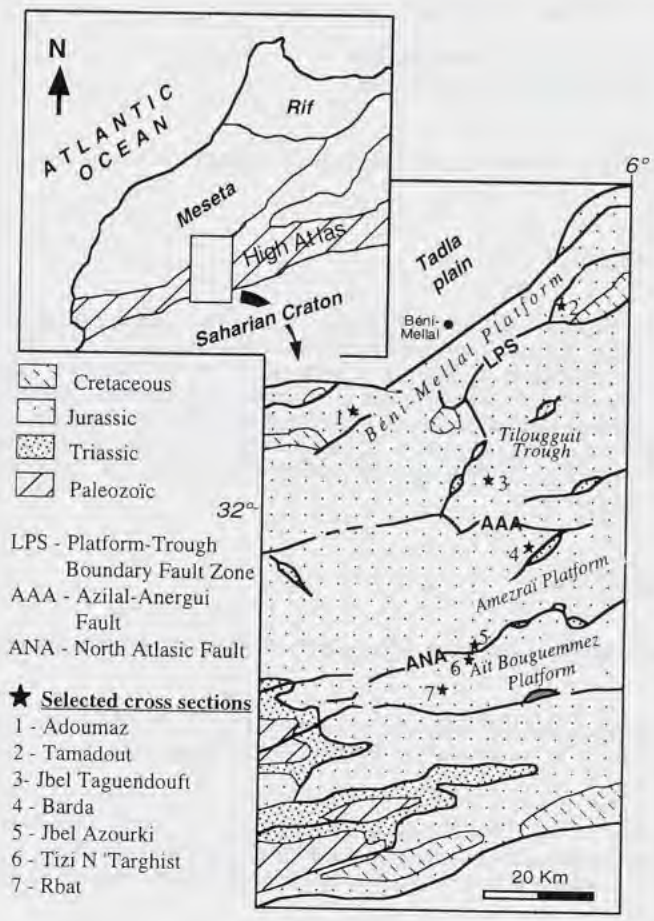

FIG. 1.— Location map of the study area.

FIG. 1.— Carte de localisation de la région étudiée.

Source : MNHN, Paris

STRATIGRAPHIC SETTING

LITHOSTRATIGRAPHY AND BIOSTRATIGRAPHY

The early to middle Liassic sedimentary supply of the study area involves nine different lithologic formations, whose age has been provided by ammonite, benthic foraminifera and brachiopod faunas (Fig. 2). These formations show important lateral sedimentary variations (Figs 2-4) leading to define three main palaeogeographic zones: Béni-Mellal platform, Tilougguit trough and central (Amezraï and Aït Bougemmez) platform, which deeply influenced the regional early and middle Liassic history. They are organised as follows:

— Aït Ras (Béni-Mellal platform) and Tighanimine (Tilougguit trough and central platform) Formations (JENNY, 1988). They correspond to the first carbonate deposits following the underlying terrigenous, evaporitic and basaltic Triassic unit. They are made up of dolomitic and marly, red coloured, decimetric beds (Aït Ras Formation) locally brecciated (Tighanimine Formation). Their stratigraphic position indicates a possible Hettangian age.

— Aït Bou Oulli Formation (JENNY, 1988). Massive, 1 to 3 m thick limestone and dolostone beds are rich in onchoids and oolites. The fauna is represented by Sinemurian brachiopods (*Terebratula moreti* Dubar, *T. marucchensis* Dubar and *Zeilleria arethusa* Di Ste. *in* JENNY, 1988), bivalves and benthic foraminifera of the A biozone (SEPTFONTAINE, 1984).

— Jbel Rat Formation (JENNY, 1988), Béni-Mellal platform. This succession shows the same stratonomic characteristics as the underlying Aït Bou Oulli Formation. Nevertheless, bird eyes, vadose pisolite and "tipi-like" stromatolitic structures are more frequent. It is Sinemurian in age, at the A and B biozone boundary (SEPTFONTAINE, 1984).

— Jbel Taguendouft Formation (JOSSEN, 1988), Tilougguit trough. This unit represents the main carbonate series developed in the central part of the Tilougguit trough. A rich ammonite fauna indicates an early to middle Liassic age (EL HARIRI *et al.*, 1996). In the type-locality, some marly intervals interfinger with the dominant limestones. The thick and dark Sinemurian limestones which involve frequent flint nodules differ from the overlying, thin, light coloured, Pliensbachian ones.

— Jbel Choucht Formation (SEPTFONTAINE, 1986), Amezraï platform. In the type-locality, on the southern boundary of the Tilougguit trough, this formation is characterised by massive reef limestones (Fig. 5). The lower part cannot be described in detail because of bad outcropping conditions related to faulting and associated gabbro intrusions. The well developed uppermost part provided "floated ammonites" indicating a late Carixian interval (DU DRESNAY *in* SEPTFONTAINE, 1986).

— Aganane Formation (SEPTFONTAINE, 1986), Béni-Mellal platform. It corresponds to a rythmic succession of marls and dolomitic limestones, rich in benthic foraminifera and algae, accumulated during the late Sinemurian-middle Domerian (early-middle Pliensbachian) (B, C, D and E biozones of SEPTFONTAINE, 1984) period. The formation often provides an heterochronous intercalated unit made up of red marls and conglomerates (marly and dolomitic member of SEPTFONTAINE, 1986 and Aït Bazzi Formation of JENNY, 1988).

— Tamadout Formation (MONBARON, 1985), Tilougguit trough. In the Tamadout area, this formation involves two different members (SOUHEL *et al.*, 1993). The lower one, Domerian (late Pliensbachian) in age, is represented in the only Tamadout sector and mainly formed of brown to red marls and shales, interbedded with decimetric bedded limestones with ammonites and calciturbidites. The following upper member, early to middle Toarcian in age, shows green to beige marls involving sandstone beds in their upper part. It overlaps the underlying member, and covers the entire Tilougguit area.

— Amezraï Formation (JOSSEN, 1988), Amezraï platform. This last unit shows a succession of thin ripple-bedded sandstones, fossiliferous (bivalves, gastropods and brachiopods) silty marls and oobioclastic oblique laminated limestones (Fig. 5). The bachiopod fauna found in the lower part indicates a Domerian age (BOUCHOUATA *et al.*, 1995).

Source : MNHN, Paris

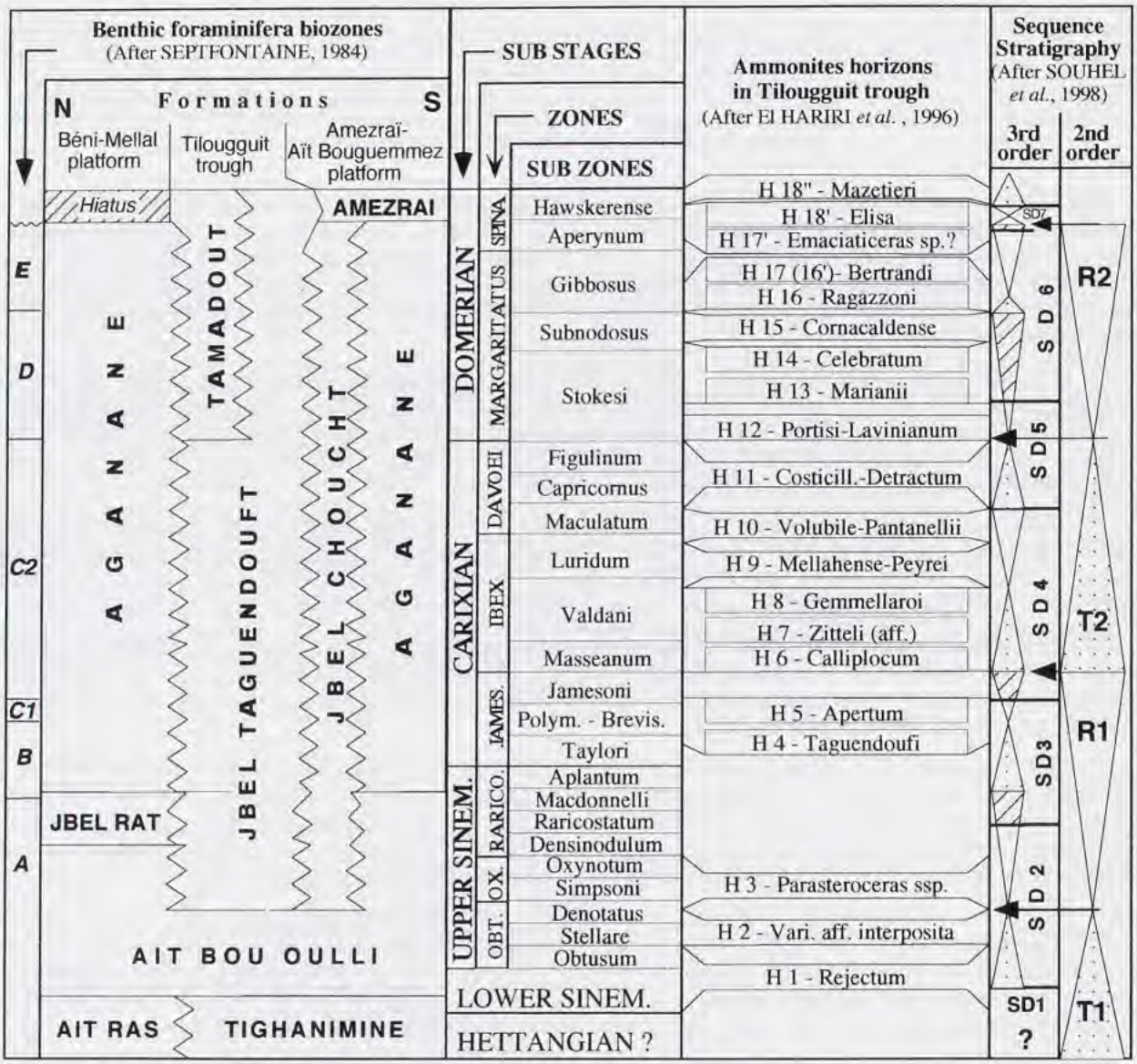

FIG. 2.— Chronostratigraphic sketch diagram involving sequence stratigraphy of the described Liassic formations and compared benthic foraminifera and ammonite zones.

FIG. 2.— Stratigraphie séquentielle et essai de corrélation des échelles d'ammonites et de foraminifères benthiques rencontrés dans les formations liasiques étudiées.

SEQUENCE STRATIGRAPHY

A detailed analysis (SOUHEL, 1996) carried out in different sections of the northern part of the study area, using sequence stratigraphy concepts, provided an interpretation of the early to middle Liassic sediments. At a third order scale (*sensu* VAIL *et al.*, 1987), eight sequences (S1 to S8, Fig. 2) have been described within the Sinemurian *pro parte* to Pliensbachian interval.

The different systems tracts which compose the middle Liassic sequences are well represented only on the platform wedge (Tamadout section, Fig. 3) where thick submarine, well dated sediments have been accumulated. The ammonite associations let us to recognise the corresponding systems tracts in the

Source : MNHN, Paris

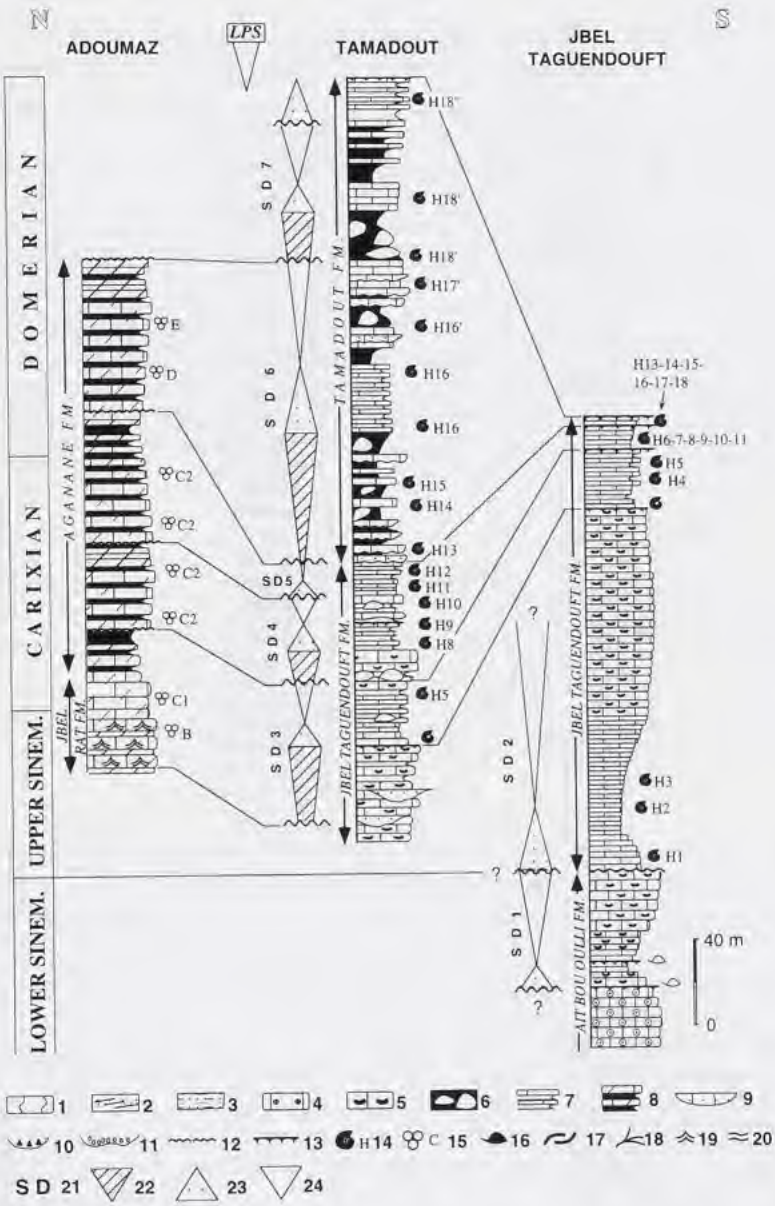

FIG. 3.— Described sections of the lower-middle Liassic formations in the northern part of the Central High Atlas (for location of the selected sections, see Fig. 1). **1**, reef limestones; **2**, shallow marine sandstones; **3**, silts and clays; **4**, oolitic limestones; **5**, flint limestones; **6**, marls involving reworked reef limestones; **7**, interbedded hemipelagic marls and limestones; **8**, interbedded peritidal marls and dolostones; **9**, carbonate turbidites; **10**, brecciated intertidal channels; **11**, brecciated coastal to continental channels; **12**, exokarstic unconformity; **13**, marine unconformity; **14**, ammonite horizon; **15**, benthic foraminifera biozone; **16**, brachiopods; **17**, large bivalves; **18**, corals; **19**, tipis; **20**, algal laminations; **21**, third order sequence; **22**, lowstand systems tract; **23**, transgressive systems tract; **24**, highstand systems tract; LPS: boundary between platform and trough; AAA: North Atlasic accident.

*FIG. 3.— Coupes des formations du Lias inférieur et moyen décrites dans la partie septentrionale du Haut Atlas central (les coupes décrites sont indiquées sur la figure 1). **1**, calcaires récifaux ; **2**, grès littoraux ; **3**, silts et argiles ; **4**, calcaires oolithiques ; **5**, calcaires à silex ; **6**, marnes englobant des blocs de calcaires récifaux ; **7**, alternances de marnes et calcaires hémipélagiques ; **8**, alternance de marnes et de dolomies péritidales ; **9**, calciturbidites ; **10**, brèches intertidales chenalisées ; **11**, brèches côtières ou continentales chenalisées ; **12**, discontinuité exokarstique ; **13**, discontinuité sous-marine ; **14**, horizon à ammonites ; **15**, biozone à foraminifères benthiques ; **16**, brachiopodes ; **17**, grands bivalves ; **18**, récifs ; **19**, tipis ; **20**, laminations algaires ; **21**, séquence de troisième ordre ; **22**, cortège de bas niveau marin ; **23**, cortège transgressif ; **24**, cortège de haut niveau marin ; LPS : limite Plate-forme - sillon ; AAA : Accident Nord-Atlasique.*

Source : MNHN, Paris

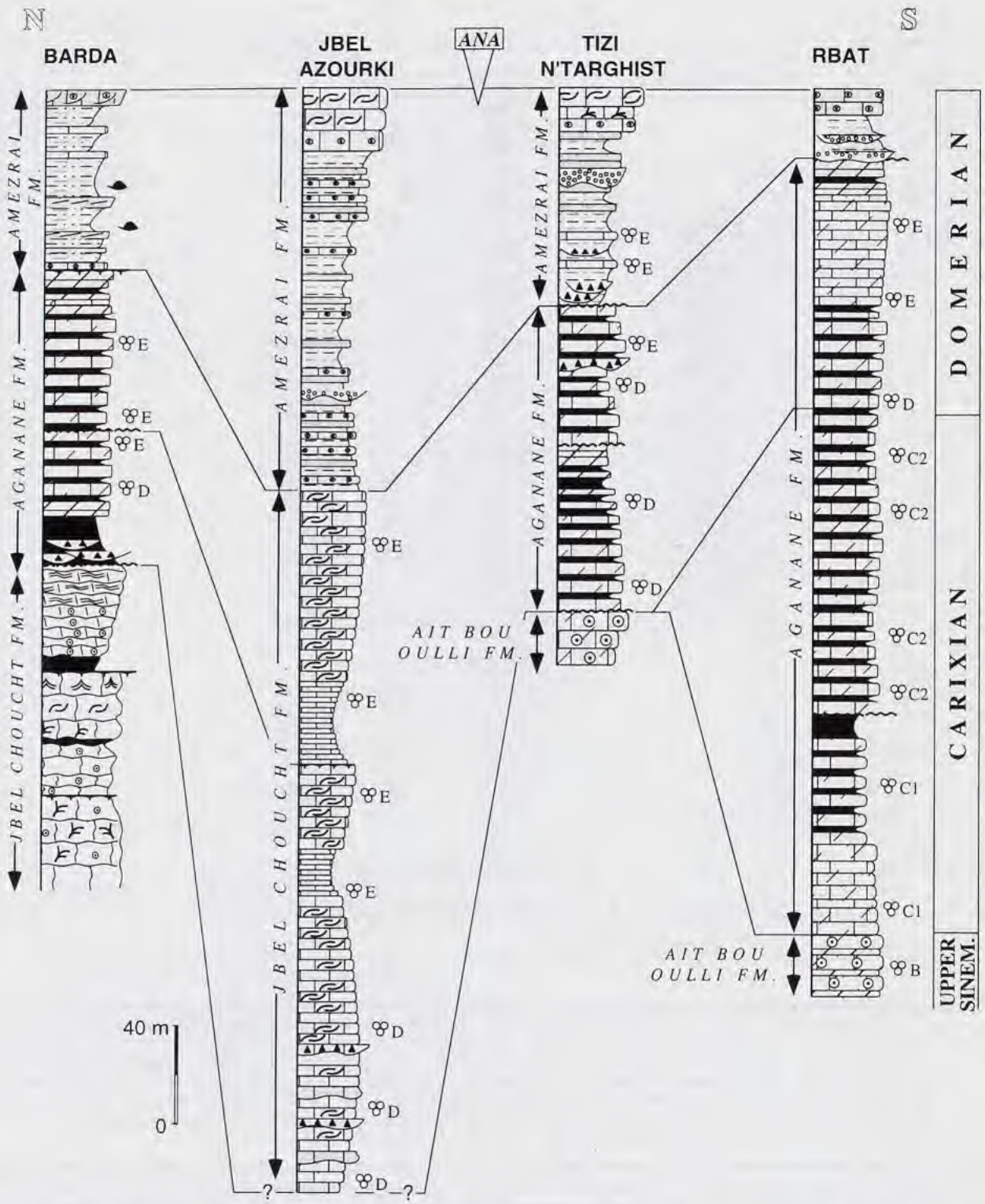

FIG. 4.— Described sections of the lower-middle Liassic formations in the central part of the Central High Atlas (for location of the sections, see Fig. 1). Legend, see Fig. 3.

FIG. 4.— Coupes des formations du Lias inférieur et moyen décrites dans la partie centrale du Haut Atlas Central (les coupes décrites sont indiquées sur la figure 1). Même légende que sur la figure 3.

Source : MNHN, Paris

thin bedded and condensed sections of the central part of the trough (Jbel Taguendouft section, Fig. 3). In the last area, the only observed unconformities involving condensed ammonite faunas (H13 to H18) correspond to the main flooding surfaces (*sensu* VAIL *et al.*, 1987).

On the platform, where nearshore, peritidal-type sedimentation occurred (Jbel Rat and Aganane Formations, Adoumaz section, Fig. 3), only the highstand systems tracts have been clearly distinguished. They correspond to carbonate series involving inter to supratidal facies made up of dolomites and clays. The lowstand systems tracts are absent or represented by supratidal dolostones associated with argilaceous palaeosoils indicating episodic emersion periods. The transgressive systems tracts are characterised by the development of peritidal, thickening upwards cycles, progressively dominated by subtidal environments related to the increase of the accommodation rate.

These sequences are organised into two second order cycles (*sensu* VAIL *et al.*, 1991; JACQUIN *et al.*, 1992; GRACIANSKY *et al.*, 1993). The drowning unconformities are located (Fig. 2) in the late Sinemurian (Obtusum zone, H1) and the Carixian-Domerian (Davoei-Margaritatus boundary, H11-H12) transition interval. The tectonically enhanced unconformities develop at the top of the early Carixian (base of Ibex zone, H5-H6) and in the late Domerian (Spinatum zone, H17'-H18').

PALAEOGEOGRAPHY

PALAEOSTRUCTURAL SETTING

Different palaeogeographic areas can be distinguished through facies and thickness changes within the formations described above. During the early-middle Liassic period, the best characterised sectors correspond to the Béni-Mellal platform, the Tilougguit trough, the Amezraï basin and the Aït Bougemmez platform (Fig. 1).

From north to south, the structural elements controlling this palaeogeographic zonation are:

— the boundary between the Béni-Mellal platform and the Tilougguit trough which corresponds to a complex flexure zone ("Limite entre Plate-forme et Sillon" = LPS, Fig. 1) involving two main elements, oriented N10 and N45 in the Béni-Mellal Atlas (CHAFIKI, 1994). Its eastward prolongation corresponds to the northern boundary of the High Atlas central part. The normal faulting along the LPS provided important debris-apron southeast dipping slopes (CHAFIKI & SOUHEL, 1993; CHAFIKI, 1994) on the Béni-Mellal platform edge;

— the Azilal-Anergui Fault Zone (AAA, Fig. 1) which corresponds to the southern boundary of the Tilougguit trough. Oriented N 70, it stretches continuously along 150 kms. Its Liassic activity induces local Toarcian wedges on the Pliensbachian slope deposits of the SW boundary of the trough (JOSSEN, 1988). In the other areas, the overlapping Middle Jurassic cover forbides field observations;

— the North Atlasic Fault (ANA, Fig. 1) which separates the Amezraï area from the Aït Bougemmez platform. Located within the large N 70 North Atlasic Fault Zone of ROCH (1939, 1950) it stretches along the northern side of the highest (more than 3000 m) atlasic mountains and corresponds to the eastern prolongation of the Tizi-N-Test fault zone. In the study area, the ANA has been generally considered as a normal fault dipping northward during the middle Liassic (BURGESS & LEE, 1978; LAVILLE, 1981). Our observations indicate several inverted polarities (thickness and facies) within the Liassic sedimentary record, related to transverse faulting (works in progress).

Source : MNHN, Paris

A

B *Domerian unconformity*

Source : MNHN, Paris

GEODYNAMIC EVOLUTION STAGES

The different stages of the palaeogeographic evolution are defined using the above presented second order cycles (Fig. 2) and complementary data collected in the Moroccan Atlasic realm (DU DRESNAY, 1979; FEDAN, 1989; BOUTAKIOUT & ELMI, 1996) and compared with the NE Moroccan and NW Algerian areas (ELMI, 1996). These cycles are considered (VAIL *et al.*, 1991; JACQUIN *et al.*, 1992; GRACIANSKY *et al.*, 1993) as tectonic and eustatic units providing the best data for basin analysis. They are from 3 to 50 Ma long and involve a transgressive stage followed by a regressive one. The first stage corresponds to a subsiding and deepening period at a regional scale whereas the second indicates a slackening of subsidence and/or a tectonic rise.

Maps of the figure 6 show the palaeogeographic history of the western part of the Central High Atlas at the end of every transgressive or regressive steps within these second order cycles. They involve data from the different authors (ROLLEY, 1973; MONBARON, 1985; JENNY, 1985; LE MARREC, 1985; JOSSEN, 1988) of the Geological maps at scale 1/100 000.

The earliest Liassic (Hettangian?-early Sinemurian, Fig. 6A) is characterised by wide dolomite and evaporite sabkhas indicating flat topography under shallow water conditions. The facies organisation testifies coastal environments involving terrigenous influence. Tectonic activity is very low or absent. The synsedimentary megabreccias of the Tighanimine Formation developed in the centre of the basin or in its southern edge (Telouet basin of JOSSEN, 1988) indicate an early subsiding step on the southern margin of the High Atlasic trough.

The late Sinemurian (Fig. 6B) corresponds to the first really open marine environments. The carbonate formations reach the limits of the Atlasic area. They indicate a huge NE slowly dipping platform which involves outlying intertidal (innershelf) sediments interfingering with subtidal (outershelf) deposits in the centre of the basin. Two subsident basins characterised by euxinic supplies can be observed: the southern one, created during the earliest Liassic period, persists in the Telouet area; the northern one is newly individualised in the Tilougguit vicinity.

Low tectonic activity leads to a progressive deepening of the sedimentary basin, except in the last central zone where faulting along the LPS and the AAA induces the creation of the Tilougguit trough .

The latest Sinemurian-early Carixian (lowermost Pliensbachian, Fig. 6C) times show a marine regression all over the Central High Atlas, specially in the bordering zones (DU DRESNAY, 1979; JOSSEN, 1987). In the Azilal (JENNY, 1988) and Zawiat Ahançal (Tizi-N-Targhist section, Fig. 4) areas the sedimentary gap reaches the Domerian (late Pliensbachian) interval.

In the late Sinemurian, the facies organisation shows two main environment types:

— intertidal to supratidal sediments with "tipi-like" structures (Jbel Rat Formation, Aganane section, Fig. 3) located on the subtidal carbonate platform of the preceeding stage;

— circalittoral carbonate deposits (H3 and H4 horizons of the Jbel Taguendouft Formation, Jbel Taguendouft section, Fig. 3), characterised by a high sedimentation rate and situated in the Tilougguit trough area.

FIG. 5.— Middle-upper Liassic sedimentation in the Central High Atlas. **A**, The Amezrai (upper Domerian-lower Toarcian) Formation in the Amezraï area (Fig. 1). The calciturbidites (right), sandstones and marls involve reworked blocks and slices (center) of the underlying Jbel choucht limestones. **B**, The Domerian (upper Pliensbachian) unconformity in the Jbel Azourki area, (section 5, Fig. 1 and Fig. 4). The massive limestones of the Jbel Choucht Formation (left) have been eroded then unconformably covered by slope breccias and calciturbidites (right), representing the Amezraï Formation.

*FIG. 5.— Sédimentation du Lias moyen-supérieur dans le Haut Atlas Central. **A**, La formation Amezrai (Domérien supérieur-Toarcien inférieur) dans la région-type (Fig. 1). Les calciturbidites (à droite), les grès et les marnes présentent des blocs et des lambeaux remaniés (au centre) appartenant aux calcaires sous-jacents du Jbel Choucht. **B**, La discontinuité domérienne (Pliensbachien supérieur) dans le secteur du Jbel Azourki (coupe 5, Fig. 1 et Fig. 4). Les calcaires massifs de la formation du Jbel Choucht (à gauche) ont été érodés puis recouverts en discordance par des brèches de pente et des calciturbidites (à droite), appartenant à la formation Amezrai.*

Source : MNHN, Paris

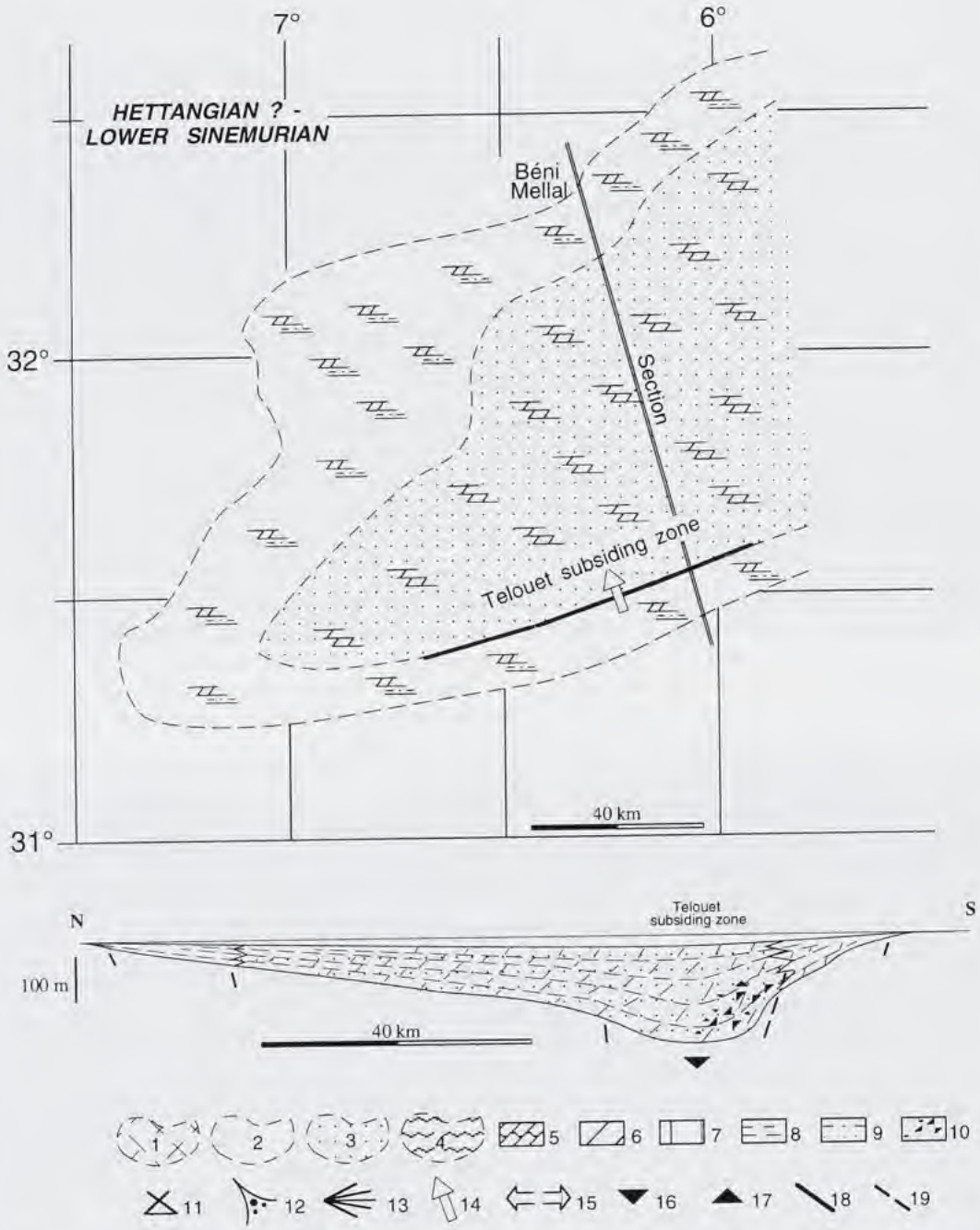

FIG. 6.— Palaeogeographic sketch maps (A to E) of the Central High Atlas during the lower-middle Liassic period. **1**, continental area; **2**, supra- to intertidal area; **3**, inter- to subtidal area; **4**, subtidal area; **5**, reef limestones; **6**, dolostones; **7**, limestones; **8**, marls; **9**, silts and clays; **10**, breccias; **11**, tipis; **12**, carbonate turbidites and slumped blocks; **13**, deltas; **14**, thickening deposits; **15**, distension; **16**, subsidence; **17**, uplift; **18**, fault zone; **19**, supposed fault.

*FIG. 6.— Cartes paléogéographiques (A à E) du Haut Atlas Central au cours du Lias inférieur et moyen. **1**, milieu continental ; **2**, zone supra- à intertidale ; **3**, zone inter- à subtidale ; **4**, zone subtidale ; **5**, calcaires récifaux ; **6**, dolomies ; **7**, calcaires ; **8**, marnes ; **9**, silts et argiles ; **10**, brèches ; **11**, tipis ; **12**, calciturbidites et blocs glissés ; **13**, deltas ; **14**, épaisseurs croissantes ; **15**, distension ; **16**, subsidence ; **17**, zones hautes ; **18**, zone faillée ; **19**, faille supposée.*

Source : MNHN, Paris

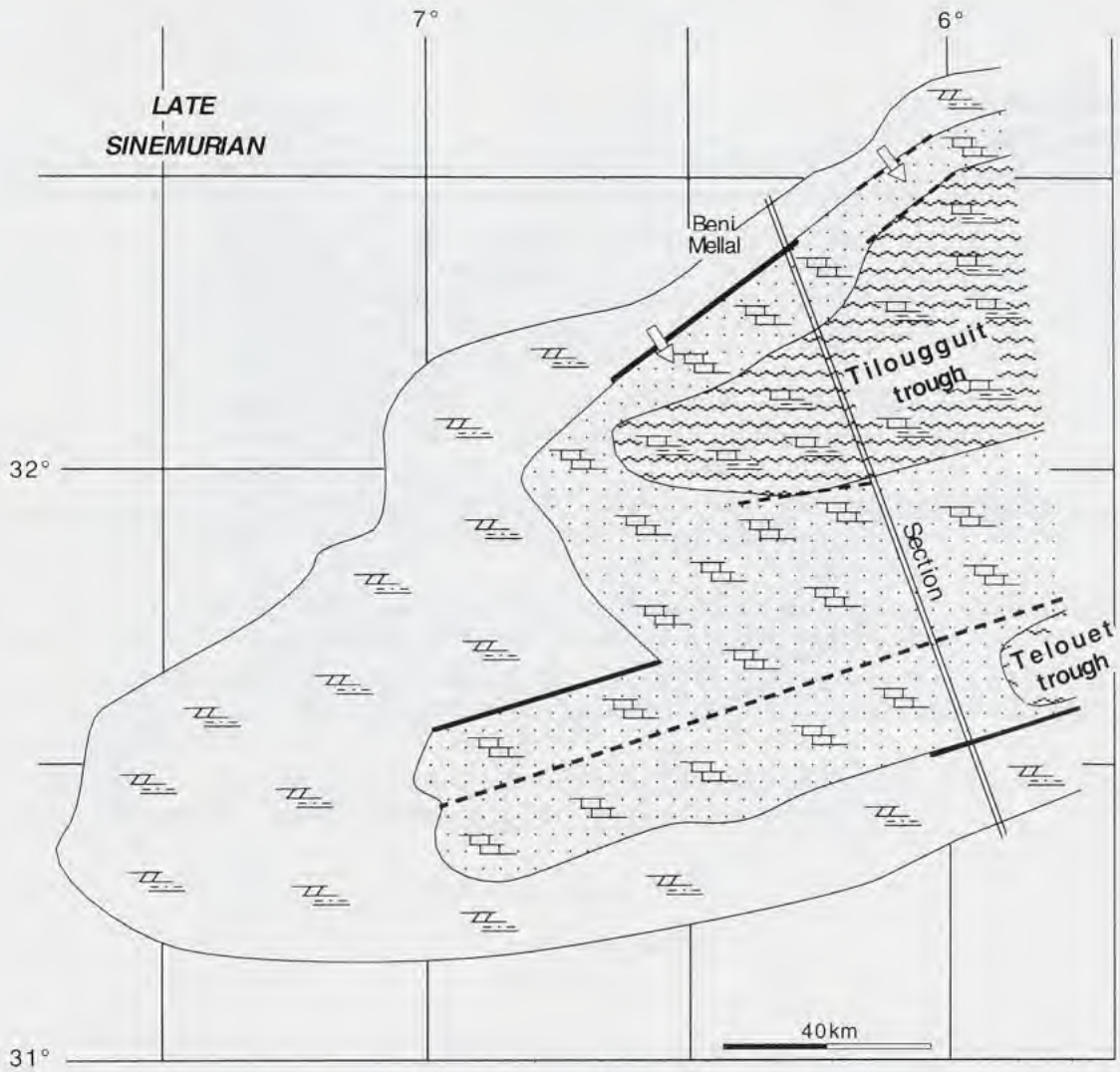

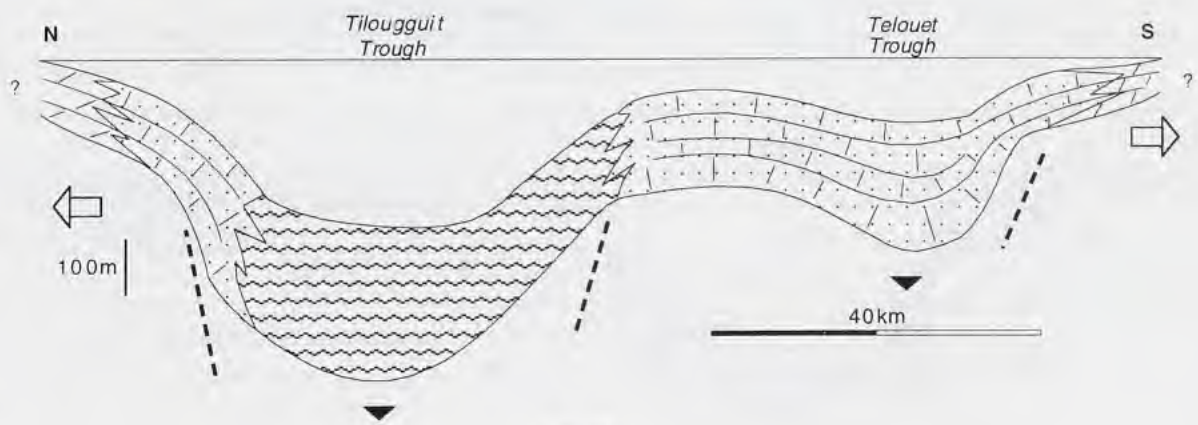

FIG. 6B

Source : MNHN, Paris

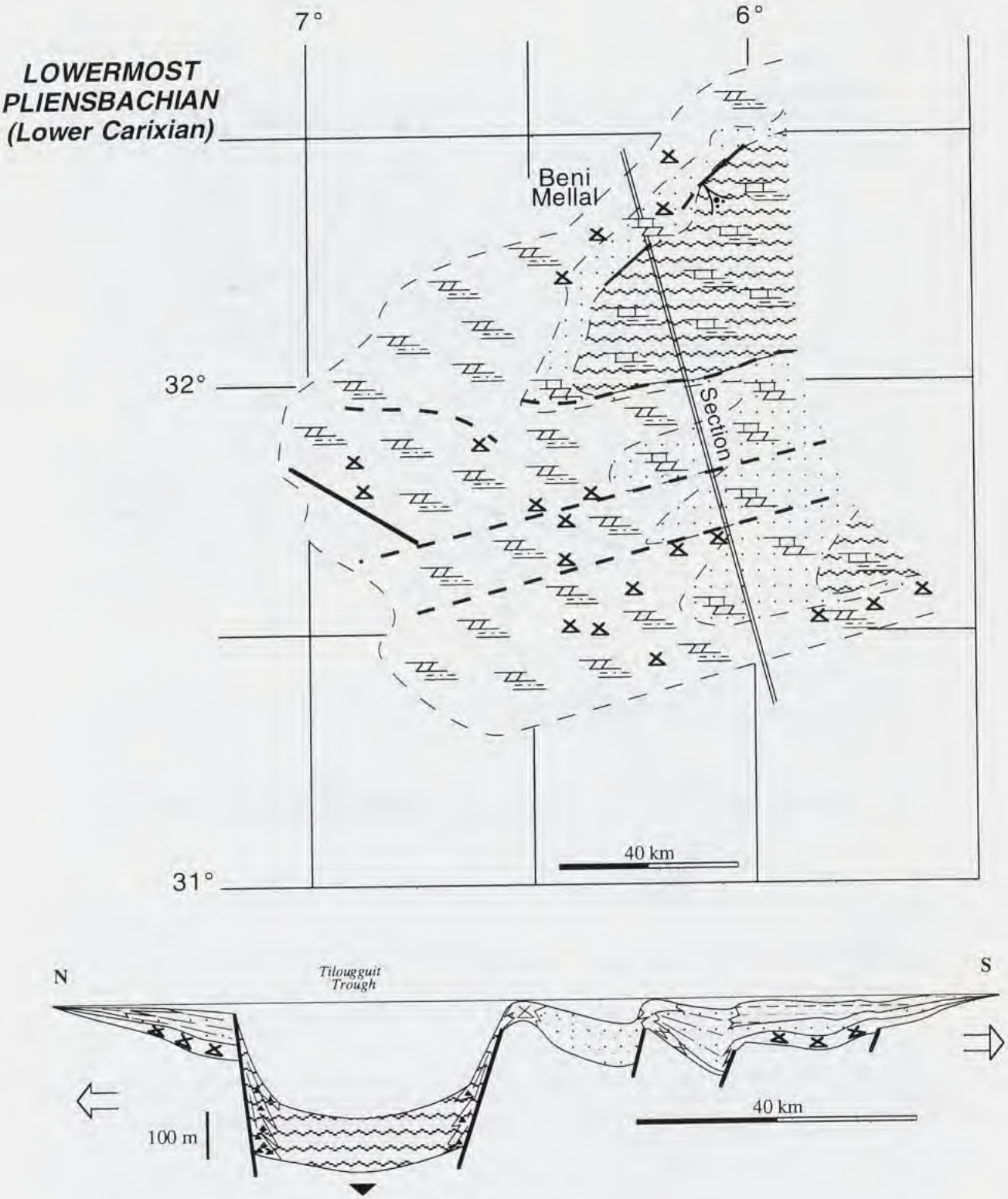

FIG. 6C

Source : MNHN, Paris

The transition between the two environments, observed in the Tamadout vicinity (Tamadout section, Fig. 3), is represented by debris apron deposits indicating a newly individualised submarine slope zone (CHAFIKI & SOUHEL, 1993). These sedimentary changes are related to the break down of the lower Liassic platform along the active LPS fault zone.

The same palaeogeographic features are preserved during the early Carixian (lowermost Pliensbachian). Temporarily emerged tidal flats with palaeosoils and karst surfaces on the northern side of the High Atlas and tipi-dolostones on the southern one develop on the late Sinemurian subtidal platform. The first Liassic large bivalve communities cover the main active fault zones.

During the middle Carixian-early Domerian (middle Pliensbachian) interval (Fig. 6D), marine sediments can be newly observed all over the western part of the High Atlasic basin. The maximum opening conditions are registered towards the Carixian-Domerian boundary, when the thin bedded marls and limestones of the Tilougguit trough interfinger with the carbonate turbidites of the SE edge of the Béni-Mellal platform and the lateral subsiding lagoons.

On the southern edge of the High Atlas, the persisting Telouet basin shows shallow marine conditions (Aganane Formation) to the west and open sea sedimentation to the east (JOSSEN, 1988; MILHI, 1992).

Towards the late (not latest) Domerian (Fig. 6E), the regional palaeogeographic setting changes (Fig. 7). The important tectonic rise of the central Tilougguit and neighbouring zones (SOUHEL *et al.*, 1995; SOUHEL, 1996) induces:

— the emersion of part of the carbonate platform leading to the development of palaeosoils, exokarst surfaces and lignitous deposits along the active fault zones (Demnat fault of JENNY, 1983);

— the carbonate and terrigenous infilling of the Tilougguit trough which involves different turbiditic basins (Tamadout section, Fig. 3) separated by isolated highs showing condensed sedimentation (Jbel Taguendouft, Fig. 3).

In the Atlasic axis, the increasing tectonic activity along the AAA leads to the deepening of the central shallow marine Amezraï platform newly converted into a turbiditic basin.

CONCLUSION

New stratigraphic and sedimentologic data allow us to separate five main stages within the palaeogeographic evolution of the Central High Atlas during the early-middle Liassic period. The lowermost Liassic sabkha conditions (stage 1) are followed by the Sinemurian extended outer carbonate platforms (stage 2), the earliest Pliensbachian regressive and diversified trough and platform environments (stage 3), the middle Pliensbachian newly transgressive and rather homogeneous sedimentation (stage 4) and finally the late Pliensbachian regressive period (stage 5).

The Liassic transgression sediments are generally deposited under low tectonic conditions, with a largest extension and a strongest depth for the Sinemurian interval. The regressive steps correspond to normal faulting periods inducing breakdown of the platforms, block tilting and creation of new subsiding basins where central deep marine sediments interfinger with bordering tidal flats.

During the considered Liassic period, the sedimentary organisation and geometries indicate a NW-SE sinistral transtensive setting (Fig. 7) involving NE-SW normal faulting and N70 inverted polarities. This interpretation fits well with the oblique opening model proposed by EL KOCHRI *et al.* (1997) for the genesis and evolution of the Central High Atlas Jurassic basins.

Extension processes seem to migrate (SOUHEL, 1996) from the south (Sinemurian in the southern side of the Central High Atlas) to the north (Middle Jurassic in the Middle Atlas).

Source : MNHN, Paris

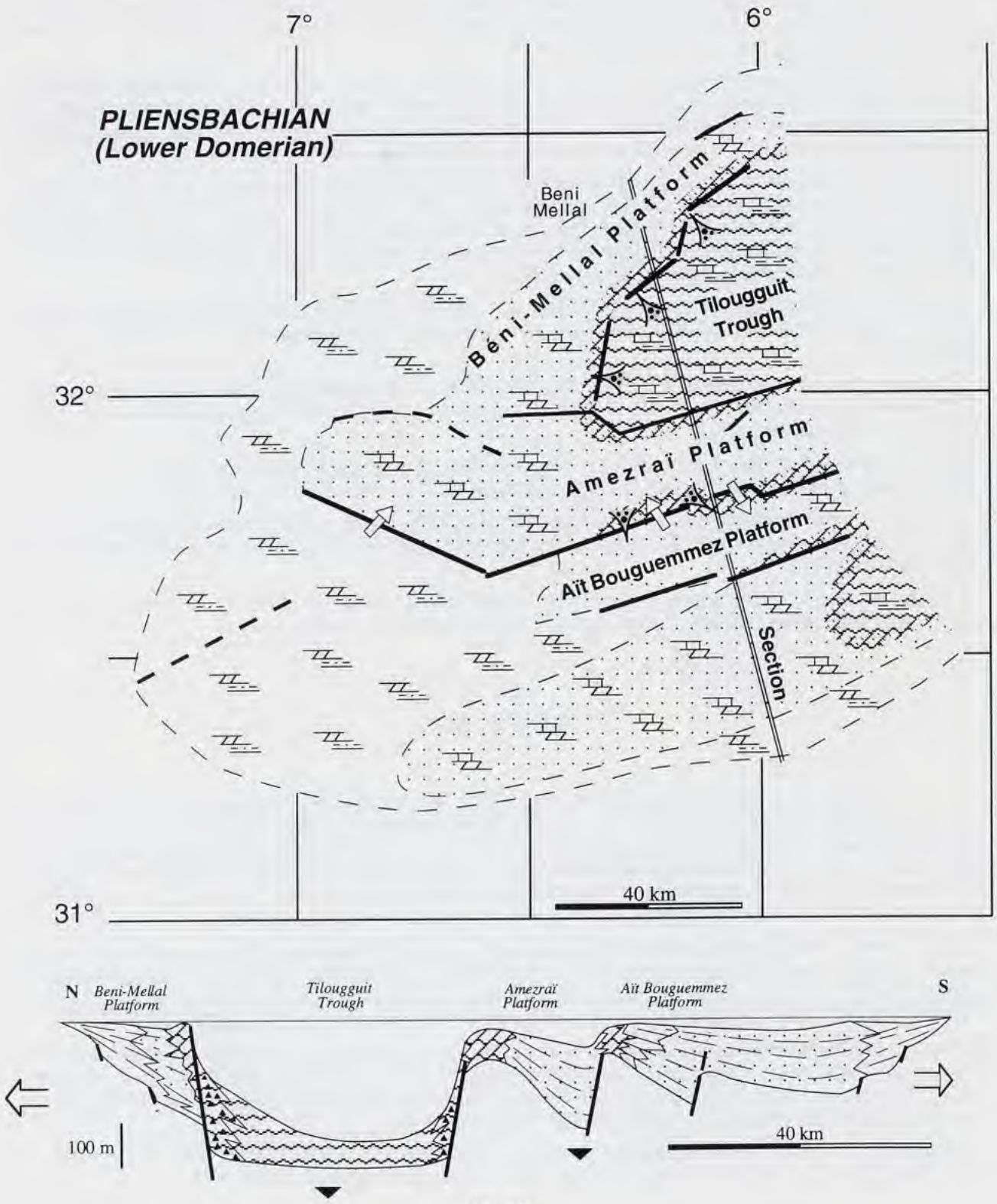

FIG. 6D

Source : MNHN, Paris

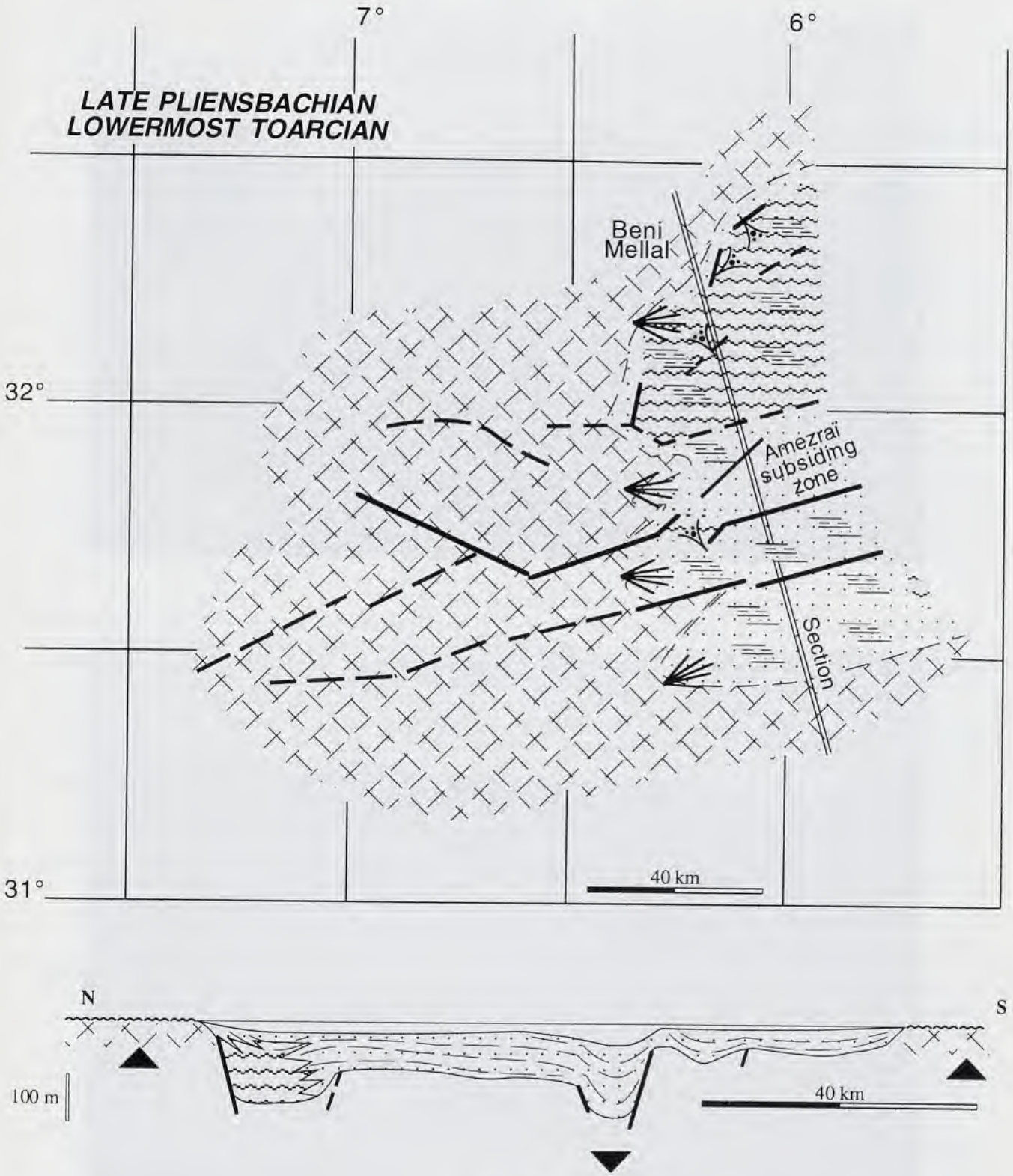

FIG. 6E

Source : MNHN, Paris

A

B

Source : MNHN, Paris

ACKNOWLEDGEMENTS

This work is a contribution to Peri-Tethys Program. The authors would like to thank the leaders of this project for financial support. S. CRASQUIN-SOLEAU, B. BIJU-DUVAL and S. ELMI who improved the first version of the text are also gratefully acknowledged.

REFERENCES

BOUCHOUATA, A., CANÉROT, J., SOUHEL, A. & ALMERAS, Y., 1995.— Stratigraphie séquentielle et évolution géodynamique du Jurassique dans la région de Talmest-Tazoult (Haut Atlas Central, Maroc). *Comptes Rendus de l'Académie des Sciences, Paris*, **320** (II): 749-756.

BOUTAKIOUT, M. & ELMI, S., 1996.— Tectonic and eustatic controls during the Lower and Middle Jurassic of the South Rif Ridge (Morocco) and their importance for the foraminifera communities. *Geological Research Forum, Zürich*, **1-2**: 237-248.

BREDE, R., HAUPMANN, M. & HERBIG H.G., 1992.— Plate tectonics and intracratonic mountain ranges in Morocco. The Mesozoic-Cenozoic development of the Central High Atlas and Middle Atlas. *Geologische Rundschau*, **81** (1): 127-141.

BURGESS, C.J. & LEE, C.W., 1978.— The Development of a Lower Jurassic carbonate tidal flat, Central High Atlas, Morocco. 1: Sedimentary history. *Journal of Sedimentary Petrology*, **48** (3): 777-794.

CHAFIKI, D., 1994.— *Dynamique sédimentaire à l'articulation plate-forme - bassin: exemple du Lias de la région de Béni-Mellal (Haut Atlas central, Maroc)*. Thèse de 3ème cycle, Université Cadi Ayyad, Marrakech, Maroc: 1-185.

CHAFIKI, D. & SOUHEL, A., 1993.— Présence d'un "debris apron" dans le Lias moyen de la région de Béni-Mellal (Haut Atlas central, Maroc). *In: 11ème Colloque des bassins sédimentaires marocains, Rabat, résumés*. Université Mohammed V, Rabat: 24.

CHOUBERT, G. & FAURE-MURET, A., 1962.— Évolution du domaine atlasique marocain depuis les temps paléozoïques. *In*: Livre à la Mémoire de Paul Fallot. *Mémoires de la Société géologique de France, Paris*, **1**: 447-527.

DUBAR, G., 1962.— Note sur la paléogéographie du Lias marocain (domaine atlasique). *In*: Livre à la Mémoire de Paul Fallot. *Mémoires de la Société géologique de France, Paris*, **1**: 529-544.

DU DRESNAY, R., 1979.— Sédiments jurassiques du domaine des chaînes atlasiques du Maroc. *In*: Symposium Sédimentation du Jurassique ouest européen, Paris, 1975. *Association des Sédimentologistes français, Publication spéciale*, **1**: 345-365.

EL HARIRI, K., DOMMERGUES, J.L., MEISTER, C., SOUHEL, A. & CHAFIKI, D., 1996.— Les Ammonites du Lias inférieur et moyen du Haut Atlas de Béni-Mellal (Maroc): taxinomie et biostratigraphie à haute résolution. *Geobios, Lyon*, **29** (5): 537-576, 15 figs.

EL KOCHKRI, A., CHOROWICZ, F. & ALEM, M. EL, 1997.— The Central and Eastern High Atlas: a Jurassic trough opening obliquely. *Peri-Tethys Programme, Annual Meeting, Rabat*. ONAREP, Rabat: 35.

ELMI, S., 1996.— Stratigraphic correlations of the main Jurassic events in the Western Mediterranean Tethys (Western Algeria and Eastern Morocco). *Geological Research Forum, Zürich*, **1-2**: 343-358, 8 figs.

FEDAN, B., 1989.— Évolution géodynamique d'un bassin intraplaque sur décrochement: le Moyen Atlas (Maroc) durant le Méso-Cénozoïque. *Travaux de l'Institut des Sciences de Rabat, Série Géologie et Géographie physique*, **18**: 1-146, 94 figs.

FIG. 7.— Uppermost Pliensbachian tectonics in the Central High Atlas. **A**, The Amezraï subsiding zone (Fig. 6E). The unconformity related to the regional NW-SE upper Domerian sinistral transtension stage separates the subvertical Hettangian-Pliensbachian limestones (foreground on the right) from the fan-shaped SE dipping uppermost Pliensbachian-Bajocian silts, sandstones and finally horizontal carbonates (foreground on the left). The scenery involves the snowy Jbel Azourki (3677 m, background on the left). **B**, The Assemsouk turbiditic basin. This basin, created by NW-SE sinistral transtension processes along the North Atlasic Fault (ANA, Fig. 1), is filled up by late Pliensbachian proximal calciturbidites generated by the Aït Bouguemmez southern (to the right) uplifted platform.

*FIG. 7.— La tectonique du Pliensbachien terminal dans le Haut Atlas Central. **A**, La zone subsidente d'Amezraï (Fig. 6E). La surface de discordance liée à la transtension régionale sénestre NW-SE sépare les calcaires couvrant l'intervalle Hettangien-Pliensbachien (premier plan à droite) des silts, grès et calcaires allant du Pliensbachien terminal au Bajocien, disposés en éventail ouvert au SE (premier plan à gauche). Le paysage englobe les reliefs enneigés du Jbel Azourki (3677 m, arrière plan à gauche). **B**, Le bassin turbiditique d'Assemsouk. Ce bassin, créé par transtension sénestre NW-SE le long de la Faille Nord-Atlasique (ANA, Fig. 1), est empli de calciturbidites proximales du Pliensbachien terminal en provenance de la plate-forme méridionale exhaussée de l'Aït Bouguemmez (à droite).*

Source : MNHN, Paris

GRACIANSKY, P.C. DE, DARDEAU, G., DUMONT, T., JACQUIN, T., MARCHAND, D., MOUTERDE, R. & VAIL, P.R., 1993.— Depositional sequence cycles, transgressive-regressive facies cycles and extensional tectonics: example from the southern Subalpine Jurassic basin, France. *Bulletin de la Société géologique de France*, **164** (5): 709-718.

JACQUIN, T., GARCIA, J.P., PONSOT, C., THIERRY, J. & VAIL, P.R., 1992.— Séquences de dépôts et cycles régressifs-transgressifs en domaine marin carbonaté. Exemple du Dogger du bassin de Paris. *Comptes Rendus de l'Académie des Sciences, Paris*, **315** (II): 353-362.

JENNY, J., 1983.— Les Décrochements de l'Atlas de Demnat (Haut Atlas central, Maroc): prolongation orientale de la zone de décrochement du Tizi-N-Test et clef de la compréhension de la tectonique atlasique. *Eclogae geologicae Helvetiae*, **77** (1): 143-152.

JENNY, J., 1985.— Carte géologique du Maroc au 1/100 000. Feuille Azilal. *Notes et Mémoires du Service géologique du Maroc, Rabat*, **339**.

JENNY, J., 1988.— Mémoire explicatif de la carte géologique du Maroc au 1/100 000. Feuille Azilal. *Notes et Mémoires du Service géologique du Maroc, Rabat*, **339 bis**: 1-104.

JOSSEN, J.A., 1987.— La Plate-forme carbonatée liasique du fond du golfe haut atlasique (Maroc). Évolution paléogéographique. *In: 112ème Congrès des Sociétés savantes, Lyon, Colloque de Géologie africaine*. Université Claude Bernard, Lyon: 45-55.

JOSSEN, J.A., 1988.— Carte géologique du Maroc au 1/100 000. Feuille Zawiat Ahançal. *Notes et Mémoires du Service géologique du Maroc, Rabat*, **355**.

LAVILLE, E., 1981.— Rôle des décrochements dans le mécanisme de formation des bassins d'effondrement du Haut Atlas marocain au cours des temps triasique et liasique. *Bulletin de la Société géologique de France*, **7**, **23** (3): 303-312.

LE MARREC, A., 1985.— Carte géologique du Maroc au 1/100 000. Feuille de Demnat. *Notes et Mémoires du Service géolologique du Maroc, Rabat*, **338**.

MILHI, A., 1992.— Les Faciès du Lias de la région du Todrha (Tinghir, versant sud du Haut Atlas central, Maroc). *Geologische Rundschau*, **81** (1): 63-68.

MONBARON, M., 1985.— Carte géologique du Maroc au 1/100 000. Feuille de Béni-Mellal. *Notes et Mémoires du Service géologique du Maroc, Rabat*, **341**.

ROCH, E., 1939.— Description géologique des montagnes à l'Est de Marrakech. *Notes et Mémoires du Service géologique du Maroc, Rabat*, **51**: 1-438.

ROCH, E., 1950.— Histoire stratigraphique du Maroc. *Notes et Mémoires du Service géologique du Maroc, Rabat*, **80**: 1-437, 77 figs, 22 pl.

ROLLEY, J.P., 1973.— *Étude géologique de l'Atlas d'Afourer, Haut Atlas central, Maroc.* Thèse de 3ème cycle, Université de Grenoble, Grenoble, France: 1-180.

SEPTFONTAINE, M., 1984.— Biozonation (à l'aide de Foraminifères imperforés) de la plate-forme interne carbonatée liasique du Haut Atlas (Maroc). *Revue de Micropaléontologie, Paris*, **27** (3): 209-229.

SEPTFONTAINE, M., 1986.— Milieux de dépôt et foraminifères (Lituolidés) de la plate-forme carbonatée du Lias moyen au Maroc. *Revue de Micropaléontologie, Paris*, **28** (4): 268-289.

SOUHEL, A., 1996.— Le Mésozoïque dans le Haut Atlas de Béni-Mellal (Maroc). Stratigraphie, sédimentologie et évolution géodynamique. *Strata, Toulouse*, **27** (2): 1-249.

SOUHEL, A., GHARIB, A., BOUCHOUATA, A. & CANÉROT, J., 1993.— Jurassic rift deposits in the Central High Atlas: platform to basin environments and sequence stratigraphy. *In: 14th International Association of Sedimentologists, Regional Meeting, Marrakech, Fieldtrip Guidebook*. University Cadi Ayyad, Marrakech, Morocco: 55-75.

SOUHEL, A., BEAUDOIN, B., CANÉROT, J. & PINAULT, M., 1995.— Analyse quantitative de la subsidence durant le Jurassique inférieur dans le Haut Atlas de Béni-Mellal (Maroc). *In: 16th Regional Meeting of Sedimentology, Abstracts. Association des Sédimentologistes français*, **22**: 136.

VAIL, P.R., COLIN, J.P., DU CHÊNE, R.J., KUCHLY, J., MEDIAVILLA, F. & TRIFILIEFF, V., 1987.— La Stratigraphie séquentielle et son application aux corrélations chronostratigraphiques dans le Jurassique du bassin de Paris. *Bulletin de la Société géologique de France*, III **8** (7): 1301-1321.

VAIL, P.R., AUDEMARD, F., BOWMAN, S.A., EISNER, P.N. & PEREZ-CRUZ, C., 1991.— The Stratigraphic signatures of tectonics, eustaty and sedimentology: an overview. *In*: G. EINSELE, W. RICHER & A. SEILACHER (eds), *Cycles and Events in Stratigraphy*. Springer, Berlin: 617-659.

Source : MNHN, Paris

4

The Jurassic events and their sedimentary and stratigraphic records on the Southern Tethyan margin in Central Tunisia

Mohamed SOUSSI [1], *Raymond ENAY* [2], *Charles MANGOLD* [2] & *Moncef TURKI* [3]

[1] Département de Géologie, Faculté des Sciences de Sfax, B.P. 3038 Sfax, Tunisie

[2] Université Claude-Bernard-Lyon 1, UFR des Sciences de la Terre
27-43, boulevard du 11 novembre 1918, F-69622 Villeurbanne Cedex, France

[3] Département de Géologie, Faculté des Sciences de Tunis, B.P. 1060, Tunis, Tunisie

ABSTRACT

The Jurassic sedimentary record of Central Tunisia comprises shallow marine peritidal carbonates, black shales, outer shelf marls and limestones, ironstone, deep marine condensed sections and hard-grounds. The faunas, especially ammonites, allow increasingly precise age estimations and correlations referred to the biochronological standard for Submediterranean Europe. The faunas show a submediterranean character in open marine environments and the South Tethyan situation is attested by abundant *Emileia* and *Oraniceras* in lower Dogger as well as the lack of boreal and sub-boreal families all along Jurassic. In fact, the Jurassic of Central Tunisia corresponds to five major transgressive-regressive tectono-eustatic second order cycles, four of which are separated by three sub-marine unconformities associated with important hiatuses. The abrupt facies changes and the frequency of condensed sections and/or hiatuses resulted from the interaction between global sea level fluctuations and local to regional tectonic activities associated with Early Mesozoic Tethyan rifting. Central Tunisia (North-South Axis) corresponded during the Jurassic to an uplifted mega-block acting as a carbonate outer shelf relayed to the north and to the south by subsident basins. Due to the intense activities of deep marine currents, occurring especially during the major rises or falls of sea level, this carbonate outer shelf has acted as a sediment-starved high. This latter has been maintained far from coarse or abundant clastic influences. Sedimentation has been recorded only during aggradational-retrogradational highstand phases.

RÉSUMÉ

Les événements jurassiques et leurs enregistrements sédimentaires et stratigraphiques sur la marge Sud-Téthysienne en Tunisie Centrale.

L'enregistrement sédimentaire du Jurassique de Tunisie centrale englobe des carbonates de plate-forme très peu profonde, des "black shales", des marno-calcaires de plate-forme externe, des oolithes ferrugineuses, des séries condensées et de nombreuses surfaces durcies. La faune d'ammonites a permis d'une part, de dater avec précision les corps sédimentaires et

SOUSSI, M., ENAY, R., MANGOLD, C. & TURKI, M., 2000.— The Jurassic events and their sedimentary and stratigraphic records on the Southern Tethyan margin in Central Tunisia. *In* : S. CRASQUIN-SOLEAU & É. BARRIER (eds), Peri-Tethys Memoir 5: new data on Peri-Tethyan sedimentary basins. *Mém. Mus. natn. Hist. Nat.*, **182** : 57-92. Paris ISBN : 2-85653-524-0.

Source : MNHN, Paris

d'autre part, d'établir des corrélations avec l'échelle biochronologique standard de l'Europe submeditéranéenne. La faune montre un caractère submeditéranéen d'environnements marins profonds et sa situation sud-Téthysienne est attestée par l'abondance des *Emilea* et *Oraniceras* ainsi que l'absence des familles boréales et sub-boréales tout le long du Jurassique. Le Jurassique de Tunisie Centrale correspond à cinq cycles transgressifs-regressifs majeurs de deuxième ordre d'origine tectono-eustatique. Quatre cycles sont séparés par des discontinuités sous-marines majeures accompagnées de lacunes stratigraphiques importantes. Les changements abrupts des faciès et la fréquence des condensations et/ou des hiatus résultent de l'interaction des effets conjoints des fluctuations eustatiques et de l'activité tectonique locale associée au rifting mésozoïque de la Téthys. En Tunisie Centrale, la région de l'Axe Nord-Sud correspondait au Jurassique à un mégabloc sous-marin élevé fonctionnant comme une plate-forme carbonatée, relayé au nord et au sud par des bassins subsidents. À cause de l'intense activité des courants profonds lors des élévations rapides ou des abaissements du niveau marin relatif, ce domaine immergé a fonctionné comme une "plate-forme affamée" qui est restée durant de longues périodes à l'écart de toute influence détritique terrigène. La sédimentation était active essentiellement pendant les phases transgressives et les périodes de haut niveau marin.

INTRODUCTION

In Tunisia, the Jurassic series crop out within the Saharan Platform (Jeffara area), along the so-called North-South Axis (NOSA) and its northern extension the "Tunisian Dorsale", and locally within the Atlasic and Tellian zones (Fig. 1B). Their subsurface analogues have been encountered in numerous wells in Southern and Central Tunisia.

Jurassic rocks of Southern Tunisia consist of mixed evaporite, carbonate and siliciclastic sediments corresponding to various depositional environments including sabkha and subaqueous evaporite basin, tidal flats, shallow and open marine carbonate platform (BUSSON, 1967; KAMOUN, 1988; BEN ISMAIL & M'RABET, 1990; BEN ISMAIL, 1991; BOUAZIZ, 1995). In Central Tunisia, the Jurassic deposits are essentially carbonates and partly shales. The lower part of the Lower Jurassic rocks are composed of peritidal shallow marine platform carbonates, while the Middle and Upper Jurassic deposits are formed of hemipelagic marls and limestones and external platform carbonates (BONNEFOUS, 1972; SOUSSI, 1990). The latter include several discontinuities associated with stratigraphic gaps (SOUSSI, ENAY *et al.*, 1991). In Northern Tunisia, the Jurassic rocks are also composed of shallow marine carbonates succeeded by Middle-Upper Jurassic hemipelagic and pelagic facies; they comprise, in addition, calciturbidites, radiolarites and local bioherms (CASTANY, 1955; BONNEFOUS, 1972; RAKUS & BIELY 1970; ALOUANI *et al.*, 1990; ALOUANI, 1991; SOUSSI *et al.*, 1992; SOUSSI *et al.*, 1994; SOUSSI, TURKI *et al.*, 1996; SOUSSI *et al.*, 1998).

This northward variation from shallow to deep marine facies is related to the Late Palaeozoic-Early Mesozoic rifting and drifting of the northern margin of the African Plate (M'RABET *et al.*, 1989; ALOUANI, 1991; PEYBERNÈS, 1992; BOUAZIZ, 1995; BEN ISMAÏL, 1991).

The reconstruction of the several palaeogeographic parts of this passive margin requires accurate and homogeneous sedimentologic, tectonic and biochronologic data.

The main objective of the present paper is to analyse the palaeogeographic framework of the Jurassic of Central Tunisia during the rifting of the Tethys. For this, we will refine the stratigraphic control using ammonites, and re-examine in detail the facies distribution and the corresponding depositional environments as well as their controlling factors.

A particular interest is reserved to the relationship between the facies record in space and time, the morpho-structural framework, and sea level changes.

The tectono-stratigraphic framework and its sedimentary record, which are emphasised by the presence of numerous condensed sections and hiatuses, will be correlated to the Jurassic of both Northern and Southern Tunisia, then it will be compared to the sea level history curves proposed by VAIL *et al.* (1987), HAQ *et al.* (1987) and HALLAM (1988). This comparison will offer the opportunity to appreciate once again the effects of the tectonic and eustatic control on sedimentation. Within Central Tunisia and especially on the NOSA, which acted as a starved platform, sedimentation has been recorded particularly during aggradational-retrogradational highstand phases. Hiatuses characterise the highest part of the tilted blocks where current activities were at a maximum during the rapid sea level rises or falls. The frequency of the discontinuities and hiatuses is due to the combined effects of the local tectonic factors and the global eustatic ones. Tectonic activities linked to the Tethyan rifting created a

Source : MNHN, Paris

pattern of tilted blocks involving palaeohighs. These latter have been isolated from the sedimentary supplies, notably during either the maximum regressive periods when sedimentation displaced towards the basin or during transgressive phase when the shoreline displaced onto continental margin.

GEOLOGICAL SETTING

The Jurassic series of Central Tunisia crop out along the so-called North-South Axis (NOSA) stretching between Jebel Rheouis in the south and Jebel el Haouareb in the north (Fig. 1 C). This area is considered as a boundary between the Central Atlas fold belt to the west and the Pelagian Sea block to the east. This NOSA constitutes a singular component of the Tunisian geology. It has acted as a relative high and unstable palaeogeographic domain, notably during the Mesozoic (BUROLLET, 1956; M'RABET, 1975; ABBES, 1983; OUALI, 1984; SOUSSI, 1990).

Along this domain, bounded by a sub-meridian fault system, the Jurassic series are generally in tectonic contact with Triassic and even Cretaceous series. The normal Upper Triassic-Lower Jurassic stratigraphic transition is locally preserved (e.g., Ain el Morra, Châabet el Attaris and Loridga sections; SOUSSI, ABBES *et al.*, 1996; SOUSSI, ABBES & BELAYOUNI, 1998).

FACIES ANALYSIS

Following the first investigations (DUMON, 1936; SCHOELLER, 1937; CASTANY, 1951), BUROLLET (1956) defined the Jurassic Nara Formation with three terms: a lower dolomitic term, a middle argillaceous term and an upper dolomitic term.

The present sedimentologic study has led to distinguish within the Nara Formation, at least, six major lithologic units, that could each have the rank of formation. These major units have a regional extent and may be easily distinguished in the field and sub-surface on the basis of their faunal and facies characteristics. Furthermore, they are separated by three major unconformities. The different lithologic units will be analysed using eight measured sections, from south to north, in Jebel Rheouis, Krechem el Kelb, Châabet el Attaris, Kef el Hassine, Kef el Khouadja, Guefaïet, Loridga and Jebel el Haouareb (Fig. 1C).

THE TYPE SUCCESSION OF RHEOUIS-LORIDGA AREA

The three terms of the Nara Formation can be observed from Jebel Rheouis to Jebel Loridga. They have been subdivided in six lithological units (Fig. 2).

— U1: first unit. The lower Nara A peritidal dolomites.

These deposits are generally in tectonic contact with the Triassic evaporites of the Rheouis Formation (BUROLLET, 1956). The transition from the Upper Triassic to the lower par of the Lower Jurassic is well exposed at Ain el Morra, Jebel Châabet el Attaris and Loridga sections (KAMOUN *et al.*, 1994; SOUSSI, ABBES *et al.*, 1996). Its lower part is dated Rhaetian at Jebel Gamgouma-Loridga (KAMOUN *et al.*, 1994), while the rest which forms the major part of the lower Nara is attributed to the Hettangian-Sinemurian (BONNEFOUS, 1972).

This unit (up to 195 m thick) is composed of massive dolomitic beds forming decimetric to metric shallowing-upwards parasequences characterised by the constancy of their sedimentary and diagenetic characteristics in Central Tunisia. The typical parasequence is composed of a basal dolomitic breccia (0.05 to 0.30 m) formed of angular dolomitic lithoclasts, pelletoids and algal debris. Locally, this term contains asymmetric ooids and pisoids encrusted by algae and it was early lithified. The middle term is generally thicker (0.70 m) and composed of homogeneous and bioturbated dolomite. The third term is

Source : MNHN, Paris

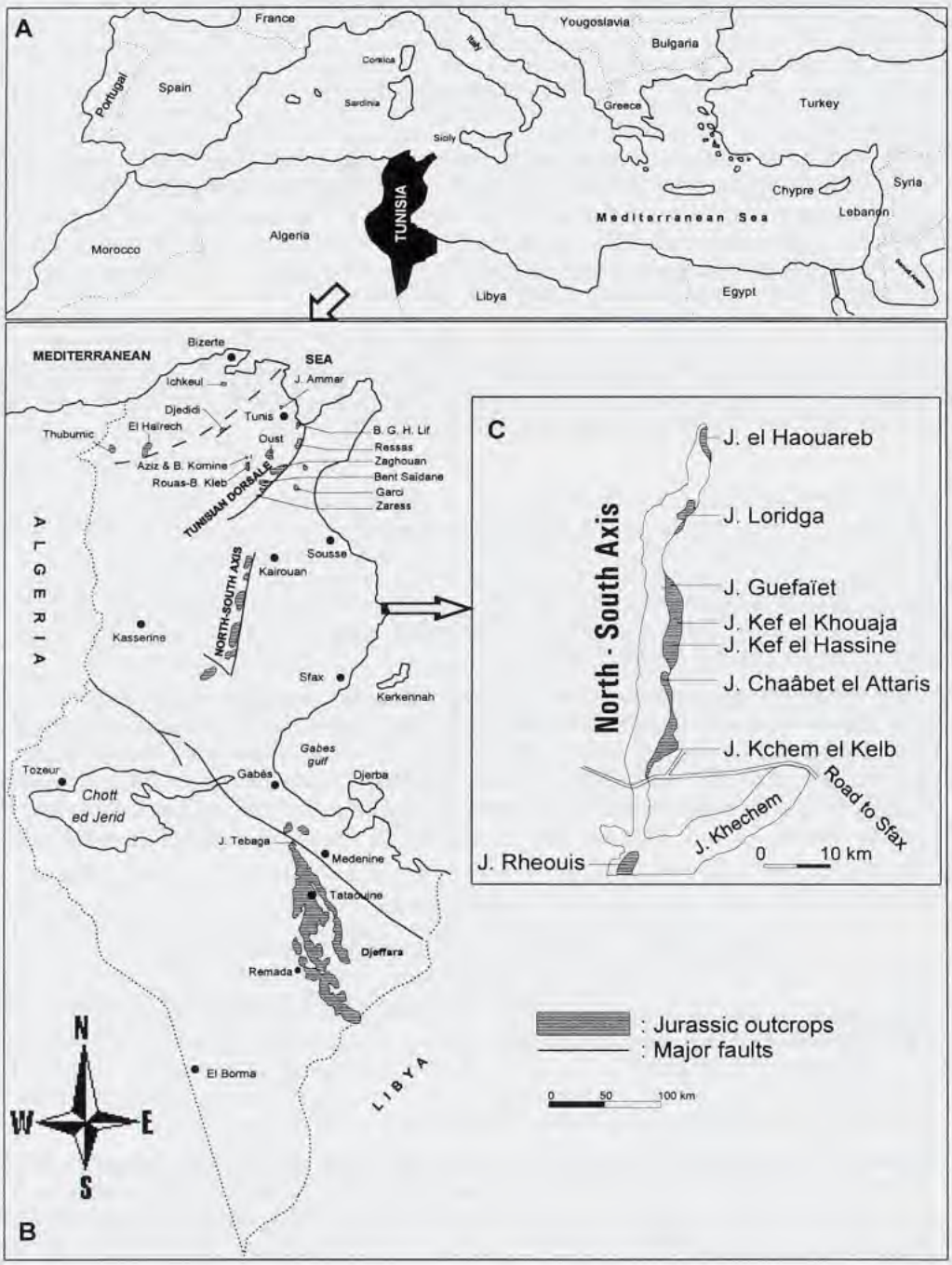

FIG. 1.— Location of the study; **A**, location map of the studied area. **B**, the main Jurassic outcrops in Tunisia; **C**, location of the studied sections along the North-South Axis (NOSA) in Central Tunisia.

*FIG.1.— Localisation de l'étude ; **A**, localisation de la zone étudiée ; **B**, principaux affleurements jurassiques de Tunisie ; **C**, localisation des coupes étudiées le long de l'Axe Nord-Sud (NOSA) en Tunisie Centrale.*

Source : MNHN, Paris

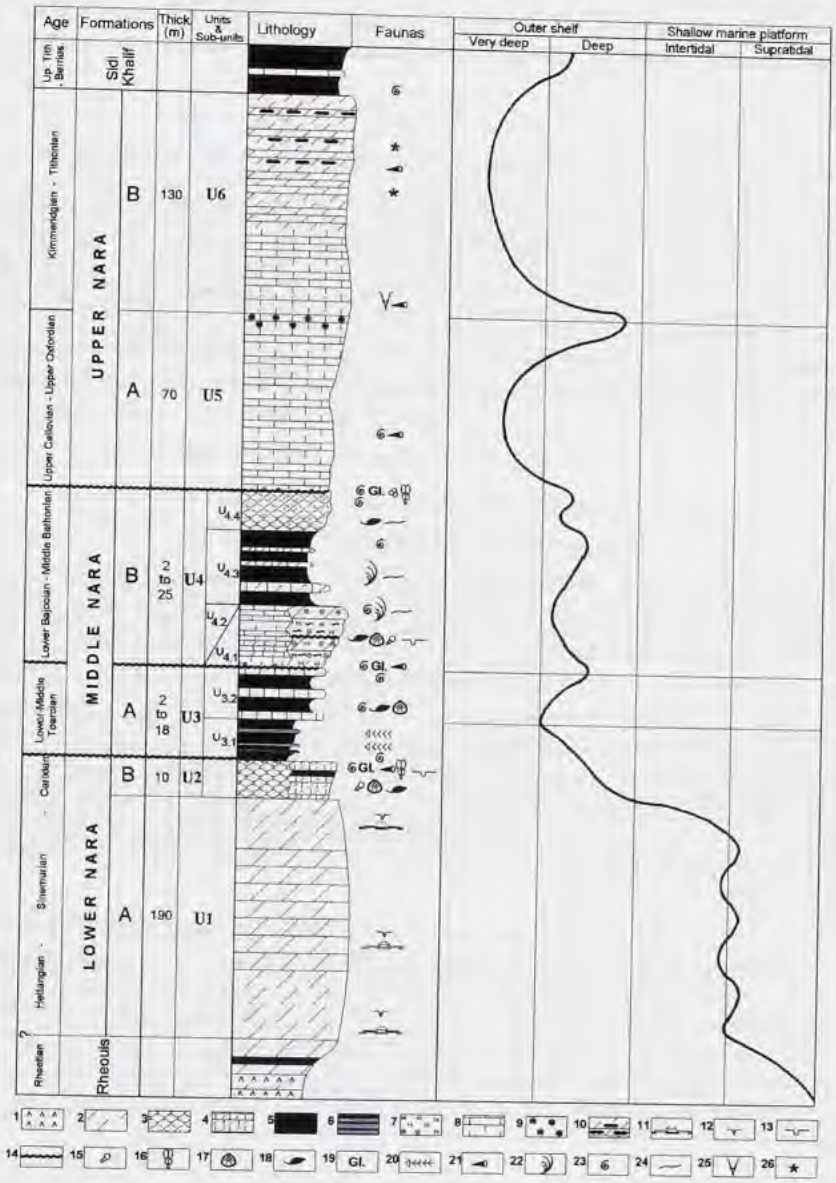

FIG. 2.— The Jurassic lithologic synthetic succession of the NOSA (Central Tunisia) and their depositional environments. **1**, gypsum; **2**, peritidal dolomites; **3**, compacted open marine carbonates; **4**, limestone partly dolomitised, **5**, shales ; **6**, laminites; **7**, ferruginous ooids; **8**, pelagic muddy limestones; **9**, calcareous ooids; **10**, cherty carbonates; **11**, stromatolite and birds-eyes; **12**, sheet cracks; **13**, borings; **14**, unconformity; **15**, gastropods; **16**, benthic foraminifera; **17**, pelycepods; **18**, brachiopods; **19**, glauconitic grains; **20**, fish bones; **21**, belemnites; **22**, *Zoophycos*; **23**, ammonites; **24**, filaments; **25**, *Saccocoma*; **26**, radiolaria.

*FIG. 2.— Succession lithologique synthétique et environnement de dépôt des séries jurassiques le long de l'Axe Nord-Sud (Tunisie centrale). **1**, gypse ; **2**, dolomies péritidales ; **3**, carbonates compactés de milieu marin ouvert ; **4**, calcaires partiellement dolomitisés, **5**, argiles ; **6**, laminites ; **7**, oolithes ferrugineuses ; **8**, calcaires "mudstones" pélagiques ; **9**, oolithes calcaires ; **10**, carbonates à silex ; **11**, stromatolites et "birds-eyes" ; **12**, fentes de dessiccation ; **13**, perforations ; **14**, discordance ; **15**, gastéropodes ; **16**, foraminifères benthiques ; **17**, pélécypodes ; **18**, brachiopodes ; **19**, grains de glauconite ; **20**, squelettes de poissons ; **21**, bélemnites ; **22**,* Zoophycos *; **23**, ammonites ; **24**, filaments ; **25**,* Saccocoma *; **26**, radiolaires.*

Source : MNHN, Paris

rich in algal stromatolitic laminations, tepees, birds-eyes, mud and sheet cracks partly filled with dolomicritic internal sediment and/or dolomite cement. Locally, this term exhibits evaporitic micronodules which are dissolved and cemented by white dolosparite. The top of the last term of the parasequence is marked by residual green argilites locally containing black pebbles. The thickness of these peritidal parasequences varies from 0.4 to 2 m while their lateral extension is a few hundred meters.

— U2: second unit. The lower Nara B bioclastic dolomites.

This unit (up to 5 m thick) constitutes the upper part of the lower Nara and is Carixian in age (SOUSSI, ENAY *et al.*, 1991). It is composed of well-bedded decimetric dolomitic beds, usually recrystallised and rich in benthic fauna (pelecypods, gastropods, textularids, ahermatypic corals and echinoderm debris). The uppermost beds which are particularly rich in ammonites and belemnites at Jebel Kef el Hassine correspond to condensed deposits. In Châabet el Attaris, these dolomites are black, compact and particularly rich in pelecypods and gastropods. In Jebel Loridga, they alternate with green shales. In all analysed sections, the top of this unit, which exhibits borings, corresponds to a submarine hard-ground (unconformity: UC1).

— U3: third unit. The middle Nara A "black shales".

This unit is composed of two distinct lithologic sub-units ($U_{3.1}$ and $U_{3.2}$).

The lower sub-unit ($U_{3.1}$) consists of black laminated marls and carbonates: "black shales" (5 to 10 m). This unit is early Toarcian in age. It consists of alternating laminated dolomitic limestone and greenish to beige coloured marls in which the clay fraction is essentially composed of illite and traces of kaolinite. The marl intervals are rich in brachiopods, pelecypods and ammonites, while the limestone beds are marked by ammonites traces. Locally, at Jebel Châabet el Attaris, these facies are dark grey to black-coloured and rich in pyrite and organic matter. They correspond to true black shales in which the total content of organic carbon is up to 12 % (SOUSSI *et al.*, 1990; SAÏDI *et al.*, 1992). Within the black shales the carbonate beds have mudstone textures, often partly dolomitised. These carbonates are poor in benthic fossils and rich in closely-spaced bituminous laminae, with carbonate or clay-organic rhythmic sequences (millimetric in thickness). Early diagenitic pyrite fabrics, such as small cubes or micro-framboidal aggregates have been observed.

The upper sub-unit ($U_{3.2}$) consists of shales and white to beige nodular limestones. In contrast to $U_{3.1}$, this sub-unit is relatively more argillaceous (with a clay fraction made essentially of kaolinite). The carbonate intervals are particularly nodular and argillaceous. They are packstone in texture and contain filaments, brachiopods, echinoderm debris, detrital quartz and abundant bioturbations. The thickness of this unit, well exposed in Krechem el Kelb (8 m), Châabet el Attaris and Kef el Hassine, decreases towards the north and is notably very reduced in the el Guefaïet area (4 m). This sub-unit terminates with a submarine erosional surface, locally encrusted by ferruginous and phosphatic horizons (unconformity: UC 2).

— U4: fourth unit. The middle Nara B ironstones and/or filaments and *Zoophycos*-rich carbonates

It is composed of four main sub-units ($U_{4.1}$- $U_{4.4}$). From bottom to top we distinguish:

The sub-unit 1 ($U_{4.1}$) consists of "ironstones" (0 to 1.6 m) rich in ferruginous ooids. It is generally Bajocian in age, but locally (Jebel Loridga), it is Aalenian-Bajocian (SOUSSI, ENAY *et al.*, 1991; SOUSSI, M'RABET & ENAY, 1991). It extends up to the middle Bathonian mainly in the northern part of the NOSA (Fig. 3). It is a few decimetres thick and formed of discontinuous lenses bodies well represented at Krechem el Kelb (1 m), Kef el Hassine (0.90 m), Demet (0.7 m) and Loridga (1.8 m) (Figs 3 and 4). In Jebel Châabet el Attaris, the ooids are rare, reworked and disseminated in a microsparitic matrix.

The "ironstone" facies has been extensively described from the Jurassic of Europe (VAN HOUTEN, 1985; HARDER, 1989). In Central Tunisia, the facies consists of muddy-carbonate horizons, reddish or bluish green in colour, very rich in phosphatic and ferruginous (goethite and hematite) pisoid- and ooid-like grains and lithoclasts encrusted by ferruginous algal laminations. The ooids and pisoids exist in

Source : MNHN, Paris

clayey or dolosparite matrix. They are 0.3 to 3 mm in size, spherical to elliptical and have a cortex composed of concentric layers enveloping a nucleus often represented by quartz grains. Some broken ooids served as nuclei for a later generation of ooids. These iron-rich grains are associated with both benthic and nektonic fauna including gastropods, pelecypods, annelids, brachiopods, ammonites and belemnites. Locally (Krechem el Kelb and Loridga), they exhibit fining-upwards sequences and low angle cross bedding.

The sub-unit 2 ($U_{4.2}$) is composed of filaments and *Zoophycos*-rich carbonates.

It is Bajocian-early Bathonian in age, 7 to 13 m thick and formed of decimetric bedded limestones or dolomites containing thin shale intercalations. Locally, at Krechem el Kelb, it is composed of reddish and compacted dolomites separated by thin clayey layers. The carbonates are mud-wackestone to packstone in texture and contain ostracods, benthic foraminifers, filaments (probably thin pelagic pelecypod shells), gastropods, brachiopods, echinoderm debris, ammonites and belemnites. These carbonates are particularly rich in bioturbations such as *Zoophycos* and *Chondrites*.

In Châabet el Attaris, this sub-unit is relatively more developed (13 m) and composed of blue grey dolomitic limestones showing erosive surfaces marked by thin siltstones particularly rich in belemnites. The thickness of this unit drastically decreases from the south to the north (Figs 3-4).

The sub-unit 3 ($U_{4.3}$) consists of pyritised ammonite-rich shales.

This sub-unit is mainly constituted of shales locally intercalated with decimetric bioturbated carbonate beds rich in *Chondrites*, *Zoophycos* and filaments. It is 1 to 3 m thick.

At Châabet el Attaris, it is exclusively formed of green shales particularly rich in small pyritised ammonites. The clay fraction consists of illite and kaolinite; the latter being progressively more abundant at the top. This sub-unit thins and disappears towards the north (Figs 3, 4 and 6).

The sub-unit 4 ($U_{4.4}$) is formed of compacted carbonates.

This sub-unit (3 m) is middle Bathonian in age and composed of compacted limestones or dolomitic beds with very thin clay intercalations. These dolomitic beds are usually coarse-grained and reddish and when preserved from dolomitisation, they are blue and particularly rich in filaments and brachiopods. This sub-unit terminates with an erosional surface encrusted by thin phosphatic layers, associated with ferruginous ooid-like grains and ammonites (unconformity: UC3).

— U5: fifth unit. The upper Nara A carbonates.

The upper Nara term is subdivided into two distinct lithologic units (U5 and U6).

The basal one which is late Callovian-Oxfordian in age and up to 70 m thick, corresponds to the fifth unit (U5). It is locally preserved from dolomitisation (Krechem el Kelb, Châabet el Attaris, Kef el Hassine and el Haouareb) and composed of decimetric bedded wack-packstone rich in ammonites, belemnites, protoglobigerines, benthic foraminifers, ostracods, echinoid debris and abundant glauconitic grains. In the northern part of Krechem el Kelb, this unit starts with a limestone lens (0.30 m in thick and 50 m in length) dated middle Callovian in age.

These condensed beds (reduced thickness, diversified fauna, glauconitic grains) are overlain by mudstone-wackstone rich in planktonic microfauna (protoglobigerines). The latter are overlain by packstone to grainstone limestone beds particularly rich in ooids.

— U6: sixth unit. The upper Nara B carbonates.

The major part of this unit (up to 130 m) is composed of decimetric dolosparitic beds, medium- to coarse-grained and showing well-preserved radiolarian.

At Châabet el Attaris, it starts with mud-wackestone containing echinoderm debris and pelagic crinoids (*Saccocoma*), calcispheres and rare ostracods.

Source : MNHN, Paris

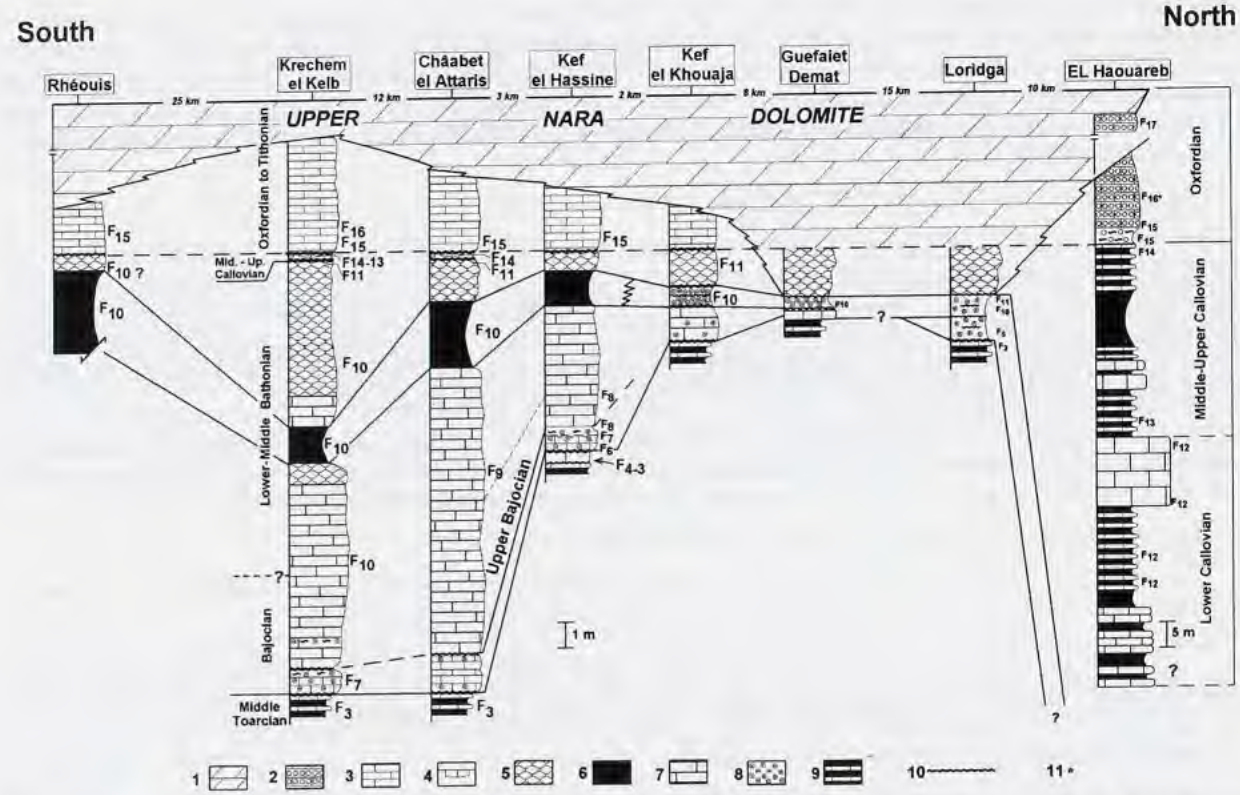

FIG. 3.— Stratigraphic correlation of the Middle Jurassic series of the measured sections along the North-South Axis (Central Tunisia). **1**, Upper Jurassic dolomites; **2**, Oxfordian "ammonitico rosso" facies; **3**, lower Oxfordian muddy-limestones; **4**, upper Callovian lense (= *Athleta* bed); **5**, middle Bathonian compacted carbonates; **6**, lower Bathonian pyritised ammonites-rich shales; **7**, Bajocian-lower Bathonian filaments and *Zoophycos*-rich limestones; **8**, Bajocian-Bathonian ironstones; **9**, middle Toarcian hemi-pelagic marls and limestones; **10**, unconformities; **11**, after GHARBI (1989).

*FIG. 3.— Corrélations stratigraphiques des unités lithologiques du Jurassique moyen des coupes étudiées le long de l'Axe Nord-Sud (Tunisie centrale). **1**, dolomies du Jurassique supérieur ; **2**, faciès "ammonitico rosso" de l'Oxfordien inférieur ; **3**, calcaires pélagiques de l'Oxfordien inférieur ; **4**, lentille calcaire du Callovien supérieur (banc à* Athleta) *; **5**, carbonates compactés à filaments du Bathonien moyen ; **6**, argiles à ammonites pyriteuses du Bathonien moyen ; **7**, calcaires à* Zoophycos *et filaments du Bajocien-Bathonien inférieur ; **8**, oolithes ferrugineuses du Bajocien-Bathonien ; **9**, marno-calcaires hémi-pélagiques du Toarcien moyen ; **10**, discordances ; **11**, d'après GHARBI (1989).*

THE LATERAL SECTION IN JEBEL EL HAOUAREB AREA

In Jebel el Haouareb area, located 9 km to the north from Jebel Loridga, the outcropping Jurassic sequence is thick and is very similar to that described within the Tunisian Dorsale (CASTANY, 1951; BONNEFOUS, 1972; GHARBI, 1989). The Lower and Middle Jurassic are not exposed. Here, the section starts with lower Callovian alternating marls and limestones particularly rich in filaments, calcispheres, and foraminifers (spirillines and lenticulines).

The overlying succession is composed of mud-wackestone carbonates rich in calcispheres (7 m), alternations of green shales and mud-wackestone carbonate beds (40 m), and the "ammonitico rosso" facies, represented by nodular limestones, reddish- to greenish-coloured and rich in protoglobigerines, calcispheres, belemnites and abundant ammonites indicating an early Oxfordian age.

Laterally to the north, the series continue with alternations of green shales and blue grey muddy-limestones locally containing numerous calciturbidite beds. The carbonate horizons contain belemnites, calcispheres, pelecypod echinoderm debris and pelagic crinoids (*Saccocoma*).

The uppermost part of the section is dolomitised and conformably overlain by the Sidi Khalif shales, the base of which is late Tithonian in age (BUSNARDO *et al.*, 1976, 1980, 1985; M'RABET, 1975, 1987).

Source : MNHN, Paris

BIOSTRATIGRAPHY AND BIOCHRONOLOGY (Figs 3 and 4)

Faunas, especially ammonites, provide the basis of the biochronological framework necessary to the interpretation of the lithosequential analysis in a regional context. It allows the estimation of the duration of the gaps in sedimentary discontinuities.

The biochronological reference framework is that used for Submediterranean Western Europe (*in* CARIOU & HANTZPERGUE, 1997). Some of the data pointed here were obtained before, but only in unpublished reports. This work incorporates the data briefly summarised in 1991 (SOUSSI, 1990; SOUSSI, ENAY *et al.*, 1991, SOUSSI, M'RABET & ENAY, 1991).

A recent work (PEYBERNES *et al.*, 1995) proposes for the same time span (Toarcian-Oxfordian) an interpretation of the depositional sequences and ammonite biochronozones of the NOSA, which recognises most of our dating. Nevertheless, differences with our data appear and the resulting ages are discussed below.

THE IDENTIFIED FAUNA

TOARCIAN ASSEMBLAGES

They were not the subject of a systematic research except at the top with the aim to precise the age of the base of the first unconformity (UC 1) and of the Middle Jurassic series above.

— The first fauna (F1), are *Paltarpites* sp. at Jebel el Guemgouma and Kef el Khouadja, *Hildaites* sp. at Jebel Châabet el Attaris from the lower Toarcian, already recognised by RAKUS (1968, unpublished) with *Paltarpites* sp. too. According to PEYBERNÈS *et al.* (1995) *Dactylioceras* sp. and *Paltarpites* sp. at Jebel Châabet el Attaris would indicate the Polymorphum Zone (earliest Toarcian).

— The presence of the Falcifer (or Serpentinum) Zone of the late early Toarcian was established (RAKUS, 1968 unpublished) with *Harpoceras* cf. *falcifer* (Sow.). *Hildaites* sp. at Jebel Châabet el Attaris; also *H.* gr. *serpentiniformis* mentioned by PEYBERNÈS *et al.* (1995) indicates the same zone (F2).

— The fauna of the Bifrons Zone, Sublevisoni Subzone (F3) (middle Toarcian) is more constant and often represented by the index species at Kef el Khouadja, Jebel Krechem el Kelb. We found *Hildoceras* cf. *sublevisoni* Fucini at Kef el Hassine a few centimetres below the unconformity UC2 (middle Nara A, U3, top of $U_{3.2}$) and the earliest Bajocian age deposits (middle Nara B, U4, base of $U_{4.1}$).

— Furthermore, at Kef el Hassine, fauna from the late Toarcian, Variabilis or Thouarsense Zone (F4), were reported by RAKUS (1968, unpublished). The phosphatised thin layer underlining the unconformity has yielded *Polyplectus* sp. from the upper Toarcian too.

North of this locality, the Toarcian does not extend above the middle Toarcian.

AALENIAN ASSEMBLAGES

Faunas of this stage and also of the upper Toarcian are everywhere nearly absent. They were recognised only at Jebel Loridga where the lowest iron oolithic levels yielded *Graphoceras (G.)* sp. and *G. (G.)* cf. *limitatum* (Buckman) from the Concavum Zone (upper Aalenian) (F5).

LOWER BAJOCIAN SONNINIA/EMILEIA AND STEPHANOCERAS/TELOCERAS ASSEMBLAGES

Two profiles, Kef el Hassine and Jebel Krechem el Kelb, allow us to characterise the lower Bajocian levels, which are undoubtedly present at other profiles according to the litho-sequential correlations, but not yet attested and dated by faunas.

Source : MNHN, Paris

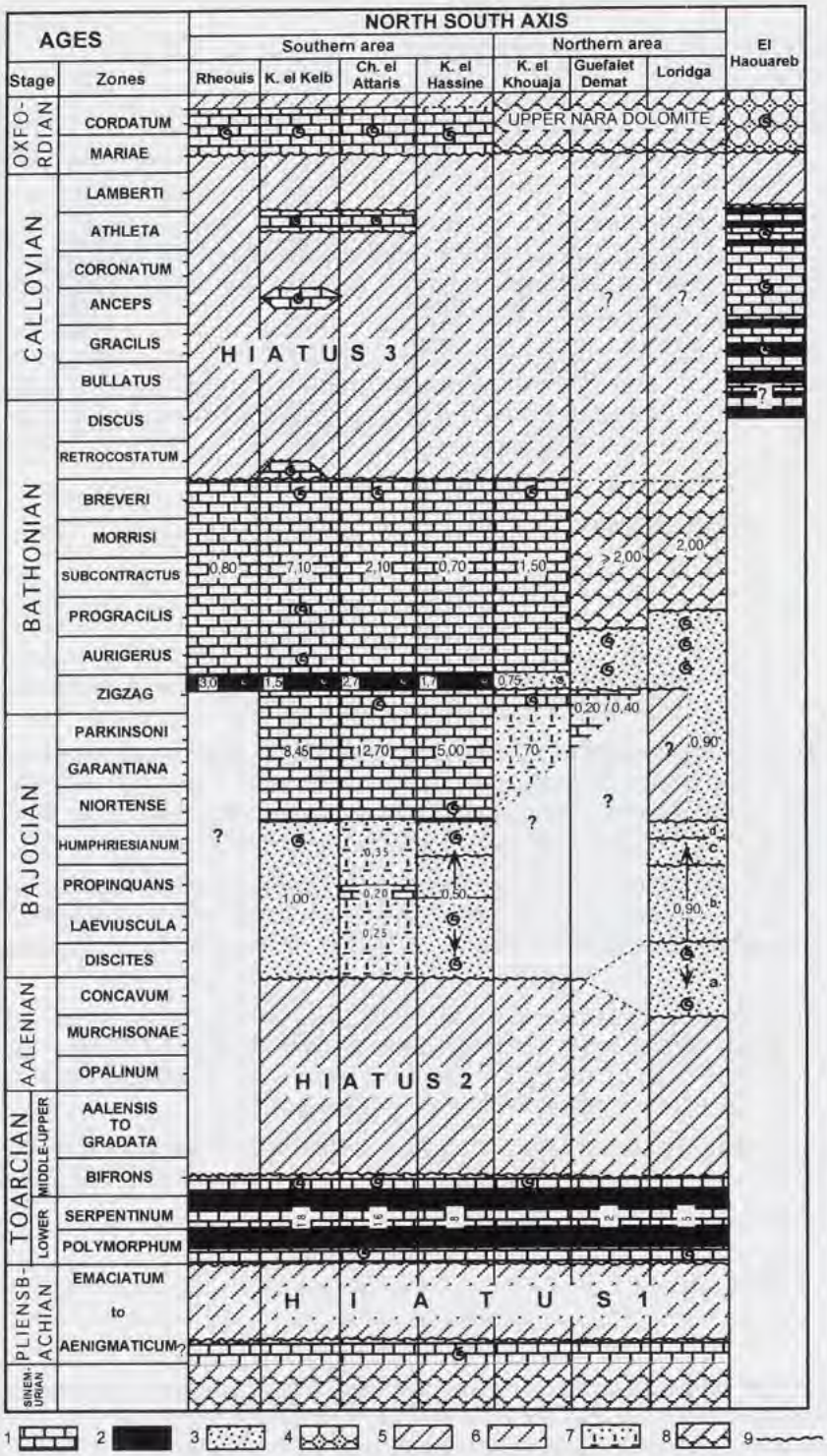

FIG. 4.— Biochronology chart of Jurassic ammonites of Central Tunisia. **1**, limestones; **2**, shales; **3**, ironstones; **4**, nodular limestones; **5**, proved hiatus; **6**, probable hiatus; **7**, ferruginous ooids-rich-limestone or "ironstones"; **8**, dolomites; **9**, unconformities.

*FIG. 4.— Charte biochronologique des ammonites du Jurassique de Tunisie Centrale. **1**, calcaires ; **2**, argiles ; **3**, oolithes ferrugineuses ; **4**, calcaires nodulaires ; **5**, lacune stratigraphique prouvée ; **6**, lacune stratigraphique probable ; **7**, calcaires à oolithes ferrugineuses ; **8**, dolomites ; **9**, discordances.*

— The first Bajocian fauna (F6) identified at Kef el Hassine within the middle Nara B (U4, Base of $U_{4.1}$) is dominated by frequent and large *Emileia* gr. *polyschides* (Waagen) associated with rare *Sonninia*: *S. (Euhoploceras) polyacantha* (Waagen) and *S. (E.) simplex* Buckman. These species are known from the Discites and Laeviuscula Zones. Throughout Europe (GABILLY *et al.*, 1971; RIOULT *et al.*, 1997), *Emileia* is rather common in the third zone (Propinquans Zone) of the lower Bajocian,

Source : MNHN, Paris

although already present in the Laeviuscula Zone. *Sonninia*, associated with the subgenus *Euhoploceras* points to an early Bajocian age. This association would also indicate a condensed sequence during Discites and Laeviuscula Zones. This is indicated by numerous phosphatised ooids and abundant belemnites both at the bottom and the top of the bed (= ammonites level).

— The next fauna with *Stephanoceras* and *Teloceras* (F7) is located at Jebel Krechem el Kelb in the uppermost beds with ferruginous ooids (middle Nara B, $U_{4.1}$): *Stephanoceras (S.)* gr. *humphriesianum* (Sow.), often of large size (0.40 m) and *Teloceras blagdeni* (d'Orb. non Sow.). At Kef el Hassine, the middle part of the same beds with ferruginous ooids, here less thick, has yielded: *Cenoceras* sp., *Chondroceras* cf. *gervillei* (Sow.), *C.* cf. *orbignyanum* (Whright), *Sphaeroceras* gr. *brongniarti* (Sow.), *Dorsetensia (Nannina)* sp., *Normannites* sp., *Epalxites* sp., *Stephanoceras (S.)* cf. *tenuicostatum* Hochstetter.

Both associations belong to the Humphriesianum Zone. It is impossible to currently recognise the subzones or horizons distinguished in Poitou (GABILLY *et al.*, 1971), in Subalpine ranges (PAVIA, 1983), in NW Germany (MASCKE, 1907) or in the Submediterranean province (RIOULT *et al.*, 1997). At Kef el Hassine, *Dorsetensia* and *Chondroceras* would indicate that the basal Romani Subzone is better-recorded.

Upper Bajocian Spiroceras assemblages

At Kef el Hassine, two levels in the filaments and *Zoophycos*-rich limestones (middle Nara B, $U_{4.2}$) have yielded: *Cadomites* sp. and *Spiroceras* sp. from the lower bed, and one metre above: *Spiroceras* sp. cf. *S. bifurcati* (Qu.) and ? *Strigoceras* sp. (F8). The second association can be referred to the Niortense Zone.

Morphoceras and Oraniceras lower Bathonian assemblages

This is the best-characterised and the most widely represented fauna from Jebel Rheouis to Jebel Loridga. Its absence at Kef el Hassine probably results from bad outcrop condition. The marls with pyritised ammonites are here covered by scree. At Jebel el Haouareb the beds below the early Callovian do not crop out.

These taxa are present in several sub-units.

— The filaments and *Zoophycos*-rich limestones (Middle Nara, $U_{4.2}$) have yielded *Oraniceras hamyanense* Flamand at Jebel Krechem el Kelb and earlier *Lobosphinctes* sp., *Planisphinctes* of the earliest Bathonian (Zigzag Zone, Parvum Subzone) at Jebel Châabet el Attaris (F9).

— The marls with pyritised fossils (Middle Nara, $U_{4.3}$) have provided the richest associations (F10): at Jebel Rheouis, *Phylloceras* sp., *Cadomites* sp. juv., *Procerites* sp. juv., *Morphoceras* sp. cf. *M. macrescens* (Buckman), *Oxycerites* cf. *yeovilensis* Roll., *Ebrayiceras* sp. (a calcareous mould perhaps from the beds situated just above); at Jebel Krechem el Kelb, *Procerites* sp. juv., *Parkinsonia* sp. juv., *Morphoceras* sp. juv. cf. *jactatum* (Buckman), *Ebrayiceras sulcatum* (Hehl *in* Zieten), *Asphinctites replictus* (Buckman), *Polysphinctites polysphinctus* Buckman, *Oxycerites* gr. *yeovilensis* Roll., *Nannolytoceras tripartitum* (Rasp.); at Châabet el Attaris: *Morphoceras* sp. juv., *M.* aff. *jactatum* (Buckman), *Cadomites* sp., *Oxycerites yeovilensis* Roll. , *O. seebachi* Wetzel.

— The compacted carbonates overlying the marls with pyritised ammonites (middle Nara, $U_{4.4}$) still contain the early Bathonian age fauna as at Krechem el Kelb: *Oraniceras hamyanense* Flamand, *Morphoceras egrediens* Wetzel, *Siemiradzkia* sp. (F10). This is perhaps the bed yielding the calcareous mould of *Ebrayiceras* found on the slope corresponding to the marls with pyritised fossils at Jebel Rheouis (see the section UC2 unconformity).

— This fauna at Kef el Khouadja was collected from two calcareous beds with phosphatised nodules and fossils below an iron ore identical with that of Oued Demet: *Oraniceras hamyanense* Flamand (juv.), *Morphoceras* sp. (cf. *M. macrescens* Buckman), *Ebrayiceras sulcatum* (Hehl *in* Zieten), *Procerites* sp. (F10).

Source : MNHN, Paris

— The iron ores spreading out from Kef el Khouadja (without fauna) to the north are not very fossiliferous: at Guefaïet, *Asphinctites patrulii* Hahn and *Procerites* gr. *tmetolobus* Buckman, at Loridga, *Oraniceras* cf. *hamyanense* Flamand.

So, except at Jebel Châabet el Attaris where ammonites from the filaments- and *Zoophycos*-rich limestones point to the base of early Bathonian, Zigzag Zone, Parvum Subzone (F9), faunas are homogeneous and nearly of the same age into the Zigzag Zone, Macrescens Subzone and Aurigera Zone pars (F10). The genus *Oraniceras* is frequent in the Moroccan Middle Atlas and on both sides of the Morocco-Algeria frontier where it is associated with European elements of these ages.

MIDDLE BATHONIAN ASSEMBLAGES

They are less frequent than lower Bathonian faunas, but well represented at Jebel Krechem el Kelb and Jebel Châabet el Attaris (F11) in the uppermost beds of the compacted carbonates below the unconformity (UC3). In the same position was discovered a single *Bullatimorphites (B.)* sp. juv.

— At Châabet el Attaris, *Hecticoceras (Prohecticoceras)* sp., *Cadomites (C.)* cf. *bremeri* Tseret. *Bullatimorphites (Sphaeroptychius) marginatus* (Ark.) and *Siemiradzkia* cf. *pseudorjasanensis* (Liss.) bring precise the age as late middle Bathonian Bremeri Zone.

— At Jebel Krechem el Kelb, the lower calcareous bed with nodules and pyritised fossils includes *Cadomites (C.) orbignyi* de Gross., the index species of the lower horizon of the Progracilis Zone. While, it contains also a Bremeri Zone assemblage: *Hecticoceras (Prohecticoceras) ochraceum* Elmi, *C. (Cadomites) bremeri* Tseret., *Bullatimorphites (B.)* sp., *Micromphalites* sp., *Choffatia (Subgrossouvria)* sp.

Above, the marly bed with phosphatised nodules has also yielded a Bremeri Zone fauna: *Cenoceras* sp., *Holcophylloceras* sp. juv., *Phylloceras plicatum* Neum., *Hecticoceras (Prohecticoceras) ochraceum* Elmi, *Oxycerites* sp., *C. (Cadomites) bremeri* Tseret., *B. (Bullatimorphites)* gr. *bullatimorphus* Buckman, *B. (Sphaeroptychius) marginatus* (Ark.), *Choffatia (Subgrossouvria)* sp., *Procerites* sp.

This assemblage also contains two forms known from the upper Bathonian, Retrocostatum Zone, Blanazense Subzone: *Hecticoceras (Prohecticoceras)* cf. *blanazense* Elmi and *H. (P.) crassum* Elmi, mixed together with the Bremeri Zone fauna.

— The only known elements of the early middle Bathonian (Progracilis Zone) were encountered at Jebel Krechem el Kelb and Jebel Loridga, and those of the late Bathonian Retrocostatum Zone, Blanazense Subzone at Krechem el Kelb. The Subcontractus and Morrisi middle Bathonian Zones and the upper Bathonian Histricoides Subzone as well as the late Bathonian Discus Zone were not identified.

PEYBERNES *et al.* (1995, p. 596, Fig. 1) mentioned a Discus Zone fauna at Jebel el Haouareb below the marls with pyritised fossils, which indicates us an assemblage of late early Callovian age. If this age can be corroborated, it would be one of the rare late Bathonian age faunas known on the Southern Tethyan margin.

LOWER AND MIDDLE CALLOVIAN ASSEMBLAGES

— The early Callovian is only present at Jebel el Haouareb, and elsewhere only the middle Callovian fauna was recognised. At Jebel Krechem el Kelb, a discontinuous level at the bottom of the upper Nara member has yielded: *Putealiceras arkelli* Zeiss, *Lunuloceras romani* (Lem.), *L.* gr. *paulowi* (de Tsyt.), *Sublunuloceras* aff. *nodosulcatum* (Lah.), *Lemoineiceras* sp., *Rehmannia (Loczyceras)* cf. *richei* (Flamand) from the middle Callovian Anceps Zone (F13).

— Lower and middle Callovian are represented by rare and badly preserved fauna only at Jebel el Haouareb. PEYBERNES *et al.* (1995) have attributed the first fauna with pyritised facies in the marls of the lower part of the interval to "Bt 5 (= late Bathonian, Discus Zone and Subzone) or to Ca 0 ? (= earliest Callovian, Macrocephalus Zone, Bullatus Subzone)". These ages are based on the presence of *Epistrenoceras* sp. and *Homoeoplanulites (H.)* gr. *furculus* (Neum.) from the alternation overlying the marls with pyritised fossils. In these alternations, we have collected *Phylloceras* sp., *Holcophylloceras* sp., *Sowerbyceras* sp. juv., *Macrocephalites* sp. juv., *Dolikephalites* gr. *gracilis* Spath, *Jeanneticeras* cf.

Source : MNHN, Paris

meridionale Elmi, *Choffatia* sp. juv., *Elatmites* sp., *Grossouvria* sp. This fauna (F12) belongs to the Gracilis Zone (late early Callovian).

If the attribution of the underlying levels to "Bathonien terminal, Retrocostatum zone or Discus" zone seems justified (see the section "Middle Bathonian assemblage"), the presence at this level of *Epistrenoceras* is a problem. J. THIERRY, author of these determinations (oral communication) has given three possibilities for this badly preserved fragment: *Garantiana* sp. (upper Bajocian), *Epistrenoceras* sp. (upper Bathonian), *Reineckeid* (Callovien). The second one (accepted *in* PEYBERNÈS *et al.*, 1995) is invalidated by the pyritised ammonite fauna. In fact, all the specimens are of small size but in excellent preservation and their generic determinations and age are beyond doubt.

The other lower Callovian fauna (Macrocephalitids ind. and *Macrocephalites* sp.) (F12) follow each other up to the limestones bar, that has yielded at its top: *Parapatoceras* sp. from lower to middle Callovian. Just 2.5 m above, *Orbignyiceras* sp. is certainly of middle Callovian age (F13) .

Upper Callovian Collotia and Peltoceras assemblages

These faunas are widely distributed both in the upper part of the limestones with filaments at Jebel el Haouareb and at the bottom of the upper member of the Nara Formation.

— At Jebel el Haouareb, the earliest bed of the alternations overlying the limestone bar has yielded: *Putealiceras* sp. cf. *P. rossiense* (Teiss.), *Collotia* sp., *Subgrossouvria* sp. (F14) from the upper Callovian Athleta Zone. The scarceness and the state of preservation of this fauna do not allow better accuracy.

— At Châabet el Attaris, a thin condensed ferruginous and nodular level (0.1 m), encrusting the surface of the "compacted carbonates" (late middle Bathonian, Bremeri Zone) contains faunas from the upper Callovian and Oxfordian. The lower, more calcareous part includes: *Holcophylloceras* gr. *mediterraneum* Neum., *Sowerbyceras* cf. *subtortisulcatum* Pomp., *Lytoceras* aff. *eudesianum* (d'Orb.), *Lunuloceras* aff. *pseudopunctatum* (Lah. *in* Jeannet), *Choffatia* sp. indet., *Collotia* sp., *Peltoceras (Metapeltoceras)* sp., *Peltoceras* cf. *diversiforme* (Waag. *in* Jeannet) (F14). This assemblage belongs to the Athleta Zone, lowermost upper Callovian. In spite of numerous ammonite sections (and belemnites) obvious on the outcrop, the "Athleta bed" of Jebel Krechem el Kelb has yielded a poor fauna difficult to extract: *Distichoceras* sp., *P. (Peltoceras)* sp., Perisphinctids indet. (F14).

Lower Oxfordian assemblages

From Kef el Hassine toward the south, the lower Oxfordian (F15) is well characterised in all the studied profiles at the base of the upper member of the Nara Formation, which has escaped dolomitisation. For the first time a fauna of this age has been recognised at Jebel Rheouis (SOUSSI, M'RABET & ENAY, 1991).

From Kef el Hassine to Jebel Rheouis

— At Kef el Hassine they are: *Holcophylloceras mediterraneum* (Neum.), *Taramelliceras pseudoculatum* (Bukow.), *Euaspidoceras* cf. *douvillei* Collot, *Perisphinctes (Otosphinctes)* sp., *Properisphinctes* gr. *bernensis* (de Lor. *in* Ark.) (F15).

— The upper part of the condensed level at Jebel Châabet el Attaris has yielded: *Phylloceras* sp., *Holcophylloceras* sp., *Campylites (C.) delmontanus helveticus* Jeannet, *Perisphinctes (Kranaosphinctes)* cf. *promiscuus* Bukow., *Euaspidoceras* cf. *knechti* Jeannet and a little above: *Lytoceras* cf. *eudesianum* (d'Orb.), *Phylloceras* gr. *plicatum* Neum (F15) .

— This fauna is richer and much diverse at Jebel Krechem el Kelb: ? *Cenoceras* sp., *Phylloceras* sp., *Ptychophylloceras* sp., *Campylites (Campylites) delmontanus* (Opp.), *C. (C.) taeniolatus* Jeann., *Taramelliceras* cf. *pseudoculatum* (Bukow.), *Prososphinctes* cf. *mazuricus* (Bukow.), *Perisphinctes (?Dichotomosphinctes)* cf. *laisinensis* (de Lor.), *Perisphinctes (?Arisphinctes)* cf. *gyrus* (Neum.), *Peltoceratoides* cf. and gr. *williamsoni* (Phill.) (F15).

Source : MNHN, Paris

— The recently discovered fossiliferous beds of Jebel Rheouis (SOUSSI *et al.*, 1991) has yielded badly preserved fossils at five levels: 1) *Peltoceratoides* sp.; 2) *Campylites* sp.; 3) *Sowerbyceras tortisulcatum* (d'Orb.), *Campylites (Campylites)* cf. *delmontanus* (Opp.), *C. (C.)* cf. *delmontanus helveticus* Jeann., *Passendorferia (Enayites) czentochovensis* (Siem.), *Euaspidoceras* gr. *williamsoni* (Phill.); 4) *Trimarginites* sp., *Perisphinctidae* ind., *Peltoceratoides* gr. *williamsoni* (Phill.); 5) *Properisphinctes* cf. *bernensis* (de Lor. *in* Arkell), and *Prososphinctes* cf. *mairei* (de Lor.), *Properisphinctes* cf. *bernensis* (de Lor. *in* Arkell), *Peltoceratoides* sp. (F15).

In summary, these assemblages which differ greatly in abundance, diversity and preservation, are in fact very homogeneous and belong to the lower Oxfordian, including forms of the Mariae and Cordatum Zones. Distinction of the subzones (to say nothing on the horizons) recognised in Submediterranean Europe is not actually possible. The absence of boreal cardioceratids and more curiously of tethyan groups like hecticoceratids obliges us to base the age determination on other groups. Such parallel zonations have been proposed or are now in use: (CARIOU *et al.*, 1997), based on *Taramelliceras* (TARKOWSKI, 1990), some Perisphinctidae (BROCHWICZ-LEWINSKI, 1981; MELENDEZ *et al.*, 1983) or Peltoceratidae and Aspidoceratidae (BONNOT, 1995).

The lower part of the Mariae Zone (Scarburgense Subzone) is not recognised and the zone is represented only by the Praecordatum Subzone. It is the same for the Cordatum Zone; its fauna points certainly to the Submediterranean equivalents of the Bukowskii and Costicardia Subzones: Claromontanus Zone of BROCHWICZ-LEWINSKI; Mirus Zone, Baccatum Subzone and Patturattensis Zone, Oculatum Subzone of TARKOWSKI. The upper Cordatum Subzone is not represented or only by its lower part.

Jebel el Haouareb

The first nodular bedded limestone ("ammonitico rosso facies") has yielded the same fauna of the early Oxfordian (F15).

— On the right bank of the wadi Souyah, 11 m thick, we found successively :

1) *Sowerbyceras* cf. *tortisulcatum* (d'Orb.), *Peltoceratoides* sp.; 2) *Passendorferia (Enayites)* cf. *birmensdorfensis* (Moesch *in* Broch.-Lew.), *Perisphinctes (Kranaosphinctes)* cf. *promiscuus* Bukow.; 3) *Euaspidoceras* sp.; 4) *Phylloceras* sp., *Campylites (Campylites) delmontanus* (Opp.), *Passendorferia (Enayites) czentochovensis* (Siem.); *Taramelliceras* aff. *T. argoviense* Jeann.; 6) *Campylites (Campylites) delmontanus helveticus* Jeann., *Lissoceratoides* sp.; 7) *Campylites (Campylites)* gr. *delmontanus* (Opp.), *Properisphinctes* sp.; 8) *Passendorferia (Enayites) czentochovensis* (Siem.); 9) *Taramelliceras argoviense* Jeann., *T. pseudoculatum* (Bukow.), *Prososphinctes* sp.; 10) *Phylloceras* sp., *Taramelliceras pseudoculatum* Bukow.; 11) *Prososphinctes sequeirosi* Broch.-Lew.; 12) *Perisphinctes (?Dichotomosphinctes)* cf. *episcopalis* de Lor., *Peltoceratoides* cf. *williamsoni constantii* (d'Orb.); 13) *Phylloceras* sp., *Holcophylloceras* sp., *Sowerbyceras tortisulcatum* (d'Orb.), *Passendorferia* sp.

— On the left bank, the upper four metres of the same sequence approximately equivalent to faunas 8 to 11 mentioned above contain: 8) Perisphinctidae ind., Aspidoceratidae ind.; 9) *Taramelliceras* cf. *baccatum* (Bukow.), *Properisphinctes* cf. *bernensis* (de Lor. *in* Arkell); 10) *Phylloceras* sp., *Taramelliceras argoviense* Jeann., *Properisphinctes* gr. *bernensis* (de Lor. *in* Arkell), *Perisphinctes (?Dichotomosphinctes)* cf. *laisinensis* de Lor., *Peltoceratoides* cf. *stephanovi* (Sap.); 11) *Taramelliceras* aff. *T. callicerum* (Opp.).

In spite of the more important thickness, the fauna of the nodular limestones leads to the same biostratigraphical conclusions as for the Cordatum Subzone. Several forms have been attributed or closely related to species with a poorly established range, often quoted from younger levels (*Taramelliceras argoviense*, *P. (?Dichotomosphinctes)* cf. *laisinensis*).

THE MIDDLE AND UPPER OXFORDIAN FAUNAS

The dolomitised limestones term of upper Nara Formation contain a poor macrofauna. The facies is unfavourable to their preservation and complete specimens are rare in good condition.

— Bad and undetermined perisphinctids, probably from the middle Oxfordian, have been found in

Source : MNHN, Paris

thick calcareous beds at Kef el Hassine and at Châabet el Attaris. The nodular levels at Jebel Krechem el Kelb are more or less rich with: *Coenoceras* sp., *Trimarginites arolicus* (Opp.) (m), *Protophites christoli* (Beaud.) (F16). The middle Oxfordian is attested at Jebel el Haouareb, according to the quotation by GHARBI (1989) of *P. christoli* (Beaud.) and *Gregoryceras riazi* (de Gross.).

— Some upper Oxfordian fauna (F17) have been collected at Jebel el Haouareb (300 m to the north of Oued Souyah) from the more calcareous intercalations of the upper Member of the Nara Formation. A first level has yielded: 1) *Orthosphinctes (Orthosphinctes)* sp.; 2) *Taramelliceras (Strebliticeras)* cf. *externnodosum* (Dorn); 3) *Orthosphinctes (Orthosphintes)*; higher, from a second outcrop we have collected: 4) *Aspidoceras circumspinosum* (Opp.); 5) *Taramelliceras* sp.; 6) *Laevaptychus* sp.; 7) *Trimarginites stenorhynchus* (Opp.); 8) *Taramelliceras* cf. *costatum* (Qu.); 9) Perisphinctidae ind. These isolated forms represent homogeneous assemblages close to those in the Bimammatum Zone.

AGE OF THE SEDIMENTARY BODIES AND ASSOCIATED UNCONFORMITIES

AGE OF THE SEDIMENTARY BODIES

Ages are constrained by new biostratigraphical data only for the upper part of the middle Nara member, from and above the second unconformity (UC 2). Uncertainties still exist on the ages of several sub-units of the series for which we use the ages established in the closest sections (Figs 3 and 4).

— *The peritidal carbonates* (lower Nara A, U1) and the bioclastic carbonates (lower Nara B, U2) are attributed to early Lower Jurassic up to the Carixian. The later is suggested by the presence of the ammonite *Metaderoceras* sp. collected 2 m below the top of U2 at Kef el Hassine (SOUSSI, ENAY *et al.*, 1991).

— *The alternation of limestones and marls* (middle Nara A, U3) includes early Toarcian age "black shales" ($U_{3.1}$) and middle Toarcian argillaceous limestones ($U_{3.2}$).

— *The ferruginous and/or phosphatised ooids limestones: "ironstones"* (middle Nara B, $U_{4.1}$) are distinguished by their fauna and ages.

In the south, from Kef el Hassine to Krechem el Kelb, the ferruginous and/or phosphatised ooids limestones are early Bajocian, ranging from Discites Zone (Kef el Hassine) to the Humphriesianum Zone (Krechem el Kelb). The same range is admitted at Châabet el Attaris where fauna are missing and the facies are poor in ferruginous or phosphatised ooids. Not all of the subzones of the recognised zones are represented and the sequence can be incomplete. So, at Kef el Hassine, a hard-ground with a ferruginous crust separates beds with *Sonninia* and *Emileia* (Discites and Laeviuscula Zones) from levels with *Chondroceras* and *Stephanoceras* (Humphriesianum Zone, mostly Romani Subzone).

The so- called ironstones, spreading out from Kef el Khouadja to the north, are restricted to the early Bathonian (Zigzag Zone, Macrescens Subzone at Kef el Khouadja and at Jebel Guefaïet; Aurigerus Zone at Demet). Thus, they are the lateral equivalent of the marls with pyritised fossils of Châabet el Attaris, Krechem el Kelb and Rheouis. On the other hand, the ironstone of the old mine of Jebel Loridga ranges up from late Aalenian (Concavum Zone) to early middle Bathonian (Progracilis Zone, Orbignyi Subzone) with the possibility of discontinuities and gaps particularly in the upper Bajocian and lower Bathonian, pars (see the section Age of the sedimentary bodies and associate unconformities).

— *The filaments- and* Zoophycos*-rich limestones* (middle Nara B, $U_{4.2}$) underlying the marls with pyritised fossils at Rheouis, Krechem el Kelb, Châabet el Attaris, ? Kef el Hassine and the ironstone at Kef el Khouadja, ? Demet, begin with the upper Bajocian at Kef el Hassine. This is the only outcrop where the upper part of the stage is recognised. Their upper part is of early Bathonian age (Zigzag Zone, Macrescens Subzone) at Kef el Khouadja. The same interval is admitted for Rheouis, Krechem el Kelb, Chaabet el Attaris and for the upper beds without fauna at Kef el Hassine.

— *The pyritised ammonites rich shales* (middle Nara B, $U_{4.3}$) are an excellent marker bed for the southern half of the NOSA from Rheouis to Châabet el Attaris, certainly also at Kef el Hassine where they are covered by scree. They occupy a constant level into the lower Bathonian: Zigzag Zone,

Source : MNHN, Paris

Macrescens Subzone. Towards the north, they laterally pass into the ironstone of Kef el Khouadja, Demet and Jebel Guefaïet.

— *The compacted carbonates* (middle Nara B, $U_{4.4}$) with the third unconformity (UC3) at the top are everywhere fossiliferous. The bottom still belongs to the lower Bathonian (Zigzag Zone, Macrescens Subzone and Aurigerus Zone) at Jebel Krechem el Kelb, where the sequence is the thickest (7 m). It is organised into several parasequences with marly or nodular intervals. At other places, the sequences are reduced and more calcareous (0.8 m at Rheouis; 0.7 m at Kef el Hassine; 1.5 m at Kef el Khouadja; 2 m at Chaabet el Attaris). The upper part is better dated from middle Bathonian, Bremeri Zone at Krechem el Kelb, Châabet el Attaris and Kef el Khouadja.

— *The dolomitised limestones of the upper Nara member* (upper Nara A, base of U5) locally begin with middle Callovian, Anceps Zone (at Krechem el Kelb), more widely within upper Callovian Athleta Zone, Collotiformis Subzone (Châabet el Attaris), and also in the whole study area within lower Oxfordian Mariae Zone, Praecordatum Subzone (Kef el Hassine, Rheouis). The upper Nara Member includes Oxfordian, Kimmeridgian and partly Tithonian, but without precise ages for the highest levels. At the top, the Sidi Khalif Formation, including Berriasian, is diachronous and begins earlier in the south (Rheouis, Bou Hedma) within the upper Tithonian (Microcanthum Zone), later (lower Berriasian, Euxinus Zone, Jacobi Subzone) at Jebel Sidi Kralif and Jebel Nara (BUSNARDO *et al.*, 1976; 1980; 1985; M'RABET, 1975, 1987).

— *The sequence of Jebel el Haouareb* is similar to these of the "Dorsale tunisienne" (Figs 3-5).

The limestones with filaments, here without *Zoophycos*, are dated upper Bathonian by PEYBERNÈS *et al.* (1995). They extend through lower and middle Callovian, and the highest beds are from upper Callovian (Athleta Zone).

The grey-green to wine-coloured nodular limestones ("ammonitico rosso" facies) underline a major lithological change during early Oxfordian time, Mariae Zone, Praecordatum Subzone), and range up into middle Oxfordian steeply invaded by secondary dolomitisation.

UNCONFORMITIES (FIG. 4)

Three unconformities have been clearly recognised within the middle Nara member. In several sections, ammonites below and above of these unconformities have allowed age correlations and the measurement of their relative duration through the biochronological reference scale.

UC1 UNCONFORMITY

UC1 falls between the bioclastic dolomites (U2) and the black shales facies (U3). This unconformity materialised by a submarine bored hard-ground is the less characterised one, because of the total lack of fauna within the bioclastic dolomites. Badly preserved fragments or moulds at the topmost of the bioclastic dolomites were determined *in situ* as *Microderoceras* sp. This unconformity underlines a stratigraphic hiatus which may correspond to a part of the Carixian and the Domerian *pro parte* (time average of 4 Ma, HAQ *et al.*, 1987). In fact, the last two metres of the bioclastic carbonates remain undated and thus could be Domerian *p.* in age.

UC2 UNCONFORMITY

UC2 passes through the middle Nara member and was unnoticed for a long time. It corresponds to a submarine erosional surface encrusted by thin phosphatic and/or ferruginous layer. The systematic collecting of fauna has allowed us to date UC2 in several places. The base of the unconformity and the sedimentary break are of middle Toarcian age (Bifrons Zone, Levisoni Subzone). The renewal of sedimentation occurred generally during the early Bajocian (Discites Zone) (Krechem el Kelb, Kef el Hassine). This unconformity marked a long hiatus varying from 4 to 12 Ma (HAQ *et al.*, 1987). At Jebel Loridga the deposition of ironstones began, exceptionally, in the late Aalenian Concavum Zone. During this time interval, locally (Kef el Hassine), encrusting layers or lenses developed in the late Toarcian.

Source : MNHN, Paris

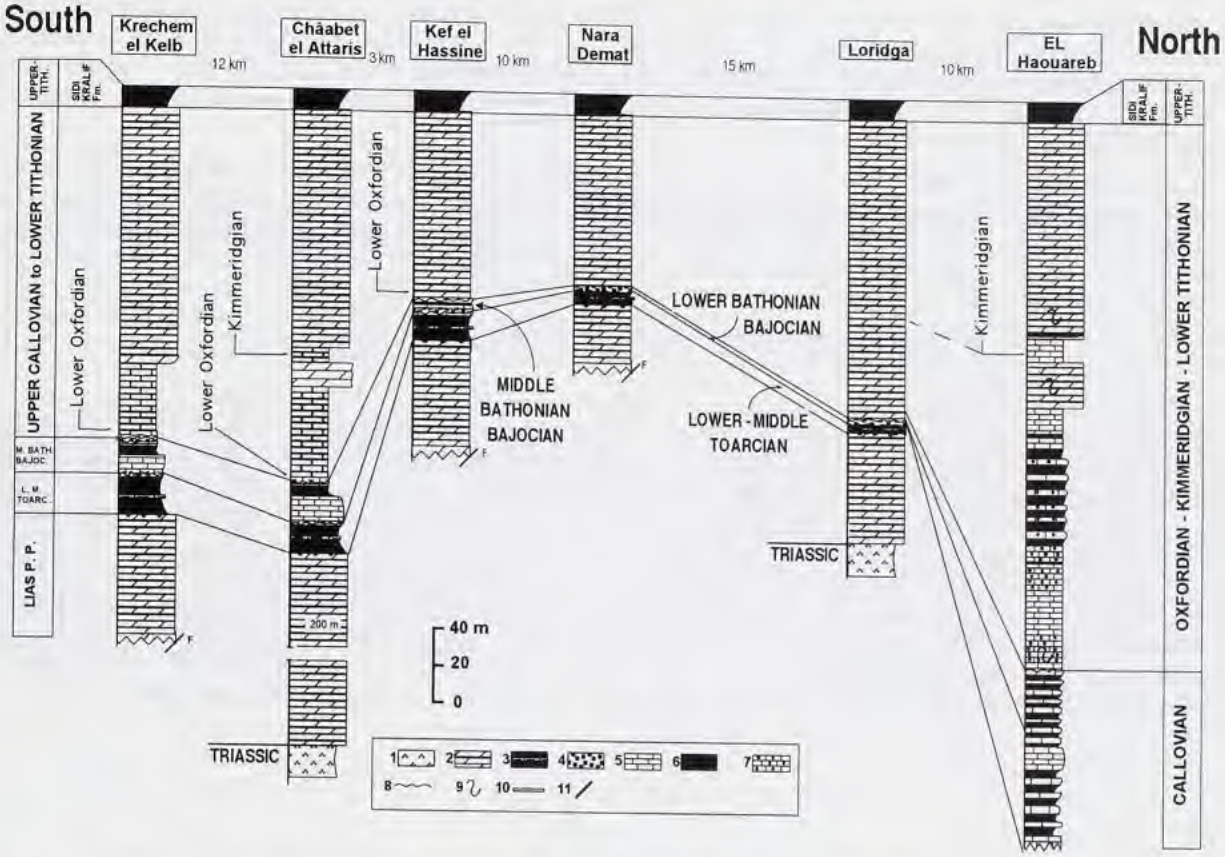

FIG. 5.— Lithostratigraphic correlation showing the thickness variation within the Jurassic series in the NOSA (Central Tunisia). **1**, Triassic gypsum; **2**, lower Liassic peritidal dolomites; **3**, Toarcian black shales; **4**, Bajocian-Bathonian ferruginous ooids or "ironstones"; **5**, Callovian-Oxfordian pelagic muddy-limestones; **6**, shales; **7**, Oxfordian calciturbidites; **8**, unconformities; **9**, slumps; **10**, hard ground; **11**, fault contact (F).

*FIG. 5.— Corrélations lithostratigraphiques montrant les variations des épaisseurs dans les séries jurassiques de l'Axe Nord-Sud (Tunisie centrale). **1**, gypses du Trias ; **2**, dolomies péritidales du Lias inférieur ; **3**, "black shales" du Toarcien ; **4**, oolithes ferrugineuses du Bajocien-Bathonien ; **5**, calcaires pélagiques du Callovien supérieur-Oxfordien ; **6**, argiles ; **7**, calciturbidites de l'Oxfordian ; **8**, discordances ; **9**, slumps ; **10**, surface durcie ; **11**, contact par faille (F).*

At Jebel Guefaïet, and probably at Demet also, the renewal of deposition began later (early Bathonian) if the marls and limestones situated below the ironstones are Toarcian. At Kef el Khouadja, UC2 was observed but has not been dated precisely. It is underlain by a clay layer with phosphatised grains resting over the limestones and marls of "Toarcian" type. Only about one metre of dolomitised limestone, beds with phosphatised ooids, scattered at the base, separate it from the bed with lower Bathonian fauna, below the ironstones. The numerous faults in the Rheouis area do not allow us to observe UC2: they also explain the differences between our observations and the sequence described by PEYBERNÈS *et al.* (1995), particularly the unit bounded by two faults and noted Bj3-Bj5. The existence of upper Bajocian beds (Bj3) agrees well with what is known elsewhere in the NOSA. The lower Bathonian marls with pyritised fossils discovered in 1988 (SOUSSI, ENAY *et al.*, 1991; SOUSSI, M'RABET & ENAY, 1991) are the marls noted Bt4 (upper Bathonian) below the "dolomies boudinées" which are overlain by D3 and the limestones with lower Oxfordian fauna (Ox2).

UC3 UNCONFORMITY

UC3, as UC2, corresponds to a submarine erosional surface encrusted by thin phosphatic and/or ferruginous layer locally rich in iron-rich ooids. It is lithologically and palaeontologically well

Source : MNHN, Paris

characterised only in the southern part of the NOSA. Beyond the Kef el Khouadja, toward the north (Guefaïet, Demet, Loridga), dolomitisation invaded the base of the upper member of Nara Formation down the contact with the ironstones (Figs 3-4). At Jebel Loridga, if a stratigraphic gap is present (see SOUSSI, ENAY *et al.*, 1991; PEYBERNÈS *et al.*, 1995) as wide as in the south, it is completely obscured by dolomitisation.

The latest deposits below the discontinuity are often condensed and locally (Krechem el Kelb) contain an earliest upper Bathonian fauna, but nearly everywhere else their age is latest middle Bathonian (Bremeri Zone) at Krechem el Kelb, Châabet el Attaris, Kef el Khouadja. We have used the same age gap for UC3 at Kef el Hassine and Jebel Rheouis but without any evidence. PEYBERNÈS *et al.* (1995) mentioned (without explanation) a fauna from the base of sequence Bt4 at Jebel Rheouis. This introduces a discontinuity essentially of middle Bathonian age (Bt1 to Bt3). This was not confirmed by our observations, in particular with the position of marls with pyritised fossils of early Bathonian, which are, for us, those designated Bt4.

The renewal of sedimentation began locally at Krechem el Kelb with a lenticular deposit of middle Callovian (Anceps zone). It developed more clearly during the late Callovian (Athleta Zone, Collotiformis Subzone) at Krechem el Kelb and Châabet el Attaris, but probably still with interruptions. The Athleta zone is unknown at Jebel Rheouis and Kef el Hassine where the earliest fauna is early Oxfordian. Moreover we do not know any fauna of the Mariae Zone, Scarburgense Subzone of the lowest Oxfordian. The renewal of sedimentation became widespread during early Oxfordian, (Mariae Zone, Praecordatum Subzone) (= Ox2 *in* PEYBERNÈS *et al.*, 1995). The nodular limestones were deposited at Jebel el Haouareb at this time (SOUSSI, ENAY *et al.*, 1991). Thus, this unconformity is accompanied by a gap of a duration which varies from 4 to 9 million years (HAQ *et al.*, 1987) which covers a relative time from Retrocostatum Zone to Lamberti Zone and also the lower part of Mariae Zone.

OTHER UNCONFORMITIES

Despite the lack of a significant faunal argument, other unconformities can be considered. In the ironstones, particularly at Jebel Loridga, several diastems made this hypothesis credible. SOUSSI, ENAY *et al.* (1991) had already considered it for the most important diastem that separates the lower part with fauna of the upper Aalenian (Concavum Zone) - lower Bajocian (Discites Zone) (Figs 3 and 4) from higher levels with lower Bathonian (Aurigerus Zone) and lowest middle Bathonian (Progracilis Zone, Orbignyi Subzone). PEYBERNÈS *et al.* (1995) went further in adding a discontinuity with a gap of a part of the middle Bathonian between lower Bathonian (SD Bt5 and Bt1 possibly) and the highest middle Bathonian (SD Bt3).

At Châabet el Attaris, the discontinuity with a lower and middle Bathonian gap suggested by PEYBERNÈS *et al.* (1995) is not justified. In fact, the lower Bathonian (Aurigerus Zone) is well characterised by fauna in the filaments and *Zoophycos*-rich limestones, and in the overlying marls with pyritised fossils. Moreover, below the beds dated from the Bremeri Zone, two metres of compacted carbonates ($U_{4.4}$) representing the rest of the middle Bathonian do exist.

In the sequence of "Dorsale tunisienne" type, at Jebel el Haouareb, no fauna was collected in the alternation of limestones and marls (7.5 m) between the latest upper Callovian fauna, Athleta Zone and the earliest lower Oxfordian fauna of the Mariae Zone. Here, a discontinuity with a gap is very probable, underlined by an important facies change. This was recognised by PEYBERNÈS *et al.* (1995), but we limit it to the Lamberti Zone and the lower part of the Mariae Zone (SD Ca5-Ox0 for Ca4-Ox1). We do not consider that a gap exists within the lower Callovian Gracilis Zone developed on 30 to 40 m, from the marls dated by a pyritised fauna (base of SD Bt5) up to the base (or the top ?) of the first calcareous bar of SD Ca2. It will be noticed that in the PEYBERNÈS *et al.* figure 1, SD "Cal ?" is wrongly situated. If their figure 2 is correct, its place would be at the top of PHN of Ca0 ? or Bt5 that we have dated as lower Callovian, Gracilis Zone.

Source : MNHN, Paris

DEPOSITIONAL ENVIRONMENTS

The vertical facies succession described here suggests that Jurassic sedimentation occurred in Central Tunisia in a full marine environment (Fig. 2).

HETTANGIAN-SINEMURIAN PERITIDAL CARBONATE PLATFORM

The sedimentary and early diagenitic characteristics recorded within the lower Liassic carbonates suggest a very shallow marine and restricted platform environment with tidal flats. The latter are characterised especially by algal (microbial) stromatolites and locally by the formation of low energy ooids and pisoids. The various terms of the peritidal cycles indicate relative fluctuation in the environments of deposition varying between shallow sub-tidal to supra-tidal (with aerial exposures) (Fig.Ê2). The various peritidal cycles have a total thickness of more than 150 m suggesting an equilibrium between subsidence and sedimentation rates. Although the depositional environments were very shallow, they appear clearly as aggradational to retrogradational over the underlying continental to paralic Triassic siltstones and evaporites (BUROLLET, 1956; SOUSSI, ABBES *et al.*, 1996). These inter-supratidal or tidal environments extend to the Atlasic zone to the north and to the Chott Basin to the south (more than 400 km). The lower Liassic sediments of Tunisia could be compared to the Holocene deposits described by SHINN *et al.* (1969) and to the Late Triassic "Dolomie Principale" in the Southern Alps (BOSELLINI & HARDIE, 1985). Relative sea level changes on a 10^3-10^5 years scale (Milankovitch-type eustasy cycles) have been evoked to explain the formation of this peritidal type cycles (GINSBURG, 1975; HARDIE *et al.*, 1986).

CARIXIAN OPEN MARINE CARBONATE PLATFORM

With the Carixian bioclastic limestones, especially those containing belemnites and ammonites, the depositional environment became slightly deeper. This deepening, caused by an important and regionally widespread marine transgression, was accompanied by a drastic slowing of sedimentation as indicated by the submarine hard-ground identified at the top of U2 over the whole study area. This transgression had been preceded, at least since the upper Sinemurian-Carixian, by the dislocation of the wide and homogeneous shallow marine platform. This first important tectonic event has been well documented both to the north within the Tunisian Dorsale (BONNEFOUS, 1972; ALOUANI, 1991; SOUSSI, DAVAUD *et al.*, 1993) and to the south within the Chott Basin (POGACSAS *et al.*, 1998; HLAIEM, 1998). The fragmentation of the "initial" platform has led to a new structural setting comprising tilted blocks and horsts and relatively subsident grabens (Fig. 7).

TOARCIAN DROWNED PLATFORM AND ASSOCIATED ANOXIC SUB-BASINS

The carbonate sedimentation of the lower Liassic was replaced in the Toarcian by shaly and laminated limestone deposition containing both pelagic and benthic faunas. The latter suggests a marine deepening in relation to a new widespread transgressive episode.

The local presence of high organic matter content within these facies, their laminated character, the absence of burrows, the presence of pyrite and the excellent preservation of fish bones indicate oxygen deficiency and signify anaerobic bottom water conditions, in association with sulphate-reducing bacterial activity. In addition, the lateral variations in thickness indicate differential and rather slow subsidence (Fig. 5). The Châabet el Attaris and the northern part of Krechem el Kelb formed a relatively subsident graben; while the Kef el Hassine-Loridga zone constituted a high and resistant horst block.

Source : MNHN, Paris

In summary, during the early Toarcian the environment of deposition corresponded to an irregular outer shelf including horsts and grabens or half grabens, which locally acted as narrow anoxic basins. On the other hand, the presence of the "black shales" confirms that the Toarcian Oceanic Anoxic Event (JENKYNS, 1985; BAUDIN *et al.*, 1988) had a worldwide extension and was recorded in numerous basins not only of the Tethyan Northern Margin but also of the Tethyan Southern Margin (SOUSSI *et al.*, 1990).

These anoxic conditions stopped during the middle Toarcian. The depositional facies became more clayey and rich in detrital quartz, abundant bioturbations and benthic fauna, thus suggesting oxic conditions in relation with the initiation of a regressive and prograding carbonate facies.

BAJOCIAN-BATHONIAN STARVED CARBONATE SHELF

During Bajocian-Bathonian time, Central Tunisia recorded the maximum variation in sediment facies and thickness and two distinct depositional environments existed simultaneously. The Bajocian ironstone deposits, following the second major stratigraphic gap (UC2), indicate a renewal of sedimentation during a transgressive phase. The origin of the Jurassic "ironstones" of NW Europe and their depositional environments have been extensively discussed (BROCHERT, 1960; HALLAM, 1975; HARDER, 1989; VAN HOUTEN, 1985; TEYSSEN, 1984).

In Central Tunisia, the lack of any evidence of emersion, the presence of mixed benthic and nektonic fauna, associated with low angle cross-bedding suggest a submarine environment characterised by high energy conditions in relation to submarine current activities. These ironstones are syngenetic in origin and reflect particular physico-chemical conditions with abnormal enrichment in iron and phosphate (SOUSSI & M'RABET, 1991).

The regional thickness and facies distribution of these "ironstones", in addition to the presence of frequent hard grounds with borings, phosphatic and ferruginous encrusting laminations, clearly demonstrate that these facies have been formed on upthrown and weakly subsiding blocks (horsts). Within the latter, the sedimentation rate was very slow, varying from 0.1 to 0.25 m per million years compared to the Bajocian-Bathonian facies which are 200 m thick (in the range of 14 m per million years) to the north within the Tunisian Trough (Bou Kornine of Hammam Lif) or in the south within the Chott Basin (BONNEFOUS, 1972; MZOUGHI *et al.*, 1992).

The adjacent and overlying Bajocian-Bathonian facies represented by filaments and *Zoophycos*-rich carbonates correspond to hemipelagic facies. During Bathonian sedimentation, detrital clay supply became more important as suggested by the increase in kaolinite. During the middle Bathonian, platform carbonate sedimentation characterised the whole area, except the palaeohigh of el Guefaïet and Loridga where ferruginous ooids continued to develop.

CALLOVIAN-TITHONIAN DEEP CARBONATE SHELF TO BASIN TRANSITION

The Callovian-Oxfordian muddy-limestones (the lower part of U5) which overlie the third major unconformity (UC3), inducing a clear angular discordance (also identified on seismic data within the Chott area), reflect a new transgressive sedimentation pattern. The depositional environments became deeper and apparently homogenous; this corresponds to a calm and deep marine carbonate platform replaced to the north by a marginal slope (el Haoureb) with mostly debris flow deposits initiated by syn-sedimentary tectonic activity.

The uppermost Oxfordian limestones become rich in benthic fauna and locally in high energy calcareous ooids, which indicate a regional shallowing-up of the depositional environment.

The upper Oxfordian temporary regression was followed by a new deepening phase, which occurred from the early Kimmeridgian. This is attested by the development of muddy limestones rich in pelagic fauna such as crinoids (*Saccocoma*), radiolarians and calpionnelids during the lower Tithonian.

Source : MNHN, Paris

PALAEOGEOGRAPHIC FRAMEWORK AND SEDIMENTATION CONTROLS

Liassic shallow marine carbonate sedimentation was replaced during the Middle-Upper Jurassic by various types of lithofacies deposited in distinct and quite different palaeoenvironments (anoxic environment, shelf and outer shelf...). In addition, the sedimentary record includes major submarine unconformities accompanied by hiatuses recorded over considerable extents. Vertical and lateral changes of thickness and facies suggest the presence of two main, but quite different, palaeogeographic domains in the studied area. A resistant block extends from Rheouis to Loridga to the south, relayed to the north by a subsident basin (el Haouareb graben). The relatively low modification of sedimentation coinciding with faunal changes between the major unconformities, in addition to the regional changes in thickness, suggests that sedimentation has been controlled both by global eustatic fluctuations and local tectonic activity.

TECTONIC CONTROL (FIG. 6)

The variations of sediment thickness and of depositional environments, observed within the upper Liassic and Middle Jurassic deposits (Fig. 5), suggest a major modification in the palaeotopography. The latter became irregular and unequally subsident. In fact, the relatively homogeneous and widespread Liassic shallow marine platform had been dislocated at least since the Lotharingian into an irregular and

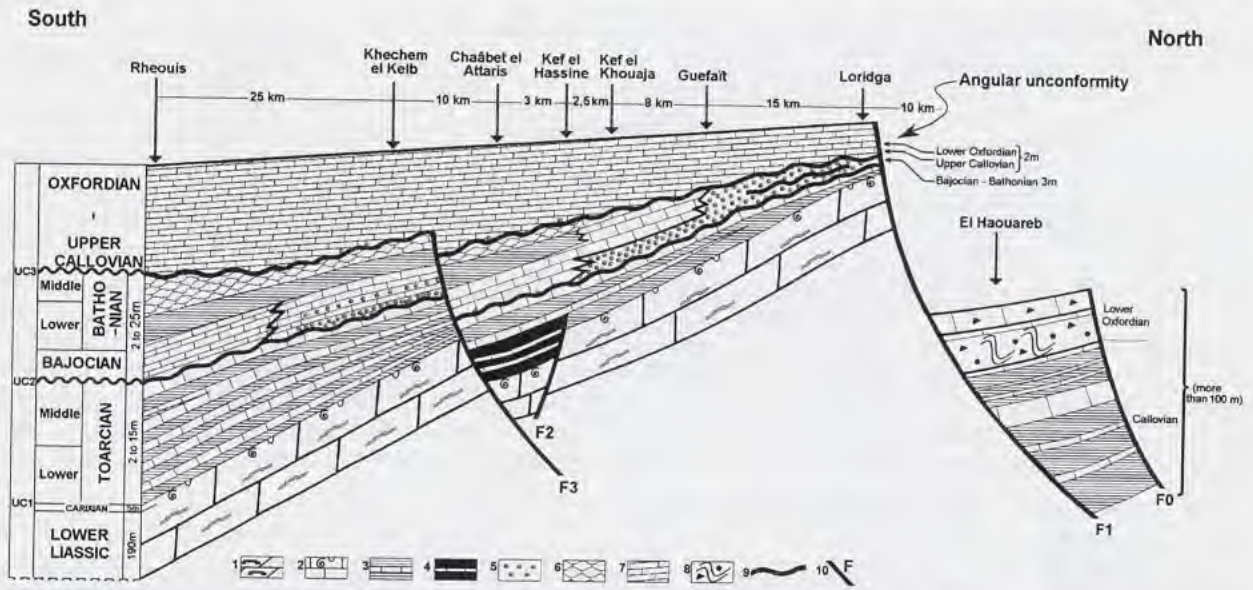

FIG. 6.— Interpretative diagram showing relationships between the Jurassic facies and the major tectonic events in the NOSA, Central Tunisia. **1**, Liassic shallow marine platform dolomites; **2**, Carixian condensed section; **3**, Toarcian marl and limestone alternations, **4**, Toarcian black shales; **5**, Bajocian-Bathonian ferruginous ooids; **6**, middle Bathonian filament-rich compacted carbonates; **7**, upper Callovian pelagic mud-limestones; **8**, early Oxfordian calciturbidites with slump; **9**, major unconformities; **F0**, M'Rhila-Kairouan fault; **F1**, Touila fault (approximately E-W trending), **F2**, Châabet el Attaris fault; **F3**, South Krechem el Kelb fault (branch of the approximately E-W Kasserine-Chorbane fault). The thickness are not proportional from south to north.

*FIG. 6.— Diagramme interprétatif montrant la relation entre les faciès du Jurassique et la structuration en blocs basculés dans le NOSA (Tunisie Centrale). **1**, dolomies de plate-forme très peu profonde du Lias ; **2**, sédiments condensés du Carixien ; **3**, alternances marno-calcaires du Toarcien ; **4**, black shales du Toarcien ; **5**, oolithes ferrugineuses du Bajocien-Bathonien ; **6**, carbonates compactés à filament du Bathonien moyen ; **7**, calcaires pélagiques du Callovien supérieur ; **8**, calciturbidites avec slumps de l'Oxfordien inférieur ; **9**, discordances majeures ; **F0**, faille de M'Rhila-Kairouan ; **F1**, faille de Touila (approximativement E-W) ; **F2**, faille de Châabet el Attaris ; **F3**, faille de Krechem el Kelb Sud (branche de la faille de Kasserine-Chorbane de direction approximative E-W). Les épaisseurs ne sont pas proportionnelles du sud au nord.*

Source : MNHN, Paris

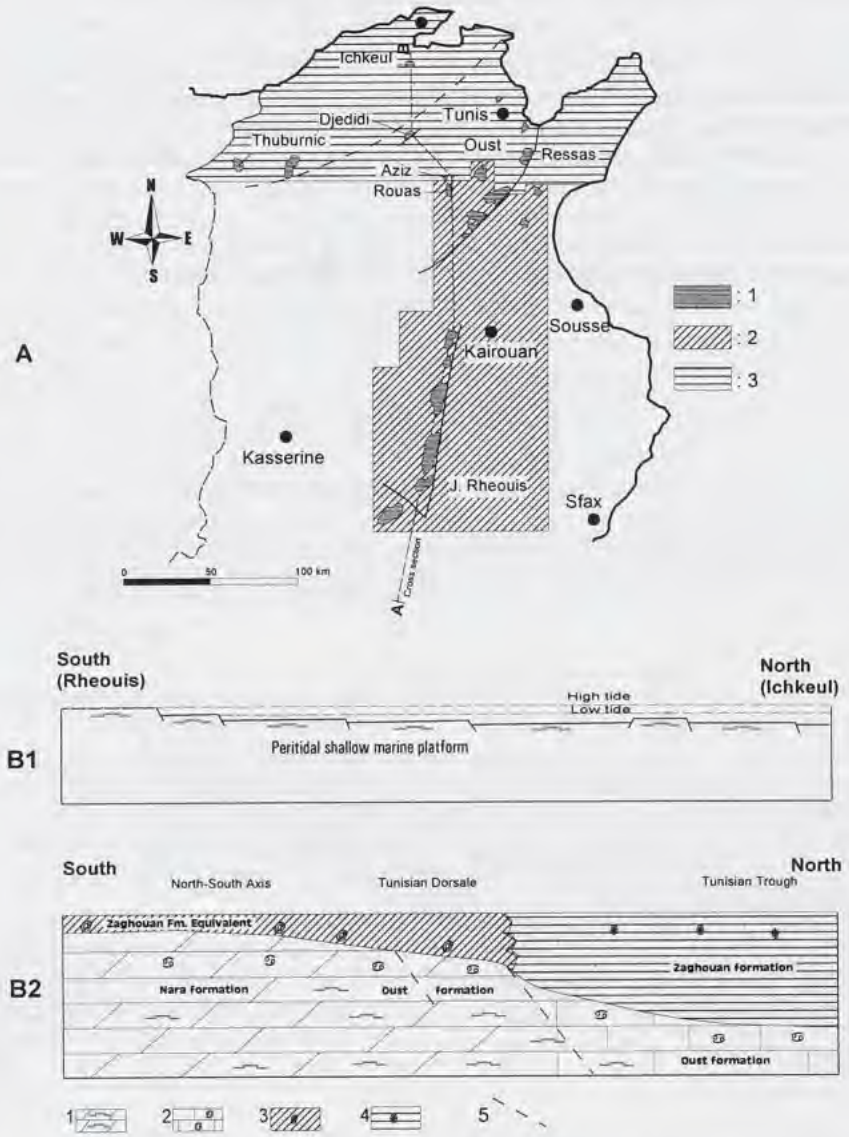

FIG. 7.— Simenurian-Carixian palaeogeography; A: The geographic distribution of the upper Sinemurian-Carixian facies. **1**, Jurassic outcrops; **2**, condensed facies; **3**, thick deep marine carbonates. B1: simplified diagram showing the Hettangian-Sinemurian palaeogeographic setting dominated by a wide peritidal shallow marine carbonate platform. B2: interpretative diagram illustrating the upper Sinemurian-Carixian facies variation. This pattern is closely related to the dislocation of the initial platform during the Liassic rifting. **1**, peritidal carbonates (Lower Nara and Oust formations); **2**, upper Sinemurian bioclastic carbonates; **3**, condensed sedimentation rich in ammonites, belemnites and glauconite; **4**, pelagic cherty muddy-limestones rich in radiolaria and schizosphers (Zaghouan formation); **5**, major faults.

*FIG. 7.— Paléogéographie du Sinémurien - Carixien ; A : distribution géographique des faciès du Sinémurien supérieur-Carixien. **1**, affleurements jurassiques ; **2**, faciès condensés ; **3**, série épaisse de calcaires profonds. B1 : diagramme simplifié montrant les différents domaines paléogéographiques durant l'intervalle Hettangien-Sinémurien, dominé par une vaste plate-forme carbonatée très peu profonde ; B2 : diagramme interprétatif montrant les variations de faciès de l'intervalle Sinémurien supérieur-Carixien. Cette évolution est étroitement associée à la dislocation de la plate-forme initiale lors du rifting du Lias inférieur. **1**, carbonates péritidaux (formations: Nara inférieure et Oust) ; **2**, carbonates bioclastiques du Sinémurien supérieur ; **3**, sédimentation condensée riche en ammonites, bélemnites et glauconite ; **4**, calcaires pélagiques à silex, riches en radiolaires et schizosphères (formation Zaghouan) ; **5**, failles majeures.*

Source : MNHN, Paris

relatively deep shelf composed of blocks tilted towards the south. This new structural pattern includes three depressions or half grabens (el Haouareb, Châabet el Attaris and Rheouis) separated by relatively resistant highs or horsts (Jebel Krechem el Kelb towards the south and Kef el Hassine-Nara Loridga block towards the north) especially during Bajocian time. The differentiation of these tilted blocks is related to E-W or near E-W synsedimentary Jurassic faults. In this connection, these E-W faults along the NOSA especially at the latitude of the El Gamgouma and Krechem el Kelb areas could correspond to the Touila E-W fault (ABBES, 1983; OUALI, 1984) and one of the branches of the Faïd faults respectively. The first could be the lateral extension towards the east of the M'rhilla fault or one of its branches while the second may be related to the nearly E-W Kasserine fault (BEN AYED, 1986). In addition local N-S synsedimentary antithetic faults are present.

The Kef el Hassine-Loridga horst is bordered towards the north by the E-W Touila fault which had been active since the Early Jurassic. This Touila fault is bordered to the north by an important down-faulted block or graben where sedimentation has been more continuous and thick during both Jurassic and Cretaceous (ABBES, 1983; OUALI, 1984). During the Jurassic the control of this fault is demonstrated by the evolution of Callovian-Oxfordian thickness and facies. The latter, reduced to the south to a few metres of mud limestones, is represented towards the north (El Haoureb area) by a thick deep marine sequence (more than 200 m) comprising debris flow deposits with slumps (Fig. 6).

Within this tectonic framework, the Châabet el Attaris graben has acted during the lower Toarcian as a narrow anoxic basin (SOUSSI *et al.*, 1990), while the Kef el Hassine-el Guefaïet and Loridga blocks corresponded to a condensed sedimentation especially during the Toarcian-Bathonian time interval. This is indicated first by the progressive thinning to the north of the several sedimentary units, secondly by the development of ironstones especially to the north and the superposition of these onto the Toarcian at el Guefaïet area.

The lack of ferruginous ooids at Krechem el Kelb during the Bathonian suggests a local readjustment of the structural system with reactivation of the Oued Abiod fault (F2) and the drowning of Krechem El Kelb block (Fig. 6).

The Jurassic tectonic activity is well illustrated at a regional scale. In fact, to the north, both in the Tunisian Dorsale and the Tunisian Trough, at least three major tectonic phases have been recognised. The first major phase occurred during the middle Liassic (upper Sinemurian-Carixian) and led to the dislocation of the initial shallow marine platform and the development of condensed horizons on the highs of the tilted blocks. Within the grabens were deposited a thick pelagic cherty muddy-limestones rich in radiolarian and schizospheres (Zaghouan Formation) (Fig. 7), (BONNEFOUS, 1972; RAKUS & BIELY, 1970; TURKI, 1988; RAÏS *et al.*, 1991; ALOUANI, 1991; SOUSSI, BUSSON *et al.*, 1993). The second tectonic event occurred during Bajocian-Bathonian time and is well recorded in Jebel Bou Garnine of Hammam Lif graben by the presence within the Bathonian deposits of two main conglomeratic horizons including resedimented Liassic dolomitic and cherty carbonates (BONNEFOUS, 1972; COSSEY & EHRLICH, 1981; TURKI, 1988). The third event is demonstrated by the resedimentation of Callovian Bent Saïdane limestones and shales within the early Oxfordian "ammonitico rosso facies".

To the west and the south of Central Tunisia, Jurassic sedimentation has also been strongly influenced by the tectonic framework characterised by E-W, N-S and NW-SE fault systems (BEN AYED & KHESSIBI, 1983; BEDIR, 1995; BOUAZIZ *et al.*, 1998). To the south of Central Tunisia, two main subsident basins have been formed in relation to the Late Palaeozoic-Early Mesozoic rifting. The Chott basin where Jurassic is up to 2000 m thick (BONNEFOUS, 1972; MZOUGHI *et al.*, 1992), and the Tataouine Remada graben also characterised by a thick Jurassic sequence (BUSSON, 1967; KAMOUN, 1988; BEN ISMAIL, 1994). These basins are separated by ridges bounded by major normal faults (BOUAZIZ *et al.*, 1998). The Medenine platform or "Tebaga high" is bordered towards the north by the E-W Tebaga fault and to the south by the E-W Zmilet el Ghar fault (Fig. 8). The Tataouine Remada graben is separated from the uplifted zone of Jebel Nefzaoua in Libya by the E-W Azizia fault (ASSERTO & BENELI, 1971; EL ZOUKI, 1980).

Some of the horsts bordered by E-W faults acted as a structural barrier blocking the terrigenous progradation phase during the Bathonian or as a platform edge favourable to the installation of sponge-coral bioherms during the Callovian (BEN ISMAIL & M'RABET, 1990).

In summary, the palaeogeographic framework of Tunisia clearly corresponds to a system of tilted blocks initiated at least since the Permian in Southern Tunisia and during the Pliensbachian in Central

Source : MNHN, Paris

and Northern Tunisia (Figs 8 and 9). Such geodynamic evolution is comparable to that outlined in Algeria (BUREAU, 1986), Morocco (WARME, 1988) and in the Western Alps (WILDI, 1983; LEMOINE, 1985; BOUILLIN, 1986) and it results from Late Palaeozoic-Early Mesozoic rifting and associated distentional drifting of the North African Tethyan margin.

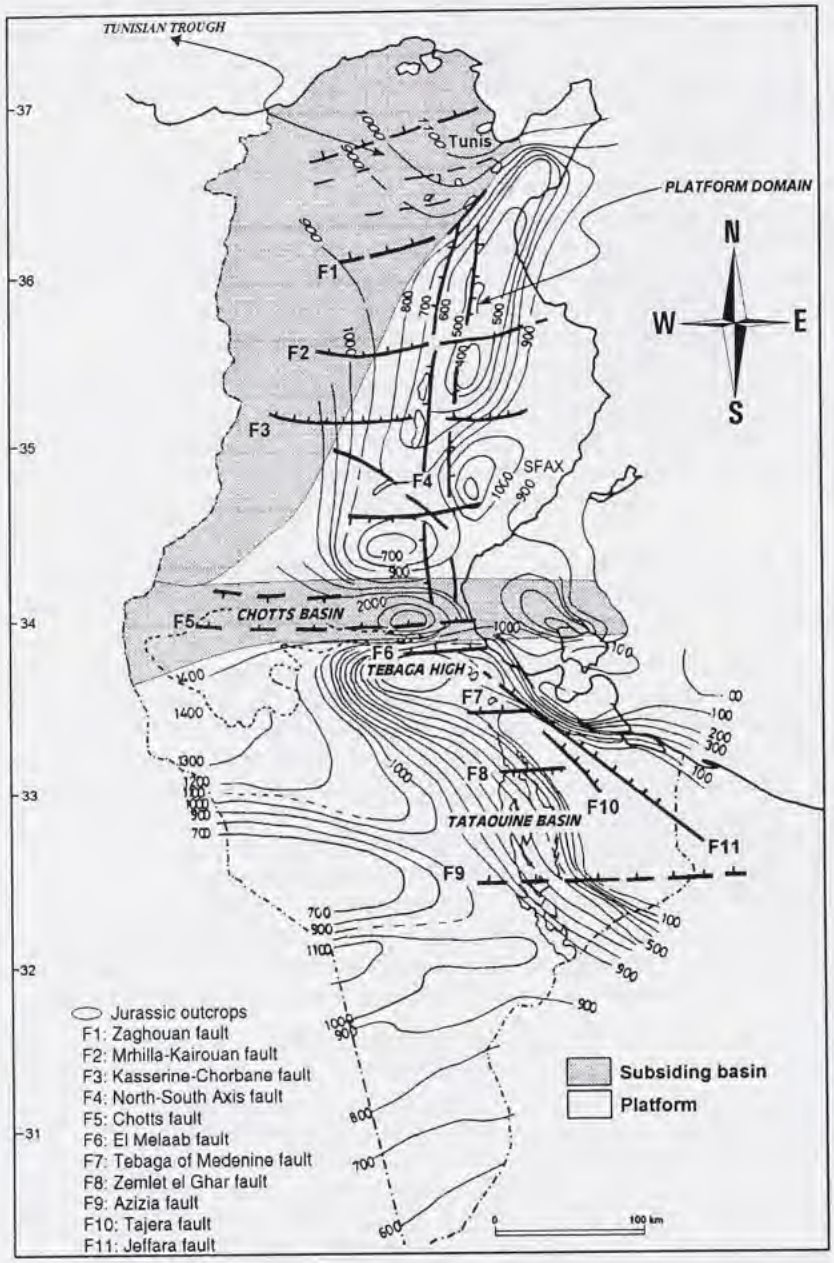

FIG. 8.— Simplified structural sketch map showing the main probable faults controlling the Jurassic palaeogeography and thickness (isopachs at 100 m intervals) in Tunisia (after BEN FERJANI *et al.*, 1990, modified).

FIG. 8.— Carte structurale simplifiée montrant les failles ayant probablement controlé la paléogéographie et les épaisseurs (isopaques tous les 100 m) du Jurassique en Tunisie (d'après BEN FERJANI et al., *1990, modifiée).*

EUSTATIC CONTROL

In addition to tectonic control, Jurassic sedimentation has been strongly influenced by sea level changes. The detailed facies analyses and accurate biostratigraphic control have led us to define with more precision the major transgressive and regressive episodes and their separating unconformities.

Source : MNHN, Paris

The major transgressive episodes which are undoubtedly linked to sea level rises occurred during late Sinemurian-Carixian, early Toarcian, early Bajocian, late Callovian and early Kimmeridgian (Fig. 2). Their corresponding deepening phases have been recorded in different ways including condensed sections, fine-grained pelagic limestones or black shales. These transgressive episodes were attested by the renewal of sedimentation and facies changes, occurring just after the starvation phases (non-deposition or submarine erosion materialised by the three major discontinuities). In Southern Tunisia, these different phases have been established not only by deepening but also by coastal onlap such as the middle Liassic Zmilet Haber and the Bajocian Krachoua carbonates. The Callovian transgression is represented in the Tebaga of Medenine mountain by a transgressive contact between the Permian and the Jurassic series.

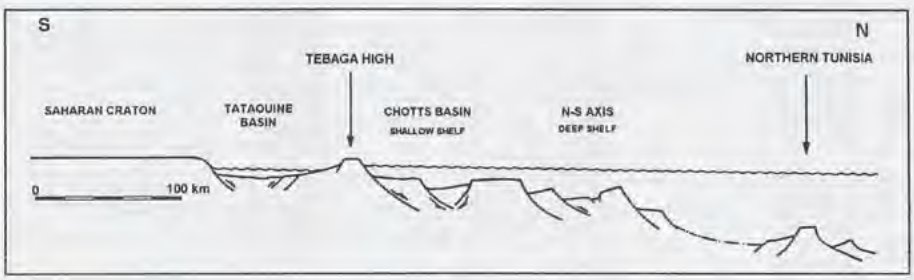

FIG. 9.— Palinspastic reconstruction of the North African margin in Tunisia along a north-south cross section during middle-late Liassic. The diagram shows the main palaeogeographic domains.

FIG. 9.— Reconstruction palinspastique de la marge Nord Africaine en Tunisie durant le Lias moyen et supérieur selon un transect nord-sud. Ce diagramme montre les principaux domaines paléogéographiques.

A number of significant regressive episodes can be also recognised. The first episode started during the middle Toarcian and continued through the late Toarcian and probably the whole Aalenian. The second started during early Bathonian and attained its maximum during late Bathonian-early Callovian. These two regressive phases were characterised by the installation of mixed (marly-calcareous) sedimentation with supply of clastics (quartz and detrital clay). The development of shallow marine carbonates particularly those rich in ooids, during the late Oxfordian indicate a shallowing-up phase of the environment of deposition in relation to a regressive episode. It is important to note that the absence of the lower and middle Callovian within the specific NOSA series could be linked to tectonic control rather than eustatic fall (see discussion).

REGIONAL CORRELATION (Fig. 10)

Before comparing the Jurassic sedimentary record of Central Tunisia to global sedimentary cycles and associated events, it is appropriate to attempt correlations with the Jurassic series of Northern and Southern Tunisia. Taking into account biostratigraphic and sedimentologic data, correlations led to the recognition of regional transgressive and regressive phases in Northern, Central and Southern Tunisia.

TRANSGRESSIVE PHASES

In Northern Tunisia (the Dorsale and adjacent areas), the upper Sinemurian-Carixian transgressive episode is recorded within the transitional series from the shallow marine peritidal limestones (Oust Formation) to the bioclastic and condensed section or their lateral equivalent facies represented by cherty muddy-limestones of the Zaghouan Formation (RAKUS & BIELY, 1970; BONNEFOUS, 1972; FAURÉ & PEYBERNÈS, 1986; SOUSSI, BUSSON *et al.*, 1993). As shown in the figure 10, the lower Nara (U1) and Oust Formation are similar and correspond to peritidal deposits. Their uppermost parts are also similar and represented by open marine carbonates particularly rich in ammonites and belemnites.

In Southern Tunisia, the sedimentary response of the first Jurassic transgressive episode was recorded within the Pliensbachian Zmilet Haber oolitic limestones (B Horizon for petroleum geologists). The latter constitutes a major onlap and could be, at least in part, the equivalent of the uppermost Carixian and ammonite-rich carbonates along the NOSA and the Dorsale zone.

Source : MNHN, Paris

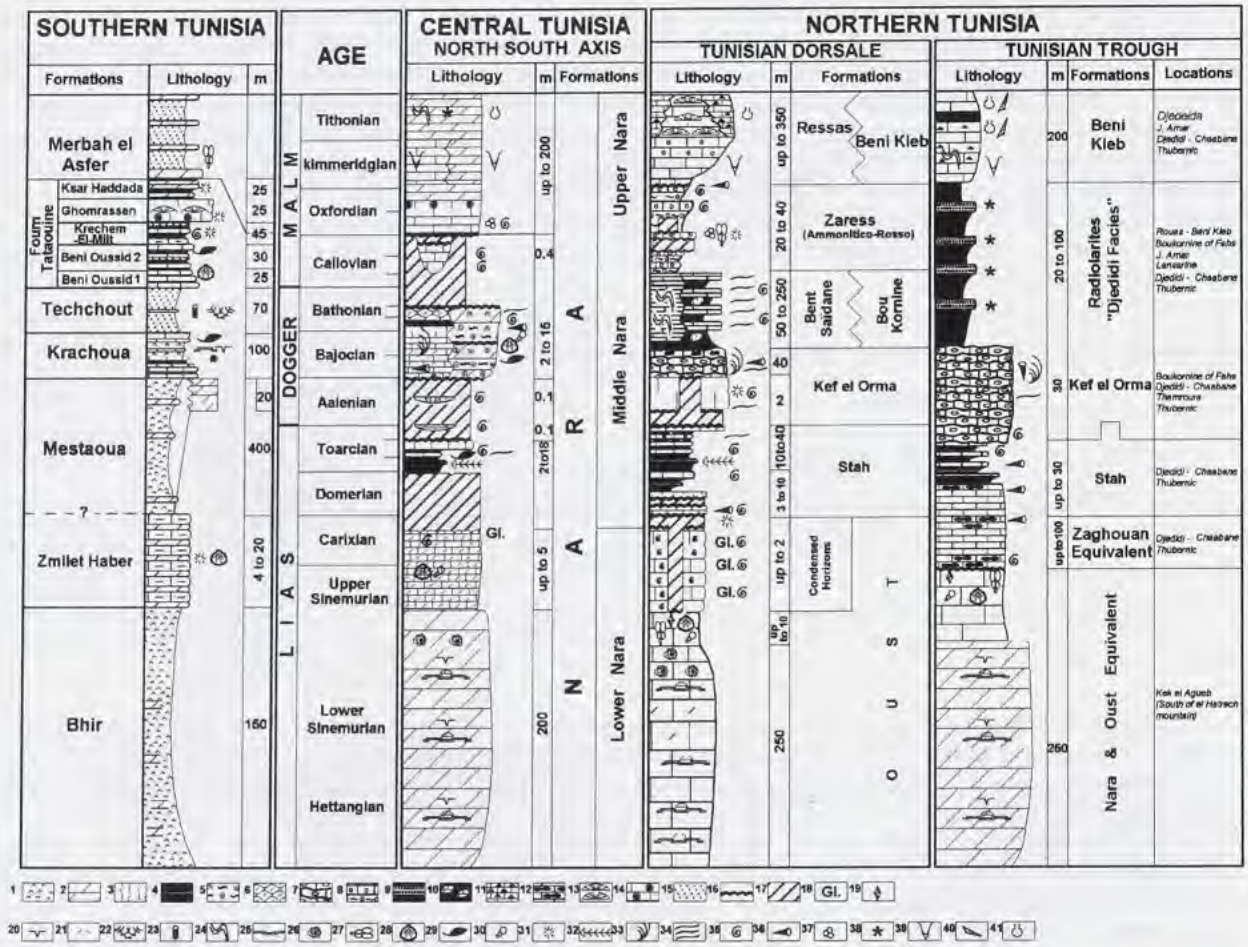

FIG. 10.— Tentative lithostratigraphic correlation between the Jurassic series of Southern, Central and Northern Tunisia. **1**, Triassic gypsum; **2**, peritidal dolomites; **3**, limestones partially dolomitised; **4**, black shales; **5**, ferruginous ooids or ironstones; **6**, compacted carbonates; **7**, nodular limestones; **8**, "ammonitico rosso" facies; **9**, radiolarites; **10**, resedimented limestones; **11**, calciturbidites; **12**, cherty limestones; **13**, reefs; **14**, calcareous ooids; **15**, sandstones; **16**, unconformities; **17**, hiatus; **18**, glauconitic grains; **19**, bipyramidal quartz cristals; **20**, sheet cracks; **21**, birds-eyes; **22**, cross-bedding; **23**, wood fragments; **24**, slump; **25**, algal laminations; **26**, oncoliths; **27**, benthic foraminifera; **28**, pelecypods; **29**, brachiopods; **30**, gastropods; **31**, echinoderms; **32**, fish bones; **33**, *Zoophycos*; **34**, filaments; **35**, ammonites; **36**, belemnites; **37**, *Protoglobigerina;* **38**, radiolaria; **39**, *Saccocoma*; **40**, *Aptycus*; **41**, calpionnellids.

*FIG. 10.— Tentative de corrélation lithostratigraphique entre les séries du Jurassique de la Tunisie Méridionale, Centrale et Septentrionale. **1**, gypses du Trias ; **2**, dolomies péritidales ; **3**, calcaires partiellement dolomitisés ; **4**, "black shales" ; **5**, oolithes ferrugineuses ou "ironstones" ; **6**, carbonates compactés ; **7**, calcaires en miches ou pseudonodulaires ; **8**, faciès "ammonitico rosso" ; **9**, radiolarites ; **10**, calcaires resédimentés ; **11**, calciturbidites ; **12**, calcaires à silex ; **13**, récifs ; **14**, oolithes calcaires ; **15**, sables et silts ; **16**, discordance ; **17**, lacune stratigraphique ; **18**, grains de glauconie ; **19**, quartz bipyramidal ; **20**, fentes de dessiccation ; **21**, "birds-eyes" ; **22**, stratifications obliques ; **23**, fragments de bois ; **24**, "slump" ; **25**, laminations algaires ; **26**, oncolithes ; **27**, foraminifères benthiques ; **28**, lamellibranches ; **29**, brachiopodes ; **30**, gastéropodes ; **31**, échinodermes ; **32**, os de poissons ; **33**, Zoophycos ; **34**, filaments ; **35**, ammonites ; **36**, bélemnites ; **37**, Protoglobigerina ; **38**, radiolaires ; **39**, Saccocoma ; **40**, Aptycus ; **41**, calpionelles.*

The lower Toarcian transgressive episode locally represented in Central Tunisia by the "black shales" ($U_{3,1}$) has been recorded in the Tunisian Dorsale and adjacent areas by black laminated marl-limestones rich in organic matter and fish traces (RAKUS & BIELY, 1970; GAUDANT *et al.*, 1972; SOUSSI *et al.*, 1992).

In Southern Tunisia, during the Toarcian(?), the sedimentation was dominated by the Mestaoua gypsum deposited in sub-aqueous evaporite basin (BEN ISMAÏL & M'RABET, 1990), but in our opinion a

Source : MNHN, Paris

part of the Zmilet Haber could correspond to the early Toarcian and the Mestaoua gypsum to the upper Toarcian-Aalenian. This hypothesis has to be confirmed by faunal arguments.

The Bajocian transgressive phase represented in Central Tunisia by the development of ironstones and hemipelagic limestones ($U_{3,1}$, $U_{3,2}$) corresponds in Northern Tunisia to the mud-limestones rich in radiolarian, filaments, calcispheres and *Zoophycos* of the Kef el Orma Formation (BONNEFOUS, 1972; FAURÉ & PEYBERNÈS, 1986). In Southern Tunisia, it corresponds to the shallow marine Krachoua carbonates overlying the Mestaoua gypsum (BUSSON, 1967; BEN ISMAÏL & M'RABET, 1990; KAMOUN, 1988; ZARBOUT & GHANMI, 1997) (Fig. 10).

The major and widespread transgressive episode, occurring at the late Callovian, is represented in Central Tunisia by the deposition of a pelagic condensed section unconformably overlying middle Bathonian rocks. In Southern Tunisia, it corresponds to the relatively deeper carbonates of Beni Oussid member (Foum Tataouine Formation; BEN ISMAÏL *et al.*, 1989), attributed to the late Bathonian by KAMOUN (1988) and recently to the Callovian on the basis of ostracods (METTE, 1997). These facies may be considered then as the equivalent of the marl and limestone alternations of the lower part of El Haouareb section in Central Tunisia. In Northern Tunisia, the Callovian transgressive event has been marked by a marine deepening illustrated by the development of pelagic and radiolarite beds (BONNEFOUS, 1972; ALOUANI *et al.*, 1990; SOUSSI *et al.*, 1998). This major transgressive phase is marked within the Chott basin by an angular unconformity and at Jebel Tebaga de Medenine by the juxtaposition of the Jurassic series to the Permian rocks.

The Kimmeridgian transgression was recorded both in Central and Northern Tunisia by the deposition of *Saccocoma*-rich muddy limestones, while in Southern Tunisia it was represented by the deposition of the Bir Miteur bioclastic carbonates overlying the Merbah el Asfer silisiclastics Formation (KAMOUN *et al.* 1994; BEN ISMAÏL, 1991).

REGRESSIVE PHASES

The major regressive phases are recorded in Southern Tunisia by: first the evaporitic deposits (upper part of the Mestaoua gypsum) upper Toarcian-Aalenian, second the ramp silisiclastic deposits of the Bathonian Techout Formation and thirdly the Oxfordian Merbah El Asfer siliciclastic deposits.

In Northern Tunisia, the regressive phases are difficult to distinguish, but they are particularly marked by an increase of detrital supply during the late Toarcian and Bathonian.

UNCONFORMITIES AND HIATUSES

The three major unconformities and their associated hiatuses identified in Central Tunisia are not yet well defined in Northern Tunisia, and particularly so in Southern Tunisia where environments of deposition were often shallow and chronostratigraphic resolution is poor. In this latter region, they correspond rather to lithologic and environmental discontinuities.

In the Tunisian Dorsale and adjacent areas, discontinuities exist but they are not marked by hiatuses as important as in Central Tunisia. They are, rather, expressed by condensed deposits with small hiatuses, notably within the upper Sinemurian-Carixian, Aalenian (FAURÉ & PEYBERNÈS, 1986) and lower Oxfordian (SOUSSI *et al.*, 1999).

In Northern Tunisia, the transition from the lower Bajocian muddy limestones to the upper Bajocian shales and packstones (Bent Saïdane Formation) is marked by centimetric conglomeratic horizons rich in reworked pebbles derived from the underlying carbonates. Locally, in Bou Garnine of Hammam Lif, the two mega-breccias composed of Liassic blocks redeposited within Bajocian-Bathonian marls, were mostly created by local tectonic activity (COSSEY & EHRLICH, 1981). The possible equivalent of the discontinuity that marks the upper Bathonian-lower Callovian in Central Tunisia is not currently identified in the Dorsale, neither by fauna nor by sedimentologic criteria.

Within the "ammonitico rosso facies" (upper Callovian-upper Oxfordian), condensed deposits are frequent and the lower Oxfordian is usually lacking.

Source : MNHN, Paris

In Southern Tunisia, due to the absence of biostratigraphic markers, hiatuses are not easy to demonstrate. The two first intra-Jurassic unconformities identified in the NOSA (UC1+UC2) could correspond in Southern Tunisia to the major lithologic changes occurring from the middle Liassic Zmilet Haber limestones to the Toarcian-Aalenian (?) Mestaoua gypsum and from the Bajocian Krachoua limestones to the Bathonian Techout sandstones.

This regional correlation demonstrates clearly that the several Jurassic deepening and shallowing episodes and their correlative transgressions and regressions have been recognised simultaneously in Northern, Central and Southern Tunisia. This implies that in Tunisia the eustatic factor has played a great part in controlling Jurassic sedimentation. Nevertheless, a number of sedimentological and stratigraphical events (hiatuses) occurring particularly in Central Tunisia, have been controlled by regional tectonics. This will be demonstrated by comparing the Central Tunisia sedimentary record to the Jurassic sea level curve of HALLAM (1988) and the global diagram of Jurassic sedimentary cycles of VAIL *et al.* (1977) and HAQ *et al.* (1987).

JURASSIC SEDIMENTARY RECORD IN CENTRAL TUNISIA AND GLOBAL SEA LEVEL CHANGES (FIG. 11)

One century ago, E. Suess recognised the importance of sedimentary cycles in stratigraphy and attributed them to fluctuations of sea level. Then, several works demonstrated that some of these cycles could have extensive repartition and could then be used as a tool in global correlation. More recently, the sequence stratigraphy approach, largely developed since the first publication of VAIL *et al.* (1977), stimulated the re-examination of basin sedimentary records. It is well established now that eustasy and tectonics constitute the major factors controlling the relative changes in sea level which create the available space for accommodation of the sediments (SARG, 1988).

On the basis of abundant data collected essentially from NW Europe, VAIL *et al.* (1977) and HAQ *et al.* (1987) constructed a global diagram or chart including a global eustatic curve and the main orders of sea level fluctuations (first, second and third order). From the lower Hettangian to the upper Tithonian, their diagrams showed seven second order cycles including 27 third orders cycles separated by 26 type 1 or 2 unconformities (HAQ *et al.*, 1987).

Our objective is not to deduce these cycles and their separating discontinuities from the chart using the ammonite zones detected in the NOSA, but to test the curve and the global cycles by reference to our data in order to distinguish the global eustatic signal from regional tectonics.

A comparison of the framework of sea level history documented by HALLAM (1975, 1988), VAIL *et al.* (1987) and HAQ *et al.* (1987) to the sedimentary record and sea level evolution of Jurassic in Central Tunisia requires the following comments.

— The overall trends of the sea level curve constructed for the NOSA, on the basis of detailed facies analysis coupled to precise dating using ammonites, compared to the curve of theses authors are closely similar. Both curves show major transgressive pulses during the Pliensbachian, the early Toarcian, the early Bajocian, the late Callovian and the Kimmeridgian (Fig. 11). The regressive tendency signalised during the Domerian, the late Toarcian, the late Bathonian and the late Oxfordian (HALLAM, 1988) in NW Europe have also been identified in Tunisia.

— The third order cycles or depositional sequences reported in the HAQ *et al.* (1987) diagram, from the Hettangian to the Tithonian, are not completely recorded in Central Tunisia. Here, only five significant (second order) major transgressive-regressive cycles have been distinguished.

These cycles extend from the Hettangian to Carixian, the early to middle Toarcian, the early Bajocian to middle Bathonian and the upper Callovian to upper Oxfordian. The fifth sequence is not well dated but may have started during the Kimmeridgian and extends to the upper Tithonian. They are separated by three major unconformities associated with hiatuses, the duration of which ranged from 4 to 12 Ma. These cycles approximately correlate with the second order cycles recognised in NW Europe by HAQ *et al.* (1987). The first, constituted of U1and U2 lithologic units, corresponds to amalgamated sequences situated since 211 to 188.5 Ma in the chart of HAQ *et al.* (1987). The Toarcian transgressive part of the second order sequence corresponds in part to the major cycle situated between 188.5 and 177

Source : MNHN, Paris

Ma, while the Aalenian cycle is completely absent within the NOSA series. The third Bajocian-Bathonian transgressive-regressive cycle, recognised in Central Tunisia, correlates quite well with the major cycle of HAQ *et al.* (1987) situated between 169 and 158.5 Ma. While the fourth and the fifth transgressive-regressive cycles in Central Tunisia could correspond to the cycles comprised between 158.5 and 138 or 136 Ma (?).

— The major sea level falls recorded during the Jurassic and shown within the HAQ and VAIL diagrams, coincide perfectly with the unconformities identified in Central Tunisia (Fig. 11).

The first unconformity (UC1), which is accompanied by the Carixian *p.p.*-Domerian hiatus, coincides with the eustatic fall noticed at 188.5 Ma. The second unconformity (UC2), accompanied by the gap of the upper Toarcian-Aalenian, coincides with the eustatic fall dated 177 Ma. The third

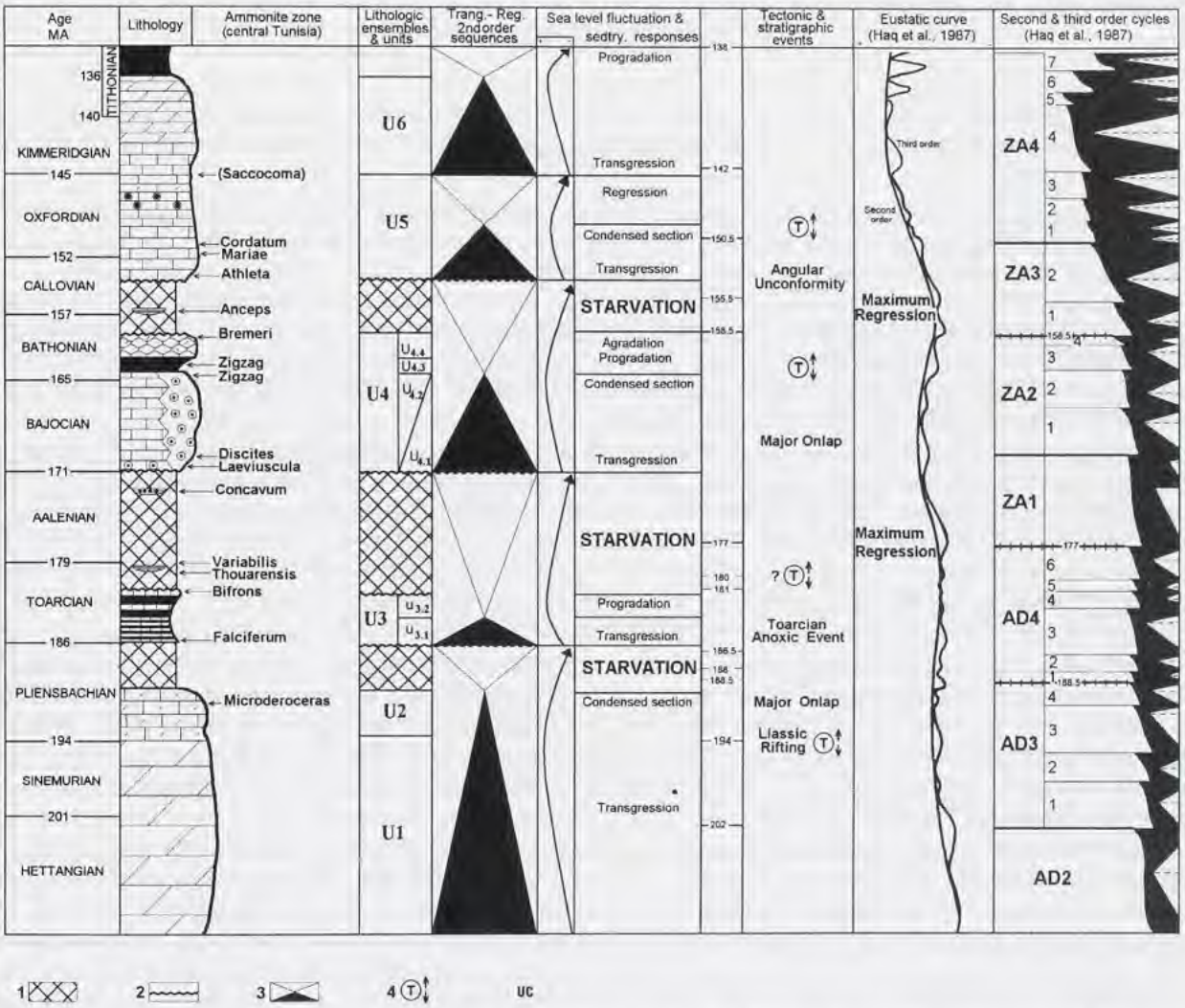

FIG. 11.— Comparison of the Jurassic stratigraphy and sedimentary cycles of Central Tunisia to the global cycles of HAQ *et al.* (1987) (for the lithological legend see figure 2). **1**, stratigraphic hiatus (submarine non-deposition/erosion); **2**, unconformity; **3**, second order tectono-eustatic transgressive–regressive cycle, black = transgressive half-cycle, grey = regressive half-cycle; **4**, major extensional tectonic event; **5**, UC: major unconformity.

FIG. 11.— Comparaison de l'enregistrement stratigraphique et des cycles sédimentaires du Jurassique de Tunisie centrale aux cycles globaux de HAQ et al., *1987 (pour la légende lithologique, voir légende de la figure 2). **1**, lacune stratigraphique ; **2**, discordance ; **3**, cycle transgressif-régressif de deuxième ordre d'origine tectono-eustatique, noir = demi cycle transgressif, gris = demi-cycle régressif ; **4**, évènement tectonique distensif majeur ; **5**, UC : discordances majeures.*

Source : MNHN, Paris

unconformity (UC3), accompanied by the hiatus of the upper Bathonian-lower Callovian, could be correlated to the eustatic fall of 158.5 Ma (HAQ *et al.*, 1987).

The sequence boundaries indicated at 188.5, 188 and 186.5 Ma converge to the major unconformity (UC1). Those dated 184, 179.5 and 177 Ma meet the unconformity UC2 and those attributed to 155.5, 158.5 and 159.5 match the unconformity UC3 (Fig. 11).

— The Jurassic condensed sections of the specific series of the NOSA (Central Tunisia), which consist in thin pelagic deposits characterised by abundant and mixed planktonic and benthic fossils associated with authigenic minerals such as glauconite, phosphate and iron oxides, occurred during Carixian, early Toarcian, Bajocian, late Callovian-early Oxfordian times. They coincide with the second order peak transgressions indicated within HAQ *et al.* (1987) at 191.5 Ma, 183.5 Ma, 170 Ma, 153.5 Ma and 150 Ma? (Fig. 11).

DISCUSSION

The sedimentary cycles of Central Tunisia are not complete and their separating unconformities are considerably longer than the duration of unconformities dividing the Jurassic supercycles of HAQ *et al.* (1987).

The hiatuses identified within the Jurassic series in Central Tunisia, separate deep marine facies and their corresponding discontinuities did not show any trace of emergence features. Thus, they have to be considered as deep marine hiatuses caused by erosion or non-deposition. The lack of sediments or the slowing of sedimentation within deep-water facies may be caused by rapid and drastic changes of sea level. Maximal of hiatuses occurred in Central Tunisia in the Domerian, late Toarcian-Aalenian and late Bathonian. Their correspondence with the major falls of sea level indicated within the HAQ *et al.* (1987) chart is remarkable and suggests at first sight that these major sea level falls should have played an important role in the development of these hiatuses.

This could be the case for the upper Toarcian-Aalenian and upper Bathonian gaps which coincide with the maximum point of the regressive parts of the second order cycles of HAQ *et al.* (1987) (Fig. 11). The gaps associated with the condensed sections occurring during the late Carixian, Bajocian and Callovian seem to be associated with the maximum water depth following a rapid rise of sea level. In fact, it is well known nowadays that during sea level high stands, especially when they follow a rapid rise of sea level, sediment supply tends to be trapped close to the shore line and the outer shelf regions become starved of sediments or characterised by slow sedimentation.

In Tunisia, the greatest hiatus abundance occurred within the NOSA and the duration of each hiatus varies from Central to Northern Tunisia and appears to depend upon the position of the section on the continental margin (Fig. 9). In addition, the studies carried out towards the west of the NOSA (BEDIR 1995) demonstrated the existence of the major second order cycles identified by HAQ *et al.* (1987) and the seismic profiles also clearly show that the Jurassic series are relatively thick and more complete to the west (Majora et Sidi Aïch blocks).

Such differences result from the tectonic configuration of Central Tunisia which corresponded during Jurassic and Cretaceous time to a platform structured into horsts and grabens delimited by N-S and nearly E-W faults. Within this platform, the NOSA has acted as an active uplift block characterised by very condensed sedimentation compared to other domains where the Jurassic series are more complete and very thick, such as the Chott Basin to the south and the Tunisian trough to the north (Fig. 9). The unconformities identified within the NOSA area, have also been identified in other areas of the Tethyan realm (HALLAM, 1978; GABILLY *et al.*, 1985), but their duration is nowhere greater than in Central Tunisia. Thus, these unconformities could be interpreted as the result of the effects of major sea level fluctuations (transgressions or regressions) enhanced by local tectonic activities.

In fact, the hiatuses identified in Northern and especially in Central Tunisia within the middle Liassic and the Dogger are very close to the tectonic movements associated with the rifting of the Tethys. On the NOSA mega-block (from Jebel Rheouis to Jebel Loridga), the sedimentation was particularly very condensed and hard-grounds coalesce to form composite condensed sections particularly on the highs of the block (Loridga area). Submarine erosional activities during the falls or rises of sea level constituted

Source : MNHN, Paris

the rule on this submerged swell. The activity of currents is recorded by the presence of reworked Toarcian lithoclasts within the Bajocian rocks, the cross bedding stratification, the association of numerous ammonite zonal marker species in the same bed, in addition to the local record of upper Toarcian, Aalenian and lower Callovian as lenses bodies delimited by erosional surfaces. Only during the highstands (maximum transgression), the NOSA block has recorded sedimentation processes. Sedimentation occurred approximately during the second order transgressive phases of the second order cycles of HAQ *et al.* (1987).

Thus, during the major falls or rises of sea level, especially those, which coincide with tectonic events, the NOSA has acted as a starved platform. The unconformities identified within the Jurassic of Central Tunisia are abruptly overlain by more marine facies. The five second order transgressive-regressive cycles identified within the NOSA Jurassic series have been clearly controlled both by sea level changes and the tectonic phases associated to the Tethyan rifting. They can be assimilated to second order tectono-eustatic cycles and their separating unconformities and hiatuses result from the combination of sea level changes with the tectonic activities (GRACIANSKY *et al.*, 1993).

CONCLUSION

THE FAUNAS

The faunas show a sub-mediterranean character and are known in open sea environments of Peri-Tethyan platforms: *Morphoceras*, *Ebrayiceras* in the Bathonian; *Rehmannia*, *Collotia* and Hecticoceratidae in the Callovian; *Taramelliceras*, *Campylites*, *Peltoceratoides* and several Perisphinctidae in the Oxfordian. Thus, they integrate well in the palaeogeographic schemes which underline the faunal homogeneity of the western part of the Tethys where the ibero-moorish strait allowed faunal exchanges. Tunisia as well as Sicily and the Malta scarp mark the eastern boundary of the extension of the dominant submediterranean faunas on the Southern Tethyan margin. Eastwards, in southern Turkey and as far as Malagasy, the submediterranean European taxa are only episodically present.

As a result, ages and correlations are referred to the biochronological standard for the submediterranean Europe. However, in the beds at the Callovian-Oxfordian boundary, boreal cardioceratids which are the basis of the zonation used in Europe are missing, especially for the Oxfordian,. So, the more typical sub-mediterranean taxa (oppeliids, perisphinctids, peltoceratids and euaspidoceratids) and the parallel zonations based on these families have been used.

Concerning biogeography, as in Algeria and Morocco, abundant *Emileia* in the lower Bajocian and *Oraniceras* in lower Bathonian attest the South Tethyan character of the faunas, as well as the lack of the boreal and sub-boreal families (cardioceratids and kosmoceratids) at the Callovian-Oxfordian boundary. The lack of sub-mediterranean hecticoceratids of the same age is not so easy to understand, as the occurrence of *Phylloceras* and *Lytoceras* from the upper Callovian up to the lower Oxfordian indicates a clear deepening of the sea which normally is auspicious for oppeliids.

The deeper marine environments of the Jurassic of the NOSA explain the lack of Arabian taxa, which are known westwards in Western Algeria and Morocco, although Tunisia is on the south Tethyan migration route often used by the Arabian taxa. The migration route was probably south of the NOSA, probably in the Chott area where environments were very shallow in which the Arabian taxa were adapted. Except for the Foum Tataouine Formation yielding upper Callovian *Pachyerymnoceras*, other South Tunisia formations do not contain ammonites. Old collections of M. Rakus include one specimen of *Ermoceras* gr. *coronatoides* (Douv.), badly preserved, especially the ventral area, from the Bajocian limestones with ferruginous ooids at Kef el Hassine. The existence of the Arabian genus *Ermoceras* in Tunisia is very probable, but needs to be confirmed by new better-preserved specimens.

Source : MNHN, Paris

THE SEDIMENTARY RECORD

Five major transgressive-regressive cycles have been at least recognised in Northern, Central and Southern Tunisia. The transgressive episodes occurred during the Pliensbachian, early Toarcian, early Bajocian, late Callovian and Kimmeridgian. The corresponding palaeogeographic evolution has been influenced by both tectonic and eustatic factors. In Central and Northern Tunisia, tectonic events occurred during the late Sinemurian, Bajocian, Callovo-Oxfordian and early Tithonian and led to the differentiation of faulted blocks with horsts and grabens.

Since the Pliensbachian, Central Tunisia acted as a pelagic platform structured into horsts and grabens limited by approximately E-W faults. Within this structural framework, the North-South Axis area has acted as a resistant block (uplift) characterised, especially during Middle Jurassic, by condensed deposits and hiatuses. The NOSA Jurassic series presents specific features compared to those of Centralwestern and Northwestern Tunisia. It is less thick and includes specific facies (ironstones) and numerous stratigraphic hiatuses. The hiatuses and discontinuities, particularly frequent in the high domains of the structural framework, are closely related to the tectonic instability and the increase of erosive activity by submarine currents on highs during the major eustatic changes. The active circulation of the deep currents and their corrosive action (sweeping and dissolution) on the biogenic material, notably on the highs of the tilted blocks during major transgressions or regressions, have notably reduced the sedimentation rate and consequently controlled the extent and duration of the sedimentary hiatuses.

The three unconformities accompanied by hiatuses correspond to the superposition of several discontinuities (VAIL *et al.*, 1987) and can be interpreted as enhanced tectonic sequence boundaries. The frequency of the unconformities and hiatuses is then due to the combined effects of the local tectonic factor and the global eustatic one. Tectonic activity which is linked to the Tethyan rifting created a pattern of tilted blocks involving palaeohighs which were isolated from sediment supplies, notably during either the maximum regressive periods when sedimentation was displaced towards the basin (progradation phase) or during rapid sea level rise when sediments were caught on the inner shelf. Sedimentation has been recorded only during the aggradational-retrogradational phases of the second order cycles.

Comparison of the NOSA Jurassic sedimentation pattern with the global cycles shows clearly that numerous third order cycles of the chart of HAQ *et al.* (1987) are not registered in this part of the margin. Only the second order ones, marked by major faunal and sedimentological changes, are recognisable. The Jurassic sedimentary and stratigraphic records of Central Tunisia represent a good illustration of the interaction between the global eustatic signal and regional tectonic activities. It demonstrates what was suggested by HALLAM (1988): "there is no region that can give a definitive picture of the sequence boundaries for the whole world, and that regional tectonics can be discounted".

Because of the abundant hiatuses and their long duration, the NOSA region cannot be used as a standard for eustatic analysis. The third order sequences recorded at a global scale are usually missing especially on the highs of the tilted blocks.

ACKNOWLEDGEMENTS

This work is a part of research projects sponsored by CONOCO, ETAP, and Peri-Tethys Program (Proposal 96/128). We are thankful to these for their logistic support. We gratefully acknowledge Mr A. M'RABET for stimulating many discussions and helpful comments. Thoughtful reviews by J. THIERRY and two anonymous reviewers greatly helped in improving the paper. We also especially thank CH. ABBES for productive discussions.

Source : MNHN, Paris

REFERENCES

ABBES, C., 1983.— *Étude structurale du Jebel Touïla: extrêmité septentrionale du chaînon N-S Sidi Khalif-Nara-El Haouareb.* Thèse de 3ème cycle, Université de Tunis, Tunis, Tunisie: 1-150.

ALOUANI, R., TLIG, S. & ZARGOUNI, F., 1990.— Découverte de radiolarites du Jurassique supérieur dans le "Sillon tunisien". Faciès et structures d'une marge SE de la Téthys maghrébine. *Comptes Rendus de l'Académie des Sciences, Paris*, **310**: 609-612.

ALOUANI, R., 1991.— *Le Jurassique du nord de la Tunisie; Marqueurs géodynamiques d'une marge transformante: turbidites, radiolarites et métamorphisme.* Thèse spécialité, Université Tunis II, Tunis, Tunisie: 1-179.

ASSERTO, R. & BENELLI, F., 1971.— Sedimentology of the pre-Cenomanian formations of Jebel Gharian, Libya. *In*: C.GRAY (ed.), *Symposium on Geology of Libya*. University of Lybia, Tripoli: 37-85.

BAUDIN, F., DERCOURT, J., HERBIN, J.P. & LACHKAR, J., 1988.— Le Lias supérieur de la zone ionienne (Grèce): une sédimentation riche en carbone organique. *Comptes Rendus de l'Académie des Sciences, Paris*, **307** (II): 985-900.

BEDIR, M., 1995.— *Mécanismes géodynamiques des bassins associés aux couloirs de coulissements de la marge atlasique de la Tunisie.* Thèse d'État, Université Tunis II, Tunis, Tunisie: 1-416.

BEN AYED, N., 1986.— *Évolution tectonique de l'avant pays de la chaîne alpine de Tunisie du début du Mésozoïque à l'Actuel.* Thèse de Doctorat d'État, Université Paris-Sud, Orsay, France: 1-328.

BEN AYED, N. & KHESSIBI, M., 1983.— Sur l'évolution géodynamique de la Jeffara tunisienne au cours du Mésozoïque. *Notes du Service géologique de Tunisie*, **47**: 41-45.

BEN FERJANI, A., BUROLLET, P.F. & MEJRI, F., 1990.— *Petroleum Geology of Tunisia*. ETAP, Tunis: 1-194.

BEN ISMAÏL, M.H., 1991.— *Les Bassins mésozoïques (Trias à Aptien) du Sud de la Tunisie: stratigraphie intégrée, caractéristiques géophysiques et évolution géodynamique.* Thèse de Doctorat, Université Tunis II, Tunis, Tunisie: 1-466.

BEN ISMAÏL, M.H., BOUAZIZ, S., ALMÉRAS, Y., CLAVEL, B., DONZE, P., ENAY, R., GHENMI, M. & TINTANT, H., 1989.— Nouvelles données biostratigraphiques sur le Callovien et les faciès "purbecko-wealdiens" (Oxfordien à Vraconien) dans la région de Tataouine (Sud-tunisien). *Bulletin de la Société géologique de France*, **8**, **V** (2): 353-360.

BEN ISMAÏL, M.H. & M'RABET, A., 1990.— Evaporite, carbonate and siliciclastic transitions in the Jurassic sequences of south-eastern Tunisia. *Sedimentary Geology*, **66**: 65-82.

BONNEFOUS, J., 1972.— *Contribution à l'étude stratigraphique et micropaléontologique du Jurassique de Tunisie (Tunisie septentrionale et centrale, Sahel et zone des Chotts).* Thèse, Université Paris VI, Paris, France: 1-397.

BONNOT, A., 1995.— *Les Aspidoceratidae (Ammonitina) en Europe occidentale au Callovien supérieur et à l'Oxfordien inférieur.* Thèse de Doctorat, Université de Dijon, Dijon, France: 1-453.

BOSELLINI, M.A. & HARDIE, L.A., 1985.— Facies e Cicli della dolomia principale delle Alpi Venete. *Memorie della Società Geologica Italiana, Modena*, **30**: 245-266.

BOUAZIZ, S., 1995.— *Étude de la tectonique cassante dans la plate-forme et l'Atlas saharien (Tunisie méridionale): évolution des paléochamps de contraintes et implications géodynamiques.* Thèse d'État, Université Tunis II, Tunis, Tunisie: 1-485.

BOUAZIZ, S., BARRIER, É., ANGELIER, J., TRICART, P. & TURKI, M.M., 1998.— Tectonic evolution of the Southern Tethyan margin in southern Tunisia. *In*: S. CRASQUIN-SOLEAU & É. BARRIER (eds), Peri-Tethys Memoir 3: Stratigraphy and evolution of Peri-tethyan platforms. *Mémoires du Muséum national d'Histoire naturelle*, **177**: 215-236.

BOUILLIN, J.P., 1986.— Le "Bassin maghrebin": une ancienne limite entre l'Europe et l'Afrique à l'ouest des Alpes. *Bulletin de la Société géologique de France*, **8**, **II** (4): 547-558.

BROCHERT, H., 1960.— Genesis of marine sedimentary iron ores. *Bulletin of the Institute of Mineralogy and Metallogeny*, **61**: 261-279.

BROCHWICZ-LEWINSKI, W., 1981.— Early Oxfordian Perisphinctids of the Czestochowa area; their stratigraphic value. *Bulletin de l'Académie polonaise des Sciences*, **28** (4): 233-242.

BUREAU, D., 1986.— *Approche sédimentaire de la dynamique structurale: évolution mésozoïque et devenir orogénique de la partie septentrionale du Fossé Saharien (Sud ouest Constantinois et Aurès, Algérie).* Thèse de Doctorat, Université Pierre et Marie Curie, Paris, France: 1-779.

BUROLLET, P.F., 1956.— Contribution à l'étude stratigraphique de la Tunisie centrale. *Annales des Mines et Géologie, Tunis*, **18**: 1-352.

BUSNARDO, R., DONZE, P., LE HÉGARAT, G., MEMMI, L. & M'RABET, A., 1976.— Précisions stratigraphiques nouvelles sur le Berriasien des Djebel Nara et Sidi Khalif (Tunisie centrale). *Geobios, Lyon*, **9** (3): 231-250.

BUSNARDO, R., DONZE, P., KHESSIBI, M., LE HÉGARAT, G. & MEMMI, L., 1980.— Interprétation biostratigraphique nouvelle de la formation des "Argiles de Sidi Kralif" au Djebel Bou Hedma (Tunisie centrale). *Geobios, Lyon*, **13** (3): 459-463.

BUSNARDO, R., DONZE, P., KHESSIBI, M., LE HEGARAT, G., MEMMI, L. & M'RABET, A., 1985.— La Formation Sidi Khalif (Tithonique-Berriasien) en Tunise centrale: Synthèse stratigraphique et sédimentologique. *In: Actes du 1er Congrès national des Sciences de la Terre, Tunis, 1981.* Société des Sciences de la Terre, Paris: 115-119.

Source : MNHN, Paris

BUSSON, G., 1967.— *Le Mésozoïque saharien.* 1ère partie: *Extrême Sud tunisien.* C.N.R.S, Paris: 1-194 (Série géologique; 8).

BUSSON, G., 1970.— Esquisses paléogéographiques du Sahara algéro-tunisien depuis le Salifère principal (Trias-Lias) jusqu'à la fin du Crétacé. *Comptes Rendus sommaires des Séances de la Société géologique de France*, **5**: 1-142.

CARIOU, É., ENAY, R., ATROPS, F., HANTZPERGUE, P., MARCHAND, D. & RIOULT, M., 1997.— Oxfordien. *In*: É. CARIOU & P. HANTZPERGUE (eds), Biostratigraphie du Jurassique ouest-européen et méditerranéen: zonations parallèles et distribution des invertébrés et microfossiles. *Elf Aquitaine Édition, Pau, Mémoire*, **17**: 144-147.

CASTANY, G., 1951.— Étude géologique de l'Atlas tunisien. *Annales des Mines et Géologie, Tunis*, **8**: 1-632.

CASTANY, G., 1955.— Les Extrusions jurassiques en Tunisie. *Annales des Mines et Géologie, Tunis*, **14**: 1-71.

COSSEY, S.P.J. & EHRLICH, R., 1981.— The Orientation of small mudy clasts in turbidites: paleoccurent indicators on a Jurassic carbonate slope, Tunisia. *Journal of Sedimentary Petrology*, **51** (3): 973-977.

DUMON, E., 1936.— *Coupe du Jebel sidi Khalif-Nara-Bou Gabrine.* Unpublished report (S.E.R.E.P.T.)

EL ZOUKI, A., 1980.— Stratigraphy and lithofacies of the continental clastics (Upper Jurassic and Lower Cretaceous) of Jebel Nefusah, NW Libya, II. *In*: M. J. SALEM & M. T. BUSREWILL (eds), *The Geology of Libya, II.* Academic Press, London: 393-418.

FAURE, J.L. & PEYBERNÈS, B., 1986.— Biozonation par Ammonites et essai de corrélation des séries réduites liasiques de la "Dorsale tunisienne". *Bulletin de la Société d'Histoire naturelle, Toulouse*, **122**: 41-49.

GABILLY, J., CARIOU, É. & HANTZPERGUE, P., 1985.— Les Grandes discontinuités stratigraphiques au Jurassique: témoins d'événements eustatiques, biologiques et sédimentaires. *Bulletin de la Société géologique de France*, **8**, **I** (3): 391-401.

GABILLY, J., ELMI, S., MATTEI, J. & MOUTERDE, R., 1971.— Toarcien. *In*: Les Zones du Jurassique en France. *Comptes Rendus sommaires des Séances de la Société géologique de France*, **6**: 82-84.

GAUDANT, J., RAKUS, M. & STRANIK, Z., 1972.— *Leptolepis* (poisson téléosteen) dans le Toarcien de la Dorsale tunisienne. *Notes du Service géologique national de Tunisie*, **38**: 5-13.

GHARBI, K., 1989.— *Les Calcaires noduleux du Callovo-Oxfordien-Kimm_ridgien de Tunisie.* Thèse de 3ème cycle, Université de Tunis, Tunis, Tunisie: 1-186.

GINSBURG, R.N., 1975.— *Tidal deposits.* Springer, New York: 1-429.

GRACIANSKY, P.C. DE, DARDEAU, G., DUMONT, T., JACQUIN, T., MARCHAND, D., MOUTERDE, R. & VAIL, P.R., 1993.— Depositional sequence cycles, transgressive-regressive facies cycles and extensional tectonics: example from the southern Subalpine Jurassic basin, France. *Bulletin de la Société géologique de France*, **164** (5): 709-718.

HALLAM, A., 1975.— *Jurassic Environments.* Cambridge University Press, Cambridge (England): 1-269.

HALLAM, A., 1988.— A Revaluation of Jurassic eustasy in the light of new data and the revised Exxon curve. *In*: C.K. WILGUS *et al.* (eds), Sea-level changes- an integrated approach. *SEPM Special Publication*, **42**: 261-271.

HAQ, B.U., HARDENBOL, J. & VAIL, P.R., 1987.— The Chronology of fluctuating sea level since the Triassic. *Science, Washington*, **235**: 1156-1167.

HARDIE, L.A., BOSSELINI, A. & GOLDAHAMMER R.K., 1986.— Repeated sub-aerial exposure of subtidal carbonate platforms, Triassic, Northern Italy: evidence for relative sea level changes on 103-105 year scale. *Paleoceanography*, **14**: 447-457.

HARDER, H., 1989.— Mineral genesis in ironstones: a model based upon laboratory experiments and petrographic observations. *In*: T.P. YOUNG & W.E.G. TAYLOR (eds), Phanerozoic Ironstones. *SpecialPublications- Geological Society of London*, **46**: 9-18.

HLAIEM, A., 1998.— *Étude géophysique et géologique des bassins et des chaînes de Tunisie centrale et méridionale durant le Mésozoïque et le Cénozoïque, évolution structurale, modélisation géothermique et implications pétrolières.* Thèse de Doctorat, Université Paris VI, Paris, France: 1-315.

JENKYNS, H.C., 1985.— The Early Toarcian and Cenomanian-Turonian Anoxic events in Europe. Comparisons and contrasts. *Geologische Rundschau, Stuttgart*, **74** (3): 505-518.

KAMOUN, F., 1988.— *Le Jurassique du Sud tunisien, témoin de la marge africaine de la Téthys; stratigraphie, sédimentologie et micropaléontologie.* Thèse de 3ème cycle, Université de Toulouse, Toulouse, France: 1-268.

KAMOUN, F., MARTINI, R., PEYBERNÈS, B. & ZANINETTI, L., 1994.— Caractérisation micropaléontologique du "Rhétien" dans l'Axe N-S (Tunisie centrale), comparaison avec le Rhétien de la Dorsale et de la plate-forme saharienne. *Rivista Italiana di Paleontologia e Stratigrafia*, **100** (3): 365-382.

LEMOINE, M., 1985.— Structuration jurassique des Alpes occidentales et palinspatique de la Téthys ligure. *Bulletin de la Société géologique France*, **8** (1): 127-137.

MASCKE, E., 1907.— *Die Stephanoceras-Verwandten in der Coronaten-Schichten von Norddeutschland.* Inaugural Dissertation der Universität Göttingen, Göttingen, Germany: 1-38.

MELENDEZ, G., SEQUEIROS, L. & BROCHWICZ-LEWINSKI, W., 1983.— Lower Oxfordian in the Iberian Chain (Spain). Part II: Ammonite fauna. *Bulletin de l'Académie polonaise des Sciences*, **30** (3-4): 173-180.

METTE, W., 1997.— Palaeoecology and palaeogeography of the Middle Jurassic ostracods of southern Tunisia. *Palaeogeography, Palaeoclimatology, Palaeoecology*, **131**: 65-111.

M'RABET, A., 1975.— *Contribution à l'étude stratigraphique, pétrographique et sédimentologique du Crétacé inférieur de l'axe Nord-Sud.* Thèse de 3ème cycle, Université Paris VI, Paris, France: 1-181.

M'RABET, A., 1987.— Stratigraphie, sédimentation et diagenèse carbonatée des séries du Crétacé inférieur de Tunisie centrale. *Annales des Mines et Géologie, Tunis*, **30**: 1-412.

Source : MNHN, Paris

M'RABET, A., BEN ISMAÏL, M.H., SOUSSI, M. & TURKI, M.M., 1989.— Jurassic rifting and drifting of North African margin and their sedimentary responses in Tunisia. *In*: 28th International Geological Congress, Washington, Abstracts. *US-Geological Survey*: 473-474.

MZOUGHI, M., DUFAURE, PH. & PEYBERNÈS, B., 1992.— Données nouvelles sur le Jurassique du Golfe de Gabes autour de l'Île de Djerba (Tunisie). *Comptes Rendus de l'Académie des Sciences, Paris*, **315** (II): 565-570.

OUALI, J.A., 1984.— *Structure et évolution géodynamique du chaînon Nara Sidi Khalif (Tunisie centrale)*. Thèse de 3ème cycle, Université Rennes I, Rennes, France: 1-114.

PAVIA, G., 1983.— *Monografie*. II: *Ammoniti e biostratigrafia del Baiociano inferiore di Digne (Francia SE, Dip. Alpes-Haute-Provence)*. Museo Regionale di Scienze Naturali, Torino: 1-254.

PEYBERNÈS, B., 1992.— The Jurassic of Tunisia: an attempt at reconstruction of the South-Neotethyan margin during and after the rifting phase. *Geology of Libya*: 1679-1766.

PEYBERNÈS, B., KAMOUN, F., THIERRY, J., BEN YOUSSEF, M., CUGNY, P., FAURÉ, P. & GHANMI, M., 1995.— Séquences de dépôt et biochronozones d'Ammonites dans l'intervalle Toarcien-Oxfordien de l'Axe N-S (Tunisie centrale). *Comptes Rendus de l'Académie des Sciences, Paris*, **321**: 593-600.

POGACSAS, G.Y., M'RABET, A., HASS, J., SAMU, L., VAKARCS, G., KHOCHTALI, T., RUMPTER, J., SZABEO, N., PAKOSDI, G., ACHECH, M.H., OUAHCHI, A., KONCZI, I., BARTHA, A. & BEN GEUCHA, A., 1998.— Palaeozoic-Mesozoic facies evolution and related hydrocarbon system of the kebylie area (central Tunisia). *In*: Proceeding of the sixth Tunisian production conference. *ETAP, Mémoire*, **12**: 285-308.

RAÏS, J., SAHIROU, G., ALOUANI, R., MOUGUINA, E.M. & TLIG, S., 1991.— Le Sillon tunisien: structuration synsédimentaire jurassique. Rift avorté et cicatrisé au Dogger supérieur-Malm, à la marge SE de la Téthys maghrébide. *Comptes Rendus de l'Académie des Sciences, Paris*, **312** (II): 1169-1175.

RAKUS, M. & BIELY, A., 1970.— Stratigraphie du Lias dans la Dorsale tunisienne. *Notes du Service géologique, Tunis*, **32**: 45-63.

RIOULT, M., CONTINI, D., ELMI, S. & GABILLY, J., 1997— Bajocien. *In*: É. CARIOU & P. HANTZPERGUE (eds), Biostratigraphie du Jurassique ouest-européen et méditerranéen: zonations parallèles et distribution des invertébrés et microfossiles. *Elf Aquitaine Édition, Pau, Mémoire*, **17**: 41-53.

SAÏDI M., ACHECHE, M.H., INOUBLI, H. & BELAYOUNI, H., 1992.— Identification et caractérisation des roches mères en Tunisie centrale. *In*: Actes des IIèmes journées de Géologie tunisienne appliquée à la Recherche des hydrocarbures. *ETAP, Mémoire*, **3**: 429-457.

SARG, J.F., 1988.— Carbonate sequence stratigraphy. *In*: C.K. WILGUS *et al.* (eds), Sea-level changes- an integrated approach. *SEPM Special Publication*, **42**: 155-181.

SCHOELLER, H., 1937.— Présence du Jurassique au Sud-Ouest de Kairouan, Tunisie. *Comptes Rendus sommaires des Séances de la Société géologique de France*: 156-157.

SHINN, E.A, LLOYD, R.M. & GINSBURG, R.N., 1969.— Anatomy of a modern carbonate tidal flat, Andros Island, Bahamas. *Journal of Sedimentary Petrology*, **39** (3): 1202-1228.

SOUSSI, M., 1990.— *Les Faciès argilo-carbonatés jurassiques en Tunisie centrale: stratigraphie, sédimentologie, diagenèse (dolomitisation) et intérêt pétrolier*. Thèse de 3ème cycle, Université Tunis II, Tunis, Tunisie: 1-281.

SOUSSI, M., ABBES, CH. & BELAYOUNI, H., 1998.— Sedimentary record of sea level changes and associated organic-rich facies on the southern Tethyan margin: the upper Triassic of central Tunisia. *Africa Geoscience Review*, **5** (3): 275-285.

SOUSSI, M., ABBES, CH., BELAYOUNI, H. & BOUKADI, N., 1996.— Sédimentologie, stratigraphie séquentielle et caractéristiques géochimiques des séries du Trias moyen et supérieur de l'Axe Nord-Sud. (Tunisie centrale), Proceedings Fifth Tunisian petroleum exploration conference. *ETAP, Mémoire*, **10**: 257-271.

SOUSSI, M., BEN ISMAÏL, M.H. & M'RABET, A., 1990.— Les "Black shales toarciens" de Tunisie centrale: témoins d'événement anoxique sur la marge sud téthysienne. *Comptes Rendus de l'Académie des Sciences, Paris*, **310**: 602-612.

SOUSSI, M., BOUGHDIRI, M., ENAY, R. & MANGOLD, CH., 1998.— Faciès à affinité ammonitico rosso d'âge Toarcien supérieur de la Tunisie atlasique nord-occidentale: conséquences pour les corrélations et la paléogéographie. *Comptes Rendus de l'Académie des Sciences, Paris*, **327**: 135-140.

SOUSSI, M., BUSSON, G., NOËL, D., BISMUTH, H., HARRAN, H., MARGIN, A.M., TURKI, M.M., CORNÉE, A. & M'RABET, A., 1993.— Schizosphères dans les calcaires fins du Lias moyen et supérieur de Tunisie nord-orientale. *In*: *14th IAS Meeting, Morocco, Abstracts*. International Association of Sedimentologists, Marrakech: 308-309.

SOUSSI, M., DAVAUD, E. & HARRAN, H., 1993.— Événement de bréchification précoce (dykes neptuniens ?) dans les calcaires du Lias de Tunisie nord-orientale. Origine et signification. *In*: *14th IAS Meeting, Morocco, Abstracts*. International Association of Sedimentologists, Marrakech: 306-307.

SOUSSI, M., ENAY, R., BOUGHDIRI, M., MANGOLD, Ch., ZAGH BIB-TURKI, D., 1999.— L'Ammotico Rosso (formation Zaress) de la Doisole tunisienne. Comptes Rendus de l'Académie des Sciences, Paris, 329 : 279-386.

SOUSSI, M., ENAY, R., MANGOLD, C., M'RABET, A., RAKUS, M. & RABHI, M., 1991.— Datations par ammonites des séries et des discontinuités du Jurassique de l'axe Nord-Sud (Tunisie centrale). *Comptes Rendus de l'Académie des Sciences, Paris*, **312**: 501-507.

SOUSSI, M., HARRAN, H., TURKI, M.M. & M'RABET, A., 1992.— Histoire tectono-sédimentaire et potentialité pétrolière du Lias (Toarcien) de la Tunisie centrale et nord-orientale. *In*: *Actes des 3èmes journées de Géologie appliquée à la recherche pétrolière*. ETAP, Tunis: 251-275.

Source : MNHN, Paris

SOUSSI, M. & M'RABET, A., 1991.— Les Faciès à oolithes ferrugineuses ("oolitic ironstones") du Jurassique moyen de l'Axe Nord-Sud (Tunisie centrale: caractéristiques et significatations). *Notes du Service géologique national de Tunisie*, **57**: 71-85.

SOUSSI, M. & M'RABET, A., 1994.— Burial dolomitisation of organic-rich and organic-poor carbonates, Jurassic of central Tunisia. *In*: B. PURSER, M. TUCKER & D. ZENGER (eds), Dolomites: A Volume in Honour of Dolomieu. *Special Publication, IAS*, **21**: 429-455.

SOUSSI, M., M'RABET, A. & ENAY, R., 1991.— Découverte du Lias et du Dogger au Jebel Rhéouis, Axe Nord-Sud (Tunisie centrale): conséquences paléogéographiques. *Notes du Service géologique national de Tunisie*, **58**: 11-19.

SOUSSI, M., M'RABET, A., TURKI, M.M., MEJRI, F. & ABBES, CH., 1994.— The Upper Jurassic carbonates of Zaghouan area, northeast Tunisia: an example of isolated platform to basin transition. *In*: *14th International Sedimentological Congress, Recife, Abstracts*. International Association of Sedimentologists, Recife: B15-16.

SOUSSI, M., TURKI-ZAGHBIB, D., OURIBANE, M. & TURKI, M.M., 1996.— Biosedimentary characteristics of Upper Tithonian Carbonate platform in Zaghouan area (NE-Tunisia). An example of isolated shallow marine platform to basin transition. *In*: *Field Trips Guide Book, 17th IAS Regional African European Meeting of Sedimentology, Sfax, Tunisia*. International Association of Sedimentologists, Sfax: 213-242.

TARKOWSKI, R., 1990.— Les *Taramelliceras* (Ammonitina) de l'Oxfordien inférieur du Jurassique cracovien, valeur stratigraphique. *In*: *1st Oxfordian Meeting, Zaragoza, 1988*. 2. Sepaz, Zaragoza: 205-221.

TEYSSEN, T.A.L., 1984.— Sedimentology of the Minette ironstones of Luxembourg and Lorraine: a Jurassic subtidal sandwave complex. *Sedimentology*, **31**: 195-211.

TURKI, M.M., 1988.— Polycinématique et contrôle sedimentaire associé sur la cicatrice Zaghouan-Nebhana. *Revue des Sciences de la Terre*, **7**: 1-228.

VAIL, P.R., MITCHUM, R.M., TODD, R.G., WIDMERRI, J.W., THOMPSON, S., SANGRE, JH. B., BUBB, J.N. & HATFIED, W.G., 1977.— Seismic stratigraphy and global changes of sea level. *In*: Seismic stratigraphy application to hydrocarbon exploration. *Memoir- American Association of Petroleum Geologists*, **26**: 49-212.

VAIL, P.R., COLIN, J.P., JAN DU CHÊNE, R., KUCHLY, J., MEDIAVILLA, F. & TRIFILIEFF, V., 1987.— La Stratigraphie séquentielle et son application aux corrélations chronostratigraphiques dans le Jurassique du bassin de Paris. *Bulletin de la Société géologique de France*, **III** (7): 1301-1321.

VAN HOUTEN, F.B., 1985.— Oolitic ironstones and contrasting Ordovician and Jurassic paleogeography. *Geology*, **13**: 722-724.

WARME, J.E, 1988.— Jurassic carbonate facies of the Central and Eastern High Atlas rift, Morocco. *In*: V.H. JACOBSHAGEN (ed.), The Atlas system of Morocco studies on its geodynamic evolution. *Lectures and Notes in Earth-Sciences*, **15**: 169-199.

WILDI, W., 1983.— La Chaîne tello-rifaine (Algérie, Maroc, Tunisie): structure, stratigraphie et évolution du Trias au Miocène. *Revue de Géologie dynamique et de Géographie physique, Paris*, **24** (3): 201-297.

WOLFGANG, M., 1997.— Paleoecology and paleogeography of the Middle Jurassic ostracods of Southern Tunisia. *Paleogeography, Paleoclimatology, Paleoecology*, **131**: 65-111.

ZARBOUT, M. & GHANMI, M., 1997.— Aperçu sur la géologie de la feuille de Dhibet à 1/100.000, n° 32. *In*: *Sixièmes Journées de Géologie tunisienne: La carte géologique au service du développement durable, Résumés*. Office national des Mines de Tunisie, Tunis: 27-30.

Source : MNHN, Paris

5

The Tethys southern margin in Morocco; Mesozoic and Cainozoic evolution of the Atlas domain

Alain PIQUÉ [1], *Mohamed CHARROUD* [2], *Edgard LAVILLE* [3], *Lahcen AÏT BRAHIM* [4] & *Mustafa AMRHAR* [5]

(1) Département des Sciences de la Terre et IUEM, Université de Bretagne Occidentale
Place Nicolas Copernic, F-29280 Plouzané Cedex, France

(2) Département de Géologie, Faculté des Sciences et Techniques du Saïs, route d'Imouzzer, B.P 2202, Fès, Maroc

(3) Département de Géologie, Université de Caen, Esplanade de la Paix, B.P. 5186, F-14032 Caen Cedex, France

(4) Département de Géologie, Faculté des Sciences, Avenue Ibn Batouta, B.P. 1040, Rabat, Maroc

(5) Département de Géologie, Faculté des Sciences Semlalia, Boulevard Amir Moulay Abdallah, B.P. 2390, Marrakech, Maroc

ABSTRACT

As the central and southern Rif, the Atlas domain of Morocco constituted the southern margin of the Tethys during the Meso-and Cainozoic. Its polyphase development recorded the geodynamic evolution of the African plate and the correlative opening of the Tethys ocean: 1) the Late Triassic-earliest Liassic times have been characterised by the initiation and development of the NE-SW trending Atlasic rift which aborted during the early Liassic; 2) the Middle and High Atlas troughs, respectively NE-SW and WSW-ENE trending, developed in response to a sinistral transtensive motion along the N 70°E trending faults, inherited from the Hercynian orogeny; 3) the Atlasic inversion was realised in two times: by a sinistral transpressive deformation during the Late Jurassic-Early Cretaceous, and by the uplift of the chain during the Neogene.

RÉSUMÉ

La marge sud de la Téthys au Maroc : évolution du domaine atlasique au Mésozoïque et au Cénozoïque.

Tout comme le Rif central et sud, le domaine atlasique du Maroc constituait la marge méridionale de la Téthys au Mésozoïque et au Cénozoïque. Son développement a donc enregistré les étapes successives de l'évolution de la plaque Afrique et de l'ouverture de l'océan Tethysien, avec notamment : 1) le développement puis l'avortement du Rift atlasique, NE-SW, au Trias supérieur-Lias basal ; 2) l'individualisation des Sillons moyen- et haut-atlasique, respectivement NE-SW et WSW-ENE, en réponse à un mouvement transtensif sénestre le long de failles N 70°E héritées de l'orogenèse hercynienne ; 3) l'inversion atlasique, elle-même réalisée en deux temps : une transpression sénestre au Jurassique supérieur-Crétacé inférieur, et le soulèvement de la chaîne au Néogène.

PIQUÉ, A., CHARROUD, M., LAVILLE, E., AÏT BRAHIM, L. & AMRHAR, M., 2000.— The Tethys southern margin in Morocco ; Mesozoic and Cainozoic evolution of the Atlas domain. *In:* S. CRASQUIN-SOLEAU & É. BARRIER (eds), Peri-Tethys Memoir 5: new data on Peri-Tethyan sedimentary basins. *Mém. Mus. natn. Hist. Nat.*, **182** : 93-106. Paris ISBN : 2-85653-524-0.

Source : MNHN, Paris

INTRODUCTION

At the beginning of the Mesozoic, the Central Atlantic ocean opened between North America and Western Africa. The continental rift was limited to the east by the unstretched continental crust of the Central Moroccan Meseta and to the north by a transform fault zone which corresponds to the eastern prolongation of the present Azores-Gibraltar zone and represented at that time the northern limit of the individualising African plate (PIQUÉ & LAVILLE, 1996). This WNW-ESE to E-W transform fault separated east-travelling Africa from Eurasia (DERCOURT *et al.*, 1993) and it corresponded to the western end of the Tethys ocean, propagating to the west (Tethyan reconquest: AUBOUIN, 1980). Consequently, Morocco corresponded to a triple point, at the intersection of a NNE-SSW continental rift — the Central Atlantic rift — and the western extremity of the Tethys, between Africa and Eurasia. Later, the eastern passive margin of the Central Atlantic ocean remained undeformed, while the southern margin of the Tethys in Morocco was affected by the Alpine orogeny. Since this transform boundary has been intensively reworked and integrated in the allochthonous units of the Rif belt, it is not possible to reconstruct the Meso- and Cainozoic palaeogeographic evolution of the southern Tethysian platform. This evolution can, however, be studied south of the Alpine Rif belt, in the relatively weakly deformed and unmetamorphosed Atlas. The aim of the present paper is to analyse the Meso- and Cainozoic evolution of the Moroccan Atlas domain, especially in its central part, through the presentation of palaeogeographic maps drawn for several key-periods. A preliminary short presentation of the Hercynian basement structures will help to discuss their control on the Mesozoic palaeogeography.

THE PALAEOZOIC INHERITED STRUCTURES

In Morocco, except in its southernmost part, the Tindouf basin, which belongs to the West African craton, the Palaeozoic sedimentary series were deformed, metamorphosed and intruded by granitoids during the second half of the Palaeozoic (PIQUÉ & MICHARD, 1989). The resulting chain corresponds to and prolongates the Hercynian (=Variscan) belt of western Europe. Its main characteristics is the inhomogeneous nature of the regional deformation: intense folding and faulting and a relatively high grade metamorphic evolution concentrated along narrow and elongate regional shear zones that separate wider areas which remained poorly deformed. The most important of these regional shear zones (Fig. 1) are :

— the Atlas Palaeozoic transform zone (APTZ). Trending 70°E to E-W, it separates the Hercynian orogenic domain to the north from the pericratonic Anti-Atlas to the south. It acted with an important transcurrent component and its dip is generally steep;

— the Marrakech-Oujda shear zone, or lineament (MOL), which trends NE-SW, parallel to the axis of the eastern belt of the Moroccan Hercynian chain. It dips at low angle to the southeast;

— the Western Meseta shear zone (WMSZ), N 20°E, characterised locally by an important metamorphism and a strong deformation (PIQUÉ *et al.*, 1980). It corresponds to the western limit of the late Dinantian-Early Carboniferous Sidi-Bettache basin;

— the Sehoul shear zone, which trends E-W. It limits to the south the Sehoul "Caledonian" belt and it was reactivated during the Hercynian orogeny.

The last period of the Palaeozoic times, i.e. the Permian, is scarcely represented by red sandstones conglomerates and felsic lavas. All of these rocks, either sedimentary or magmatic, yielded Early Permian ages (e.g., BROUTIN *et al.*, 1989; YOUBI *et al.*, 1995; etc.) and, as far as we presently know, neither Late Permian nor Early Triassic are represented.

Source : MNHN, Paris

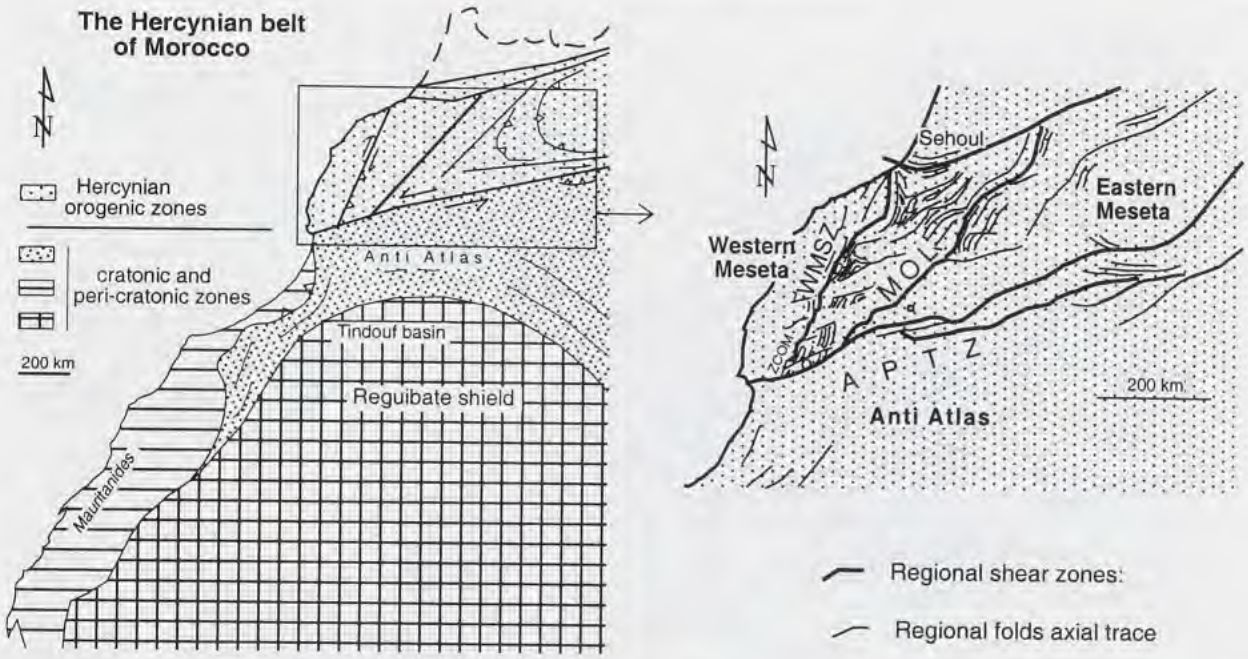

FIG. 1.— The Hercynian regional structures in Morocco. APTZ: Atlas Palaeozoic Transform Fault; MOL: Marrakech-Oujda Lineament; WMSZ: Western Meseta Shear Zone

FIG. 1.— Les structures hercyniennes d'importance régionale au Maroc. APTZ : Zone transformante paléozoïque de l'Atlas ; MOL : Linéament Marrakech-Oujda ; WMSZ : Zone cisaillée de Meseta occidentale.

LATE TRIASSIC-EARLY LIASSIC: THE ATLANTIC AND ATLASIC RIFTING

The Mesozoic sedimentary rocks known in Morocco unconformably cover the folded and eroded Palaeozoic rocks. The oldest Triassic sedimentary sequences are Carnian in age (locally late Ladinian in northeast Morocco: OUJIDI *et al.*, 1997). They are found: i) in faulted basins distributed in the present Atlantic margin. They correspond to the synsedimentary deposits of the Atlantic rift (LE ROY, 1997; LE ROY *et al.*, 1997) and they are not considered here; ii) in halfgrabens located from Middle to Central High Atlas (Fig. 2). Their active border faults, mainly NE-SW trending, are reactivated Hercynian thrusts and reverse faults (LAVILLE *et al.*, 1995). The left-lateral oblique faults like the Tizi n'Test fault correspond to Hercynian N 70° strike-slip faults (BEAUCHAMP, 1988). The synsedimentary activity of the halfgrabens is indicated by the facies distribution and the thickness lateral changes of the sedimentary sequences. The subsidence decreased during the Norian and the halfgraben border faults were sealed up by the lower Liassic carbonates. Contemporaneously with this crustal extension, tholeiitic magmas were emplaced (BERTRAND *et al.*, 1982) and a thermal flow occurred, indicated by the alteration of the uppermost Triassic-lowermost Liassic basalts and by the development of a very low grade paragenesis (BENCHEKROUN *et al.*, 1987), probably hydrothermal, dated at about 200 Ma (HUON *et al.*, 1993; CLAUER *et al.*, 1995; RAIS, work in progress). All of these structural, metamorphic and magmatic arguments suggest that an intracontinental rift, the Atlasic rift, developed from the Middle Atlas to Central High Atlas, in a NE-SW direction parallel to the Atlantic rift. Contrary to the Atlantic rift, which led to the oceanic accretion, the Atlasic rift aborted during the earliest Liassic.

The postrift early and mid-Liassic carbonate shelf extended over a large part of northern Morocco, far from the limits of the former Atlasic rift. During the Carixian for instance, various sedimentary facies characterised this shelf (Fig. 3):

— chert limestones which sometimes graded laterally to reefal buildings. These limestones are restricted to the axis of the future Atlasic troughs;

— oolitic limestones;

Source : MNHN, Paris

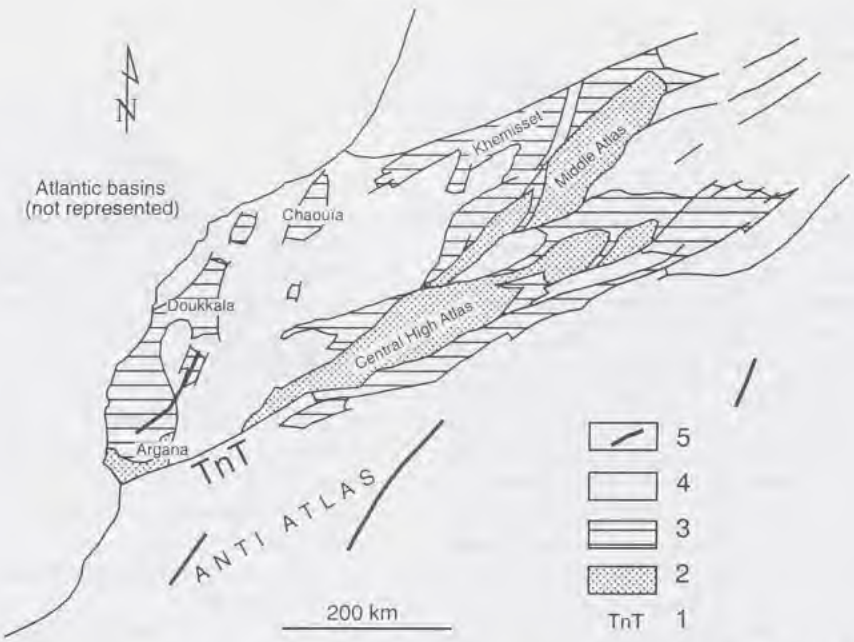

FIG. 2.— The Late Triassic-earliest Liassic Atlasic rift (from LAVILLE & PIQUÉ, 1991). **1**, TnT: Tizi n'Test Fault; **2**, Lower sequences (Carnian); **3**, Upper sequences (Norian); **4**, post-Triassic; **5**, doleritic dike.

*FIG. 2.— Le rift atlasique du Trias supérieur-Lias basal (d'après LAVILLE & PIQUÉ, 1991). **1**, Tnt : Faille du Tizi n'Test ; **2**, séries inférieures (Carnien) ; **3**, séries supérieures (Norien) ; **4**, terrains post-triasiques ; **5**, dykes doléritiques.*

— transitional facies: dolomitic limestones and shelly *Hesperithyris* limestones with argillaceous intercalations. These "Itzer beds" are located on some intrabasinal highs, as the Haute Moulouya threshold, in the Midelt area.

LATE LIASSIC-BATHONIAN: THE ATLAS TROUGHS

At the limit between the Domerian and the Toarcian, a transtensive fracturation of the former carbonate shelf occurred, individualising the Middle Atlas and High Atlas troughs made of coalescent lozange-shaped depocentres which were limited by synsedimentary normal and transcurrent faults, N 50°E in the Middle Atlas and N 70°E in the High Atlas (Fig. 4). The fracturation of the mid-Liassic shelf was contemporaneous with the beginning of the oceanic accretion in the Central Atlantic. At that time, the eastward drift of Africa was triggered, inducing new intracontinental stresses in the northern part of the Africa plate. As a result, the crustal weakness zones were reactivated in this new stress field and, as for the Late Triassic rifting episode, in many cases one can effectively demonstrate that the border faults of these basins correspond to Hercynian structures. This is obvious for the southern limit of the High Atlas basin, which corresponds to the former Atlas Palaeozoic transform fault, and for the southeastern limit of the Middle Atlas trough, parallel to the former Marrakech-Oujda shear zone.

In the two subsident troughs a thick pile of marine sedimentary sequences was deposited from the late Liassic to the end of Dogger, in contrast with thin or even absent contemporary deposits outside the troughs. The main sedimentary facies which characterise this period are:

— yellow cephalopods marls which often contain turbiditic horizons, deposited in the Atlasic trough axis;

— encrinitic limestones indicative of inner shelf conditions at the margins of the Atlasic troughs;

— red clays (Mibladen series), which were deposited in the Moulouya and Oranese Meseta areas in a lagoonal environment with tidal flats and frequent emersions.

Source : MNHN, Paris

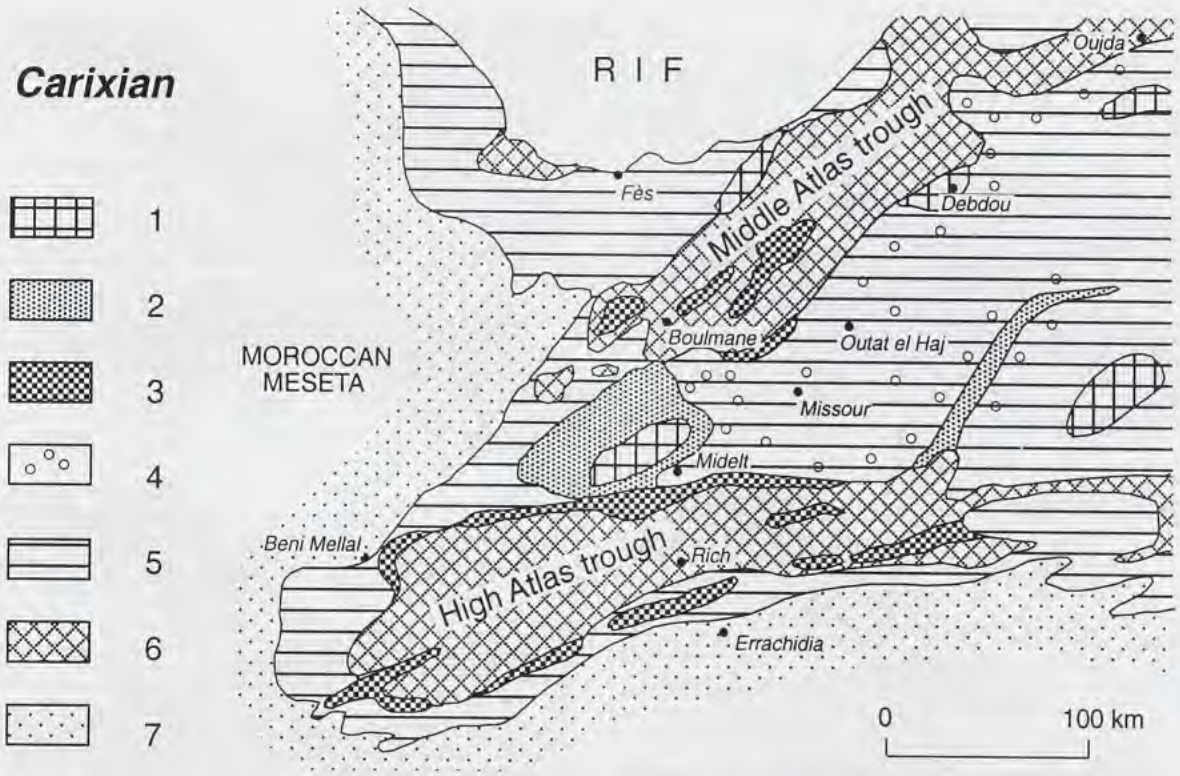

FIG. 3.— Palaeogeography of the central Atlasic domain during Carixian times from CHARROUD (unpublished). Location of the represented area: see Fig. 4. **1**, intrabasinal heights; **2**, transitional facies (Itzer beds); **3**, reefal formations; **4**, inner shelf; **5**, inner shelf : oolitic limestones with continental influences; **6**, outer shelf and basinal facies. Bedded and chert limestones; **7**, continental inland.

*FIG. 3.— Paléogéographie du domaine atlasique central au Carixien, d'après CHARROUD (inédit). Localisation de la zone représentée : voir Fig. 4. **1**, hauts-fonds ; **2**, faciès de transition (faciès d'Itzer) ; **3**, récifs ; **4**, plate-forme interne ; **5**, plate-forme interne : calcaires oolitiques à influences continentales ; **6**, plate-forme externe et faciès de bassin. Calcaires en plaquettes et à cherts ; **7**, terres émergées.*

The maximum depth of the basins was attained between the early Aaleno-Bajocian and the late Bajocian, with the deposition of deep basin facies: the early Aaleno-Bajocian *Posidonomya* Boulemane marls with turbiditic intercalations. The deposition of the late Bajocian, so-called "Calcaire corniche", a reefal and oolitic limestone indicative of open shelf environments, marked the progressive filling of the troughs. However, deep basin conditions persisted as long as the late Bajocian in the northeastern part of the Middle Atlas trough where they are represented by the "Marnes de Sakka supérieures".

In the Middle Atlas domain deposition of the the late Bajocian "Calcaire corniche" marked the beginning of the northeastward retreat of the sea. In the main part of the Atlas trough, the "Calcaire corniche" was covered by red beds, mostly aerial, deposited in a para-deltaic and deltaic system (Fig. 5). The numerous dinosaur tracks which were found in these strata indicate that they correspond to the Late Jurassic and part of the Early Cretaceous. The orientation of the palaeo-currents and the nature of the clasts suggest that they were originated from the Saharian domain like the contemporary Algerian Ksour sandstones (DELFAUD & ZELLOUF, 1993). However, other source lands were represented by several physiographically high areas which furnished relatively immature clasts. Meanwhile, marine conditions persisted in northeastern Morocco, where deep deltaic sediments were deposited (CATTANEO, 1991) and in the western part of the High Atlas, connected to the young Atlantic (e.g., AMRHAR, 1995).

From a structural point of view, the rhomboidal shape of the depocentres and the arcuate shape of the plutonic alkaline bodies (ZAYANE, 1992 and Fig. 6) emplaced in the central High Atlas during the Late Jurassic argue for a strong transcurrent, sinistral component in the Atlasic troughs along N 70°E faults (LAVILLE, 1988), perhaps associated with a normal N-S extension (WARME, 1988). In the eastern High

Source : MNHN, Paris

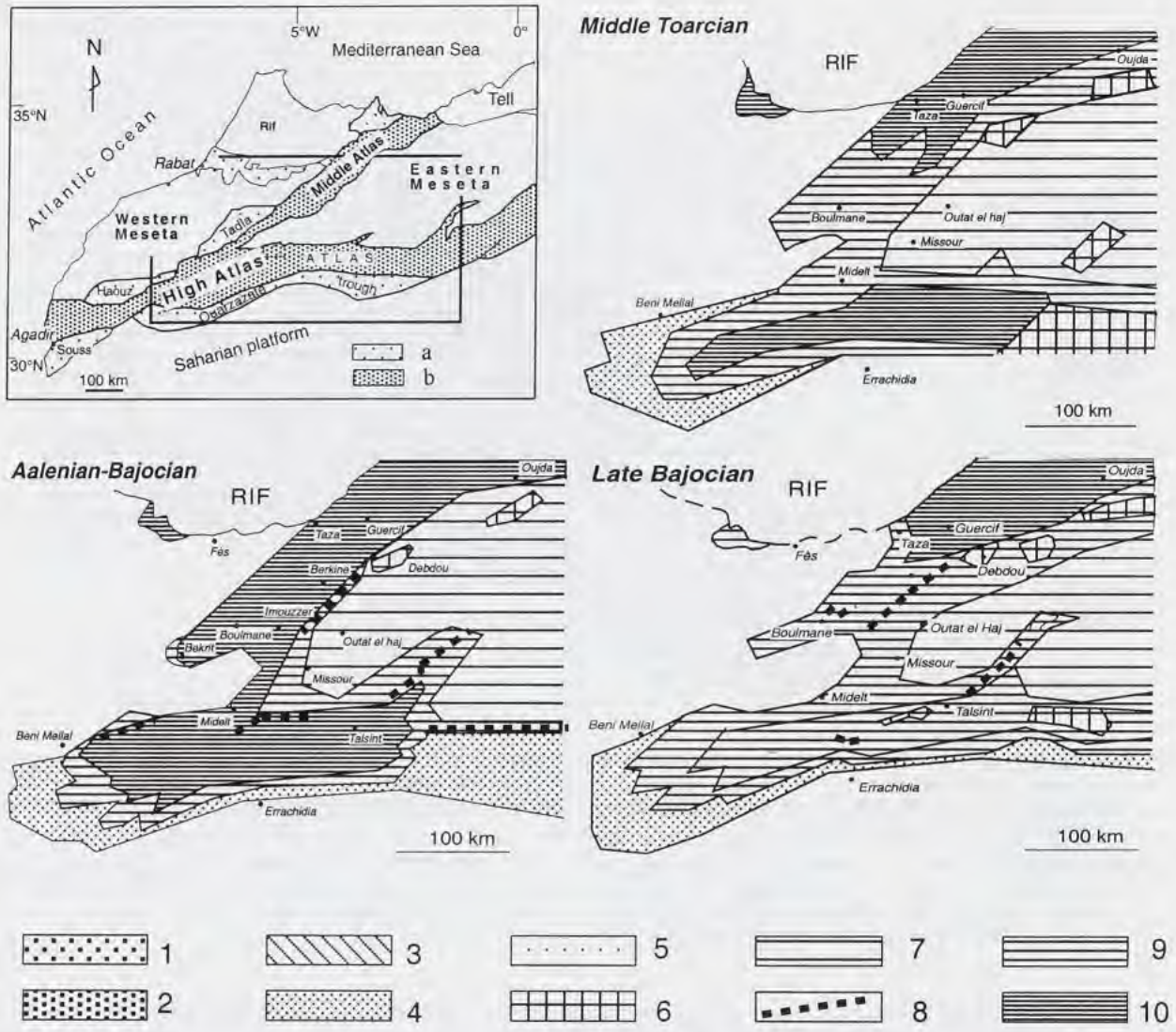

FIG. 4.— "Palaeostructural maps" of the central Atlasic domain from middle Toarcian to late Bajocian from CHARROUD (unpublished, modified). Cartoon: studied area; **a**, marginal basins; **b**, Atlasic belt. **1**, deltaic; **2**, paradeltaic; **3**, residual shelf; **4**, continental basins; **5**, emerged area; **6**, intrabasinal height; **7**, tidal flats and lagoonal facies; **8**, reefs; **9**, shelf; **10**, basin.

*FIG. 4.— "Cartes paléostructurales" du domaine atlasique central du Toarcien moyen au Bajocien supérieur d'après CHARROUD (inédit, modifié). Cartouche : zone étudiée ; **a**, bassins marginaux ; **b**, chaîne atlasique. **1**, deltaïque ; **2**, paradeltaïque ; **3**, plate-forme résiduelle ; **4**, bassins continentaux ; **5**, terres émergées ; **6**, hauts-fonds ; **7**, faciès lagunaires et tidal flats ; **8**, récifs ; **9**, plate-forme ; **10**, faciès de bassin.*

Atlas, El KOCHRI & CHOROWICZ (1996) suggested that the N 70°E trending faults were normal faults, connected by NW-SE transfer faults. On the other hand, it is important to note that the Palaeozoic basement is practically never represented in the Atlasic anticlines, where Triassic siltstones and/or plutonic massifs crop out. This suggests that the deformation of Central Atlas was coeval with a general décollement of the Mesozoic cover at the level of the Late Triassic sequences.

The main shortening in the Atlas axis was expressed by open folds locally accompanied by the development of an incipient cleavage (Fig. 8). It occurred during the Late Jurassic-Early Cretaceous, since the eroded hinges of some folds (in particular those which contain plutonic rocks) were unconformably covered by transgressive strata of late Early Cretaceous age (Fig. 7). This tectogenesis was not followed by any uplift of the mountain range.

Source : MNHN, Paris

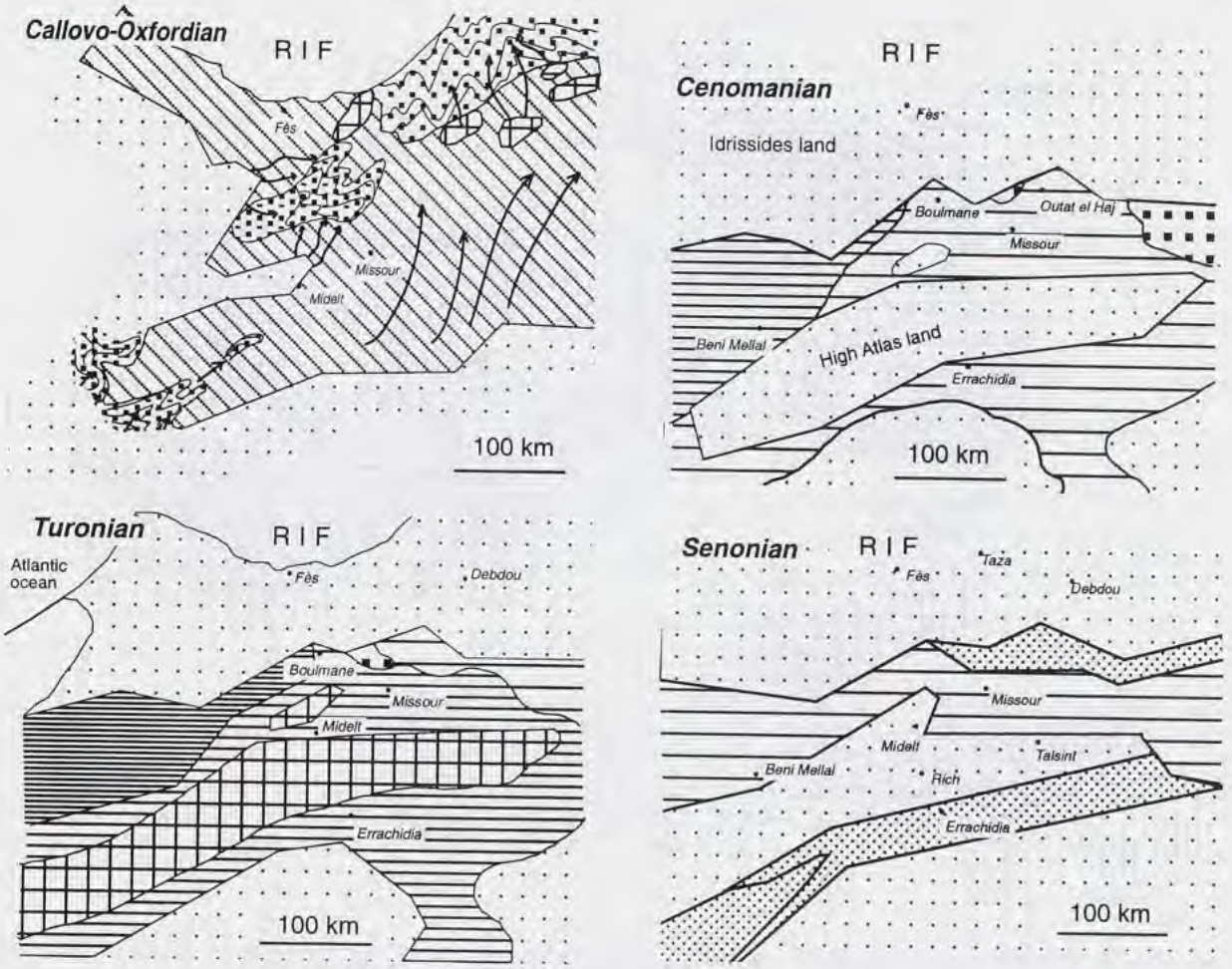

FIG. 5.— "Palaeostructural maps" of the central Atlasic domain from Callovo-Oxfordian to Senonian from CHARROUD (unpublished, modified). Same legend as Fig. 4.

FIG. 5.— "Cartes paléostructurales" du domaine atlasique central du Callovo-Oxfordien au Sénonien d'après CHARROUD (inédit, modifié). Même légende que Fig. 4.

THE EARLY-LATE CRETACEOUS AND PALAEOCENE-EOCENE

This period was dominated by the general eustatic transgression which, in Morocco, proceeded northeastward from the Atlantic and southwestward from the Tethys.

On the basis of sedimentological evidence (presence of marine sedimentary rocks in the western part of the Atlasic domain and littoral conditions in the east), the marine Albo-Aptian deposits of Beni-Mellal (Ouaouizart and Ait Attab basins) in the High Atlas and Boulemane (Tighboula-Oudiksou and Ain Nokra basins) in the Middle Atlas are classically considered as Atlantic-related, although faunal similarities would suggest Tethysian affinities (CHARRIÈRE & VILA, 1991).

Evaporitic sediments with colored marls and gypsum were deposited during the early and middle Cenomanian (Fig. 5). They grade westward into the marls and limestones of the inner carbonate shelf. During the late Cenomanian-early Turonian, the transgression attained its maximum and the shelf facies became homogeneous within the whole Atlasic domain. To the west, they covered the western Meseta although small areas remained however emerged. To the north, the Idrissides land (CHOUBERT & FAURE-MURET, 1962) constituted the northern border of the seaway.

Source : MNHN, Paris

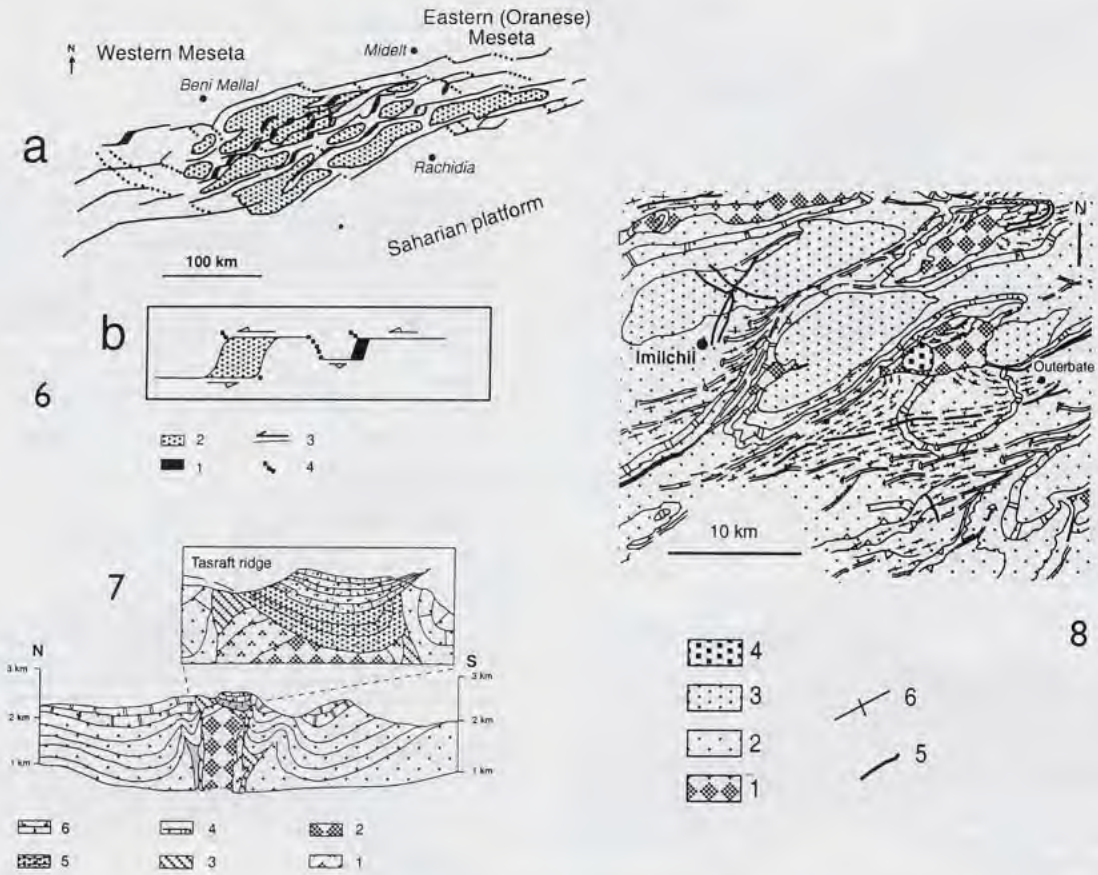

FIGS 6-8.— **6**.—The Atlasic structures in the central High Atlas. Depocentres and plutonic massifs in the central High Atlas (a) and schematic structural model of their distribution (b). From LAVILLE (1988). **1**, depocentre; **2**, plutonic massif; **3**, transcurrent fault; **4**, synsedimentary fold.
7.— The Tasraft ridge and anticline, central High Atlas, from LAVILLE (1988). **1**, Late Triassic-early Liassic doleritic basalts; **2**, Jurassic pluton; **3**, Triassic siltstones; **4**, Jurassic carbonates; **5**, Callovian-Lower Cretaceous; **6**, Upper Cretaceous.
8.— Distribution of the cleavage in the central High Atlas from LAVILLE *et al.*, (1991). **1**, pluton; **2**, Liassic to Bajocian; **3**, Bathonian; **4**, Upper Jurassic-Lower Cretaceous; **5**, cleavage trajectory; **6**, dyke.

*FIGS 6-8.— **6**.— Les structures atlasiques dans le Haut Atlas central. Dépocentres et massifs plutoniques dans le Haut Atlas central (a) et modèle structural schématique de leur disposition (b). D'après LAVILLE (1988). **1**, dépocentre ; **2**, massif plutonique ; **3**, faille transcurrente ; **4**, pli synsédimentaire.*
*7.— La ride et l'anticlinal de Tasraft, Haut Atlas central, d'après LAVILLE (1988). **1**, basaltes doléritiques du Trias terminal-Lias basal ; **2**, pluton jurassique ; **3**, siltites triasiques ; **4**, carbonates jurassiques ; **5**, Callovien-Crétacé inférieur ; **6**, Crétacé supérieur.*
*8.— Répartition de la schistosité dans le Haut Atlas central, d'après LAVILLE et al., 1991. **1**, pluton ; **2**, Lias à Bajocien ; **3**, Bathonien ; **4**, Jurassique supérieur-Crétacé inférieur ; **5**, trajectoires de la schistosité ; **6**, dyke.*

The Senonian palaeogeography remained practically similar to that of the Turonian, the facies changes resulting from the general regression. In the Atlasic domain, the fracturation of the Turonian shelf produced small basins where confined facies (bituminous marls) were deposited between uplifting and emerging areas characterised by phosphorite sediments (CHARROUD *et al.*, 1993). These Atlasic bituminous marls (BENALIOULHAJ, 1991) were coeval with the Western Meseta phosphoritic deposits indicative of the Atlantic shallow shelf. The Eocene marls, dolomites and gypsum are the last marine deposits in the Atlas domain, sometimes covered by sandstones attributed to the Oligocene.

Noteworthy is the emplacement of Eocene alkaline magmas in two massifs, Taourirt (AGARD, 1950) and Tamazert (BOUABDELI, 1987) of the Atlas domain (Fig. 9).

Source : MNHN, Paris

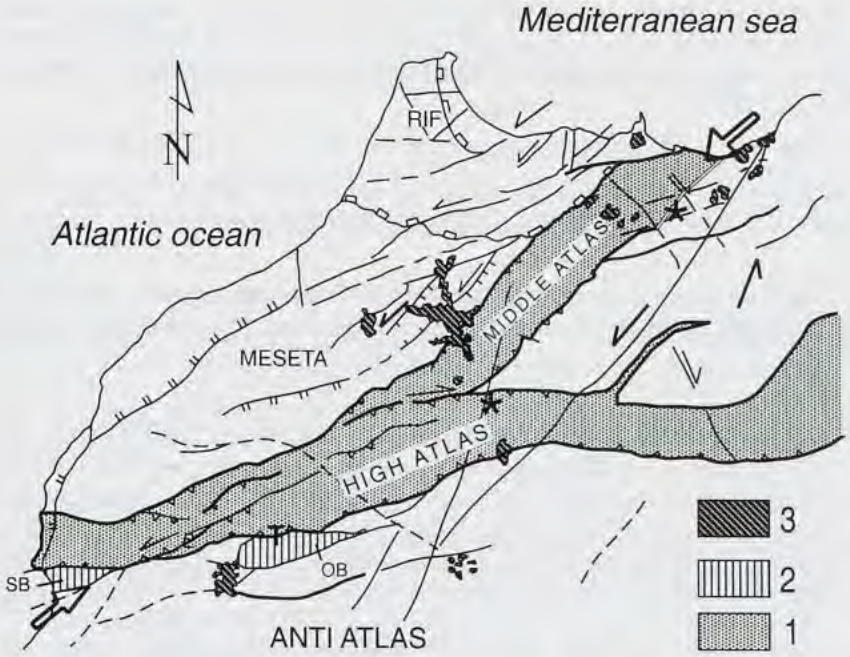

FIG. 9.— Eocene magmatic rocks, Neogene and Quaternary structures and volcanic rocks in the Atlasic domain (from AÏT BRAHIM, unpublished, modified). 1, Atlas belt; 2, Neogene basins (SB: Souss basin, OB: Ouarzazate basin); 3, Neogene alkaline volcanic rocks. Arrow: Transmoroccan lineament; T: Toundoute nappe; *: Eocene alkaline rocks.

*FIG. 9.— Roches magmatiques éocènes, structures néogènes et quaternaires dans le domaine atlasique (d'après AÏT BRAHIM inédit, modifié). **1**, Atlas ; **2**, Bassins néogènes (SB : Bassin du Souss ; OB : Bassin de Ouarzazate ; **3**, roches volcaniques alcalines néogènes ; Flèche : linéament transmarocain ; T : nappe de Toundoute ; * : roches alcalines éocènes.*

THE NEOGENE

In northern Morocco, the Africa-Europe convergence during the Neogene was at the origin of the Rif orogeny, with the development of south- and southwest-vergent nappes, HP metamorphism, etc. The late Miocene "post-nappes" basins of the Rif (e.g., AÏT BRAHIM & CHOTIN, 1989) register the successive stress fields acting from the Tortonian to Present.

Meanwhile, the Atlas domain reacted to the same regional N-S shortening. South of the High Atlas, the Souss and Ouarzazate basins filled up with detrital sandstones and conglomeratic sequences. At the base of the Ouarzazate sequences, the Hadida Formation (GÖRLER *et al.*, 1988) represents the Oligocene (and early Miocene?). The clasts have a southern (Anti-Atlas) origin. The overlying sequence, the Kandoula Formation, represents the early -(?)middle Miocene. It exhibits proximal alluvial fans originated from the north, registering henceforth the surrection of the High Atlas. Laterally, these clastic sequences correspond to the Toundoute pellicular and gravity-driven nappe (LAVILLE *et al.*, 1977), itself issued from the High Atlas domain. The upper part of the Kandoula Formation represents the middle Miocene-early Pleistocene and it is composed of fluviatile and torrential sequences of northern (High Atlas) origin. Final emplacement of the clastic sequences was contemporaneous with the development of flat-lying and south-vergent shear zones (OUTTANI *et al.*, 1995). The High Atlas northern border is represented by north-vergent, E-W trending reverse faults, with a right-lateral component (MOREL *et al.*, 1993).

Like the High Atlas, the Middle Atlas is limited by reverse faults, here NE-SW, often showing a left-lateral component (DUÉE *et al.*, 1977; LAVILLE & FEDAN, 1989). Some of them, e.g., the Ait Oufella fault at the southeastern limit of the Middle Atlas, are flat-lying thrusts related to a décollement at the base of the Mesozoic cover (MOREL *et al.*, 1993).

Source : MNHN, Paris

The Neogene and Quaternary volcanism is distributed along the Transmoroccan lineament (AÏT BRAHIM, 1986) which runs from Oujda to Agadir (Fig. 9). Its alkaline nature is attributed to a mantellic origin and its emplacement along the NE-SW axis has been related to the left-lateral motion along this lineament (PIQUÉ *et al.*, 1998a).

DISCUSSION AND CONCLUSIONS

The Moroccan Atlas displays several particular points which distinguish it from the other segments of the Maghrebian Atlas chain. Their enumeration sheds light on its particular geodynamic evolution.

THE ATLASIC RIFT OF MOROCCO AND THE DEVELOPMENT OF THE ATLASIC TROUGHS

WARME (1988) among others described the Jurassic "Atlasic rift" of Morocco as the result of N 70°E to E-W trending normal faults which merge into a crustal detachment zone weakly dipping to the North. A similar model was developed later for the Algerian Atlas (VIALLY *et al.*, 1994). Others argued, on the contrary, for an oblique opening of the Moroccan Atlasic basins. In the Middle Atlas and the central High Atlas, LAVILLE & PETIT (1984) and LAVILLE *et al.* (1995) showed that, since the end of Triassic times, the NE-SW Hercynian directions (e.g., the Marrakech-Oujda shear zone) were reactivated as normal faults which delimitated halfgrabens while the N 70°E to E-W faults (e.g., those which constituted the Atlas Palaeozoic Transform Zone) acted as sinistral transcurrent faults. Later, during Jurassic times, the distribution of the depocentres and the plutonic massifs suggest their en-échelon pattern along the sinistral transcurrent N 70°E trending faults.

The important lateral component of the motion along the N 70°E to E-W faults during the Jurassic, already proposed by MATTAUER *et al.* (1977), implies that the "Atlasic rift" of WARME (1988), SOUHEL *et al.* (1993) and CANÉROT *et al.* (1996) corresponds rather to a transtensive zone referred to above as the "Atlasic troughs". Between the northern limit of the Africa plate, parallel to the present Rif mountain, and the south-Atlasic line, the Atlas domain was a sinistral mega-shear zone where the development of the Middle and High Atlas troughs resulted from sinistral motions along the N 70°E to E-W faults, while the NE-SW faults acted preferentially as normal faults. At that time, the Atlasic domain was connected to the Atlantic, to the southwest, and the Tethys, to the northeast. The filling of the Atlasic troughs occurred during the end of the Jurassic, when the sinistral transcurrent, probably transtensive, movement decreased progressively.

THE CENTRAL ATLAS MAIN DEFORMATION

Along the axis of the High Atlas, the main tectogenesis, i.e. the development of the penetrative structures, occurred during the Late Jurassic-Early Cretaceous, certainly before the deposition of the marine Cretaceous sequences (LAVILLE & FEDAN, 1989). Since the Cretaceous transgression covered at least parts of the Atlas domain, it is clear that the orogenesis (i.e. the uplift of the Atlas mountain range) did not immediately follow its tectogenesis (LAVILLE *et al.*, 1991). The explanation for the absence of post-tectonic uplift is that the tectogenesis did not create a crustal thickening and a subsequent isostatic rebound, that is compatible with a transpressive regime for the Late Jurassic-Early Cretaceous tectonism.

Now, it is important to note that the Mesozoic shortening of the Moroccan Atlas did not affect the other segments of the Maghrebian Atlas which were deformed later, during the Eocene in Algeria (e.g., VIALLY *et al.*, 1994) and the Neogene in Tunisia (e.g., PHILIP *et al.*, 1986). Reasons for this diachronous deformation are not clear yet. The oblique convergence between Africa and Europe could have been realised earlier in Morocco, in front of the Iberian microplate, than in easternmore segments of the Atlas (PIQUÉ *et al.*, 1998b).

Source : MNHN, Paris

THE ALKALINE MAGMATISM IN THE ATLAS DOMAIN

The alkaline magmatic activity occurred during three periods in the Moroccan Atlas:

— during the Late Jurassic, alkaline magmas emplaced in the central High Atlas. The geometry of the small plutons suggests that they emplaced in connection with the sinistral transcurrent motion along N 70°E trending faults (Fig. 6);

— during the Eocene in the Taourirt and Tamazert massifs;

— during the Neogene and the Quaternary. The three main volcanic provinces, i.e. Oujda Mountains, Middle Atlas and Siroua are aligned along the NE-SW Transmoroccan lineament (Fig. 9).

The Jurassic alkaline rocks are not represented in the western nor the eastern High Atlas, but only in the Central High Atlas axis, along the former Atlasic rift. It is thus probable that their emplacement has been favoured, within the Atlas transcurrent domain, by the earlier crustal thinning previously realised during the Late Triassic-early Liassic rifting.

The Eocene and Neogene-Quaternary alkaline rocks are distributed along NE-SW trending zones. It is suggested that their emplacement is related to a N-S regional shortening, attributed to the Africa-Europe convergence.

THE ATLAS UPLIFT

In the course of the continuing Africa-Europe collision, the uplift of the High Atlas and at a lesser degree the Middle Atlas was due to the reactivation of the crustal faults in a roughly N-S compressive stress field (GOMEZ *et al.*, 1996). The High Atlas N 70°E faults acted then as reverse faults, north- and south-vergent thrusts developed along the borders of the chain, and a sinistral component was present on the Middle Atlas NE-SW faults.

In conclusion, the main tectonic event (i.e. the development of regional folds, themselves derived from sedimentary ridges and depocenters) in the Central Atlas was achieved prior to the deposition of the Cretaceous transgressive beds. It resulted from the adaptation of the Mesozoic cover to a transpressive reactivation of Hercynian faults and a general décollement of this cover from its Hercynian basement.

By contrast, along the Atlas borders, the main deformation occurred later, during Neogene times. It was characterised by reverse faults and flat-lying thrusts divergent with regard to the Atlas axis. The kilometric-scale thrusts (LAVILLE *et al.*, 1977; MOREL *et al.*, 1993; LOWELL, 1995; OUTTANI *et al.*, 1995; etc.) are of particular interest since they are the manifestation of a décollement tectonics, perhaps initiated during the Mesozoic and strongly reactivated during the Neogene. Whether or not they are limited to the Atlas borders or played a significative role in the deformation and the uplift of the whole chain is not determined yet.

ACKNOWLEDGEMENTS

The paper is the result of a grant from the Peri-Tethys program. It has been improved thanks to thorough scientific reviews made by Drs G. DUEE and D. FRIZON DE LAMOTTE and a careful editorial review by Dr. S. CRASQUIN-SOLEAU.

Source : MNHN, Paris

REFERENCES

AGARD, J., 1950.— Sur l'âge et le mode de gisement des aïounites et mestigmérites du Maroc oriental. *Notes et Mémoires du Service géologique du Maroc, Rabat*, **76**: 189-196.

AÏT BRAHIM, L., 1986.— La Zone de fracture trans-marocaine Agadir-Nekor: critères géophysiques, données de terrain et analyse de documents Landsat. *Bulletin de l'Institut scientifique de Rabat*, **10**: 27-40.

AÏT BRAHIM, L. & CHOTIN, P., 1989.— Genèse et déformation des bassins néogènes du Rif central (Maroc) au cours du rapprochement Europe-Afrique. *Geodinamica Acta*, **3**: 295-304.

AMRHAR, M., 1995.— *Tectonique et inversions géodynamiques postrift dans le Haut Atlas occidental. Structures, instabilités tectoniques et magmatismes liés à l'ouverture de l'Atlantique central et la collision Afrique-Europe*. Thèse, Université de Marrakech, Marrakech, Maroc: 1-253.

AUBOUIN, J., 1980.— De la tectonique des plaques à la genèse des chaînes de montagne. *Mémoire hors série de la Société géologique de France*, **10**: 163-180.

BEAUCHAMP, J., 1988.— Triassic sedimentation and rifting in the High Atlas (Morocco). *In*: W. MANSPEIZER (ed.), *Triassic-Jurassic Rifting: Continental Breakup and the Origin of the Atlantic Ocean and Passive Margins*. Elsevier, Amsterdam; Oxford; New-York: 477-497 (Developments in geotectonics; 22).

BENALIOULHAJ, N., 1991.— *Les Formations à phosphates et à schistes bitumineux du bassin des Oulad Abdoun et du bassin de Timahdit (Maroc): pétrographie, minéralogie, géochimie et environnement de dépôt*. Thèse, Université Louis Pasteur, Strasbourg, France: 1-238.

BENCHEKROUN, S., PIQUÉ, A., LUCAS, J., BESNUS, Y. & ROBILLARD, D., 1987.— Les Argiles triasiques au Maroc et leur évolution diagénétique et métamorphique. *Sciences géologiques, Bulletin*, **40**: 285-293.

BERTRAND, H., DOSTAL, J. & DUPUY, C., 1982.— Geochemistry of early Mesozoic tholeiites from Morocco. *Earth and Planetary Sciences Letters*, **58**: 225-239.

BOUABDELI, A., 1987.— *Étude pétrologique et géochimique des lamprophyres et roches associées de la région de Tamazert (Haut Atlas de Midelt, Maroc)*. Thèse, Université de Montpellier, Montpellier, France: 1-162.

BROUTIN, J., FERRANDINI, J. & SABER, H., 1989.— Implications stratigraphiques et paléogéographiques de la découverte d'une flore permienne euraméricaine dans le Haut Atlas occidental (Maroc). *Comptes Rendus de l'Académie des Sciences, Paris*, **308** (II): 1509-1515.

CANÉROT, J., SOUHEIL, A., EL HARIRI, K., BOUCHOUATA, A. & GHARIB, A., 1996.— Geodynamic evolution of the central High Atlas (Morocco). *In*: *30th International Geological Congress, Beijing*. Geological Publishing, House Beijing, Pekin: 1-190.

CATTANEO, G., 1991.— Évolution sédimentaire et paléogéographie du Jurassique supérieur et du Crétacé basal de l'avant-pays rifain oriental (Maroc). *Bulletin de la Société géologique de France*, **162**: 69-78.

CHARRIÈRE, A. & VILA, J.M., 1991.— Découverte d'Aptien marin à foraminifères dans le Moyen Atlas (Maroc): un golfe mésogéen à travers la "Terre des Idrissides"?. *Comptes Rendus de l'Académie des Sciences, Paris*, **313** (II): 1579-1586.

CHARROUD, M., AÏT SLIMANE, A. & FEDAN, B., 1993.— Répercussions de la tectonique locale et des transgressions-régressions atlantiques sur l'évolution crétacée et paléogène de la bordure sud-ouest du Moyen Atlas (Maroc). *In*: *14th International Meeting of Sedimentology, Marrakech, Avril 1993, Abstract*. Université de Marrakech, Marrakech: 97-98.

CHOUBERT, G. & FAURE-MURET, A., 1962.— Évolution du domaine atlasique marocain depuis les temps paléozoïques. *In*: Livre à la Mémoire de Paul Fallot. *Mémoires de la Société géologique de France, Paris*, **1**: 447-527.

CLAUER, N., RAIS, N., SCHALTEGGER, U. & PIQUÉ, A., 1995.— K-Ar systematics of clay-to-mica minerals in a multi-stage low-grade metamorphic evolution. *Chemical Geology (isotope geoscience section)*, **124**: 305-316.

DELFAUD, J. & ZELLOUF, K., 1993.— Existence, durant le Jurassique et le Crétacé inférieur, d'un Paléo-Niger coulant du sud vers le nord au Sahara occidental. *In*: *4ème Colloque de Géologie africaine, Pau*. Comité des Travaux historiques et scientifiques, Paris: 93-104.

DERCOURT, J., RICOU, L.E. & VRIELYNCK, B., 1993.—*Atlas Tethys Paleoenvironmental Maps*. Gauthier-Villars, Paris: 1-307, 14 maps, 1 pl.

DUÉE, G., HERVOUET, Y., LAVILLE, E., LUCA, P. DE & ROBILLARD, A., 1977.— L'Accident nord-Moyen Atlasique dans la région de Boulemane (Maroc): une zone de coulissement synsédimentaire. *Annales de la Société géologique du Nord*, **98**: 145-162.

EL KOCHRI, A. & CHOROWICZ, J., 1996.— Oblique extension in the Jurassic trough of the Central and Eastern High Atlas (Morocco). *Journal of Canadian Earth-Sciences*, **33**: 84-92.

GOMEZ, F., BARAZANGI, M. & BENSAÏD, M., 1996.— Active tectonism in the Middle Atlas mountains of Morocco: synchronous shortening and extension. *Journal of the Geological Society, London*, **153**: 389-402.

GÖRLER, K., HELMDACH, F.F., GAEMERS, P., HEISSIG, K., HINSCH, W., MÄDLER, K., SCHWARZHAUS, W. & ZUCHT, M., 1988.— The Uplift of the central High Atlas as deduced from Neogene continental sediments of the Ouarzazate province, Morocco. *In*: V.H. JACOBSHAGEN (ed.), The Atlas system of Morocco studies on its geodynamic evolution. *Lectures and Notes in Earth-Sciences*, **15**: 361-404.

Source : MNHN, Paris

HUON, S., CORNÉE, J.J., PIQUÉ, A., RAIS, N., CLAUER, N., LIEWIG, N. & ZAYANE, R., 1993.— Mise en évidence au Maroc d'événements thermiques d'âge triasico-liasique liés à l'ouverture de l'Atlantique. *Bulletin de la Société géologique de France*, **164**: 165-176.

LAVILLE, E., 1988.— A Multiple releasing and restraining stepover model for the Jurassic strike-slip basin of the Central High Atlas (Morocco). *In*: W. MANSPEIZER (ed.), *Triassic-Jurassic Rifting: Continental Breakup and the Origin of the Atlantic Ocean and Passive Margins*. Elsevier, Amsterdam; Oxford; New-York: 499-523 (Developments in geotectonics; 22).

LAVILLE, E., LESAGE, J.L. & SEGURET, M., 1977.— Géométrie, cinématique (dynamique) de la tectonique atlasique sur le versant sud du Haut Atlas marocain. Aperçu sur les tectoniques hercyniennes et tardi-hercyniennes. *Bulletin de la Société géologique de France*, **19** (7): 527-539.

LAVILLE, E. & PETIT, J.P., 1984.— Role of synsedimentary strike-slip faults in the formation of Moroccan Triassic basins. *Geology*, **12**: 424-427.

LAVILLE, E. & FEDAN, B., 1989.— Le Système atlasique marocain au Jurassique: évolution structurale et cadre géodynamique. *Sciences géologiques, Strasbourg, Mémoires*, **84**: 3-28.

LAVILLE, E. & PIQUÉ, A., 1991.— La Distension crustale atlantique et atlasique au Maroc au début du Mésozoïque: le rejeu des structures hercyniennes. *Bulletin de la Société géologique de France*, **162** (6): 1161-1171.

LAVILLE, E., FEDAN, B. & PIQUÉ, A., 1991.— Déformation synschisteuse jurassique, orogenèse cénozoïque: deux étapes de la structuration du Haut Atlas (Maroc). *Comptes Rendus de l'Académie des Sciences, Paris*, **312** (II): 1205-1211.

LAVILLE, E., CHARROUD, A., FEDAN, B., CHARROUD, M. & PIQUÉ, A., 1995.— Inversion négative et rifting atlasique: l'exemple du bassin triasique de Kerrouchène (Maroc). *Bulletin de la Société géologique de France*, **166**: 364-374.

LE ROY, P., 1997.— *Les Bassins ouest-marocains; leur formation et leur évolution dans le cadre de l'ouverture et du développement de l'Atlantique central (marge africaine)*. Thèse, Université de Bretagne occidentale, Brest, France: 1-327.

LE ROY, P., PIQUÉ, A., LE GALL, B., AÏT BRAHIM, L., MORABET, M. AL. & DEMNATI, A., 1997.— Les Bassins côtiers triasico-liasiques du Maroc occidental et la diachronie du rifting intra-continental de l'Atlantique central. *Bulletin de la Société géologique de France*, **168**: 637-648.

LOWELL, J., 1995.— Mechanics of basin inversion from worlwide examples. *In* : J. BUCHANAN & P. BUCHANAN (eds), Basin inversion. *Special Publication- Geological Society of London*, **88**: 39-57.

MATTAUER, M., TAPPONNIER, P. & PROUST, F., 1977.— Sur les mécanismes de formation des chaînes intracontinentales: l'exemple des chaînes atlasiques du Maroc. *Bulletin de la Société géologique de France*, **7, 19** (3): 521-526.

MOREL, J.L., ZOUINE, E.M. & POISSON, A., 1993.— Relations entre la subsidence des bassins moulouyens et la création des reliefs atlasiques (Maroc): un exemple d'inversion tectonique depuis le Néogène. *Bulletin de la Société géologique de France*, **164**: 79-91.

OUJIDI, M., COUREL, L., BENAOUISS, N., EL MOUSTAINE, M., EL YOUSSI, M., ET TOUHAMI, M., JALIL, N., OUAHRACHE, D., SABAOUI, A. & TOURANI, A., 1997.— La Marge péri-téthysienne marocaine pendant le Trias. *In*: *Les Marges téthysiennes d'Afrique du Nord: séance spécialisée 16-17 décembre 1997*. Société géologique de France, Paris: 34.

OUTTANI, F., ADDOUM, B., MERCIER, E., FRIZON DE LAMOTTE, D. & ANDRIEUX, J., 1995.— Geometry and kinematics of the South Atlas Front (Algeria-Tunisia). An analysis emphasising the structural role of the fault-propagation folds. *Tectonophysics*, **249**: 233-248.

PHILIP, H., ANDRIEUX, J., DLALA, M., CHIHI, L. & BEN AYED, N., 1986.— Évolution tectonique mio-plio-quaternaire du fossé de Kasserine (Tunisie centrale): implications sur l'évolution géodynamique récente de la Tunisie. *Bulletin de la Société géologique de France*, **8** (4): 559-568.

PIQUÉ, A., JEANNETTE, D. & MICHARD, A., 1980.— The Western Meseta Shear Zone, a major and permanent feature of the Hercynian belt of Morocco. *Journal of Structural Geology*, **2**: 55-61.

PIQUÉ, A. & MICHARD, A., 1989.— Moroccan Hercynides: a synopsis. The Palaeozoic sedimentary and tectonic evolution at the northern margin of West Africa. *American Journal of Science*, **289**: 286-330.

PIQUÉ, A. & LAVILLE, E., 1996.— The Central Atlantic rifting: reactivation of Palaeozoic structures?. *Journal of Geodynamics*, **21**: 235-255.

PIQUÉ, A., AÏT BRAHIM, L., EL AZZOUZI, M'H., MAURY, R., BELLON, H., SEMROUD, B. & LAVILLE, E., 1998a.— Le Poinçon maghrébin: contraintes structurales et géochimiques. *Comptes Rendus de l'Académie des Sciences, Paris*, **326**: 575-581.

PIQUÉ, A., AÏT BRAHIM, L., AÏT OUALI, R., AMRHAR, M., CHARROUD, M., GOURMELEN, C., LAVILLE, E., REKHISS, F. & TRICART, P., 1998b.— Évolution structurale des domaines atlasiques du Maghreb au Méso- et Cénozoïque; le rôle des structures héritées dans la déformation du domaine atlasique de l'Afrique du Nord. *Bulletin de la Société géologique de France*, **169**: 797-810.

SOUHEL, A., CANÉROT, J., BOUCHOUATA, A., CHAFIKI, D., EL HARIRI, K. & GHARIB, A., 1993.— Le Rift atlasique sur la transversale de Beni-Mellal (Haut Atlas central). VI. Essai de synthèse géodynamique. *In*: *14th International Meeting of Sedimentology, Marrakech, Avril 1993, Abstract*. Université de Marrakech, Marrakech: 305-306.

VIALLY, R., LETOUZEY, J., BENARD, F., HADDADI, N., DESFORGES, G., ASKRI, H. & BOUDJEMA, A., 1994.— Basin inversion along the North African margin: the Saharan Atlas (Algeria). *In*: F. ROURE (ed.), *Peri-Tethyan Platforms: Proceeding of the IFP Peri-Tethys Research Conference held in Arles, France, March 23, 1993*. Technip, Paris: 79-118.

Source : MNHN, Paris

WARME, J.E., 1988.— Jurassic carbonate facies of the Central and Eastern High Atlas rift, Morocco. *In*: V.H. JACOBSHAGEN (ed.), The Atlas system of Morocco studies on its geodynamic evolution. *Lectures and Notes in Earth-Sciences*, **15**: 169-199.

YOUBI, N., CABANIS, B., CHALOT-PRAT, F. & CAILLEUX, Y., 1995.— Histoire volcano-tectonique du massif permien de Khenifra (Sud-Est du Maroc central). *Geodinamica Acta*, **8**: 158-172.

ZAYANE, R., 1992.— *La Série plutonique du Haut Atlas central marocain (région d'Imilchil): pétrographie et géochimie; aspects métamorphiques et structuraux de sa mise en place*. Thèse, Université de Bretagne occidentale, Brest, France: 1-201.

Source : MNHN, Paris

6

The Southern Tethyan margin in Northeastern Morocco; sedimentary characteristics and tectonic control

Pierre CHOTIN [1], *Lahsen* AÏT BRAHIM [2] & *Hassan* TABYAOUI [2]

(1) Université Pierre et Marie Curie, Département de Géotectonique, Tour 26-16, E1
4, place Jussieu, F-75252 Paris Cedex 05, France

(2) Université Mohamed V, Département de Géologie, Avenue Ibn Batouta, Rabat, Maroc

ABSTRACT

Palaeostress analysis in northeastern Morocco allows the reconstruction of the tectonic and palaeogeographic evolution of northeastern Morocco from Triassic to Eocene. The studied area is part of the West African Tethyan margin. From field work and from space imagery analysis, we establish maps of the main regional faults and examine their movement in each succeeding tectonic phase. Stress tensor calculation has showed that these faults acted as normal faults during the period comprised between the Triassic and the Late Cretaceous. The extensive stress was oriented NNW-SSE to N-S during the Triassic and NNW-SSE to N-S and E-W during the Late Jurassic to the Early Cretaceous. During the Liassic and the Dogger the faults created horsts and grabens structure on the Tethyan margin and from Late Jurassic to Early Cretaceous, north verging tilted blocks appeared. In the Late Cretaceous sequences, a strike-slip tectonic regime prevailed. The calculated tensors show a maximal compressive stress oriented E-W. A last stress pattern reconstructed from faults in the Eocene formations gives a maximal compressive stress oriented N-S. Three successive stages mark the evolution of the Tethyan margin: the creation of an horts and grabens structured margin during the Triassic and the related effusion of basalts; a transgression during the Liassic accompanied by an important subsidence; the creation of a tilted blocks structured margin from Late Kimmeridgian to Early Cretaceous. At the end of the Early Cretaceous the whole region emerged. During the Late Cretaceous a compressive stress regime led to the formation of ENE-WSW and NW-SE strike-slip faults and N020° folds. Finally, during the Eocene, a compressive event created NNE-SSW and NW-SE strike-slip faults and ENE-WSW to E-W folds. In conclusion, the northeast Moroccan margin of the Tethys evolved during the period comprised between the Triassic to the Early Cretaceous as a passive margin related to the breakup of the Pangea and the opening of the Atlantic and Atlasic domains. This margin evolved later in an active compressed zone from Late Cretaceous to Neogene.

CHOTIN, P., AÏT BRAHIM, L. & TABYAOUI, H., 2000.— The Southern Tethyan margin in Northeastern Morocco; sedimentary characteristics and tectonic control. *In*: S. CRASQUIN-SOLEAU & É. BARRIER (eds), Peri-Tethys Memoir 5: new data on Peri-Tethyan sedimentary basins, *Mém. Mus. natn. Hist. nat.*, **182** : 107-128. Paris ISBN : 2-85653-524-0.

Source : MNHN, Paris

RÉSUMÉ

La marge sud-téthysienne au Maroc nord-oriental : caractéristiques sédimentaires et contrôle tectonique.

L'analyse des paléocontraintes dans le Maroc nord-oriental permet de reconstruire l'évolution tectonique et paléogéographique de ces régions, du Trias à l'Eocène. La zone étudiée fait partie de la marge téthysienne nord-africaine. Nous avons établi la carte des failles principales à partir de travaux sur le terrain et de l'analyse des images spatiales et nous avons examiné leur mouvement au cours de chaque phase tectonique. Ces failles ont un mouvement normal entre le Trias et le Crétacé supérieur. La contrainte en extension est alors orientée NNW-SSE à N-S pendant le Trias et NNW-SSE à N-S et E-W pendant la période qui s'étend du Jurassique supérieur au Crétacé inférieur. Au cours du Lias et du Dogger, des horsts et grabens se forment sur la marge téthysienne et, du Jurassique supérieur au Crétacé inférieur, des blocs basculés à vergence Nord y apparaissent alors. Dans les séries du Crétacé supérieur, c'est un régime tectonique en décrochement qui se met en place. Les tenseurs calculés montrent que la contrainte compressive est orientée E-W au cours de cette période. Enfin, dans les formations éocènes nous observons une contrainte compressive orientée N-S. Le contrôle tectonique de l'évolution de la marge téthysienne nous permet de reconnaître le scénario suivant : la création d'une marge structurée en horst et grabens pendant le Trias et l'effusion simultanée de basaltes ; une transgression au cours du Lias accompagnée par une importante subsidence ; la création de blocs basculés du Jurassique supérieur au Crétacé inférieur. A la fin du Crétacé inférieur, la région émerge. Au cours du Crétacé supérieur, une phase compressive conduit à la formation de failles décrochantes orientées NNE-SSW et NW-SE ainsi que de plis orientés ENE-WSW à E-W. En conclusion, la marge téthysienne du Maroc nord-oriental évolue du Trias au Crétacé inférieur comme une marge passive en relation avec la rupture de la Pangée et l'ouverture des domaines atlantique et atlasique. Cette marge évolue en zone de compression au cours du Crétacé supérieur et de l'Eocène.

INTRODUCTION

The studied area is located in northeastern Morocco (Fig. 1), between the Oranesan meseta in the south and the Rif-Tell belt in the north. Within this area, the Beni Snassen mounts are located in the

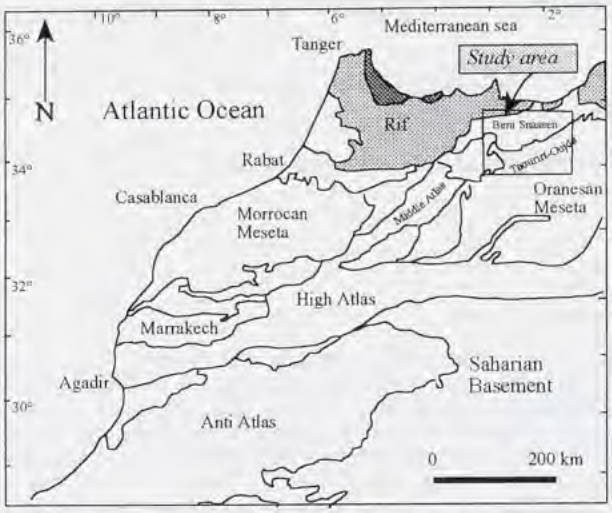

FIG. 1.— Geographical map with the studied area in northeastern Morocco.

FIG. 1.— Carte géographique et situation de la zone étudiée dans le Maroc nord-oriental.

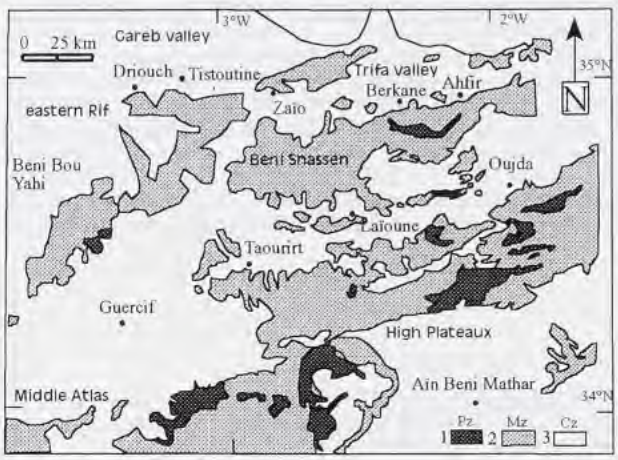

FIG. 2.— Geological sketch map of the studied area. **1**, Palaeozoic basement; **2**, Mesozoic sediments; **3**, Cainozoic sediments.

FIG. 2.— Schéma géologique de la zone étudiée. 1, socle paléozoïque ; 2, sédiments mésozoïques ; 3, sédiments cénozoïques.

Source : MNHN, Paris

north, and the Taourirt-Oujda mounts in the south, following an ENE-WSW direction over a distance between 80 to 120 km and are separated by the Taourirt-Oujda basin (Fig. 2). These mounts are essentially constituted by a Mesozoic sedimentary cover (an average altitude of 1200 m) in which the Palaeozoic appears in antiforms. In the east, we find the Tlemcen mounts (outside the map, in the Algerian regions) and in the west, the Beni Bou Yahi mounts and the Guercif basin (Fig. 2). Previous studies in the region were largely concerned with the biostratigraphy and the sedimentology of the Triassic to Early Cretaceous series (CATTANEO, 1984, 1987, 1991; NACIRI, 1994; OUAHHABI, 1994; OUJIDI, 1994; MEHDI, 1995; OUAHBI, 1996). These detailed studies have greatly increased the understanding of the organisation and dating of the different sedimentary facies.

The cartography of faults in this region is based on the analysis of Landsat, SPOT and ERS1 SAR space imagery (AÏT BRAHIM *et al.*, 1994, 1996; TABYAOUI *et al.*, 1996) and field work (Fig. 3). The aim of this paper is, (1) to constrain the timing of the tectonic evolution, (2) to clarify the tectonic control of sedimentation, (3) to determine the succession of palaeostress fields and (4) to relate these data with geodynamic setting.

REVIEW OF THE SEDIMENTARY CARACTERISTICS OF THE TETHYAN SERIES

THE TRIASSIC PERIOD

The Triassic deposits contain red beds with a coarse detritical basal level composed of Palaeozoic elements, overlaying unconformably the hercynian basement (Fig. 4). This sedimentation has been perturbed by the effusion of volcanic dolerites (BERTRAND & PRIOTON, 1975; CHEROTSKY, 1973; OUJIDI, 1994) and basalts (LAPIERRE *et al.*, 1984) which are 215 Ma old (MANSPEIZER *et al.*, 1978). This tholeiitic magmatism originated under tidal conditions characteristic of brackish water domain (COGNEY & FAUGÈRES, 1975). This can be deduced from the presence of inter-stratified dolomitic limestones containing gasteropods and lamellibranchs in particular *Annaplophora littica* Quenst. of the late Ladinian (OWODENKO, 1946). The distribution and thickness of the Triassic series testify to a palaeo-relief, structured by relatively rapid subsident zones (Taourirt, Oujda and Tiouli areas) (Fig. 3) and by shallow zones. Outside these areas, the deposits are either very reduced, corresponding to local palaeoreliefs (Tanouralt and Bourdine areas) (Fig. 3), or are absent (uplifted blocks of Touissit, Rhar Roubane, Debdou and Boudoufoud).

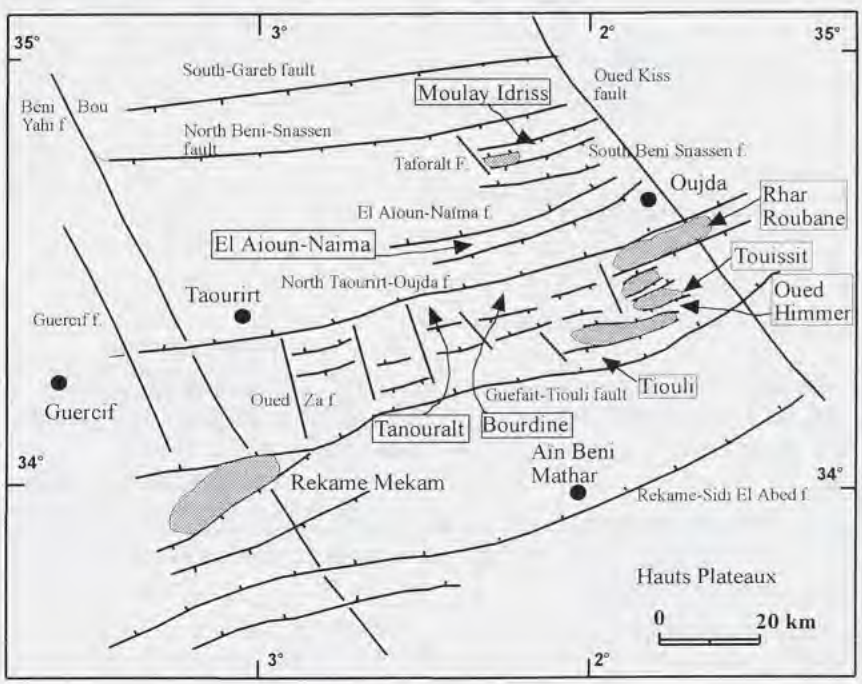

FIG. 3.— Map of the faults identified by space imagery analysis and field observations. Location of the horsts and grabens.

FIG. 3.— Carte des failles identifiées par l'imagerie spatiale et les observations de terrain. Localisation des horsts et grabens.

Source : MNHN, Paris

THE EARLY JURASSIC PERIOD

The installation of a uniform and shallow carbonate shelf took place during the early Liassic. It is characterised by the deposition of conglomerates and limestones (Fig. 4). The nature and the distribution of these deposits reflect the persistence of palaeo-highs as in the northern part of the Beni Snassen mounts (CATTANEO, 1987; NACIRI, 1994) and in the Touissit, Titeft and Debdou areas (Fig. 3).

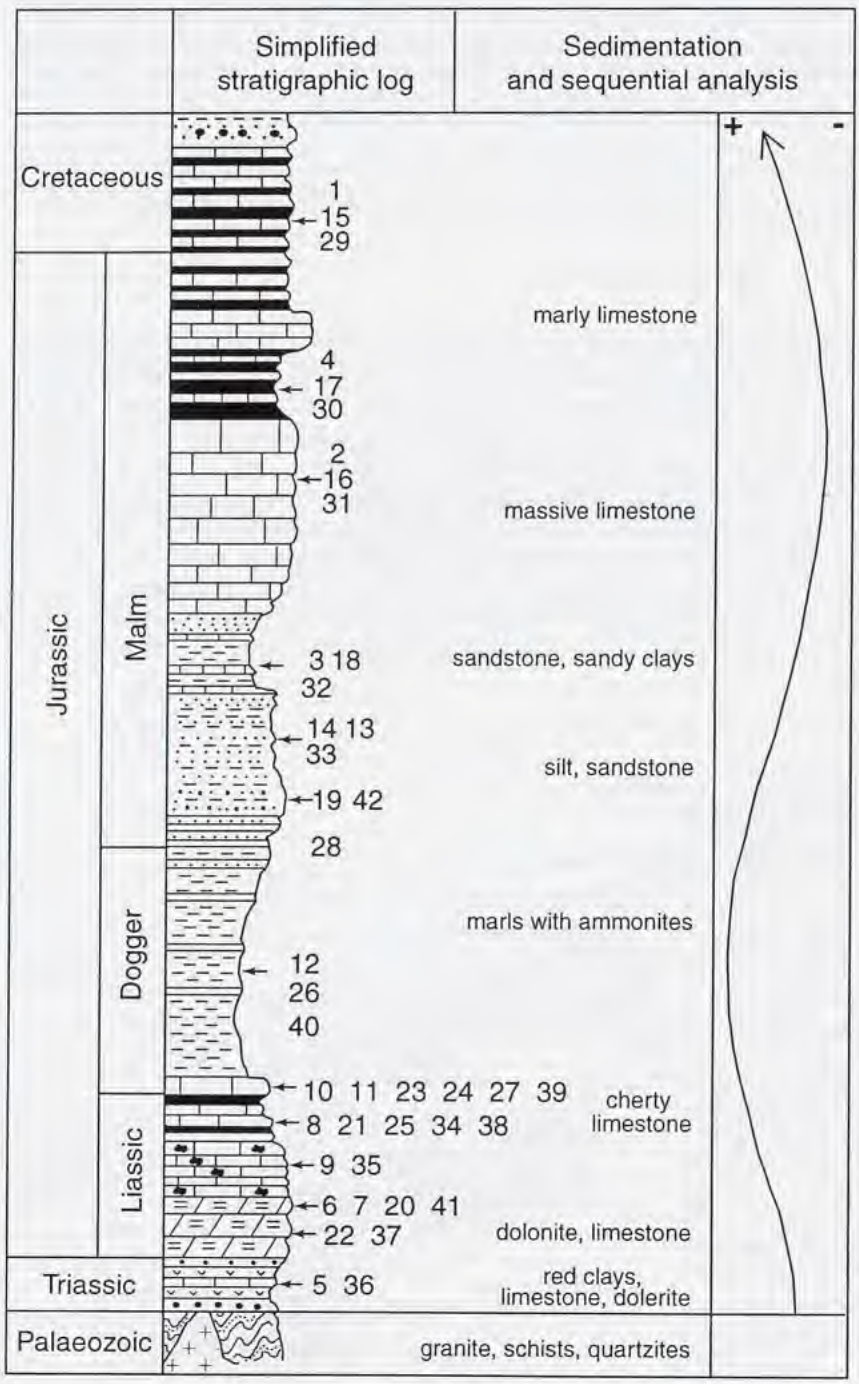

FIG. 4.— Lithostratigraphic column and simplified sequencial analysis of the Mesozoic formations in northeastern Morocco (CATTANEO, 1987).

FIG. 4.— Colonne lithostratigraphique et analyse séquentielle simplifiée des formations mésozoïques du Maroc nord-oriental (CATTANEO, 1987).

Source : MNHN, Paris

During the Carixian times, this carbonated shelf changed (Fig. 5). In the Beni Snassen area, three zones of deposits develop from north to south. In the north, the first zone now presents proximal platform facies where we find Megalodontidae limestones; in the central part, the second one shows facies of external, proximal to distal platform represented by cherty limestones and the third one, in the south presents deep deposits of external platform of mud type (CATTANEO, 1987; NACIRI, 1994). In the Taourirt-Oujda area, the cherty limestone facies testifies to a north and westwards deepening. To the east and to the south, limestones of shallow intra- to supratidal environment are found (limestones with Megalodontidae, oolitic limestones, subrecifal limestones). Their thickness decreases quickly to the Touissit horst (Fig. 3). Further to the south, a brackish water domain sets up in the High Plateaux.

The Domerian time is characterised by a general spreading of the transgression. The deposit environment is now becoming increasingly deeper and is evolving in an outer carbonaceous shelf or basin. In the Taourirt-Oujda axis and in the Beni Snassen area, a marly limestone facies with ammonites can be found. South and northwards, the deposits are replaced by a reduced sequence of limestones and dolomites of outer distal shelf. Southwards, in the High Plateaux, clays and red marls are deposited in a inner epi-continental shelf.

The Toarcian time is characterised by the "ammonitico-rosso" facies developed in an outer shelf environment. We find it in the Beni Snassen area and in the Taourirt-Oujda axe. Southwards, the deposits consist of marls and sandy limestones of shallow distal shelf with a strong continental influence.

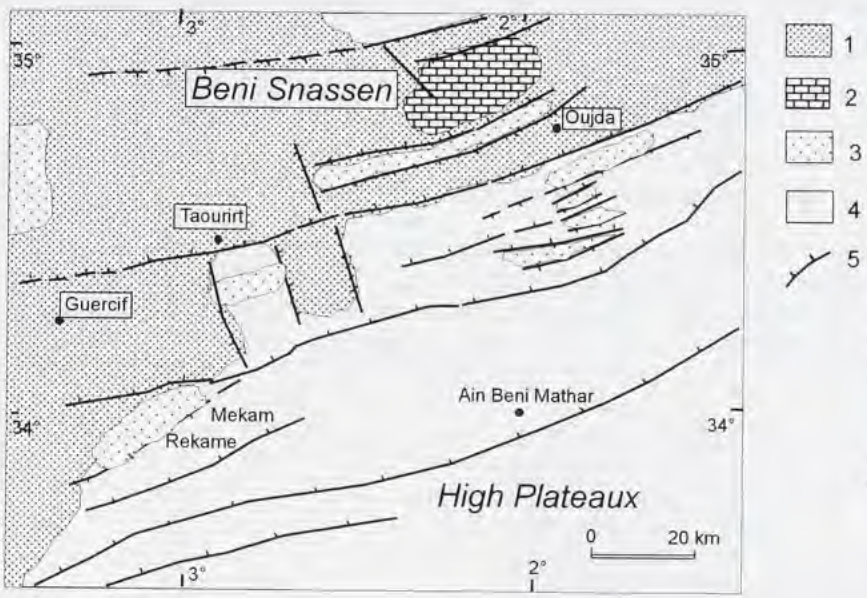

FIG. 5.— Palaeogeographical map during the Carixian. **1**, proximal shelf; **2**, outer shelf; **3**, epi-continental shelf; **4**, emerged land; **5**, faults.

*FIG. 5.— Carte paléogéographique au Carixien. **1**, plate-forme proximale ; **2**, plate-forme externe ; **3**, plate-forme épicontinentale ; **4**, terres émergées ; **5**, failles.*

THE MIDDLE JURASSIC PERIOD

During the Aalenian and the middle Bajocian times, the decrease of subsidence in the Taourirt-Oujda area permitted the development of inner to supratidal shelf facies (Fig. 4). north and westwards of the Taourirt-Oujda axis, these facies changed into *Zoophycos* marls and black limestones deposited in an open outer shelf (NACIRI, 1994).

During the Bathonian and Callovian times, the sedimentary environment changed suddenly and the detritical sedimentation came back (Fig. 6). These deposits marked an important filling phase of the subsident areas.

During the Bathonian times, the facies were both deeper and more diverse, containing organo-detritical marls and 800 m thick limestones, north of the Taourirt-Oujda axis. South of Oujda,

Source : MNHN, Paris

limestones with iron oolites and ammonites were simultaneously being deposited (LUCAS, 1942; ELMI, 1973). Further to the south, in the High Plateaux, gypsum marls developed.

The Callovo-Oxfordian time is characterised by a flysch sedimentation of deep sea fan type, which is well developed south of Oujda. Deposits are thicker in the grabens (200 to 250 m in Jebel Azira and Bou Beker) than in the horsts (12 to 15 m)(CLAVEAU, 1952).

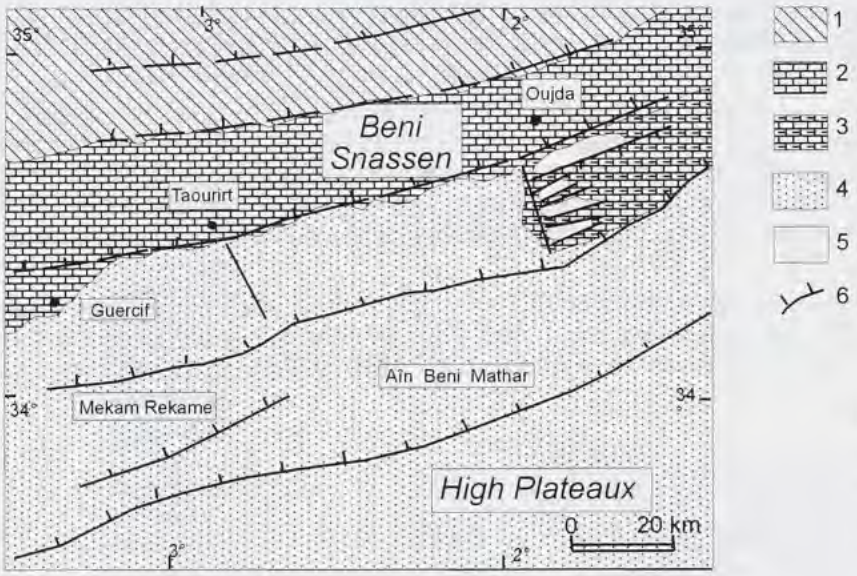

FIG. 6.— Palaeogeographical map during the Bathonian-Callovian. **1**, basin (marls); **2**, marls and organo-detritical limestones; **3**, iron oolitic limestones; **4**, marls and sandy limestones; **5**, emerged lands; **6**, faults.

*FIG. 6.— Carte paléogéographique au Bathonien-Callovien. **1**, bassin (marnes) ; **2**, marnes et calcaires organo-détritiques ; **3**, calcaires oolithiques ferrugineux ; **4**, marnes et calcaires sableux ; **5**, terres émergées ; **6**, failles.*

THE UPPER JURASSIC PERIOD

From the middle Oxfordian to the early Kimmeridgian, a deltaic structure formed by several hundred meters of sandstones and sandy marls developed south of Oujda (Figs 4 and 7). These deposits were interrupted at the end of the early Kimmeridgian by a shallow water calcareous episode which ends to the Mesozoic sedimentary cycle in the Taourit-Oujda region. Benio Ourimeuch sandstone formations were simultaneously being deposited in the Beni Snassen area (CATTANEO, 1987).

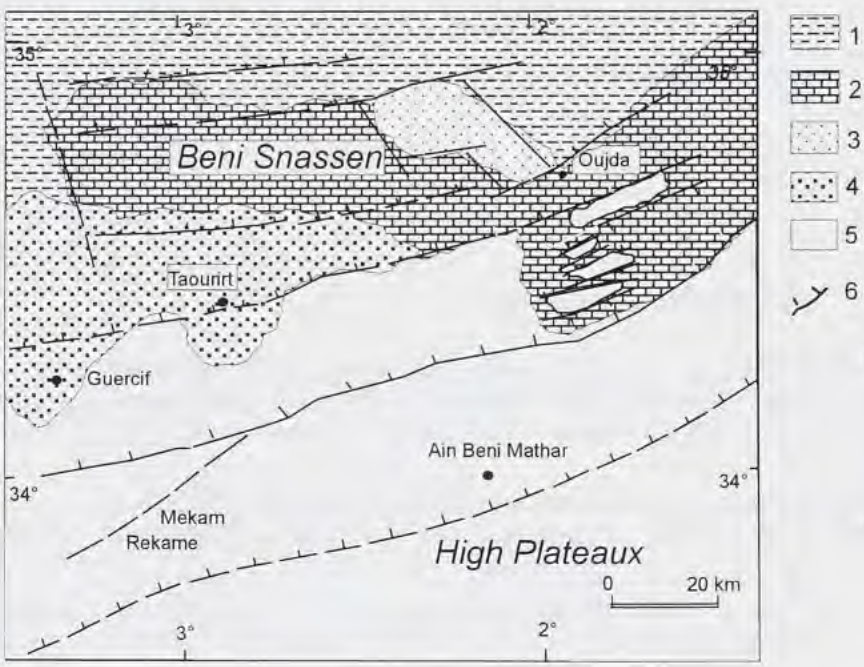

FIG. 7.— Palaeogeographical map during the Oxfordian-early Kimmeridgian. **1**, basin; **2**, carbonate margin; **3**, littoral domain; **4**, deltaïc plain; **5**, emerged lands; **6**, faults.

*FIG. 7.— Carte paléogéographique à l'Oxfordien-Kimméridgien inférieur. **1**, bassin ; **2**, bordure carbonatée ; **3**, domaine littoral ; **4**, plaine deltaïque ; **5**, terres émergées ; **6**, failles.*

Source : MNHN, Paris

THE LATE KIMMERIDGIAN AND THE EARLY BERRIASIAN PERIODS

During this time, a return of the carbonated sedimentation can be observed (Figs 4 and 8). These deposits are organised in three series (CATTANEO, 1987): the limestones of Mechraa Klila from the late Kimmeridgian, the marly limestones and limestones of Ahmer Akhdar from the early Portlandian and the marly limestones of Bou Rhennja from the late Portlandian to early Berriasian ages. The thickness of the early Kimmeridgian sedimentary sequence increases from south to north. Deposits are thicker in the Beni Snassen area (550 m) than in the Taourirt-Oujda axe where they do not exceed 180 m (OUAHBI, 1996). To the south, they are reduced or absent. These series show also lateral variations of facies. These deposits testify to the installation of an inner carbonated shelf organised in a sub-tidal zone which pass southwards to an estran regime. The Taourirt-Oujda region has emerged definitely.

By the end of the early Berriasian, the whole of northeastern Morocco had emerged.

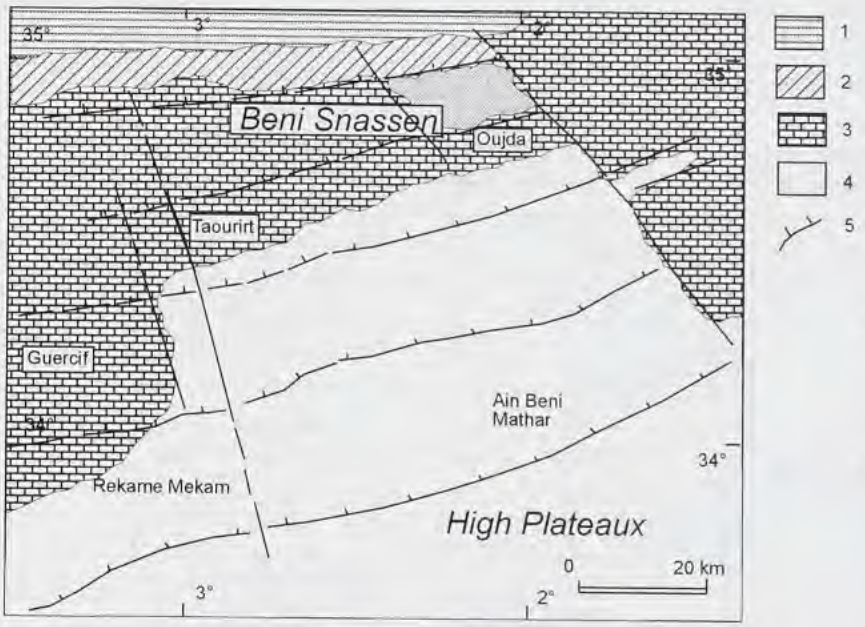

FIG. 8.— Palaeogeographical map during the late Portlandian. **1**, carbonated outer shelf; **2**, barrier; **3**, epicontinental carbonated shelf; **4**, emerged lands; **5**, faults.

*FIG. 8.— Carte paléogéographique au Portlandien supérieur. **1**, plate-forme externe carbonatée ; **2**, barrière ; **3**, plate-forme carbonatée épicontinentale ; **4**, terres émergées ; **5**, failles*

STUDY OF FAULT SYSTEMS AND STRESS PATTERNS

Detailed investigation of the brittle fracturing were carried out in the research area to establish the stress pattern from Triassic to Eocene. It led to the reconstruction of the palaeostresses responsible for the deformation of eastern Morocco. The analysis of fault planes and slickenside lineations from field measurements enables us to reconstruct the orientations (trend and plunge) of the principal stress axes. More than 600 measurements of slip data were collected in the Beni Snassen mounts and in the Taourirt-Oujda mounts. In most of the sites we characterised two or more successive episodes of deformation. We separated the successive tectonic events using observations of field relative chronology criteria, the fossilised structures, crosscutting relationships between faults and superposition of slickensides on a fault plane. We used the ANGELIER (1979, 1984, 1989, 1990) inversion method to reconstruct the orientation of the maximum, intermediate and minimum principal stress axes ($\sigma 1$, $\sigma 2$, $\sigma 3$) and shape ratio Φ. The results are reported on the synthetical stratigraphic column (Fig. 9), on the Table 1 and on structural maps of the Beni Snassen and the Taourirt-Oujda regions.

Source : MNHN, Paris

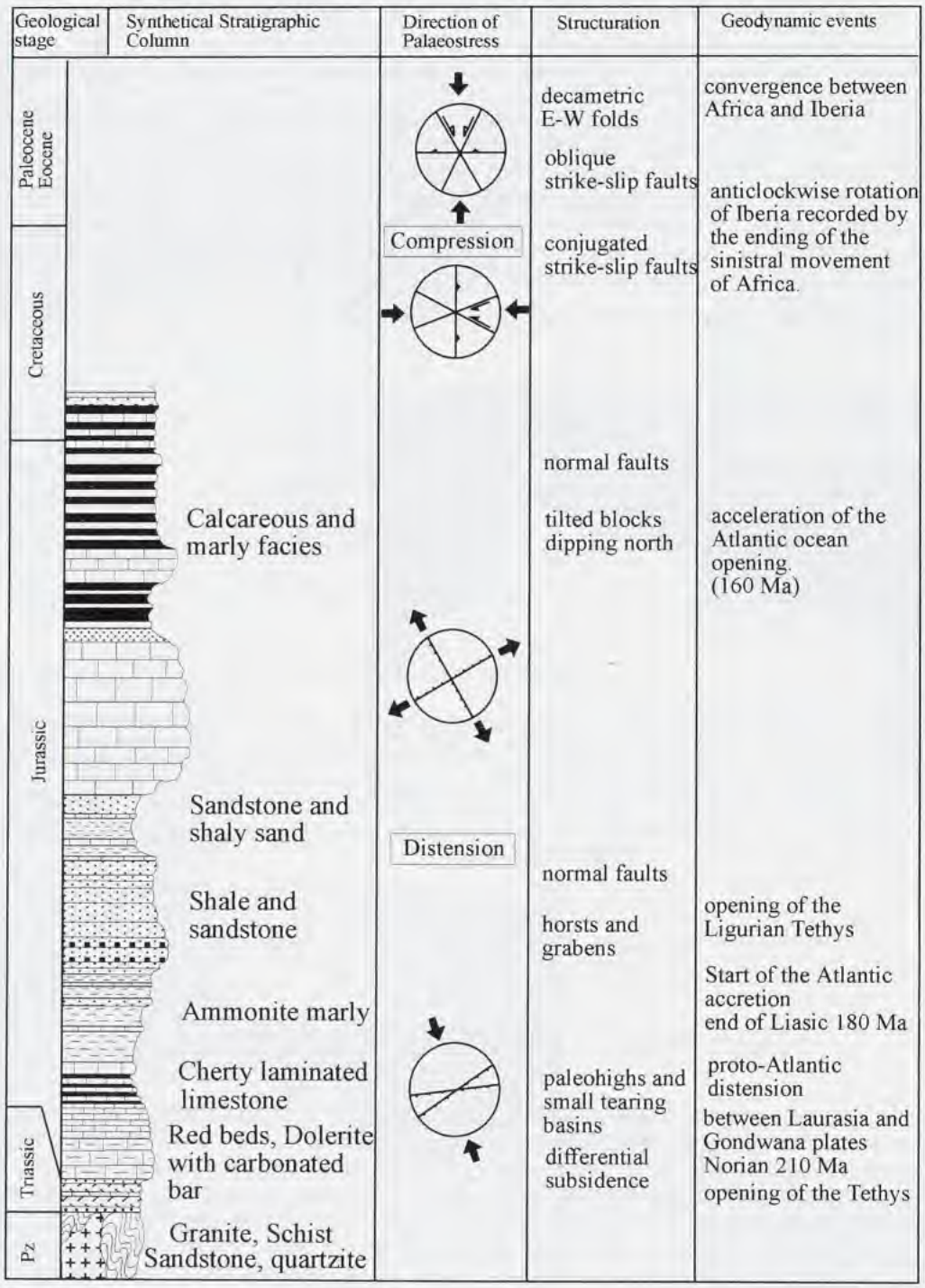

FIG. 9.— Palaeostress fields and geodynamical setting in the southern tethyan margin of northeastern Morocco.

FIG. 9.— Champs de contraintes et évolution géodynamique de la marge sud téthysienne du Maroc nord oriental.

Source : MNHN, Paris

TABLE 1.— Location of fault stations (Nbr: number of measured faults) and reconstruction of stress tensors that correspond to the orientation of stress axes and to the ratio $\Phi = (\sigma2-\sigma3)/(\sigma1-\sigma3)$ between principal stress values ($\sigma1>\sigma2>\sigma3$) (ANGELIER, 1984). ANG: average angle between computed shear stress and observed slickenside lineations (α in degrees). Average RUP: ratio upsilon (ranging from 0 to 200%) of the INVDIR method (ANGELIER, 1990); values below 50% correspond to good fits between actual fault slip data distribution and computed shear distribution. T= type of predominant faulting (N: normal faults; I: reverse faults; D: strike-slip faults).

TABLEAU 1.— Localisation des stations de mesures (Nbr : nombre de failles mesurées) et reconstruction du tenseur des contraintes qui correspond à l'orientation des axes de contraintes et au ratio $\Phi = (\sigma2 - \sigma3) / (\sigma1 - \sigma3)$ entre les valeurs des axes principaux ($\sigma1>\sigma2>\sigma3$) (ANGELIER, 1984). ANG : angle moyen entre la contrainte tangentielle et la strie mesurée (α en degrés). RUP : ratio (entre 0 et 200%) de la méthode INVDIR (ANGELIER, 1990) ; les valeurs en dessous de 50% donnent une bonne correspondance entre la distribution des données des stries mesurées et la distribution de la contrainte calculée. T : type de failles (N : faille normale ; I : faille inverse ; D : faille décrochante).

Site number	Lat./Long. in degrees	Number of faults	σ1 trend	σ1 plunge	σ2 trend	σ2 plunge	σ3 trend	σ3 plunge	Meth	ϕ	ANG	RUP %	stress Regime
1	34.40/2.53	11	204	77	74	8	342	10	INVD	0.158	8	35	N
2	34.43/2.48	10	106	72	12	1	282	18	INVD	0.334	4	27	N
3	34.44/2.43	7	331	69	211	11	117	17	INVD	0.275	4	21	N
4	34.48/2.25	7	339	71	71	1	162	19	INVD	0.277	10	31	N
5	34.53/2.18	8	187	66	283	3	15	24	INVD	0.250	7	34	N
6	34.55/2.03	6	273	74	178	2	87	16	INVD	0.227	3	13	N
7	34.46/2.17	15	291	77	122	13	31	2	INVD	0.305	20	60	N
8	34.13/2.45	12	27	69	127	4	218	21	INVD	0.069	5	16	N
9	34.20/2.48	9	274	75	179	1	88	15	INVD	0.211	21	6	N
10	34.18/2.15	10	106	72	12	1	282	18	INVD	0.334	15	4	N
11	34.30/2.05	8	266	83	58	6	148	3	INVD	0.536	18	6	N
12	34.37/1.53	11	342	73	74	1	165	16	INVD	0.191	5	25	N
13	34.30/1.47	8	350	80	149	9	240	4	INVD	0.646	7	6	N
14	34.24/1.50	9	322	73	232	0	142	14	INVD	0.244	5	20	N
15	34.40/2.55	9	281	8	30	65	188	23	INVD	0.367	10	33	D
16	34.50/2.51	12	85	17	287	72	177	6	INVD	0.369	10	37	D
17	34.44/2.38	12	171	7	160	73	3	17	INVD	0.312	13	35	D
18	34.48/2.25	12	276	5	116	85	6	2	INVD	0.417	11	27	D
19	34.51/2.24	12	88	7	316	80	179	7	INVD	0.350	8	16	D
20	34.55/2.03	14	282	8	24	55	187	33	INVD	0.199	11	34	D
21	34.47/2.21	15	83	8	222	79	352	7	INVD	0.300	8	25	D
22	34.2/2.48	8	83	15	309	69	117	15	INVD	0.202	32	12	D
23	34.14/2.35	13	83	23	191	33	327	48	INVD	0.132	46	15	D
24	34.17/2.14	41	96	0	195	90	6	0	INVD	0.356	14	7	D
25	34.2/2.16	14	100	15	281	75	190	0	INVD	0.475	11	38	D
26	34.35/1.52	19	108	0	200	85	18	5	INVD	0.220	13	36	D
27	34.29/1.47	14	106	1	204	79	16	11	INVD	0.400	28	12	D
28	34.21/1.52	12	94	8	207	60	1	20	INVD	0.282	47	19	D
29	34.40/2.56	8	187	17	1	72	97	2	INVD	0.427	3	24	D
30	34.43/2.49	10	356	2	133	87	266	2	INVD	0.286	14	56	D
31	34.45/2.46	6	190	9	334	79	99	7	INVD	0.361	7	23	D
32	34.42/2.34	13	190	19	53	65	286	16	INVD	0.138	10	32	D
33	34.47/2.55	11	185	0	93	82	275	8	INVD	0.469	8	31	D
34	34.55/2.04	9	14	9	239	78	106	8	INVD	0.398	7	30	D
35	34.46/2.14	11	181	10	271	2	14	79	INVD	0.698	8	35	I
36	34.20/2.48	17	173	6	279	71	81	18	INVD	0.329	16	53	D
37	34.22/2.44	13	184	2	331	87	94	1	INVD	0.346	17	36	D
38	34.26/2.17	17	187	0	94	87	277	3	INVD	0.393	18	6	D
39	34.17/2.14	11	190	7	305	73	98	15	INVD	0.302	9	31	D
40	34.34/1.51	25	179	1	294	87	88	2	INVD	0.338	4	5	D
41	34.29/1.47	14	192	9	314	74	100	13	INVD	0.314	15	9	D
42	34.21/1.52	11	359	1	188	89	89	0	INVD	0.375	16	10	D

Source : MNHN, Paris

NORMAL FAULTING TECTONIC REGIMES

The Triassic volcanic and sedimentary series are affected by normal synsedimentary faults oriented N70°E to N90°E. These faults gave rise to the effusion of tholeiitic volcanism and the structure of subsident basins limited by highs. In this extensional regime we calculate a minimum principal stress of σ3 oriented NNW-SSE to N-S (Figs 10 and 11).

Late Jurassic to Early Cretaceous series are affected by metric to decametric ENE-WSW to E-W and NW-SE groups of normal faults. The fault slip data analysis allows the reconstruction of two palaeostress tensors with an horizontal σ3 axis oriented NNW-SSE to N-S and NE-SW to E-W respectively. During the Liassic and the Dogger, the faults with ENE-WSW and E-W directions are again active and permit the development of ENE-WSW to E-W directed horsts and grabens. During the Late Jurassic and the Early Cretaceous, the same faults were responsible for the formation of northwards verging tilted blocks of the Tethyan margin. Normal faults which are progressively damped, variation of thickness at each side of the faults, synsedimentary block tilting, intraformational breccias,

STRIKE-SLIP FAULTING REGIMES

A conjugated system of dextral strike-slip faults trending ENE-WSW and sinistral strike-slip faults trending NW-SE is present throughout the investigated area. The stress pattern registered in the pre-Miocene series shows that the maximum principal stress σ1 was oriented E-W and the σ3, N-S (Figs 12 and 13). Some of these faults are neoformed, others correspond to normal faults which have undergone strike-slip reactivation. This is illustrated by the presence of vertical slickensides intersected by horizontal ones. Locally, some normal synsedimentary faults trending NW-SE were reactivated as reverse faults. A maximum compressive stress oriented E-W with a permutation between σ2 and σ3 was calculated. This stress pattern is discrete in the Beni Snassen and the Taourirt-Oujda Mounts and it is better registered in the Terni Masgout Mounts by N20°E folds related to sinistral strike-slip faults trending N160°E. Some E-W directed faults were reactivated as sinistral strike-slip faults.

A second stress pattern has been registered with the maximal horizontal compressive stress σ1 trending N-S and σ3, trending E-W (Figs 14 and 15). This is showed by dextral strike-slip faults trending NW-SE, sinistral ones trending NE-SW and folds trending E-W. Some normal faults oriented ENE-WSW to E-W were reactivated as reverse faults. Some NW-trending faults of the preceding stage of E-W compression were also remobilized into dextral strike-slip faults under this N-S compression.

FIG. 10.— Location of fault stations and orientation of the principal stress axes during the Triassic to Early Cretaceous in the Beni Snassen mounts. Geological space imagery sketch map of the Beni Snassen mounts. **1**, Quaternary; **2**, Neogene to Quaternary volcanism; **3**, Mio-Pliocene; **4**, Miocene; **5**, Cretaceous; **6**, Callovian, Oxfordian; **7**, Oxfordian, Kimmeridgian; **8**, Kimmeridgian, Portlandian; **9**, Dogger; **10**, Liassic; **11**, Triassic; **12**, granite; **13**, Palaeozoic; **14**, faults; **15**, normal faults; **16**, strike-slip faults; **17**, reverse faults; **18**, stratigraphic bedding. 1 to 7: stereographic projections in this and subsequent figures, illustrate fault plane solutions in Schmidt lower hemisphere projection: fault planes are shown as curves and poles as open squares, slickenside lineations as small centrifugal arrows (normal faults), centripetal arrows (reverse faults) or double arrows (strike-slip faults). 5 branchs star: σ1; 4 branchs star: σ2; 3 branchs star: σ3; centrifugal black arrows indicate the direction of extension and centripetal ones, the direction of compression, in the horizontal plane.

*FIG. 10.— Localisation des stations de mesures et détermination des directions de contraintes principales du Trias au Crétacé supérieur dans les monts Beni Snassen. **1**, Quaternaire ; **2**, volcanisme néogène à Quaternaire ; **3**, Mio-Pliocène ; **4**, Miocène ; **5**, Crétacé ; **6**, Callovien-Oxfordien ; **7**, Oxfordien-Kimméridgien ; **8**, Kimméridgien-Portlandien ; **9**, Dogger ; **10**, Lias ; **11**, Trias ; **12**, Granite ; **13**, Paléozoïque ; **14**, faille ; **15**, faille normale ; **16**, faille décrochante ; **17**, faille inverse ; **18**, bancs stratigraphiques ; 1 à 7 : projection stéréographique des plans de failles sur diagramme de Schmidt, hémisphère inférieur : les plans de faille sont représentés par des courbes et les pôles par des carrés blancs, les stries par des petites flèches centrifuges pour les failles "normales", des flèches centripètes pour les failles inverses ou des flèches doubles pour les failles pour les décrochements ; étoile à 5 branches : σ1 ; étoile à 4 branches : σ2 ; étoile à 3 branches : σ3.*

Source : MNHN, Paris

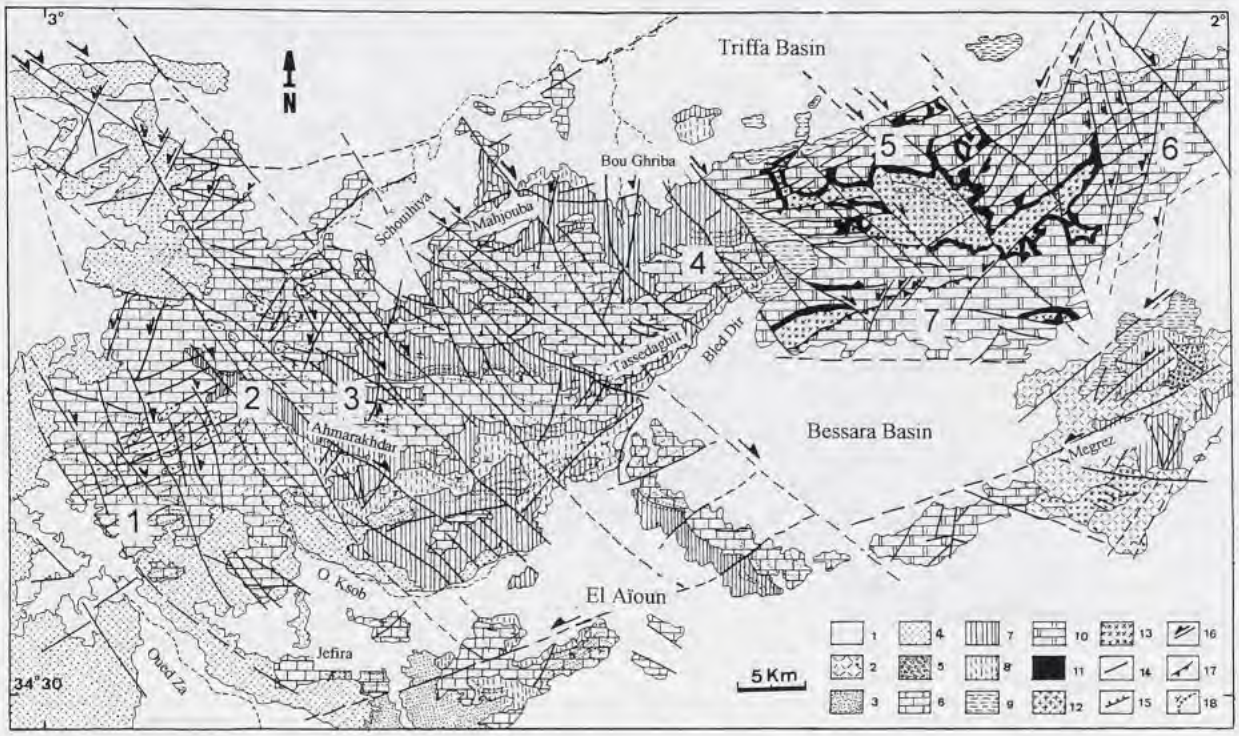

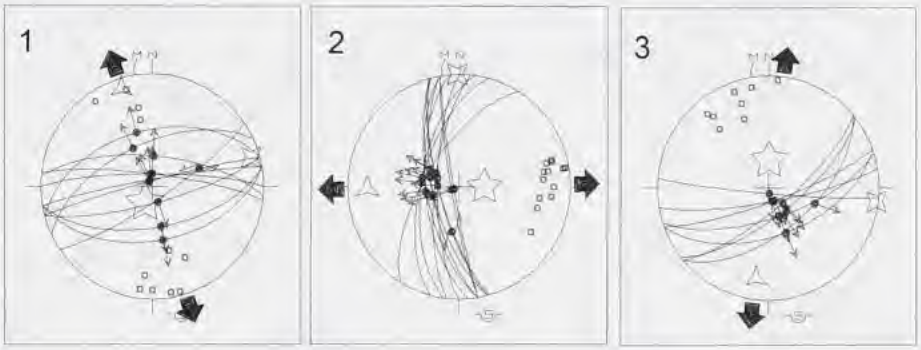

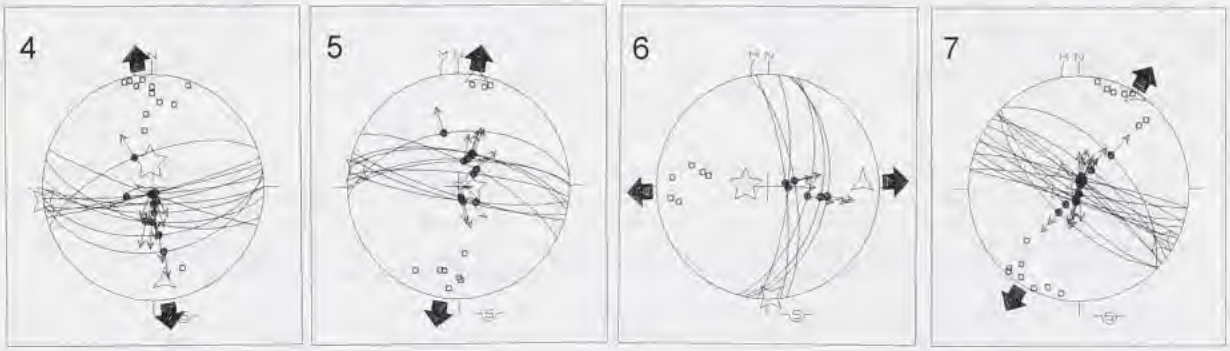

Source : MNHN, Paris

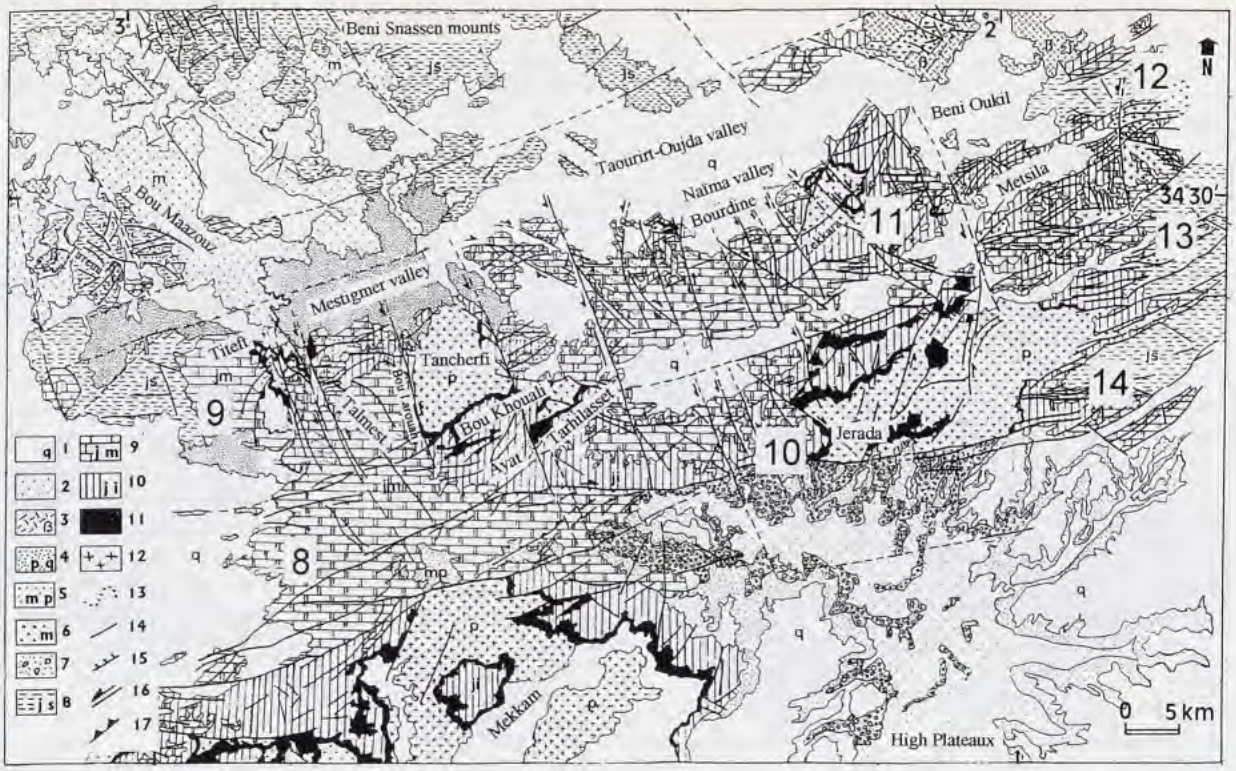

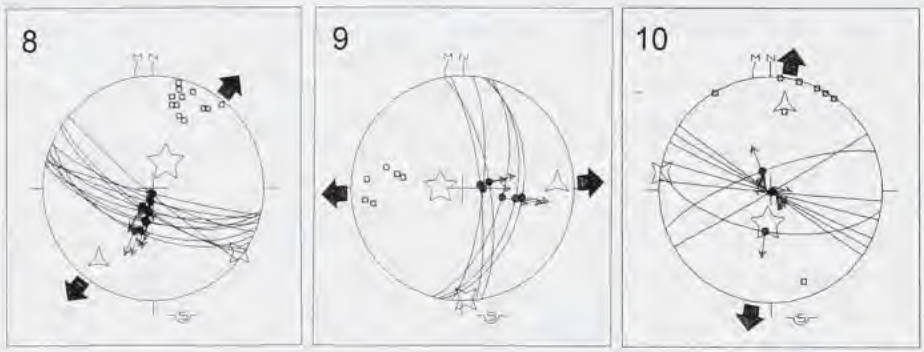

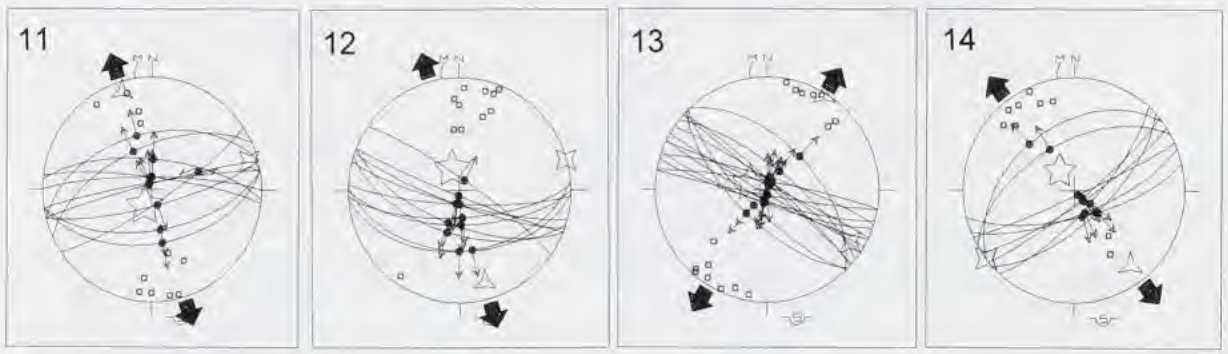

FIG. 11.— Location of fault stations and orientation of the principal stress axes during the Triassic to Early Cretaceous extension in the Taourirt-Oujda mounts geological sketch map. **1**, Quaternary; **2**, Moulouyan surface; **3**, Neogene to Quaternary volcanism; **4**, Plio-Quaternary; **5**, Mio-Pliocene; **6**, Miocene; **7**, Aquitanian; **8**, Malm; **9**, Dogger; **10**, Liassic; **11**, Triassic; **12**, Palaeozoic; **13**, stratigraphic bedding; **14**, faults; **15**, normal faults; **16**, strike-slip faults; **17**, reverse faults. 8 to 14: Schmidt lower hemisphere projection of fault planes (same legend as figure 10).

*FIG. 11.— Localisation des stations de mesures et détermination des directions de contraintes principales du Trias au Crétacé supérieur dans les monts de Taourirt-Oujda. **1**, Quaternaire ; **2**, surface du Moulouyen ; **3**, volcanisme néogène à quaternaire ; **4**, Plio-Quaternaire ; **5**, Mio-Pliocène ; **6**, Miocène ; **7**, Aquitanien ; **8**, Malm ; **9**, Dogger ; **10**, Lias ; **11**, Trias ; **12**, Paléozoïque ; **13**, bancs stratigraphiques ; **14**, faille ; **15**, faille normale ; **16**, faille décrochante ; **17**, faille inverse ; 8 à 14 : projection de Schmidt hémisphère inférieur (même légende que figure 10).*

Source : MNHN, Paris

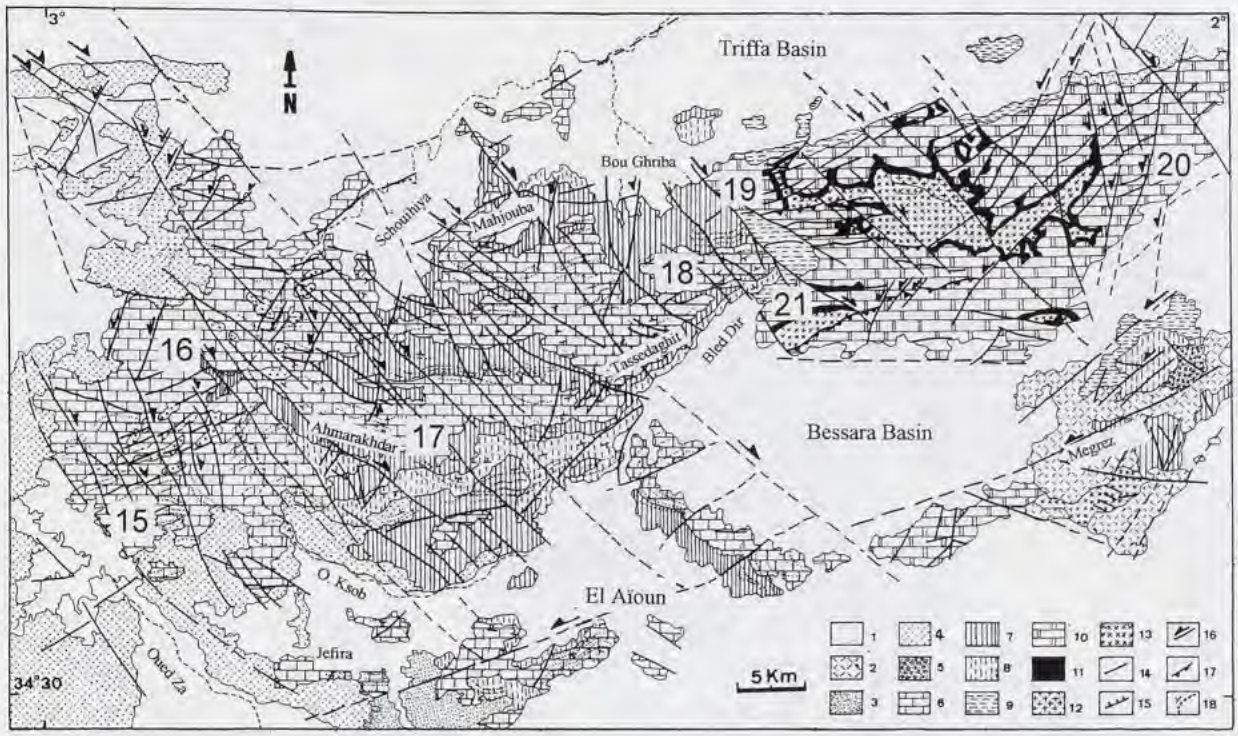

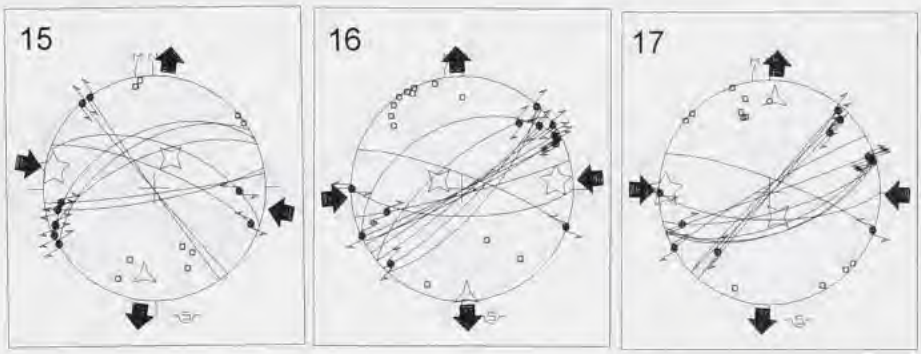

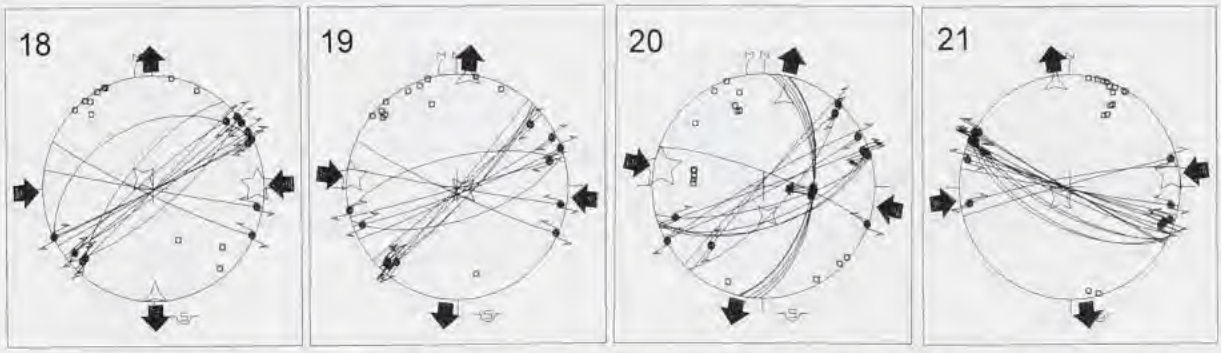

FIG. 12.— Location of fault stations and orientation of the principal stress axis during the Late Cretaceous in the Beni Snassen mounts. 15 to 21: Schmidt lower hemisphere projection of fault planes (same legend as figure 10).

FIG. 12.— Localisation des stations de mesure des failles et détermination de la direction de contrainte principale au cours du Crétacé supérieur dans les monts Beni Snassen. 15 à 21 : projection de Schmidt hémisphère inférieur (même légende que figure 10).

Source : MNHN, Paris

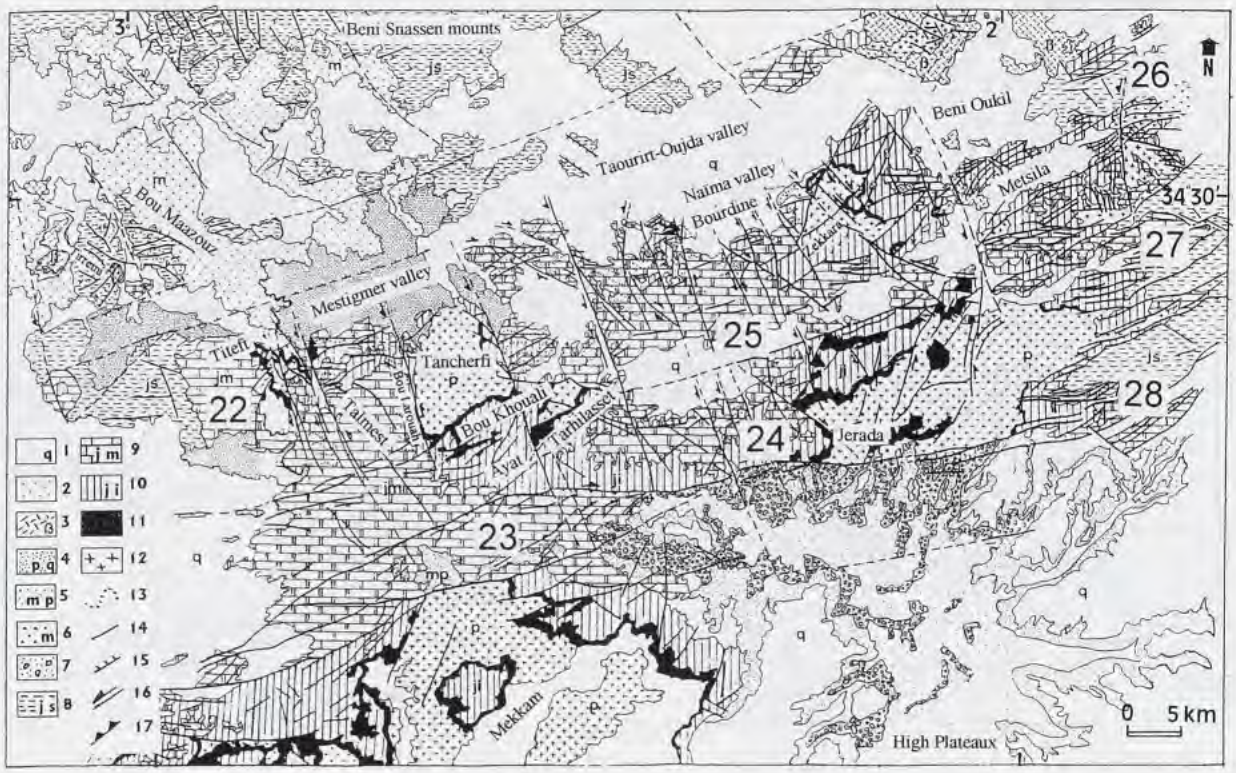

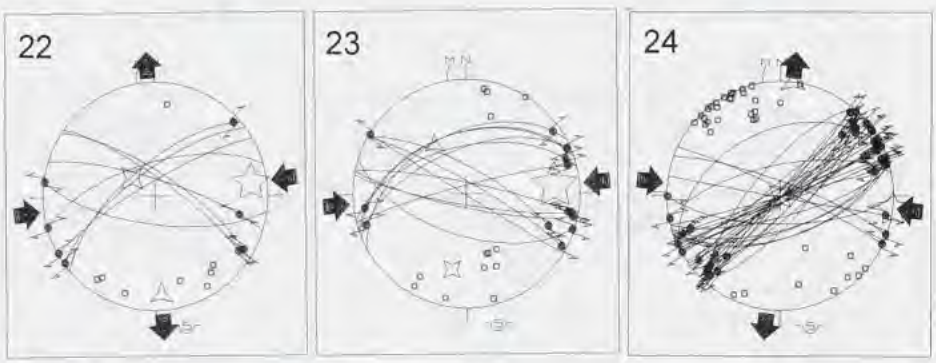

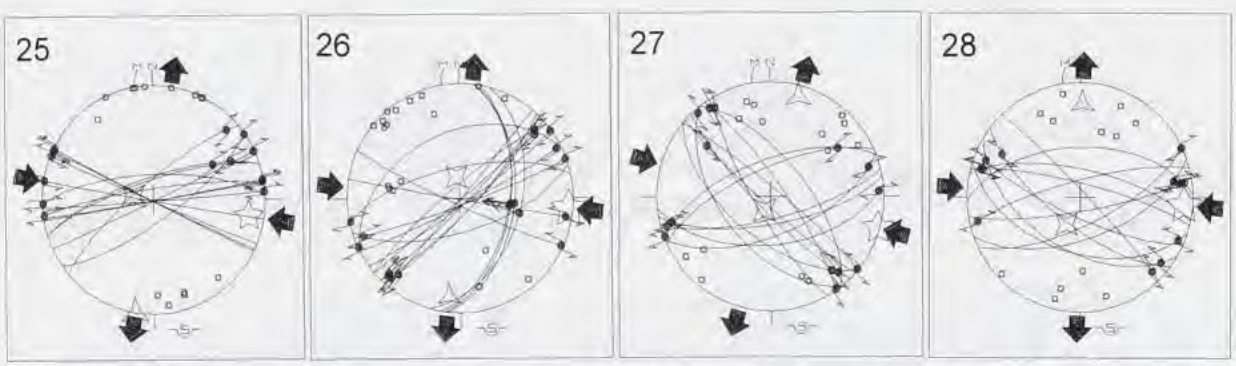

FIG. 13.— Location of fault stations and orientation of the principal stress axis during the Late Cretaceous in the Taourirt-Oujda mounts. 22 to 28: Schmidt lower hemisphere projection of fault planes (same legend as figure 11).

FIG. 13.— Localisation des stations de mesure des failles et détermination de la direction de contrainte principale au cours du Crétacé supérieur dans les monts de Taourirt-Oujda. 22 à 28 : projection de Schmidt hémisphère inférieur (même légende que figure 11).

Source : MNHN, Paris

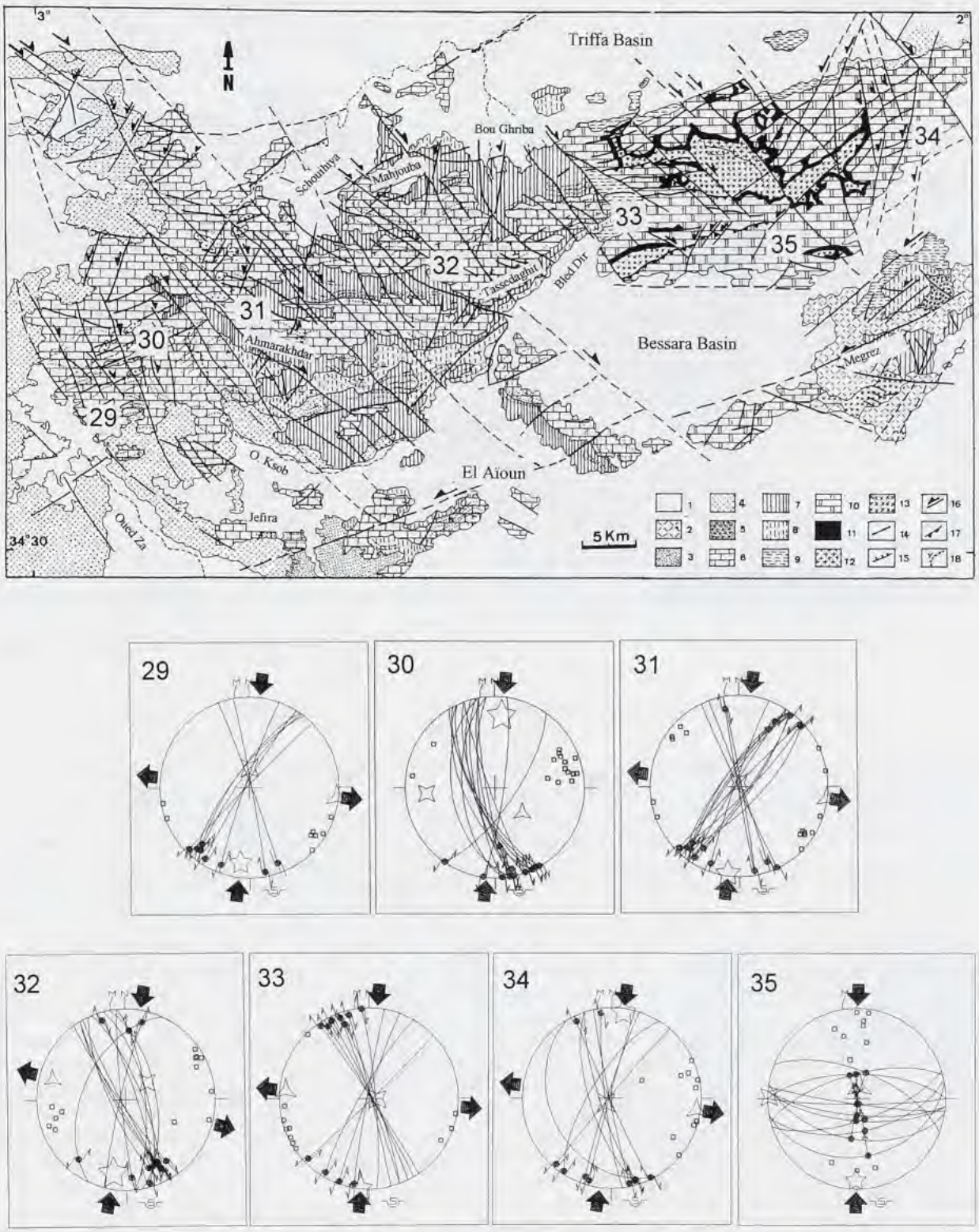

FIG. 14.— Location of fault stations and orientation of the principal stress axis during the Eocene compression in the Beni Snassen mounts. 29 to 35: Schmidt lower hemisphere projection of fault planes (same legend as figure 10).

FIG. 14.— Localisation des stations de mesure des failles et détermination de la direction de contrainte principale au cours de l'Eocène dans les monts de Beni Snassen. 29 à 35 : projection de Schmidt hémisphère inférieur (même légende que figure 10).

Source : MNHN, Paris

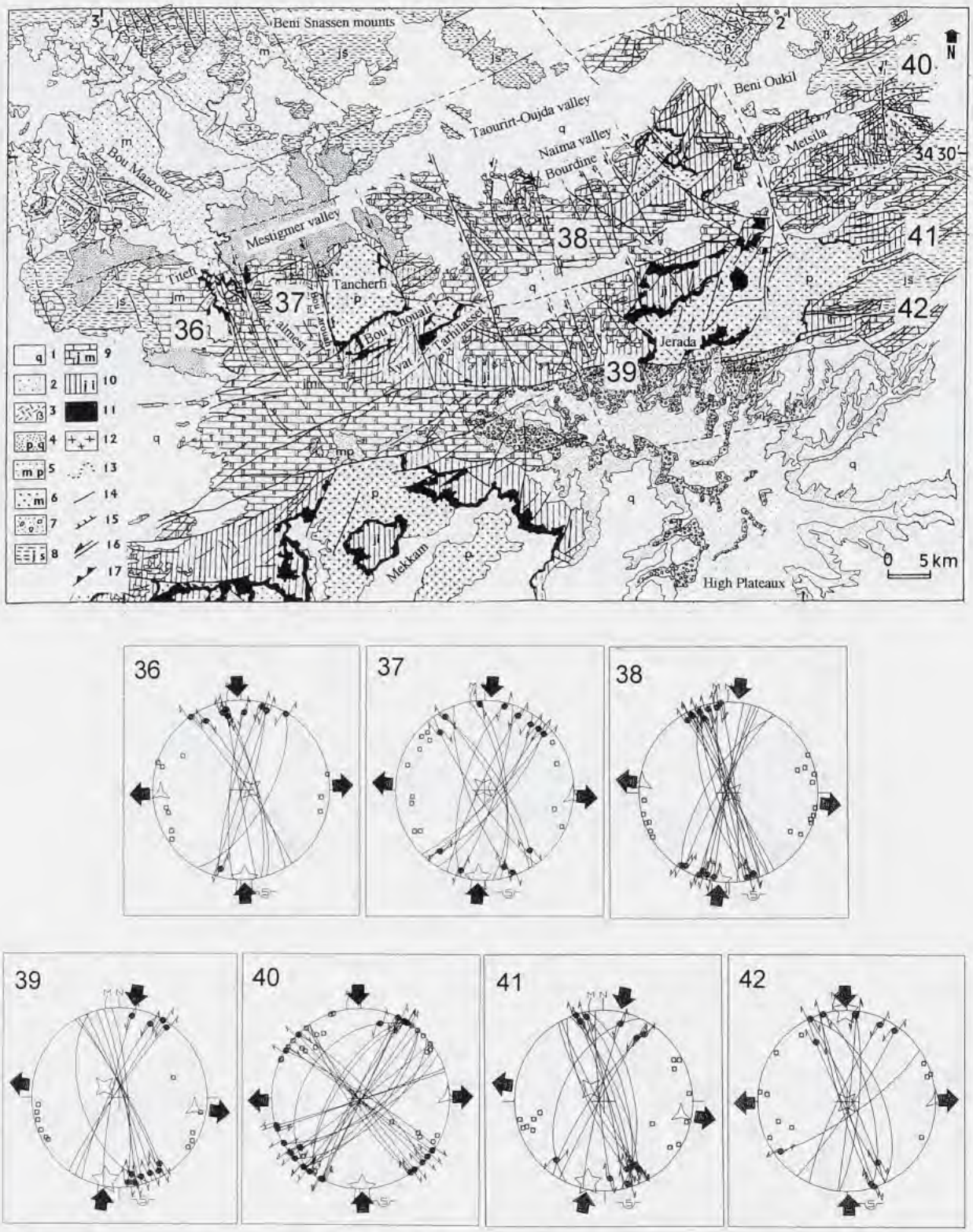

FIG. 15.— Location of fault stations and orientation of the principal stress axis during the Eocene compression in the Taourirt-Oujda mounts. 36 to 42: Schmidt lower hemisphere projection of fault planes (same legend as figure 11).

FIG. 15.— Localisation des stations de mesure des failles et détermination de la direction de contrainte principale au cours de l'Eocène dans les monts de Taourirt-Oujda. 36 à 42 : projection de Schmidt hémisphère inférieur (même légende que figure 11).

Source : MNHN, Paris

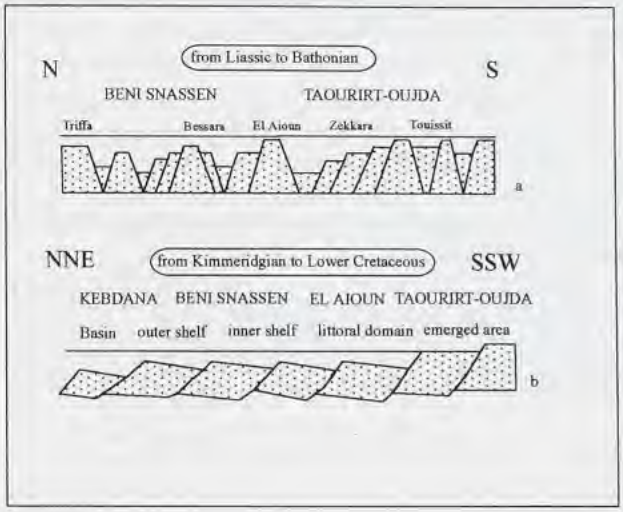

FIG. 16.— Palaeogeographic synthetic profiles through the studied area showing: **a**, the horsts and grabens structure from Liassic to Bathonian; **b**, the tilted blocks structure during Kimmeridgian to Early Cretaceous.

*FIG. 16.— Coupe paléogéographique synthétique au travers de la zone étudiée montrant : **a**, la structure en horsts et grabens se mettant en place du Lias au Bathonien ; **b**, la structure en blocs basculés formés du Kimméridgien au Crétacé supérieur.*

TECTONIC CONTROL OF THE EVOLUTION OF THE TETHYAN MARGIN IN NORTHEASTERN MOROCCO

From the data presented above, we can infer that the evolution of the northeastern Morocco from the Triassic to the Eocene periods occurred in several steps. The correlations between global and detailed biostratigraphic, sedimentary and major tectonic events and the key periods of the Tethys evolution show that these main steps are as follows.

BI-DIRECTIONAL DISTENSION FROM THE TRIASSIC TO THE EARLY CRETACEOUS

During the Late Triassic period, the tectonic regime was characterised by extensional deformation caused by the principal minimum stress $\sigma 3$ oriented NNW-SSE to N-S. Old inherited ENE-WSW to E-W oriented late-hercynian faults have been reactivated as normal faults. This event led to the formation of horts (Debdou, Touissit, Rhar Roubane, Tanouralt, Bourdine) and basins with differential subsidence (Tiouli, Oujda, Taourirt, Metroh, Oued Himmer, Guercif, High Plateaux) (Figs 3 and 16a). This extensive regime induced the effusion of basalts and dolerites within the red clays and the evaporites, marking the beginning of the rifting at 215 Ma.

During the early Liassic, northeastern Morocco was structured by narrow and elongated horsts (Touissit, Debdou and El Aïoun-Naïma) and by narrow graben in a ENE-WSW direction (Figs 3 and 16a). It corresponds to an unstable subsident area located between two stable and shallow zones namely the northern border of the Beni Snassen area and the High Plateaux in the south. Among the normal faults oriented ENE-WSW which controlled the structure of these zones, we find (Fig. 3) the fault of Rekame-Sidi El Abid, Guefait-Tiouli, Taourirt-Oujda, the faults of El Aïoun-Naïma, the fault south of the Beni Snassen area, the fault north of the Beni Snassen area, the fault south of the Gareb area, and the fault of Tafouralt (Fig. 3). The extensional stress responsible for the reactivation of these faults trends NNW-SSE, and is secondly associated with a new extension trending NE-SW to E-W. This fault activity coincides with the transgressive deposition of carbonates in the grabens where we can observe an important accumulation. This event is related to the eastwards translation of the African plate. The opening of the Atlantic rift goes ahead and the separation between Africa and America is effective (JANSAL & WADE, 1975; LANCELOT & WINTERER, 1980).

During the middle Liassic, the effect of generalised eustatism (VAIL *et al.*, 1977) is associated with an important subsidence brought about by the reactivation of synsedimentary faults oriented ENE-WSW to E-W and NW-SE as a result of a bi-directional extension NNW-SSE to N-S and ENE-WSW to E-W. This tectonic and sedimentary transgressive evolution is materialised by the progressive advance of the

Source : MNHN, Paris

Tethyan Sea onto the coastal or emerged palaeo-highs (El Aïoun-Naïma horst, Moulay Idriss horst, High Plateaux, northern border of the Beni Snassen area) and the deepening of subsident zones (Beni Snassen graben, Taourit-Oujda graben, Guercif graben) (Fig. 3).

During the late Liassic the tectonic regime underwent no change. Most of the faults oriented as ENE-WSW to E-W and NW-SE, previously active, were remobilised as normal faults and contributed to the fragmentation of the Tethyan margin. This tectonic period was characterised by terrigenous flows relatively moderate and the generalisation of the marly facies deposits, indicating a modification of the climate which became more temperate. Progressive filling up of grabens is related to the beginning of oceanic accretion in the Central Atlantic Ocean at around 180 Ma (OLIVET *et al.*, 1984).

From the Aalenian to the Bajocian times, and owing to marine advance, the tectonic of horsts and grabens was accentuated under the same distensive regime. The palaeogeographic scheme shows the deposition of an external carbonated shelf facies, open onto the slope in the Beni Snassen area and in the Guercif basin, and a carbonated neritic facies in the Taourirt-Oujda axis and in the High Plateaux regions.

During the middle Bathonian times, the opened deposit areas evolved in restrained environments in which argillaceous and sandy materials had been deposited, attesting the retreat of the sea toward the NE. During that time, the Moroccan Atlasic basins and the Moroccan High Plateaux emerged. The northeastern Morocco was integrated to the Rif-Tell domain and constituted its southern margin. The distensive movements created a more rapid deepening of the basement, compensated by a more important sedimentary drift. Most of the syn-sedimentary deformations are concentrated along the major normal faults oriented ENE-WSW and NW-SE. The permanent movement of these faults is responsible for the facies variation and the thickness of the sedimentary series.

During the Callovian, the subsidence continued to take place in the whole of northeastern Morocco. During the Oxfordian, horsts and grabens were structured by ENE-WSW to E-W normal faults. We observe within the sedimentary series, slumps, syn-sedimentary normal faults, and brecciated levels. Numerous normal faults were reactivated during the early Kimmeridgian and brought about the instability of the Rif foreland in these areas (DE LUCA, 1982; HERVOUET, 1985). During this period, the relative movement of Africa always occurred eastwards and coincided with the first phase of acceleration of the Atlantic oceanic accretion.

From the late Kimmeridgian to the Early Cretaceous, the structural control led to an important increase in the subsidence of these areas. The reactivation of the ENE-WSW to E-W and the NW-SE normal faults induced to the formation of tilted blocks in the northeastern Morocco (Fig. 16b). The thickness of the sedimentary series increases from south to north. This tectonic regime induced the formation of carbonated sedimentation which was deposited in the whole maghrebian margin of the Tethys. The Taourirt-Oujda and High Plateaux areas emerged. The reactivation of the faults is also attested by the superposition of filling sequences which correspond to alternative periods of downlift and stability. This new structural scheme was conserved until the end of Early Cretaceous. Therefore, during the late Kimmeridgian the deposits vary in thickness; they are thicker in the Beni Snassen area (550 m) than in the Taourirt-Oujda area (180 m) (OUAHBI, 1996). In the south, they are less thick in the Taourirt-Oujda Mounts and absent in the High Plateaux. The extension controlled the tilting of the blocks, the formation of breccias and the collapse of cliffs in the Mechraa Klila formation. NW-SE directed faults such as the Tafouralt or the Oued Kiss fault (Fig. 3) with an horizontal slip component, controlled the shape of the sedimentation area. During the early Portlandian, the palaeogeographic scheme and the structural framework were comparable to those of the late Kimmeridgian because of the polarity and the orientation of palaeogeographic lines and direction of tectonic lines. The dislocation of the late Kimmeridgian carbonated shelf and the installation of a new subtidal carbonated shelf was initially caused by the reactivation of the faults in the Beni Snassen and the Taourirt-Oujda areas. The High Plateaux and the Taourirt-Oujda mounts corresponded to emerged areas. This contrast between the depth of the deposit and the thickness of the sedimentary series implies a progressive subsidence which lasted throughout the Portlandian under the control of subvertical normal faults oriented N70° to N90°E. These faults, fossilised by the upper layers, indicate the existence of a distensive tectonic activity.

The dislocation of the early Portlandian carbonated shelf induced the birth of high zones and subsident ones. Then we observe the formation of a shallow epi-continental carbonated shelf materialised by the generalisation of marly-calcareous facies of Bou Rhennja.

Source : MNHN, Paris

After the last argillaceous and sandy terrigenous deposits of the Early Cretaceous, northeastern Morocco emerged definitely. The deposit area is displaced by progradation toward the Rif Basin in the north, as a result of the Purbeckian regression (CATTANEO, 1987).

LATE CRETACEOUS E-W COMPRESSION

This compression direction, attributed to the Late Cretaceous, is the oldest compressive tectonic event registered in this part of the Tethyan African margin. It is represented in the Beni Snassen and Taourirt-Oujda mounts. It postdates the Early Cretaceous deposits and predates the first Miocene deposits. It is recorded by conjugate dextral strike-slip faults trending ENE-WSW and sinistral strike-slip faults trending NW-SE and by N20°E folds related to N160°E sinistral faults. This tectonic event is related to an contre-clockwise rotation of the regional direction of Iberia, registered by the stopping of the sinistral strike-slip movement of Africa along E-W fractures, which became dextral strike-slip motion (between 80 ± 5 Ma) (BIJU-DUVAL *et al.*, 1977; PATRIAT *et al.*, 1982)

EOCENE N-S COMPRESSION

This compressive direction corresponds to the main tectonic event in the maghrebian regions. It is recorded by NNE-SSW dextral and NW-SE sinistral strike-slip faults. It also caused the creation of decametric folds oriented ENE-WSW to E-W the organisation of which will be perturbed by Neogene to Quaternary tectonic events. The Miocene series overlay unconformably the Jurassic series which are affected by this event. This tectonic event, attributed to the Eocene is directly related to the main direction of the maghrebian orogeny. It is linked to the close-up between Africa and Eurasia lithospheric plates.

CONCLUSION

Northeastern Morocco registered the main tectonic events which occurred onto the Tethyan African margin. First an opening attempt during the Triassic allowed the effusion of tholeiitic basalts. This period, characterised by active distension, allowed the transgression of the Tethyan sea onto the African margin. This distensive regime is related to the break up of the Pangea, the opening of the Tethyan sea and the formation of the Atlantic margins. Then, during the Liassic and the Dogger, the sedimentation is typically Atlasic. The synsedimentary fracturing, induced by ENE-WSW to E-W and NW-SE directed faults, led to the creation of a horst and graben system in a bi-directionnal N-S and E-W extensional regime which affected the whole area. This fracturing is directly related to the proto-Atlantic rifting. Finally, from the middle Oxfordian to the Early Cretaceous, the shelf sedimentary systems registered the effect of a distensive tectonic regime, leading to the formation of tilted blocks and rapid downlifting. This allowed the transgression on the Tethyan margin. The structures were controlled by ENE-WSW to E-W and NW-SE directed faults which were in permanent motion during that period. Thus, the distribution of sedimentary areas from the Triassic to the Cretaceous in the northeastern Morocco, was produced by the conjugate effect of tectonic and eustatism.

REFERENCES

AÏT BRAHIM, L., TABYAOUI, H., CHOTIN, P. & GÉLARD, J.P., 1994.— Apport des données satellitaires SPOT-XS contrôlées par une étude de terrain à l'élaboration de la carte géologique des monts de Taourirt-Oujda au 1/200 000. *In*: *Actes du 12ème Colloque sur les Bassins sédimentaires marocains*. Université Hassan II Mohammedia, Casablanca.

AÏT BRAHIM, L., TABYAOUI, H., CHOTIN, P. & GÉLARD, J.P., 1996.— Apport des données satellitaires SPOT-XS contrôlées par une étude de terrain à l'élaboration de la carte géologique des monts des Beni Snassen au 1/200 000. *In*: *Actes du 13ème Colloque sur les Bassins sédimentaires marocains, Marrakech, 19-22 mars 1996*. Université Cadi Ayad, Marrakech: 13.

Source : MNHN, Paris

ANGELIER, J., 1979.— Determination of the mean principal directions of stress for a given fault population. *Tectonophysics*, **56**: 17-26.

ANGELIER, J., 1984.— Tectonic analysis of fault slip data sets. *Journal of Geophysical Research*, **89** (B7): 5835-5848.

ANGELIER, J., 1989.— From orientation to magnitudes in paleostress determinations using fault slip data. *Journal of Structural Geology*, **11** (1/2): 37-50.

ANGELIER, J., 1990.— Inversion of field data in fault tectonics to obtain the regional stress. II: A New rapid direct inversion method by analytical means. *Geophysical Journal International*, **103**: 363-376.

BERTRAND, H. & PRIOTON, J.M., 1975.— *Les Dolérites marocaines et l'ouverture de l'Atlantique. Étude pétrologique et chimique*. Thèse de 3ème cycle, Université Claude Bernard, Lyon, France, **425-426**: 1-320.

BIJU-DUVAL, B., DERCOURT, J. & LE PICHON, X., 1977.— From the Tethys ocean to the Mediterranean sea: a plate tectonic model of the evolution of the western alpine system. *In*: B. BIJU-DUVAL & L. MONTADERT (eds), *International Symposium of the Structural History of the Mediterranean Basins*. Technip, Paris: 143-164.

CATTANEO, G., 1984.— La Marge téthysienne de la bordure nord-occidentale du Maghreb au Jurassique supérieur; un modèle de plate-forme à sédimentation carbonatée et terrigène deltaïque (massif des Beni Snassen, Maroc nord oriental). *Revue de Géologie dynamique et de Géographie physique, Paris*, **25** (1): 45-57.

CATTANEO, G., 1987.— *Les Formations du Jurassique supérieur et du Crétacé inférieur de l'avant-pays rifain oriental (Maroc)*. Thèse, Université de Bourgogne, Dijon, France: 1-300.

CATTANEO, G., 1991.— *f*volution sédimentaire et paléogéographie du Jurassique supérieur et du Crétacé basal de l'avant-pays rifain oriental (Maroc). *Bulletin de la Société géologique de France*, **162** (1): 69-78.

CHEROTSKY, G., 1973.— Nouvelles données sur les aïounites. *Notes et Mémoires du Service géologique du Maroc, Rabat*, **33** (249): 125-133.

CLAVEAU, J., 1952.— Existence dans les environs d'Oujda d'une discordance dans le Jurassique supérieur, établie grâce à des niveaux repères récemment reconnus. *Comptes Rendus de l'Académie des Sciences, Paris*, **234**: 1796-1798.

COGNEY, G. & FAUGÈRES, J.C., 1975.— Précision sur la mise en place des épanchements basaltiques des formations triasiques de la bordure septentrionale du Maroc central. *Bulletin de la Société géologique de France*, **17** (5): 721-733.

ELMI, S., 1973.— Décrochements et mouvements atlasiques dans la région frontalière algéro-marocaine (Monts de Rhar Roubane). *Comptes Rendus de l'Académie des Sciences, Paris*, **276**: 1521-1524, 1 fig.

HERVOUET, Y., 1985.— *Géodynamique alpine (Trias-Actuel) de la marge septentrionale de l'Afrique, au nord du bassin de Guercif (Maroc oriental)*. Thèse, Université de Pau, Pau, France: 1-367.

JANSAL, L.F. & WADE, J.A., 1975.— Geology of the continental margin off Nova Scotia and Newfoundland. *In*: J.M. VAN DER LINDENW & J.A. WADE (eds), Offshore geology of eastern Canada. 2: Regional Geology. *Paper- Geological Survey of Canada*, **74-30**: 51-106.

LANCELOT, Y. & WINTERER, E.L., 1980.— Evolution of the Moroccan oceanic basin and adjacent continental margin. A synthesis. *In*: *Initial Report Deep Sea Drilling Project, III*. Washington U.S. Government, Printing Office: 801-821.

LAPIERRE, H., MANGOLD, C., ELMI, S. & BROUXEL, M., 1984.— Deux successions volcano-sédimentaires dans le Trias d'Oranie (Algérie Occidentale): témoins de la fracturation d'une plate-forme continentale. *Revue de Géologie dynamique et de Géographie physique, Paris*, **25** (5): 361-373.

LUCA, P. DE, 1982.— L'Unité chaotique des Kebdana (région de Zaïo, Maroc). Relation structurale avec l'avant-pays du Rif oriental. *Bulletin de la Société géologique de France*, **20** (3): 339-343.

LUCAS, G., 1942.— *Description géologique et pétrographique des monts du Rhar Roubane et de Sidi El Abed*. Thèse, Université de Paris, France. Also published as 1942.— *Service géologique de l'Algérie, Alger*, **16** (2): 1-539.

MANSPEIZER, W., PUFFER, J.H. & COUSMINER, H.L., 1978.— Separation of Morocco and Eastern North America: a Triassic-Liassic stratigraphic record. *Geological Society of America Bulletin*, **89**: 901-920.

MEHDI, M., 1995.— *Stratigraphie intégrée, analyse séquentielle et micropaléontologique du Jurassique et du Crétacé inférieur de l'avant pays rifain oriental (Maroc)*. Thèse Doctorat, Université Mohammed I, Oujda, Maroc: 1-471.

NACIRI, T., 1994.— *Évolution sédimentaire, environnements et contrôles dans le Lias-Dogger des Beni Snassen orientaux (Maroc nord oriental)*. Thèse Doctorat, Université Mohammed I, Oujda, Maroc: 1-410.

OLIVET, J.L., BONNIN, J., BENZART, P. & AUZENDE, J.M., 1984.— Cinématique de l'Atlantique nord et central. *Rapport scientifique et technique CNEXO*, **54**: 1-108.

OUAHBI, W., 1996.— *Stratigraphie, sédimentologie et micropaléontologie des dépôts jurassico-crétacés de l'avant-pays rifain nord-oriental. Comparaison avec les régions voisines et place dans la marge sud-tethysienne*. Thèse de 3ème cycle, Université Mohamed V, Rabat, Maroc: 1-317.

OUAHHABI, B., 1994.— *Le Lias et le Dogger inférieur des Beni Snassen orientaux (Maroc). Stratigraphie, Paléontologie, Dynamique de Bassins, comparaisons avec les Monts d'Oujda*. Thèse de Doctorat, Université Mohamed I, Oujda, Maroc: 1-425.

OUJIDI, M., 1994.— *Le Complexe volcano-sédimentaire rouge du Trias et de la base du Lias du Pays des Horsts (Maroc Oriental). Géodynamique du bassin, dynamique sédimentaire et phénomène de silicification*. Thèse de Doctorat, Université Mohamed I, Oujda, Maroc: 1-332.

OWODENKO, B., 1946.— Mémoire explicatif de la carte géologique du bassin houiller de Djerada et de la région du Sud d'Oujda. *Mémoires de la Société géologique de Belgique, Liège*, **70**: 1-162.

Source : MNHN, Paris

PATRIAT, P.H., SEGOUFIN, J., SCHLICH, R., GOSLIN, J., AUZENDE, J.M., BEUZART, P., BONNIN, J. & OLIVET, J.L., 1982.— Les Mouvements relatifs de l'Inde, de l'Afrique et de l'Eurasie. *Bulletin de la Société géologique de France*,**7, XXIV** (2): 363-373.

TABYAOUI, H., AÏT BRAHIM, L., CHOTIN, P. & GÉLARD, J.P., 1996.— Exemples d'artefact à l'utilisation de l'imagerie radar SAR-ERS-1: effet du rabattement au sommet; faille de l'Oued Za, monts de Taourirt-Oujda. *In*: *Actes du 13ème Colloque sur les Bassins sédimentaires marocains, Marrakech, 19-22 mars 1996*. Université Cadi Ayad, Marrakech: 192.

VAIL, P.R., MITCHUM, M.R. & THOMPSON, S., 1977.— Seismic stratigraphy and global changes of sea level. *Memoirs of the American Association of Petroleum Geologists*, **26**: 63-82.

Source : MNHN, Paris

Source : MNHN, Paris

Subsidence history of the Essaouira basin (Morocco)

Kamal LABBASSI [1], *Fida* MEDINA [2], *Abdelkrim* RIMI [3], *Hosna* MUSTAPHI [4] & *Rkia* BOUATMANI [5]

[1] Département de Géologie, Faculté des Sciences, B.P. 20, El Jadida, Maroc

[2] Département de Géologie, Institut Scientifique, B.P. 703, Agdal, Rabat, Maroc

[3] Département de Physique du Globe, Institut Scientifique, B.P. 703, Agdal, Rabat, Maroc

[4] Centre régional de la Géologie, B.P. 421, Laâyoune, Maroc

[5] ONAREP, 34, avenue Al Fadila et Département de Géologie, Faculté des Sciences, B.P. 1040, Rabat, Maroc

ABSTRACT

Subsidence history of the Essaouira basin from the Triassic to present times was studied on the base of data from 28 wells and newly determined decompaction curves. The general (average of 25 curves) and selected local curves (4) include several phases of rapid subsidence: (1) a synrift phase during the Late Triassic-earliest Liassic associated with the extensional tectonism; (2) postrift phases during the late Liassic, in Late Jurassic-Early Cretaceous times, and from Hauterivian to Aptian. The synrift apparent amount of extension inferred from subsidence curves is 1.56 to 3.8 for a uniform stretching model and between 1.19 and 2.26 for a non-uniform extension model. This amount reduces to 1.17 when the area of Triassic sediments is distributed in a uniform basin upon the basement top, and is then similar to that calculated from fault restoration. These curves constitute a database for studying the thermal evolution of the basin, which led to hydrocarbon generation.

RÉSUMÉ

L'histoire de la subsidence du bassin d'Essaouira (Maroc).

L'histoire de la subsidence du bassin d'Essaouira du Trias à l'Actuel a été étudiée à partir des données de 28 forages et de nouvelles courbes de décompaction. Les courbes générales (moyenne de 25 courbes) et locales (4 courbes choisies) comportent plusieurs phases de subsidence rapide : (1) une phase syn-rift pendant le Trias supérieur-Lias basal, liée à la tectonique distensive ; (2) des phases post-rift pendant le Lias supérieur, au Jurassique supérieur-Crétacé inférieur et de l'Hauterivien à l'Aptien. La quantité d'extension apparente au cours de la période syn-rift déterminée à partir des courbes est de 1,56 à 3,8 pour un modèle d'étirement uniforme et entre 1,19 et 2,26 pour un modèle d'extension non-uniforme. Cette quantité se réduit à 1,17 quand la surface occupée par les sédiments triasiques est répartie sur un bassin uniforme au dessus du toit du socle; la quantité d'extension obtenue est alors similaire à celle calculée à partir de l'équilibrage des failles. Ces courbes constituent une base de données pour l'étude de l'évolution thermique du bassin qui a conduit à la génération d'hydrocarbures.

LABBASSI, K., MEDINA, F., RIMI, A., MUSTAPHI, H. & BOUATMANI, R., 2000.— Subsidence history of the Essaouira basin (Morocco). *In*: S. CRASQUIN-SOLEAU & É. BARRIER (eds), Peri-Tethys Memoir 5: new data on Peri-Tethyan sedimentary basins, *Mém. Mus. natn. Hist. nat.*, **182** : 129-142. Paris ISBN : 2-85653-524-0.

Source : MNHN, Paris

INTRODUCTION

The birth and later evolution of the Central Atlantic Ocean has led to the development of several coastal basins on both margins of the rift, i.e. along the present-day margins of northwestern Africa and northeastern North America. Along the Moroccan coast, the productive Essaouira (sub-) basin (DORREEN, 1987; BOUCHTA, 1992), structurally classified by petroleum geologists as a pull-apart basin (CHATELLIER & SLEVIN, 1988), is located in the central part of the larger El Jadida-Agadir basin (MEDINA, 1989a), which represents a Mesozoic-Cainozoic platform that was uplifted during the collision between Africa and Europe in Late Cretaceous and Tertiary times (Fig. 1).

The major stages of the structural evolution of the Essaouira basin during Mesozoic times can be retraced using seismic profiles (e.g., BROUGHTON & TRÉPANIER, 1993; MEHDI, 1994) and gravimetry, which gives the shape of the faulted basement top (MEHDI, 1994), but these methods remain insufficient for constraining the tectonic and thermal processes that may have controlled the evolution of the basin and hydrocarbon generation within it. They require quantitative studies, such as subsidence analysis which appears to be a powerful technique, as already shown by its application to surface and subsurface sections of the El Jadida-Agadir basin (MEDINA, 1992; MUSTAPHI & BOUATMANI, 1996; MUSTAPHI, 1997). However, the database used in the previous studies was too small for being conclusive, since isolated sections, which represent one-dimensional evolution, may only reflect local phenomena – such as a horst structure, for instance – , and cannot be used for thermal modeling and setting subsidence maps. Therefore, we analyse in this paper the structural aspects of the subsidence history of the Essaouira basin, with the help of a large database, collected mainly from subsurface information (boreholes and fictitious wells) supplied by ONAREP (Rabat), within the productive zone of the basin.

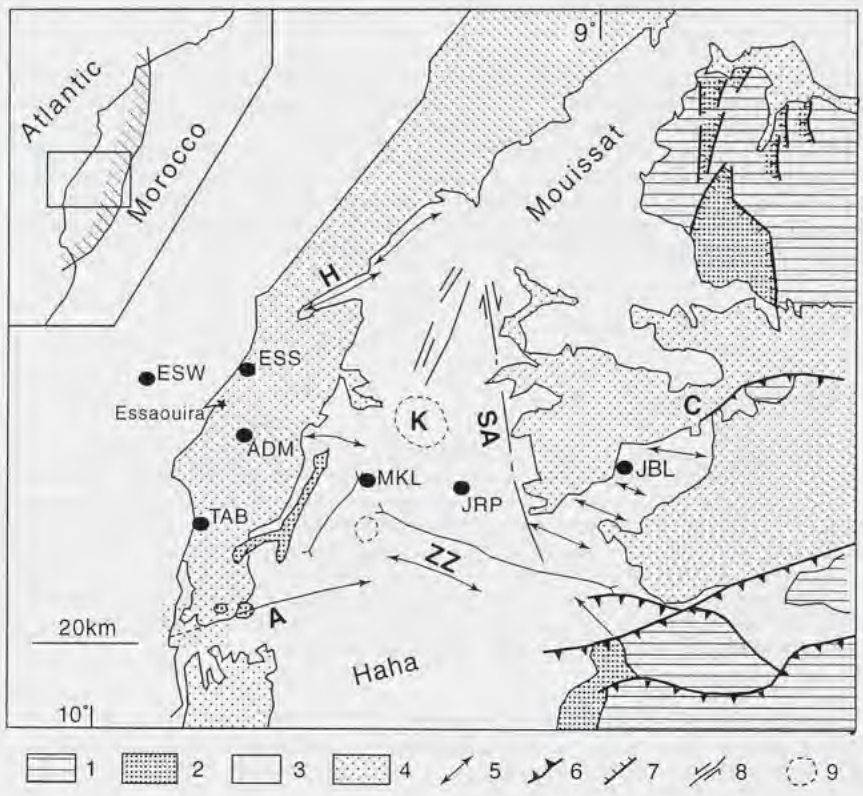

FIG. 1.— Simplified structural map of the Essaouira basin and adjacent areas, and location of the studied wells. **1**, Precambrian and Palaeozoic; **2**, Triassic (and Permian *p.p.*); **3**, Jurassic to Early Tertiary; **4**, Pliocene and Quaternary; **5**, anticlinal axis; **6**, thrust; **7**, normal fault; **8**, strike-slip fault; **9**, diapir. **H**, Jbel Hadid anticline; **K**, Kechoula diapir; **T**, Tidsi diapir; **A**, Amsitten anticline; **ZZ**, Zem Zem anticline; **SA**, Sidi Amara fault; **C**, Chichaoua. Fictitious well ESPRF is located west of the area shown in the figure.

*FIG. 1.— Carte structurale simplifiée du bassin d'Essaouira, et localisation des forages étudiés. **1**, Précambrien et Paléozoïque ; **2**, Trias (et Permien* p.p.*) ; **3**, Jurassique à Tertiaire inférieur ; **4**, Pliocène et Quaternaire ; **5**, axe anticlinal ; **6**, faille inverse ; **7**, faille normale ; **8**, décrochement ; **9**, diapir. **H**, anticlinal du Jbel Hadid ; **K**, diapir de Kechoula ; **T**, diapir de Tidsi ; **A**, anticlinal d'Amsitten ; **ZZ**, anticlinal du Zem Zem ; **SA**, faille de Sidi Amara ; **C**, Chichaoua. Le puits fictif ESPRF est situé à l'ouest de la région représentée dans la figure.*

Source : MNHN, Paris

STRUCTURAL SETTING

The Essaouira basin (Fig. 1) appears as an east-west trending synclinorium with Mesozoic (mainly Cretaceous) sediments, affected by weak deformations (SOUID AHMED, 1983; MEDINA, 1989b; MEHDI, 1994) consisting of NE-SW to WNW-ESE folds at the basin edges (Amsitten, Zem Zem, Chichaoua and Hadid shear zones), diapiric structures (e.g., Kechoula) and NNW-SSE to ENE-WSW strike-slip faults or fault zones injected or not by Triassic salt (Sidi Amara, Tidsi). All these deformations were produced by the Late Cretaceous to Quaternary compressions related to the collision between Africa and Europe.

The older Mesozoic structures appear along E-W seismic sections, which show: (i) a Late Triassic to earliest Liassic synrift series deposited within westwards-dipping half-grabens bounded by N-S-trending, moderately-dipping, normal faults, and (ii) a relatively undeformed Jurassic and Cretaceous post-rift sequence disrupted by salt diapirs (Fig. 2). The half grabens are isolated from the final rift zone, located westwards, by horsts such as the Meskala-Zelten horst structure (BROUGHTON & TREPANIER, 1993; BOUATMANI, 1995). The amount of extension at the surface, calculated by restoration of cross-sections attains 17% (BOUATMANI, 1995). Some of the seismic sections clearly show that the faults merge into a detachment plane at 4 sTWT (MEDINA, in press), as in the Souss basin located southwards (MEDINA *et al.*, 1996; MUSTAPHI *et al.*, 1997). Contrary to the synrift period, deposition and palaeogeography during the postrift stage was mainly controlled by sea level changes, diapirism, and some mild tectonics (e.g., WIEDMANN *et al.*, 1982; TAJ-EDDINE & BEN ABBES TAARJI, 1996).

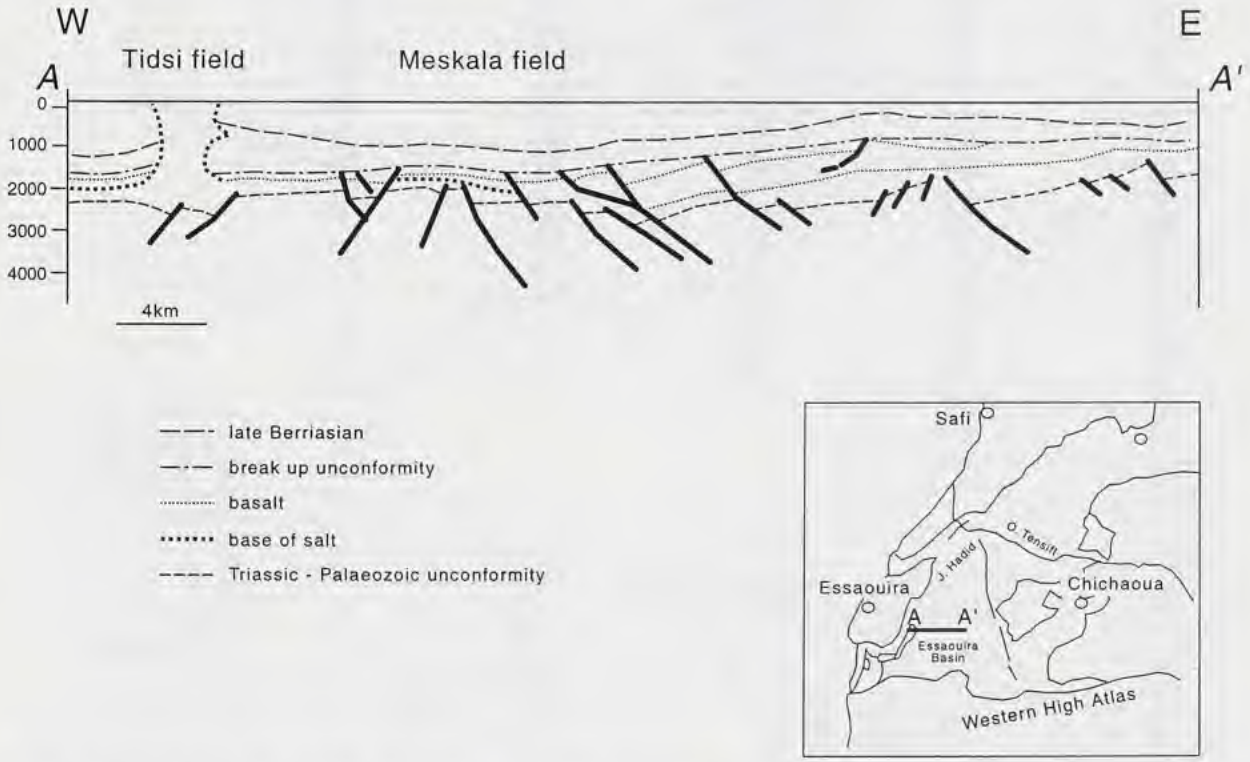

FIG. 2.— Interpretation of an E-W oriented seismic profile across the Essaouira basin (from BOUATMANI & AIT SALEM, unpublished). Vertical scale in metres.

FIG. 2.— Interprétation d'un profil de sismique-réflexion, de direction E-W, à travers le bassin d'Essaouira (d'après BOUATMANI & AIT SALEM, inédit). Échelle verticale en mètres.

Source : MNHN, Paris

SUBSIDENCE HISTORY

Subsidence history of the Essaouira basin can be visualised through burial and thermo-tectonic curves and subsidence rate histograms. Computation was carried out with the help of the computer program BURSUB (STAM *et al.*, 1987) for 28 wells (two are offshore) and one fictitions well. For clarity, only the three most complete wells (JRP1, MKL1 and ADM1), which are those that reach the basement, and a fictitions well (ESPRF1) are shown (Fig. 1).

INPUT PARAMETERS

Lithostratigraphic column. The Mesozoic series drilled in the Essaouira basin (see DUFFAUD *et al.*, 1966; BROUGHTON & TRÉPANIER, 1993) can be simplified as the following, according to biostratigraphic datings (Fig. 3): (1) Late Triassic to earliest Liassic syn-rift detritics (mainly sandstones and siltsones with halite) and volcanic rocks located within the half-grabens (levels T1 to J0); and (2) Jurassic (J1 to J9), Cretaceous (C1 to C6) and Eocene postrift deposits, consisting of carbonates, clastics and minor evaporites. Thickness of the formations generally increases westwards. It may be noted that the biostratigraphic datings given by ONAREP reports have not been revised; therefore, the formations encountered in the wells may show some sligth diachronism with the surface formations that have been extensively studied during the last years. However, the presumed difference has not an important influence on our study, because we work at a relatively large scale.

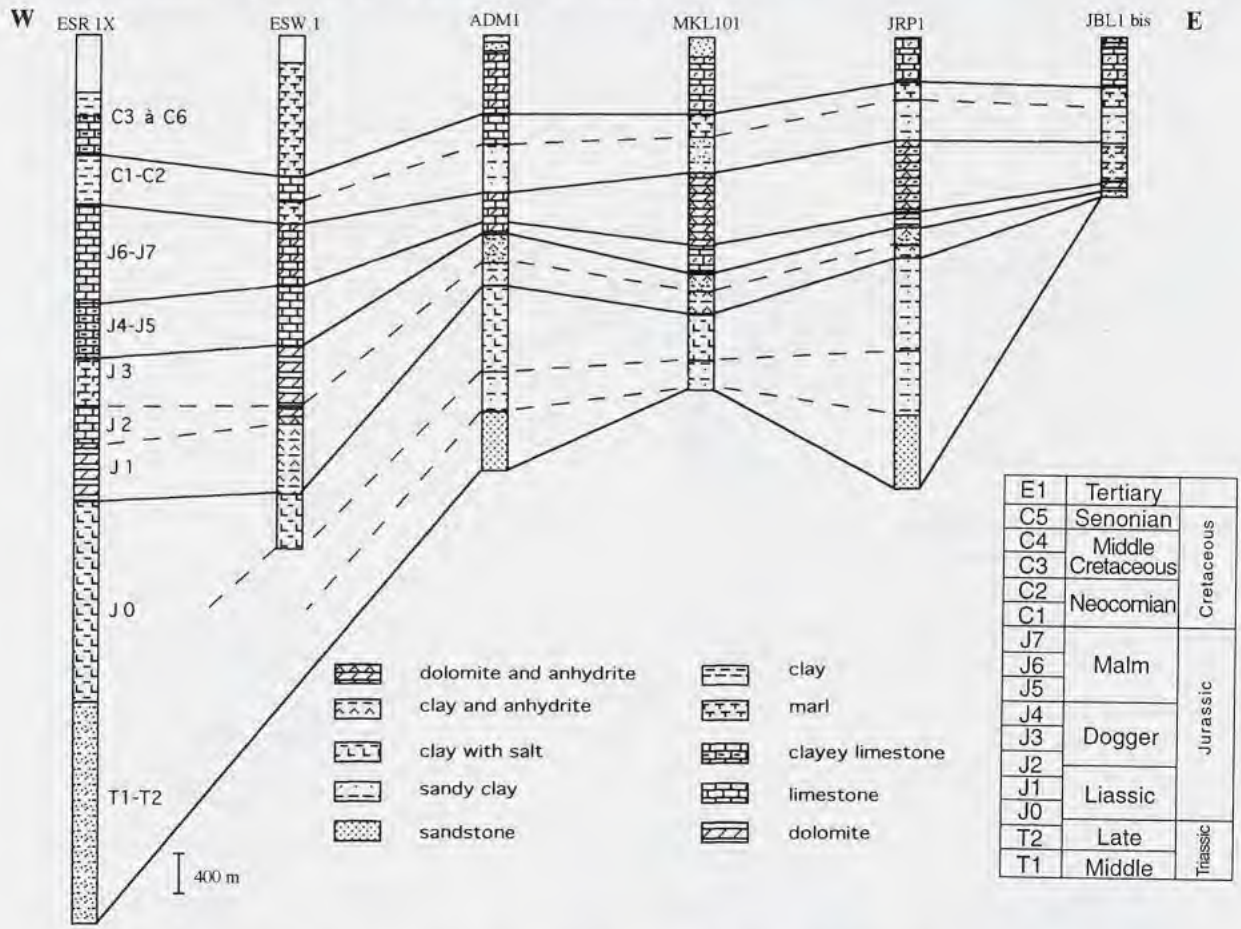

FIG. 3.— Lithologic columns of the Mesozoic formations in Essaouira basin (location on figure 1).

FIG. 3.— Colonnes lithologiques des formations mésozoïques du bassin d'Essaouira (localisation sur la figure 1).

Source : MNHN, Paris

Decompaction parameters. Decompaction curves and parameters were newly determined on the base on 2680 datapoints obtained from sonic logs (LABBASSI, in press) for five different lithologies: clay, sandy clay, sandstones, limestones and dolomites. The values obtained for surface porosity (Φo) and for constant c (Fig. 4) appear to be reliable since they are not very different from those determined by other

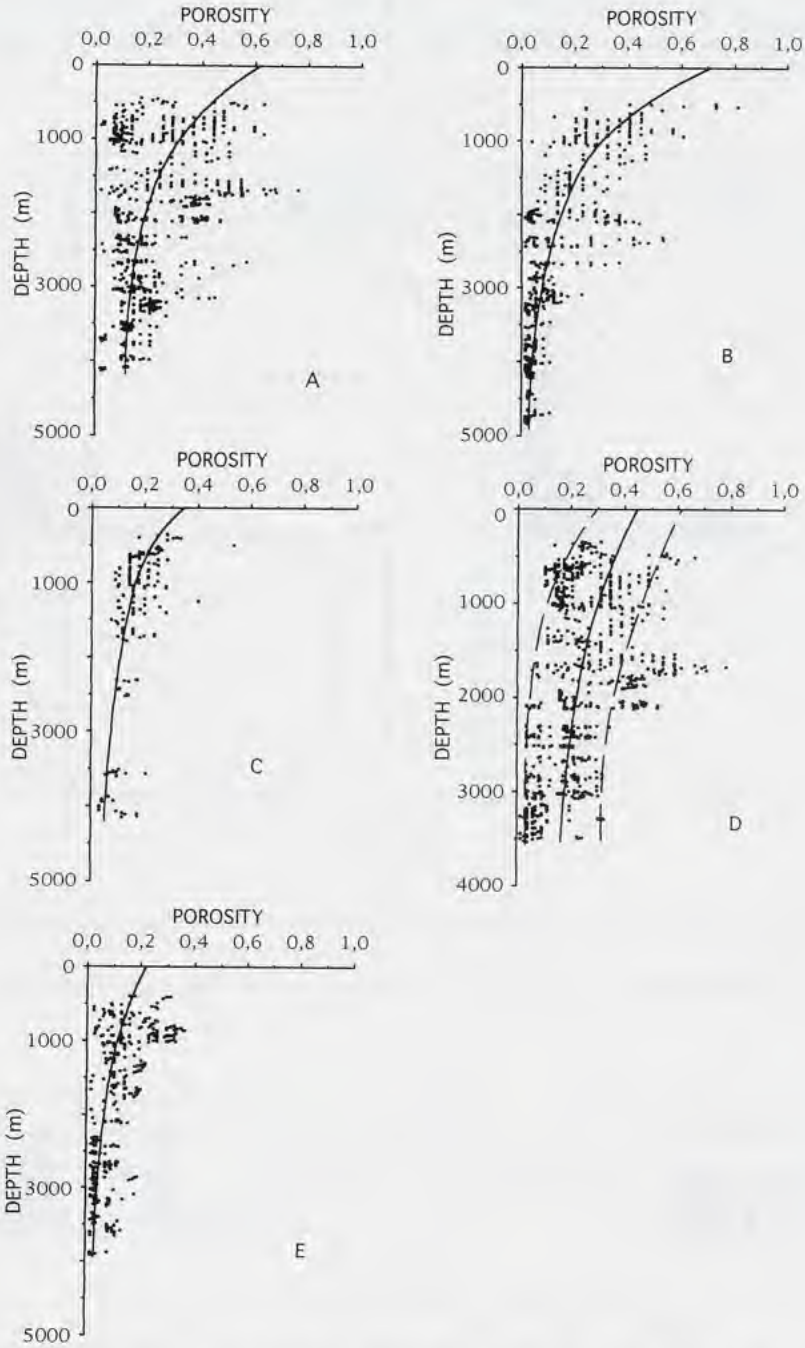

FIG. 4.— Porosity vs. depth datapoints and curves for 5 lithologies, determined from sonic logs. **A**, sandy clay (Φo=0.62; c=0.57); **B**, clay (Φo=0.71; c=0.77); **C**, sandstones (Φo=0.35; c=0.59); **D**, limestones (Φo=0.46; c=0.23); **E**, dolomites (Φo=0.21; c=0.6).

*FIG. 4.— Points de mesure et courbes de porosité en fonction de la profondeur pour 5 lithologies, déterminés à partir des diagraphies. **A**, argiles gréseuses (Φo=0,62 ; c=0,57) ; **B**, argiles (Φo=0,71 ; c=0,77) ; **C**, grès (Φo=0,35 ; c=0,59) ; **D**, calcaires (Φo=0,46 ; c=0,23) ; **E**, dolomies (Φo=0,21 ; c=0,6).*

Source : MNHN, Paris

authors in the same area (MEDINA & RIMI, 1992) or in other regions (ROYDEN & KEEN, 1980; SCLATER & CHRISTIE, 1980; BRUNET, 1991).

Depth of deposition. According to sedimentological and palaeontological data, sediments in Essaouira basin were deposited in a shallow environment, the depth of which did not exceed 100 m, as indicated for instance by the ubiquitous presence of evaporites in Late Jurassic and Middle to Late Cretaceous times (ETTACHFINI *et al.*, 1989; ALGOUTI *et al.*, 1993). These depth values do not therefore introduce large estimation errors. Maximal depths were recorded during Late Jurassic and Middle Cretaceous times (Fig. 5, A).

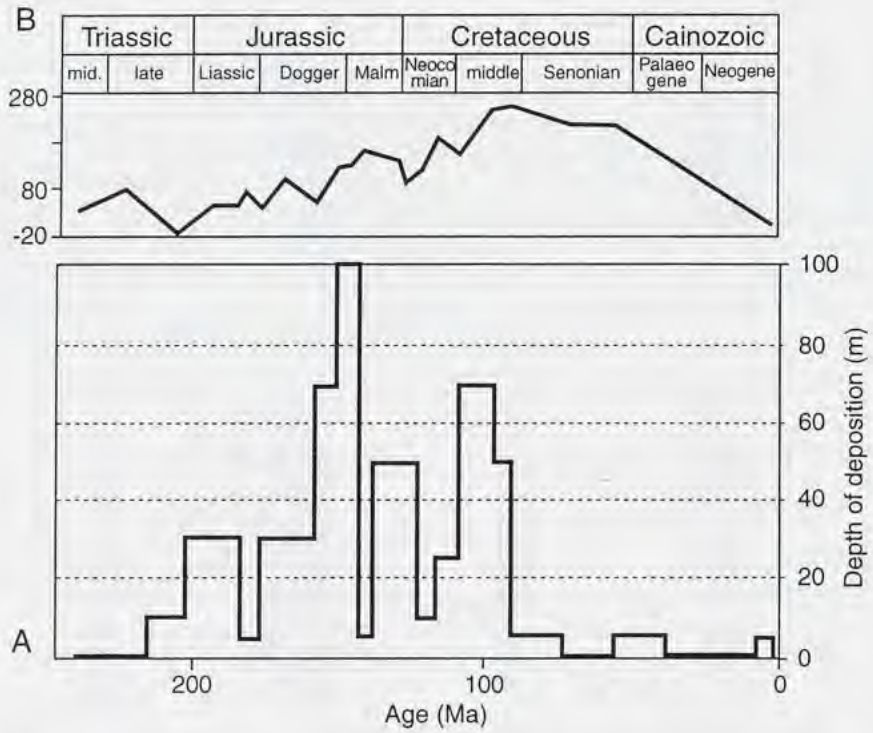

FIG. 5.— Depth of deposition values for the Essaouira basin formations (A) and sea level changes (B). B from HAQ *et al.* (1987).

FIG. 5.— Profondeur de dépôt des formations du bassin d'Essaouira (A) et variations du niveau marin (B). B d'après HAQ et al. *(1987).*

Sea level changes. Values of sea level changes were taken from the long-term curves of HAQ *et al.* (1987), which show a maximum of about 270 m during the Middle Cretaceous (Fig. 5, B).

Chronostratigraphic scale. In order to maintain homogeneity with chronology of sea level changes, the chonostratigraphic scale was also taken from HAQ *et al.* (1987).

RESULTS

SUBSIDENCE CURVES

Subsidence curves were established for the top of the Palaeozoic basement in each well (Fig. 6). The lower and upper curves respectively represent burial (with or without compaction) and unloaded thermo-tectonic subsidence for a local, Airy-type isostatic compensation. We also present histograms of tectonic subsidence rates, which allow visualising the main phases.

Source : MNHN, Paris

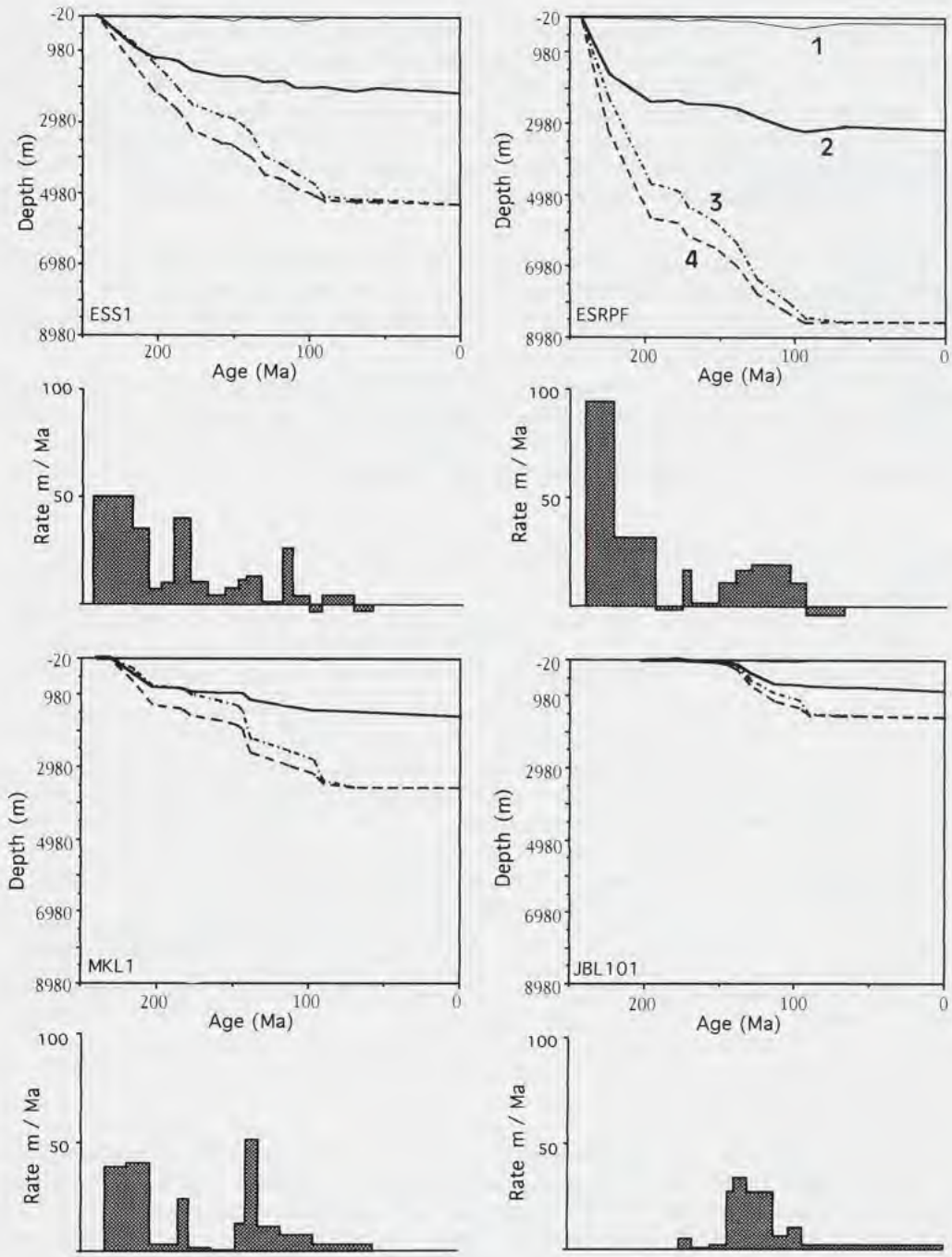

FIG. 6.— Total and thermo-tectonic subsidence curves and histograms of rates of subsidence for wells JRP1, MKL1 and ADM1 and fictitious well ESPRF1. **1**, depth of deposition; **2**, thermo-tectonic subsidence; **3**, total subsidence without decompaction; **4**, total subsidence with decompacted sediments.

*FIG. 6.— Courbes de subsidence totale et thermo-tectonique, et histogrammes de taux de subsidence pour les forages JRP1, MKL1 et ADM1, et le puits fictif ESPRF1. **1**, profondeur de dépôt ; **2**, subsidence thermo-tectonique ; **3**, subsidence totale sans décompaction ; **4**, subsidence totale avec sédiments décompactés.*

Source : MNHN, Paris

Analysis of subsidence curves shows several rapid (tectonic) phases which, however, are not necessarily common to all the sections.

Thus, the first phase of rapid subsidence was recorded during the Triassic (probably Late Triassic)-earliest Liassic (230-194 Ma). Initial fault-controlled subsidence reaches 1200 m to 1500 m and represents 40% to 70% of the total tectonic subsidence. We note that well MKL shows a slight uplift before the inception of subsidence, which may be interpreted as due to footwall uplift related to extensional faulting. During the Liassic and Middle Jurassic (194-143 Ma), subsidence generally slows down, although some anomalies, expressed by a steep slope during the late Liassic (183-177 Ma) may disturb this calm period. During the Callovian-Oxfordian (158-143 Ma) some wells show no subsidence at all.

In Late Jurassic-Early Cretaceous times (143-129 Ma), a second major phase is recorded in all the sections. This rapid subsidence is followed by a calm period with an acceleration phase during the Hauterivian (113 Ma). During Middle and Late Cretaceous times, there is generally no tectonic subsidence, but rather some tendency to uplift.

The figure 7 shows the spatial evolution of subsidence through the plot of the four tectonic curves; thus, well MKL, located on the Meskala-Zelten horst structure, has undergone less subsidence than ADM and JRP which are located on either side of the horst. On the contrary, fictitious well ESPRF shows a very large amount of subsidence reflecting its distal position.

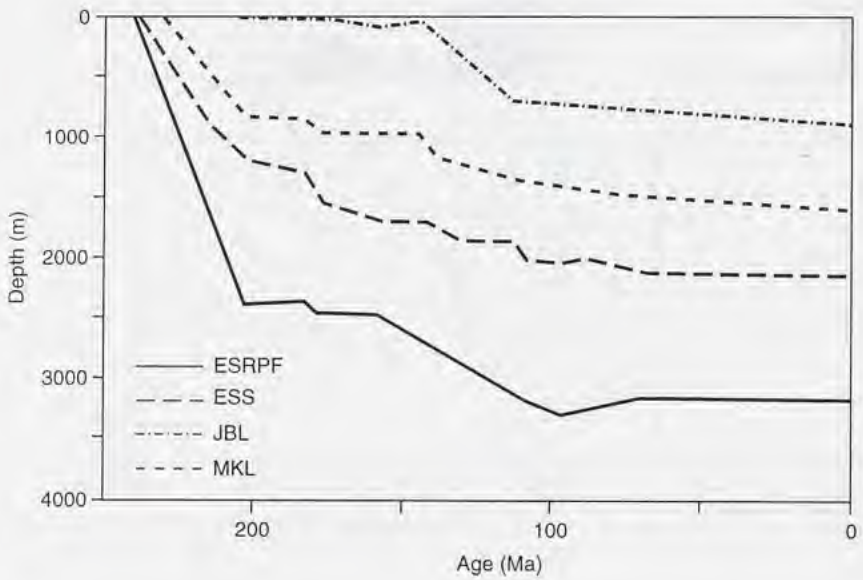

FIG. 7.— Plot of the studied four thermo-tectonic curves.

FIG. 7.— Diagramme des quatre courbes thermo-tectoniques étudiées.

Since almost all subsidence curves show differences that may be caused by different effects, we have tried to remove the latter by constructing a "regional" smoothed curve for tectonic subsidence, based on averaging the data of 25 curves (Fig. 8). It is important to note that because most wells do not reach the basement, we are only interested in the variation of the subsidence, not in its absolute value, which needs normalizing the curves with respect to the oldest level that can be found in all wells (e.g., BRUNET & LE PICHON, 1981). The smoothed curve, which may best reflect the subsidence history of the Essaouira basin, shows four stages of rapid (tectonic) subsidence followed by a slow (thermal) subsidence; the rapid subsidence stages are recorded during the Triassic (240-201 Ma), from the Toarcian to the Bajocian (187-167 Ma), during the Tithonian-Berriasian (141-130 Ma), and from the late Hauterivian to the Aptian (120-108 Ma). As we have indicated before, the chronology of these stages is strongly dependent on the biostratigraphic dates made by ONAREP, which have not been revised.

Source : MNHN, Paris

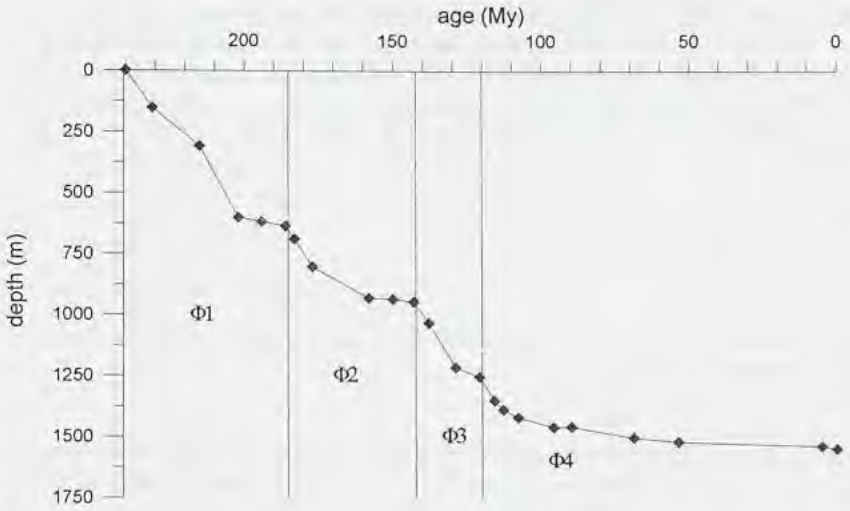

FIG. 8.— Average thermo-tectonic subsidence curve for the Essaouira basin, based on data from 25 subsidence curves. Φ1 to Φ4, stages of subsidence.

FIG. 8.— Courbe de subsidence thermo-tectonique moyenne du bassin d'Essaouira, basée sur les données de 25 courbes de subsidence. Φ1 à Φ4, stades de subsidence.

AMOUNT OF EXTENSION

The amount of extension, expressed by the parameters β and δ, was evaluated by comparing the observed curves to the theoretical ones established for different models, especially the uniform (MCKENZIE, 1978) and non-uniform (ROYDEN & KEEN, 1980; HELLINGER & SCLATER, 1983; LISTER *et al.*, 1991) stretching models, assuming normal thicknesses of the crust (30-35 km) and the lithosphere (125 km) for the synrift phase, and an attenuated crust and lithosphere during the post-rift stages.

SYNRIFT PHASE.— Comparison of the observed subsidence curves to the theoretical ones for a uniform stretching model, shows that the amount of extension is variable, attaining 3.8 in the west, and 1.56 at the eastern border. These values appear to be too high with respect to estimations from fault restoration (BOUATMANI, 1995), and are not common to continental proximal areas. In addition, most subsidence curves show an amount of thermal subsidence much smaller than that expected from the value of initial tectonic subsidence. We conclude that the use of the uniform extension model may not be adequate, and we investigate in the following the use of a non-uniform extension model. Although the estimation of crustal and subcrustal extension in this case is made difficult by the second subsidence phase (Liassic-Middle Jurassic), which breaks the trend of the thermo-relaxation curve, the very small amount of thermal relaxation during the Liassic (only 10 m during the 10 Ma that immediately follows the rapid subsidence phase), suggests very small amounts of subcrustal streching, and even no subcrustal stretching at all; so if we fix the latter to unity ($\beta=1$), then the amounts of crustal stretching δ are, depending on the adopted models (HELLINGER & SCLATER, 1983; ROYDEN, 1986), between 1.19 and 1.56 onshore and 1.97 and 2.26 offshore. It can be readily noticed that this amount is much smaller than that obtained using the uniform extension model, and are closer to – although still higher than– the values obtained from faults. We will review this point in the discussion. Another explanation for the almost flat thermal relaxation phase could be a border effect, according to which the walls of extensional basins cool very rapidly because of lateral conduction of heat. Thus, narrow basins and borders of wider basins may show little thermal subsidence. In the case of Essaouira basin, we believe that both mechanisms (simple shear and border effect) have taken place.

POST-RIFT PHASES.— Post-rift subsidence phases are relatively less important as can be seen on the different curves, and excepting ESPRF1, even the rapid subsidence observed during the Late Jurassic becomes difficult to discern when reducing the vertical scale, as in figure 6. Assuming that the lithosphere has been sufficiently weakened by the previous event, as indicated by the extrusion of volcanics, a uniform stretching model seems to be more adequate than a non-uniform one. Taking into account the previous event for the calculations, i.e. a stretched crust and no subcrustal stretching, the values of β ($=\delta$) are around 1.05 for well MKL as well as for the other sections where the event is clear. The same can be said for the Late Jurassic-Early Cretaceous event, which shows larger values of β (1.11). The apparent cumulative stretching since the onset of rifting is about 1.3. However, one must

Source : MNHN, Paris

keep in mind that the Cretaceous events may not be indicative of any real tectonic stretching, since: (1) the faults sole out into detachment levels located within the sedimentary cover, and therefore can be considered as growth faults, the effects of which are recorded by the sedimentary column, and (2) the region comprises several diapiric structures that had some important influence on the sedimentary record, especially in Cretaceous times (e.g., TAJ-EDDINE & BEN ABBES TAARJI, 1996).

DISCUSSION

In the following, we discuss the obtained results, by comparison to those obtained with the help of other methods such as gravimetry and seismic reflection.

According to gravimetric data taken from TADILI *et al.* (1986) and BERNARDIN (1988), thickness of the crust beneath the Essaouira basin is roughly 30 km in the east and 25 km in the west. Although the basin is located at the foreland of the Atlas chain, no major thickening of the crust can be inferred from gravimetry (BERNARDIN, 1988). The value of crustal thinning is then 0 to 17% for an initial crustal thickness of 30 km, and 14 to 28% for a 35 km-thick crust. The maximum value of δ is 1.28.

Restoration of cross-sections by removal of the offsets induced by the activity of normal faults gives stretching values of 15-17% only (BOUATMANI, 1995), which fit well with those determined through gravimetry. Unfortunately, no other measurements can be made on fault blocks since the synrift sequence becomes deeply buried westwards.

Although we admit that most stretching occurred during the synrift phase, the values of crustal thinning determined from subsidence curves (1.19 and 1.56 onshore and 1.97 and 2.26 offshore) remain too high.

Some similar disparities have been found by several authors, in the North Sea (COWARD, 1986), in the Celtic basin (DYMENT, 1989) and in the Gulf of Lions (BURRUS, 1989). Different explanations have been suggested, such as: (1) variable amounts of stretching at different levels of the crust (North Sea), (2) neoformation of the Moho discontinuity (Celtic basin) removing the effects of crustal thinning during the previous extension, and (3) phase changes at the deepest levels of the crust (Gulf of Lions).

We think that evaluation of the extension in Essaouira basin from subsidence curves is overestimated, because it only takes into account particular sections, which may not be representative of the whole basin; on the other hand, petroleum exploration wells are drilled on particular structures. The amount of extension obtained is then only *apparent*. A much better approximation could be the estimation of the area produced by the extension, and then a mean thickness of the Triassic strata. In our case, it appears obvious that initial subsidence determined from thickness of the synrift section within more or less triangular half-grabens will lead to overestimated amounts of extension when the borehole crosses the thickest part of the half-graben, and to underestimated values in the thinnest parts. If we replace the triangular basin by a rectangular one with the same area, we obtain a uniformly stretched shape, to which the uniform stretching model can be compared.

We have applied this method to the studied section. From the figure 9, the total area covered by synrift sediments within the triangular half-grabens is about 50 km^2. When converting the area from triangles to a single rectangle, the depth of the sediment-filled basin becomes 1 km. For a sediment of density 2.2 g/cm^3, the value of β obtained is 1.17 which fits exactly with that measured through normal faults.

From gravimetric data, the Moho raises from approximately 30 km in the east to 25 in the west; the created area is about 125 km^2, which is larger than that created at the surface. The difference can be explained by the uncertainties on density contrasts, which may lead to large errors on Moho depth.

A more important problem is the occurrence of basalts within the Triassic series and at its top, since adiabatic decompression and subsequent melting beneath a normal lithosphere, i.e. the base of which is at 1333°C need large amounts of extension (>2 according to LE PICHON & SIBUET, 1981). This can be readily solved by admitting that subcrustal extension occurred westwards, in the direction of the final

Source : MNHN, Paris

rift axis, so the basalts were generated at some distance of the basin. The overall absence of feeder dykes or necks in the area is in good agreement with this assumption.

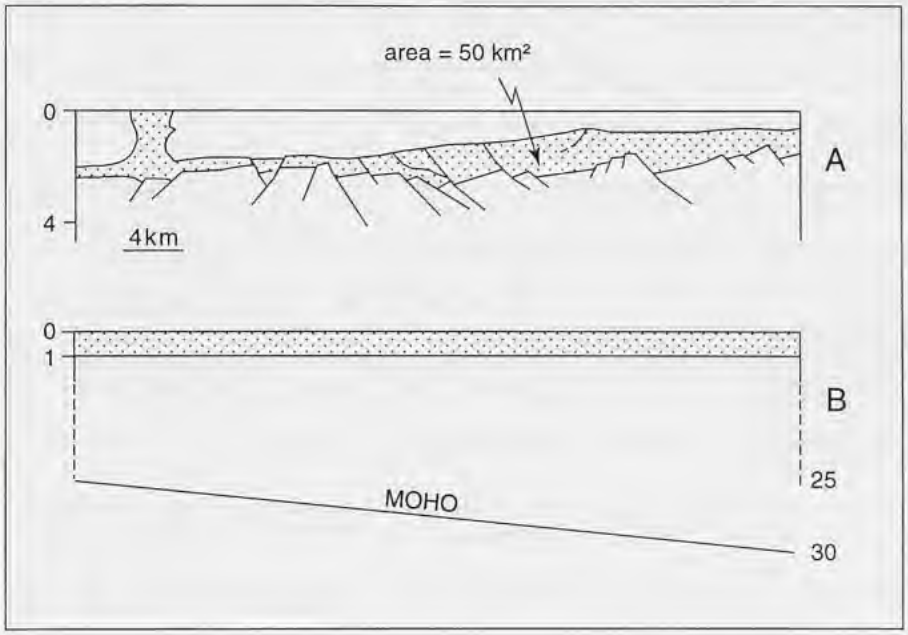

FIG. 9.— Sketch showing the effect of distributing the area occupied by the Triassic formations on a rectangle instead of triangles (half grabens).

FIG. 9.— Schéma montrant l'effet de répartition de la surface occupée par les formations triasiques sur un rectangle au lieu d'un triangle (demi-graben).

CONCLUSION

Subsidence history of the Essaouira basin reveals several phases of rapid subsidence: (1) a synrift phase during the Triassic-earliest Liassic (240-201 Ma) associated with the extensional tectonism; (2) postrift phases during the late Liassic (187-167 Ma), in Late Jurassic-Early Cretaceous times (141-130 Ma), and during the Hauterivian to Aptian (120-108 Ma). The synrift *apparent* amount of extension inferred from subsidence curves is 1.56 to 3.8 for a uniform stretching model and between 1.19 and 2.26 for a non-uniform extension model. This amount falls to 1.17 when the area of Triassic sediments is distributed in a uniform basin upon the basement top, and is then similar to that calculated from fault restoration.

ACKNOWLEDGEMENTS

This paper is part of the State Thesis of one of us (K. LABBASSI), which was funded in part by the Peri-Tethys Program. We would like to thank ONAREP (Rabat) for providing the well data, and R. STEPHENSON and an anonymous reviewer for their comments.

REFERENCES

ALGOUTI, AH., ALGOUTI, AB., CHBANI, B. & AZZAOUI, K.A., 1993.— Turonien supérieur et Sénonien dans la région d'Imin'Tanout (Haut Atlas, Maroc): sédimentologie, diagenèse, analyse séquentielle. *Revue de la Faculté des Sciences Marrakech-Semlalia, section Sciences de la Terre*, **7**: 183-196.

BERNARDIN, C., 1988.— *Interprétation gravimétrique et structure profonde de la Meseta marocaine et de sa marge atlantique*. Thèse, Université St-Jérôme, Marseille, France: 1-162.

BOUATMANI, R., 1995.— *Étude préliminaire du Trias du bassin d'Essaouira*. Mémoire de DEA, Université Mohammed V, Rabat, Maroc: 1-40.

Source : MNHN, Paris

BOUCHTA, R., 1992.— Prospects pétroliers et miniers liés à la marge passive atlantique du Maroc. *Notes et Mémoires du Service géologique du Maroc, Rabat*, **366**: 103-112.

BROUGHTON, P. & TRÉPANIER, A., 1993.— Hydrocarbon generation in the Essaouira basin of western Morocco. *AAPG Bulletin*, **77** (6): 999-1015.

BRUNET, M.F., 1991.— *Subsidence et géodynamique du Bassin d'Aquitaine. Relations avec l'ouverture de l'Atlantique.* Thèse d'État, Université Paris VI, Paris, France: 1-287.

BRUNET, M.F. & LE PICHON, X., 1981.— Subsidence of the Paris Basin. *Journal of Geophysical Research*, **87** (B10): 8547-8560.

BURRUS, J., 1989.— Review of geodynamic models for extensional basins; the paradox of the gulf of Lions. *Bulletin de la Société géologique de France*, **8**, **V** (2): 377-393.

CHATELLIER, J.-Y. & SLEVIN, A., 1988.— Review of African petroleum and gas deposits. *Journal of African Earth-Sciences*, **7** (3): 561-578.

COWARD, M.P., 1986.— Heterogeneous stretching, simple shear and basin development. *Earth & Planetary Science Letters*, **80**: 325-336.

DORREEN, J.M., 1987.— Petroleum exploration in the coastal basins and offshore Morocco. *In*: C.D. CORNELIUS, M. JARNAZ & E.P. LEHMANN (eds), *Geology and Culture of Morocco* Earth-Sciences Society of Libya, Damas: 111-116.

DUFFAUD, F., BRUN, L. & PLAUCHUT, B., 1966.— Le Bassin du Sud-Ouest marocain. *In*: D. REYRE (ed.), Bassins sédimentaires du littoral africain: symposium de New Delhi. *Bulletin d'information et de liaison de l'Association des services géologiques africains*, **I**: 5-26.

DYMENT, J., 1989.— SWAT et les bassins celtiques: relations avec la croûte hercynienne, néoformation du Moho. *Bulletin de la Société géologique de France*, **8**, **V** (3): 477-487.

ETTACHFINI, E.M., EL KAMALI, N. & BILOTTE, M., 1989.— Essai de caractérisation bio- et lithostratigraphique des séquences sédimentaires dans le Crétacé moyen de la région d'Imi n'Tanout (Haut Atlas occidental, Maroc). *Sciences géologiques, Strasbourg, Mémoires*, **84**: 71-81.

HAQ, B.U., HARDENBOL, J. & VAIL, P.R., 1987.— Chronology of fluctuating sea level since the Triassic. *Science*, **235**: 1156-1167.

HELLINGER, S.J. & SCLATER, J.G., 1983.— Some comments on two-layer extensional models for the evolution of sedimentary basins. *Journal of Geophysical Research*, **88** (B10): 8251-8269.

LABBASSI, K., in press.— Détermination des lois de compaction dans le bassin d'El Jadida-Agadir. *Gaia*.

LE PICHON, X. & SIBUET, J.-C., 1981.— Passive margins: a model of formation. *Journal of Geophysical Research*, **86** (B5): 3708-3720.

LISTER, G.S., ETHERIDGE, M.A. & SYMONDS, P.A., 1991.— Detachment models for the formation of passive continental margins. *Tectonics*, **10**: 1038-1064.

MCKENZIE, D.P., 1978.— Some remarks on the development of sedimentary basins. *Earth & Planetary Science Letters*, **40**: 25-32.

MEDINA, F., 1989a.— Extensional tectonics in the El Jadida-Agadir (Morocco) Triassic-Liassic basin during the early rifting of the Central Atlantic. *Garcia de Orta, Lisboa, série Geologia*, **12** (1-2): 21-36.

MEDINA, F., 1989b.— Landsat imagery interpretation of Essaouira basin (Morocco). Comparison with geophysical data, and structural implications. *Journal of African Earth-Sciences*, **9** (1): 69-75.

MEDINA, F., 1992.— La Subsidence jurassique à éocène dans le bassin d'El Jadida-Agadir (Maroc): essai de quantification. *Comunicaçoes dos Serviços geologicos de Portugal*, **78** (2): 133-144.

MEDINA, F., in press.— Structural Styles of the Morrocan Triassic Basins. *In*: I. LERCHE & G. H. BACHMANN (eds), *The Epicontinental Triassic*. Springer, Berlin.

MEDINA, F., MUSTAPHI, H., JABOUR, H., HOEPFFNER, CH., AHMAMOU, M., ERRAMI, A. & EL FARIATI, A., 1996.— Structure des formations triasiques le long du segment occidental de la zone de faille du Tizi n'Test. *In:* F. MEDINA (ed.), *Le Permien et le Trias du Maroc: état des connaissances*. Pumag, Marrakech: 291-305.

MEDINA, F. & RIMI, A., 1992.— Détermination des coefficients de compaction pour les calcaires et les argilites du bassin côtier mésozoïque marocain. *Bulletin de l'Institut scientifique*, **16**: 60-64.

MEHDI, K., 1994.— *Analyse et synthèse des études géologiques et géophysiques de la partie orientale du bassin d'Essaouira (Maroc).* Thèse de Doctorat, Université Bordeaux I, Bordeaux, France: 1-300.

MUSTAPHI, H., 1997.— *Apport des données de subsurface (sismique-reflexion et forages) et de modélisation à l'étude de l'évolution structurale du bassin du Souss du Trias à l'Actuel*. Thèse de 3ème cycle, Université Mohammed V, Rabat, Maroc: 1-248.

MUSTAPHI, H. & BOUATMANI, R., 1996.— Analyse de la subsidence dans les bassins d'Agadir et d'Essaouira. *In*: *Actes du 13ème Colloque sur les Bassins sédimentaires marocains, Marrakech, 19-22 mars 1996*. Université Cadi Ayad, Marrakech: 147-148.

MUSTAPHI, H., MEDINA, F., JABOUR, H. & HOEPFFNER, CH., 1997.— Le Bassin du Souss (Haut Atlas occidental, Maroc): résultat d'une inversion tectonique contrôlée par un détachement profond. *Journal of African Earth-Sciences*, **24** (1-2): 153-168.

Source : MNHN, Paris

ROYDEN, L., 1986.— A Simple method for analyzing subsidence and heat flow in extensional basins. *In*:J. BURRUS (ed.), *Thermal modeling in sedimentary basins*. Technip, Paris: 49-73.

ROYDEN, L. & KEEN, C.E., 1980.— Rifting process and thermal evolution of the continental margin of Eastern Canada determined from subsidence curves. *Earth & Planetary Science Letters*, **51**: 343-361.

SCLATER, J.G. & CHRISTIE, P.A.F., 1980.— Continental stretching: an explanation of the post mid-Cretaceous subsidence of the Central North Sea graben. *Journal of Geophysical Research*, **85** (B7): 3711-3739.

SOUID AHMED, K., 1983.— *Étude tectonique et microtectonique des injections de Trias dans le bassin d'Essaouira pendant les compressions alpines dans l'avant-pays atlasique (Maroc)*. Thèse de 3ème cycle, Université de Montpellier, Montpellier, France: 1-101.

STAM, B.E., GRADSTEIN, F.M., LLOYD, P. & GILLIS, D., 1987.— Algorithms for burial and subsidence history. *Computers and Geosciences*, **13** (2): 317-342.

TADILI, B., RAMDANI, M., BEN SARI, D., CHAPOCHNIKOV, K. & BELLOT, A., 1986.— Structure de la croûte dans le Nord du Maroc. *Annales geophysicae*, (B)**4**: 99-104.

TAJ-EDDINE, K. & BEN ABBES TAARJI, R.K., 1996.— Halocinèse et sédimentation dans le bassin d'Essaouira (Atlas atlantique, Maroc). *In*: *Actes du 13ème Colloque sur les Bassins sédimentaires marocains, Marrakech, 19-22 mars 1996*. Université Cadi Ayad, Marrakech:197-198.

WIEDMANN, J., BUTT, A. & EINSELE, G., 1982.— Cretaceous stratigraphy, environment and subsidence history of the Moroccan continental margin. *In*: U. VON RAD, K. HINZ, M. SARNTHEIN & E. SEIBOLD (eds), *Geology of the Northwest African Continental Margin*. Springer, Berlin: 366-395.

Source : MNHN, Paris

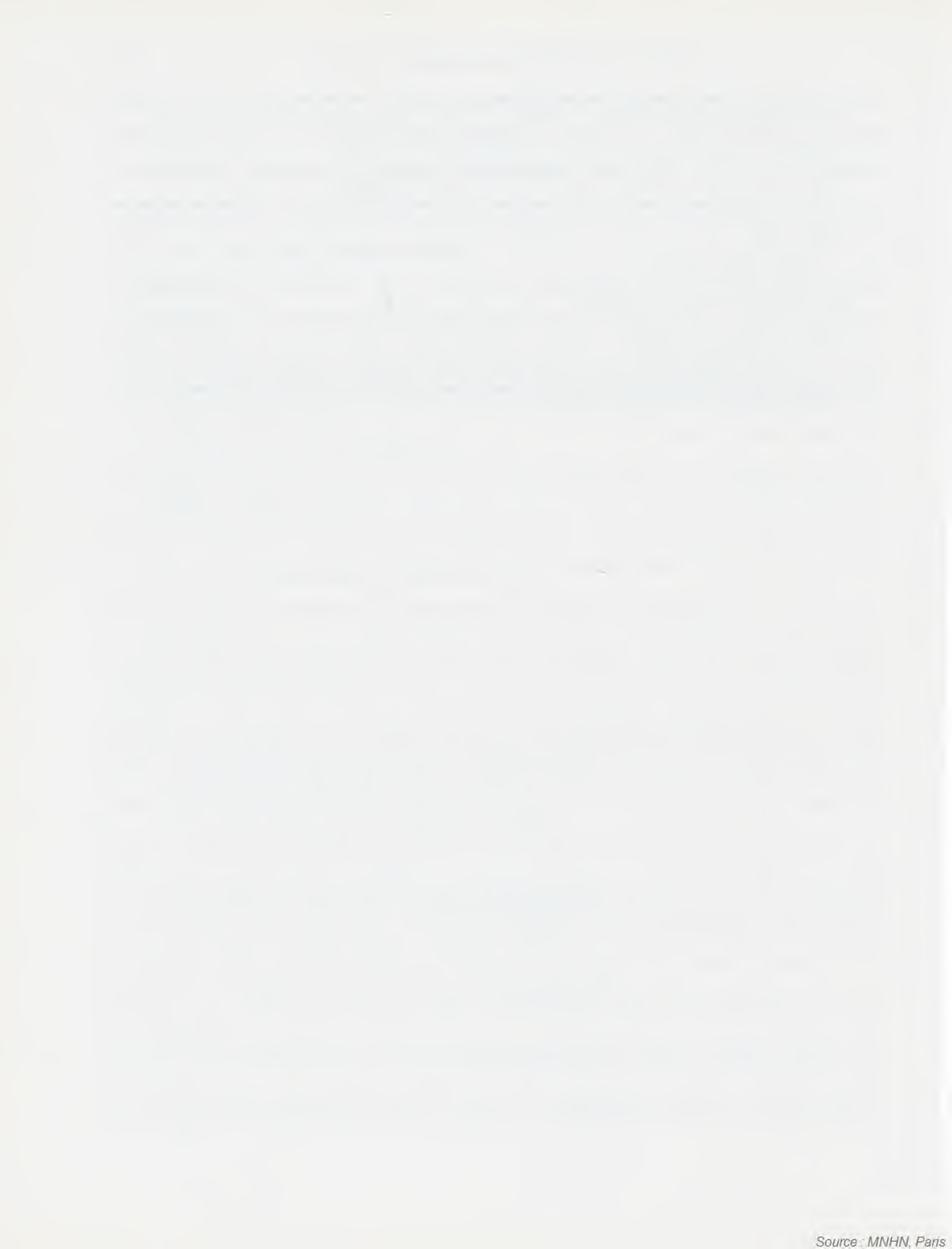

Source : MNHN, Paris

8

Hydrocarbon systems of Morocco

Haddou JABOUR, Al Moundir MORABET & Rabah BOUCHTA

ONAREP, P.O. Box 8030, Rabat, Maroc

ABSTRACT

Available data base interpretation along with MAGOON & DOW's (1994) petroleum system concept is utilised in this paper to evaluate the origin of the proven hydrocarbon resources of Morocco, which lie chiefly in the Essaouira, Pre-Rif, Rharb and offshore Tarfaya Basins. Several systems are interpreted, in which the confidence in the source/petroleum tie varies from "known" to "hypothetical", involving charge from Silurian (eastern Essaouira), Palaeozoic-Liassic (Sidi Fili trend of Pre-Rif), Liassic (Bou Draa and Haricha fields of Pre-Rif), Oxfordian (western Essaouira), Cretaceous (Aïn Hamra) and an intra-Miocene biogenic system in the Rharb Basin. The origin of the Cap Juby heavy oil accumulation in the offshore Tarfaya basin is uncertain, we favour an offshelf Jurassic and/or Cretaceous sources interpretation. The hydrocarbon system concept is extended in this paper to predict further, currently undrilled or unproven, systems. These include areas where the proven source rocks referred to above are likely to be developed and be mature, plus systems that can be predicted on the basis of analogues from surrounding regions. An example of the latter is a series of postulated Triassic systems developed in lacustrine deposits in Atlantic offshore and coastal half graben. Palaeozoic source rocks may be regionally developed and may still be in the oil and gas windows over wide, generally unexplored, regions. Early to Middle Jurassic source rocks occur mainly in lagoonal, platform sags and outer shelf environments while Cretaceous-Eocene source beds occur in continental rift complexes and deltaïc basins. Biogenic gas potential is probably confined to Neogene deposits in foreland and divergent margin basins. Further application of the hydrocarbon system concept should help to significantly reduce geologic risk particularly in frontier exploration areas.

RÉSUMÉ

Les systèmes pétroliers au Maroc.

L'interprétation de la base de données disponibles et le concept de système pétrolier établi par MAGOON & DOW (1994) sont utilisés dans cet article pour évaluer les origines des ressources d'hydrocarbures prouvées au Maroc. Ces ressources se situent essentiellement dans les bassins d'Essaouira, du Pré-Rif, du Rharb et dans l'offshore de Tarfaya. Plusieurs systèmes, dont le degré de confiance de corrélation huile-roche mère varie de "connu" à "hypothétique", sont également interprétés. Ces systèmes impliquent des charges du Silurien (Est d'Essaouira), du Paléozoïque-Lias (trend de Sidi-Fili dans le Pré-Rif), du Lias (champs de Bou Draâ et Haricha dans les rides prérifaines), de l'Oxfordien (Ouest d'Essaouira), du Crétacé (Aïn Hamra) et d'un système intra-Miocène de gaz biogénique dans le bassin du Rharb. L'origine de l'huile lourde accumulée dans la structure de Cap Juby dans l'offshore de Tarfaya est incertaine. Notre interprétation favorise une origine de roche mère de type bassin du Crétacé et/ou Jurassique. Le concept de système pétrolier est étendu, dans cet article, pour inclure les systèmes non encore prouvés ou non encore testés par forage. Ces systèmes comprennent des zones où les roches mères sus-mentionnées peuvent être

JABOUR, H., MORABET, AL M. & BOUCHTA, R., 2000.— Hydrocarbon systems of Morocco. *In*: S. CRASQUIN-SOLEAU & É. BARRIER (eds), Peri-Tethys Memoir 5: new data on Peri-Tethyan sedimentary basins, *Mém. Mus. natn. Hist. nat.*, **182** : 143-158. Paris ISBN : 2-85653-524-0.

Source : MNHN, Paris

développées et matures ainsi que les systèmes pouvant être anticipés par analogie avec les zones avoisinantes. Un exemple de ces systèmes consiste en une série de structures en demi-graben dans l'offshore atlantique et dans les bassins côtiers dans lesquels se sont développées des roches mères lacustres. Les roches mères paléozoïques peuvent être régionalement développées et dans de larges régions non encore explorées; ces régions peuvent se situer dans la fenêtre à huile. Les roches mères du Jurassique inférieur et moyen se sont déposées essentiellement dans des environnements lagunaires, de sillons de plate-forme ou de plate-forme externe. Les roches mères du Crétacé-Eocène sont des dépôts de rifts continentaux complexes et de bassins deltaïques. Les roches mères à l'origine du gaz biogénique sont des sédiments probablement limités au Néogène déposés dans les bassins type foreland ou de marge passive. L'application future du concept des systèmes pétroliers devrait aider à réduire, de façon significative, le risque géologique et particulièrement en limite des zones d'exploration.

INTRODUCTION

Although most of Moroccan sedimentary basins are still largely unexplored and justifiably considered frontier exploration areas, the database so far acquired in the exploration of these basins requires a modern conceptual interpretation. As more geological, geophysical and geochemical information about known petroleum occurrences is acquired, there is a need to adequately document and review the models and geologic processes pertinent to these proven systems and use these as analogues to accurately and adequately assess the hydrocarbon potential of less explored basins or those in which hydrocarbons have yet to be proven.

Basin evaluation to date in Morocco has relied on analytical studies that emphasise structural evolution and sediment fill, regardless of their relationship to any petroleum deposits. The petroleum system concept, as proposed by MAGOON & DOW (1994) is a more holistic approach, which emphasises the genetic relation between a particular source rock and the resulting petroleum accumulation. These basic elements include the petroleum source rock, migration path, reservoir rock, seal, and trap and the geologic processes that create each of these basic elements.

The purpose of this paper is to define, where the data base allows, the established petroleum systems in Morocco, to determine the level of certainty of a specific system and attempt a classification, and additionally to predict where further, currently unproven, petroleum systems may lie elsewhere in the country.

The terminology used in this paper is a composite of that applied by MAGOON & DOW (1994), by MAGOON (1988) and by DEMAISON & HUIZINGA (1991). The definition of the key-terms used is given below.

An established petroleum system (one in which the occurrence of hydrocarbons is proven) can be identified at three levels of certainty in terms of the geochemical correlation of petroleum and source rocks (MAGOON & DOW, 1994). These can be listed as follows:

— known petroleum system; where a good geochemical match must exist between the active source rock and oil or gas accumulation.

— hypothetical petroleum system, in which geochemical information is sufficient to identify a source rock but where no geochemical match exists between source and petroleum deposits.

— speculative petroleum system, where the existence of both source rock and petroleum accumulation is postulated entirely on the basis of geologic and/or geophysical evidence.

MAGOON & DOW (1994) proposed naming systems based on the predominant source and reservoir within the relevant system, using lithostratigraphic schemes. The absence of a common accepted lithostratigraphy throughout Morocco presents problems here, therefore, chronostratigraphic terms are used. These have to be used in conjunction with the basin name concerned.

The migration system can be further described using the following defined terms: a pure-bred petroleum system exists in a geological setting in which the structural framework has not changed significantly during the geological life of that system; a hybrid system exists in areas of major structural reorientation, without which the petroleum system would not occur in its current form; high-impedance migration systems are characterised by laterally continuous seals coupled with a moderate to high degree of structural deformation; low-impedance migration systems are characterised by either a high

Source : MNHN, Paris

degree of regional seal continuity or a low degree of structural deformation. Data available on the petroleum systems of Morocco at this stage are generally not sufficient to estimate charge factor or gross accumulation efficiency (GAE). However, in some cases, observations on trap fill allow an evaluation of whether the system is under, normally or super-charged.

BASIN DEVELOPMENT, REGIONAL STRATIGRAPHY AND SOURCE FACIES OCCURRENCES

A large number of discrete sedimentary basins are recognised in Morocco (Fig. 1), varying in their style from intramontane through inverted rifts to thrust belts, forelands and passive margin. Most of these basins remain underexplored, with as a result, their potential petroleum systems and resources ill-understood. Production is currently limited to onshore basins in the coastal area of northern and central Morocco.

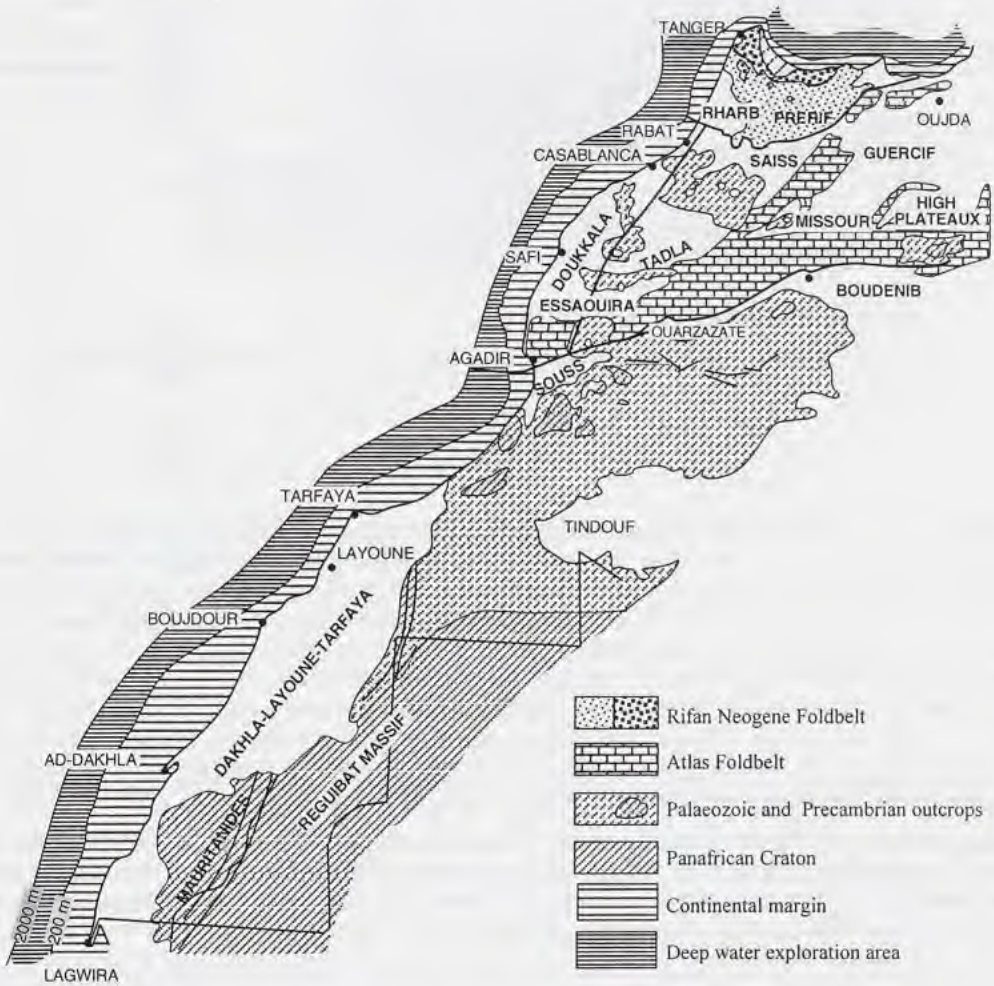

FIG. 1.— Structural units and major sedimentary basins of Morocco.

FIG. 1.— Les unités structurales et les principaux bassins sédimentaires du Maroc.

Our current state of knowledge of the history of basin development and stratigraphy of the country is summarised below. The figure 2 presents a summary of the most important tectonic events within a typical onshore Moroccan basin.

A stratigraphic section of the area of fullest control, the Atlantic Coastal basins, is illustrated (Fig. 2).

Source : MNHN, Paris

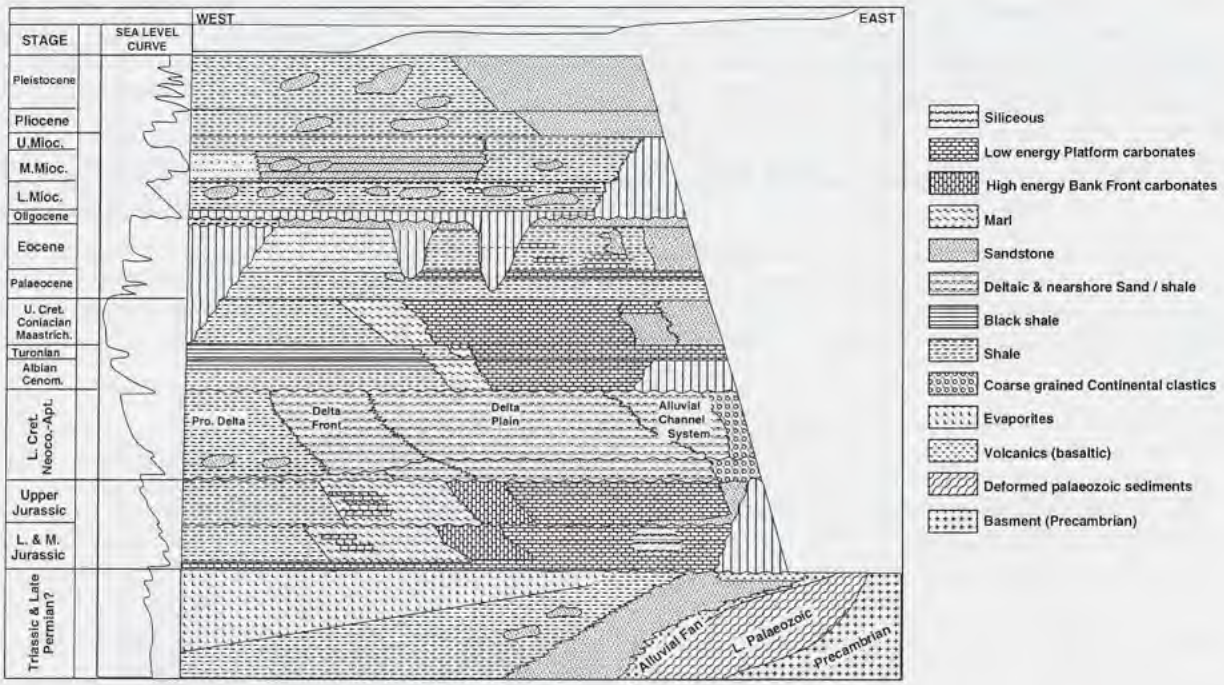

FIG. 2.— Lithostratigraphic column of the atlasic coastal basins to the South of Agadir.

FIG. 2.— Colonne lithostratigraphique des bassins côtiers atlasiques au Sud d'Agadir.

PALAEOZOIC

The oldest rocks encountered in Morocco belong to the Precambrian and outcrop in the Anti-Atlas. Lower and Middle Cambrian strata have not been drilled but geophysical data, tied to surface geological control, suggest that the succession is 100 to 3000 m thick; consisting of grey green shales, sandstones, quartzites, and volcanoclastics. The Ordovician is represented by 1000 to 2500 m of grey to black shales, siltstones, sandstones and quartzites and the Silurian by 100 to 200 m of graptolitic, locally carbonaceous, black shales. Devonian rocks are mostly shales, often black, with thin sandstones and deeper water reefal limestones locally developed. The Carboniferous succession, up to 4000 m thick in depocenters, is represented by Visean, Namurian and Westphalian shales, sandstones, conglomerates, turbidites and platform carbonates. Thin carbonaceous shales and coal beds are also present locally. The Carboniferous rocks are bounded by the overlying erosive Hercynian unconformity.

The main potential Palaeozoic source rock is the Silurian sapropelic, radioactive graptolitic black shales, rich in kerogen of Type II. Black carbonaceous shales also occur frequently in the Late Ordovician and Early Devonian locally in the Westphalian. These systems are tightly controlled and determined by the geodynamic characteristics of the basins.

The tectonic evolution of the onshore intracratonic basins, where the Palaeozoic succession is best represented, is complex and results from successive tectonic episodes (Fig. 3). The first main event, the Hercynian orogeny, caused strong deformation of the Palaeozoic sequence. Hercynian events begun at the end of the Devonian with very large scale folding, and strike-slip faulting resulting in the creation of a number of deep Carboniferous basins. Subsequent deformation occurred during late Westphalian and with tight folding, thrusting, nappe development and strike-slip faulting, associated with dyke emplacement and granite intrusions.

These compressional events have a crucial and positive impact on the maturity history of Palaeozoic source rocks in many of the intracratonic basins. In the Tadla Basin, Early Palaeozoic source rocks are still present within the oil window in uplifted and thrusted blocks (Fig. 3), generally in areas which not

Source : MNHN, Paris

suffer from deep Carboniferous burial. It is likely that recent burial (Tertiary) resulted in renewed hydrocarbon generation in at least some of these basins. Examples are the western Meseta, High Plateaux, Pre-Rif, western Tindouf and part of Errachidia-Boudenib areas.

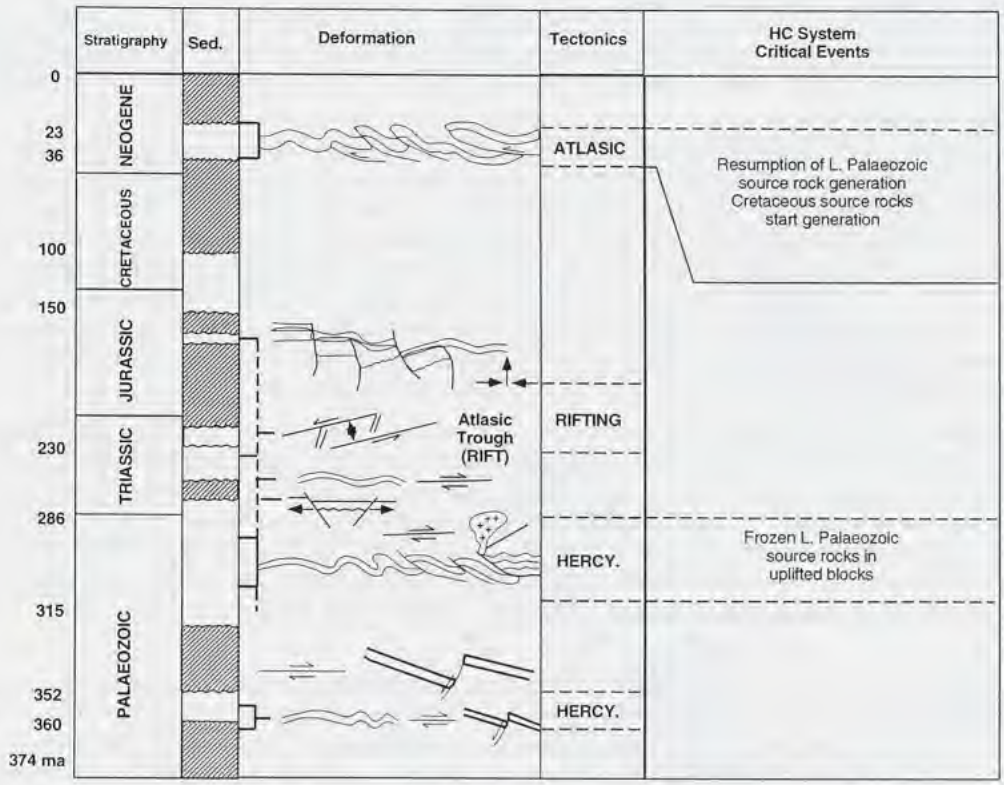

FIG. 3.— Tectonic evolution and subsequent critical events of petroleum systems in Morocco based on the example of theTadla and other basins bordering the Atlas foldbelt.

FIG. 3.—L'évolution tectonique et les événements critiques conséquents des systèmes pétroliers au Maroc, basés sur le bassin de Tadla et les bassins en bordure de la chaîne atlasique.

MESOZOIC

Triassic grabens and half grabens associated with fragmentation of the continents occur throughout Morocco, filled with continental coarse clastics, red beds and locally by lacustrine deposits (BROWN, 1980). Crustal extension and rifting started in the latest Triassic massifs and Hercynian highs. Transgressive sediments associated with the Tethys seaway spilled into the proto-Atlantic oceanic rift later in the Triassic, leading to the development of hypersaline lagoon conditions over a large part of coastal Morocco and the formations of thick salt deposits in, for example, the Essaouira Basin, Pre-Rif and High Plateaux. These should provide excellent seals for hydrocarbons generated from both Palaeozoic and Triassic source rocks.

The opening of the Atlantic Ocean was preceded by further (Triassic-Early Jurassic) rifting. This was followed by massive regional subsidence during the Jurassic as is well illustrated in the Tarfaya region and along the Atlantic shelf. Tethyan-related rifting occurs during the Jurassic in the Atlas Such Tethyan rift are often discordant to the Atlantic-related rifts, with the former trending NE-SW and the latter N-S. The Tethyan rift system was later inverted during the Alpine orogeny to form the mountains of the High and Middle Atlas.

Liassic and Dogger (pre-Callovian) sedimentation is dominated by intertidal to supratidal conditions, extending across most of the coastal basins. A sediment pil of carbonates, anhydrite and red-brown to

Source : MNHN, Paris

green shales accumulated. The Bajocian (Middle Jurassic) is characterised by an important clastic influx especially in the Pre-Rif ridges areas. Open subtidal carbonates and minor grey shale were deposited during the Callovian and early Oxfordian times. A gradual regression began in middle Oxfordian time. This resulted in renewed intertidal to supratidal facies deposition. A marked drop occured in sea level during the Late Jurassic.

Jurassic potential source rocks range in age from Early Jurassic (Tarfaya) margin, Pre-Rif and the Inter-Atlasic basins) to Oxfordian (Essaouira basin). These source rocks contain predominantly sapropelic Type II kerogen.

Early Cretaceous rocks, which are particularly well-represented in the Dakhla-Layoune-Tarfaya basin, are characterised by thick regressive cycles, thick continental and deltaïc clastics accumulated unconformably over Jurassic platform carbonates. The Aptian and Albian succession is composed of a thick interval of shallow marine, lagoonal and intertidal sediments represented by lithofacies such as shales, sandstones and shelly limestones. Thick marls, that may be rich in organic matter, are also widespread. The Late Cretaceous throughout Morocco is composed of carbonates and shales, with common minor transgressive events. Potential source rock development is tied to these transgressions, with an extensive organic rich shale recognised in the Turonian organic shale is seen as a 50 m (gross) in the onshore Tarfaya Basin with TOC of 6-19 % (EINSELE & WIEDMANN, 1982).

As the Atlantic Ocean widened and deepened, the relative movement between the African and Eurasian plates reversed direction by Late Cretaceous time. Collision and subduction in Early Tertiary time resulted in the Alpine orogeny which had a major impact on northern Morocco. The Rif Domain developed Alpine style nappes at this time. Subsidence continued in several marginal sedimentary troughs, associated with continued opening of the Tethys seaway, such as the Pre-Rif Ridges and the Morocco-Algeria Atlas. A thick sedimentary pile in the Atlas sedimentary trough, which may have developed above earlier incipient rifts, was inverted during the Early Tertiary, when the Atlas Mountains were overthrust to the west and south.

Tertiary sediments are represented by marine and continental deposits. Palaeocene to Eocene marine clastics are overlain by Oligocene continental clastics. During the Tortonian the Pre-Rif nappe was emplaced. This appears on seismic reflection profiles as an interval of chaotic internal structures. The Pre-Rif nappe, which is up to 3000 m thick, contains Triassic salt and volcanics together with Late Cretaceous and Early Tertiary strata. Post-nappe sediments up to 2000 m thick, are mostly fine-grained foreland basin clastics. Miocene transgressive sandy carbonates are present in the sub-nappe.

TABLE 1.— Petroleum systems (established hydrocarbon accumulation).

TABLEAU 1.— Systèmes pétroliers (accumulations d'hydrocarbures établies).

BASIN	Petroleum system name (source age/main reservoir age)	Reservoir facies	Representative discovery	Status of geochimical correlation	Migration path
Prerif	Cretaceous-Miocene	Clastic deposits	Ain Harma	Good	Faults
	Lias-Domerian	Dolomite	Haricha	Good	Faults
	Lias-Palaeozoic	Granite + Wash Quartzite	Sidi Fili trend	Fair	Faults
Rharb	Miocene-Miocene	Turbidite Sands	Ksiri	Fair	Local expulsion
Essaouira	Oxfordian-Oxfordian Silurian-Triassic (also Oxfordian reservoir)	Dolomite	Sid Rhalem	Good	Lateral faults, subcrop
		Non - marine sands	Meskala	Fair	
Tarfaya	Lias-Upper Jurassic (?)	L.& M. Jurassic carbonate bank	MO-2 heavy oil (Cap Juby)	Poor but carbonate source favoured	Lateral

Source : MNHN, Paris

ESTABLISHED PETROLEUM SYSTEMS (WITH PROVEN HYDROCARBONS)

This section of the paper presents the current level of understanding of the established petroleum systems of Morocco (i.e. where moveable hydrocarbons have been encountered) and classifies these (Table 1) in terms of our confidence in the source to oil tie according to the terminology of MAGOON & DOW (1994).

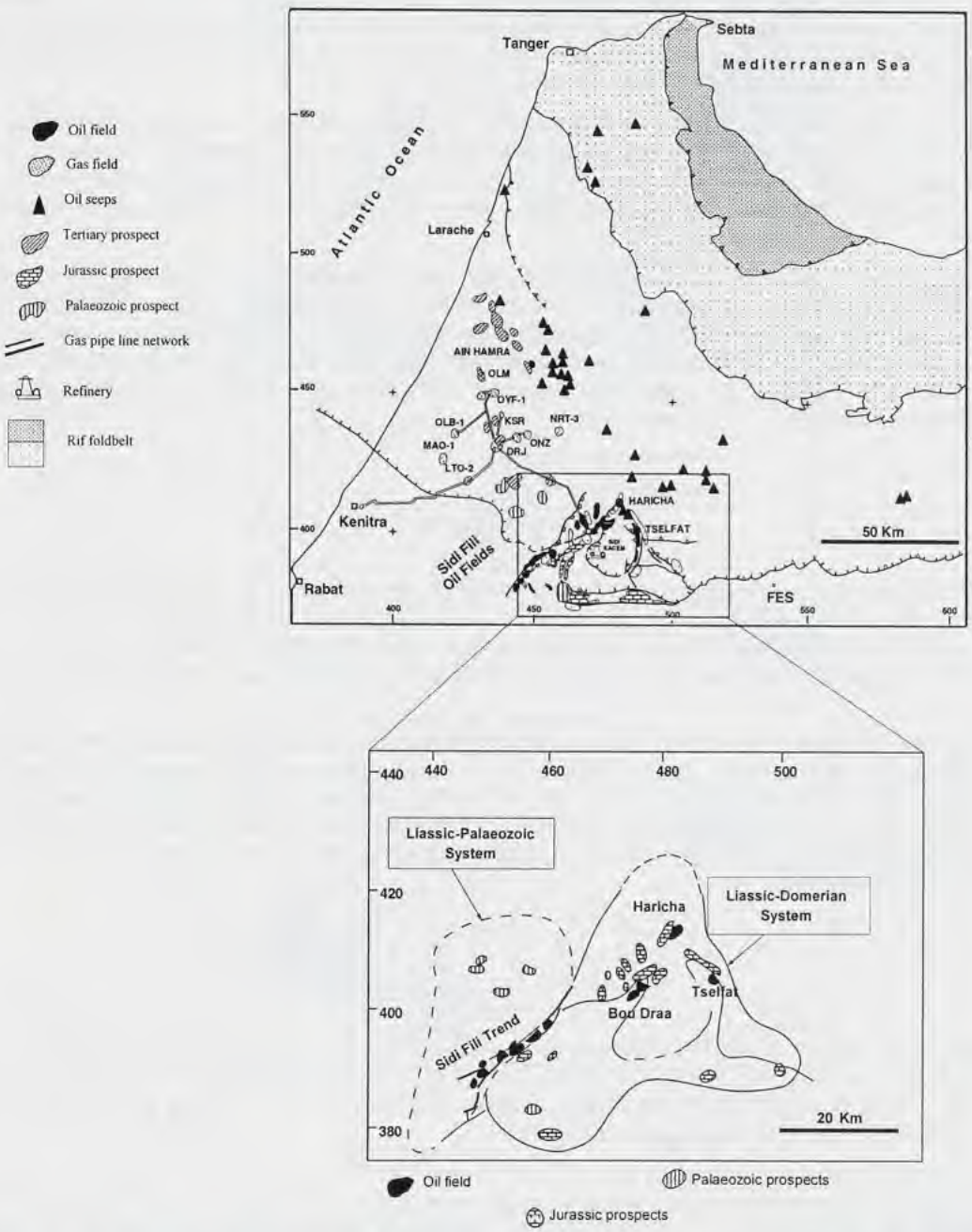

FIG. 4.— Map showing the areal extends of two petroleum systems defined in the Pre-Rif ridges area. The Liassic-Domerian system may extend to the north whereas the Palaeozoic-Liassic system may extend to the northwest.

FIG. 4.—Carte montrant l'extension des deux systèmes pétroliers définis dans la zone des rides prérifaines. Le système Lias-Domérien peut s'étendre plus au nord tandis que le système Paléozoïque-Lias peut s'étendre dans la partie nord-west.

Source : MNHN, Paris

PRE-RIF PRODUCING BASIN

In the Pre-Rif compressional belt, developed basinward of the Rif Nappe, available data is used to define 3 petroleum systems.

The first (Cretaceous-Miocene) lies to the north of the Rharb Basin, and is represented by the first oil discovery in North Africa, Aïn Hamra, made in 1923. Oil is reservoired in shallow late Miocene sand lenses (200 m), within steep compressional structures in the post-nappe series and has been typed to a Late Cretaceous source. The complex structural setting suggests a hybrid system. The two other systems occur in the Pre-Rif Ridges, as illustrated on the figure 4.

A series of oil occurrences in structures along the northeast-southwest trending Sidi-Fili fault (Fig. 4) is reservoired in washed/weathered hercynian granites and fractured Palaeozoic sandstone reservoirs. The most likely source is the Early Jurassic though Triassic and Palaeozoic contributions can also be postulated. A hybrid system is suspected. This system is labelled as the Palaeozoic system on the figure 4.

The third system (Liassic-Domerian) occurs in the eastern part of the Pre-Rif (Fig. 5). Oil is sourced mainly from Early Jurassic and reservoired in Domerian reefal carbonates and Middle Jurassic arkosic sands. Some oil may also be reservoired in early Miocene sandy carbonates. Oil is produced, as tar, in hanging wall anticlines and imbricate ramps at a relatively shallow depth. Recent studies suggest that the oil so far produced could be a product of dismigration via major faults from deeper accumulations within sub-thrust anticlines.

RHARB PRODUCING BASIN

The Rharb Basin is a Neogene foreland basin filled by a thick Miocene-Pliocene clastic series deposited coeval with uplifting of the Rif and Pre-Rif. Palaeozoic and Mesozoic basement outcrops along its southern edge and is drilled in the basin centre and in the northeast, where the basin passes into the Pre-Rif folded belt. The Rharb basin deep contains several sub-basins developed along major listric faults.

A significant amount of biogenic gas is reservoired and produced from Tertiary rocks deposited in this foreland basin. This geologic setting is classified as a purebed system. Biogenic gas is expelled from thermally immature Miocene source rock into adjoining medium- to fine-grained, well-sorted Late Miocene sand reservoirs. Recent seismic processing techniques have considerably improved the success ratio in exploring for biogenic gas in this petroleum system. More than 80 seismic amplitude anomalies are identified in this region.

ESSAOUIRA PRODUCING BASIN

A detailed description of the Essaouira basin is provided by BROUGHTON & TRÉPANIER (1993). This basin, which is currently the most important producing basin in Morocco, is a Mesozoic-Cainozoic earlier trend basin passive margin basin developed over earlier fault trends. The basin trend basin contains numerous extensional salt-related structures.

In the Essaouira Basin, two petroleum systems are identified (Fig. 6). Wet gas is sourced from Silurian (cf. CLIFFORD, 1986) and possibly additional Ordovician and Devonian source rocks and reservoired below a Triassic salt seal in siliciclastic sediments (termed Silurian-Triassic system). Highly mature west gas is vertically drained from source to reservoir in the Meskala-Zelten horst. The system is interpreted to be normally charged. We also favour a Palaeozoic source for the gas fields in the eastern part of the basin, reservoired in fractured Oxfordian dolomites, as these fields are distant from any conceivable Oxfordian gas kitchen.

Source : MNHN, Paris

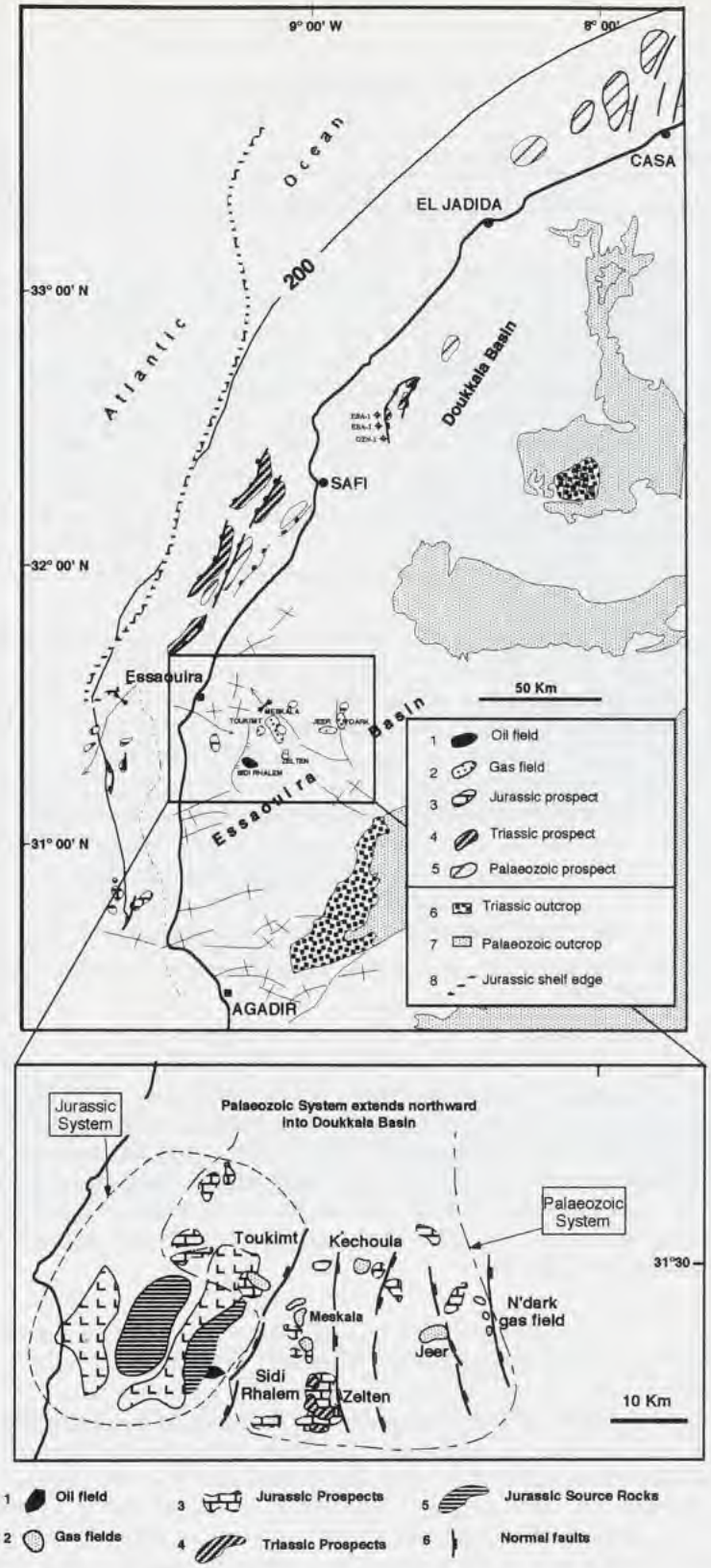

FIG. 5.— Map showing the area extends of the two petroleum systems defined in the Essaouira basin. The Silurian–Triassic system most likely extends to the north into the Doukkala and Casablanca basins. Note the mapping of an additional kitchen in the west of the Oxfordian system, which has, as yet, no discoveries associated.

FIG. 5.— Carte montrant l'extension des deux systèmes pétroliers définis dans le bassin d'Essaouira. Le système Silurien-Trias peut vraisemblablement s'étendre plus au nord pour inclure les bassins de Doukkala et de Casablanca offshore. A noter la cartographie d'une cuisine à huile supplémentaire, à l'ouest du système Oxfordien, qui n'est pas encore associée à une découverte.

Source : MNHN, Paris

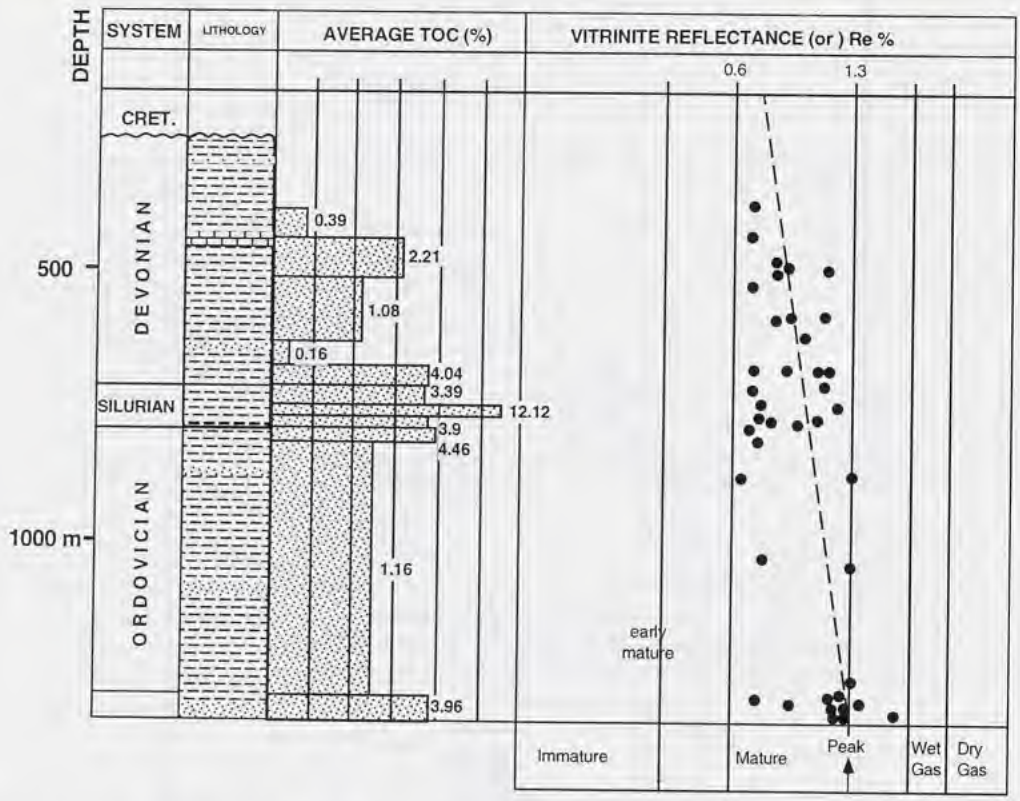

FIG. 6.— Geochemical data on the KAT-1 well (Tadla basin), illustrating good quality source rocks still within the oil window.

FIG. 6.— Les données géochimiques du puits KAT-1 du bassin de Tadla illustrent une roche mère paléozoïque de bonne qualité à l'intérieur de la fenêtre à l'huile.

The oil in the Essaouira Basin is formed in a purebred petroleum system (Oxfordian-Oxfordian). The entire petroleum system, including the seal, is confined to the Oxfordian, with the source developed in the early Oxfordian (BROUGHTON & TRÉPANIER, 1993). The reservoir in a late Oxfordian (Argovian) fractured sandy dolomite is sealed by late Oxfordian anhydrite. Data from the Sidi Rhalem oil field suggest this system to be undercharged. Recent studies, however, suggest a normally charged portion of the system to the west in Neknafa syncline where oil and/or wet gas accumulations may be found against salt walls and overhangs (Fig. 5).

TARFAYA BASIN (CAP JUBY DISCOVERY)

Well MO-2 offshore Cap Juby in the Tarfaya basin discovered a significant heavy oil (11° API) accumlation in a fractured Late Jurassic carbonate bank,which was unfortunately partially breached on an Oligocene shelf collapse unconformity. Jurassic petroleum system defined in Tarfaya Basin is classified as purebred system. A small amount of light oil is also found in Middle Jurassic reservoirs, Many attempts have been made at source to oil correlation, none of which have been conclusive, though the bulk of the evidence tends to favour a Jurassic carbonate source rock. This seems most likely developed in the Early Jurassic either in intra-platform sags behind the shelf edge. An alternative interpretation of a shalier facies source, developed in the present day adjoining deep water area, cannot be ruled out. Exploration drilling carried out in this area has mainly targetted the Late Jurassic shelf edge. Recent studies, however, tend to favor Early and Middle Jurassic objectives surrounding the possible interior platform source rock depocenter, which are less likely to have suffered from reservoir breaching or input of groundwater.

Source : MNHN, Paris

PREDICTED PETROLEUM SYSTEMS IN FRONTIER BASINS

This section of the paper presents an interpretation of where further petroleum systems and resources lie undiscovered in the underexplored basins of Morocco. As the occurrence of petroleum has yet to be proven in these cases, the term petroleum system as applied by MAGOON & DOW (1994) cannot be used. Therefore, these interpretations will be presented as "predicted petroleum systems". The evidence supporting these included identification of source rocks from geochemical analysis, extrapolations of source rock extents from palaeogeographic mapping, extrapolations based on regional analogue basins, basin modelling and in some cases, the occurrence of shows and/or seeps. The predicted systems are grouped by the age of the inferred source rock.

PREDICTED PALAEOZOIC SOURCED SYSTEMS

The main regional Palaeozoic source rocks, particularly those in the Silurian and Devonian are predicted to have extended over Morocco, being effective source rocks in adjoining areas of Algeria and in the Appalachian Basin (USA), which originally lay in close palaeotectonic position to Morocco where stratigraphic data is available, the Silurian source rock can usually be identified, though at a wide range of possible levels of maturity. The highest levels of maturity would be expected to occur over uplifted Carboniferous depocentres, and it may be the tendency for such areas to present good outcrop data that has led to a perception that the Palaeozoic of Morocco is regionally overcooked. This is clearly not the case in the Essaouira and Tadla (Fig. 6) basins and it remains possible that large areas of Morocco contain Palaeozoic source rocks that retained and generated much of their potential in post-Hercynian time (Fig. 3). Such regions include the following.

TADLA BASIN

A scarcity of exploration boreholes in this basin (1 well per 3000 sq km) places the emphasis for exploration on geological, geochemical and geophysical evidence. Geochemical analyses show that oil-prone Silurian and Early Devonian source rocks (TOC up to 12%) are still within the oil window on uplifted blocks (Fig. 6) (JABOUR & NAKAYAMA, 1988). Generation of oil and gas is predicted to have occurred from Carboniferous to Cretaceous (JABOUR & NAKAYAMA, 1988). Resevoir objectives occur in basal Triassic and Middle Jurassic siliciclastics which display excellent reservoir characteristics.

DOUKKALA BASIN

In the Doukkala Basin, a Palaeozoic petroleum system is predicted as an extension of that developed in the Essaouira basin (Fig. 5). Oil and gas produced from Silurian-Lower Devonian source rocks could be reservoired, as in Essaouira, in Permo-Triassic siliciclastic reservoirs. Such sub-system would be vertically drained and normally charged. A further potential reservoir is a postulated Middle Devonian reef complex.

CASABLANCA OFFSHORE BASIN

The Doukkala Basin passes northwards into the Casablanca offshore area, in which large structural closures are defined on seismic. No wells have been drilled in this large exploration area. Oil is postulated to be sourced from Silurian-Early Devonian oil prone source rocks and reservoired in fractured and weathered Ordovician quartzitic sandstones. The system is laterally drained and postulated to be normally charged with a high impedance entrapment style. The system is very similar in both size and system components to the Hassi-Messaoud oil field in Algeria.

Source : MNHN, Paris

INTERATLASIC BASINS

Additional Palaeozoic petroleum systems are predicted in the Inter-Atlasic Basins. Oil and/or gas probably originates from Carboniferous and Silurian source rocks (which are still in the generating stage, particularly on uplifted blocks). Shows have been observed in basal Triassic sands and conglomerates. The oil and/or gas is thought to be vertically drained and sealed by a thick, high impedance salt sequence.

The Palaeozoic petroleum system of the interatlasic basins may be developed in three areas, namely the High Plateaux, the Missour Basin and the Zekkara-Jerada area. No direct correlation has yet been found between the oil and gas seen as shows and seeps and the likely source rock. Currently, no data is available to confidently map the areal extend of these plays, though kitchens can crudely be defined from sparse geochemical data.

PREDICTED TRIASSIC SOURCED SYSTEMS

The postulated Triassic system is comprised of lacustrine deposits rich in type I similar to these recorded in the coeval Newark basin (OLSEN & SCHLISCHE, 1990). This oil prone source can be expected to charge alluvial fan and fluvial clastic reservoirs in both the hanging wall and the footwall of the half graben (Fig. 7). Thick Late Triassic-early Liassic salt provides adequate sealing for this system. The Triassic systems are predicted to have the character of pure-bred systems with a high impedance associated with a mainly vertically drained system. The areal extent of these systems is very limited, and in most cases corresponds only to the area encompassed by the half graben.

A study integrating seismic, gravity and magnetic data has identified at least 8 such buried Triassic half-grabens along segments of the Atlantic margin between Casablanca and Tarfaya.

PREDICTED JURASSIC SOURCED SYSTEMS

Early Jurassic source rocks, as established in the Tarfaya marin and Pre-Rif are expected to extend into the Inter-Atlasic Basins, including the southeastern part of the High Plateaux, the southeastern and western parts of the Missour basin, and the Guercif Basin and the Zekkara area. Here again, the extent of the kitchen and petroleum system is speculative, due to lack of seismic coverage.

PREDICTED CRETACEOUS SOURCED SYSTEMS

Regional source rocks tied to transgressions and oceanic anoxic events are predicted in the Albian and Turonian. Interest is focused on the former due to maturity consideration. The main areas of interest are those in which a thick cover is developed of maturity above potential Cretaceous source rocks. These are the following:

DAKHLA-LAAYOUNE BASIN

In the Layoune-Dakhla basins, Early Cretaceous source rocks matured below a thick deepwater argillaceous section may charge Albian rollover structures generated along listric faults. In addition, Late Cretaceous source rocks, if mature, may charge Maastrichtian carbonate reservoirs. Such Cretaceous sources may be the origin of residual oil stains observed in the 51 A-1 well, within Senonian and Eocene carbonates.

Source : MNHN, Paris

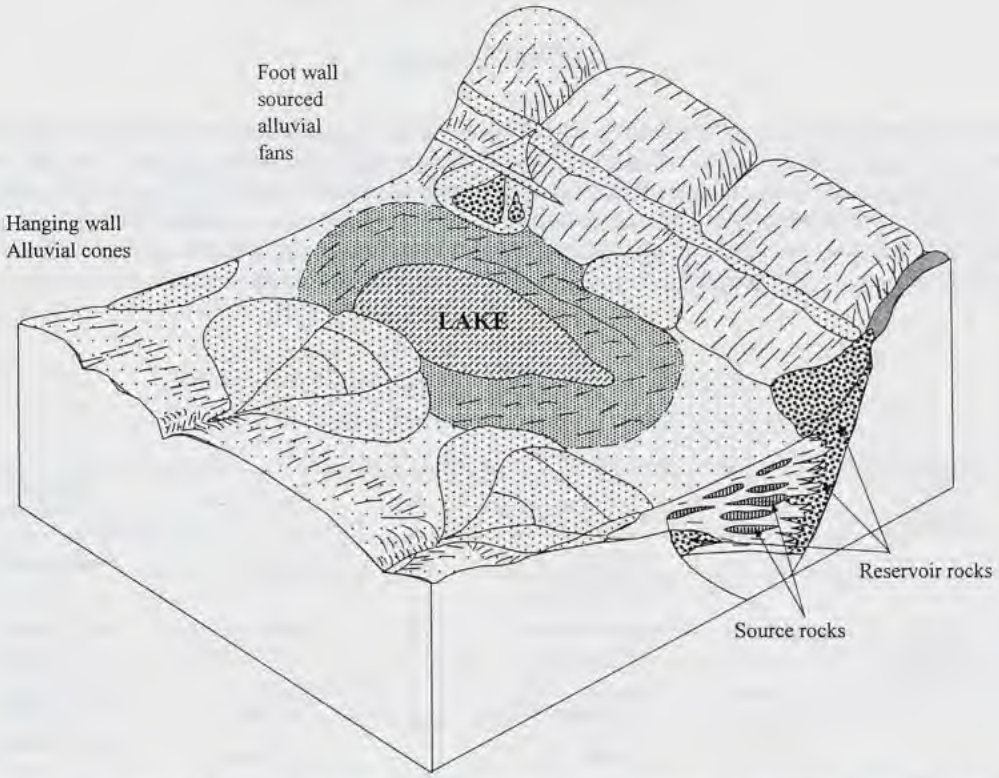

FIG. 7.— Sedimentary model of a Triassic Newark-style half-graben illustrating the various components of the postulated Triassic petroleum system.

FIG. 7.—Modèle sédimentaire d'un hémi-graben triasique type Newark illustrant les différentes composantes d'un système pétrolier triasique postulé.

AGADIR-ESSAOUIRA OFFSHORE BASINS

Cretaceous petroleum systems are predicted to exist in offshore Agadir-Tarfaya segment. Excellent Apto-Albian source rocks, mature basinward, potentially charging a Jurassic faulted and karstified bank edge in Agadir and parts of the Tarfaya offshore basins.

In the Agadir-Essaouira offshore area, recent study has developed a new exploration concept. The primary exploration objective is a faulted carbonate shelf edge where porosity is enhanced by subareal exposure and consequent karstification. A hypothetical source rock would be Early Cretaceous shales deposited beyond the Jurassic shelf edge. Geochemical basin modeling has defined a possible kitchen area from which oil is generated. No exploration drilling has tested this concept yet.

TADLA BASIN

For the Cretaceous system, rich (up to 13% TOC) oil prone Cretaceous source rock are interpreted to enter the oil window under an interpreted low angle thrust marking the Atlas front. The additional loading and burial acquired is predicted to be sufficient for maturity to be attained.

PREDICTED NEOGENE SOURCED SYSTEMS

By analogy to the established Neogene hydrocarbon systems of the Rharb and Pre-Rif basins, shallow biogenic gas systems are predicted in areas of high Neogene subsidence rate in offshore Rharb, the offshore Mediterranean and Laayoune-Dakhla basins.

Source : MNHN, Paris

CONCLUSION

The present geological, geochemical and geophysical coverage has permitted us to predict a number of petroleum systems in Morocco (Table 2) in addition to those already established as producing provinces. These are defined on rather general information over relatively large areas. Any petroleum system identified on a subsurface data, be subdivided into smaller sub-systems. Furthermore, some areas such as the Atlas domain, Rif domain and south Atlas and Sahara domain where little or no seismic coverage is acquired, will probably provide, once investigated, a large variety of additional petroleum systems.

TABLE 2.— Predicted petroleum systems (no discoveries to date).

TABLEAU 2.— Systèmes pétroliers prédits (pas de découvertes à ce jour).

Age of proposed source	Basin	Proposed reservoir age	Shows	Comments/critical factors	Proposed migration path
Paleozoic (Silurian,+ ? Ordovician)	Tadla	Triassic(Ci.) Middle Jurassic (Ci.) Caboniferous(ci.)	Shows	Timing of generation	Vertically drained
	Doukkala	Permo-Triassic(Ci.) Devonian Build-Ups(Cb.)	Shows	Extention of Essaouira system	Vertically up-faults Laterally drained
	Casablanca	Factured Ordovician sst.(Ci.)		Timing + ? overmaturity	Laterally drained
	Boudenib	Devonian carbonates(Cb.)		Timing + ? overmaturity	Vertically up-faults
Triassic Lacustrine	Coastal Rift half-grabens	Triassic fluvial clastic deposits (Ci.)		Based on Newark rift system analogue	Laterally and vertically drained
Lower Jurassic	Interatlasic Basins (Guercif,Missour, High Plateau)	Mid Jurassic(Cb.)	Shows Seeps	Timing of generation w.r.t. trap formation	Laterally drained
Cretaceous (Albian+ ? Turonian if mature)	Tarfaya	Cretaceous, U. Jurassic(Cb./Ci.)	Shows		Laterally drained
	Agadir	L. Cretaceous (Ci.)	Shows		Laterally drained
	Dakhla	Cretaceous(Ci.+ Cb.)	Shows residual oil in 51-A-1)	No	Laterally drained
	Tadla	Late Cretaceous (Ci.)		Maturity predicted below Atlas overthrust	
Neogene biogenic systems	Dakhla	Neogene sand lenses		Compare Rharb analogue	Local generation & expultion
	Mediterranean	Neogene sand		Compare Rharb analogue	Local generation & expulsion

Several large basins in Morocco still have much unexplored acreage. Drilling to date has tended to concentrate on relatively shallow objectives, drilling large, often recent structures without the modern appreciation of petroleum system concepts or the benefit of high quality seismic. The application of these concepts leads one to concentrate on very specific plays and regions, often unexplored, where petroleum is most likely to have been generated and preserved, e.g., in Palaeozoic-sourced plays over areas not deeply buried in pre-hercynian times and in regions close to potential Jurassic and Cretaceous kitchens, that may because of limited source facies extent or maturity considerations, be of limited lateral extent. Very little is known about deep offshore plays. The results so far obtained from the Campos Basin on the western side of the Atlantic ocean illustrate the potential attractiveness of such areas. In salt basins, great strides have been made with new technology in deciphering the architecture of subsalt formations. A better knowledge of the petroleum systems and the characterisation of the geology of the Moroccan sedimentary basins should therefore considerably enhance the chances of eventual exploration drilling success.

Source : MNHN, Paris

ACKNOWLEDGEMENTS

This work, presented as an oral communication in its first version during the Hydrocarbon geology of North African conference held in London (1995) then in the Peri-Tethys conference held in Rabat (1997) expresses ideas evolved from discussion with several individuals working in both academia and industry. The authors would like to acknowledge the comments of ALTON BROWN, who refereed the manuscript, and DUNCAN MACGREGOR, who made the publication of this work possible. The authors are grateful to the last comments of a peer reviewer and the editing of the manuscript by SYLVIE CRASQUIN-SOLEAU of the Peri-Tethys program.

REFERENCES

BROUGHTON, P. & TRÉPANIER, A., 1993.— Hydrocarbon generation in the Essaouira basin of western Morocco. *AAPG Bulletin*, **77** (6): 999-1015.

BROWN, R, 1980.— Triassic Rock of the Argana Valley south Morocco and their regional structural implication. *AAPG Bulletin*, **64** (7): 988-1003.

CLIFFORD, A.C., 1986.— African oil past, present & future. *In*: M.T HALBOUTY (ed.), Future petroleum provinces of the world. *AAPG Memoir*, **40**: 339-372.

DEMAISON, G. & HUIZINGA, B.J., 1991.— Genetic classification of petroleum systems. *AAPG Bulletin*, **75** (10): 1626-1943.

EINSELE, G. & WIEDMANN, J., 1982.— Turonian black shales in the Moroccan coastal basins. *In*: U. VON RAD, K. HINZ, M. SARNTHEIN & E. SEIBOLD (eds), *Geology of the Northwest African Continental Margin*. Springer, Berlin: 396-414.

JABOUR, H. & NAKAYAMA, K., 1988.— Basin Modelling of Tadla Basin, Morocco, for Hydrocarbon potential. *AAPG Bulletin*, **72** (6): 1059-1073.

MAGOON, L.B., 1987.— The Petroleum system-a classication scheme for research, resource assessment and exploration. *AAPG Bulletin*, **71** (5): 587.

MAGOON, L.B., 1988.— The Petroleum system-a classification scheme for research, exploration, and resource assessment. *In*: L.B. MAGOON (ed.), Petroleum systems of the United-States. *Bulletin- Geological Survey of America*, **1870**: 2-15.

MAGOON, L.B. & DOW, W.G. (eds), 1994.— The Petroleum system: from source to trap. *AAPG- Memoir*, **60**: 1-655.

OLSEN, P.E. & SCHLISCHE, R.W., 1990.— Transtensional arm of early Mesozoic Fundy rift basin: penecontemporaneous faulting and sedimentation. *Geology*, **18**: 695-698.

Source : MNHN, Paris

Source : MNHN, Paris

The Jurassic in Syria: an overview. Lithostratigraphic and biostratigraphic correlations with adjacent areas

Mikhail MOUTY

Department of Geology, Damascus University, Damascus, Syria

ABSTRACT

The carbonated Jurassic sediments in Syria and the adjacent areas are generally dominated by limestones, dolomitic limestones and restricted marly intercalations, precipitated in shallow marine environments. Since the Jurassic marine onset, transgressions covered the entire region of Syria with the exception of two NE-SW elongated uplifts in the E-SE (Hamad Uplift) and in the N-NE of the country (Aleppo-Mardin High). Before the end of the Middle Jurassic (early Bathonian), the sea regressed from the interior of Syria northwards, moving the Tethyan Ocean shore line westward to the Levantine zone. There, subsidence continued and the Jurassic sediments are locally thicker than 1300 m (Mount Hermon, Galilee). Before the end of the Upper Jurassic (late Kimmeridgian), the sea further regressed from the last submerged areas. Consequently, the entire Syrian platform remained emerged until the Cretaceous transgression initiated in the Barremian-Aptian time. As elsewhere in the Levant, volcanic activity characterises locally the beginning and the end of the Jurassic serie in Syria.

RÉSUMÉ

Le Jurassique de Syrie : une vue d'ensemble. Corrélations lithostratigraphiques et biostratigraphiques avec les régions avoisinantes.

Les sédiments carbonatés du Jurassique de Syrie et des régions adjacentes sont généralement dominés par des calcaires, des calcaires dolomitiques et de façon moindre par des intercalations de marnes, déposés dans des environnements marins peu profonds. Depuis le début du régime marin au Jurassique, les transgressions couvrent l'ensemble de la Syrie à l'exception de deux zones surélevées allongées, de direction NE-SW, dans l'est-sud est (zone surélevée de Hamad) et dans le nord-nord est du pays (zone surélevée d'Aleppo-Mardin). Avant la fin du Jurassique moyen (Bathonien inférieur), la mer régresse de l'intérieur de la Syrie vers le nord, déplaçant la ligne de rivage de la Téthys vers l'Ouest, vers la zone Levantine. Là, la subsidence continue et les sédiments jurassiques, localement, ont une épaisseur supérieure à 1300 m (Mont Hermon, Galilée). Avant la fin du Jurassique supérieur (Kimméridgien supérieur), la mer se retire des dernières zones submergées. En conséquence, la totalité de la plate-forme syrienne reste émergée jusqu'à la transgression du Crétacé, débutant au Barrémien-Aptien. Comme ailleurs dans le Levant, l'activité volcanique caractérise localement le début et la fin du Jurassique.

MOUTY, M., 2000.— The Jurassic in Syria: an overview. Lithostratigraphic and biostratigraphic correlations with adjacent areas. *In*: S. CRASQUIN-SOLEAU & E. BARRIER (eds), Peri-Tethys Memoir 5: New data on Peri-Tethyan sedimentary basins. *Mém. Mus. natn. Hist. nat.*, **182** : 159-168. Paris ISBN : 2-85653-524-0.

Source : MNHN, Paris

INTRODUCTION

Jurassic strata crop out in the main chains in Syria: the Anti-Lebanon Chain, the Coastal Chain (Jibal As-Sahilyeh), the Kurd Dagh Chain and the Palmyrides Chain (Fig. 1). A large number of boreholes penetrating the Jurassic in different areas, and the sections measured in the Jurassic outcrops give an important insight on its development in Syria.

The earliest works on the Jurassic of Syria date from the 19th century (LARTET, 1869; FRAAS, 1877; NOETLING, 1887). Several important studies have described the Jurassic sequences in Syria (VAUTRIN, 1934; DUBERTRET, 1949-1975; PONIKAROV, 1966; MOUTY, 1976, 1978).

The recent lithological and palaeontological studies conducted on several formations, units and biozones within the Jurassic series (MOUTY, 1997a, b; FOURCADE & MOUTY, 1995; FOURCADE *et al.*, 1997) gave precise correlations between different Jurassic sections in Syria and in the neighbouring countries, allowing an accurate palaeogeographic reconstruction of the Syrian platform during the Jurassic.

The aim of the present paper is to correlate Jurassic formations in Syria and other neighbouring countries on lithological and palaeontological basis.

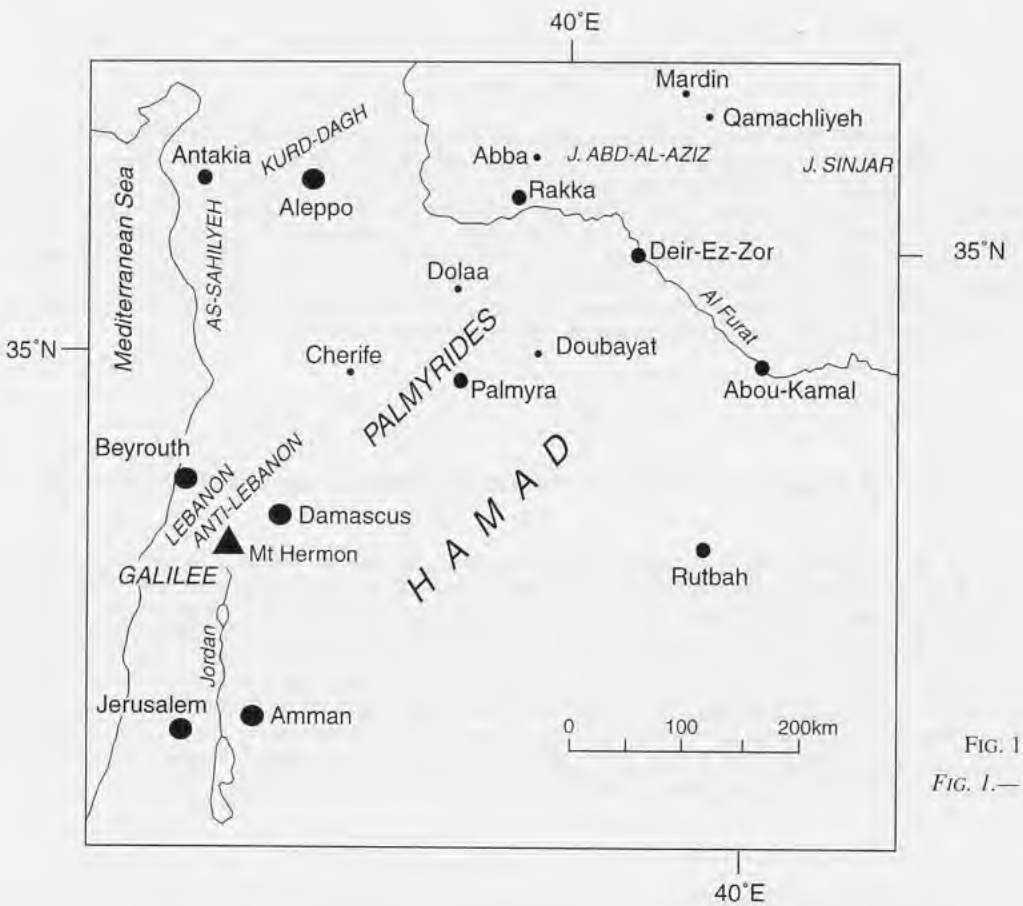

FIG. 1.— Location map.

FIG. 1.— Carte de localisation.

Source : MNHN, Paris

STRATIGRAPHY (Fig. 2)

EARLY JURASSIC (LIASSIC)

The Early Jurassic in Mount Hermon (Anti-Lebanon) is represented by the Aarne Formation (MOUTY, work in progress). It is essentially composed of numerous thin beds of multicoloured (black, yellow,...) argillaceous marls with thin beds of limestones which predominate in the upper part of the formation. A 50 m thick volcanic layer (spilite) is interbedded within this formation. Some limestone beds in the upper part of the formation contain *Pseudocyclammina liasica* Hottinger Foraminifera which is characteristic of the late Liassic (Pliensbachian-Toarcian).

The thickness of this formation in the type section (Mount Hermon) reaches 150 m. It overlies intercalations of black argillaceous marls and black thin bedded limestones (Rime Formation, DUBERTRET, 1960) with *Aulotortus sinuosus* (Weynschenk) which characterises the Late Triassic (Norian-Rhaetian).

The Aarne Formation is correlated in Lebanon with the lower part of "niveau 2" of Wadi Nahr Ibrahim (RENOUARD, 1951) which is composed of limestones, dolomitic limestones with rare marl intercalations and overlies a 300 m thick of dolomites and dolomitic limestones ("niveau 1") with probable Triassic Nodosaridae (NOUJEIM-CLARK & MOUTY, work in progress).

The Early Jurassic in the Palmyrides Chain is represented by the lower part (Unit A) of Satih Formation (MOUTY, 1997a), which is composed of thin beds of limestones and dolomitic limestones with some marl intercalations containing Liassic Foraminifera (*Mayncina termieri* Hottinger) in its upper part.

In the boreholes drilled in central, north and northeast Syria, the Early Jurassic is represented by limestones in the upper part of the Dolaa Group (DUBERTRET & DANIEL, 1962, according to DUBERTET, 1963).

The Early Jurassic in the Coastal Chain (Jibal As-Sahilyeh) is represented by Treize Formation (MOUTY, 1997b) which is composed of thin beds of light yellow marls, marly limestones and limestones. Fossils found in this formation are Brachiopoda, *Liospiriferina undulata* (Seguenza), and Foraminifera, *Pseudocyclammina liasica* Hottinger which indicate a Pliensbachian-Toarcian age. The thickness of this formation in its type locality reaches 40 meters. It underlies a thick serie of dolomites and dolomitic limestones (200-300 m) with Late Triassic Foraminifera: (*Galeanelia* aff. *laticarinata* Al Shaibani, *Gsollbergella spiriloculiformis* (Oroveczne-Scbeffer).

In the Kurd Dagh Chain, the Early Jurassic is represented by thick beds of micritic and pelbiomicritic limestones (the lower part of the Dodo Formation: "*Lithiotis* Limestone") (MOUTY, work in progress), with big, undulated and plated Pelecypoda: *Lithiotis* sp., which characterises the basal beds of the Jurassic in Iran (KENT *et al.*, 1951).

The numerous boreholes, which penetrated the Jurassic series, are located in the interior of Syria. The Early Jurassic encountered in these boreholes is undifferentiated in the upper part of Dolaa Group (DUBERTRET & DANIEL, 1962, according to DUBERTRET, 1963), and consisting in limestones underlying evaporates with some intercalations of thin beds of marls and marly limestones containing Late Triassic microfossils (BASH IMAM & SIGAL, 1985).

In this respect, it is very important to mention that the entire Jurassic serie is missing on the Aleppo-Mardin High (PONIKAROV, 1966; KAMMAR, 1994) and on the Hamad Uplift (MOUTY & AL MALEH, 1983; MOUTY, 1997a).

The Early Jurassic formations or units in Syria are correlated with the Ubaid Formation (DUNNINGTON, 1954, according to DUBERTRET, 1959) in west Iraq (Rutbah area) which is composed of limestones, dolomitic limestones and rare marl intercalations containing Liassic Foraminifera (DUNNINGTON, 1954 cited *in* DUBERTRET, 1959). They are correlated, in the northwestern Iraq, with the

Source : MNHN, Paris

lower part of the Sargelu Formation which is composed in its type locality of "thin bedded black, bituminous limestones, and black laminated shales" containing Liassic fauna at the base (BELLEN cited *in* DUBERTRET, 1959). They are also correlative with the upper part of the "Grès à plantes de Subeihi" (WETZEL & MORTON, 1959) in the northwest Jordan (Wadi Nahr Az-Zarqua).

The Early Jurassic volcanic serie, which outcrops in the Mount Hermon, reaches its maximum thickness in the Galilee to the west and southwest where it is represented by Asher volcanic Formation (GARFUNKEL & DERIN, 1985). The dolerite flow in the Abba borehole, 54 km NE by N of Raqqa (DANIEL cited *in* DUBERTRET, 1963) and the volcanic flow in the SE of Turkey (ALTINLI, 1966) are about of the same age.

<table>
<tr><th>Locality / Age</th><th>Galilee</th><th>Hermon</th><th>Lebanon</th><th>Coastal Chain J. As Sahilyeh</th><th>Kurd Dagh</th><th>Palmyrides</th><th>West Iraq</th><th>Jordan</th></tr>
<tr><td>Aptian - Cenomanian</td><td>Tayasir</td><td>Grès de base</td><td>Grès de base</td><td>Bab Janneh</td><td>Grès de base</td><td>Palmyra</td><td>Rutbah</td><td>Hathira</td></tr>
<tr><td>Tithonian</td><td>absent</td><td>absent</td><td>absent</td><td>absent</td><td rowspan="3">absent</td><td rowspan="3">absent</td><td rowspan="3">absent</td><td rowspan="3">absent</td></tr>
<tr><td>Kimmeridgian</td><td rowspan="2">Haifa Bay</td><td>Batroun</td><td>Salima</td><td rowspan="2">Nasirah</td></tr>
<tr><td>Oxfordian</td><td>Bloudane</td><td>Bikfaya</td></tr>
<tr><td>Callovian</td><td rowspan="6">Haifa</td><td>Majdal Chams</td><td>Bhanness</td><td>Wadi Al Ouyoun</td><td rowspan="2">absent</td><td rowspan="2">absent</td><td rowspan="2">Muhaiwir</td><td rowspan="2">Huni</td></tr>
<tr><td>Bathonian</td><td>Hermon</td><td>Kesrouane</td><td rowspan="2">Machta</td></tr>
<tr><td>Bajocian</td><td>Bqassem</td><td>niveau 4a
niveau 3</td><td rowspan="2">Dodo
Lithotis limestones
C
B
A</td><td rowspan="2">Sath
C
B
A</td></tr>
<tr><td>Aalenian</td><td>Kalaat Jandal</td><td rowspan="3">niveau 2</td><td>Ouyoun</td><td rowspan="2">Ubaid</td><td rowspan="2">Subeihi</td></tr>
<tr><td>Toarcian</td><td rowspan="3">Aarne</td><td rowspan="3">Treize</td></tr>
<tr><td>Pliensbachian</td><td rowspan="2">Asher</td></tr>
<tr><td>Lower Triassic</td></tr>
<tr><td>Norian-Rhaetian</td><td>Mohilla</td><td>Rime</td><td>niveau 1</td><td>Jweikhate</td><td>Smalek</td><td>Hayan</td><td>Zor Hauran</td><td>Zarqa</td></tr>
</table>

FIG. 2.— Correlation of the Jurassic formations in Syria and neighbouring countries.

FIG. 2.— Corrélations des formations jurassiques en Syrie et dans les régions avoisinantes.

MIDDLE JURASSIC (DOGGER)

The Middle Jurassic is the thickest serie of this stage in Syria. It is represented by many formations and units, especially along the coasts of the Eastern Mediterranean, from the Coastal Chains in Syria, all the way down to northern Sinai (Egypt).

The Kalaat Jandal Formation in the Mount Hermon was first defined by DUBERTRET (1960), as "Calcaire de Kalaat Jandal". It was modified recently (MOUTY, work in progress) by the separation of its lower part (Aarne Formation), due to the fact that it is lithologically different. It is essentially composed, in its type section, of medium to thick beds of micritic and pelbiomicritic limestones which are partly dolomitised. Its facies indicates a shallow marine environment of low energy. Its thickness is approximately 400 m.

The formation yields relatively abundant fossils, mainly Foraminifera. The most important ones are: *Timidonella sarda* Bassoullet, *Haurania deserta* Henson, *Amijiella amiji* (Henson). These fossils indicate an Aalenian-Bajocian age.

This formation is correlated with the Ouyoun Formation in the Coastal Chain in the NW Syria

Source : MNHN, Paris

(MOUTY, 1997b) which is composed of thick beds of limestones, dolomites, and dolomitic limestones containing *Timidonella sarda* Bassoullet, *Haurania deserta* Henson, *Amijiella amiji* (Henson). It is correlated with the B unit of Dodo Formation (MOUTY *et al.*, work in progress) in the Kurd Dagh, which consists in micritic and pelbiomicritic limestones containing *Timidonella sarda* Bassoullet, and with the B unit of Satih Formation in the Palmyrides Chain (MOUTY, 1997a) which consists in massive dolomicritic limestone containing *Haurania deserta* Henson and *Amijiella amiji* (Henson).

The correlation of this formation with its rivals in the neighbouring countries bears some problems. It could be preliminarily correlated in age with the lower part of Haifa Formation (DERIN, 1974) in Galilee, with the upper part of "Niveau 2" in Lebanon (RENOUARD, 1951), with the limestones and marly sandstones of the Huni Formation in Wadi Az-Zarqa (WETZEL & MORTON, 1959), in the northwest Jordan, with the lower part of Muhaiwir Formation (WETZEL, 1951 cited *in* DUBERTRET, 1959) in the southwest Iraq, which contains *Haurania deserta* Henson, *Amijiella amiji* (Henson) and with the middle part of Sargelu Formation (WETZEL, 1951 cited *in* DUBERTRET, 1959) in the northwest Iraq, which contains abundant macrofossils (ammonites, Rhynchonellidae).

Bqassem Formation, in the Mount Hermon, overlies the Kalaat Jandal Formation. It was first defined by DUBERTRET (1960) as "Calcaire jaune de Bqassem". It is composed of limestones with marl intercalations, very thick in the lower part of the formation. It represents shallow marine environment sediments of relatively high energy. It overlies an important hard ground surface on the top of Kalaat Jandal Formation. Its thickness in its type locality is 150 m. According to VAUTRIN (1934) and DUBERTRET (1960), fossils are abundant. The formation fossil assemblage consists of *Rhynchonella hopkinsi* McCoy, *R. absoleta* Sowerby, *Terebratula superstes* Douville, *T. quillyensis* Bayle. The presence of characteristic Foraminifera, *Haurania deserta* Henson, *Amijiella amiji* (Henson), indicates an upper Bajocian-Bathonian age.

The formation has no proved correlation except the age with its rivals in the neighbouring countries. It could be correlated with the upper part (Unit C) of Satih Formation (MOUTY, 1997a) in the Palmyrides Chain which contains brachiopods, *Daghanirhynchia subversabilis* (Weik), and Foraminifera, *Haurania deserta* Henson, *Amijiella amiji* (Henson), with the lower part of Machta Formation (MOUTY, 1997b) in the Coastal Chain in the NW Syria, which consists in few metres of marl and limestone intercalations with a typical surface of emersion (palaeosoil surface). This surface is marked in the interior Syria, in the west of Iraq and in the northwest of Jordan, by an erosion surface, covered by clastic continental sediments of Early Cretaceous.

The Hermon Formation overlies the Bqassem Formation in Mount Hermon. It was first defined by DUBERTRET (1960) as "Calcaire de l'Hermon". It consists in thick beds of micritic, biomicritic and pelbiomicritic limestones. The depositional environment of this formation is neritic and normal saline, subject to long period of subsidence. Its thickness, in its type locality, is about 700m.

Fossils in the type locality are relatively frequent, consisting in lower part of *Paleopfenderina salernitana* (Sartoni & Crescenti), *P. trochoidea* (Smouth & Sugden), *Kilianina blancheti* Pfender, *Endersonella palastiniensis* (Henson), and in the upper part, are rich in *Steinekella steinekei* Redmond, *S. crusei* Redmond, *Praekurnubia crusei* Redmond, *Redmondoides lugeoni* (Septfontaine) with Dasycladacea: *Salpingoporella annulata* Carozzi, *Thaumatoporella parvovesiculifera* (Raineri).

Fossil assemblages mentioned above indicate a Bathonian-lower Callovian age.

The formation can be correlated with the upper part of the Haifa Formation in the Galilee area (DERIN, 1974). It is correlated with massive limestones of the Kesrouane Formation in Lebanon (DUBERTRET, 1960).

The Hermon Formation has no proper lithologic correlation with the Coastal Chain in the northwest Syria. It is correlated, essentially in age, with the upper part of the Machta formation, and the lower part of Wadi Al-Ouyoun formation (MOUTY, 1997b), since Machta Formation consisted in an alternation of thick lithological units of limestones and marls, that contain, from the base to the top, *Paleopfenderina trochoidea* (Smouth & Sugden), *P. salernitana* (Sartoni & Crescenti), *Kilianina blancheti* Pfender, which indicate a Bathonian age, and the lower part of Wadi Al-Ouyoun formation which contains *Steinekella steinekei* Redmond, *S. crusei* Redmond and which indicate a Callovian age.

The Hermon Formation is missing in the entire interior Syria, except for west Palmyrides Chain (Sherifeh area) which contains *Valvulinella jurasica* (Henson).

Source : MNHN, Paris

LATE JURASSIC (MALM)

The Majdal Chams Formation overlies the Hermon Formation in the southwest flank of Mount Hermon (Majdal Chains village). It was first defined by DUBERTRET (1960) as "Marnes gris-clair de Mejdel Chems" (in Hermon geological map). It is composed of argillaceous marls with limonitic concretions at the base and intercalations of thin beds of limestone and marl.

Fossils are abundant throughout, specially in ammonites and brachiopods. According to NOETLING (1887), VAUTRIN (1934), HAAS (1955), ARKELL (1956), DUBERTRET (1960), RAZVALYAEV (1966), CARIOU & HANTZPERGUE (1997), CARIOU *et al.* (1997), this fauna indicates an Oxfordian age.

The thickness of Majdal Chams Formation in its type locality is about 150-200 m. It decreases in thickness northwards. It drops to 50 m in Wadi Al-Karn, 40 km northeast of Mount Hermon: "Marne jaune de Wadi Al-Karn" (DUBERTRET, 1950), yielding abundant fossils: stromatopora, corals, echinoids, brachiopods (*Somalirhynchia africana* Uhlig, *Bihenithyris weiri* Muir-Wood) which indicate a middle Callovian age (*Erymnoceras* and *Pachyerymnoceras* horizon) (ALMÉRAS, personal communication).

The upper part of the Majdal Chams Formation is partly correlated in age with the upper part of Wadi Al-Ouyoun Formation (MOUTY, 1997b) in the Coastal Chain, in the northwest Syria, which yields Foraminifera, *Steinekella steinekei* Redmond, *S. crusei* Redmond, and brachiopods, *Bihenithyris* sp., *Kutchirhynchia indica* (d'Orbigny), indicating a middle Callovian age.

A 30 m thick remarkable volcanic horizon termed "Niveau volcanic de Bhanness" (DUBERTRET, 1950) occurs in Lebanon.

The Late Jurassic is represented in the Levantine coastal chains. Above the Majdal Chams Formation follows the Bloudane Formation (MOUTY, work in progress) which is the "Calcaire à *Balanocidaris glandifera*" (VAUTRIN, 1934). It consists in massive limestones presenting a very distinctive 15-25 m high cliff. It yields relative abundant fossils, mainly echinoids (*Balanocidaris glandifera* Munster) and Foraminifera. The most important Foraminifera is *Levantinella egyptiensis* (Fourcade, Mouty & Teherani) which indicates an Oxfordian age (Levantinella egyptiensis biozone). The alga *Clypeina jurassica* Favre characterises this formation.

The depositional environment of the formation is clearly neritic.

It is followed by the "calcaires jaunes supérieurs". This formation is correlated with the "Falaise de Bikfaya" (DUBERTRET, 1949, 1950) which forms in the Lebanon a high cliff (80 m) of massive limestone. The absence of micropalaeontological analysis makes difficult a precise correlation. It is probably equivalent to the Haifa Bay Formation.

Nevertheless, the Bloudane Formation is correlated in age with the lower part of Nasirah Formation (MOUTY, 1997b) in the Coastal Chain, in northwest Syria, which consists in pelbiomicritic limestone with *Levantinella egyptiensis* (Fourcade, Mouty & Teherani) and *Alveosepta jaccardi* (Schrodt). It is also correlative with the Haifa micrite levels containing *Levantinella egyptiensis* (Fourcade, Mouty & Teherani) in the Galilee (PICARD & HIRSCH, 1987).

The Late Jurassic is represented in the Anti-Lebanon by the Batroun Formation or "Calcaire jaune de Batroun" (DUBERTRET, 1950) which is composed of light yellow micritic, pelbiomicritic and oolitic limestones with abundant marl intercalations. In the SW flank of Mount Hermon, near Hadar village, two 20 cm thick basalt beds are present at the top of upper part of the formation.

The thickness of this formation in the Anti-Lebanon is about 20-40 m.

Fossils in the Hermon area are, according to VAUTRIN (1934): *Terebratula subsella* Leym., *Pyguropsis noetlingi* De Loriol. Near the Batroun locality (Rawda), SW of Zebdani plain, the fossils are abundant: *Alveosepta jaccardi* (Schrodt), *Kurnubia palastiniensis* Henson, *Alveosepta (Iberina) prealusitanica* (Maync). The presence of the latter species characterises the Kimmeridgian in this region.

The formation is correlated with the Calcaire de Salima (DUBERTRET, 1950) in Lebanon which is

Source : MNHN, Paris

composed of light yellow oolithic and clastic limestones (150 m thick) locally interbedded by some volcanic levels.

The formation is correlated in age with the upper part of Nasirah Formation (MOUTY, 1997b) in the Coastal Chain in the northwest Syria, which yields *Alveosepta jaccardi* (Schrodt), *A. (Iberina) prealusitanica* (Maync) and *Kurnubia palastiniensis* Henson.

It is also correlated with the Haifa Bay Formation in Galilee which contains *Alveosepta (Iberina) prealusitanica* (Maync) (MAYNC, 1966).

The Late Jurassic is missing in the entire interior Syria, except for the Sherifeh area (W of Palmyrides Chain), which was submerged during that time: its sediments contain *Levantinella egyptiensis* (Fourcade, Mouty & Teherani) (HENSON, 1948).

It is also missing in west Iraq (BUDAY, 1980) and in Jordan (WETZEL & MORTON, 1959).

The Late Jurassic is restrictively present along the coastal chains of the East Mediterranean: Jabal Akraa, Coastal Chain (Jibal As-Sahilyeh), Lebanon Chain, Anti-Lebanon Chain and Galilee (Coastal Basin).

The Tithonian is missing in Syria and probably in the neighbouring areas due to an important hiatus which reaches the end of Neocomian.

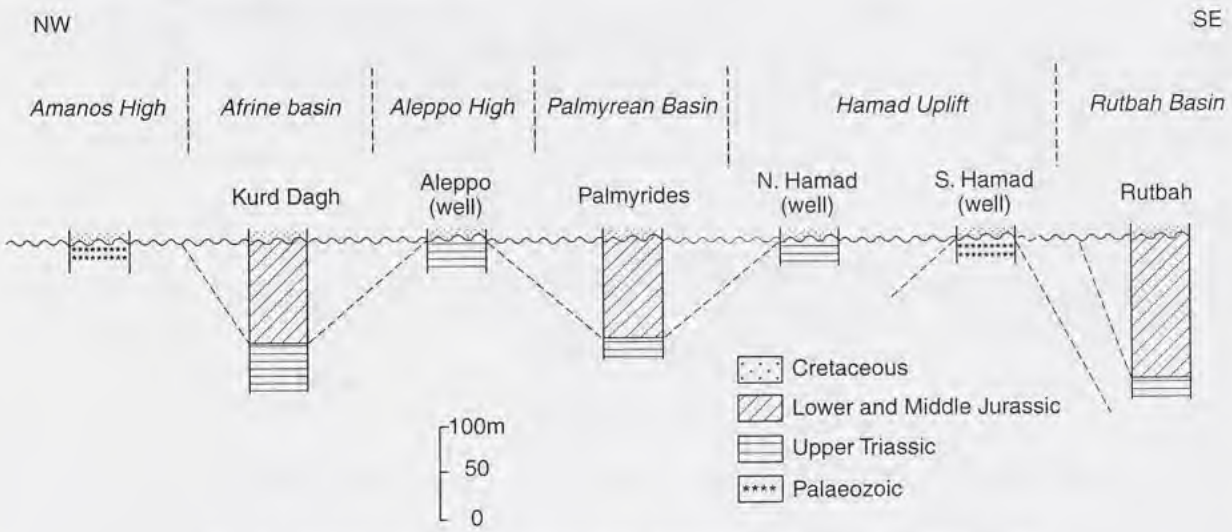

FIG. 3.— Correlation between sections from Amanos High to Rutbah Basin (NW-SE).

FIG. 3.— Corrélations entre les coupes depuis la surrélévation d'Amanos jusqu'au Bassin de Rutbah (NW-SE).

CONCLUSION

The palaeogeographic development during the Early and Middle Jurassic in Syria is controlled by two ENE-SW oriented huge uplift zones:

Hamad Uplift (MOUTY & AL MALEH, 1983; MOUTY, 1997a), Aleppo-Mardin high (PONIKAROV, 1966; KAMMAR, 1994) and Amanos High (LOVELOK, 1984) within the Syrian platform, separated by intracratonic rifted zones: the Rutbah basin (SW Iraq), the Palmyrid basin, the Afrine basin; and bordered in the west by the western margin of a N-E oriented rift zone (the Coastal basin) which represent the oldest manifestation of the Levant Fault-Zone (Dead Sea Fault) well developed at Late Tertiary (MOUTY, work in progress) (Figs 3 and 5).

These structures were the result of the Gondwana breakup, reflected by the opening of the Tethyan Ocean at the end of Upper Triassic.

Source : MNHN, Paris

The palaeogeographic development during the Early Jurassic is characterised by progressive transgression started just before the end of Late Triassic (MOUTY, 1997a) onto the Syrian platform, that did not submerge the huge uplifted zones. The evaporitic sediments precipitated under lagoonal conditions during the Triassic were replaced by marine sediments. The volcanic rocks within the Early Jurassic sediments (Mount Hermon, Galilee, Dolaa well) indicate the activity of these rifted zones at that time.

These marine conditions were continued during the Dogger, represented by frankly marine sedimentation, mostly neritic calcareous-micritic, pelitic or arenaceous sedimentation. The west marginal rift zone (Levantine basin) differs from the other basins, especially in its southern part (Lebanon, Anti-Lebanon and Galilee) which was being of more expressive mobility and subsidence (VAUTRIN, 1934; RENOUARD, 1951; DUBERTRET, 1966; PICARD & HIRSCH, 1987; HIRSCH & PICARD, 1988).

The Dogger sedimentation locally ended by an emergent phase. Before the end of the Dogger, at the base of the Bathonian, a regressive phase marks the end of the marine cycle on the entire interior Syrian platform.

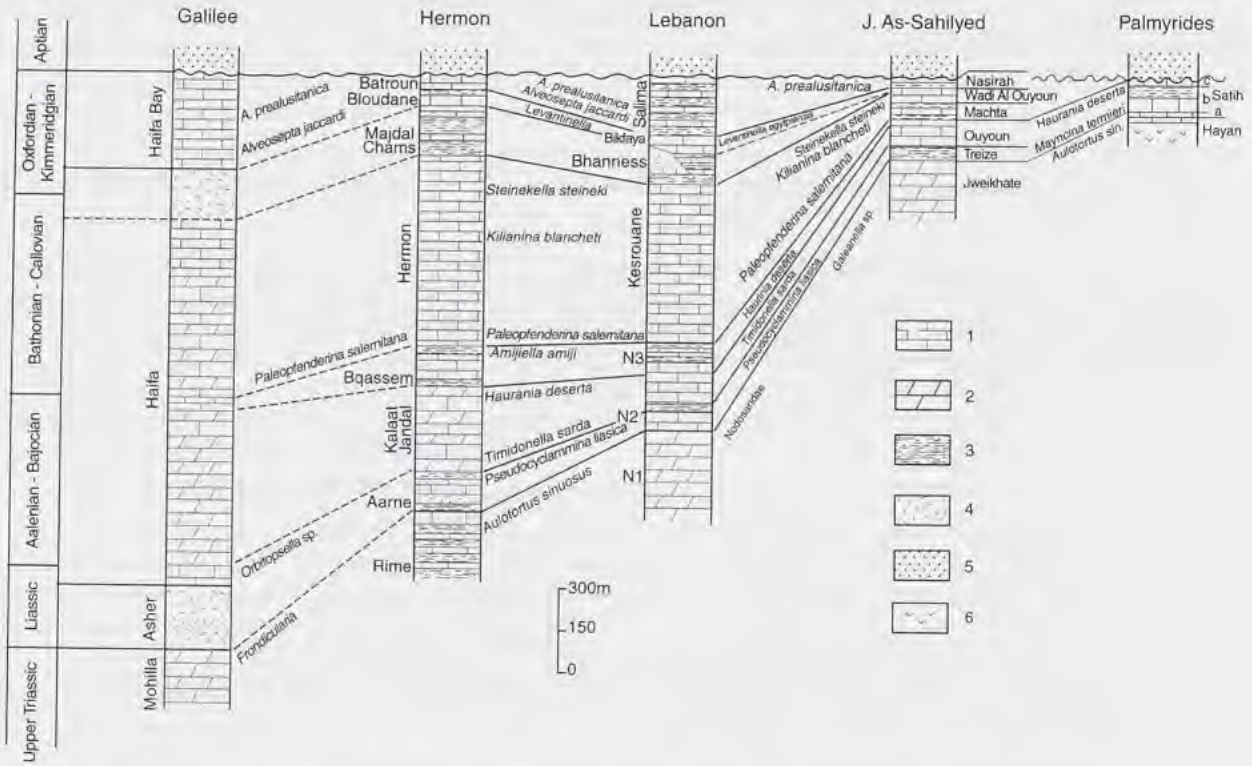

FIG. 4.— Stratigraphic sections of East Mediterranean Chains. **1**, limestones; **2**, dolomites; **3**, marls; **4**, basalts; **5**, sandstones; **6**, gypsum.

*FIG. 4.— Corrélations stratigraphiques des Chaînes est-méditerranéennes. **1**, calcaires ; **2**, dolomies ; **3**, marnes ; **4**, basaltes ; **5**, grès ; **6**, gypse.*

The regressive phase began at the base of the Bathonian. The Jurassic sea withdrew from the interior rifted basins to the Tethyan Ocean in the north and to the East Mediterranean basin in the west forming an embayement in the Sherifeh area. This basin on the western margin of the Syrian platform continues to subsidise, especially in its southern part (Lebanon, Anti-Lebanon and Galilee) until the end of Kimmeridgian (Fig. 4) where the latest regressive phase began, with some volcanic activity locally (Mount Hermon and Lebanon), and the entire Syrian platform became emerged during the Tithonian stage.

Source : MNHN, Paris

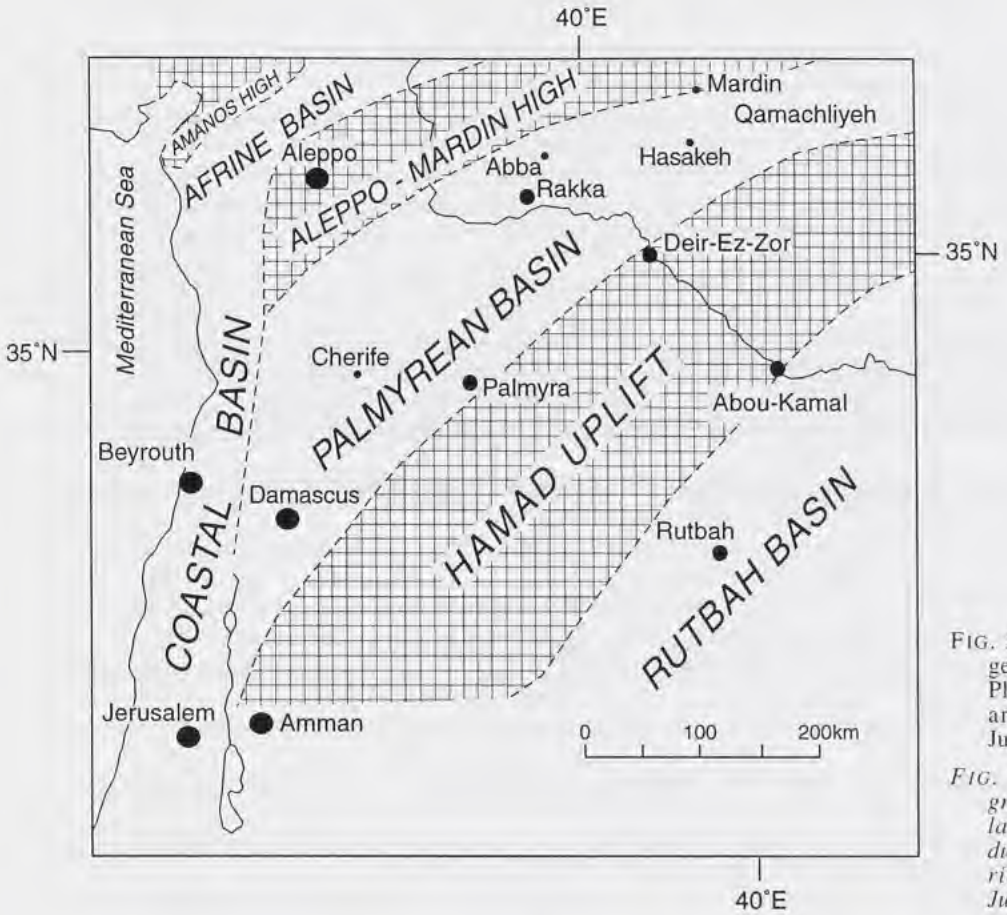

FIG. 5.— Schematic palaeogeographic map of Syrian Platform during the Early and the early Middle Jurassic.

FIG. 5.— Carte paléogéographique schématique de la plate-forme syrienne durant le Jurassique inférieur et le début du Jurassique moyen.

REFERENCES

ALTINLI, I.E., 1966.— Geology of eastern and southeastern Anatolia. *Bulletin of Mineral Exploration Institute, Foreign Edition, Ankara*, **60**: 36-76.

ARKELL, W.J., 1956.— *Jurassic Geology of the World*. Oliver & Boyd, London: 1-806.

BASH IMAM, I. & SIGAL, J., 1985.— Précisions nouvelles sur l'âge triasique et non jurassique de la majeure partie des formations évaporitiques des forages de l'Est syrien. *Revue de Paléobiologie*, **4** (1): 35-42.

BUDAY, T., 1980.— *The Regional Geology of Iraq*. Tome 1. State Organization for Minerals, Baghdad: 1-445.

CARIOU, É., BASSOULLET, J.-P., GROSSOWICZ, L., HIRSCH, F., 1997.— Le Callovo-Oxfordien du Sud Levant: données biostratigraphiques nouvelles (Ammonites, Foraminifères) endémisme et corrélations stratigraphiques. *In*: *De la biostratigraphie à la paleobiogéographie: réunion spécialisée APF-SG*. Lyon, Société géologique de France: 21.

CARIOU, É. & HANTZPERGUE, P., 1997.— Biostratigraphie du Jurassique ouest-européen et méditerranéen: zonations parallèles et distribution des invertébrés et microfossiles. *Elf Aquitaine Édition, Pau, Mémoire*, **17**: 1-440.

DERIN, B., 1974.— *The Jurassic of Central and Northern Israel*. Ph. D. Thesis, Hebrew University, Jerusalem, Israel: 1-70 (in Hebrew, English summary).

DUBERTRET, L., 1949.— *Carte géologique au 1: 200 000. Feuille de Tripoli. Notice explicative*. République libanaise, Ministère des Travaux publics, Beyrouth: 1-64.

DUBERTRET, L., 1950.— Sur le Jurassique du Liban et de l'Anti-Liban. *Comptes Rendus sommaires de la Société géologique de France*, **2**: 12-13.

DUBERTRET, L. (ed.), 1959.— *Lexique stratigraphique international*. 3: *Asie, Iraq*. CNRS, Paris, Fasc. 10a: 1-333.

DUBERTRET, L., 1960.— *Feuille Hermon, Notice explicative*. République libanaise, Ministère des Travaux publics, Beyrouth: 1-46.

DUBERTRET, L. (ed.), 1963.— *Lexique stratigraphique international*. 3: *Asie, Syrie*. CNRS, Paris, Fasc. 10cl: 1-437.

DUBERTRET, L., 1966.— Liban, Syrie et bordure des pays voisins. *Notes et Mémoires sur le Moyen-Orient*, **8**: 251-358.

Source : MNHN, Paris

DUBERTRET, L., 1975.— Introduction à la carte géologique à 1/50 000 du Liban. *Notes et Mémoires sur le Moyen-Orient*, **13**: 345-403.

FOURCADE, E. & MOUTY, M., 1995.— Découverte d'un nouveau grand Foraminifère du Jurassique de la marge sud téthysienne: *Syriana khouryi* n.gen. n.sp. *Revue de Micropaléontologie*, **38** (3): 217-227.

FOURCADE, E., MOUTY, M. & TEHERANI, KH., 1997.— *Levantinella* nov. gen. et révision du genre *Mangashtia* Henson, grands Foraminifères du Jurassique et du Crétacé du Moyen-Orient. *Geobios, Lyon*, **30** (2): 179-192.

FRAAS, O., 1877.— Juraschichten am Hermon. Neues Jahrbuch fur Mineralogie, Geologie und Palaeontologie, **1**: 17-30.

GARFUNKEL, Z. & DERIN, B., 1985.— Permian-Early Mesozoic Tectonism and Continental margin formation in Israel and its implications for the history of the eastern Mediterranean. *Special Publications - Geological Society of London*, **17**: 187-201.

HAAS, O., 1955.— Revision of the Jurassic ammonite fauna of Mount Hermon, Syria. *Bulletin of the American Museum of Natural History*, **108**: 1-210.

HENSON, F.R.S., 1948.— *Larger Imperforate Foraminifera of South-Western Asia, Families Lituolidae, Orbitolinidae, Meandropsinidae*. British Museum, London: 1-127.

HIRSCH, F. & PICARD, L., 1988.— The Jurassic facies in the Levant. *Journal of Petroleum Geology*, **11** (3): 277-308.

KAMMAR, N., 1994.— *The Triassic and Jurassic in Aleppo Plateau*. M. Sc. Thesis, Damascus University, Damascus, Syria: 1-114 (in Arabic).

KENT, P.E., SLINGER, F.C. & THOMAS, A.N., 1951.— Stratigraphical exploration surveys in SW Persia. *In: Proceedings of the 3rd World Petroleum Congress, Section 1*. E. J. Brill, Leiden: 141-159.

LARTET, L., 1869.— *Essai sur la géologie de la Palestine*. Thèse, Faculté des Sciences de Paris, Paris, France, **316**: 1-229, 29 figs. Publiée également par Masson et Fils.

LOVELOK, P.E.R., 1984.— A Review of the tectonics of the Northern Middle East region. *Geological Magazine*, **121**: 577-587

MAYNC, W., 1966.— Microbiostratigraphy of the Jurassic of Israel. *Israel Geological Survey, Bulletin*, **40**: 1-56.

MOUTY, M., 1976.— Présence du Lias dans le Massif Alaouite, Syrie. *Comptes Rendus sommaires de la Société géologique de France*, **3**: 104-105.

MOUTY, M., 1978.— Données nouvelles sur le Jurassique dans les Palmyrides. *Syrian Geological Magazine, Damas*, **2**: 20-22 (en arabe).

MOUTY, M., 1997a.— Le Jurassique de la Chaîne des Palmyrides (Syrie Centrale). *Bulletin de la Société géologique de France*, **168** (2): 181-186.

MOUTY, M., 1997b.— Le Jurassique de la Chaîne Côtière (Jibal As-Sahilyeh) de Syrie: essai de biozonation par grands foraminifères. *Comptes Rendus de l'Académie des Sciences, Paris*, **325**: 207-213.

MOUTY, M. & AL MALEH, A.KH., 1983.— *Geological Study of Palmyrides Chain (Syria)*. Ministry of Petroleum and Mineral Resources, Damascus: 1-257.

NOETLING, F., 1887.— *Der Jura am Hermon*. E. Schweizerbart'sche Verlagsbuchhandlung, Stuttgart: 1-46.

PICARD, L. & HIRSCH, F., 1987.— *The Jurassic Stratigraphy in Israel and the Adjacent Countries*. The Israel Academy of Sciences and Humanities, Jerusalem: 1-106.

PONIKAROV, V.P., 1966.— *Geological Map of Syria, Scale 1: 1 000 000*. Ministry of Petroleum and Mineral Resources, Damascus.

RAZVALYAEV, A.V., 1966.— *Explanatory Notes to the Geological Map of Syria, 1: 200 000*. Syrian Arab Report of the Ministry of Industry, Department of Geological and Mineral Research, Damacus: 1-122.

RENOUARD, G., 1951.— Sur la découverte du Jurassique inférieur (?) et du Jurassique moyen au Liban. *Comptes Rendus de l'Académie des Sciences, Paris*, **232**: 992-994.

VAUTRIN, H., 1934.— Contribution à l'étude de la série jurassique dans la chaîne de l'Anti-Liban et plus particulièrement dans l'Hermon (Syrie). *Comptes Rendus de l'Académie des Sciences, Paris*, **198**: 1438-1440.

WETZEL, R. & MORTON, D.M., 1959.— Contribution à la géologie de la Transjordanie. *Notes et Mémoires sur le Moyen-Orient*, **7**: 95-191.

Source : MNHN, Paris

10

Basin development and tectonic history of the Euphrates graben (Eastern Syria): a stratigraphic and seismic approach

Cécile CARON [1], *Maher* JAMAL [2]
Hassan ZEINAB [3] & *Francis* CERDA [1]

[1] Mazzeh Dar Es Saada, 16 Villat Gharbia, BP 9645, Damas, Syrie
[2] Ministry of Petroleum and Mineral Resources, Adawi Autostrade, Damas, Syrie
[3] Syrian Petroleum Company, P.O. Box 2849 – 668, Damas, Syrie

ABSTRACT

The Euphrates graben (Eastern Syria) is a E-W to NW-SE trending basin developed during the Late Cretaceous within the northern Arabian platform. This basin holds significant hydrocarbon reserves and is a major petroleum province in Syria. The present study intends to reconstruct the structural evolution of this graben system from the Early Cretaceous to the Oligocene, on the basis of detailed isopach maps and regional 2 D seismic profiles. Early NE-SW extension and associated basaltic activity are attested in Eastern Syria as soon as in Albian times. Intense block-faulting and graben formation are reported later, during the Turonian-Coniacian. After a period of relative tectonic quiescence by the Santonian, the main pulse of "rifting" occured in Campanian times, with the opening of a deep N120-140E trough, filled with a 1500 m thick "syn-rift" sequence. At that time, major northeast-vergent listric faults formed in the southern part of the Euphrates graben. This graben may correspond to a flexural basin induced by the obduction of the Tethyan oceanic crust onto the northern margin of the Arabian plate during the Late Cretaceous. The early Maastrichtian period is characterised by an counterclock-wise rotation of stress orientation (from NE-SW to N15E). This change may be explained either by the stopping of lateral eastward expulsion (folding of the Zagros foreland) or by the obduction stage along the Bitlis axis. N-S compressive movements in late Maastrichtian times caused the Euphrates "rift" system to abort. Structural inversion was particularly active in the northwestern part of the Euphrates graben, at the junction with the Palmyrides belt, Mesozoic basin first inverted at that time. Palaeogene is the time of global compressive tectonics. The response of the Euphrates graben to compression is diachronous over the northwestern area, with a propagation of structural inversion from north to south. Northern grabens are inverted in the Palaeocene, whereas southern grabens are inverted later in the Eocene. This pattern is consistent with the global tectonic setting of the Northern Arabian plate at that time, implying southward migration of deformation from the site of the Bitlis convergent zone to the foreland domains. The Oligocene period corresponds to the reactivation of N120E normal faults in the northwestern part of the study area.

CARON, C., JAMAL, M., ZEINAB, H. & CERDA, F., 2000.— Basin development and tectonic history of the Euphrates graben (Eastern Syria): a stratigraphic and seismic approach. *In* : S. CRASQUIN-SOLEAU & É. BARRIER (eds), Peri-Tethys Memoir 5: new data on Peri-Tethyan sedimentary basins, *Mém. Mus. natn. Hist. nat.*, **182** : 169-202. Paris ISBN : 2-85653-524-0.

Source : MNHN, Paris

RÉSUMÉ

Développement du bassin et histoire tectonique du graben de l'Euphrate (Syrie orientale): approche stratigraphique et sismique.

Le graben de l'Euphrate (Syrie orientale), d'orientation E-W à NW-SE, se développe au Crétacé supérieur au sein de la plate-forme arabe septentrionale. Ce bassin renferme d'importantes réserves d'hydrocarbures qui en font une province pétrolifère majeure en Syrie. La présente étude se propose de reconstituer l'évolution structurale de ce graben du Crétacé inférieur à l'Oligocène, sur la base de cartes en isopaques détaillées et de profils sismiques régionaux 2 D. Dès l'Albien, l'est de la Syrie est le siège d'une extension NE-SW s'accompagnant d'une activité basaltique marquée. L'intense morcellement en blocs marquant la formation du graben de l'Euphrate se produit cependant plus tard, au cours du Turonien-Coniacien. Après une période de relative stabilité tectonique au Santonien, la phase de "rifting" atteint son climax au Campanien, avec l'ouverture d'un graben N120E où les dépôts "syn-rift" excèdent une épaisseur de 1500 m. A cette époque, des failles listriques majeures à vergence nord-est s'individualisent dans la partie sud du graben. Le graben de l'Euphrate pourrait correspondre à un bassin flexural induit par l'obduction de la croûte téthysienne sur la marge nord de la plaque arabe au cours du Crétacé supérieur. Une rotation anti-horaire de la direction d'extension (NE-SW à N15E) est observée au Maestrichtien inférieur, peut-être liée à un blocage de l'extension vers l'est (plissement de l'avant-pays de la chaîne du Zagros) ou bien à l'obduction de la croûte téthysienne qui intervient à cette époque le long de la zone de suture de Bitlis. Le Maestrichtien supérieur voit l'arrêt de l'activité du "rift" de l'Euphrate et son inversion locale, sous l'effet d'une compression N-S. L'inversion du graben est surtout sensible dans sa partie nord-ouest, à la jonction avec la chaîne des Palmyrides, bassin mésozoïque majeur en Syrie, qui connaît sa première phase d'inversion à cette époque. Cette inversion se poursuit au Paléogène et se propage dans le graben de l'Euphrate du nord vers le sud. Les grabens les plus méridionaux s'inversent à l'Eocène, alors que ceux du nord s'inversent dès le Paléocène. Ce résultat est cohérent avec le cadre géodynamique général de la bordure nord de la plaque arabe à cette époque, impliquant une migration de la déformation depuis la zone de convergence de Bitlis vers l'avant-pays au sud. La période oligocène correspond à la réactivation des failles normales N120E dans le secteur nord-ouest de la zone d'étude.

INTRODUCTION AND SCOPE

The Euphrates graben (Eastern Syria) is commonly described as an intracratonic E-W to NW-SE trending rift developed within the northern Arabic Platform during the Late Cretaceous. This basin is totally hidden by a "post-rift" sequence reaching more than 3000 m in thickness. It holds significant petroleum reserves that have been discovered during the past decade. The main proven play is a Triassic/Early Cretaceous clastic reservoir (Mulussa/Rutbah formations) covered and laterally oil-sourced by Late Cretaceous limestones.

Despite the great amount of structural and sedimentological studies carried out at the scale of the field, no comprehensive analysis of the development of this graben system was available up to now. The produced maps are regional structural maps drawn on top of selected levels. No detailed isopach mapping has been published, even though it can provide substantial information about the tectono-sedimentary evolution of this basin. Moreover, the global geotectonic setting is not fully understood. How to explain for example the occurrence of a rifting phase during a period dominated by plate convergence in the Late Cretaceous?

The present study intends to elucidate this question or, at least, to propose clues for understanding. The main data used for this study include 4 seismic reflection profiles (7 regional 2D lines) and information from up to 100 exploratory and appraisal wells distributed over some 5600 km^2.

GEOLOGICAL SETTING OF THE EUPHRATES GRABEN

The Euphrates graben is located in the northwestern part of the Arabian plate, at the eastern edge of the Syrian territory (Fig. 1). This basin extends approximately 160 km from the E-W trending Anah graben in Iraq to the northeastern edge of the Palmyrides fold belt (Fig. 2) with 90 km in width. This graben is bounded to the south by the Hamad high and to the north by the Derro high (Fig. 2), which could represent the northeastern extension of the Palmyra belt into the Sinjar trough region lying to the north (SAWAF *et al.*, 1993). The Euphrates graben shows a bi-directional fault pattern resulting from a multiphase history of deformation (LITAK *et al.*, 1998). The northwestern tracts of the basin show

Source : MNHN, Paris

predominantly east-west oriented normal faults, whereas its southern portion displays a northwest-oriented array of normal faults.

GLOBAL GEODYNAMIC FRAMEWORK

The Arabian plate was separated from the African plate in the early to the middle Miocene along the Read Sea rift (Fig. 1). The western boundary of the Arabian plate is marked by the left-lateral Levant fault system, which extends from the Gulf of Aqaba in the south to the Bitlis suture zone in the north. The Levant transform fault marks the boundary between the Arabian plate to the east and the Levantine (Eastern Mediterranean) sub-plate to the west. The Bitlis suture is the site of convergence between the Arabian and Eurasian plates. Continuing movement along the northern boundary is accommodated by thrusting along this suture as well as extension along the left-lateral east Anatolian fault zone (Turkey block). To the east of the Arabian plate, the Neogene-Quaternary Zagros fold belt represents the collision zone of the African/Arabian plate with Iran.

GLOBAL STRUCTURAL SETTING: A REVIEW

The Euphrates graben is one of the three major basins active during the Mesozoic in Syria (Fig. 2). The Palmyrides and Sinjar troughs are organised along an ENE/WSW trend whereas the Euphrates graben follows a NW/SE trend (Fig. 2). Palmyrides and Euphrates trends are believed to represent suture or shear zones along which the northern Arabian platform accreted during Late Proterozoic time. This is suggested by the difference in metamorphic basement depth on both sides of the Palmyrides and

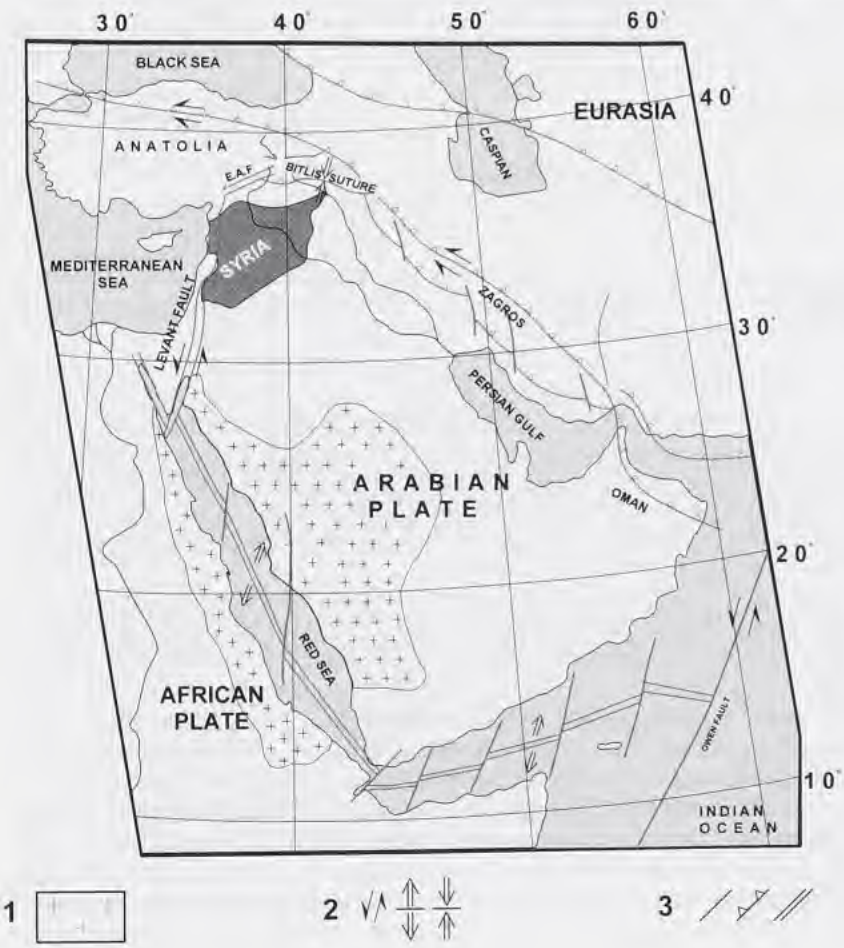

FIG. 1.— Geodynamical setting of the Arabian plate. **1**, crystalline basement; **2**, relative movements at plate boundaries; **3**, major tectonic lineaments. EAF, East Anatolian Fault.

*FIG. 1.— Cadre géodynamique de la plaque arabe. **1**, socle cristallin ; **2**, mouvements relatifs aux limites de plaques ; **3**, linéaments tectoniques majeurs. EAF, faille est-anatolienne*

Source : MNHN, Paris

the Euphrates graben system (BREW *et al.*, 1997). These suture/shear zones could have acted as zones of weakness that still control the intracontinental deformation in Syria. Between these Mesozoic intracratonic basins (Palmyrides, Euphrates, and Sinjar) are located several uplifted areas: the Aleppo plateau to the north, the Hamad uplift to the south, the Khleissia and Mardin highs to the east and northeast respectively (Fig. 2).

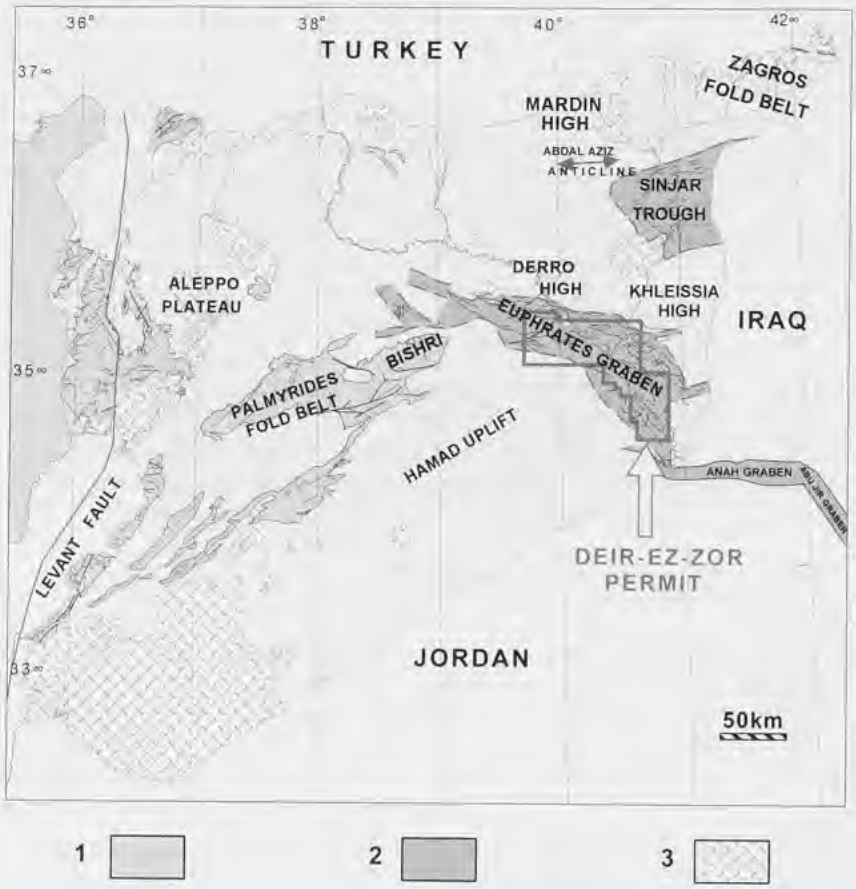

FIG. 2.— Geological setting of the Euphrates graben (East Syria). **1**, Mesozoic outcrops; **2**, grabens/troughs; **3**, volcanic outcrops.

*FIG. 2.— Cadre géologique du graben de l'Euphrate (Syrie orientale). **1**, affleurements mésozoïques ; **2**, grabens/dépressions ; **3**, affleurements volcaniques.*

The Palmyrides trough has been a centre of deposition from Carboniferous times onwards, with two major phases of rifting: from Carboniferous to Triassic times and from Aptian to Late Cretaceous (LOVELOCK, 1984). The second subsidence episode accompanied the development of the Levant passive margin to the west, in relation with the opening of the Eastern Mediterranean basin (BEST *et al.*, 1993). The Palmyrides rift was first inverted and deformed by the Late Cretaceous (N110E compression) until the Upper Eocene (SALEL, 1993; CHAIMOV *et al.*, 1993).

The Sinjar trough, on trend with the Palmyrides depression to the northeast and continuing into the Mesopotamian basin in Iraq, is contemporaneous with the second phase of rifting in the Palmyrides (BEST *et al.*, 1993; RUITER *et al.*, 1994).

The Sinjar trough and the northern part of the Euphrates graben (E-W trending basin) are believed to develop as a northeastern dependence of the Palmyrides trough (BEST *et al.*, 1993). The southern part of the Euphrates graben (N140E-trending basin) is conceived to develop later, during the Late Mesozoic (BEST *et al.*, 1993). According to LITAK *et al.* (1998), N140E-striking faults of the southern area appear to accommodate more strike-slip movement than the E-W normal faults of the northern part of the Euphrates graben. These authors conclude that Late Cretaceous extension may have been initially accommodated by the N140E inherited fault system (Proterozoic shear zone), but later broke through a new set of more favourably oriented structures (N100E). This is in line with LOVELOCK's interpretation

Source : MNHN, Paris

(1984) in which the Euphrates graben is viewed as a transtensional fault system which, after an eastward step at the Anah graben, continued along the southeast-striking "Abu Jir" N140E trend in Iraq (Fig. 2). Alternately, LITAK *et al.* (1998) suggested that the bi-directional fault pattern of the Euphrates graben might reflect a change in the pre-existing structures when approximating the Palmyrides N50E structural trend. Hence, the structural pattern of the northwestern area, with predominantly N100E faults, would result from the overprint of east-west oriented structures associated with Cainozoic compression, over a set of mostly northwest-trending Mesozoic normal faults.

The Euphrates graben as a whole is conceived as an aborted intracontinental rift system. A Coniacian age is proposed for the beginning of block faulting and the development of a regional unconformity (LITAK *et al.*, 1998). Rifting activity is shown to culminate during the Campanian-Maastrichtian.

LITAK *et al.* (1998) also noted that the Euphrates graben displays several features, which are unusual within classical rift structures:

— its aspect ratio length/width (160 x 90 km) is approximately one-half that of typical rifts;

— the estimated maximum total extension (about 6 km; β=1.06) is lower than that reported in the literature for most other continental rifts. Stretching factor β ranges from 1.1 to 1.3 in the Rhine graben, from 1.55 to 1.9 in the North Sea central graben, from 1.1 to 2.0 in the Gulf of Suez (see LITAK *et al.*, 1998 for references);

— the Euphrates graben does not exhibit sharp edges characterised by major listric bounding faults. Instead, numerous high-angle, planar normal faults are distributed over a broad zone to accommodate minimal extension.

LITAK *et al.* (1998) considered that this peculiar configuration is a common feature of rift basins in their initial formation stages. Therefore, the Euphrates rift is suggested to have aborted early in its history. RUITER *et al.* (1994) proposed that the Euphrates graben developed as a result of the subduction of the Arabian plate beneath the Eurasian plate. BEST *et al.* (1993) suggested to connect this rifting phase to the obduction events operating around the periphery of the Arabian plate during the Late Cretaceous.

STRATIGRAPHICAL SETTING OF THE EUPHRATES GRABEN

The generalised stratigraphical succession within the Euphrates graben is shown in the figure 3. The lithostratigraphic nomenclature adopted in this study is the one used since 1980 by the Pecten/Shell oil company in Syria, which introduces Iraqi formation names. The Palaeozoic to recent sedimentary sequence over the Euphrates graben is composed of a number of discrete depositional cycles separated by periods of erosion and/or non-deposition. Only during the Late Cretaceous and Tertiary has deposition been relatively continuous.

In the Euphrates graben, the maximum depth to the top of the "pre-rift" sequence is about 5 km (LITAK *et al.*, 1998). The sequences deposited prior to the "rifting" event and reached by exploration drilling range from Early Silurian to Lower Cretaceous in age and correspond to various depositional environments.

The oldest deposits drilled in the Euphrates graben (Fig. 3) are composed of black micaceous shales with minor silstones and thin beds of fine-grained sandstones of the so-called Abba formation. These organic-rich graptolite shales, of Silurian age, record deep marine conditions. No Devonian deposits are known in the Euphrates graben. More generally, the Devonian stratigraphic record is very sparse in Syria (BEST *et al.*, 1993). Whether it is absent by non-deposition, by erosion at the base Carboniferous unconformity or by a combination of both is still unclear. The Carboniferous Doubayat formation, composed of sandy shales and minor terrigenous carbonates, overlies the Lower Palaeozoic section with a slight angular unconformity. The Carboniferous sedimentary cycle is a transgressive-regressive sequence. The transgression starts with the sandy marine shale of the Lower Doubayat and evolves to a fully marine dolomite interval (intra-Carboniferous Dolomite). The Upper Doubayat section is a regressive sequence of sandstones and interbedded shales, deposited in a deltaic environment grading upwards into a continental one.

Source : MNHN, Paris

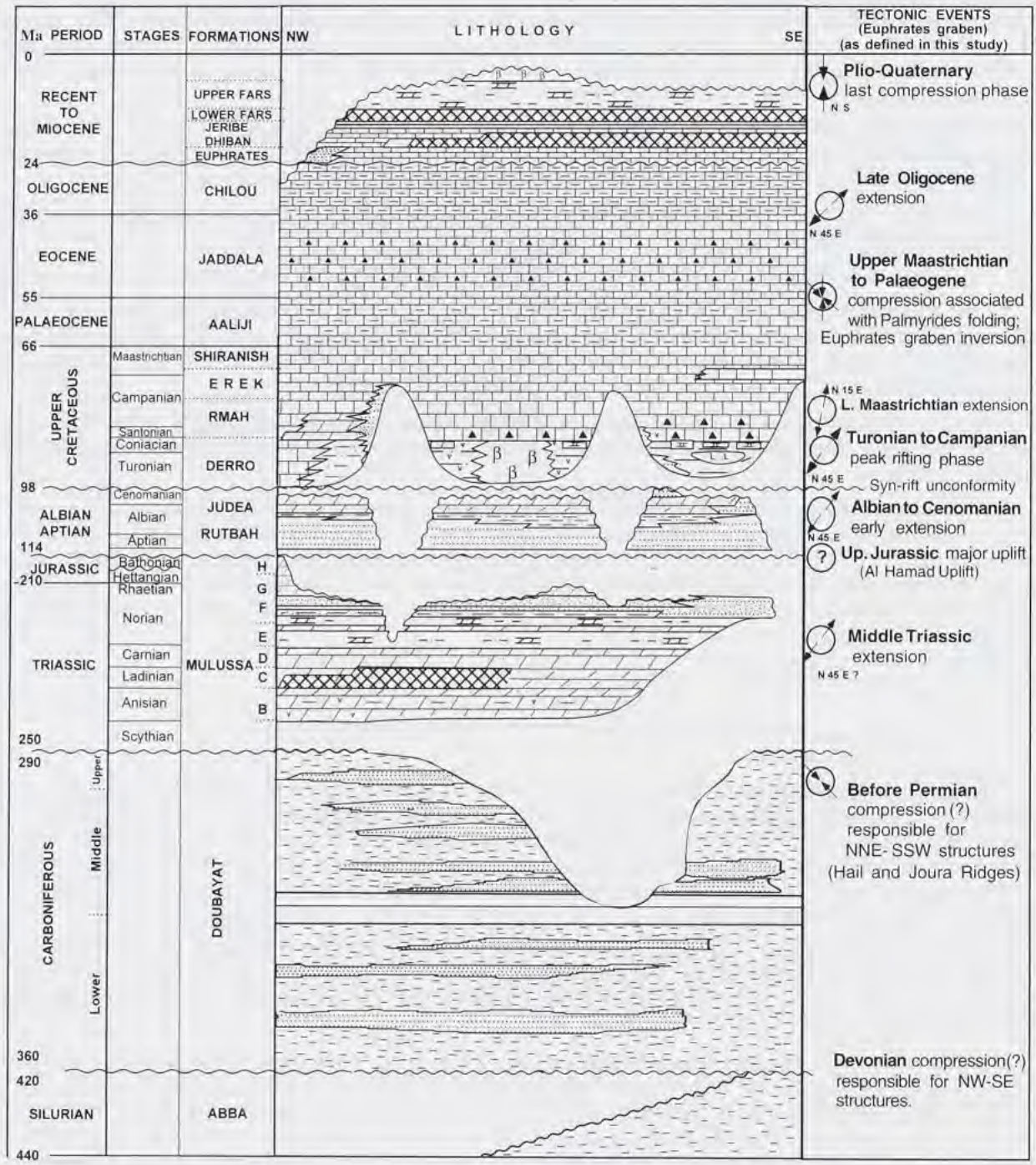

FIG. 3.— Chronostratigraphic chart of the Euphrates graben.

FIG. 3.— Charte chronostratigraphique du graben de l'Euphrate.

Source : MNHN, Paris

The Palaeozoic-Mesozoic boundary is characterised by a Carboniferous/Triassic unconformity, as no Permian deposits are recorded in the Euphrates graben and more generally in Eastern Syria. This time boundary also corresponds to a change from clastic to carbonate sedimentation. As a matter of fact, the Upper Permian-Lower Triassic period is marked by the creation of the Eastern Mediterranean basin to the west and by the development of the Levantine passive margin (BEST *et al.*, 1993). Within the Triassic interval, marine to supratidal dolomite and anhydrite (Mulussa B to E members) evolved upwards into a fluvial channel sand-dominated unit (Mulussa F formation, average thickness: 200 m) that forms the lowermost part of the reservoir-bearing sequence in the Euphrates oil province (Fig. 3). Following the deposition of the Triassic sequence (700 m thick in the deepest parts of the Euphrates depression), a major stratigraphic gap covers the period from Jurassic to Lower Cretaceous (some 110 Ma). In most of the studied wells, Lower Cretaceous series (Rutbah clastics) directly overlie the Triassic sediments. These deltaic to interdeltaic sandstones, up to 250m thick, constitute with the Mulussa F sandstones, the main reservoir of the Euphrates graben oil province. They are conformably overlain by a Cenomanian carbonate 10-90 m thick sequence (Judea formation).

The base of the Turonian in the Euphrates graben is marked by the presence of an unconformity which dates the onset of rifting in that area (Fig. 3). This unconformity is overlain by a thick Upper Cretaceous section, which reaches more than 2200 m in the deepest parts of the Euphrates rift system. The Palaeogene sedimentary package, 500-1500 m thick, mainly consists of argillaceous limestones interbedded with claystones. The final depositional stage is represented by shelf and shallow water carbonates, lagoonal deposits, continental sands and conglomerates of Neogene and Quaternary age with cumulative thicknesses increasing northeastward in the Euphrates graben, from 400 m to 1400 m.

DATABASE - METHODOLOGY

The zone under study has been constrained to the "Deir Ez Zor permit" area (Fig. 2), as this permit covers most of the Euphrates graben.

WELL DATA

Well data are widely used in this study. Among these wells, 46 were drilled either by Elf (EAS/EHS) or by the operating company DEZPC (Deir-Ez-Zor Petroleum Company). 36 wells were drilled either by the Pecten Shell/SSPD/AFPC group or by SAMOCO before 1988. On December 15th, 1988, Elf Aquitaine Syrie secured exploration rights in the Deir Ez Zor contract area and duly acquired information on the 36 wells drilled before that date. 6 wells drilled after 1988 by the AFPC/SSPD group were obtained by well data exchange in 1994 and 1996. Complementary set of wells has been provided with the kind authorisation of SPC (Syrian Petroleum Company), owner of the data.

Within each studied period of the graben history, the successive horizons are described step by step, following the chronology of sediment deposition. For each horizon considered, formation tops picked on electric logs are contoured as isopach maps. In most of the presented maps, the structural framework is taken at the Late Cretaceous/Early Cretaceous unconformity (Fig. 4). The base of the Late Cretaceous (Turonian) corresponds to the "syn-rift" unconformity located at the top of the Mesozoic "pre-rift" series (Fig. 3). This framework is used as a guideline to extrapolate isopach curves wherever well data coverage is scarce, except for the Palaeogene period, for which the iso-contouring method is applied.

SEISMIC DATA

The database used in this study is shown in the figure 4 and consists of 190 km of conventional seismic, respectively 155 km of dip and 35 km of strike sections. Among the seven 2D seismic lines interpreted in this work, 3 were shot by Pecten Shell in 1985 and 1986 and 4 by Elf from 1989 to 1992. Pecten Shell seismic data were duly acquired on December 15th, 1988, when Elf Aquitaine Syrie held exploration rights on the Deir Ez Zor permit area. 2D surveys were acquired and processed by various contractors: GSI, CGG, and GECO-PRAKLA. The main acquisition source was vibroseis, but dynamite was also employed when crossing the Euphrates River.

Source : MNHN, Paris

The 2D grid is wide and irregular (Fig. 4), about 6 to 20 km spacing between dip lines (NE-SW). However, this grid covers most of the graben extension. It was mainly chosen to define NE-SW transects spanning the width of the Euphrates graben, with cross-line control across the Hamad uplift to the south and the Derro high to the north.

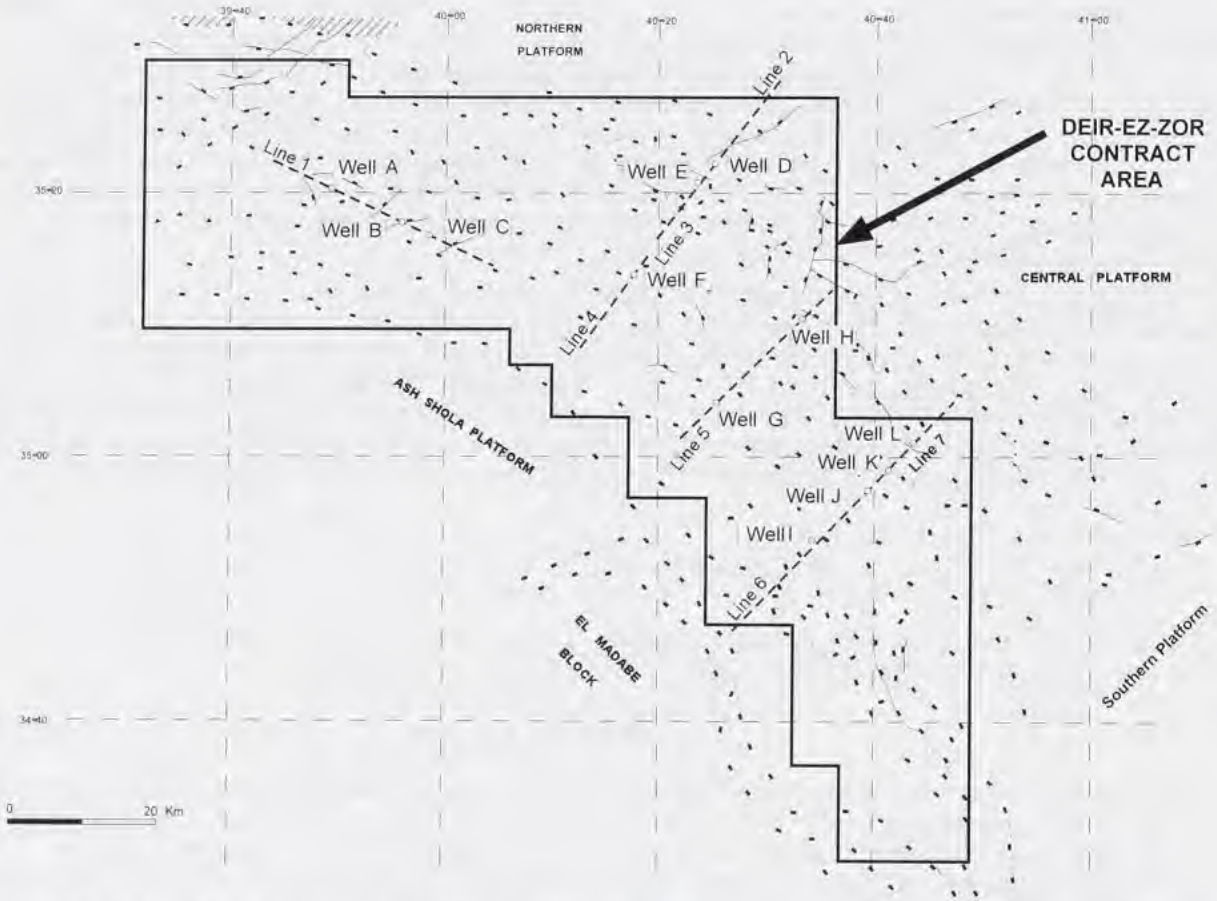

FIG. 4.— Location of the selected seismic lines and calibration wells on the Upper Cretaceous structural map of the Euphrates graben.

FIG. 4.— Localisation des lignes sismiques sélectionnées et des puits de calibration sur le schéma structural du graben de l'Euphrate au Crétacé supérieur.

Time/depth calibrations were provided by Well A, Well B, Well C, Well D, Well E, Well F within the northern area. Wells G to L were used as drill-hole controls within the southern area. 2D seismic lines have been scanned and directly loaded on Schlumberger-Charisma workstation. Picked horizons were chosen for their interest in delineating the major structures.

Finally, NE-SW geo-seismic sections have been drawn, with special focusing on the successive stages of the structural evolution of the Euphrates graben. This sketch scenario is obtained by flattening the cross-sections at representative time levels.

GEOLOGICAL EVOLUTION OF THE EUPHRATES GRABEN: SEDIMENTARY APPROACH

In this section, we attempt to document the structural evolution of the Euphrates graben on the basis of the stratigraphic approach, i.e. by integrating successive isopach maps into a comprehensive

Source : MNHN, Paris

cinematic history. Note that this broad approach will serve as a basis for a more detailed discussion of the whole tectono-sedimentary evolution, when dealing with seismic data.

THE "EARLY RIFTING" PHASE: WHERE TO PLACE THE "FIRST RIFT PULSE"?

The first "rift" pulse is commonly reported at the Late Cretaceous/Early Cretaceous unconformity (LITAK *et al.*, 1998) (Fig. 3). However, initiation of the "rift" system as early as in Albian times is manifested by isopach mapping of the late Albian deposits (Upper Rutbah shales) (Fig. 5). Mapping of the shaly-silty sequence reveals that the "Upper Rutbah" isopachs exhibit a clear NW-SE trend with a well-defined central depression where the shales may be up to 100 m thick. These shales are of marine affinity, as their palynofloral assemblages contain a mass occurrence of dinoflagellates. The decrease in thickness appears symmetrical on either side of that depression. We interpret this feature as suggestive of early tectonic faulting at the site of the future Late Cretaceous graben rather than post-depositional erosion.

The absence of Upper Rutbah shales in the northwestern part of the Deir Ez Zor permit area suggests the emergence of a positive structure (Fig. 5). This structure, hereafter named "Joura Ridge" will play an important role in the subsequent depositional history of the Euphrates basin. This NE-SW tectonic high will divide the northern part of this basin into two zones showing distinct tectono-sedimentary evolutions: an eastern zone controlled by N120E faults (graben opening) and a western zone mainly influenced by the sedimentary dynamics of the westerly Bishri trough. The latter corresponds to the northeastern part of the Palmyrides rift formed during the Triassic (Fig. 2) and later inverted to form a broad (approximately 75 km wide) northeast-plunging anticlinorium that terminates in a domal uplift

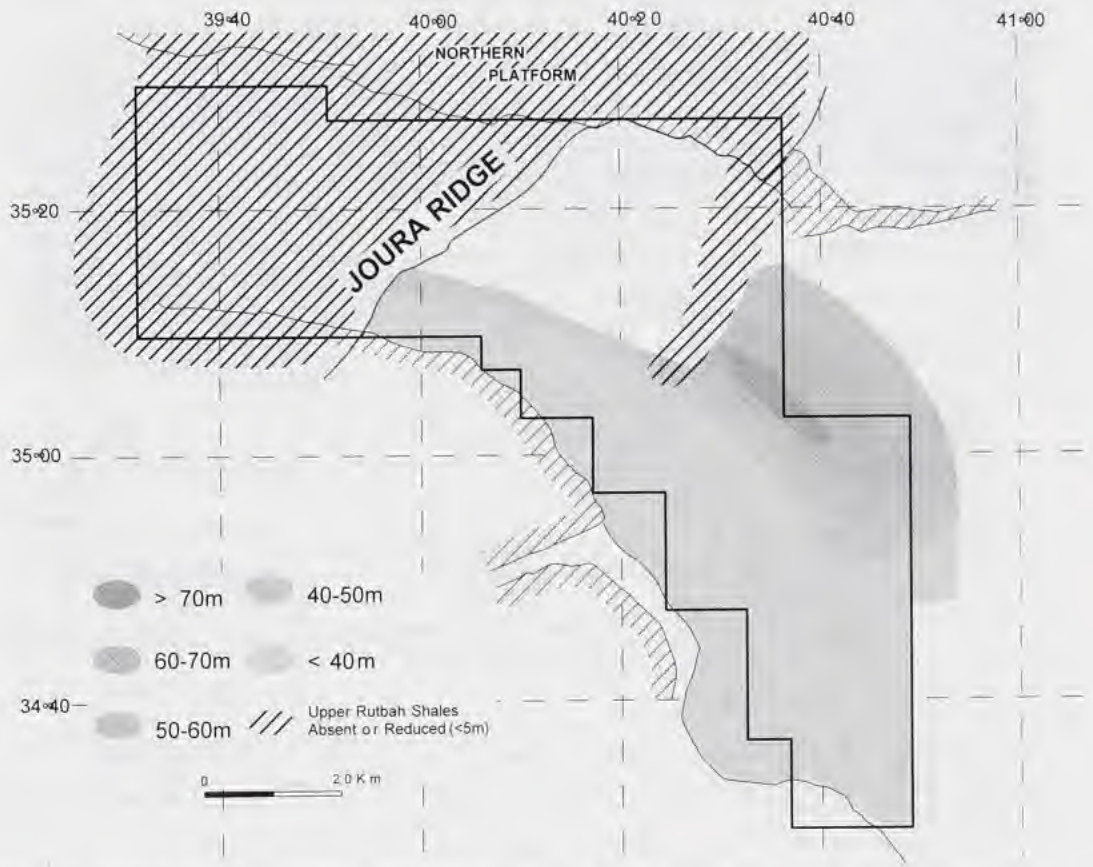

FIG. 5.— Isopach map of the upper Albian deposits (Upper Rutbah formation) within the Euphrates graben.

FIG. 5.— Carte en isopaques des dépôts de l'Albien supérieur (formation du Rutbah supérieur) dans le graben de l'Euphrate.

Source : MNHN, Paris

(Jebel Bishri, MC BRIDE *et al.*, 1990). The Joura Ridge could be the northeastern expression of the Al Hamad uplift (MOUTY, 1997). The NE-SW trending Al Hamad uplift, recognised from Jordan to NE Syria, separated from the Late Triassic to the Early Cretaceous two subsiding sedimentary basins in Syria: the Palmyrides basin to the northwest and the Rutbah basin to the southeast (MOUTY, 1997).

The following period corresponds to the deposition of the Judea carbonates during the Cenomanian transgression (MAY, 1991) that flooded the Joura Ridge (Fig. 6). In the northwestern part of the Euphrates graben, the thickness of the Judea formation increases towards the west. This depositional pattern illustrates the proximity of the Bishri subsiding trough to the west. The Judea carbonates are notably thicker over the southeastern area, i.e. over the zone of incipient "rifting", and contain marine palynoflora.

At that time, the early "rifting" phase (NE-SW extension) is yet accompanied by basaltic activity. K-Ar ages as old as late Albian-early Cenomanian (95 Ma) have been obtained on the volcanics associated with the "syn-rift" unconformity (in-house ELF data). In the Abd Al Aziz trough, which is on trend with, and possibly of similar origin as, the Sinjar trough (KENT & HICKMAN, 1997) (Fig. 2), the first "rift" pulse is also recorded at the base of the Early Cretaceous sequence (KENT & HICKMAN, 1997).

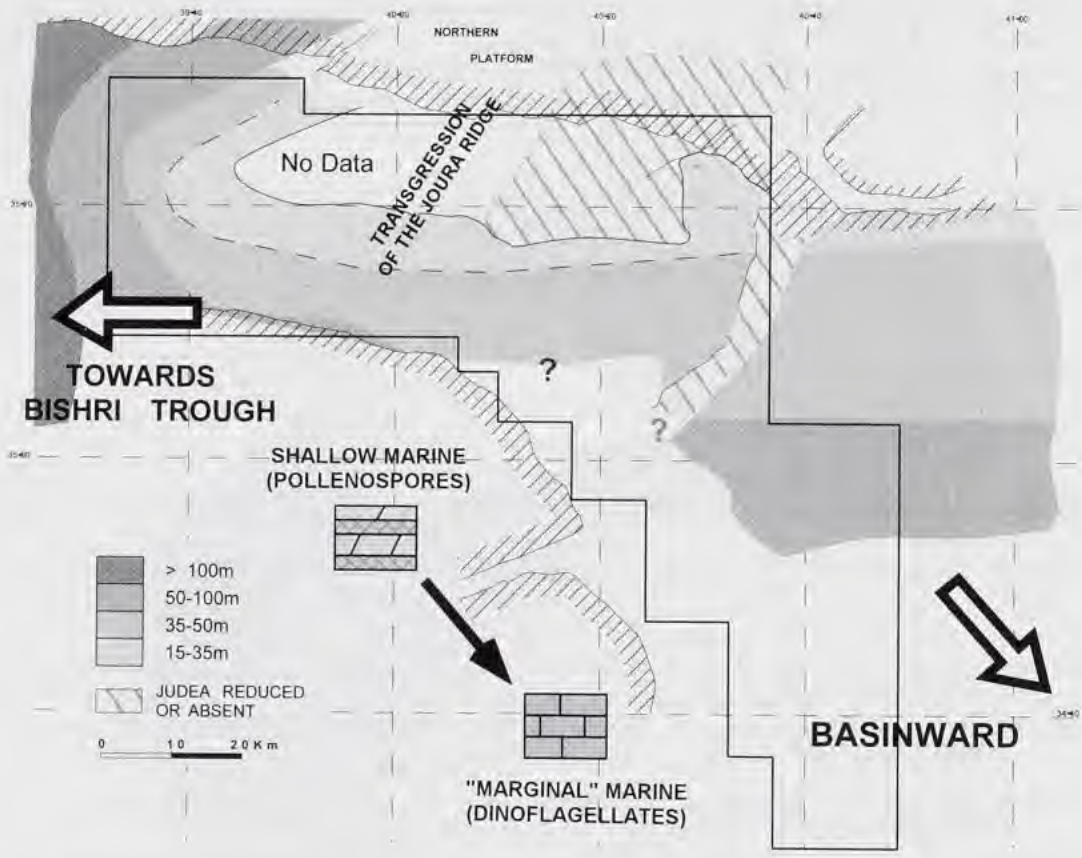

FIG. 6.— Facies and isopach map of the Cenomanian deposits (Judea formation) within the Euphrates graben.

FIG. 6.— Carte montrant la répartition des faciès et les variations d'épaisseur des dépôts du Cénomanien (formation Judea) dans le graben de l'Euphrate.

Source : MNHN, Paris

THE "SYN-RIFT" PHASE: TURONIAN TO EARLY MAASTRICHTIAN PERIOD

THE TURONIAN TO CONIACIAN PERIOD: DEPOSITION OF THE DERRO-KOMETAN FORMATION

The Derro and Kometan formations correspond to distinct depositional environments but are considered as time-equivalent units of Turonian to Coniacian age (in-house ELF reports).

The Derro formation consists in thick layers of volcanic ashes interbedded with and crosscut by abundant laminae and veins of crystalline dolomite. This unit is also made of volcanoclastic sediments corresponding to a mixing of tuffaceous siltstones and tuffaceous sandstones. The Derro is described as continental "red beds" interlayered with shales, tuffaceous silts and lavas, highly variable sands and locally evaporitic deposits (interlayered shale and anhydrite). The Kometan marine formation is composed of dolomites and argillaceous limestones.

The facies and isopach maps shown on the figures 7 and 8 reveal that, by the Turonian, the Joura Ridge was reactivated and acquired a NNE-SSW shape. This high divides the northern part of the Euphrates graben into two zones showing contrasting tectono-sedimentary evolutions. The western zone is characterised by the deposition of the dolomites and argillaceous limestones of the Kometan formation, which are thickest towards the West (from 25 m to 160 m) (Fig. 8). This depositional pattern is similar to that of the preceding period (Cenomanian Judea carbonates, Fig. 6) and illustrates the

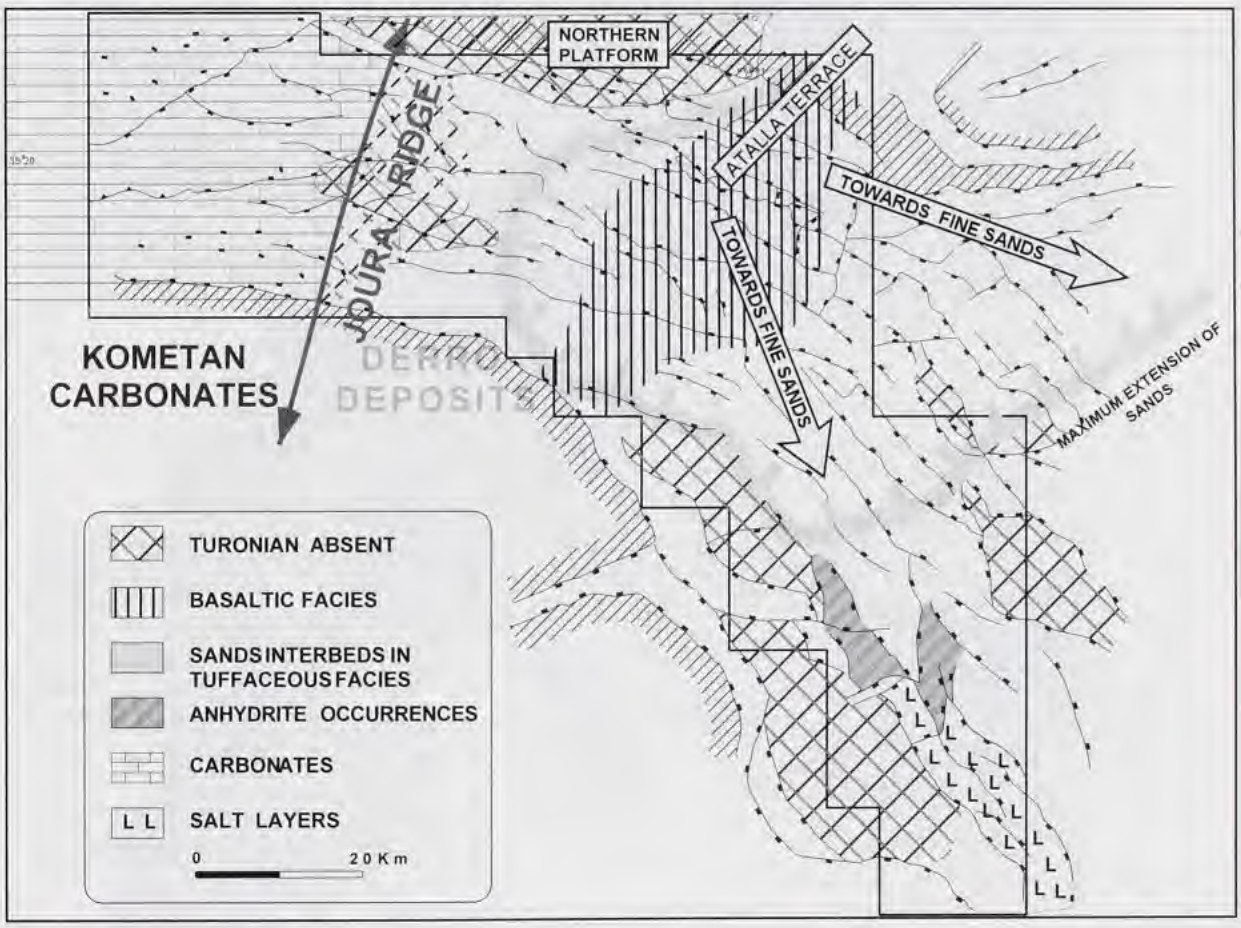

FIG. 7.— Facies map of the Turonian deposits (Derro-Kometan formations) within the Euphrates graben.

FIG. 7.— Carte de répartition des faciès du Turonien (formations Derro-Kometan) dans le graben de l'Euphrate.

Source : MNHN, Paris

proximity of the Bishri subsiding trough to the west. East of the Joura Ridge, Turonian deposits consist of the so-called Derro volcanoclastic series. In the northeastern and central areas, sandstones interbeds are recorded within the Derro formation. They show a limited spatial extent to the South and a coarsening trend to the north-northwest (Fig. 7). Very coarse to conglomeratic sands are recorded over the Atalla Terrace. These sands are probably derived from a north-northwestern source, located at the present site of the northern platform of the Euphrates graben. Anhydrite occurrences in the Derro formation are also described in the northernmost reference wells. As a whole, these features point to regressive conditions, which are also found in the southern part of the study area, with the occurrence of numerous salt layers in the Derro deposits (Fig. 7). Weathered basalts are exclusively encountered in the northeastern area, all along a NNE-SSW trend mostly parallel to the Joura Ridge at that time. Elsewhere, the Derro formation consists of tuffaceous claystones and volcanic tuffs.

On a regional scale, the thickest Derro deposits (>200 m) are distributed along elongated depressions associated with normal faulting (Fig. 8). These grabens develop along a N160E to submeridian direction over the southern area (Jido, Shwema, El Ward grabens) and along a N140E to N120E direction over the central and western parts of the study area (Al Furat-Khabour and Thayyem-El Liel grabens). Derro deposits are absent on top of tilted blocks and horsts (Maezalieh block, El Ward block, Tanak-Jido high, El Hamra block, Joura high; Fig. 8). Deposition of the Derro formation is synchronous with a major structuration phase responsible for the formation of horsts and grabens in a global NE-SW extensional regime.

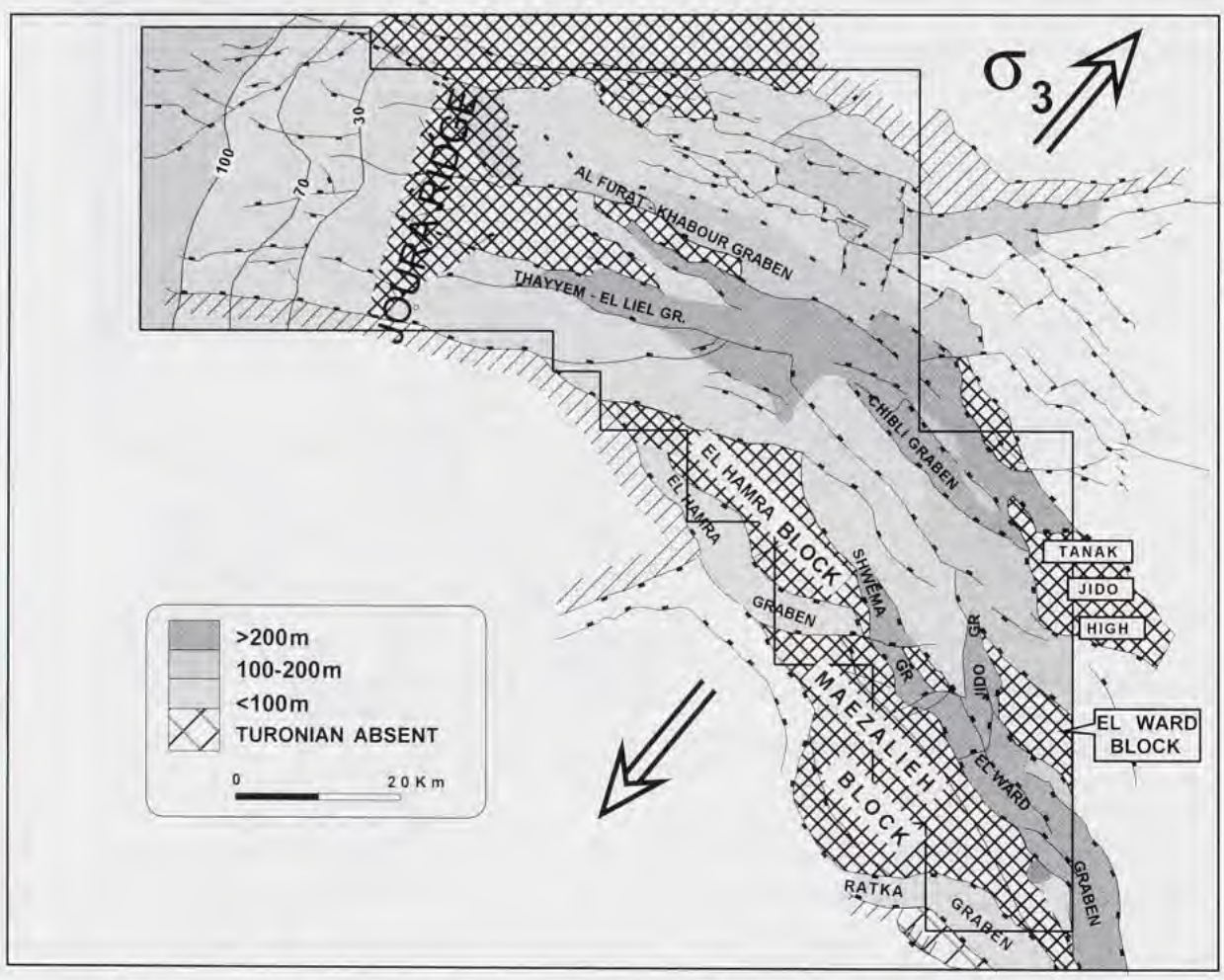

FIG. 8.— Isopach map of the Turonian deposits (Derro-Kometan formations) within the Euphrates graben.

FIG. 8.— Carte en isopaques des dépôts du Turonien (formations Derro-Kometan) dans le graben de l'Euphrate.

Source : MNHN, Paris

THE SANTONIAN TO CAMPANIAN PERIOD: DEPOSITION OF THE R'MAH FORMATION

The R'mah formation, of Santonian to Campanian age, is composed of a lower dolomitic unit often containing a basal sandy layer and an upper unit made of cherty limestones. In the northwestern part of the Euphrates graben, the R'mah unit may contain well-developed sandy levels (up to 160 m thick). These sands are coarse-grained, clean and massive with less permeable bioturbated intervals enriched in organic matter and clay minerals. They constitute an oil-bearing unit located above the classical Early Cretaceous reservoir.

Isopach mapping of the R'mah deposits is expected to provide substantial informations concerning the "rifting" stage itself, as these deposits directly overlie the Derro-Kometan units. From NW to SE, three zones may be distinguished (Fig. 9):

— a western zone where the R'mah carbonates are more than 100 m thick and where they thicken gradually towards the NW (>450 m in westernmost wells). In that zone, the sedimentation is clearly controlled by NE-SW structures, mimetic of the Joura Ridge orientation at that time;

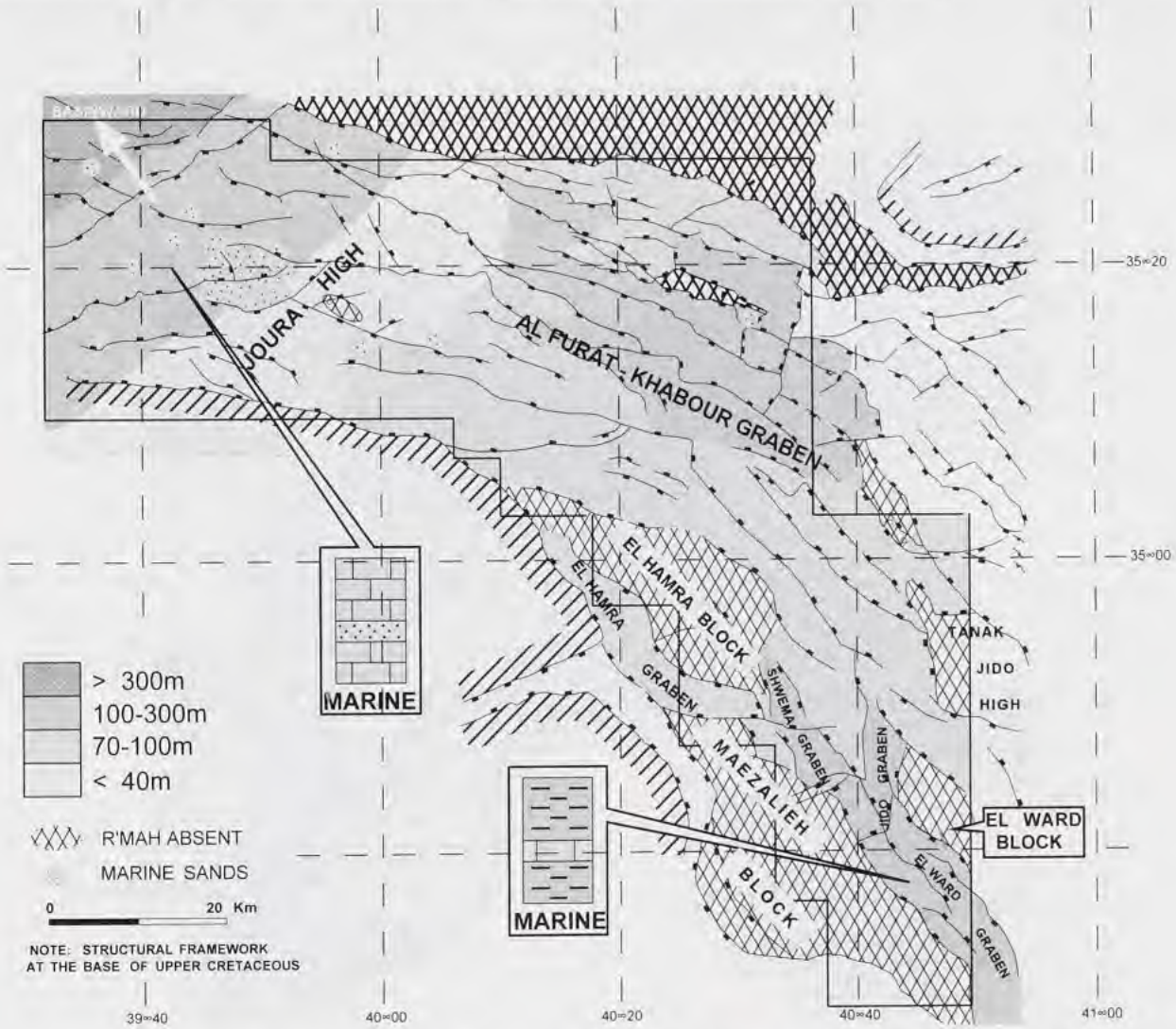

FIG. 9.— Facies and isopach map of the Santonian deposits (Rmah formation) within the Euphrates graben.

FIG. 9.— Carte en faciès et isopaques des dépôts du Santonien (formation Rmah) dans le graben de l'Euphrate.

Source : MNHN, Paris

— an intermediate zone where the R'mah carbonates do not exceed 40 m in thickness. This zone defines a NE-SW belt of some 20 kilometres in width. It corresponds to the so-called "Joura Ridge";

— an eastern and southern area, where the deposition of the R'mah carbonates is apparently controlled by NW-SE structures linked to the "rifting" phase (Al Furat-Khabour, Jido, Shwema and El Ward grabens).

Sands are deposited at the footwall of the Joura Ridge and are progressively dispersed towards the Bishri mobile zone to the west. They probably come from the erosion of temporarily emergent areas over the Joura High.

THE CAMPANIAN TO EARLY MAASTRICHTIAN PERIOD: DEPOSITION OF THE EREK FORMATION

The Campanian to early Maastrichtian Erek formation directly overlies the R'mah cherty limestones. This unit is composed of dark brown/blackish argillaceous limestones with interbeds of sparitic recrystallised white limestones.

The Campanian to early Maastrichtian period is the time of substantial changes in the sedimentary dynamics of the Euphrates graben. The comparison between isopach maps of Erek (Fig. 10) and R'mah (Fig. 9) formations shows a completely distinct distribution in carbonate deposits.

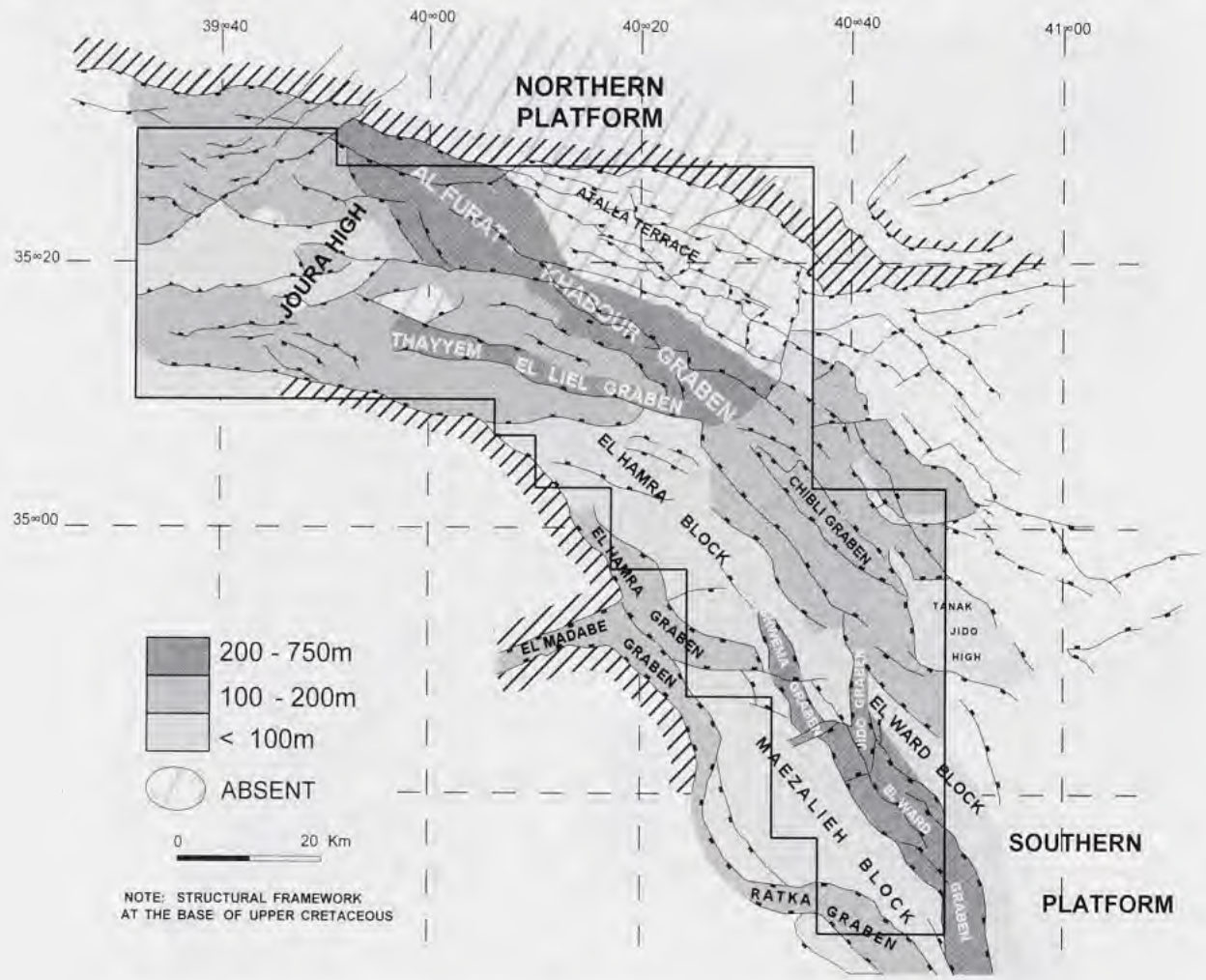

FIG. 10.— Isopach map of the Campanian deposits (Erek formation) within the Euphrates graben.

FIG. 10.— Carte en isopaques des dépôts du Campanien (formation Erek) dans le graben de l'Euphrate.

Source : MNHN, Paris

Rather isopach limestones fill in the northwestern area, which behaved since the Albian as a dependence of the Bishri trough and was characterised by high sedimentation rates. In other words, the NE-SW (structural?) control on R'mah deposits no longer existed during the deposition of the Erek limestones.

Actually, the Joura high is entirely transgressed by Erek carbonates. In its northern part, this ridge is incised by a NW-SE deep trough (Al Furat-Khabour graben). Along this narrow trough, Erek deposits are composed of argillaceous, partly silicified limestones containing abundant planktonic microforaminifera. This N140E depression may be interpreted as a northern esxtension of the Al Furat Khabour graben initiated in Turonian times (Fig. 8).

In the northeastern area, a complex terrace (Atalla terrace) forms between the deep mobile Al Furat-Khabour graben and the stable northern platform. No Erek deposits are found in that area (Fig. 10). In the southern area, the Tanak-Jido, El Hamra and El Ward blocks are completely transgressed at that time (Erek deposits <100 m). The Campanian period corresponds to the maximum extension of the Euphrates graben system and may be viewed as the peak "rifting" phase in that area during the Late Cretaceous.

THE EARLY MAASTRICHTIAN PERIOD: DEPOSITION OF THE LOWER SHIRANISH FORMATION

The Lower Shiranish formation, of early Maastrichtian age, consists in brown argillaceous limestones (mudstones, wackestones) overlain by withish limestones (Tayarat formation).

Isopach mapping of the Lower Shiranish deposits (Fig. 11) shows a considerable widening of regional subsidence throughout the Euphrates graben. The global broadening of depocenters and gradual

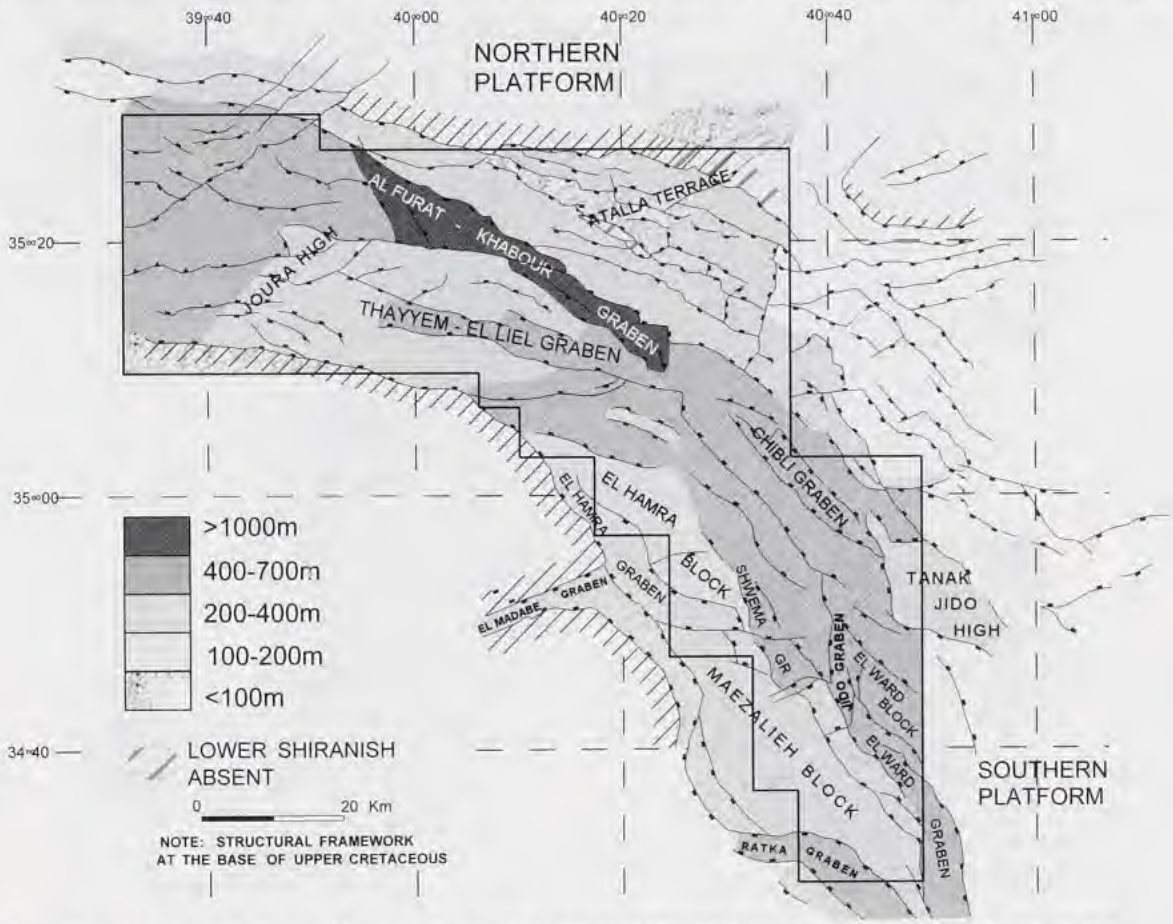

FIG. 11.— Isopach map of the lower Maastrichtian deposits (Lower Shiranish formation) within the Euphrates graben.

FIG. 11.— Carte en isopaques des dépôts du Maestrichtien inférieur (formation Shiranish inférieur) dans le graben de l'Euphrate.

Source : MNHN, Paris

blanketing of the Atalla Terrace, which corresponded to a low-relief area in the preceding Erek period, suggest this interpretation. As such, the northwestern area (west of the Joura high) and the domains located between the Chibli and Shwema grabens are strongly deepening and filled with a 400 to 700 m thick Lower Shiranish section. To the northeast, a depression is highly active along N120E to N140E master faults (Al Furat-Khabour graben), with a Lower Shiranish section more than 1000 m thick. However, its extension to the NW is rather limited, at least when compared to the Erek configuration (Fig. 10).

Moreover, the Lower Shiranish isopach map shows a considerable reduction of fault-induced subsidence along N140E-N160E faults of the southern area (El Ward, Jido, Schwema grabens). These faults are much less active than the N100-120E faults of the northern area. This suggests a change in stress orientation, from N45E to N15E.

THE "POST-RIFT" PHASE

THE LATE MAASTRICHTIAN PERIOD: DEPOSITION OF THE UPPER SHIRANISH FORMATION

The Upper Shiranish formation, of Maastrichtian age, is composed of argillaceous limestones (mudstones-wackestones) grading to marl, with local interbeds of white limestone (packestone) containing calcite and glauconite.

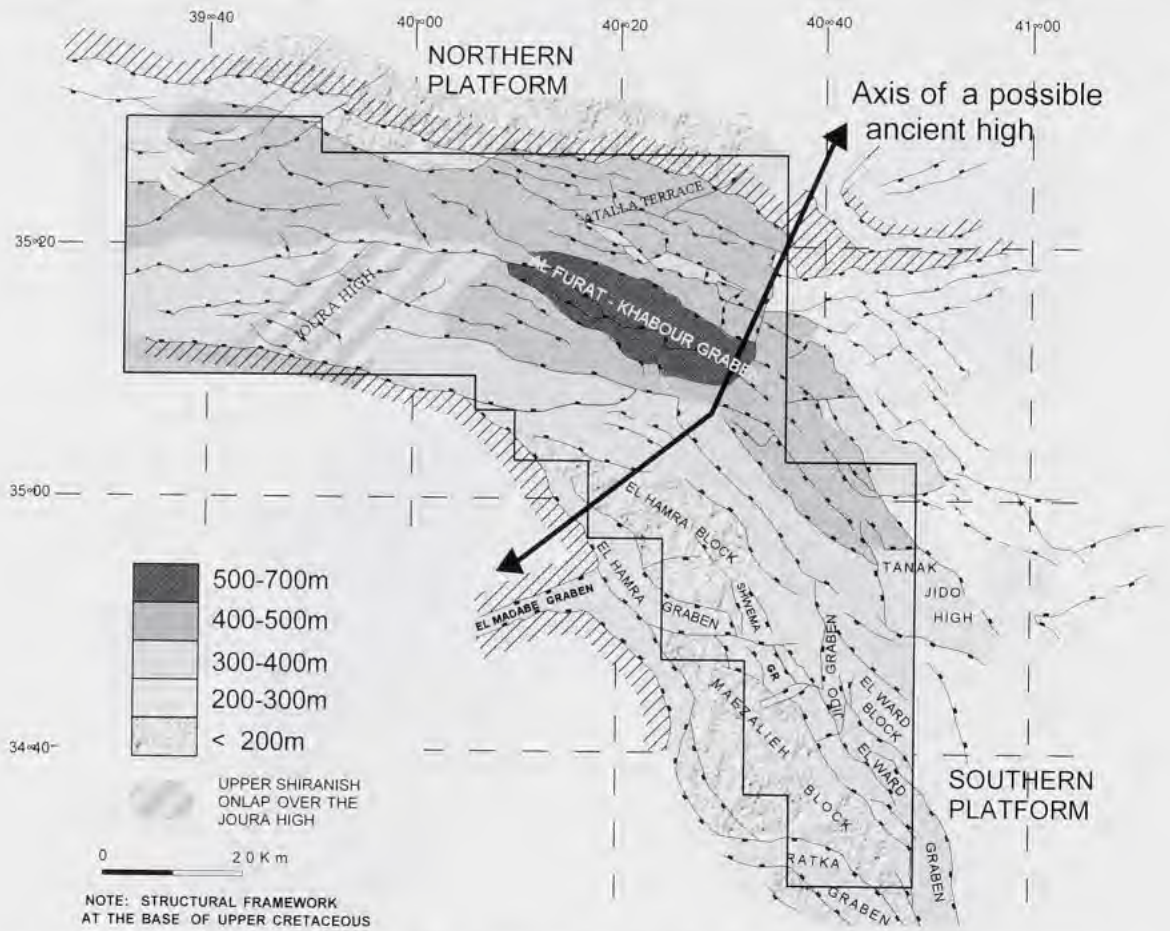

FIG. 12.— Isopach map of the upper Maastrichtian deposits (Upper Shiranish formation) within the Euphrates graben.

FIG. 12.— Carte en isopaques des dépôts du Maestrichtien supérieur (formation Shiranish supérieur) dans le graben de l'Euphrate.

Source : MNHN, Paris

The Upper Shiranish marks the end of fault-induced subsidence throughout the Euphrates graben. This configuration is visible in the northeastern area, where the Atalla terrace is overstepped by Upper Shiranish limestones. At that time, the thickest deposits (>500m) developed within a very localised basin, centered along the axis of the former graben system (N120E-trending Al Furat-Khabour graben) (Fig. 12). Noticeable is the limited extent of this basin to the southeast. From Campanian to late Maastrichtian times, this basin appeared to terminate against a N45E to N20E zone, which corresponds to a structural high on the Albian and Cenomanian maps (Figs 5 and 6). Moreover, this trend is globally parallel to the Joura Ridge and appears to guide the extension of Derro volcanics (Fig. 7).

The Late Maastrichtian period corresponds as well to the renewed uplift of the El Ward, Tanak-Jido and El Hamra blocks and onlap pattern of the Upper Shiranish against these blocks. A residual block of the Joura high (its southern edge) was also reactivated at that time. The movements associated with the first phase of the Palmyridian orogeny (first inversion stage of the Mesozoic Bishri basin, SALEL, 1993) may account for this change in sedimentary dynamics over the Euphrates graben. This hypothesis will be further tested with the seismic data.

THE PALAEOCENE PERIOD: DEPOSITION OF THE AALIJI FORMATION

The Aaliji formation, of Palaeocene age, consists in grey to grey-brown argillaceous limestones (mudstones/wackestones) often grading to calcareous claystones and shales.

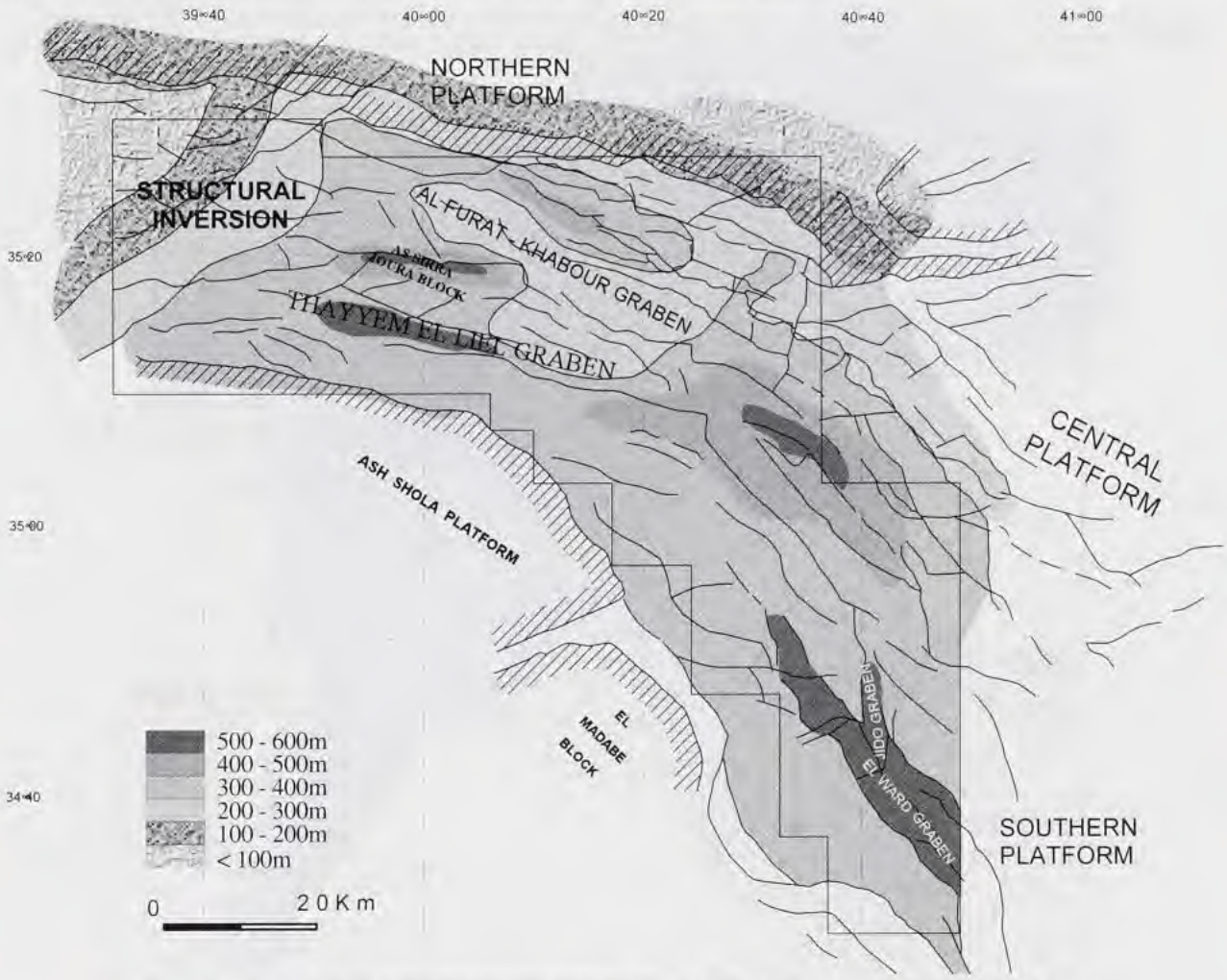

FIG. 13.— Isopach map of the Palaeocene deposits (Aaliji formation) within the Euphrates graben.

FIG. 13.— Carte en isopaques des dépôts du Paléocène (formation Aaliji) dans le graben de l'Euphrate.

Source : MNHN, Paris

The depocenters, which were active during the Late Cretaceous (Thayyem-El Liel, El Ward, Shwema grabens), were continuously active by the Palaeocene (Fig. 13). Localised horsts and long-lived interior highs (Maezalieh, Jido-Tanak, El Hamra blocks), which were so far partly submergent blocks, are buried by the Palaeocene below an isopach series (300-400 m). Regular infilling of subbasins and smoothing of the former dissected "rift" bathymetry characterise the Aaliji stage.

In the northwestern area, a clear NE-SW zonation is evidenced, with a global trend opposite to that of the Late Cretaceous period (Fig. 9). Actually, Palaeocene deposits display a gradual decrease in thickness with proximity to the Bishri trough. Anomalous high thicknesses are recorded at the footwall of tilted blocks and over updip zones (northern part of the residual As Sirra Joura block in Fig. 13). Moreover, the axis of the Al Furat-Khabour graben, which was so far the main depocenter, corresponds to a relative sediment-starved basin in Aaliji times.

In order to explain this peculiar configuration, we suggest that the basin inversion occured during Aaliji time. The Aaliji section is thicker over previous positive structures and thinner over older depositional sinks (Fig. 13). We propose the following scheme: reverse displacement took place on the same fault as the initial normal movement. In that frame, normal faults bounding horsts and tilted blocks were reactivated as reverse faults and induced a relative thickening of the Aaliji section over the downthrown panel of the inverted fault. Conversely, downdip areas were capped by relatively thinner

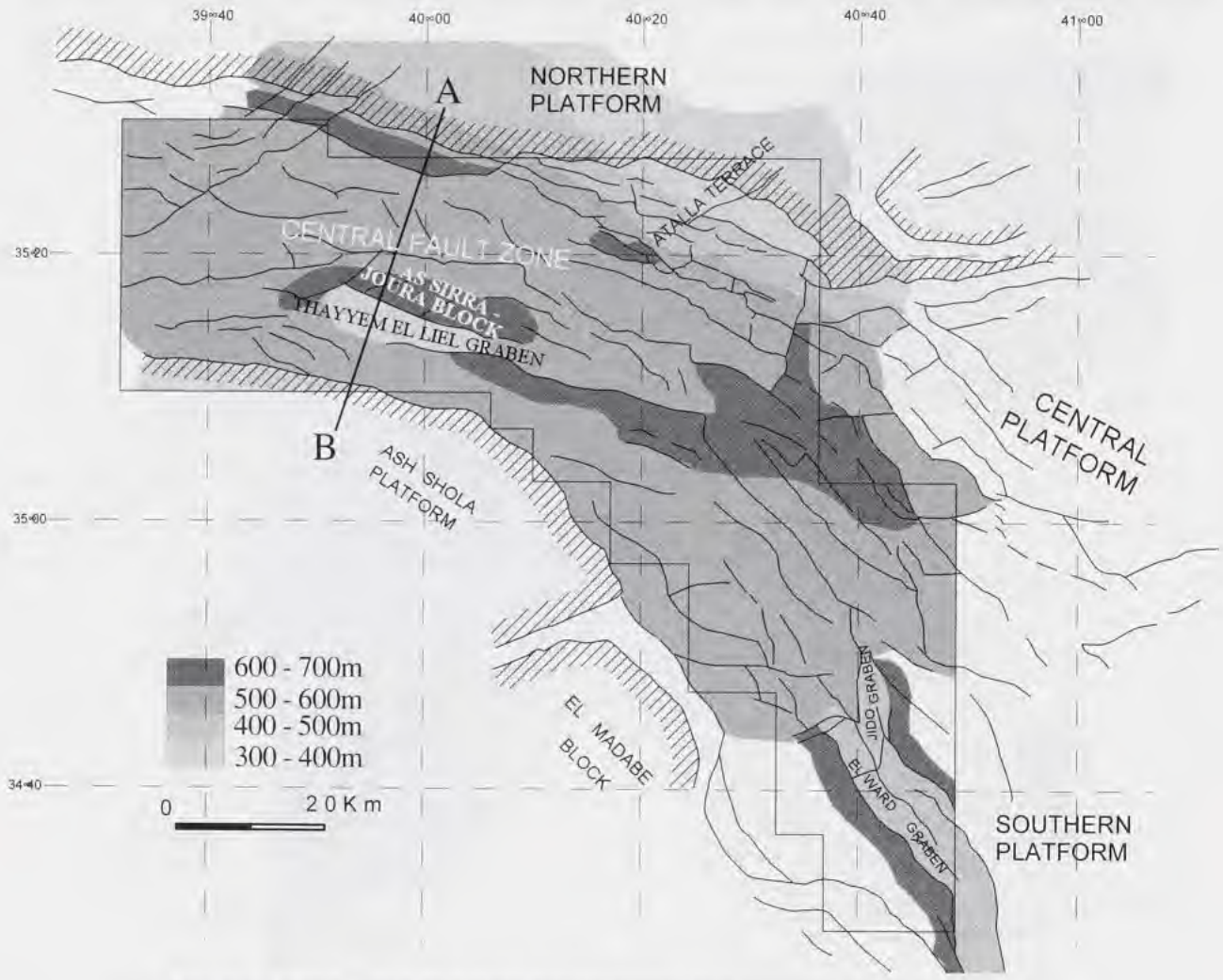

FIG. 14.— Isopach map of the Eocene deposits (Jaddala formation) within the Euphrates graben.

FIG. 14.— Carte en isopaques des dépôts de l'Éocène (formation Jaddala) dans le graben de l'Euphrate.

Source : MNHN, Paris

deposits, over the upthrown panel of the inverted faults. As a whole, an anticline-shaped structure was created. This pattern is illustrated by the idealised cross-section in the figure 16. This configuration will be exemplified in the foregoing seismic section.

In Palaeocene times, the northern part of the Euphrates graben as a whole was probably subject to tectonic inversion. This structural inversion could have begun as soon as in Upper Shiranish times and could be related to the first phase of deformation in the Palmyrides area (SALEL, 1993). The normal faults bordering the Al Furat-Khabour depression were presumably reactivated as reverse faults at that time. This would explain the unexpected low thickness values recorded along this structure (Fig. 13).

Aside from the NE-SW zonation of Aaliji isopachs in the northwestern part of the study area, the high rates of subsidence persisting along N140E normal faults in the southern part of the Euphrates graben further suggest that compression was NW-SE orientated in Palaeocene time.

THE EOCENE PERIOD: DEPOSITION OF THE JADDALA FORMATION

The Jaddala formation, of Eocene age, is composed of whitish to medium-grey argillaceous limestones (mudstones, packestones) grading to packestones. A basal term is identified consisting of marls to very argillaceous limestones. Abundant light brown to brown cherts are encountered in the middle portion of the interval.

Comparison of Aaliji and Jaddala isopach maps (Figs 13 - 14) reflects the completely different distributions of relative depositional highs and lows between the two periods. In the southern part of the

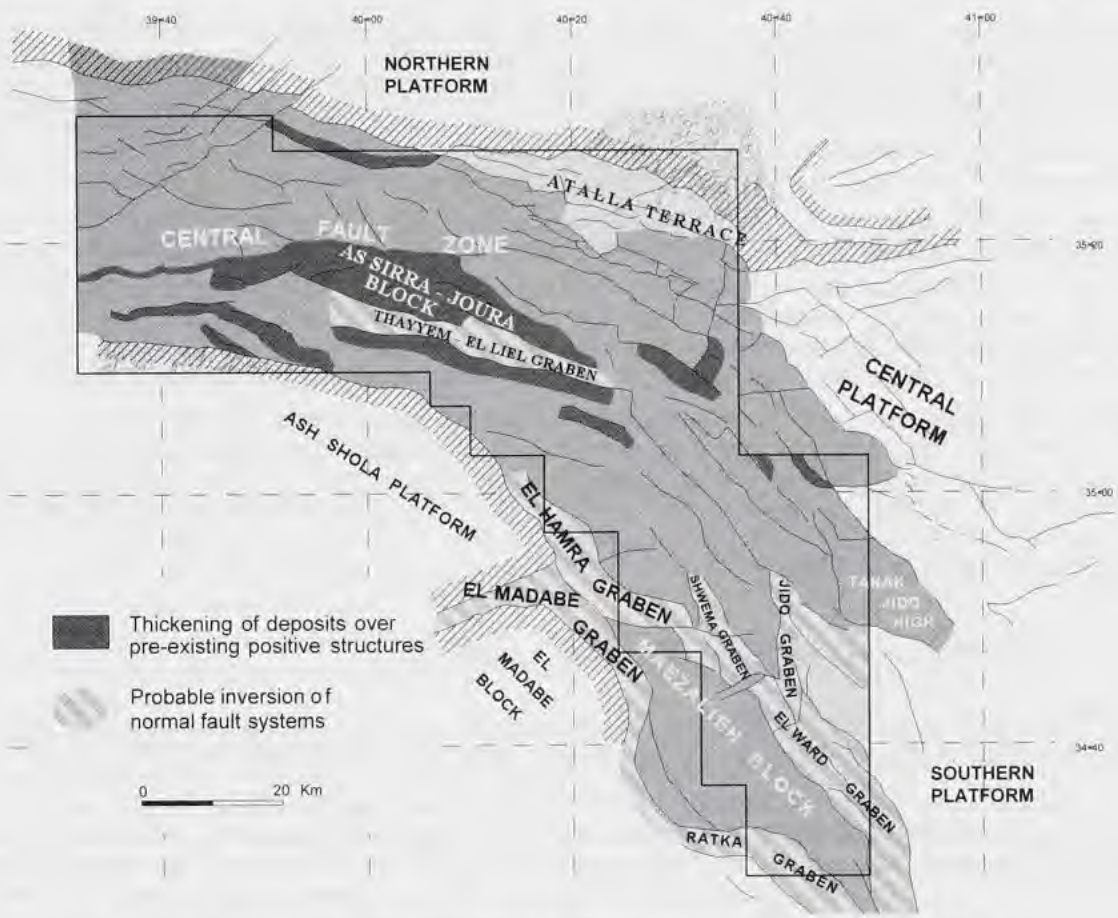

FIG. 15.— Interpretative structural map of the Eocene period within the Euphrates graben.

FIG. 15.— Schéma structural interprétatif à l'Éocène dans le graben de l'Euphrate.

Source : MNHN, Paris

study area, the El Ward graben was less active than in Palaeocene times. The NE-SW zonation that characterised the northwestern part of the Euphrates graben in Palaeocene times is no more apparent on the Eocene isopach map. This configuration suggests the local transgression of the Palaeocene folds and a global change in stress orientation. Furthermore, from south to north, one can notice that:

— in Aaliji times, the Thayyem-El Liel graben received the thickest deposits (>500 m). In Jaddala times, the sedimentation was reduced along this depression (<400 m) and could be compared to the sedimentation growth over the Atalla Terrace;

— in Aaliji times, the Al Furat-Khabour graben acted as a sediment-starved basin with a sedimentation rate fairly comparable to that taking place over the Atalla terrace. In Jaddala times, this graben showed average sedimentation rates with the development of a 500-600 m section;

— in Aaliji times, the As Sirra–Joura block was characterised by moderate sedimentation rates, fairly comparable to those observed at a regional scale over the entire Euphrates graben system. In Eocene times, this block was overfilled by Jaddala deposits, which are, there, the thickest recorded throughout the Euphrates graben (> 660 m).

The figure 16 is an idealised N-S cross-section showing the contrasting evolutions between Aaliji and Jaddala times.

In Aaliji times, the north-dipping Central Fault Zone (CFZ) that bounded the As Sirra-Joura block to the north was reactivated by tectonic inversion and delineates to the north an upthrown, sediment-starved panel, which was, up to that time, the site of maximum subsidence (Al Furat-Khabour graben)(Fig. 16). In the meantime, normal fault-induced subsidence was proceeding within the Thayyem-El Liel graben, not yet affected by structural inversion.

In Jaddala times, ongoing reverse motion along the Central Fault Zone caused the southern compartment (As Sirra-Joura block) to downwarp and the Jaddala unit to thicken at that site. The As Sirra-Joura block is bounded to the south by a south-dipping master fault, which corresponds to the northern bounding fault of the Thayyem-El Liel graben (Fig. 16). In Jaddala times, this fault experienced reverse motion, resulting in the deposition of a sequence thinner within the southern upthrown panel (Thayyem–El Liel graben) than in the northern compartment (As Sirra-Joura block).

On the structural interpretative map of the Eocene period (Fig. 15), relative mobile and stable areas are shown, as well as the local thickening of Eocene deposits at the footwall of tilted blocks. The global inversion of the As Sirra-Joura block and the Thayyem-El Liel graben suggests that these E-W structures were favourably oriented with respect to Eocene compression. Stopping of subsidence along the El Ward graben and interruption of N45E inversion over the northwestern area (Fig. 15) further suggest a change in stress orientation from NW-SE (Palaeocene) to N-S (Eocene) compression.

One important result relies in the delay observed between the timing of inversion over the northwestern area. The response of the Euphrates graben to compression was diachronous there, with a propagation of structural inversion from north to south. This pattern is consistent with the global tectonic setting of the Northern Arabian plate at that time, implying southward migration of deformation from the site of subduction (suture zone recognised along the frontier between Syria and Turkey) to the foreland domains (SALEL, 1993).

THE OLIGOCENE PERIOD: DEPOSITION OF THE CHILOU FORMATION

The Chilou formation, of Oligocene age, is composed of cream to light grey argillaceous limestones (mudstones/wackestones), with traces of very fine to fine bioclasts, interbedded with claystones.

The distribution of Oligocene deposits over the Euphrates graben is quite similar to that of the Eocene period, with the persistence of the same depositional highs and lows. However, a global N140E depression newly appeared over the northern area, involving the northern part of the previous Al-Furat Khabour graben (Fig. 17). We suggest that the Oligocene was the time of change in stress regime, from NW-SE to N-S compression in Palaeocene - Eocene to NE-SW extension in Oligocene. This extension is limited to the northwestern part of the study area and possibly implies the reactivation of pre-existing N120E faults.

Source : MNHN, Paris

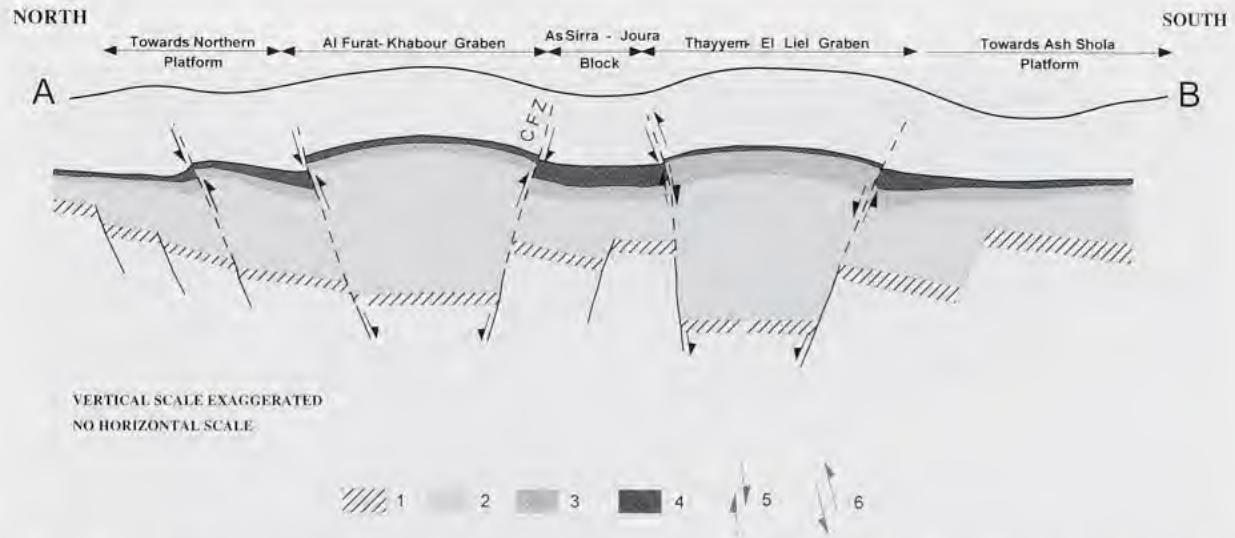

FIG. 16.— Schematic cross-section showing the tectonic control on Palaeocene and Eocene deposition in the northwestern part of the Euphrates graben. Location of this section is given in Fig. 14. **1**, "pre-rift" section; **2**, "syn-rift" to "late-rift" sequence; **3**, Palaeocene (Aaliji deposits); **4**, Eocene (Jaddala deposits); **5**, tectonic control on Palaeocene deposition; **6**, tectonic control on Palaeocene and Eocene deposition by reverse motion of pre-existing normal faults. CFZ: Central Fault Zone.

*FIG. 16.— Coupe schématique illustrant le contrôle tectonique de la sédimentation au Paléocène et à l'Éocène dans la partie nord-ouest du graben de l'Euphrate. La localisation de cette coupe est donnée sur la Fig. 14. **1**, séquence "pré-rift" ; **2**, séquence "syn à post-rift" ; **3**, Paléocène (dépôts Aaliji) ; **4**, Éocène (dépôts Jaddala) ; **5**, contrôle tectonique de la sédimentation au Paléocène (Aaliji) ; **6**, contrôle tectonique de la sédimentation au Paléocène et à l'Éocène par inversion des failles normales préexistantes. CFZ : zone de la Faille Centrale.*

GEOLOGICAL EVOLUTION OF THE EUPHRATES GRABEN: THE SEISMIC APPROACH

The aims of this section are to precise and eventually criticise the structural scenario proposed in the previous section by integrating the interpretation of 2D seismic data. The objective is threefold:

— to check the validity of the morphostructural schema issued from isopach mapping (location of the main rotated fault blocks and stable domains);

— to precise the structural relationships between the Mesozoic active blocks and the Tertiary tectonically inverted areas;

— to obtain by horizontal flattening an image of the Euphrates graben at different key-phases of its evolution and over selected areas.

The choice of the seismic lines has been guided by their location with respect to the calibration wells. Location map of these lines is exhibited on the figure 4.

Whenever possible, up to 16 horizons have been followed. Silurian, Intra-Carboniferous, Carboniferous, Norian (Mulussa E formation), Albian (Rutbah formation) and Cenomanian (Judea formation) tops provide interpretation of the pre-Late Cretaceous structures. Picking of the Turonian (Derro), Santonian (R'mah), Campanian (Erek), early and late Maastrichtian (Intra-Shiranish and Shiranish) tops is expected to reflect the evolution of the "syn-rift" sequence. Palaeocene (Aaliji), Eocene (Jaddala), Oligocene (Chilou) and early Miocene (Euphrates, Jeribe) tops enable to interpret the evolution of the "post-rift" sequence.

Source : MNHN, Paris

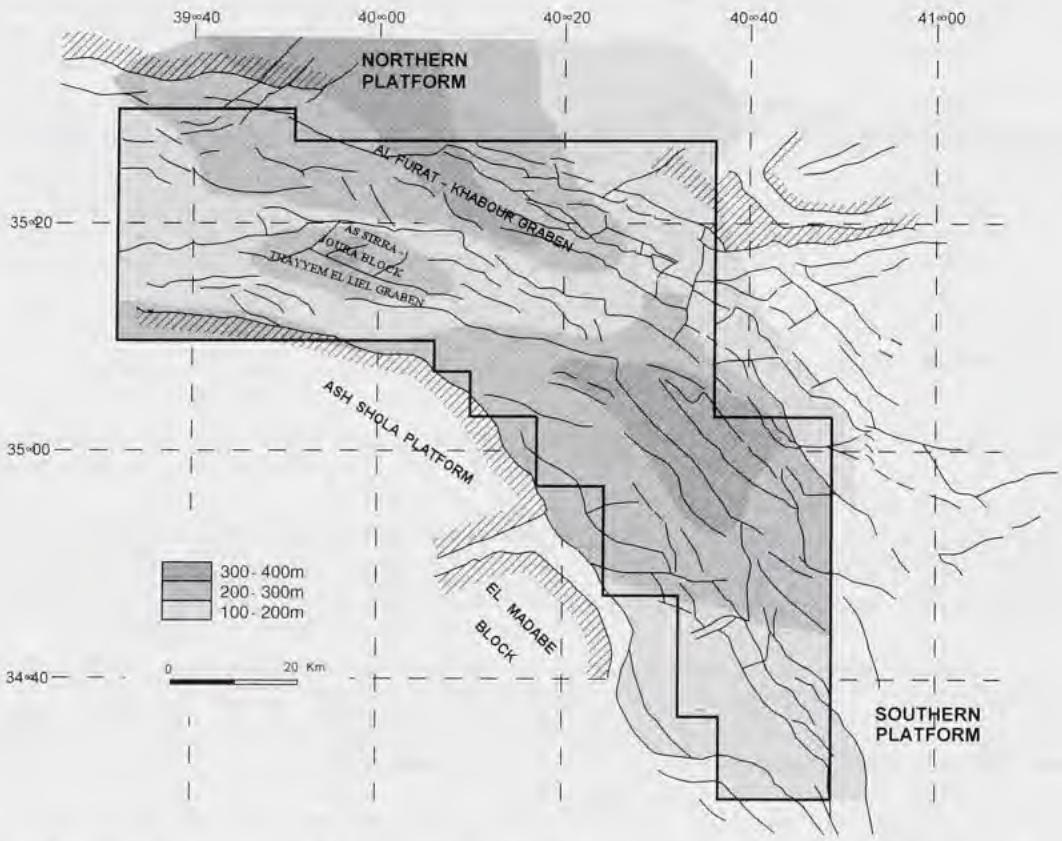

FIG. 17.— Isopach map of the Oligocene deposits (Chilou formation) within the Euphrates graben.

FIG. 17.— Carte en isopaques des dépôts de l'Oligocène (formation Chilou) dans le graben de l'Euphrate.

DESCRIPTION OF THE STRUCTURAL STYLES

STRUCTURAL STYLES IN THE NORTHWESTERN AREA

Seismic line 1 (Fig. 18) is a strike line, about 35 km long, which covers most of the northwestern part of the study area (see location on Fig. 4). This line transects the Joura-As Sirra block and part of the southern border of the Al Kharrata graben. Calibration of line 1 has been possible after production of synthetic seismograms and time-converted logs for three wells, which are from west to east: Well A, Well B and Well C (purple vertical lines on Fig. 18).

Seismic line 1 shows that the As Sirra-Joura block is dissected into a series of tilted blocks bounded by northwest dipping master faults. Southeast-dipping antithetic faults develop within individual blocks. Block tilting and normal faulting operate within the pre-Maastrichtian section and reach down to the Palaeozoic units. Fault network is very dense with generally planar and steep contact surfaces. Top of Silurian shales (in brown on Fig. 18) is shifted down on the eastern side of the section. Prominent faults extend within the Cainozoic section, up to the Miocene. Large-scale folding of the post-Miocene series traduces the last and major structuration phase in that area (Fig. 3), contemporaneous with the Plio-Quaternary orogeny that produced the present Taurus and Zagros ranges (LOVELOCK, 1984).

Source : MNHN, Paris

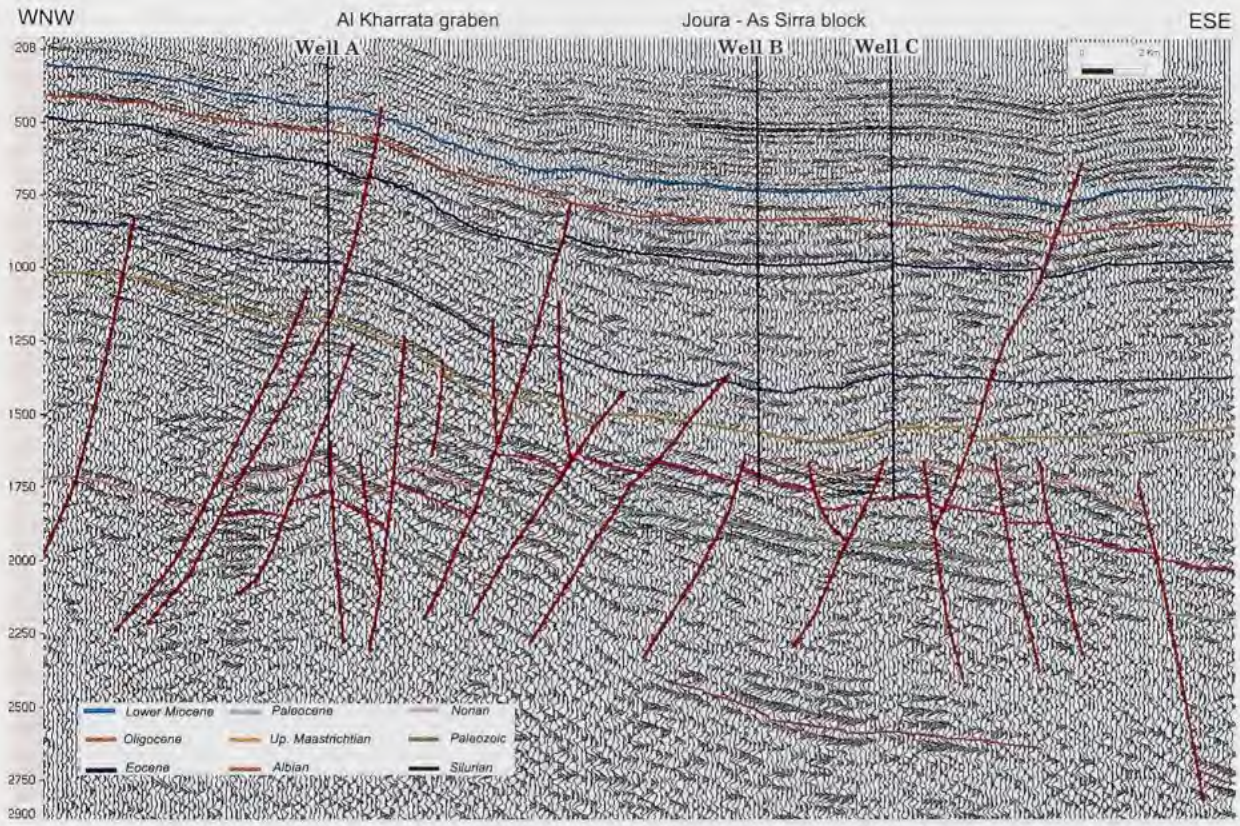

FIG. 18.— Seismic interprétation of line 1. Vertical scale is two-way travel time in ms. Datum plane is 300 m amsl.

FIG. 18.— Interprétation du profil 1. L'échelle verticale est en ms temps double. Le plan de référence sismique est de 300 m niveau mer.

STRUCTURAL STYLES IN THE NORTHEASTERN AREA

The northeastern part of the Deir Ez Zor contract area covers a complex terrace area (Atalla Terrace) located between the deep mobile Euphrates graben to the south (Al Furat-Khabour graben) and the stable northern platform to the north. The figure 19 shows a geo-seismic cross-section elongating from southwest to northeast over the area covered by the 2D data. Three 2D seismic lines have been composed to obtain this cross-section over the northeastern area (lines 2, 3 and 4). Well D, Well E and Well F were used for seismic calibration of the seismic lines 2, 3 and 4 respectively.

The outstanding structural style is a complex system of tilted blocks, horsts and grabens (Figs 20 and 21). However, in opposition to the northwestern area, faults rarely extend up to the Palaeocene section.

From north to south, several relevant structural features may be discussed:

— within the northern platform (line 2, Fig. 20), the top Palaeozoic marker is found at around 1750 ms twt and is quite easy to follow over this area. This zone is characterised by the lack of Cenomanian to early Maastrichtian deposits. The late Maastrichtian formation is directly overlapping the Albian sandstones;

— immediately south of the northern platform lies a master normal fault, which offsets the top Palaeozoic marker at 2400 ms twt. This master fault flattens with depth, causing collapse of the hanging wall and formation of inclined antithetic panels. Synthetic dip development adjacent to the fault plane (A on Fig. 20) and tilting of pre-Turonian units indicate that this fault was active from the Turonian to

Source : MNHN, Paris

the early stages of upper Mastrichtian, with a break of activity during the Santonian (B on Fig. 20). This fault activated a northeastern upthrown panel (northern platform) over which the Albian section is partly eroded. The platform was therefore a structural high continuously emergent during most of the "syn-rift" phase of the graben evolution;

— to the south (Fig. 20), the structural pattern consists in the so-called Atalla Terrace, characterised by a series of narrow horsts, grabens and half grabens with horizontal dips and a top Carboniferous marker at 2250 ms;

— line 4 (Fig. 21) illustrates the deepest parts of the Al Furat-Khabour graben system, where the Late Cretaceous time isopach reaches 1500 ms twt, whereas this section may be less than 600 ms in thickness over the upthrown El Liel panel. The steep master normal fault that bounds this panel to the northeast is inverted in late Maastrichtian-early Palaeocene times.

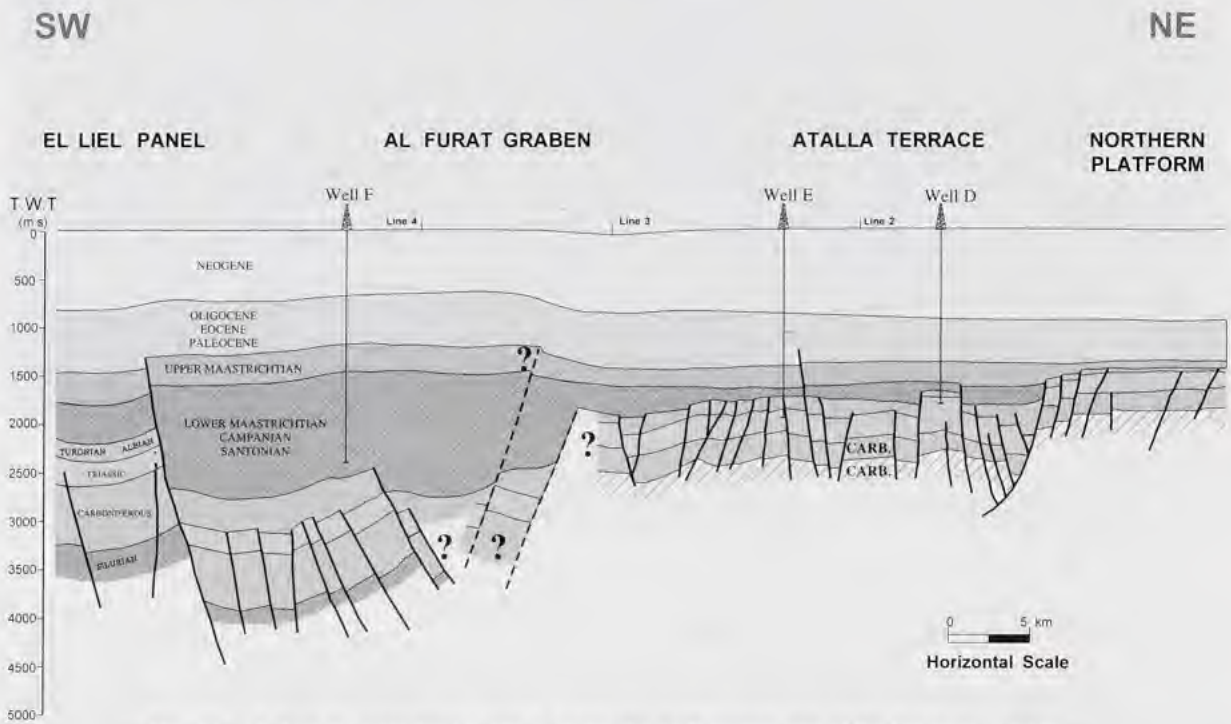

FIG. 19.— Schematic geoseismic section across the northeastern part of the Euphrates graben.

FIG. 19.— Coupe géosismique schématique de la partie nord-est du graben de l'Euphrate.

STRUCTURAL STYLES IN THE CENTRAL AREA

Seismic line 5 (Fig. 22) is a dip line that transects the central part of the Euphrates graben (Fig. 4). Calibration was obtained by wells G and H. 12 horizons have been followed up. The "pre-rift" sequence is dissected into grabens, horsts and tilted blocks. Major normal faults that offset the "pre-rift" markers up to 350 ms twt are typically NE-vergent and reactivated as reverse faults in late Palaeocene times. They typically flatten at depth and control planar roll over processes (SHAW *et al.*, 1997) within associated antithetic panels.

Source : MNHN, Paris

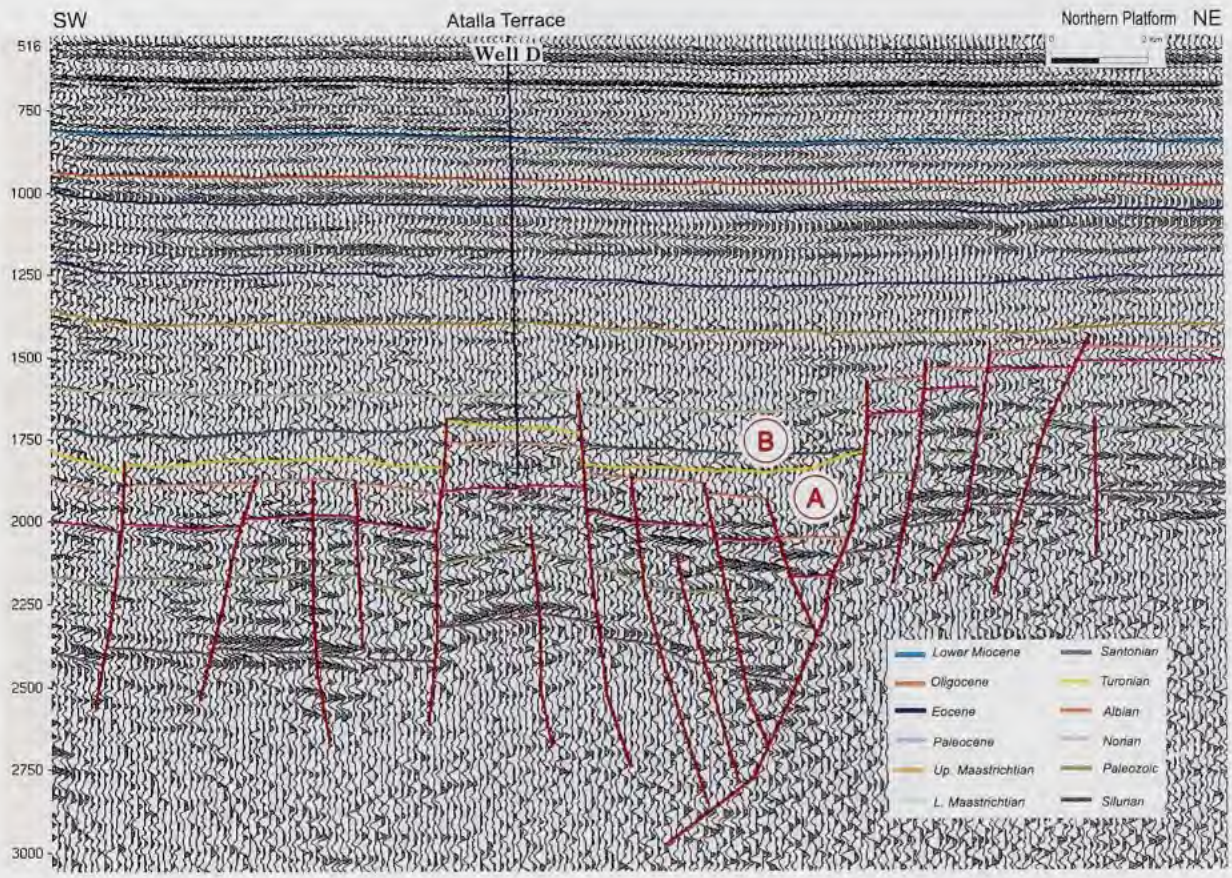

FIG. 20.— Seismic interpretation of line 2. Vertical scale is two-way travel time in ms. Datum plane is 300 m amsl. **A**: fault-controlled deposition of Turonian deposits. **B**: Onlap pattern of the Santonian section against the underlying Turonian strata.

*FIG. 20.—Interprétation du profil 2. L'échelle verticale est en ms temps double. Le plan de référence sismique est de 300 m niveau mer. **A** : contrôle par faille du dépôt du Turonien. **B** : onlap du Santonien sur les unités turoniennes sous-jacentes.*

STRUCTURAL STYLES IN THE SOUTHERN AREA

Line 6 (Fig. 23) transects from NE to SW the Dablan-Shwema High and the Shwema- El Ward South graben. Within the Shwema-Dablan High, the "pre-rift" sequence is dissected into horsts and half-grabens delineated by a system of planar steep faults with no or moderate offset. The Shwema-El Ward South graben is a well-defined graben structure with bounding master faults characterised by offsets no more than 200 ms twt. The northeastern side of line 6 shows the reactivation of a syn-rift fault resulting in a newly formed reverse fault implying the whole post-rift sequence, reflecting the Plio-Quaternary last structuration phase.

Line 7 (Fig. 24) clearly shows antithetic and roll-over features along NE-facing master normal faults, characterised by a maximum offset of 250 ms twt.

The figure 25 is a geo-seismic section elongating from SW to NE over the area covered by 2 regional seismic lines (line 6 with Well I as calibration well, line 7 with Well J, Well K and Well L as control wells).

Source : MNHN, Paris

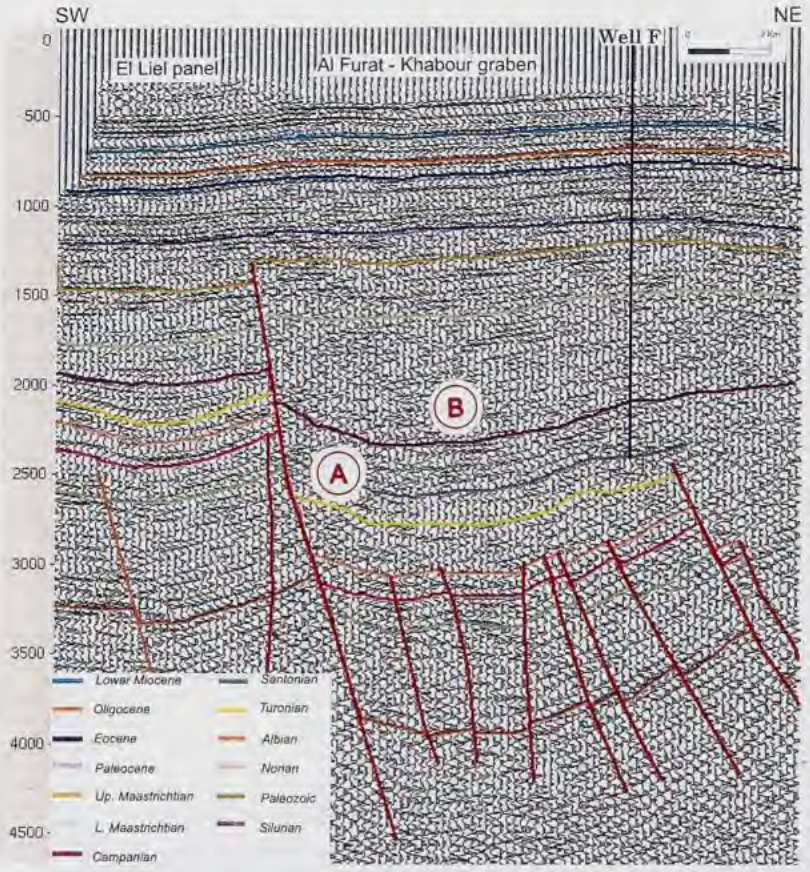

FIG. 21.— Seismic interpretation of line 4. Vertical scale is two-way travel time in ms. Datum plane is 300 m amsl. **A**: fault-controlled deposition of Turonian to Campanian deposits. **B**: onlap pattern of the early Maastrichtian section against the underlying Campanian strata.

FIG. 21.— Interprétation du profil 4. L'échelle verticale est en ms temps double. Le plan de référence sismique est de 300 m niveau mer. ***A*** *: contrôle par faille des dépôts du Turonien au Campanien.* ***B*** *: onlap du Maestrichtien inférieur sur les unités campaniennes sous-jacentes.*

RECOGNITION OF SUCCESSIVE TECTONIC PHASES WITHIN THE PRE-OLIGOCENE SECTION

This section attempts to characterise the successive tectonic phases by horizontal flattening of selected seismic lines at representative time levels. For that purpose, the recognition of onlap patterns, truncations, fan-shaped deposition, structural erosion on top of tilted blocks, character of fault motion is fundamental.

Turonian to Santonian interval

The thickness of the Turonian Derro formation is highly changing and largely fault-controlled in the northern part of the Euphrates graben (Figs 20 and 21). Derro deposits are typically eroded on top of tilted blocks (see Well J block on Fig. 24, see Santonian onlap on Well D block on Fig. 20). Their deposition is synchronous with the first structuration phase of the study area into horsts, grabens and tilted blocks. However, on line 7 (Fig. 24) and more generally over the southeastern area, the Derro sequence is rather isopach within antithetic zones and conformably overlies the Early Cretaceous ("pre-rift") sequence. This pattern suggests that, in the southeastern area, the antithetic phase occured in post-Turonian times and even after the Santonian. Actually, tectonic activity seems to slightly resume after the Derro deposition, as evidenced by the unconformable deposition of the Santonian formation onto the Turonian strata and the moderate thickness variations of this section along master normal faults (Figs 20 and 22).

Campanian interval

The northeastern sides of lines 6 and 7 (Figs 23 and 24) show that Campanian deposits are notably thicker within graben and half-graben structures and reduced on top of tilted blocks. The important thickness variations observed between the top Santonian and top Campanian markers traduce the onset

Source : MNHN, Paris

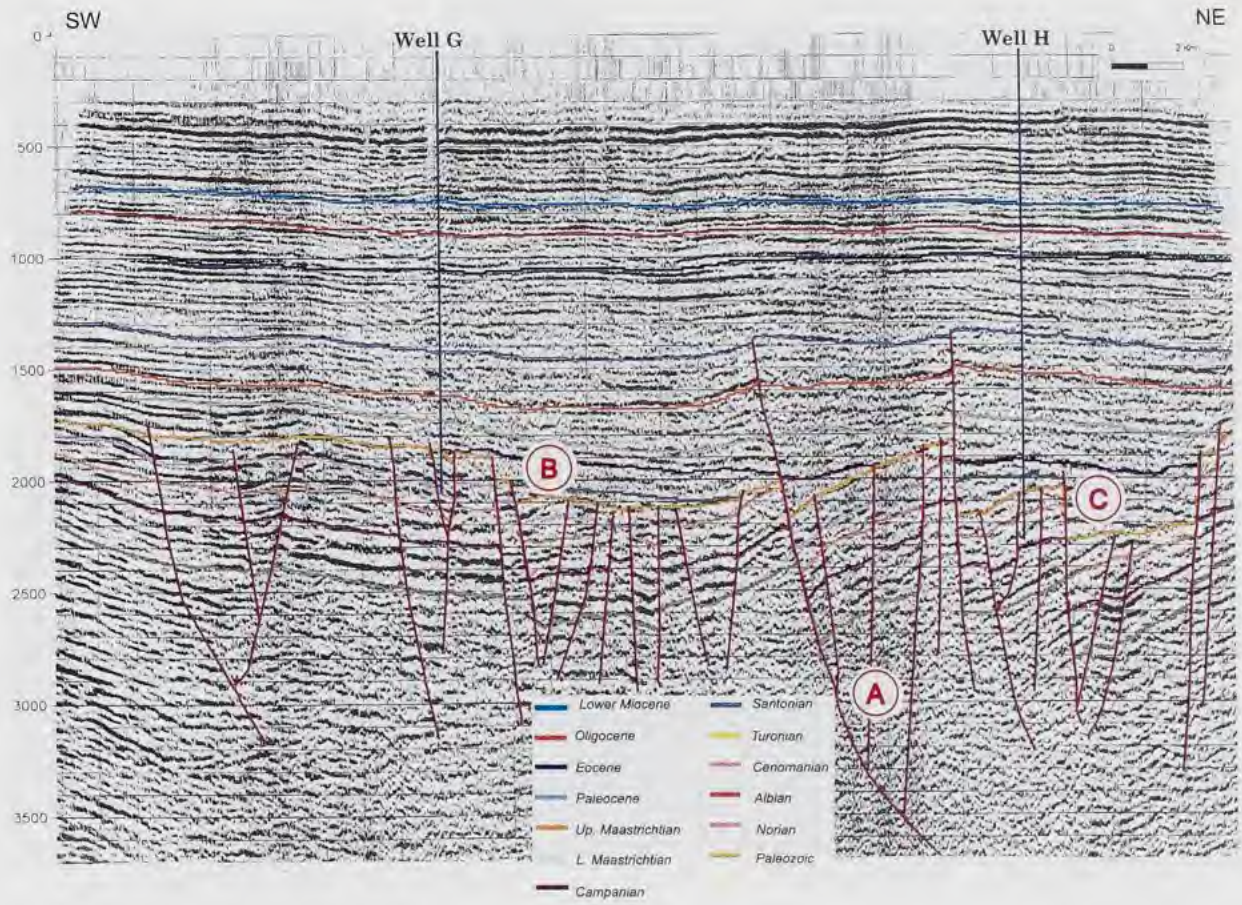

FIG. 22.— Seismic interpretation of line 5. Vertical scale is two-way travel time in ms. Datum plane is 300 m amsl. **A**: NE-vergent listric fault with associated antithetic panels. **B**: onlap pattern of the Santonian section against the underlying Turonian strata. **C**: Campanian major phase of "rifting".

FIG. 22.— Interprétation du profil 5. L'échelle verticale est en ms temps double. Le plan de référence sismique est de 300 m niveau mer. ***A*** *: faille listrique à vergence NE et panneaux antithétiques associés.* ***B*** *: onlap du Santonien sur les unités turoniennes sous-jacentes.* ***C*** *: Phase majeure de "rifting" au Campanien.*

of a major "rifting" phase in the southeastern area by the Campanian. Antithetic panels correlatively developed (line 7, Fig. 24) and are always connected at depth with NE-vergent listric faults.

Early Maastrichtian interval

No thickening of the early Maastrichtian series is observed along the N140E master normal fault bordering the Well J block to the northeast nor along the N140E fault bordering the Well L block (Fig. 24). The two major N140E-trending normal faults of the northeastern side of line 5 (Fig. 22) inverted by the late Palaeocene also did not guide the early Maastrichtian sedimentation. These N140E-trending faults probably acted as transfer fault zones at that time. Concomitantly, in the northern area, seismic data reflect high rates of subsidence along mostly E-W to N120E normal faults (Fig. 4), guiding the deposition of a thick early Maastrichtian section (Line 4, Fig. 21). Line 4 (Fig. 21) also shows the onlap pattern of the early Maastrichtian markers over Campanian strata. As the El Liel panel is entirely transgressed by the Campanian series (no residual relief), this onlap was caused by the reactivation of the fault system during a new tectonic phase of early Maastrichtian age. This configuration as a whole suggests a change from NE-SW extension in Campanian times to N15E extension by the early Maastrichtian. This result is in line with the stratigraphic data previously discussed.

Source : MNHN, Paris

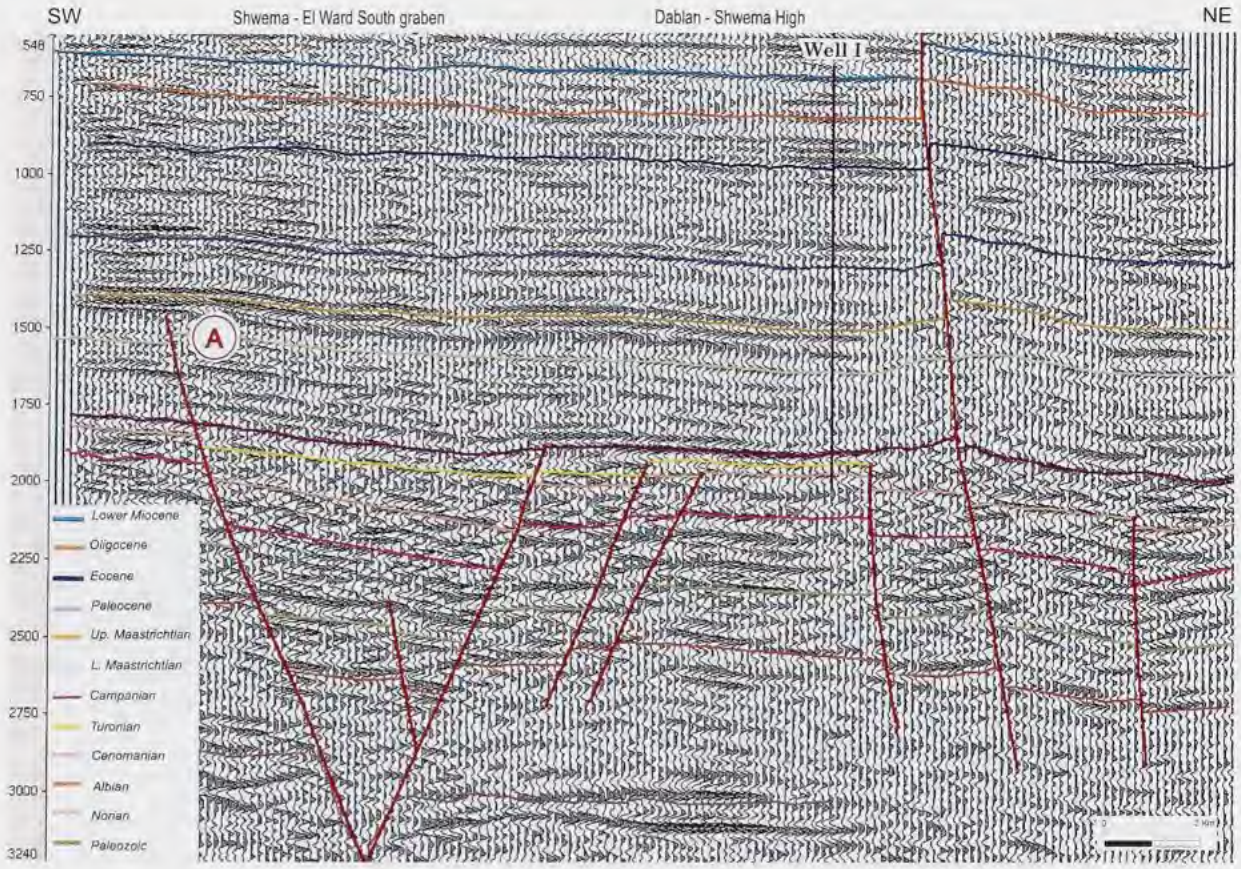

FIG. 23.— Seismic interpretation of line 6. Vertical scale is two-way travel time in ms. Datum plane is 300 m amsl. **A**: First phase of graben inversion during the late Maastrichtian.

*FIG. 23.— Interprétation du profil 6. L'échelle verticale est en ms temps double. Le plan de référence sismique est de 300 m niveau mer. **A** : Première phase d'inversion des grabens au cours du Maestrichtien supérieur.*

Late Maastrichtian interval

Picking of the top Maastrichtian horizon shows a characteristic pattern, with the Upper Shiranish marker blanketing the "rift"-interior highs and platforms (Fig. 20). This capping of the topography might represent the late "syn-rift"/early "post-rift" stage. Moreover, the southwestern side of line 6 (Fig. 23) shows that the late Maastrichtian series are gradually thinner over a tectonically inverted N140E master normal fault. Inversion occured prior to the deposition of the latest Maastrichtian deposits, which are clearly sealing the inverted fault. This is the older evidence of structural inversion of the pre-existing grabens and half-graben systems. The late Maastrichtian and following periods may thus be considered as taking part of the "post-rift" stage. This inversion stage is not detected over the northwestern area. As N140E-trending interior highs and the N45E-trending Joura Ridge are reactivated (Fig. 12), we might infer that the direction of the late Maastrichtian compression is NW-SE.

Post-rift interval

Globally, picking of the "post-rift" sequence in the northwestern area (Figs 18 and 23) shows numerous evidence of graben and half-graben inversion, resulting from the compressive movements that prevailed from Late Mesozoic to Quaternary. Numerous Late Cretaceous normal faults were propagated up into the "post-rift" section and reactivated as reverse faults, causing inversion of the previous grabens and formation of broad anticlines (Fig. 18). However, this configuration does not apply to the central

Source : MNHN, Paris

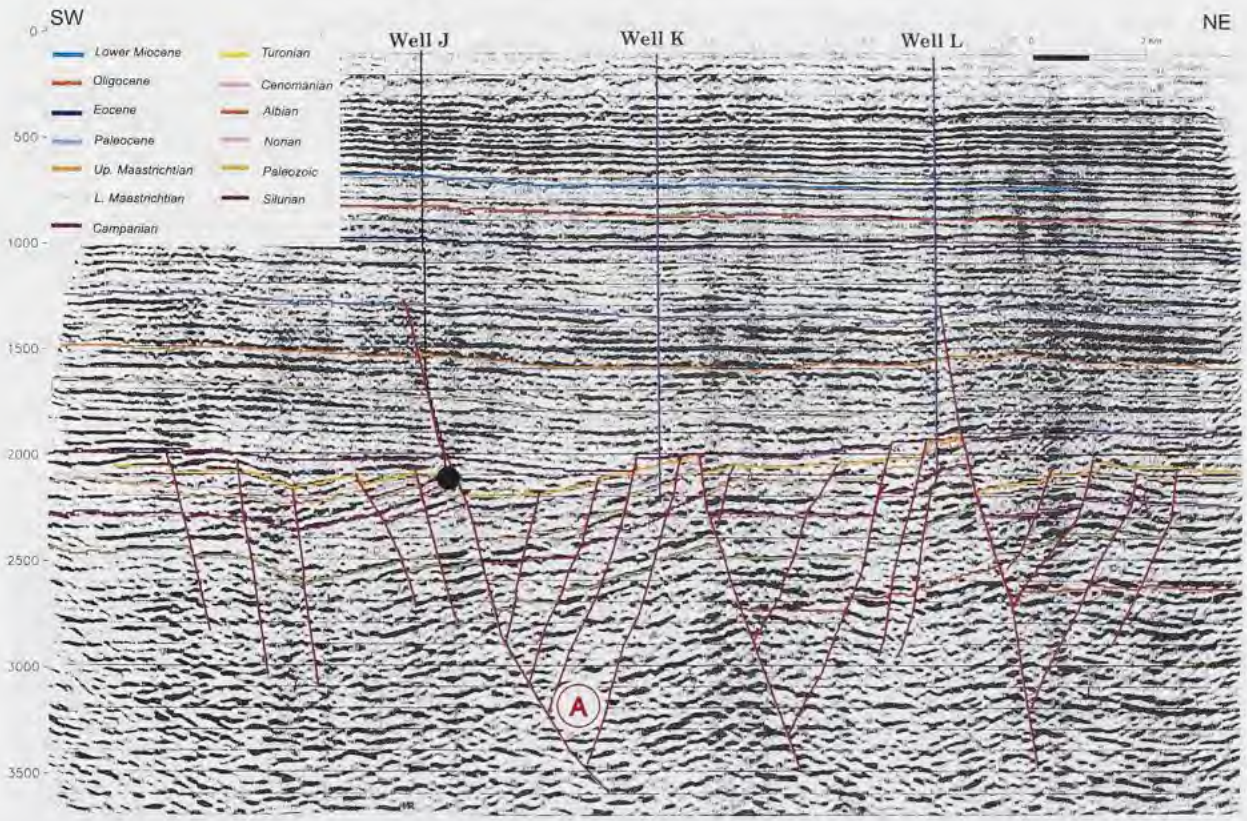

FIG. 24.— Seismic interpretation of line 7. Vertical scale is two-way travel time in ms. Datum plane is 300 m amsl. A: NE-vergent listric fault with associated antithetic panels.

FIG. 24.— Interprétation du profil 7. L'échelle verticale est en ms temps double. Le plan de référence sismique est de 300 m niveau mer. A : faille listrique à vergence NE et panneaux antithétiques associés.

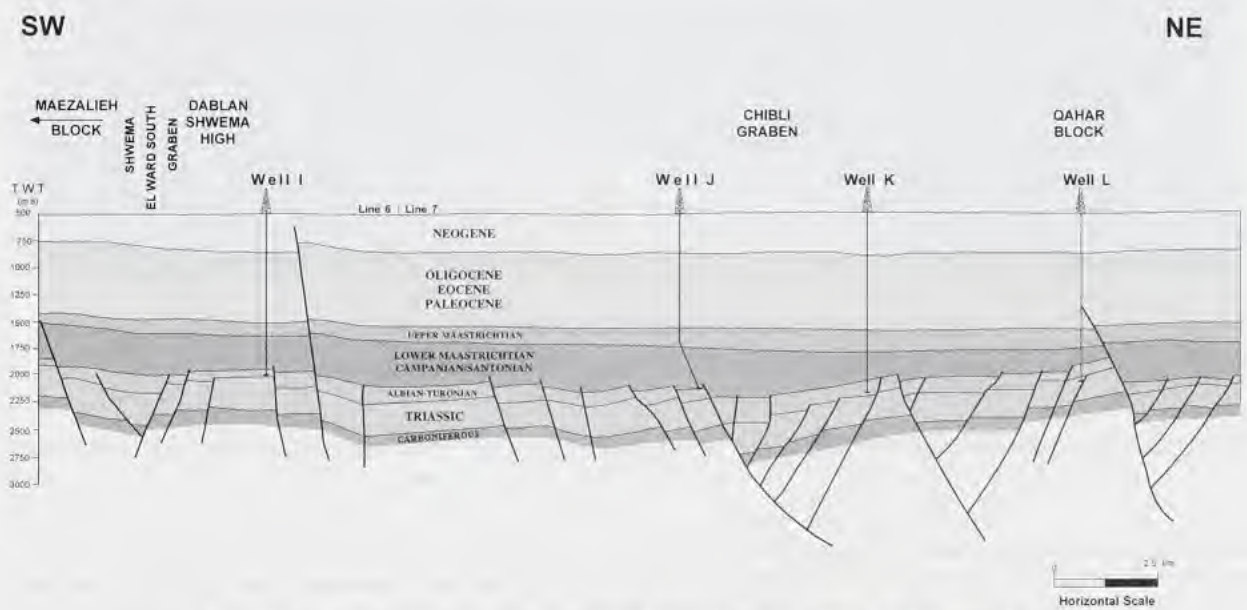

FIG. 25.— Geoseismic cross-section across the southern part of the Euphrates graben.

FIG. 25.— Coupe géosismique de la partie sud du graben de l'Euphrate.

Source : MNHN, Paris

and southern parts of the Euphrates graben, where the base of the Eocene series (Jaddala formation) seals most of the faults (Figs 22 and 24).

The figure 26 corresponds to a flattening of the line 1 (Fig. 18) at top of Eocene. This section illustrates the discussion held in the stratigraphic section of this paper (Fig. 16). The thickening of the Eocene Jaddala section over the pre-existing Joura block is explained by reverse motion of normal faults.

The Palaeocene-Eocene transition is imaged on seismic by an unconformity characterised by onlap termination (Figs 22 and 24). This pattern traduces the local sealing of Palaeocene faults and the global change in stress orientation between the Palaeocene and Eocene periods, as already discussed in the stratigraphic section.

The NE-SW extension suspected to occur in Oligocene times (Chilou deposition) is confirmed by flattening of line 1 (Fig. 18) at top Chilou (Fig. 27). The Cretaceous Al Kharrata graben inverted in Late Cretaceous-Palaeocene-Eocene times was reactivated by normal faulting in Oligocene times.

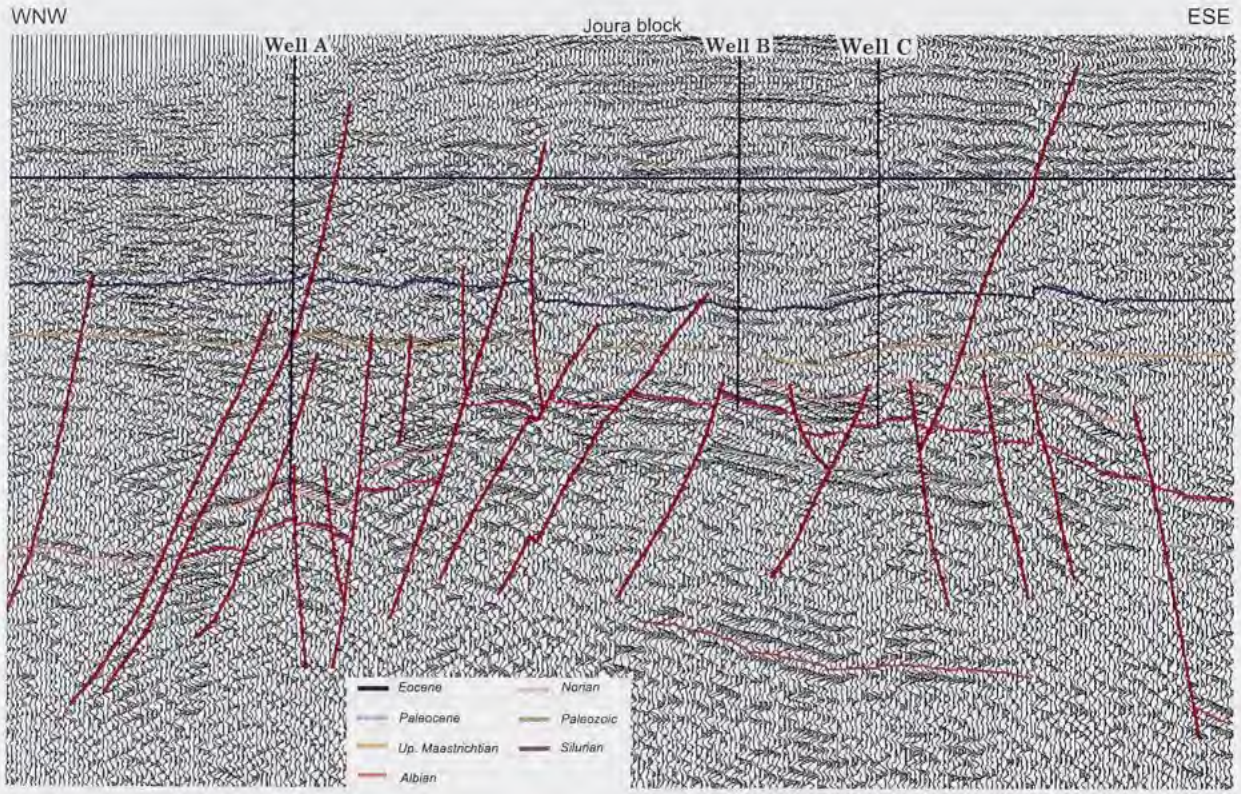

FIG. 26.— Seismic interpretation of line 1 flattened at top of Eocene.

FIG. 26.— Interprétation du profil 1 horizontalisé au toit de l'Éocène.

CONFRONTATION OF STRATIGRAPHIC AND STRUCTURAL DATA: TECTONIC EVOLUTION

First movements announcing the major phase of "rifting" and associated basaltic activity are recorded at the future site of the Euphrates graben as soon as in Albian times, along the southern segment of the depression. The NE-SW extension was maintained in Turonian times (Fig. 28), with the development of N160E to N120E-trending grabens and associated volcanic activity. A period of relative tectonic quiescence followed the Turonian phase, with the deposition of Santonian limestones in a global transgressive context.

Source : MNHN, Paris

The main pulse of "rifting" occured in Campanian times, with NE-SW extension and block tilting. A deep N120-N140E trough opened, extending to the northern platform of the Euphrates graben. Northeast vergent listric faults developed at that time in the southern part of the Euphrates graben. This northeastward tilting was contemporaneous with the obduction of the Tethyan oceanic crust onto the northeastern margin of the Arabian plate (Oman and Zagros ophiolites; KAZMIN *et al.*, 1986; DERCOURT *et al.*, 1993). As the fault network within the Euphrates graben (N140E) roughly parallels the obduction axis (Zagros trend), the Euphrates graben could represent a flexural basin formed in response to the loading of the subducting Arabian plate (Fig. 28).

The early Maastrichtian period is characterised by a change in the direction of extension, from NE-SW (from Turonian to Campanian) to N15E. Extension occured along N100-N120E faults and transtension along N160E faults. This structural setting accords with the tectonic evolution described by KENT & HICKMAN (1997) in the Abd Al Aziz and Sinjar areas. An early stage of Zagros folding at the eastern margin of the Arabian plate may have stopped the lateral eastward tilting and caused the direction of extension to rotate. Alternately, the N15E extension recorded during the Early Maastrichtian

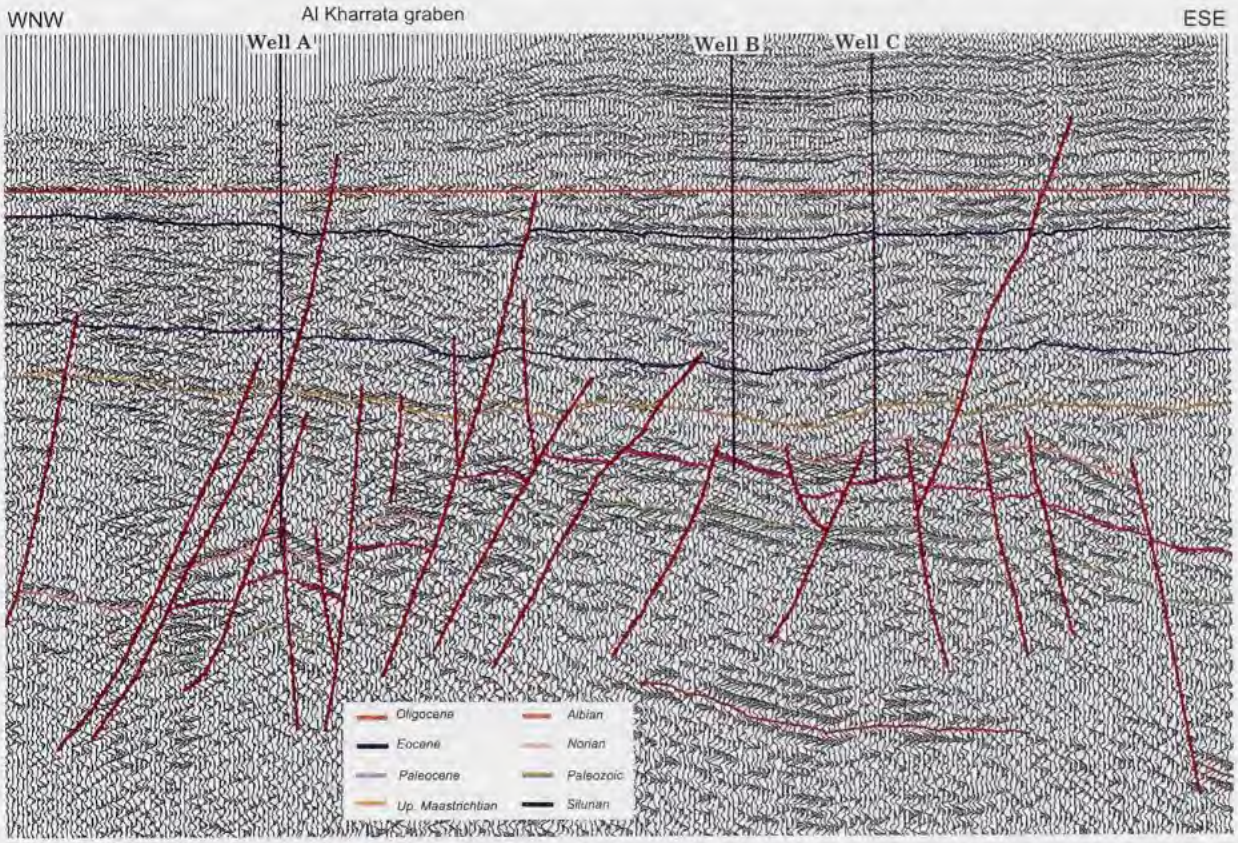

FIG. 27.— Seismic interpretation of line 1 flattened at top of Oligocene.

FIG. 27.— Interprétation du profil 1 horizontalisé au toit de l'Oligocène.

may have been induced by the obduction stage strongly active at that time along the globally E-W Bitlis axis, with the tectonic emplacement of ophiolites (KAZMIN *et al.*, 1986; ORSZAC-SPERBER *et al.*, 1989; SAGE & LETOUZET, 1990; DERCOURT *et al.*, 1993).

In late Maastrichtian and early Palaeogene times, NW-SE compressive movements caused the Euphrates "rift" system to abort. Structural inversion occured west to the Joura Ridge, mainly along NE-SW structural trends. The area of structural inversion covers the hinge zone of two megatectonic trends: the NW-SE trend of the Euphrates graben and the northeastern part of the Palmyra fault zone (inverted Bishri trough) with predominantly SW-NE structures. Early Palaeogene was the time of global

Source : MNHN, Paris

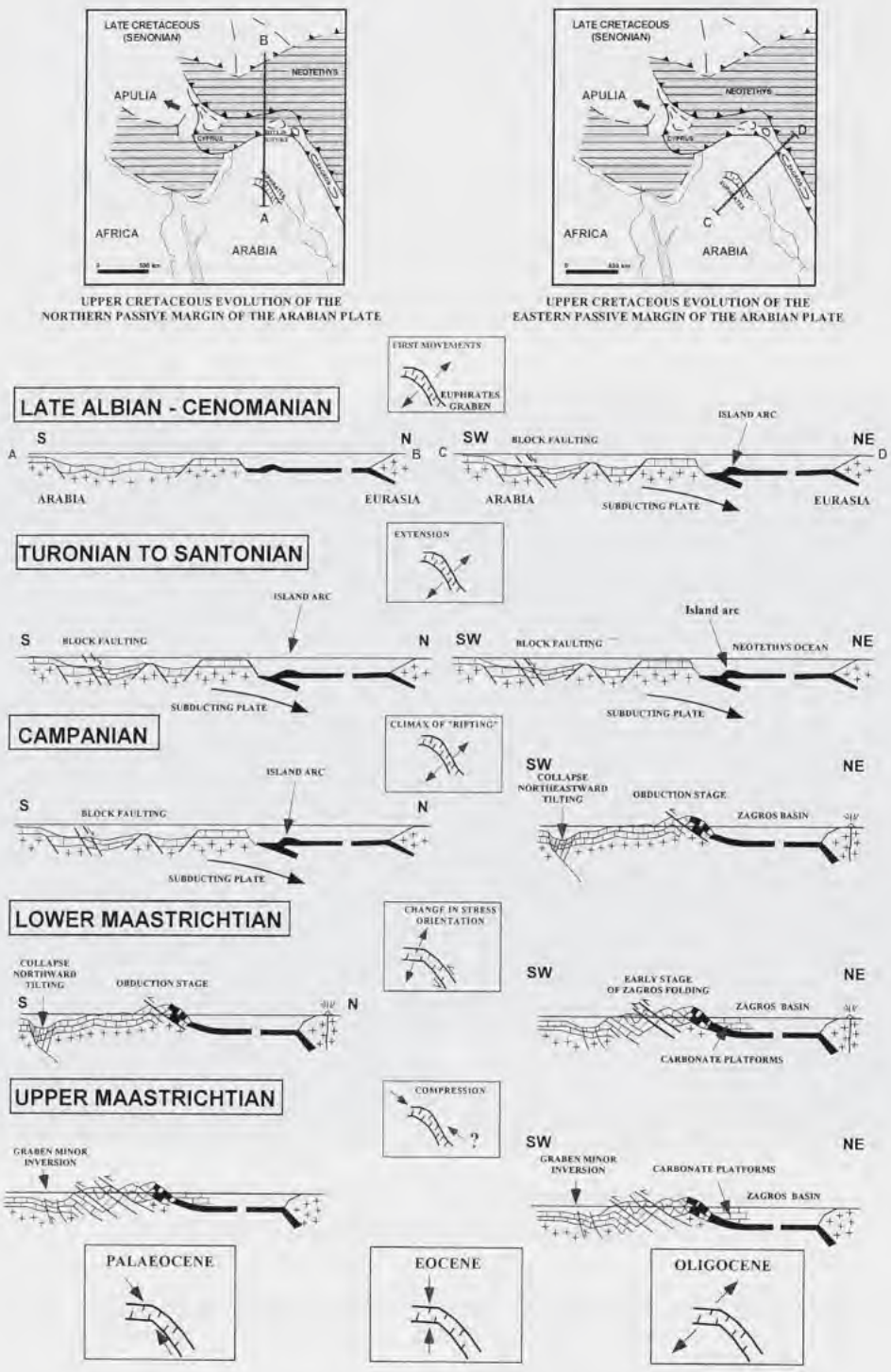

FIG. 28.— Conceptual model for the structural evolution of the Euphrates graben.

FIG. 28.— Modèle schématique d'évolution structurale du graben de l'Euphrate.

Source : MNHN, Paris

compressive tectonics. This compression is clearly associated with the subduction of the Afro-Arabian plate beneath the Eurasia plate, along the Bitlis suture zone to the north and Zagros suture zone to the northeast. Structural inversion locally affected the depositional trends over the northwestern part of the Euphrates graben and migrates in time from north to south. However, the Euphrates graben appears to be moderately deformed with respect to adjacent Mesozoic basins (Palmyrides, Sinjar and Abd El Aziz troughs).

Palaeostress orientation changed from N-S compression to NE-SW extension by the Oligocene, inducing over the northernmost part of the Euphrates graben the reactivation of Late Cretaceous N120E faults.

REFERENCES

BEST, A.J., BARAZANGI, M., AL SAAD, D., SAWAF, T. & GEGRAN, A., 1993.— Continental margin evolution of the Northern Arabian Platform in Syria. *AAPG Bulletin*, **77**: 173-193.

BREW, G.E., DOGAN, R.K., SEBER, L., AL IMAM, A. & SAWAF, T., 1997.— Basement depth and sedimentary velocity structure in the Northern Arabian platform, Eastern Syria. *Geophysical Journal International*, **128**: 617-631.

CHAIMOV, T.A., BARAZANGI, M., AL SAAD, D., SAWAF, T. & KHADDOUR, M., 1993.— Seismic fabric and 3D structure of the Southwestern Intracontinental Palmyride fold belt, Syria. *AAPG Bulletin*, **77**: 2032-2047.

DERCOURT, J., RICOU, L.E. & VRIELYNCK, B., 1993.— *Atlas Tethys Paleoenvironmental Maps*. Gauthier-Villars, Paris: 1-307, 14 maps, 1 pl.

KAZMIN, Y., RICOU, L.E. & SBORTSHIKOV, I.M., 1986.— Structure and evolution of the passive margin of the Eastern Tethys. *Tectonophysics*, **123**: 153-179.

KENT, N. & HICKMAN, R.G., 1997.— Structural development of Jebel Abd Al Aziz, Northeast Syria. *GeoArabia*, **2**: 307-330.

LITAK, R.K., BARAZANGI, M., BREW, G., SAWAF, AL IMAM, A. & AL YOUSSEF, W., 1998.— Structure and Evolution of the Petroliferous Euphrates Graben System, Southeast Syria. *AAPG Bulletin*, **82**: 1173-1190.

LOVELOCK, P.E.R., 1984.— A review of the tectonics of the northern Middle East region. *Geological Magazine*, **121**: 577-587.

MCBRIDE, J.H., BARAZANGI, M., BEST, J., AL SAAD, D., SAWAF, T., AL OTRI M. & GEBRAN, A., 1990.— Seismic reflection structure of the intracratonic Palmyride fold-thrust belt and surrounding Arabian platform in Syria. *AAPG Bulletin*, **74**: 238-259.

MAY, P.R., 1991.— The Eastern Mediterranean Mesozoic Basin : evolution and oil habitat. *AAPG Bulletin*, **75**: 1215-1232.

MOUTY, M., 1997.— Le Jurassique de la chaîne des Palmyrides (Syrie centrale). *Bulletin de la Société géologique de France*, **168** (2): 181-186.

ORSZAC-SPERBER, F., ROUCHY, J.M. & ELION, P., 1989.— The Sedimentary expression of regional tectonic events during the Miocene-Pliocene transition in the Southern Cyprus basins. *Geological Magazine*, **126**: 291-299.

RUITER, R.S.C., LOVELOCK, P.E.R. & NABULSI, N., 1994.— The Euphrates graben of Eastern Syria : a new petroleum province in the Northern Middle East. *In*: M.I. AL HUSSEIN (ed.), *Geo' 94: The Middle East petroleum geosciences*. Volume 1: *Maname, Bahrain*. Gulf Petrolink: 357-368.

SAGE, L. & LETOUZEY, J., 1990.— Convergence of the African and Eurasian plate in the Eastern Mediterranean. *In*: J. LETOUZEY (ed.), *Petroleum and Tectonics in Mobile Belts*. Technip, Paris: 49-68.

SALEL, J.F., 1993.— *Tectonique de chevauchement et inversion dans la chaîne des Palmyrides et le graben de l'Euphrate (Syrie). Conséquences sur l'évolution de la plaque arabe*. Thèse, Université de Montpellier, Montpellier, France: 1-288.

SAWAF, T., AL SAAD, D., GEBRAN, A., BARAZANGI, M., BEST, J.A. & CHAIMOV, T.A., 1993.— Structure and stratigraphy of Eastern Syria across the Euphrates depression. *Tectonophysics*, **220**: 267-281.

SHAW, J.H., HOOK, C.S. & SITOHANG, E.P., 1997.— Extensional fault-bend folding and synrift deposition: an example from the central Sumatra basin, Indonisa. *AAPG Bulletin*, **81**: 367-379.

Source : MNHN, Paris

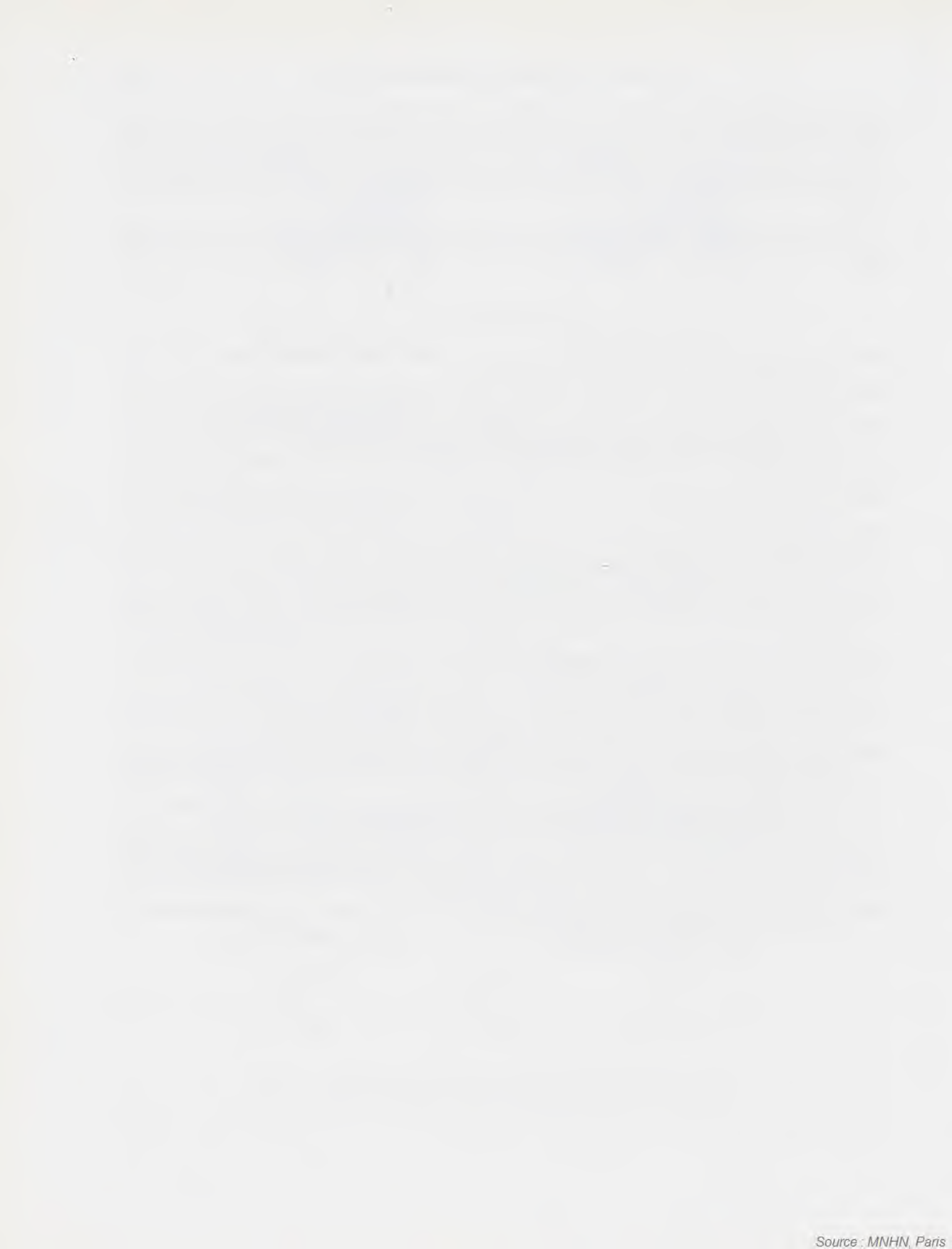

Source : MNHN, Paris

11

Palaeogeography and palaeotectonic of the jointing area between the Eastern European Basin and the Tethys Basin during Late Carboniferous (Moscovian) and Early Permian (Asselian and Artinskian)

Boris I. CHUVASHOV [1] *& Sylvie CRASQUIN-SOLEAU* [2]

[1] Institute of Geology and Geochemistry of the Urals Branch of Russian Academy of Sciences
Pochtovy pereulok 7, 620 151, Ekaterinburg, Russia

[2] CNRS UPRES-A 7073, Université Pierre et Marie Curie, Département de Géologie sédimentaire
T.15-25, E.4, case 104, F-75252 Paris Cedex 05, France

ABSTRACT

During the Moscovian, the Eastern European sedimentary Basin (EEB) occupied an extensive territory on the Eastern European continent, from the meridian of Arkhangelsk to the west up to the Urals to the east. On the territory of the present eastern slope of Urals, the narrow and long Eastern Uralian Gulf (EUG) incorporated to the south the basins of Turansk Plate and Precaspian Depression. In its southwestern part, the EEB is separated from the Donetsk gulf by the Voronezh Peninsula. The EEB territory was subdivided in two unequal seas: the Volga-Kama Sea and Preuralian Sea (the last one included the Eastern Uralian Gulf). In the Volga-Kama Sea, the carbonate shallow-water sediments prevail. In the rather deep-water Preuralian Sea, lateral facies belts are present from coarse clastic marine and continental facies to the east, passing to mainly carbonated to the west. The uplift of the Palaeouralian mountain system separated the Preuralian Basin from the Eastern Uralian Gulf. During the Asselian, the main changes in the palaeogeography of the considered territory marine realms occurred. The reduction of the EUG took place at the end of the Carboniferous. During the middle Asselian, the sea left the Donetsk Gulf. The isolation and deepening of Precaspian Basin step up, allowing the connection between the Preuralian Basin and the northern part of the Tethys Ocean. The important feature of the Asselian palaeogeography is the built up of a strong reef barrier, which surrounds the Precaspian Basin and in a north-south direction (≈ along 60°E meridian). It separated the Volga-Kama Sea from the Preuralian Sea. In the Preuralian Sea territory, lateral sediment belts, similar to the Moscovian ones, occur from coarse clastic sediments to the east to mainly carbonated sediments to the west. On the immersed edge of the platform, the most thick reef barrier for the whole Early Permian history was generated. During middle Asselian, the maximum transgression level was reached, then, from Shikhanskian time, began the regression and the quick reduction of the Volga-Kama Sea. During the Artinskian, the last existence of a marine basin with normal salinity is recorded. The EEB width was strongly reduced (500 km against 1500 km during Asselian). On a great part of the Volga-Kama Sea territory, the salinity increased: the dolomites and anhydrites set down everywhere. During the first half of the Artinskian, the sea left the Turansk plate territory and its southern adjacent parts. During the late Artinskian, the marine transgression occured in the south, where the Tethyan belt reached the Precaspian area. This geological history for these three time-slices is presented on three pairs of palaeogeographic maps. The palaeobiogeographical relationships and palaeoclimatic conditions are considered.

CHUVASHOV, B.I. & CRASQUIN-SOLEAU, S., 2000.— Palaeogeography and palaeotectonic of the jointing zone between the Eastern European Basin and the Tethys Basin during Late Carboniferous (Moscovian) and Early Permian (Asselian and Artinskian). *In*: S. CRASQUIN-SOLEAU & É. BARRIER (eds), Peri-Tethys Memoir 5, new data on Peri-Tethyan sedimentary basins. *Mém. Mus. natn. Hist. nat.*, **182** : 203-238, Paris ISBN : 2-85653-524-0.

Source : MNHN, Paris

RÉSUMÉ

Paléogéographie et paléotectonique d'une zone de jonction entre le Bassin Est Européen et le Bassin de la Téthys au cours du Carbonifère supérieur (Moscovien) et du Permien inférieur (Assélien et Artinskien).

Au cours du Moscovien, le Bassin sédimentaire Est Européen (EEB) occupe un large territoire sur le Continent Est-Européen, depuis le méridien d'Arkhangelsk à l'ouest jusque l'Oural à l'est. Sur le versant oriental actuel de l'Oural, existe l'étroit et long Golfe Est Ouralien (EUG), intégrant, vers le sud, les bassins de la plaque de Turan et de la Dépression Précaspienne. Dans sa partie sud-ouest, le Bassin Est Européen est séparé du Golfe du Donetz par la péninsule de Voronezh. Le Bassin Est-Européen est subdivisé en deux mers de superficies inégales : la Mer de Volga-Kama et la Mer Préouralienne (cette dernière incluant le Golfe Est-Ouralien). Dans la Mer de Volga-Kama, les sédiments carbonatés d'eau peu profonde dominent. Dans la Mer Préouralienne, relativement profonde, se développent des ceintures de faciès depuis des sédiments grossiers clastiques marins et des faciès continentaux à l'est jusqu'à des dépôts principalement carbonatés à l'ouest. La surrection de l'Oural sépare le Bassin Préouralien du Golfe Est Ouralien. Durant l'Assélien, se produisent les principales modifications paléogéographiques des domaines marins de cette région. A la fin du Carbonifère, l'EUG s'est notablement réduit. A l'Assélien moyen, la mer se retire du Golfe du Donetz. L'isolement et l'approfondissement du Bassin Précaspien et de la partie nord de la Téthys se produisent. Le caractère important de la paléogéographie de l'Assélien est la construction d'une barrière récifale majeure sur le pourtour du Bassin Précaspien et en direction nord-sud, le long du méridien 60°E. Cette barrière sépare la Mer de Volga-Kama de la Mer Préouralienne. Dans la Mer Préouralienne, des ceintures de faciès, similaires à celles du Moscovien, se développent depuis des faciès grossiers clastiques à l'est jusqu'à des faciès principalement carbonatés à l'ouest. Sur la partie immergée de la plate-forme, la plus importante barrière récifale de toute l'histoire du Permien inférieur s'édifie. Durant l'Assélien moyen, le maximum de transgression est atteint puis, à partir du Shikhanskien, commence la régression avec une rapide réduction de la Mer de Volga-Kama. Au cours de l'Artinskien, le dernier bassin marin à salinité normale est reconnu. Le Bassin Est-Européen est considérablement réduit (500 km de large pour 1500 à l'Assélien). Sur la majeure partie du territoire de la Mer de Volga-Kama, la salinité augmente fortement: des dolomies et des anhydrites se déposent partout. Durant la première moitié de l'Artinskien, la mer quitte la plaque de Turan et ses régions méridionales adjacentes. A l'Artinskien supérieur, la transgression marine se produit au sud, là où la Téthys rejoint la zone Précaspienne. Cette histoire géologique pour les trois intervalles de temps est présentée sur trois paires de cartes paléogéographiques. Les relations paléobiogéographiques et les conditions paléoclimatiques sont abordées.

INTRODUCTION

We discuss here the relations between the Eastern European Basin (EEB) and the seas of the Tethys Basin for three time slices: Moscovian (Late Carboniferous), Asselian and Artinskian (Early Permian). The historical study of the Carboniferous-Permian communications between the Urals and Russian Platform, on one side, and the Tethyan Basin, on the other, was previously published (CHUVASHOV, 1977).

The EEB was divided here in two parts: the Volga-Kama Sea to the west and the Preuralian Sea alongside the Urals.

The Moscovian was marked by wide biogeographical connections and large transgression of the ocean on shallow-water carbonate platforms. Some important geological events occured during this period: the development of the Preuralian Sea: the Uralian Basin, uniform before, was divided by the uplift of Palaeourals Mountain system in two parts: Preuralian Sea and Eastern Uralian Gulf; the Precaspian Depression was perfectly delimited at this moment.

During the Asselian, the Early Permian had a maximum variety of biota, due to the maximum of the transgression. During this period, several important geological events occured: the Donetsk Gulf was closed, the Preuralian Sea and the Precaspian Basin had their maximum of extension. The strong influence of Tethyan biota is displayed on the organic communities of southern Preuralian Sea and could be followed up to 55°N.

During the Artinskian, a significant reduction of the EEB area occurred and its Volga- Kama part was transformed in an extensive very shallow-water lagoon with poor and uniform fauna. The typical marine basin with diverse sediments and biotopes was preserved on the borders of the Preuralian Sea and it's nearest western frame. The communications with the Tethys Basin at this time were reduced to the minimum.

Source : MNHN, Paris

FIG. 1.— Location, on a present day map, of the main geographical terms used in this paper.

FIG. 1.— Localisation, sur une carte géographique actuelle, des principaux termes utilisés dans cet article.

Source : MNHN, Paris

The general palaeogeographic map of the Eastern-European Basin is established on the base of 1: 5 000 000 map, the palaeogeographic map of Preuralian Sea on the basis of 1: 2 500 000 map and map of the jointing zone of Preuralian Sea and Tethyan Basin, scale 1: 5 000 000. All the geographic localities are reported on a present day map (Fig. 1). The legend used for all palaeogeographic maps and profiles is drawn on the figure 2.

Our approach to restore the palaeogeographic situation is defined by the study of the Preuralian Sea sediments and biota as well as data on the Volga-Kama Sea. In terms of tectonic, the Volga-Kama Sea corresponds to the eastern rim of the Russian Platform and the Preuralian Foredeep. All facial zones (belt of sediments) of this territory are traced from the Polar Urals and Preuralie to the Precaspian Depression. The most difficult problem is the reconstruction of the Precaspian Depression and Turansk Plate palaeogeography, where the studied formations are reached at significant depth, and drilled by far separate boreholes, with very partial selection of cores. All direct and indirect informations are used.

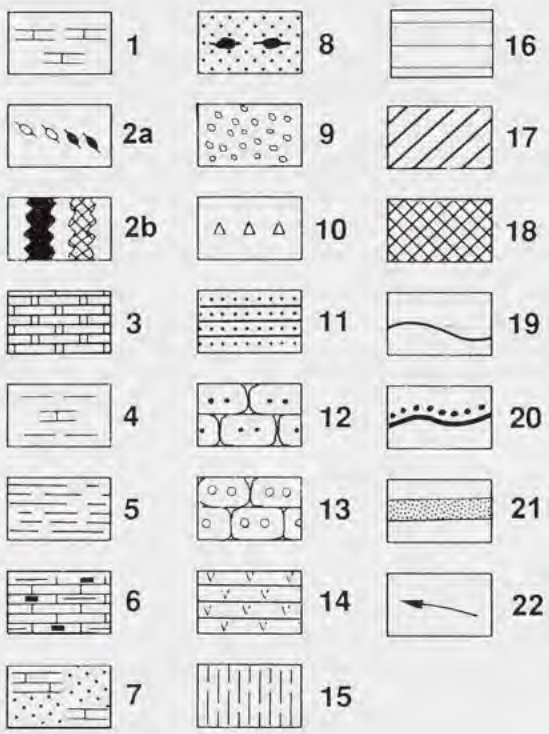

FIG. 2.— Legend for palaeogeographic maps and profiles. **1**, shallow-water limestones (carbonated platform); **2a**, organic buildups for palaeogeographic maps: established (black) and suggested (white); **2b**, organic buildups for profiles: established (black) and suggested (hachures); **3**, dolomites; **4**, deep water argilites with limestone and marl interlayers; **5**, deep water argilites; **6**, coal-bearing paralic deposits; **7**, sandstones with shallow-water limestones; **8**, organic buildups on the sandy basement; **9**, pebble and boulder conglomerates; **10**, volcanic rocks; **11**, sandy flysh; **12**, sandstones (for profiles); **13**, gravelstone (for profiles); **14**, evaporates; **15**, suggested areas of marine sediments distribution; **16**, land and island with hilly relief; **17**, land and island with middle mountain (1-2000 m) relief; **18**, high mountain (above 2000 m) relief; **19**, limits of facial zones; **20**, area of shore - line shifting during the map time slice; **21**, emerged land with low relief; **22**, direction of distribution of denuded material.

*FIG. 2.— Légende pour les cartes paléogéographiques et les profils. **1**, calcaires d'eau peu profonde (plate-forme carbonatée) ; **2a**, contructions organiques sur les cartes paléogéographiques : prouvée (noir) et supposée (blanc) ; **2b**, contructions organiques sur les profils : prouvée (noir) et supposée (hachures) ; **3**, dolomies ; **4**, argilites d'eau profonde avec niveaux intercalés de calcaires et de marnes ; **5**, argilites d'eau profonde ; **6**, dépôts paraliques avec charbon ; **7**, grès avec des calcaires d'eau peu profonde ; **8**, contructions organiques sur un sous-bassement sableux ; **9**, conglomérats à blocs et galets ; **10**, roches volcaniques ; **11**, flysch sableux ; **12**, grès sur les profiles ; **13**, roches gravelleuses (sur les profils) ; **14**, évaporites ; **15**, aire de répartition supposée de faciès marins ; **16**, terres émergées et îles avec un relief de collines ; **17**, terres émergées et îles avec un relief de moyenne montagne (1200 m) ; **18**, relief de haute montagne (supérieur à 200 m) ; **19**, limites des zones de faciès ; **20**, zone de déplacement de la ligne de rivage dans l'intervalle de temps de la carte ; **21**, zones émergées avec faible relief ; **22**, sens de distribution du matériel détritique.*

Source : MNHN, Paris

The "Atlas of the lithological and palaeogeographic maps of the Russian platform ..." (VINOGRADOV, 1961) is used for the reconstruction of Russian Platform, and for the Urals, the "Atlas of Palaeozoic-Mesozoic lithological-palaeogeographic maps of the Cis-Urals" (CHERMNYSK, 1972). The palaeogeographic reconstruction of the Pamir and Tyan Shan region areas largely take in account the work of BENSH (1982) and informations were extracted from numerous publications about stratigraphy and lithology, as well as being the results of private investigations. Only a small part of the publications used are mentioned in the reference list. The characteristics of palaeogeographic situation for the three time slices are given below.

THE MOSCOVIAN

The Moscovian stage is subdivided in two substages (Table 1): lower and upper. For the lower Moscovian, the Vereiskian and Kashirskian horizons are recognised. The upper Moscovian is subdivided in Podolskian and Maychkovskian horizons. All horizons have other names in the Urals, but we use above divisions because they are relatively well known and well correlated with Uralian horizons. A correlation table between Donetz, Moscow and Urals formations is proposed (Table 2, modified after IZART *et al.*, 1998) for Late Carboniferous and Early Permian.

TABLE 1.— Correlations of the formations and units used in the text.

TABLEAU 1.— Corrélation des formations et unités appelées dans le texte.

<table>
<tr><td rowspan="4">Artinskian</td><td rowspan="2">upper</td><td colspan="2">Saraninskian</td><td rowspan="2"></td><td rowspan="2">Timaksk suite</td></tr>
<tr><td colspan="2">Sarginskian</td></tr>
<tr><td rowspan="2">lower</td><td colspan="2">Irginskian</td><td rowspan="2">Tabolask suite
Visikovsk suite</td></tr>
<tr><td colspan="2">Burtsevskian</td></tr>
<tr><td colspan="5">Sakmarian</td></tr>
<tr><td rowspan="4">Asselian</td><td>Shikhanskian</td><td colspan="2">S. sphaerica - P. firma zone</td><td>Skosyrsk suite</td><td>Kramatorsk suite</td></tr>
<tr><td rowspan="3">Kholodnolozhskian</td><td colspan="2">S. moelleri - P. fecunda zone</td><td rowspan="2"></td><td rowspan="2">Slavyaksk suite</td></tr>
<tr><td colspan="2">S. fusiformis zone</td><td rowspan="2">Kalitvensk suite</td><td rowspan="2">Nikotovsk suite</td></tr>
<tr><td colspan="2">D. bosbytauenis - D. robusta zone</td><td>Kartamishsk suite</td></tr>
<tr><td colspan="5">Kazimovian - Gzelian</td></tr>
<tr><td rowspan="5">Moscovian</td><td rowspan="2">upper</td><td colspan="2">Maychkovskian</td><td rowspan="5">Bukhana suite</td><td>C2me</td></tr>
<tr><td colspan="2">Podolskian</td><td>C2md</td></tr>
<tr><td rowspan="3">lower</td><td colspan="2">Kashirskian</td><td>C2mc</td></tr>
<tr><td rowspan="3">Vereiskian</td><td>Ordynsk mb</td><td>C2mb</td></tr>
<tr><td>Alyutovsk mb</td><td></td></tr>
<tr><td>Shazk mb</td><td>C2ma</td></tr>
</table>

MOSCOVIAN PALAEOGEOGRAPHY OF THE EUROPEAN EASTERN BASIN

The Moscovian Eastern European Basin covered a large territory of the Eastern Russian Platform. The width of this basin is almost 1500 km on the Moscow latitude. Northern part of the EEB was located in recent Arctic Ocean.

The EEB can be divided in different seas and gulfs (Fig. 3), according to their size, depth, and type of sediments. The large Donetsk Gulf, filled by a thick sequence of coal-bearing paralic deposits, connected with the EEB in the south. A very large western part of the EEB could be treated like Volga-

Source : MNHN, Paris

TABLE 2.— Correlation table of the formations used in Russia (after IZART *et al.*, 1998).
TABLEAU 2.—Tableau de corrélation des formations utilisées en Russie (d'après IZART et al., *1998).*

Western European stages	Eastern European horizons			Eastern European stages	
	Donetsk Basin	Russian Platform	Ural		
Saxonian			Irenskian Philippovskian	Kungurian	Early Permian
			Saraninskian Sarginskian Irginskian Burtsevskian	Artinskian	
	Kramatorsk		Sterlitamakskian Tastubskian	Sakmarian	
Autunian	Slavjansk Nikitovsk Kartamysh	Shikhanskian Sukoljegorskian	Shikhanskian Kholodnolozhskian	Asselian	
Stephanian	Mironovsk Kalinovsk	Noginskian Klyazminskian	Mortukskian Azantashskian	Gzhelian	Late Carboniferous
	Torezk	Dorogomilovskian Khamovnichinskian Krevyakinskian	Kerzhakovskian Orlovskian	Kasimovian	
Westphalian D	Sanjarovsk Sabovsk	Myachkovskian Podolskian		Moscovian	Middle Carboniferous
Westphalian C	Mariesvk Kamensk	Kashizskian Vereiskian			
Westphalian B	Krasnodonsk	Upper Aza: Melekeskian	Asatauskian	Bashkirian	
Westphalian A	Makeevsk Zuevsk	Upper Aza: Cheremshanskian	Tashastinskian		
Namurian C	Blagodatnensk Manuilovsk	Lower Aza: Prekamskian Severokeltmenskian	Askynbashkian Akavaskian		
Namurian B	Feninsk	Lower Aza: Kzasnopolyanskian	Siuranskian		

Source : MNHN, Paris

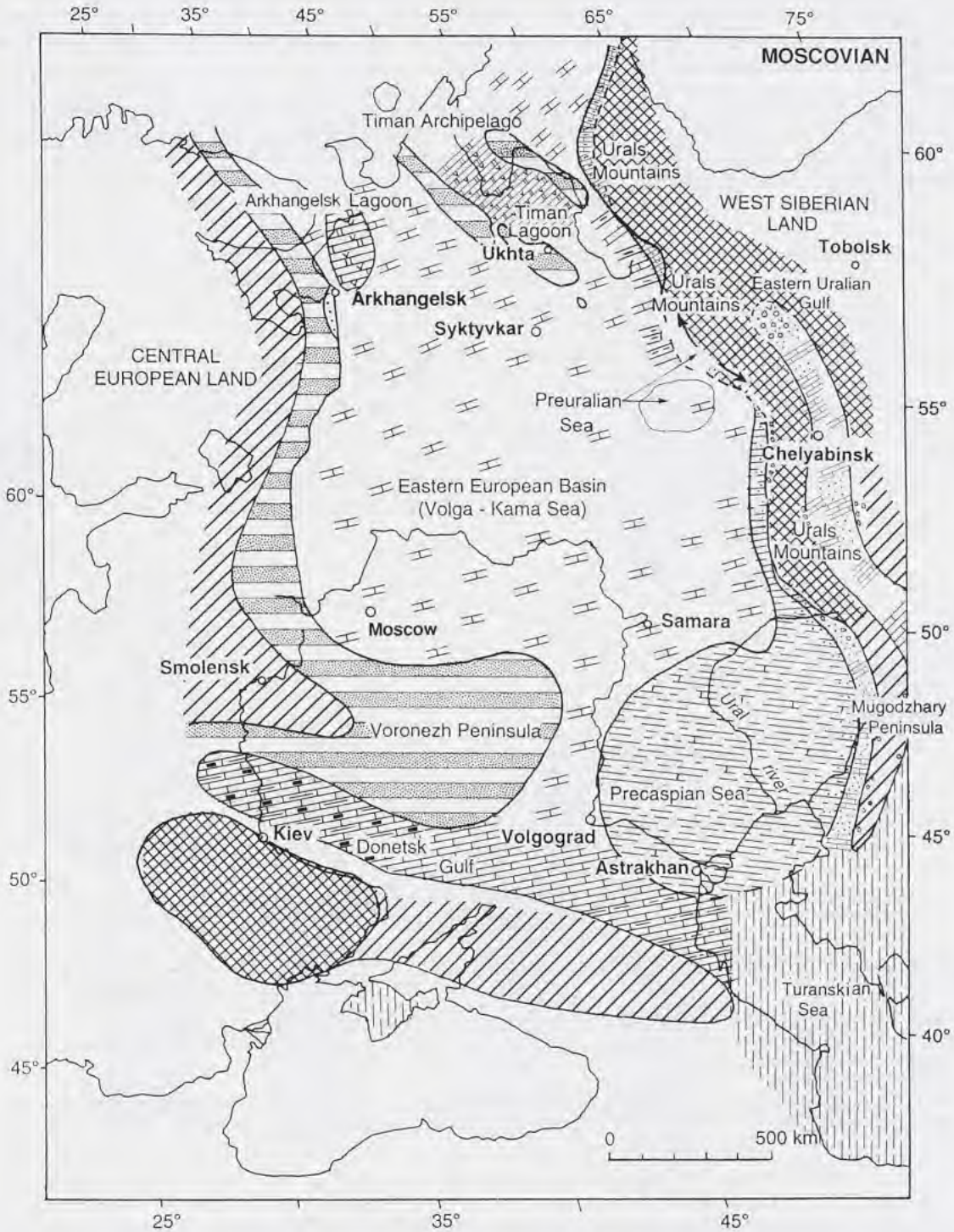

FIG. 3.— Palaeogeography of the Eastern European Basin during the Moscovian. See legend on Fig. 2.

FIG. 3.— Paléogéographie du Bassin Est-Européen durant le Moscovien. Légende voir Fig. 2.

Source : MNHN, Paris

Kama Sea with essentially shallow-water carbonate sediments and rather diverse biota. A very long and narrow Preuralian Foredeep was occupied by the deep-water of Preuralian Sea. Its southern part was connected with the large and deep-water Precaspian Sea. The growing mountain chains of the Palaeourals have separated Preuralian Sea from the Eastern Uralian Gulf (Fig. 3). Both were united to the south with Precaspian and Turanskian Seas.

Within the Preuralian Sea, there was a general uniformity of the sediments distribution: coarse-grained terrestrial and near-shore sediments in the east and replaced in western direction by the deep-water mainly clay sediments, themselves gradually replaced by shallow water carbonates. A very concise description of facial belts is given below (Figs 3-5).

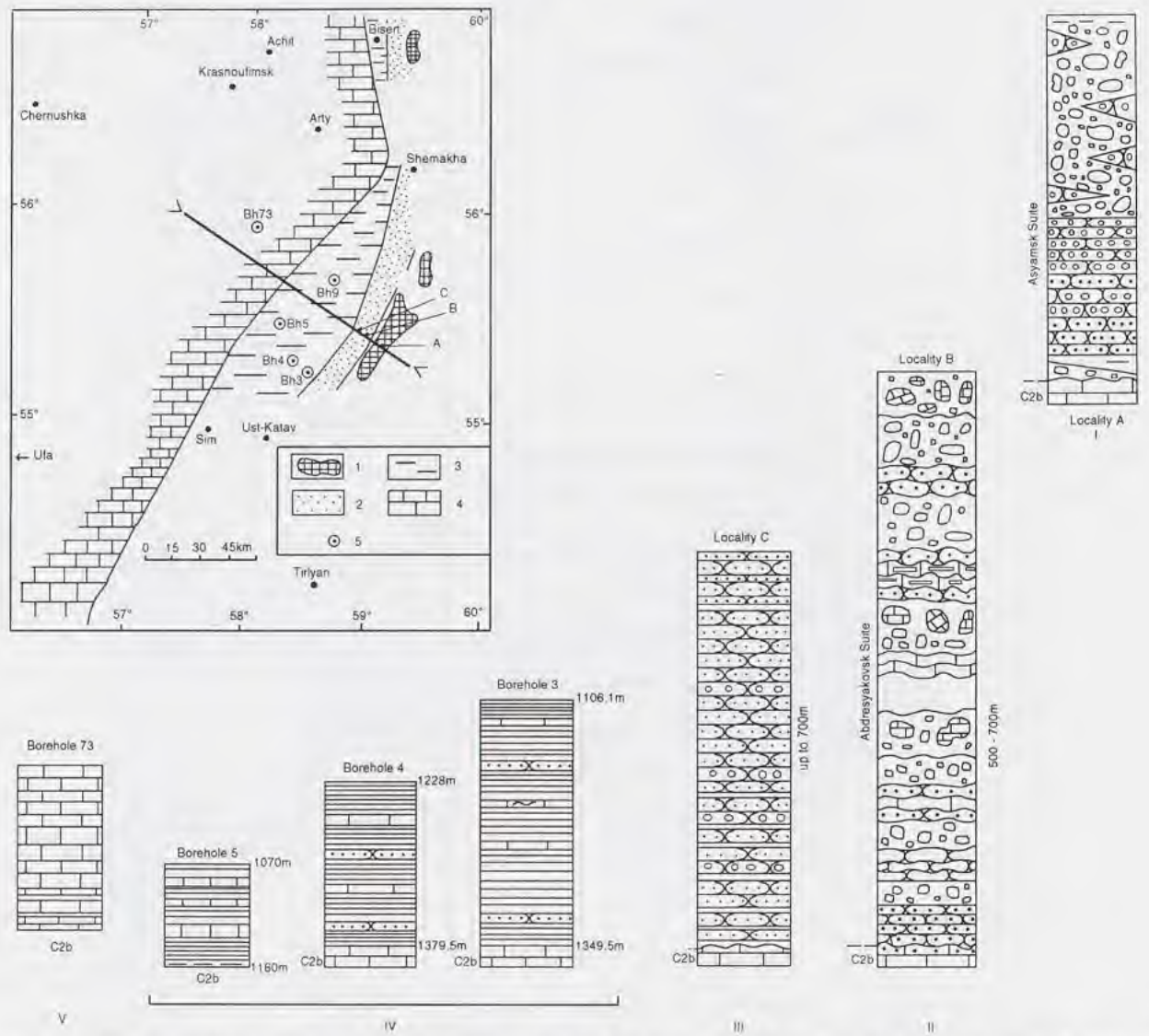

FIG. 4.— Main types of Moscovian sequences of the Preuralian Sea and their distribution within Ufa Amphitheatre . **1**, fields of Asyamsk Suite distribution; **2**, belt of distribution of types II (to the east) and III (to the west); **3**, area of type IV distribution; **4**, distribution of type V sediments - shallow water carbonates. **C2/b**, limestones of Bashkirian. Section see figure 5.

*FIG. 4.— Principaux types de faciès dans les séquences du Moscovien de la Mer Préouralienne et leur distribution dans l'Amphithéâtre d'Ufa. **1**, zone de distribution de la suite d'Asyamsk ; **2**, zone de distribution des faciès de types II (à l'est) et III (à l'ouest) ; **3**, zone de dsitribution des faciès de type IV ; **4**, zone de distribution des faciès de type V - carbonates d'eau peu profonde ; **C2/b**, calcaires du Bashkirien. Trait de coupe voir figure 5.*

Source : MNHN, Paris

— The terrestrial coarse-grained sediments are distributed within restricted and separated areas: in the eastern shore line of the north island of Novaya Zemlya archipelago (76°10N), in the Polar Urals (between 69°N and 67°10N), within the Ufa Amphitheatre (from 57°10N up to 55°N). The local distribution of the type of sediments along the Urals can be explained by the post Palaeozoic erosion. Sandstones, gravelstones and conglomerates compose the Eksinsk suite in the North Island (MATVEEV *et al.*, 1989). The Moscovian stage of Polar Urals is composed by similar sediments. The Moscovian carbonate breccias, sandstones, gravelstones and conglomerates are distributed along of the Ufa Amphitheatre. The thickness is 200-400 m.

— The near-shore marine coarse-grained sediments are also located in restricted areas along the western slope of the Urals, but are more widely distributed. Along the eastern slope of the Pay-Khoy Mountains within the Karsk Depression (between 69°N and 69°20N; Fig. 1), there are mainly sandstones (200-250 m) with fusulinids (CHERMNYKH, 1976). Similar sediments are distributed in the Pechora River upper stream area (between 60° and 60°20N). A rather thick sequence of conglomerates, gravelstones and sandstones, with marine fauna in some sandstone interlayers, occurs in the Ufa Amphitheatre (Figs 4-5). These sediments are considered as Abdresyakovsk Suite (Fig. 4) with a thickness up to 1000 m. Locally, this suite includes levels with large (up to 5-7 m) carbonate blocks, which represent partly the destroyed near-shore reefs and bioherms (CHUVASHOV, 1980). A similar sandstone-conglomerate sequence was studied in the Ural and Ilek Rivers basins (Fig. 1), between 52° and 51°N (KHVOROVA, 1961; RAUSER-CHERNOUSSOVA & KOROLUK, 1981). Some large (100-200 m) and thick (up to 15 m) lenses of alga and stromatolite limestones are included in this section with a total thickness averaging 800 m. Similar sandstone-conglomerate sediments with blocks of the biohermal limestones (2-3 m of diameter) have been found 30 km eastwards from Aktyubinsk.

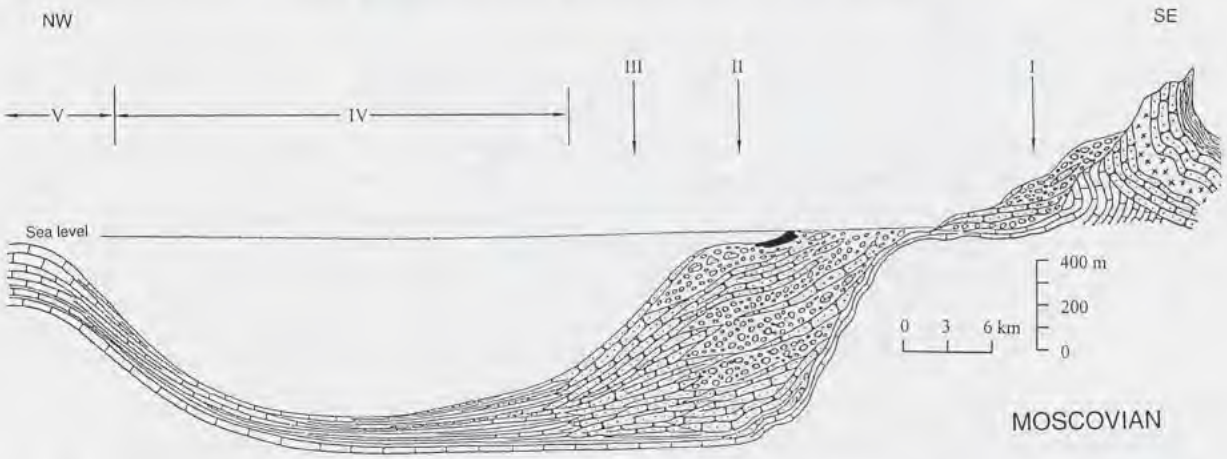

FIG. 5.— Palaeotectonical and facial profile of Moscovian sediments along the line of the figure 4, crossing different facial zones (roman numerals) from northwest to southeast.

FIG. 5.— Profil paléotectonique et faciologique des sédiments du Moscovien, le long de la ligne de la figure 4, recoupant les différentes zones de faciès (chiffres romains) du nord-ouest au sud-est.

— Flysh-like sediments. On the Polar Urals (between 69° 40N and 66°N), the lower part of Kech-Pel Suite (ROGOV *et al.*, 1988), a regular repetition of rather thin interlayers of fine-grained sandstones and argilites, could be dated as Moscovian (thickness up to 200 m). To the south, on a large extent of the western slope of the Urals (between 60°N and 55°50N) this facial zone was destroyed by the post-Permian erosion. The thick (up to 700-800 m) marine sequence of sandstones, argilites with rare interlayers of pelitic and detrital limestones, carbonate breccias, is traced to south till 56°50N (Figs 4-5). Southernmost, this type of sediments is present in the Sakmara and Ural Rivers basin (between 51°50N and 50°N). The thickness of sandstones, argilites with rare bed of detrital and micritic limestones could be up to 1500 m near the eastern boundary of this facial belt. The thickness decreases near the western boundary (400 m in the borehole at the latitude of Samara; TSCHEKOTOVA, 1990). Similar sediments are distributed between the Mugodzhary Mountains and the Precaspian Depression (Fig. 3) where they were drilled by numerous prospecting holes (Fig. 6) in oil fields: Alibek-Mola (17a on Fig. 6), Zhanazhol (17

Source : MNHN, Paris

on Fig. 6), Tortay (9 on Fig. 6), Emba (GRACHEV, 1956; AVROV *et al.*, 1962; AVROV & KROSMACHEVA, 1963; IVANOV, 1962 and 1966; DNEPROV, 1962; BULEKBAEV *et al.*, 1967; KARSTSEVA *et al.*, 1985). Usually, the Moscovian stage is here underlayered by limestones of the Serpukhovian and different levels of the Bashkirian. In Alibek-Mola area (17a on Fig. 6) the lower part of Moscovian is mainly represented by limestones (Vereiskian horizon: 48 m and Kashirskian: 160 m; Table 1). Essentially terrigenous sediments are distributed in the upper Moscovian, but significant (thickness up to 60 m) limestone packets are present in this part of the section. The thickness of the Podolskian horizon is close to 300 m and that of Myachkovskian to 129 m. In Tortay area (9 on Fig. 6), the terrigenous sediments are prevailing in the lower part of the Moscovian and carbonates are concentrated in the upper part.

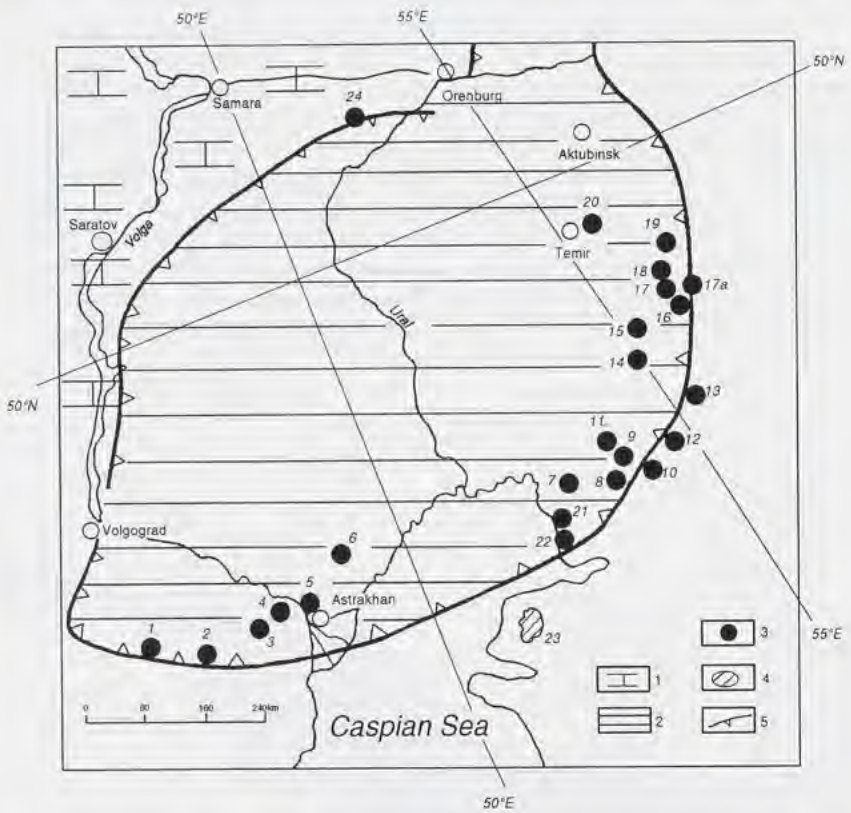

FIG. 6.— Location of main prospecting areas on the territory of Precaspian Depression. **1**, Carbonate frame of the Precaspian Depression; **2**, Precaspian Depression; **3**, boreholes and prospecting areas; **4**, large prospecting area; **5**, boundaries of Precaspian Depression.

*FIG. 6.— Localisation des principaux gisements de prospection sur le territoire de la Dépression Précaspienne. **1**, cadre de la Dépression Précaspienne, roches carbonatées ; **2**, Dépression Précaspienne ; **3**, forages et zones de prospection ; **4**, zones étendues de prospection ; **5**, limites de la Dépression Précaspienne.*

1, Sukhotinsk ; **2**, Karakulsk ; **3**, Vysokovsk ; **4**, Dolgozhdann ; **5**, Astrakhansk ; **6**, Zavolzhsk ; **7**, Karaton ; **8**, Tugarakchan ; **9**, Tortay ; **10**, Turesay ; **11**, Biikzhal ; **12**, Zhanasu ; **13**, Teresken ; **14**, Severny Kindisay ; **15**, Kursay ; **16**, Kokpekty ; **17**, Zanazhol ; **17a**, Alimbek - Mola ; **18**, Blansay ; **19**, Ostansuk ; **20**, Temir ; **21**, Krasnokhuduksk ; **22**, Tengiz ; **23**, Buzachi ; **24**, Karachaganak.

— The essentially clay and cherty-clayey sediments (depressional type) are traced almost everywhere from the Novaya Zemlya archipelago up to the Precaspian Sea. On the southern island of Novaya Zemlya archipelago, undivided Middle Carboniferous sediments are represented by very thin sequence (6-28 m) of cherty argilites, argilites and manganese bearing carbonates (PLATONOV *et al.*, 1992). These sediments are present in the Vaigach Island (Fig. 1) and on the eastern slope of the Pay-Khoy Mountains (between 70° and 68°N).

Source : MNHN, Paris

In the Lemva River area (between 68° and 66°N), from east to west, are recognised the series of undivided Middle-Upper Carboniferous (CHERMNYKH, 1976; ELISEEV, 1973, 1978). In the eastern part of this zone, the Moscovian stage is a part of Kharotsk series, a sequence of argilites and cherty argilites, deep-water limestones and dolomites; the thickness of this series exceeds 500 m. Next to west, the Kharutsk series is represented by a very thin (20-30 m) repetition of cherty and argilites. And westwards, the Worgashor series is composed of argilites and cherty argilites with interlayers of spongy limestones and silts (150 m). These sediments can be found in the upper stream of Pechora, Kolva, Vishera Rivers (Fig. 1) in the Northern Urals (between 62° and 61°N).

This type of Moscovian sediments is distributed without interruption from 56°40N to the Precaspian Basin. The depressional and other types of Moscovian sediments are shown on the figures 4 and 5. The relatively narrow belt of depressional sediments, distributed along the Urals, becomes very wide within the Precaspian Depression. On the perimeter of the Precaspian Depression (oil fields of Karachaganak in the north; Astrakhan Dome in the southwest; Yuzhno-Embensk uplift in the southeast; Tengis in the east; Fig. 6) is observed, above the Bashkirian shallow-water limestones, a monotonous sequence (60-250 m) of black argilites, marls, micrites with very rare and uniform fauna (radiolaria, sponges, ammonoids, fish remains, conodonts; KARIMOV *et al.*, 1990). Miospores were identified in some intervals. Within this sequence, there are thin grainstone beds with Middle and Late Carboniferous and Early Permian foraminifera. Usually, these organic remains are considered as reworked.

The Artinskian dating of the uppermost part is generally acknowledged. For the lower part, the age attributed could be: Artinskian (MOVSHOVICH, 1977; LAPKIN & MOVSHOVICH, 1978, 1994; LATSKOVA, 1976, and others), adopting a long time break between Bashkirian limestones and clay and marl sediments; late Bashkirian-Sakmarian (DALYAN, 1990; this paper) if we consider a continuous sedimentation. We shall consider each hypothesis in light of available material.

To the south of Karachaganak oil field reef formation (24 on Fig. 6) (ILYN *et al.*, 1987), above Bashkirian limestones, there are black argilites and marls (up to 60 m). Early Asselian conodonts were found in its middle part; the upper part contains Artinskian radiolaria and miospores.

In the Astrakhan uplift area (MOVSHOVICH, 1977) above Bashkirian limestones, was drilled a formation of black argilites and marls in the lower part; the numerous silt and sandstone interlayers occur in the top formation (whole thickness is 160 m). Some thin grainstone interlayers, with Middle-Late Carboniferous and Asselian foraminifera, are found in lower and middle part of the formation. The upper part contains Artinskian radiolaria and miospores and the age of the formation as a whole is adopted as Artinskian (MOVSHOVICH, 1977; LAPKIN & MOVCHOVICH, 1994). All above mentioned foraminifera are considered as reworked, according to existing pattern. Similar situation is observed everywhere along the borders of the Precaspian Depression.

The depressional sediments of the Preuralian foredeep were gradually replaced westwards by the shallow-water, sequence, mainly carbonated, representing deposits of the Volga-Kama basin (Figs 3-5). It is very important to note that on the border of the Russian Platform and Foredeep, organic build-ups did not exist and the transitional zone is rather narrow (1-3 km). Numerous islands, with low relief, were present on the Volga-Kama territory at the beginning of Moscovian as a result of the Bashkirian regression. These islands were baring areas during the early Moscovian. Such conditions of sedimentation have defined lithological composition of the lower substage (Vereiskian and, at a smaller scale, Kashirskian horizon sediments): usually argilites and marls, less often sandstones, gravelstones and carbonate breccias. At the top of the Moscovian, except with prevailing detrital and biogenic carbonates, dolomites became rather common and locally evaporates are present.

In the Pechora River basin (on right bank), the thickness of Moscovian shallow water carbonates could reach 200-300 m (CHERMNYKH, 1976). The numerous packets of carbonate breccias, with blocks up to 1-5 m, are present in this area (CHUVASHOV, 1994). The upper Moscovian contains significant thickness of dolomites and anhydrite along of the left side of the Pechora valley near Timan (Fig. 3).

On the large territory of the Western Urals and Cis-Urals, from the Kolva River to the Ay River (between 61°20 and 56°N) (Fig. 1), there are two folded types of Moscovian. The lower one (Vereiskian and Kashirskian horizons in whole) is represented by argilites and marls with interlayers of limestones, silts and sandstones. The upper part is composed mainly of detrital and biogenic limestones with rich and diversified fauna (RAUSER-CHERNOUSSOVA, 1961b). To the west of the Urals, secondary dolomites

Source : MNHN, Paris

significantly increase. The most important thickness of the Moscovian stage (350-400 m) is recorded near Staroutkinsk Settlement (Chussovaya River Basin; Fig. 1, ≈57°N; PAKHOMOV & DOSORTSEV, 1966; TSCHERBAKOV & TSCHERBAKOVA, 1966).

Along of the Middle Volga (north of Samara, Fig. 3), the Vereiskian horizon (25 m) is a sequence of the reddish and greenish-grey argilites with dolomites, silts and sandstones. Dolomites and limestones prevail in the Kashirskian horizon (80 m); silts and sandstones at the bottom. Podolskian (113 m) and Myachkovskian (124 m) horizons are represented by limestones and dolomites with prevalence of first one (RAUSER-CHERNOUSSOVA, 1961a).

In the Volgograd region (Figs 1-3), contiguous with the northwestern Precaspian Depression, there is the next sequence of Moscovian (SEMIKHATOVA, 1961). Vereiskian horizon (22-125 m) is composed of argilites and silts with sandstone and limestone interlayers. The thickness of this horizon decreased to the northwest. The Kashirskian horizon (100-324 m) is represented by argilites and marls with numerous carbonate beds. Both Podolskian (140 m) and Myachkovskian (124 m) horizons are represented by limestones and dolomites with beds of marls and argilites.

Within the Moscow Synclinal, the Moscovian stage is represented by such sequence (IVANOVA & SHIK, 1978; MAKHLINA *et al.*, 1997). The Vereiskian horizon contains three members (from bottom to top; Table 1): Shazk member (3-10 m), argilites and sandstones with thin limestone and marl interlayers containing brachiopods and fish remains; Alyutovsk member (5-19 m), argilite-limestone alternation with sandstones in the middle part of section; Ordynsk member (5-10 m), argilites and clayey limestones.

The Kashirskian horizon (60-70 m) combines carbonates with some interlayers of red and pink argilites and silts. Fusulinids, corals and brachiopods are recognised. A conglomerate bed marks the bottom of the stratotype of the Podolskian horizon near Podolsk (Fig. 1); above, thin-bedded limestones with rich and diverse fauna of foraminifera (including fusulinids), corals, brachiopods, crinoids and calcareous algae. The Myachkovskian horizon (19-24 m) is represented by white and white-grey detritic and biogenic limestones with algae and a very rich fauna.

The original sequence of Moscovian sediments is present in the Donetsk Gulf (Fig. 3), where coal-bearing paralic deposits are accumulated (1800-3000 m thick). The rare and wonderful combination of normal marine (fusulinids, corals, brachiopods, bivalves, ammonoids, ostracods and conodonts) and terrestrial (bivalves, plants, miospores) organic remains could be noted for this section. A short summary description is given below (after AISENVERG & ROTAY, 1978).

At the basis of the Moscovian stage, the sediments belong to the biostratigraphic zone C2 m/a (450-600 m): alternation of sandstones and argilites with 6 or 7 limestone beds. Some coal seams (part of them industrial) occur in this sequence. The next zone C2m/b (150-500 m) differs from the underlying by smaller development of sandstones. The zone C2m/c (250-450 m) contains 5 thick limestone beds, some industrial coal seams and a lot of coal interlayers. The zone C2m/d (250-400 m) contains 5-8 limestone beds. The highest Moscovian zone C2m/e (360-600 m) includes up to 10 limestone beds 5-6 of which are widely distributed.

At the east of Palaeourals, the Eastern Uralian Gulf (EUG) is traced along the mountain system on more than 1000 km (Figs 3-5). The width of this gulf (before folded and thrusting shortening) was about 200-250 km. Biostratigraphy and palaeogeography of the EUG were previously described (CHUVASHOV *et al.*, 1984). A very concise conclusion is presented below.

A thick sequence of coarse-grained terrestrial sediments (red argilites, silts, sandstones and conglomerates), with locally lenses of gypsum and anhydrite, could be followed along western and eastern shore lines of the EUG. On the eastern border of gulf (Tobol River Basin, latitude 52°30N; Figs 1, 3, 9), volcanic rocks and tuffs with clastic terrestrial sediments, are recognised with a thickness up to 1000 m.

The inner part of the EUG, in its northern half, is filled by marine flysh-like sediments. Beds and packets of limestones, conglomerates and gravelstones are distributed locally within the flysh-like sequence. The carbonates increase southwards and the Moscovian in whole is composed by shallow-water carbonates with prolific fauna and calcareous algae near the southern end of the EUG (Figs 3, 9).

To the east of the EUG (Figs 3, 9), an extensive continent took place. In the restricted intermountain

Source : MNHN, Paris

depressions, occur red-coloured clay-sandstone deposits or conglomerates and gravelstones-sandstones. In numerous areas of the recent West-Siberian plate, those sediments are associated with the thick blocks of volcanic rocks and tuffs. The poor palaeontological data (bivalves, plants and miospores) permit, after all, to consider that these terrigenous sediments and volcanic rocks were accumulated during a long time, from the second half of Bashkirian up to the end of the Permian.

The southern edge of the EUG (Figs 3, 9) was separated from the Precaspian Sea by the Mugodzhary Peninsula. To the south of the Precaspian Sea, the EUG was merged in the Turanskian Sea. There are some arguments to follow the EUG to the south in the region of Aral Sea, where, on geophysical data (PAK, 1988; BABADZHANOV *et al.*, 1989; PILIPENKO, 1990), the Aralo-Murgabsk rifts dissected, from north to south, the middle part of the Turansk plate. The northern branch of this zone passed along the western shore line and jointed the middle part of the Aral Sea. In this graben, Upper Palaeozoic-Mesozoic sediments are recognised with a total thickness up to 8-10 km. Amongst this sequence, under the Jurassic, are defined by geophysical methods, the Upper Palaeozoic-Triassic rocks with a thickness

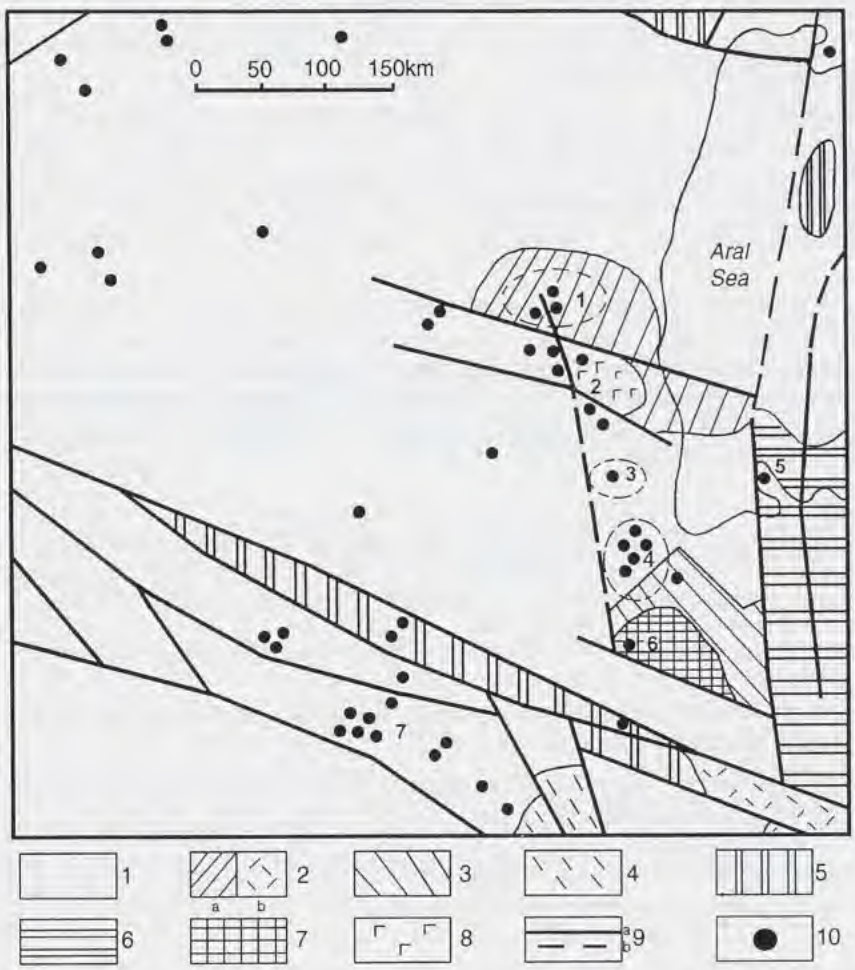

FIG. 7.— Geological map of the Usturt territory without Jurassic-Quaternary deposits (after KARTSEVA & KIRUKHIN, 1974). **1**, Upper Permian-Triassic; **2**, Upper Carboniferous-Lower Permian; **2a**, slates; **2b**, volcanic rocks; **3**, Lower Carboniferous; **4**, Lower-Middle Carboniferous; **5**, Middle Palaeozoic (Silurian - Lower Carboniferous); **6**, Precambrian and Palaeozoic; **7**, Precambrian only; **8**, diabases of porphyrite; **9**, faults: a- real and b- suggested; **10**, boreholes: 1- Baiterek; 2- Sarytekis; 3- Karakunduk; 4- Priozerny; 5- Kisylshaly; 6- Koskala; 7- Shakhpakhty.

*FIG. 7.— Carte géologique écorchée du territoire d'Usturt, sans les dépôts du Jurassique au Quaternaire (d'après KARTSEVA & KIRUKHIN, 1974). **1**, Permien supérieur - Trias ; **2**, Carbonifère supérieur - Permien inférieur ; **3**, Carbonifère inférieur ; **4**, Carbonifère inférieur et moyen ; **5**, Paléozoïque moyen (Silurien à Carbonifère inférieur) ; **6**, Précambrien et Paléozoïque ; **7**, Précambrien seul ; **8**, diabases de porphyrites ; **9**, failles: a - prouvées, b - suggérées ; **10**, forages : 1 - Baiterek ; 2 - Sarytekis ; 3 - Karakunduk ; 4 - Priozerny ; 5 - Kisylshaly ; 6 - Koskala ; 7 - Shakhpakhty.*

Source : MNHN, Paris

0.4-0.2 km. In this interval, there is a zone (2-3 km in width) with very irregular reflection of the seismic waves, related to reef distribution. This suggestion is supported by the drilling data. In the Karakuduk bore-hole (3 on Fig. 7), the Upper Palaeozoic carbonates are reached. Marine clayey silts are penetrated by Priozerny borehole (4 on Fig. 7). The exact age of the formations is not established, but the general regularity of more wide Moscovian sediments distribution compared with Upper Carboniferous-Asselian, suggests the existence of Moscovian polyfacial sediments near and within the Aral Sea area.

The synthesis on Upper Palaeozoic of the Aral region according to drilling data was made by KARTSEVA & KIRUKHIN (1974). They have shown (Fig. 7) that, under Jurassic sediments, are widely distributed Asselian-Upper Carboniferous and Triassic-Upper Permian deposits. The regularity of sediments permits to assume a wide distribution of Moscovian stage here.

The palaeogeography of the southeastern part of the Turanskian Sea is reconstructed mainly prospectively (Fig. 9) (COOK *et al.*, 1994). The very thick, mainly carbonated, Famennian-Bashkirian sequence has been studied in the Kara-Tau Ridge. To the west, a borehole drilled, on more than 1 km, evaporates (gypsum), which are considered as the higher part of the section. The Moscovian and younger sediments could be amongst the evaporites. This kind of deposits could be accumulated only within a large lagoon (Kara-Tau Lagoon).

The western extremity of this lagoon was represented by the shallow-water marine carbonate-terrigenous sediments of the Nura-Tau Mountains area, which was located immediately to the west of Kara-Tau Lagoon (Fig. 9; IBRAGIMOV *et al.*, 1989). Above the late Bashkirian conglomerates and sandstones, the lower Moscovian bioherms, up to 50 m in thickness, are overlapped by a thick (up to 700 m) sequence of argilites, silts, sandstones with lenses and beds of conglomerates, tuffs and limestones.

In the central Kisyl-Kum (area of Tokhtinikhtau Mountains; Fig. 9), the Moscovian stage is represented by Tokhtatausk series, subdivided into three members. The lower (490 m) is composed by sandstones, gravelstones and conglomerates with rare limestone beds. The middle member (700 m) is represented by sandstones, gravelstones, silts, argilites and limestones. The upper member (650 m) is very similar to the lower one. All this sequence could be considered as marine near-shore sediments (KALASHNIKOV & ASKAROV, 1989).

Very sketchy data exist on the Moscovian of the western part of the Turansk Sea on the Busachy Peninsula (Fig. 6; KARTSEVA, 1979). A borehole (23 on Fig. 6) drilled (interval 2000-3500 m) dark-grey micritic and detrital limestones with interlayers of carbonate breccias and rudstones. Upper Carboniferous and Asselian foraminifera are determined in the interval 2172-2924 m.

In the Bukhara-Karsha region (right side of the Amu-Darya River Valley; Figs 8-9), the Upper Palaeozoic deposits were drilled by numerous boreholes (USAKOV, 1985) with Moscovian limestones holding foraminifera. For other prospecting areas, the Moscovian stage could be supposed under the Upper Carboniferous and Lower Permian.

The Moscovian stage in the region of Balkhash Lake or within the Balkhash Bay (Fig. 9) is subdivided into three palaeogeographic members (BOGUSH *et al.*, 1976; YUFEREV & SOKOLOV, 1976):

— with *Choristites fritchi* (118-183 m): alternation of sandstones, silts, cherty argilites and tuff beds and packets; organic remains are represented by foraminifera, corals, brachiopods, bivalves, gastropods and ammonoids;

— with *Alljutovella* (35-47 m): represented in the southern area by limestones with foraminifera, corals and brachiopods. In the northern part, the coeval sediments are composed of sandstones and tuffs. A limestone packet (27-32 m) with foraminifera, solitary and colonial corals, brachiopods and algae overlies them;

— with *Profusulinella rhomboides*; this member, on the southern part of synclinal, is represented by alternation of cherty-clays, argilites, silts and sandstones, detrital limestone beds and packets (78 m). On the northern edge of this structure, there are three groups. The lower one (31 m) is composed of the silts with tuffs and sandstones. The middle one (77 m) is represented by calcareous silts with brachiopods and numerous cephalopods. The upper one (92 m) is composed of coarse-grained sandstones and tuffs with small pebbles. Brachiopods, gastropods, cephalopods and large wood trunks are present.

Source : MNHN, Paris

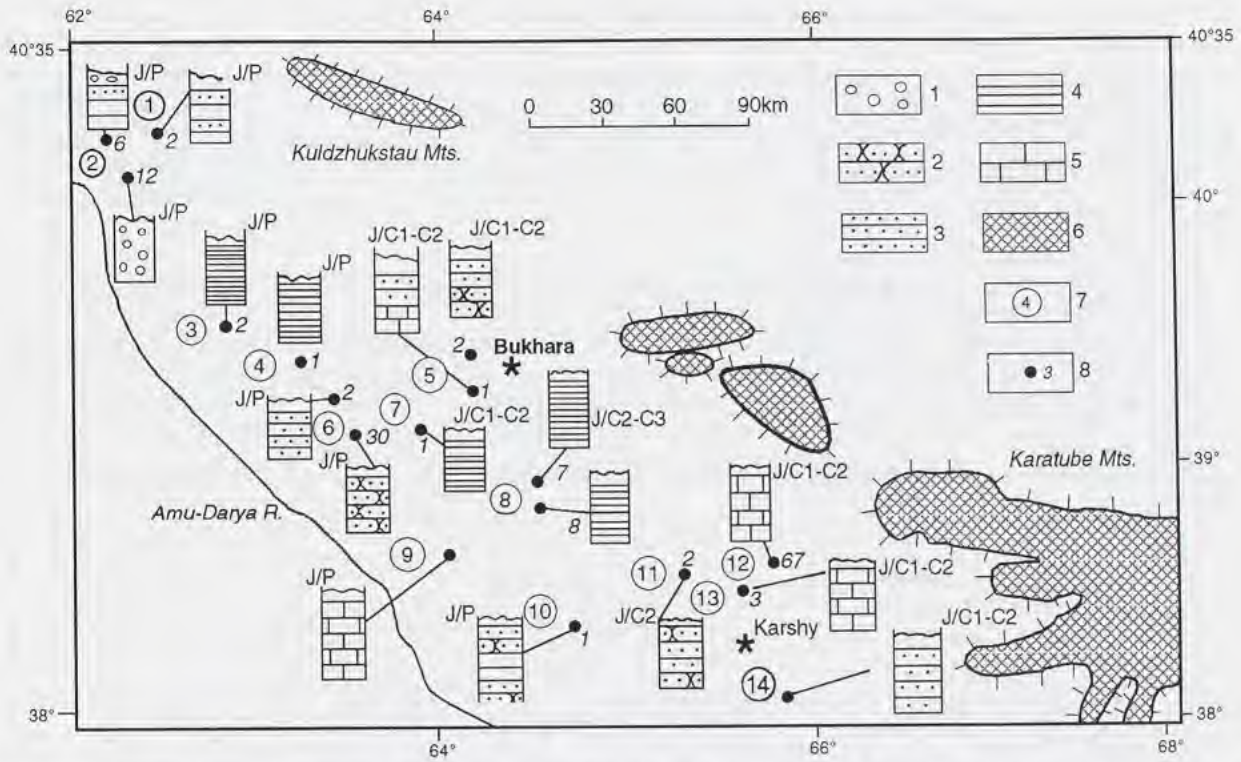

FIG. 8.— Area of Upper Palaeozoic distribution on the right side of the Amu-Darya River (after USAKOV, 1985). **1**, conglomerates, gravelstones; **2**, sandstones; **3**, silts; **4**, argilites; **5**, limestones; **6**, outcrops of pre-Mesozoic rocks; **7**, Prospecting areas: 1- Dautepe; 2- Yankikasgan; 3- Khatar; 4- Sverdlov; 5- Kandym; 6- Chandyr; 7- Zekry; 8- Bayshirin; 9- Pamuk; 10- Severny Mamanak; 11- Severny Karaktay; 13- Sapadny Karaktay; 14- Shurtan. **8**, numbers of boreholes with Upper Palaeozoic; C1- Lower Carboniferous; C2- Middle Carboniferous; C3- Upper Carboniferous; P- Permian; J- Jurassic.

*FIG. 8.— Zone de distribution du Paléozoïque supérieur sur la rive droite de l'Amu-Darya (d'après USAKOV, 1985). **1**, conglomérats, graviers ; **2**, grès ; **3**, silts ; **4**, argilites ; **5**, calcaires ; **6**, affleurements de roches anté-mésozoïques ; **7**, zones de prospections: 1 - Dautepe ; 2 - Yankikasgan ; 3 - Khatar ; 4 - Sverdlov ; 5 - Kandym ; 6 - Chandyr ; 7- Zekry ; 8 - Bayshirin ; 9 - Pamuk ; 10 - Severny Mamanak ; 11 - Severny Karaktay ; 13 - Sapadny Karaktay ; 14 - Shurtan ; **8**, numéros des forages avec du Paléozoïque supérieur ; C1 - Carbonifère inférieur ; C2 - Carbonifère moyen ; C3 - Carbonifère supérieur ; P - Permien ; J - Jurassique.*

YUFEREV & SOKOLOV (1976) considered that the marine Balkhash Gulf was merged to the south with the Ob-Saisan Sea (to the east on the map, Fig. 9) and was surrounded to the west, the north and the northeast by the mountainous land with active volcanic activity. If the second part of this assertion can be adopted without any comment, the first one, about gulf communications, can not be accepted. The whole fauna and alga assemblages of the Moscovian Balkhash Gulf show the connection of this gulf with biotas of both Tethyan and Eastern European Basins (Fig. 9) without any incursion of the very specific fauna of the Ob-Saisan Sea.

MOSCOVIAN PALAEOBIOGEOGRAPHY

The Moscovian palaeogeographic situation is supported by the biogeographic data, showing the wide and free communications between Tethyan and Uralian biotas. The results of fusulinid study were used for restoration of the connection ways between Arctic, Eastern European and Tethyan Basins (IVANOVA & CHUVASHOV, 1990). The fusulinid fauna of the Preuralian Sea shows a significant influence of the Northern American biota (genera *Pulchrella*, *Pseudofusulinella*, *Wedekindellina*). A migration way of those fusulinids along of the Palaeourals shoreline is distinctly traced. The southernmost distribution of these American genera is limited to 53°N. To the south of this latitude, the fusulinid fauna are closer to Tethyan and Donetsk Gulf ones (some genera as *Putrella*, *Eofusulina*, *Hemifusulina*).

Source : MNHN, Paris

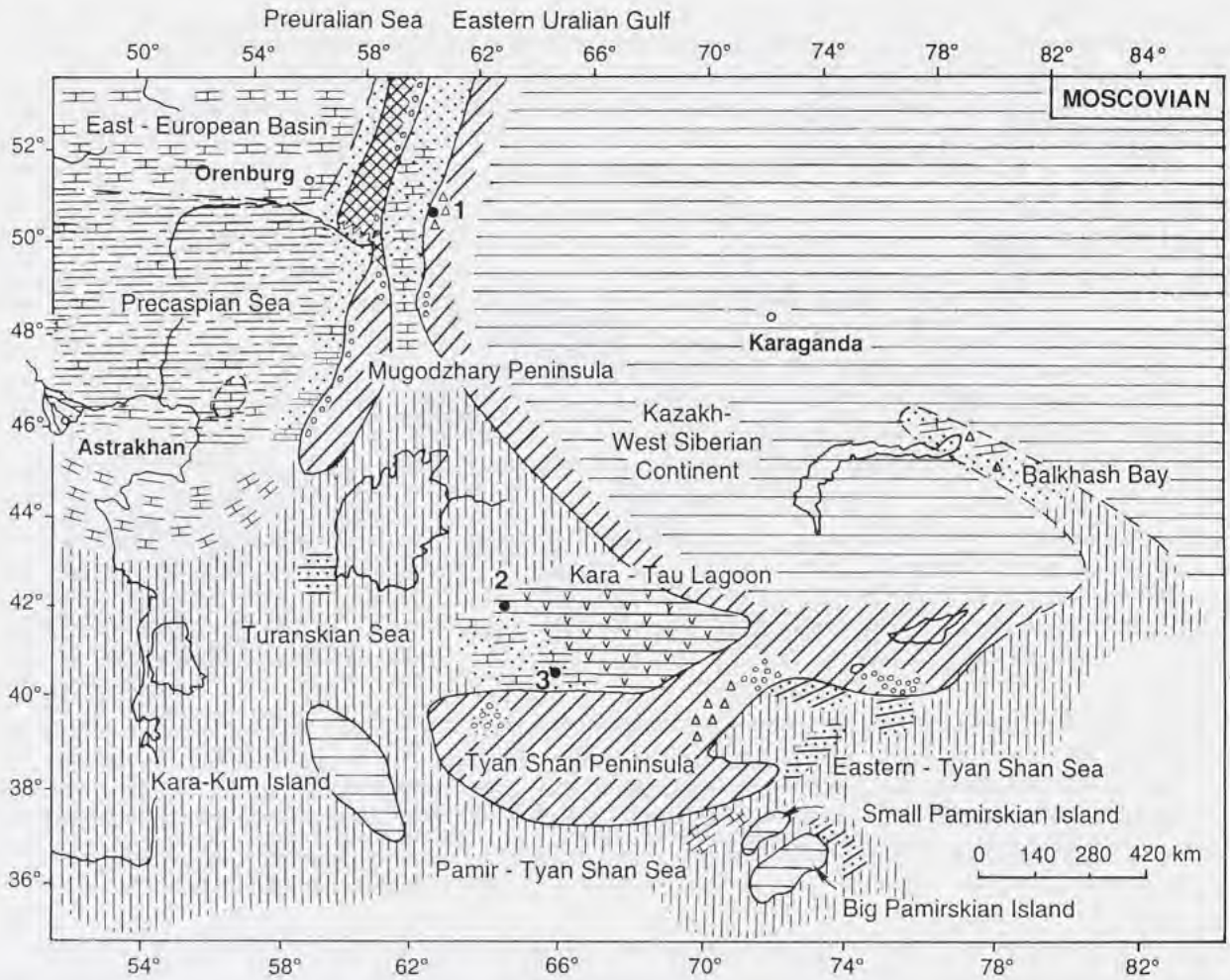

FIG. 9.— Palaeogeographic map of jointing zone of the Eastern European and Tethyan Basins during Moscovian (late Moscovian). **1**, area of Tobol River - terrestrial terrigenous sediments with volcanic rocks. **2**, Toktynyktau Mountains; **3**, Nura-Tau Mountains. Legend: see Fig. 2.

*FIG. 9.— Carte paléogéographqiue de la zone de jonction du Bassin Est Européen et de la Téthys au Moscovien (Moscovien terminal). **1**, région de la rivière Tobol, sédiments continentaux terrigènes avec roches volcaniques ; **2**, Montagnes de Toktynyktau ; **3**, Montagnes de Nura-Tau. Légende : voir Fig. 2.*

New results on the Moscovian fusulinids of southwestern Darvaz, Pamir were recently published (LEVEN, 1998). Most of Moscovian fusulinid genera and species of this area are identical with fusulinid biota of the Eastern European Basin. Only some genera are endemic. *Undatofusulina* is known in the Pamir and the Middle Asia in whole and in the Donetsk Basin. *Putrella* is distributed within the same territory and in the southern part of Eastern Uralian Gulf.

A great similarity could be noted between Moscovian fusulinids of Eastern European and Tethyan Basins. For example, Moscovian foraminifera of Vietnam (NGUEN VAN LIEM, 1982) and Thailand (TORIYAMA *et al.*, 1975), according to the present genera, are very close to fusulinid biota of the Russian Platform or, in other words, of the Volga-Kama Sea.

Taxonomic assemblages between the Moscovian brachiopods of Near-Polar Urals and Central Kisyl-Kum (KALASHNIKOV & ASKAROV, 1989) share a lot of genera and species: *Choristites priscus* (Eichw.), *Ch. sowerby* (Fish.), *Brachithyrina subcarnica* (Ilov.), *Chaoiella gruenewaldti* (Krotov), *Linoproductus simensis* (Tchernyshew), *Meekella eximia* (Eichw.), *Enteletes lamarcki* (Fish.), *Neospirifer postriatus* Nik.

Source : MNHN, Paris

Three biogeographic assemblages of calcareous algae are recognised (CHUVASHOV *et al.*, 1995). One of them characterises both slopes of the Southern Urals in the basin of the Urals and in Mugodzhary Mountains (CHUVASHOV & ANFIMOV, 1988). A specificity of this assemblage is a great diversity of green algae (*Anchicodium, Neoanchicodium, Epimastopora, Gyroporella, Macroporella*, different Beresellids) and similarity with coeval Tethyan assemblages (Middle Asia, KHODZHANYAZOVA, 1991; Pyrenees Mountains, RA'CZ, 1966). It is possible to assume, that the distribution of this Uralian alga association goes up to 53°N.

The importance of the green algae and their diversity is regularly decreasing to the north, along the Urals. The Middle Urals and the most part of the Russian Platform at the same latitudes show assemblages belonging to the Beresellid realm (*Dvinella, Beresella, Uraloporella*). Mainly red algae (*Ungdarella, Komia, Pechoria*) were recognised in the northern part of the Urals and northeastern part of the Russian Platform. This alga distribution could be explained by the decrease of the temperature from south to north along the Palaeourals Mountains.

All these data show the mutual and stable connections between Tethyan and Eastern-European Basin biotas.

THE ASSELIAN

The Asselian stage is subdivided into two horizons (from bottom to top): Kholodnolozhskian and Shikhanskian. In the first one, the following fusulinid zones are identified: Daixina bosbytauensis - Daixina robusta zone; Sphaeroschwagerina fusiformis zone; Sphaeroschwagerina moelleri - Pseudofusulina fecunda zone. The Shikhanskian horizon corresponds to the Sphaeroschwagerina sphaerica - Pseudofusulina firma zone. The maximum of the Asselian transgression is linked with the "moelleri-fecunda" zone. The palaeogeographic situation shown on the maps (Figs 10-12), basically reflects this phase of the geological history.

ASSELIAN PALAEOGEOGRAPHY OF EASTERN EUROPEAN BASIN

During the Asselian, the area of Eastern European Basin is reduced; its width, at Moscow latitude, does not exceeded 1000 km (Fig. 10). Some very important geological events between the Moscovian and the Asselian and during the Asselian should be pointed out. At the beginning of the Late Carboniferous, the Eastern Uralian Gulf, and at the end of middle Asselian, Donetsk Gulf, were closed. With the development of the Preuralian Foredeep, the Preuralian Sea boundaries received a more sharp geomorphological impression; a reef barrier arose on the boundary with Volga-Kama Sea or, in other words, on the border of the Russian Platform. This barrier is traced from the Arctic Ocean to the northern rim of the Precaspian Depression. This last one is deepening in relation with the structural environment (Palaeourals and Mugodzhary Mountains, Russian and Turansk Plates).

On the borders of the Preuralian Sea, from east to west, some facial zones could be traced. They are defined before for the Moscovian, but for the Asselian the differentiation between facial zones is clearer and the preservation of the eastern facies is better. All the Asselian facies of the Preuralian Sea can be described as follow (Figs 11-12).

— Mainly sandstone sequence with lenses and packets of the boulder-pebble conglomerates; numerous interlayers of silts and argilites, and some beds of detritic limestones. A grading bedding is typical for sandstones and detritic limestones. Among this sequence, rather thin (up to 3-2 m) stromatolite, brachiopod, bryozoan, algae and *Palaeoaplysina* organic build-ups could occur. Significant olistostromes (2-20 m) are sometimes present. Rather thick (up to 250 m) carbonates breccias could be recognised in uppermost part of the sequence. The thickness of the serie reaches 1500 m in the Southern Urals and 700-800 m in the Middle Urals.

Source : MNHN, Paris

Fig. 10.— Palaeogeographic map of the Eastern European Basin during the Asselian. Legend: see Fig. 2.

Fig. 10.— Carte paléogéographique du Bassin Est Européen durant l'Assélien. Légende : voir Fig. 2.

Source : MNHN, Paris

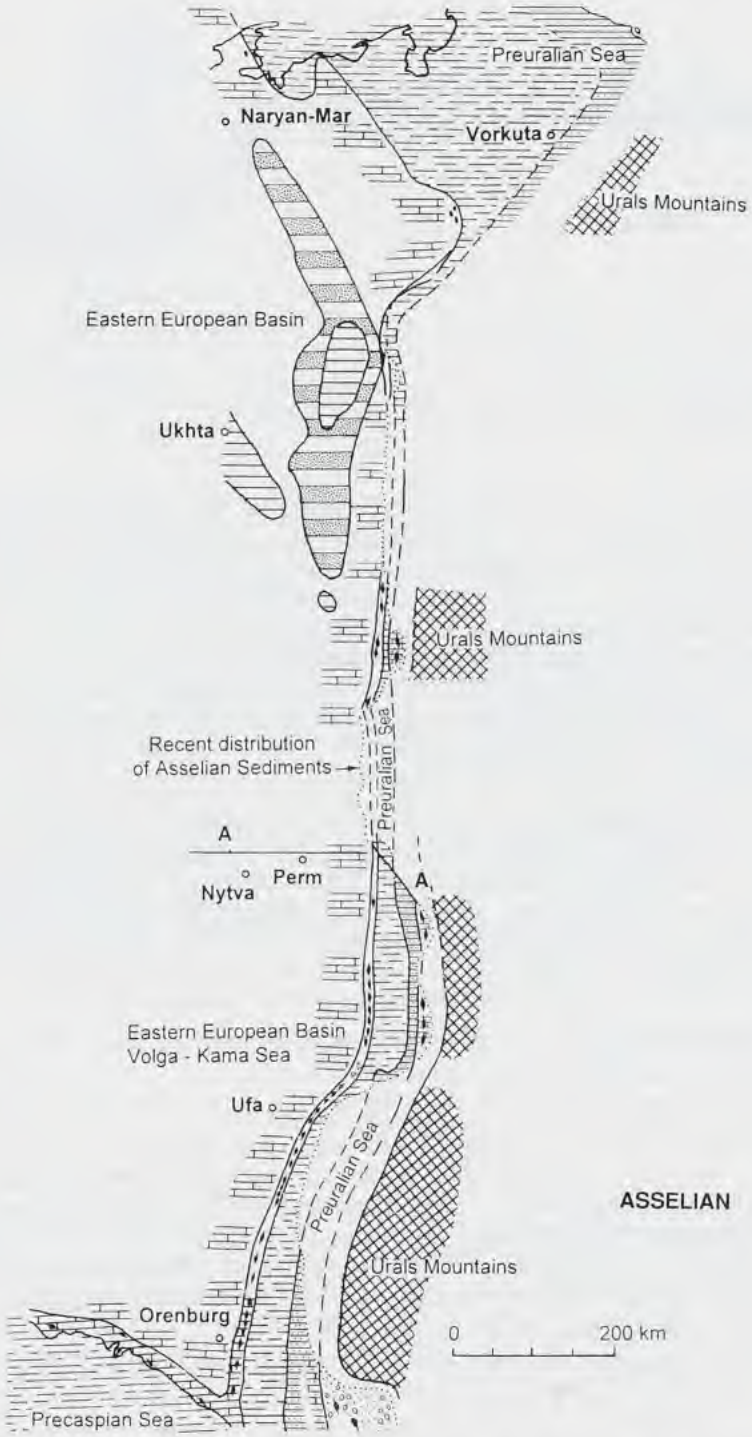

FIG. 11.— Palaeogeographic map of the Preuralian Sea during the Asselian. Section A-A1: see figure 12; Legend: see Fig. 2.

FIG. 11.— Carte paléogéographique de la Mer Préouralienne durant l'Assélien. Coupe A-A1 : voir figure 12. Légende : voir Fig. 2.

Source : MNHN, Paris

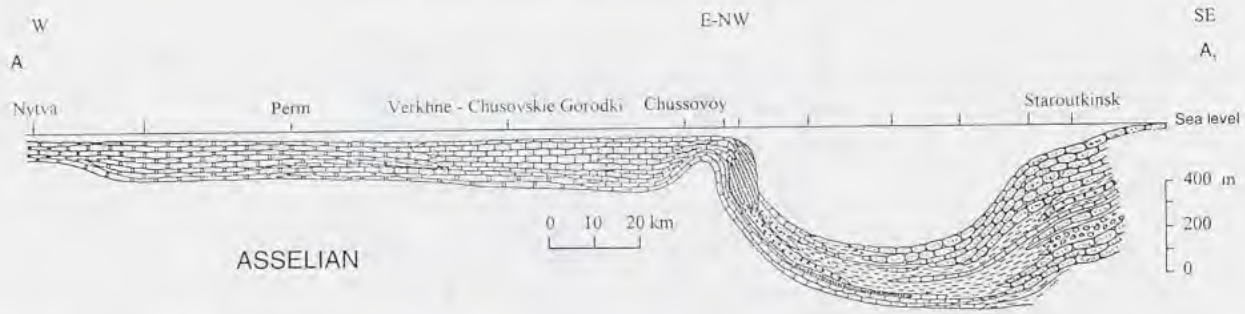

FIG. 12.— Palaeotectonical and facial profile of Asselian sediments on the Perm latitude (section A-A1 on Fig. 11). Legend: see Fig. 2. Arrows show the used sections.

FIG. 12.— Profil paléotectonique et faciologique des sédiments de l'Assélien à la latitude de Perm (coupe A-A1 sur la figure 11). Légende : voir Fig. 2. Les flèches montrent les forages utilisés.

This type of section differs by richness and diversity of the organic communities. The detritic limestones contain small foraminifera, fusulinids, corals, fragment of brachiopods and bryozoans, crinoids, ostracods, algae, which were displaced by grainflows from shallow water coastal areas to the deeper parts of the basin. The set of marls, argilites and micritic limestones, cherts, which are intersected by the turbidite beds, contain an another autochthonous association of organisms: radiolaria, sponges, bivalves, ammonoids, nautiloids, trilobites, conodonts, fish remains, worm trails. This facial type is distributed within two restricted areas. The northern one is located (Figs 10-11) between 57°30 and 56°50N, and the southern area corresponds to the basin of the Sakmara and Ural Rivers (between 52° and 50°N). This belt of the coarse-grained sediments is traced on the eastern rim of the Precaspian Depression (BOGATYREV & EVENTOL, 1962) (Fig. 13).

— To the west, the next facial zone is also represented mainly by sandstones, but there is here a rather regular alternation of thin (5-15 cm, seldom up to 50-70 cm) sandstone beds with silt and argilite interlayers. Usually, rare beds of detrital limestones, thinner than in the eastern facial zone, are included in this uniform sandstone-argilite sequence. Organic remains could be divided into two groups: allochtonous in turbidites (foraminifera, including fusulinids, corals, brachiopods, bryozoans, crinoids and algae) and autochthonous, within clay interlayers between sandstone beds: radiolaria, sponges, bivalves, ammonoids, fishes, conodonts. The thickness of this type seldom exceeds 500 m.

The distribution of these deposits is more uniform than for the first type. This type is absent only in a restricted area located between 58° and 60°N (Fig. 10).

— Further west, the third facial zone is distributed almost everywhere from the Novaya Zemlya archipelago to the north up to the Precaspian Depression to the south. The most significant width in the latitudinal direction is 70-75 km. This type of section is represented mainly by argilites, cherty argilites, marls and micritic limestones. Three subtypes could be recognised amongst these deposits (CHUVACHOV & DYUPINA, 1973; TSCHERBAKOVA *et al.*, 1979; CHUVASHOV *et al.*, 1990): eastern, central and western (Fig. 12). The eastern subtype is characterised by presence of the sandstone beds, packets and a small increase of thickness (up to 120 m). The central subtype is composed mainly of marls and argilites with cherts and has an insignificant thickness (20-50 m). The western subtype is characterised by limestones and marls with carbonate breccias and conglomerate packets and lenses. The thickness of this type could be up to 150 m.

The biota could be divided into two assemblages: allo- and autochthonous. The first group contains the shallow-water organisms: foraminifera (including fusulinids), single and fragment of colonial corals, brachiopods, bryozoans, crinoids, algae, which are transported in the deep part of basin by the sandy grainflows from the premountain shallow-water. Similar assemblage is present within carbonate turbidites and breccias, which are displaced from the western rim of Russian Platform to the east by grainflows.

Source : MNHN, Paris

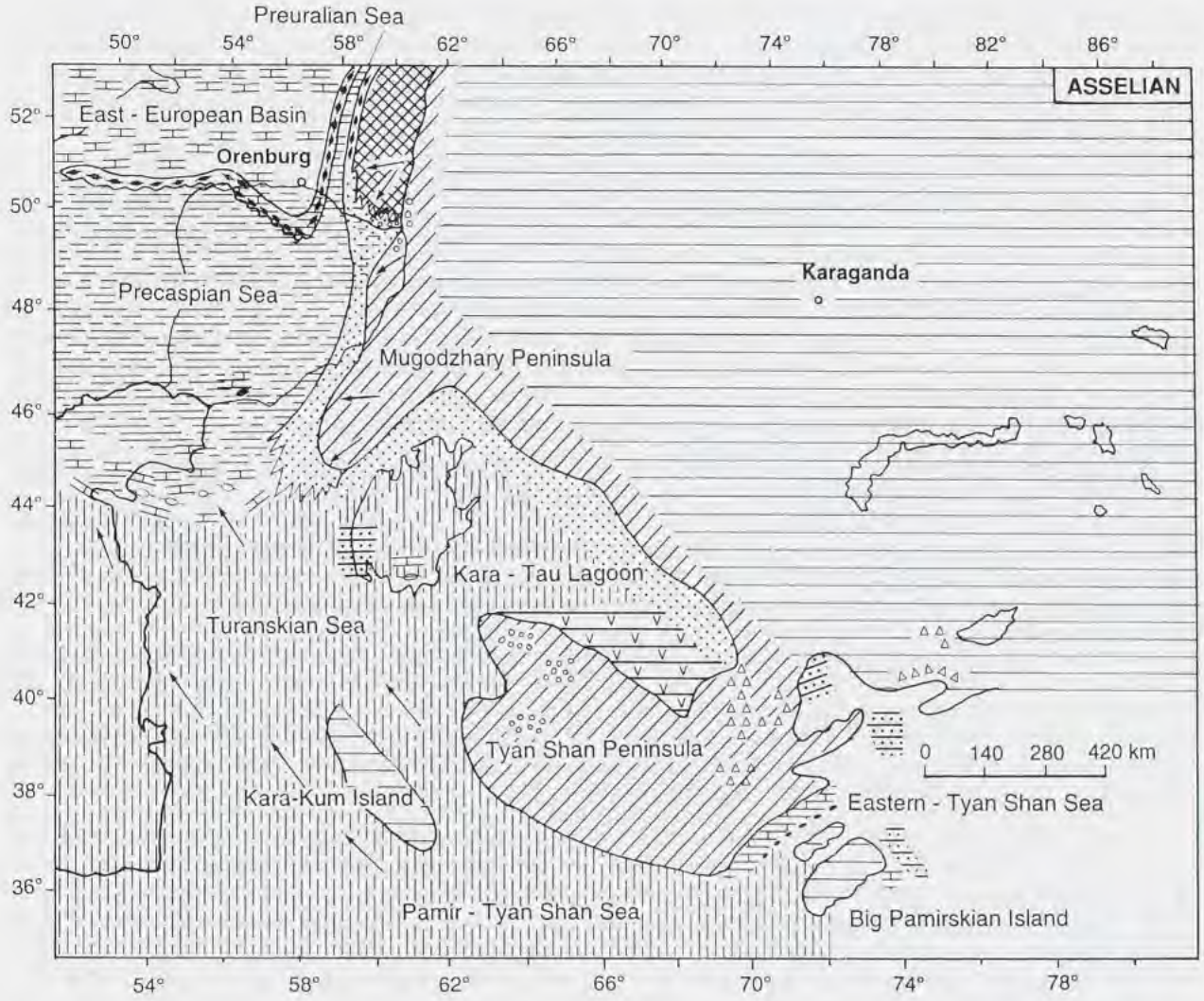

FIG. 13.— Palaeogeographic map of the Eastern European and Tethyan Basins jointed area during the Asselian. Legend: see Fig.2.

FIG. 13.— Carte paléogéographique de la zone de jonction des Bassins Est Européen et Téthysien à l'Assélien. Légende : voir Fig. 2.

The autochthonous group is represented by some genera of small foraminifera, radiolaria, siliceous sponges, small-size solitary corals, bivalves, trilobites, thin-shelled brachiopods, ammonoids and nautiloids, fishes, conodonts, worm-trails. According to the whole data, those sediments could be interpreted as deep-water, compared with other Asselian facies. This type of the sequence is named below as depressional.

The depressional type of sediments along of the Precaspian Depression rim was established on numerous prospecting fields. Some informations were given before in the description of the Moscovian sediments and palaeogeography. The idea of depressional deposits distribution on the whole territory of the Precaspian Depression is now really validated.

— The Asselian reef is the most important during all the Early Permian and can be followed from the Kolguev Island (Fig. 1) in the Barents Sea (PREOBRAZHENSKAYA *et al.*, 1993), along the western edge of the Pechorsk Depression (KONOVALOVA *et al.*, 1995; KUZKOKOVA & CHERMNYSKH, 1987) and, further to the south, along the eastern rim of the Russian Platform until the Orenburg latitude. Southern, the reef belt is turning westwards along the northern border of the Precaspian Depression

Source : MNHN, Paris

(YAROSHENKO, 1985). The Asselian reefs outcrop in the basins of the Pechora, Kolva, Vishera Rivers (between 61°50 and 60°30N), along the Chussovaya River (58°10N). The most impressive outcrops of these build-ups are present near Sterlitamak and Ishimbay (53°30N - 53°40N). The Sterlitamak reefs were described by SHAMOV (1958), KOROLUK (1985) and RAUSER-CHERNOUSSOVA & KOROLUK (1993). The general characteristics of the Early Permian reefs were given by CHUVASHOV (1983).

The relationships between the Asselian reefs and the under- and overlying formations, as well as their thickness, are variable in the different parts of the reef belt. They lie down on Upper Carboniferous reefs, or locally with unconformity on Middle Carboniferous limestones. Usually, the Asselian build-ups are shifted to the west, at least on 10 km, from the Late Carboniferous organic constructions. The reefs of the northern border of the Precaspian Depression have a thickness up to 250 m. The thickness could reach 500 m on the western border of the Preuralian Foredeep between Orenburg and Ufa latitudes. In the Middle Urals (at Perm latitude), the thickness of Asselian reefs is 300-350 m. A similar thickness is recorded in the Northern Urals, between the Vishera and Kolva Rivers, and in the upper and middle streams of the Pechora River. The organic build-ups of the western border of the Pechorsk depression are represented by biostromes and bioherms (5-25 m), composed of *Palaeoaplysina*.

The Asselian reefs are usually composed by a rather stable assemblage of organisms: sponges, bryozoans, brachiopods, *Palaeoaplysina* and problematic algae (*Tubiphytes*). The importance of *Palaeoaplysina*, as reef-building organism, is more significant in Near-Polar and Northern Urals. In Middle and Southern Urals, these organisms have a rock-building importance only at the beginning of late Kholodnolozhskian (Table 1). A very rich and diverse assemblage of the calcareous algae is connected with the Asselian organic build-ups. Some levels are composed of stromatolites.

— To the west, the Asselian reef belt is replaced by a rather thick sequence of bedded limestones with some dolomites in the lower part of section. Most part of this sequence is represented by the detritic limestones; *Palaeoplysina* and colonial coral bioherms are locally distributed (no more than 1-5 m). The organic limestone components are small foraminifera, fusulinids, corals, bryozoans, brachiopods, crinoids and *Tubiphytes*. Other algae are very unusual in this facial zone (THEODOROVICH, 1949; CHUVACHOV & DYUPINA, 1973; ZOLOTOVA *et al.*, 1973).

In these detritic and biogenic limestones, rather thick (2-5 m usually; up to 10 m) packets of dark-grey and black thin-bedded bituminous marls, clayey limestones and argilites with concretion and lenses of black cherts are developed. Such deposits were laid down in rather small (some metres deep and up to 100-300 m long) quite-water depression, where clay and carbonate material enriched by the organic matter were accumulated. The assemblage of fauna is represented by numerous fusulinids, small (up to 20-30 cm in diameter) colonial corals, bryozoan colonies (usually complete and large, up to 20 cm).

These Asselian deposits are distributed to the west of the coeval reef belt on 80 to 100 km. A change in deposits distribution is shown on the profile along the Chussovaya River (Figs 1 and 11). The Asselian thickness in the eastern part is about 170-220 m, decreased to 100-120 m near Perm (110 km westwards of the reef belt) and reached 50-65 m further to the west (mainly with dolomites). On the Oka-Zna uplift (250 km eastwards of Moscow), the Asselian stage (40-45 m in thickness; SEMINA, 1961) is composed by an alternation of limestones and dolomites. Further westwards, a section of the Asselian (about 80 km to the east from Moscow) presents mainly dolomites (MAKHLINA, 1978) with a thickness of 25 m.

These data could be used for the interpretation of change in the bedded carbonates from east to west in the Volga-Kama Sea territory:

— gradually decrease of thickness from east to west (200 m to 25 m); disappearance of biogenic beds;

— increase of dolomite content as result of salinity rising;

— standardisation and poverty of fauna become more significant to the west. These data emphasise the stronger differentiation (biological and sedimentological) in the Asselian than in the Moscovian, near eastern and western boundaries of the Volga-Kama Sea.

The Donetsk Gulf, with normal salinity, exists only during the Kholodnolozhskian (lower Asselian). In the central part of the gulf, a next sequence exits, with from bottom to top (NESTERENKO, 1978; ALEKSEEVA *et al.*, 1983) (Table 1):

Source : MNHN, Paris

— Kartamishsk Suite: mainly red sandstones with packets and beds of argilites and some limestone beds; it disappears northwards; 500-1200 m thick.

— Nikitovsk Suite: grey sandstones and argilites with packets and beds of dolomites, limestones and anhydrites; in the northern part of the gulf, rock-salt lenses (40 m) are recognised; 100-250 m thick.

— Slavyansk Suite: mainly anhydrites, gypsum, rock salts, packet of limestones (10-15 m) containing a very diverse and rich fauna: foraminifera (small ones and fusulinids), corals, bryozoan, brachiopods, crinoids and algae. The thickness is up to 600 m. These three suites, on the whole, could be correlated with Asselian Kholodnolozhskian horizon.

— Kramatorsk Suite: mainly evaporates (anhydrites and rock-salts); in the upper part of the suite there is a packet of potash salts. Rather thick alternation of red sandstones and argilites subdivide evaporates; thickness of this suite is 530 m. The Kramatorsk Suite is compared with the upper Asselian (Shikhanskian Horizon) and lower Sakmarian (Tastubskian Horizon).

In the northern part of the Donetsk Gulf was established an other Asselian sequence based on Skosyrsk borehole example (ALEKSEEVA *et al.*, 1983). It is located at the junction zone of the southern slope of the Voronezh dome and the Donetsk Folded belt or, in other words, at the junction of the Russian and Scythian Plates. The Asselian deposits are composed as follow (from bottom to top).

— Kalitvensk Suite: dark-grey silts and argilites with interlayers and blocks of sandstones and micrites or detritic limestones (1-3.5 m). The detritic limestones contain: small foraminifera, fusulinids, brachiopods, crinoids, conodonts and algae; plant remains and miospores are present in argilites and sandstones. This suite corresponds to the two lowermost Asselian biozones: Ultradaixina bosbytauensis-Daixana robusta zone (Orenburgian *in* IZART *et al.*, 1998) and Sphaeroschwagerina fusiformis zone; thickness of the suite is 118 m.

— Skosyrsk Suite: mainly limestones with thin (up to 1.2 m) argilite and marl interlayers. The limestones as well as in the Kalitvensk Suite contain diverse fauna and calcareous algae. The suite corresponds to the two biostratigraphical zones: Sphaeroschwagerina moelleri-Pseudofusulina fecunda zone and Sphaeroschwagerina sphaerica-Pseudofusulina firma zone; thickness are 81.6 m and 42.6 m. The usual thickness of the Asselian here is about 242 m.

In the Precaspian Depression, a deep water Asselian basin is now well known. The reef belt is traced along the northern and northwestern border of the Precaspian depression. On palaeogeographic maps (Figs 10, 11, 13), is shown a shallow-water sea with essentially carbonate sediments and organic build-ups. As we saw before, in the Astrakhan borehole, in the middle part of the argilite-marl sequence (in stratigraphical interval between early Bashkirian and Artinskian), there are many reef limestone fragments without any mixture of the terrigenous material. The area of baring should be located very close to the south of the Precaspian depression border. It is important to note also, that some horizons of carbonate breccias with numerous reef fragments were established within Asselian interval of the borehole on Busachi Peninsula (23 on Fig. 6) immediately to the south of the discussed area (KARTSEVA, 1979).

The distribution of the Asselian marine sediments in the region of western and southern parts of the Aral Sea (Turanskian Sea in palaeogeographic mean) is also rather probable from results of geophysical researches. There are direct borehole data (Figs 7, 13) which prove the existence of carbonate and terrigenous Asselian rocks in the western and south-western areas of Aral Sea (KARTSEVA & KIRUKHIN, 1974). The wide distribution of them in Tyan Shan-Pamir region is supported by series of sections in Fergana and Darwas areas (BENSH, 1982; LEVEN & TSCHERBOVICH, 1978).

ASSELIAN PALAEOBIOGEOGRAPHY

The palaeogeographic situation (Figs 10 and 13) is supported by the biogeographical data. During the Asselian, very diversified and rich fauna and algae flora exist and the basin have its largest expansion. The diversity falls down during the middle Asselian ("moelleri-fecunda" time). The taxonomic variety of the biota is favoured by the wide biogeographical communications. An homogeneous fauna is present

Source : MNHN, Paris

on whole Preuralian Sea (CHUVASHOV, 1991) with slight differentiation to the north which could be explained by a low decreasing of water temperature in south-north direction. Indeed, almost same sediments are deposited along the western flank of Urals Mountains with a general similar fauna. The main differentiation is recorded in fusulinids with two assemblages.

A typical Tethyan genus (*Ultradaixina*) from the base of the Asselian, is distributed only in the south of the Urals and Preuralie and is not known north of 51°30N. A group of the Tethyan genera (*Dutkevichia, Likharevites, Dutkevichites*) grows at 55°N. Between 55° and 58°N, the species diversity of the genera *Rugosofusulina* and *Paraschwagerina* is strongly reduced. Quite the reverse, *Pseudofusulinella* and *Globifusulina* (*G. krotowi, G. nux, G. caudata*), rare or absent in southern latitudes, become very abundant, especially in the Middle, Northern and Polar Urals. This differentiation between fusulinid fauna of the northern and southern flanks of the Preuralian Sea becomes more marked during the Sakmarian.

The fusulinids of the Donetsk Gulf (*Ultradaixina, Dutkevichia, Likharevites* without *Pseudofusulinella* and *Globifusulina*) have a significant similarity with the South Uralian and Tethyan assemblages. A free communication between the Donetsk Gulf and the Tethyan Sea and a rather complicated relation with the Preuralian Sea (through Precaspian deep-water sea and waters with high salinity of the Volga-Kama Sea) can explain this phenomenon.

Almost the same regularity could be noted in the distribution of calcareous algae. Rich assemblage is established within the reef facies and it is possible to compare them along the Preuralian Sea and with other basins. There is a more diversified algae association in the Asselian-Sakmarian reefs of the Southern Preuralie (KULIK, 1978; KULIK *et al.*, 1978). This association is recognised (CHUVASHOV, 1974) as far as the latitude of Perm (58°N) with the genera: *Tubiphytes, Anchicodium, Eugonophyllum, Neoanchicodium, Globuliferoporella, Epimastopora, Pseudoepimastopora, Gyroporella, Sphaenoporella,* etc. In the North Urals, this list is reduced to *Tubiphytes, Epimastopora* and *Pseudoepimastopora.* At least, in the Near-Polar Urals (65°40N), only numerous *Tubiphytes* are found in the reef limestones.

An interesting conclusion could be drawn from the comparisons of the Uralian alga assemblages with the associations from other parts of the Asselian ocean. The richest Asselian alga assemblage has been studied in the Karachatyr Mountains (KHODZHANYAZOVA, 1991). This alga flora is close to Carnic Alps (FLUGEL, 1966) and Slovenia (KOKHANSKY & HERAK, 1960) coeval assemblages. There is a possibility to adopt for these points the same palaeolatitude. The Southern and Middle Uralian alga association could be compared with the assemblage of the Arctic Canada (MAMET *et al.*, 1987) and the palaeolatitudes of both areas could be similar.

The penetration of some Tethyan brachiopod genera and species, along the Preuralian Sea up to 58°N (KALASHNIKOV, 1998), can give an additional information about free relation and permanent exchanges between the Tethyan and Eastern European faunas.

ARTINSKIAN AGE

The Artinskian stage is subdivided into two substages: lower and upper (Table 1). The lower substage includes (from bottom to top) two horizons, Burtsevskian (Pseudofusulina concavutas - P. pedissequa zone) and Irginskian (Pseudofusulina juresanensis zone). The upper substage contains Sarginskian (lower) and Saraninskian horizons. The Sarginskian horizon corresponds to the Parafusulina solidissima zone. The Saraninskian horizon does not contain fusulinids and its bottom is marked by the first occurrence of the conodont *Neostreptognathodus pnevi*. This level could be used for interregional correlation. In the Preuralian Sea, the Saraninskian horizon could be defined by small foraminifera, bryozoans, ostracods and miospores. The complete correlations of the Artinskian fusulinid, ammonoid, ostracod and conodont zones were given by CHUVASHOV *et al.* (1994).

Source : MNHN, Paris

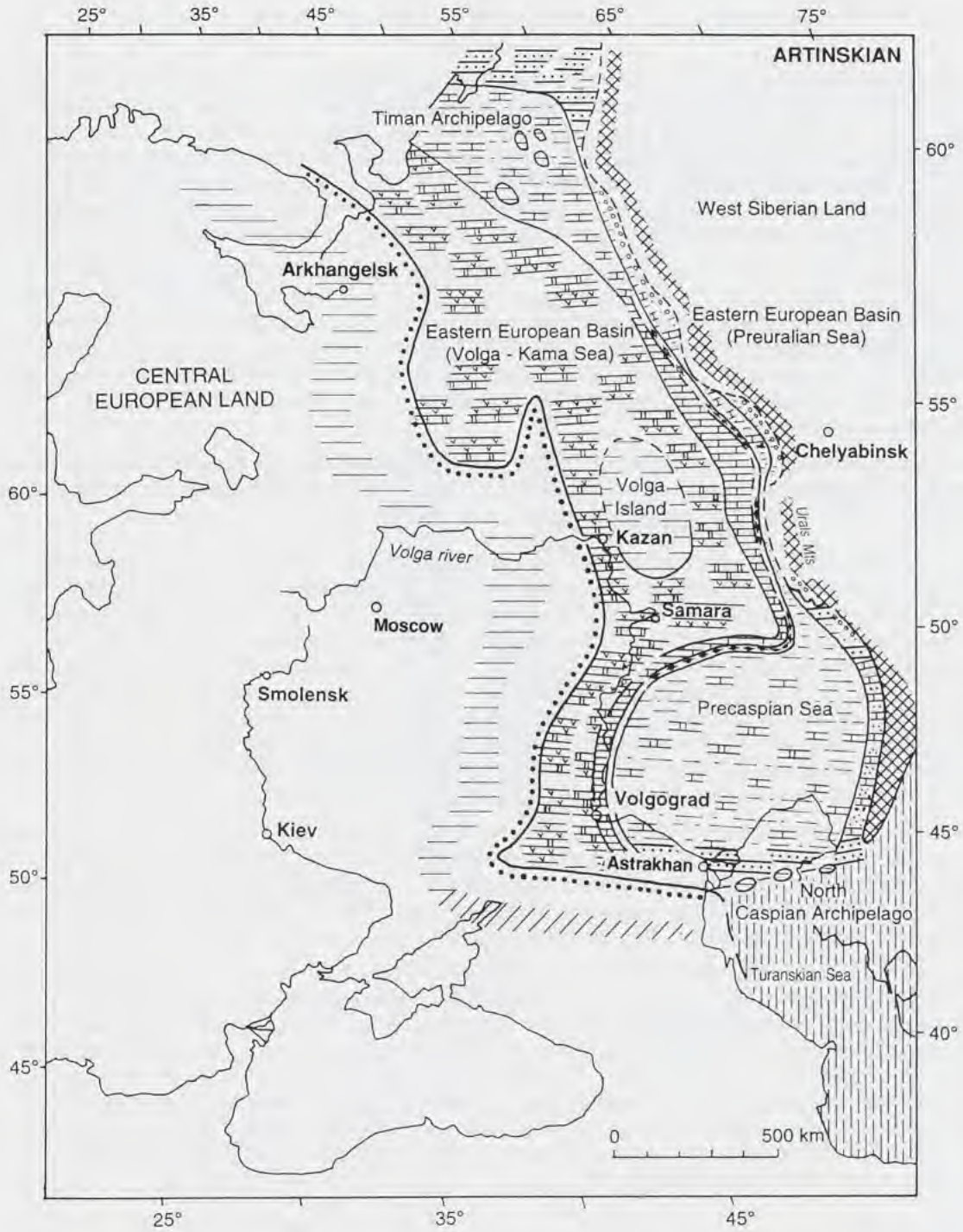

Fig. 14. Palaeogeographic map of the Eastern European Basin during the Artinskian. Legend: see Fig. 2.

FIG. 14.— Carte paléogéographique du Bassin Est Européen durant l'Artinskien. Légende : voir Fig. 2.

Source : MNHN, Paris

ARTINSKIAN PALAEOGEOGRAPHY OF EASTERN EUROPEAN BASIN

During the Artinskian, there is the strong reduction of the Eastern European Basin area; its width at Moscow latitude is up to 500 km including about 100 km of the Preuralian Sea, where deep-water conditions of sedimentation and relatively rich biota are preserved (Figs 14 and 15). Important palaeogeographic changes took place in the junction area of the Preuralian Sea and Tethys Basin. During the second half of the Sakmarian and the early Artinskian, the sea left a large part of the modern Tyan Shan and Pamir territories, except its southeastern part. Most part of the Turanskian Sea (near the Aral Sea) also disappeared. Marine conditions were probably saved in the south of the Precaspian Sea.

In the second half of the Artinskian, an extensive transgression of the Tethys began, but its influence did not carry on for long, and at the beginning of the Kungurian, on the whole territory of the Eastern European Basin, an extensive shallow-water lagoon with evaporite accumulation is established. A deep-water evaporite sedimentation took place in the Precaspian Depression: anhydrites, potash and salt. Exceptionally, in a narrow stripe of the Preuralian Sea, contiguous to the Palaeourals, the influence of fresh water and periodical transgression from the north (Arctic Basin) established, for a short time, normal marine conditions.

The characteristic Artinskian facies of the Eastern European Basin are present along the Palaeourals Mountains. A regular east-west row of facial zones (I to V; Figs 16-17) could be traced along of the Preuralian Sea (Figs 15-17). A concise description is given below.

The first facial zone (I) is composed of an alternation of coarse-grained sandstones, gravelstones, pebble and boulder conglomerates with some packets of sandstones, silts and argilites. Numerous olistostromes (2-50 m thick) could be present in this sequence. These sediments contain a rather rich and diversified fauna (fusulinids and small foraminifera, colonial and solitary corals, bryozoans, bivalves, brachiopods, ammonoids and nautiloids, crinoids, trilobites, ostracods, fish and conodont remains). Large (up to 3-5 m) wood trunk and numerous leaves could be met locally. This series, which can be named "coarse flysh", is distributed in wide areas (Figs 14-17). From north to south, in some areas, these sediments are replaced by a sandstone-silt-argilite sequence: area between the Vaigach Island and the Tschugor River (from 70°15 to 64°10N); area between the Vishera and Kosva Rivers (from 60°20 to 58°30N); basin of the Jurusan and Ay Rivers (between 55°30 to 55°N).

The whole territory of the Western Urals could be divided into two large areas, the boundary between them is located at 61°N. The southern part of this area is characterised by relatively rich and diversified fauna. The Artinskian sediments of the large territory north of 61°N (Pechora River Basin) contain uniformly very rare organic remains (CHUVASHOV, 1991). It could be explained by the gradual decrease of the water temperature. The thickness of this sequence varies from 700 to 2000 m.

For the Preuralian Sea whole territory, a very important regularity can be marked in the construction of Artinskian terrigenous sequence. Its lower part, which corresponds to Burtsevskian and Irginskian horizons (Table 1), is represented by relatively thin-grained sediments, argilites, silts and sandstones. The Sarginskian horizon is composed by more coarse-grained deposits: conglomerates and gravelstones, coarse-grained sandstones; to the west, this sequence is formed essentially by sandstones. In the uppermost horizon, Saraninskian, relatively thin-grained terrigenous sediments prevailed in the eastern part of the facial zone; argilites, marls and limestones are common westwards. This sediment fineness reflects two very important events: tectonic movements in the Palaeourals folded belt and change of the ocean level and the late Artinskian transgression.

The next facial belt (II) is represented by "thin flysh", an uniform alternation of sandstones and argilites with rare thin (5-15 cm) micrite, marl, detritic limestone and silt interlayers. Thickness of sandstone and argilite beds are usually 5-30 cm and could reach sometimes 50-70 cm. The organic remains are rarer in this facial zone than in the previous one and can be divided into two groups: allochthonous in sandstone turbidites beds with foraminifera (including fusulinids), bryozoan and brachiopod fragments, ammonoids, crinoids, calcareous algae; autochthonous in argilites, marls and limestones with small foraminifera, radiolaria, sponges, bivalves, trilobites, ostracods, fish remains and conodonts.

Source : MNHN, Paris

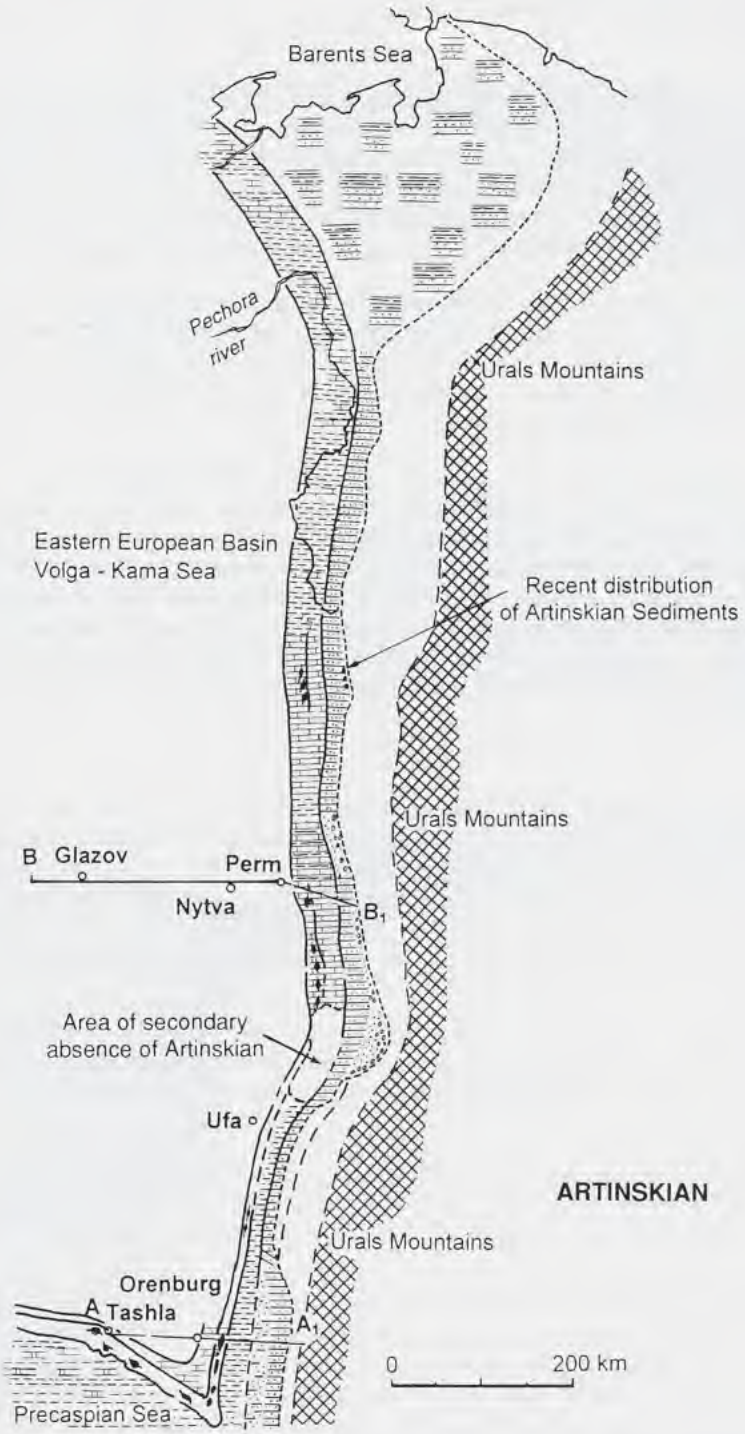

Fig. 15.— Palaeogeographic map of the Preuralian Sea during the Artinskian. A-A1 and B-B1: position of profiles represented on Figs 16 and 17. Legend: see Fig. 2.

FIG. 15.— Carte paléogéographique de la Mer Préouralienne durant l'Artinskien. A-A1 et B-B1 : position des profils des Figs 16 et 17. Légende : voir Fig. 2.

Source : MNHN, Paris

These more deep-water sediments are traced throughout the Preuralian Sea. The thickness of sections near the eastern border of this zone is up to 1000-1200 m. The western boundary of this belt is defined by dominance of argilites, marls and micritic limestones with rare interlayers of sandstones and silts; the thickness is about 150-200 m.

To the west, a next facial zone (III) is represented mainly by carbonate-clay sediments; in the eastern part of this belt, there are some interlayers of sandstones and silts; the western sequence contains numerous beds of limestones and marls. A very rich and diversified fauna exists on the western part of the zone: small foraminifera and fusulinids, radiolaria (locally), calcareous and siliceous sponges, corals, brachiopods, bivalves, bryozoans, ammonoids and nautiloids, trilobites, fishes, crustaceans, ostracods, conodont-bearing organisms. The thickness of the upper Artinskian substage varies from 80 to 200 m.

Westwards, the fourth zone (IV) is composed of similar carbonate-clay deposits, but here they contain locally numerous organic build-ups, which could be treated like patch-reefs. The reef thickness, in the eastern part of the zone, can be up to 300 m, in the western part it decreases to 10-20 m and locally only some metres. These reefs are constructed by numerous *Tubiphytes*, stromatolites, and (more rare) phylloid algae, bryozoans and brachiopods.

The westernmost facial zone (V) is considered as part of the Volga-Kama Sea. The Artinskian is represented by an uniform sequence of dolomites and dolomitic limestones with small foraminifera, single and colonial corals, bivalves and brachiopods. The thickness is about 100-150 m and quickly decreases to the west. The western territory, on the whole, is occupied by a shallow-water sea with significant increase of salinity. The sediments of the Volga-Kama Sea area are represented by dolomites only, with uniform and scanty organic remains: rare levels with small foraminifera, colonial corals, brachiopods and bivalves. Anhydrite beds and packets are locally distributed in the Artinskian sections of the Volga-Kama Sea eastern and central parts and are present almost everywhere near the western border of the basin (Figs 14-17).

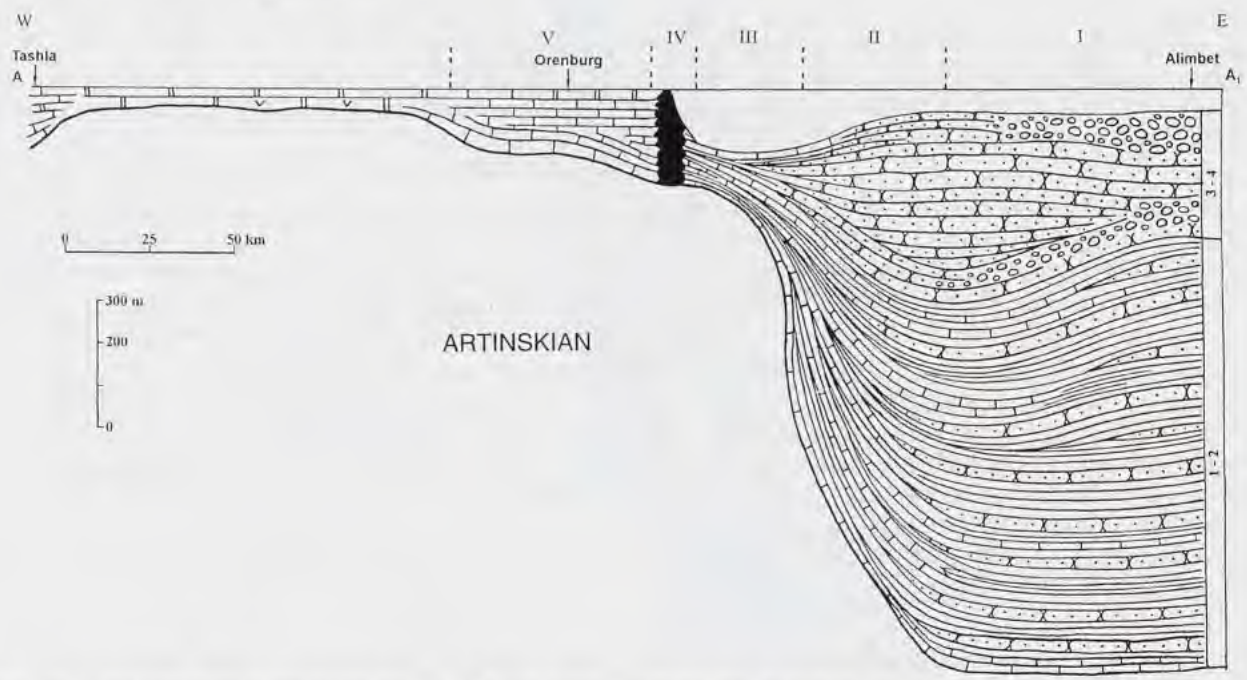

FIG. 16.— Palaeotectonical and facial profile (W-E) of sediments during the Artinskian, through southern part of the Preuralian and eastern part of Volga-Kama Seas (Orenburg latitude). A-A1: position of profile on Fig. 15. Legend: see Fig. 2. Arrows show most important sections. Roman numbers locate the different facial belts.

FIG. 16.— Profil paléotectonique et faciologique des sédiments de l'Artinskien à travers la partie médiane de la Mer Préouralienne et de la partie orientale de la Mer de Volga-Kama. A-A1 : position du profil sur la Fig. 15. Légende : voir Fig. 2. Les flèches positionnent les coupes les plus importantes. Les chiffres romains positionnent les différentes zones de faciès.

Source : MNHN, Paris

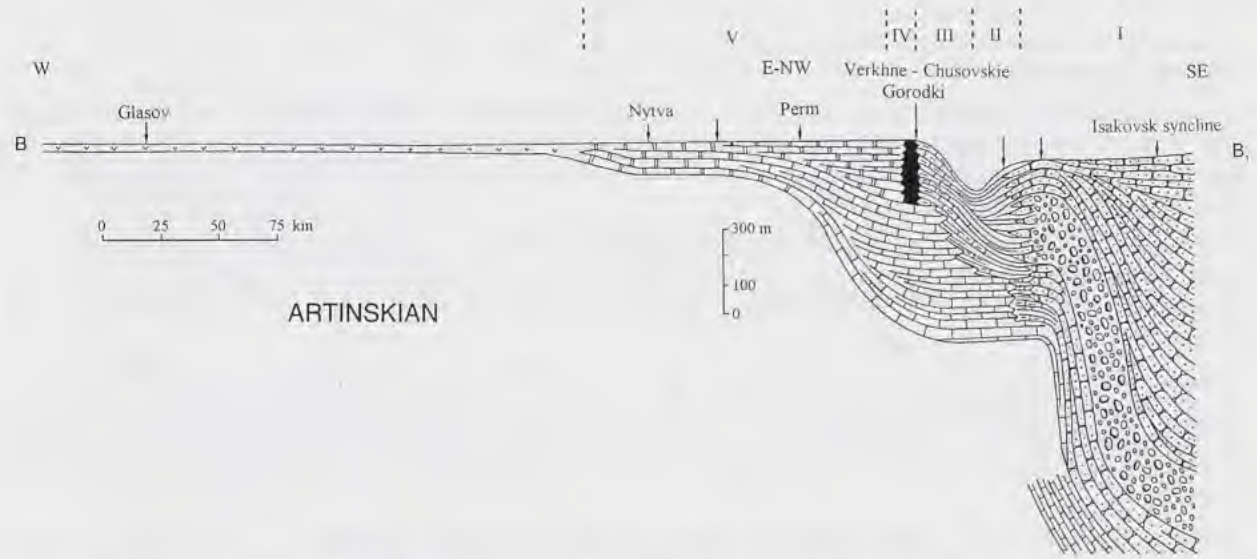

FIG. 17.— Palaeotectonical and facial profile (W-E; NW-SE) through the middle part of the Preuralian and eastern part of Volga-Kama Sea (Perm latitude). The position of this profile (B - B1) on Fig. 15. Legend see Fig. 2. Arrows show most important sections. Roman numbers locate the different facial belts.

FIG. 17.— Profil paléotectonique et faciologique des sédiments de l'Artinskien à travers la partie méridionale de la Mer Préouralienne et de la partie orientale de la Mer de Volga-Kama. B-B1 : position du profil sur la Fig. 15. Légende voir Fig. 2. Les flèches positionnent les coupes les plus importantes. Les chiffres romains positionnent les différentes zones de faciès.

These facial zones (I-V) are traced from the southern part of the Preuralian and Volga-Kama Seas as far as the region of the Precaspian Sea. The facial zones I and II are followed along the eastern boundary of the Precaspian Depression (AVROV *et al.*, 1962; AVROV & KOSMACHEVA, 1963; AISENSTADT & PINCHUK, 1961; TURKOV & UMIRSHIN, 1980) (Fig. 18). The very large central part of the Precaspian Depression is filled by sediments very similar to the deposits of facial zone III. The facial zones IV and V could be easily recognised along the northern and northwestern rims of the Precaspian Depression (Fig. 14).

Along the edges of the Precaspian Depression, the Artinskian sequences were studied in numerous boreholes. We give below concise informations, because the stratigraphy problem of the depressional-type sequence was discussed before during description of the Moscovian and Asselian stratigraphy and palaeogeography.

To the south of the reef formation of the Karachaganak oil field (ILYN *et al.*, 1987) on the northern border of the Precaspian Depression, above the Bashkirian limestones, there are black argilites with rare interlayers of micrite, marls; the thickness is 14-57 m. The upper part contains Artinskian radiolaria and miospores.

Similar sediments, drilled by the Astrakhan borehole (MOVSHOVICH, 1977) reach 160 m; some beds of silts and fine-grained sandstones are present in the upper part of the sequence. Artinskian radiolaria, ammonoids and miospores were recognised here. The presence of terrigenous sediments in the southern part of the Precaspian Depression is explained by the appearance of the low mountain ridge (Karpinsky Kryazh) along the southern border of the Precaspian Depression. Between this border and the Karpinsky Kryazh, the next Artinskian terrigenous sediment sequence, from bottom to top, is the following (LEVINA *et al.*, 1991):

— Visikovsk Suite (50-1000 m): alternation of sandstones, silts and argilites; with early Artinskian fusulinids and ammonoids;

— Tabolassk Suite (80-500 m): silts and sandstones with fusulinids and ammonoids;

Source : MNHN, Paris

— Tinaks Suite (50-300 m): argilites, marls and limestones with marine organic remains. The wide distribution of carbonate sediments could prove that the Karpinsky Kryazh was covered by the sea at end of the Artinskian.

The boundary between lower and upper Artinskian is located in the middle part of the Tabolassk Suite. It is very important to note that the three Artinskian terrigenous sequences are easily recognisable also near the Precaspian Depression. It can be used as an additional feature for correlation and reconstruction of the geological history.

Near the eastern border of the Precaspian Depression (Yuzhno-Embensk uplift, Fig. 6) above the lower Bashkirian limestones, there is a rather thick (225 m) member of black argilites, marls and micrites (LAPKIN & MOVSHOVICH, 1994). Artinskian miospores were found in the upper part of this sequence.

Along the eastern border of the Precaspian Depression, in Tengiz (22 on Fig. 6) and Karaton (7 on Fig. 6) oil fields, above the Bashkirian limestones, numerous boreholes drilled a sequence of black argilites, marls, spongy limestones and carbonate breccias with a maximal thickness of 300 m (ZOLOTUKHINA *et al.*, 1989; COOK *et al.*, 1994). The upper part belongs, without doubt, to the Artinskian.

This information allows to conclude that the Precaspian Depression, on the whole, is filled essentially by clay sediments with rare interlayers of cherts, marls and limestones. Some sandstones and silts are present in the lower and in the lower upper Artinskian substages along of the southern, southeastern and eastern rims of the depression. The thickness of Artinskian, near the outer border of depression, could be some dozens of metres; a thicker section should exist along southern and eastern borders. In the central part of the depression, the thickness of the Artinskian, essentially clayey, could be some metres only.

ARTINSKIAN PALAEOBIOGEOGRAPHY

There is an important problem for the reconstruction of the Artinskian palaeogeography in the area located south of the Eastern European Basin edge. All informations given above confirm the thesis that a continuous sedimentation took place during the Artinskian in the Preuralian Sea. In the Tethyan Basin, the situation is totally different. The nearest best studied sequence (Fergana Valley; BENSH, 1982) shows that the upper part of the Dangibulak Horizon (early Sakmarian) is represented by lagoon facies, but at the same time, in the Darvaz region (Western Pamir), Dangibulak and Uluk (late Sakmarian) horizons are represented by marine sediments. These data could be used to assess the slow retreat of the Tethys (Turanskian and Pamir-Tyan Shan Seas) shore line to the south.

We have no data about the lower Artinskian sediments on the eastern territories presented in the figure 18. The suggestion of a wide distribution of a sedimentation break on the territory of the Middle Asia and Pamir during early Artinskian could be realistic. The large scale of this break could be confirmed by biostratigraphic researches in China (CHUVASHOV, 1984; LEVEN *et al.*, 1996).

The next Tethyan transgression northwards could be dated from late Artinskian or, more exactly, from Sarginskian and Saraninskian. The significant similarities between some groups of late Artinskian fauna (brachiopods, bryozoans, ammonoids) could be used for reconstruction of the communications between the Eastern European and Tethyan Basins. A possible way for these connections could be a narrow strait in the jointed area between Karpinsky Kryazh and Mugodzhary Peninsula. This palaeogeographic situation is represented on the map (Fig. 18).

CONCLUSION

The palaeogeographic situation for an investigated series of time slices (Moscovian, Asselian and Artinskian) reflects, in full, the evolution of biota and sedimentogenesis of the Eastern European sedimentary basin and its connection with the Tethys.

Source : MNHN, Paris

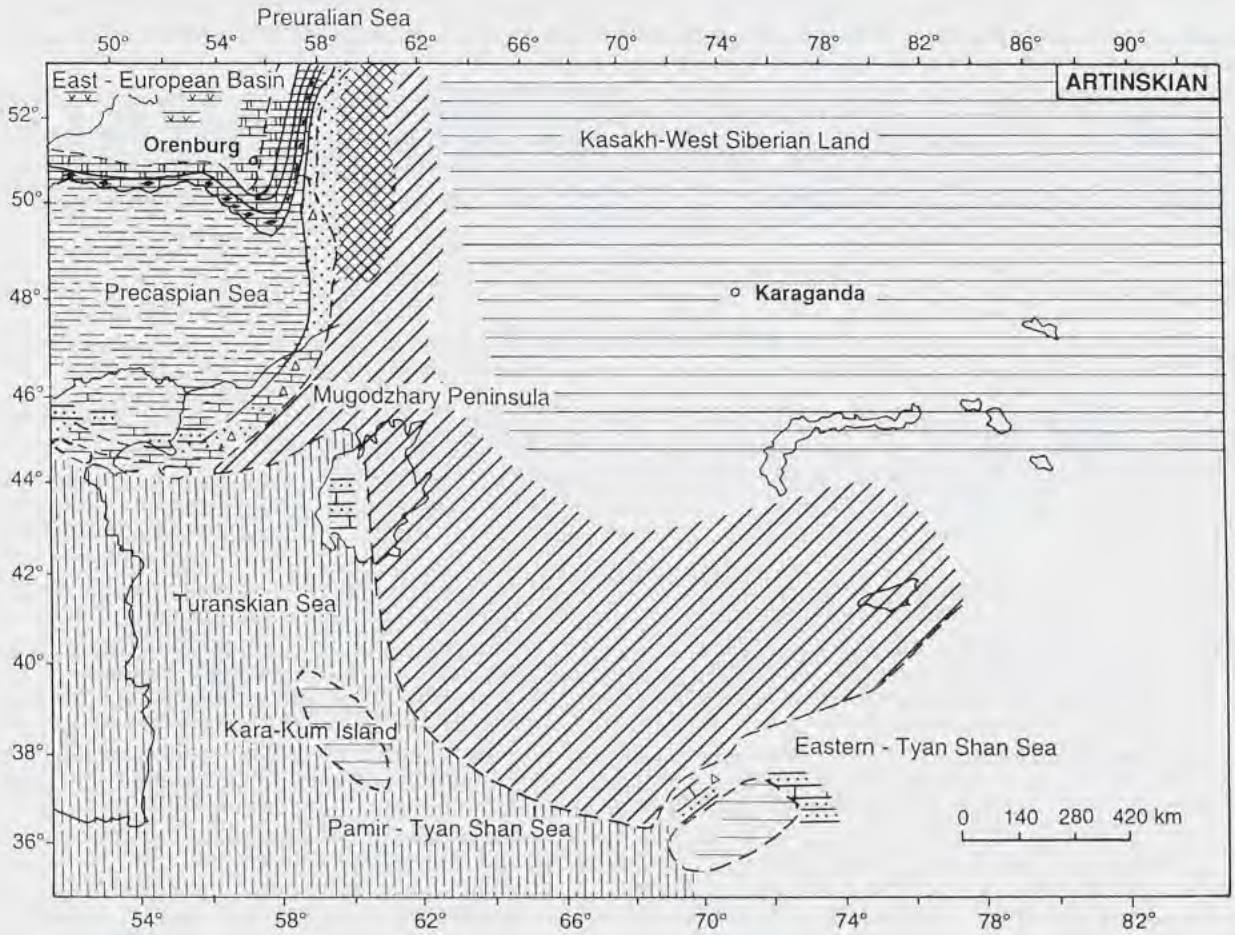

FIG. 18.— Palaeogeographic map of jointing area of the Eastern European and Tethyan Basins during the Artinskian. Legend: see Fig. 2.

FIG. 18.— Carte paléogéographique de la zone de jonction des Bassins Est Européen et Téthysien à l'Artinskien. Légende : voir Fig. 2.

The Moscovian stage is characterised by wide and free connections between EEB and Tethyan seas; the communications between these two large global Carboniferous and Permian water-bearing domains are significantly reduced during Early Permian. The boundary between the Eastern European Basin and the Tethyan Basin can be determined on the basis of biogeographical data. For the Moscovian, it can be traced on 55°N latitude. To the south of this latitude, the composition of fusulinid assemblage varies; among brachiopods and algae, there are numerous Tethyan genera and species. During the Asselian, some typical Tethyan fusulinid genera reach the 55°N latitude, but the ammonites community of the Eastern European Basin stays different from Tethyan association. According to these data, the boundary between the Eastern European and Tethyan Basins for the Moscovian and the Asselian can be traced on 55°N latitude. During the second half of Sakmarian and Artinskian, the boundary between these basins is displaced to the south. The fusulinids of the Eastern European Basin (up to the southern margins of the Precaspian sea) are clearly different from Tethyan ones. For the Artinskian, the boundary between the EEB and Tethyan Basin biotas can be traced on 40°N latitudes.

The palaeogeographic reconstructions allow to assume the wide development of marine, including carbonated, Middle-Late Carboniferous sediments on territory of the Caspian Sea (from the Karpinsky Kryazh, to the south, and on the whole area of Caspian up to Aral); that significantly increases the potential for oil and gas fields of this age on the extensive territory of the Turansk plate.

Source : MNHN, Paris

New studies confirm that a Precaspian deep water basin was generated during late Bashkirian time and remained up to the end of Artinskian; during the Kungurian, this deep water depression was filled by thick Kungurian and Late Permian evaporates.

During the second half of the Sakmarian and the first half of Artinskian, the EEB were almost completely isolated from the influence of Tethyan biota, due to the appearance of an extensive land on the modern territories of Northern Precaspian, Prearalian and Tyan Shan. Mutual palaeobiogeographical isolations of EEB and Tethyan seas was also determined by the depth of Precaspian Basin and the salinity increase in the greatest part of the Volga-Kama sea.

ACKNOWLEDGEMENTS

The authors are very grateful to the reviewers of the paper, Pr Maurizio GAETANI (University of Milano) and Dr Alain IZART (Université de Metz). We thank very sincerely Michel PETZOLD (Université Pierre et Marie Curie, Paris) for the drawing of maps and profiles.

REFERENCES

ALEKSEEVA, I.A., GLUSHENKO, N.V., IVANOV, V.K., INOSOVA, K.I., KALMYKEVA, M.A., KASHIK, D.S., KOSITSKAYA, R.J., KRUSINA, A.K.H., MOVSKOVICH, E.V., REDITCHIN, N.A. & SHVARTSMAN, E.G., 1983.— Key section of the Carboniferous-Permian boundary beds of the Southern part of Eastern-Europian Platform (Gzhelian and Asselian, borehole 4199, Skosyrskaya). *Transactions of Stratigraphical Commitee of USSR*, **12**: 5-135 (in Russian).

AISENVERG, D.E. & ROTAY, A.P., 1978.— The General sketch on Donetsk Basin. stratigraphy of carboniferous. *In*: D.E. AISENVERG, V.V. LAGUTINA, M.L. LEVENSTEIN & V.S. POPOV, *Field excursion guidebook for the Donets Basin: compte rendu du 8ème Congrès international sur la stratigraphie du Carbonifère, Moscow, 1975*. Nauka, Moscow: 9-29.

AISENSTADT, G.A. & PINCHUK, I.A., 1961.— Yuzhno-Embensk. 2 and Tugarakchan- 5 prospecting boreholes. Permian deposits. *In*: *The Reference Boreholes of USSR. 184*. Gostoptekhizdat, Leningrad: 59-65 (in Russian).

AVROV, P.YA., BULEKBAEV, Z.E. & KOSMACHEVA, L.G., 1962.— A Geological structure, oil and gas potential of eastern and south-eastern frames of the Precaspian Depression. *In*: A.S. BOGATYREV & YA.S. EVENTOV (eds), *Geological Structure, Oil and Gas of the Eastern Part of Precaspian Depression and its Frame*. Gostoptekhizdat, Moscow: 57-71 (in Russian).

AVROV, P.YA. & KOSMACHEVA, L.G., 1963.— *A Geological Structure, Oil and Gas Potential of the Aktubinskian Preuraliae and Western Mugodzhary Area*. Kazakh Academy of Sciences, Alma-Ata: 1-52 (in Russian).

BABADZHANOV, T.L., RZHAEVA, V.A. & SHAIKHSADE, E.R., 1989.— A Deep structure of the earth crust under Aral Sea. *Petroleum and Gas Geology*, **1**: 80-86 (in Russian).

BENSH, F.R., 1982.— *Upper Carboniferous and Lower Permian Stages and Fusulinid Zones*. Fan, Tashkent: 1-272 (in Russian).

BOGATYREV, A.S. & EVENTOV, YA.S. (eds), 1962.— *Geological Structure, Oil and Gas of the Eastern Part of Precaspian Depression and its Frame*. Gostoptekhizdat, Moscow: 1-367 (in Russian).

BOGUSH, O.I., STAROSTIN, V.A. & JUFEREV, O.V., 1976.— Biostratigraphy of the Bashkirian and Moscovian of the Northern Pre-Balkhash area. *In*: V. DUBATOLOV (ed.), *Pre-Balkhash Region-Transitional Zone of Late Carboniferous Biogeographical Belts*. Nauka, Moscow: 6-26.

BULEKBAEV, Z.E., GANELINA, P.A. & GAREZKY, R.G., 1967.— Carboniferous and Permian deposits of the eastern board of the Precaspian Depression. *Bulletin of Moscovian Society of Ispitateley prirody*, **42** (6): 32-43 (in Russian).

CHERMNYKH, V.A. (ed.), 1972.— *Atlas of Palaeozoic and Mesozoic Palaeogeographic Maps of the Cis-Urals*. Academy Sciences of USSR, Leningrad: 1-46 (in Russian).

CHERMNYKH, V.A., 1976.— *Carboniferous Stratigraphy of the Northern Urals*. Nauka, Leningrad: 1-304 (in Russian).

CHUVASHOV, B.I., 1974.— Permian calcareous algae of the Urals. *In*: G. PAPULOV & B. CHUVASHOV (eds), *Algae, Brachiopods an Miospores of the Urals Permian*. Uralian Scientific Center of Academy Sciences of USSR, Sverdlovsk: 1-76 (in Russian).

CHUVASHOV, B.I., 1977.— Biogeographical communication of the Early Permian Basin of the Urals and Cis-Urals. *In*: V. DUBATOV & O.JUFEREV (eds), *Palaeobiogeography and Biostratigraphy*. Nauka, Novosibirsk: 116-131 (in Russian).

CHUVASHOV, B.I., 1980.— Calcareous algae within Uralian Palaeozoic near-shore bioherms. *In*: G. VYALUKHIN & M. KLUZHINA (eds), *Lithology and Conditions of Sedimentation of the Palaeozoic Deposits*. Uralian Scientific Center of Academy Sciences of USSR, Sverdlovsk: 87-107 (in Russian).

Source : MNHN, Paris

CHUVASHOV, B.I., 1983.— Permian reefs of the Urals. *Facies, Erlangen*, **8**: 191-212.

CHUVASHOV, B.I., 1984.— *Artinskian Stage of Early Permian; Problems of Dividing and Correlation*. Uralian Scientific Center of Academy Sciences of USSR, Sverdlovsk: 1-64 (in Russian).

CHUVASHOV, B.I., 1991.— Influence of palaeogeography and biogeography on the precision of the biogeographical correlation. *Izvestia of Academy Sciences of USSR, Geological Series*, **7**: 47-59 (in Russian).

CHUVASHOV, B.I., 1994.— Origin of the carbonate breccia horizons within Upper Palaeozoic of Preuralian foredeep. *In*: V. KOROTEEV (ed.), *Ezhegodnik-1993*. Urals Branch of Russian Academy Sciences, Ekaterinburg: 53-63 (in Russian).

CHUVASHOV, B.I. & ANFIMOV, A.L., 1988.— New calcareous algae from Middle Carboniferous-Early Permian of the Urals. *In*: V. DUBATOLOV & T. MOSKALENKO (eds), *Calcareous Algae and Stromatolites: Taxonomy, Biostratigraphy and Correlation*. Nauka, Novosibirsk: 54-70; 183-186 (in Russian).

CHUVASHOV, B.I. & DYUPINA, G.V., 1973.— *Upper Palaeozoic Terrigenous Deposits of the Western Slope of the Urals*. Nauka, Moscow: 1-208 (in Russian).

CHUVASHOV, B.I., DYUPINA, G.V., MIZENS, G.A. & CHERNYKH, V.V., 1990.— *The Reference Sections of Upper Carboniferous-Lower Permian of the Western Urals and Cis-Urals*. Uralian Branch of Academy Sciences of USSR, Sverdlovsk: 1-368 (in Russian).

CHUVASHOV, B.I., IVANOVA, R.M. & KOLCHINA, A.N., 1984.— *Upper Palaeozoic of the Eastern Slope of the Urals. Stratigraphy and Geological History*. Uralian Branch of Academy Sciences of USSR, Sverdlovsk: 1-230.

CHUVASHOV, B.I., SOFRONITSKY, P.A., MOLIN, V.A., KANEV, G.P., MOLOSTOVSKAYA, I.I., USTRYTSKY, V.I. & SEGEDIN, R.A., 1994.— The Stratigraphy of Permian system of the Urals. *In*: B. POPOV & N. ANCYGIN (eds), *Explanatory Note to the Stratigraphic Charts of the Urals: Precambrian and Palaeozoic*. Urals Geological Expedition, Ekaterinburg: 128-152 (in Russian).

CHUVASHOV, B.I., SHUYSKY, V.P. & IVANOVA, R.M., 1995.— Biogeography of Palaeozoic Calcareous Algae. *In*: *Abstracts of 6th International Symposium on Fossil Algae and Carbonate Platforms*. Hagetepe University, Ankara: 6.

COOK, H.E., ZHEMCHUZHNIKOV, V.G., BUVTYSHKIN V.M., GOLUB, L.Y., GATOVSKY, Y.A. & ZORIN, A.Y., 1994.— Devonian and Carboniferous passive margin Carbonate platform of Southern Kasakhstan. *In*: A.F. EMBRY, B. BEAUCHAMP & D.J. GLASS (eds), Pangea: global environments and resources. *Memoir- Canadian Society of Petroleum Geologist*, **17**: 363-381.

DALYAN, I.B., 1990.— About before-Asselian break on the eastern border of the Precaspian Depression. *Petroleum and Gas Geology*, **7**: 34-36 (in Russian).

DNEPROV, V.S., 1962.— *A Geological Structure, Oil and Gas of the Yuzhno-Embensk Uplift and Northern Usturt*. Gostoptekhizdat, Leningrad: 1-124 (in Russian).

ELISEEV, A.I., 1973.— *The Carboniferous of Lemvinsk Zone (Near-Polar Urals)*. Nauka, Leningrad: 1-95 (in Russian).

ELISEEV, A.I., 1978.— *The Formations of Northern-East Rim of the Eastern-European Platform*. Nauka, Leningrad: 1-204 (in Russian).

FLUGEL, E., 1966.— Algen aus dem Perm der Karnishen Alpen. *Sonderhefte of Carinthia, Klagenfurt*, **II**: 1-80.

GRACHEV, R.I., 1956.— A Geological structure and history of Yuzno-Embensk uplift development. *In*: *Geological Sbornik*. VNIGRI, Leningrad: 215-265 (in Russian).

IBRAGIMOV, R.N., NISHANKHODZHAEV, R.N. & ASKAROV, R.N., 1989.— Stratigraphy and tectonic of Upper Palaeozoic (Karakuduk Area, Northern Nuratau). *Uzbeksk Geological Journal*, **5**: 20-24 (in Russian).

ILYIN, V., GUBAREVA, V.S., SAMILATSKAYA, T. & KLENINA, L.N., 1987.— Under rock-salt stratigraphic sequence of Karachaganak Oil Field. *In*: V. ILYIN & B. SMILATSKAYA (eds), *Palaeozoic Stratigraphy and Palaeontology of the Precaspian Depression*. VNIGNI, Moscow: 5-25 (in Russian).

IVANOV, YU.A., 1962.— Stratigraphy, oil and gas potential of Carboniferous, Sakmarian and Artinskian of the Aktubinsk Preuralye and Western Premugodzharye. *In*: A. BOGATYREV & YA.S. EVENTOV (eds), *Geological Structure, Oil and Gas of the Eastern Part of Precaspian Depression and its Frame*. Gostoptekhizdat, Moscow: 108-127 (in Russian).

IVANOV, YU.A., 1966.— *The Characteristic, Structure, Oil and Gas Potential of the Carboniferous and Permian of Northern, East and South-East areas of the Precaspian Depression and its Frame: Abstract of Master Thesis*. Petroleum Institute, Moscow: 1-24 (in Russian).

IVANOVA, R.M. & CHUVASHOV, B.I., 1990.— Biogeographical and facial specialties of the Middle Carboniferous fusulinids assemblages of the Urals and adjacent regions. *In*: *Biostratigraphical Boundaries of the Carboniferous Units of the Urals*. Uralian Branch of Academy Sciences of USSR, Sverdlovsk: 130-142 (in Russian).

IVANOVA, E.A. & SHIK, E.M., 1978.— A Middle Carboniferous. Moscovian Stage. *In*: D.E. AISENVERG, V.V. LAGUTINA, M.L. LEVENSTEIN & V.S. POPOV, *Field excursion guidebook for the Donets Basin: compte rendu du 8ème Congrès international sur la stratigraphie du Carbonifère, Moscow, 1975*. Nauka, Moscow: 28-32 (in Russian).

IZART, A., VASLET, D., BRIAND, C., BROUTIN, J., COQUEL, R., DAVYDOV, V., DONSIMONI, M., EL WARTITI, M., ENSEPBAEV, T., GELUK, M., GOREVA, N., GÖRÜR, N., IQBAL, N., JOLTAEV, G., KOSSOVAYA, O., KRAINER, K., LAVEINE, J.P., MAKHLINA, M., MASLO, A., NEMIROVSKAYA, T., KORA, M., KOZITSKAYA, R., MASSA, D., MERCIER, D., MONOD, O., OPLUSTIL, S., SCHNEIDER, J., SCHÖNLAUB, H., STSCHEGOLEV, A., SÜSS, P., VACHARD, D., VAI, G.B., VOZAROVA, A., WEISSBROD, T. & ZDANOWSKI, A., 1998.— Stratigraphic correlations between the continental and marine Tethyan and Peri-Tethyan basins during the Late Carboniferous and the Early Permian. *In*: S. CRASQUIN-SOLEAU, A. IZART, D. VASLET & P. DE WEVER (eds), Peri-Tethys: stratigraphic correlations 2. *Geodiversitas*, **20** (4): 521-596.

Source : MNHN, Paris

KALASHNIKOV, N.V., 1998.— *Permian Spiriferidae of the Europe-an North*. GEOS, Moscow: 1-139 (in Russian).

KALASHNIKOV, N.V. & ASKAROV, R.N., 1989.— The Comparative characteristic of the Late Moscovian brachiopod assemblages of the Northern Urals and Middle Asia. *In*: V. MOLIN (ed.), *Palaeozoic Biostratigraphy of the Timan-Pechora Province*. Komi Scientific Center of Russian Academy Sciences, Syktyvkar: 50-59 (in Russian).

KARIMOV, B.YU., GADZHIEV, A.N., KHALILOV, E.A. & MEKHTIEV, N.YU., 1990.— Karaton-Southern Emba ring-like structure and its oil and gas potential. *Petroleum and Gas Geology*, **4**: 9-12 (in Russian).

KARTSEVA, O.A., 1979.— Upper Carboniferous and Lower Permian of the Busachi peninsula. *Bulletin of Moskovian Society of Ispytateley Prirody, Geological Section*, **54** (6): 56-59 (in Russian).

KARTSEVA, O.A. & KIRUKHIN, L.G., 1974.— Upper Palaeozoic of Ustyurt. *Bulletin of Moscovian Society of Ispytateley Prirody, Geological Section*, **49** (6): 5-12 (in Russian).

KHODZHANYAZOVA, R.R., 1991.— Stratigraphy and correlation of Upper Carboniferous and Early Permian of Southern Fergana area according to Calcareous Algoflora. *In*: *Permian System of the World: Abstract Volume of International Congress*. Uralyan Branch of Academy Sciences of USSR, Sverdlovsk: 84 (in Russian).

KHVOROVA, I.V., 1961.— *Flysh and Molassa Formations of Southern Urals*. Academy Sciences of USSR, Moscow : 1-352 (in Russian).

KOKHANSKY, V. & HERAK, M., 1960.— On the Carboniferous and Permian Dasicladaceae of Yugoslavia. *Goloski Vestnik, Zagreb*, **13**: 65-96.

KONOVALOVA, M.B., CHERMNYKH, V.A. & IGONIN, V.M., 1995.— Carbonate essentially reef facies of Upper Carboniferous and Lower Permian on the right side of Kozhim River (Near-Polar Urals). *In*: A. ROZANOV, M. BOGOSLOVSKAYA, T. GRUNT, T. LEONOVA & I.MOROZOVA (eds), *Guidebook of excursion on Permian deposits of Kozhim River*. Palaeontological Institute of Russian Academy of Sciences, Moscow: 16-20.

KOROLUK, I.K., 1985.— *Method and Results of Permian Reef Shakh-Tau Study*. Nauka, Moscow: 1-112 (in Russian).

KULIK, E.L., 1978.— Calcareous green (Siphonales) Asselian and Sakmarian algae of Shakh-Tau reef. *Problems of Micropalaeontology, Moscow*, **21**: 182-215 (in Russian).

KULIK, E.L., KOROLUK, I.K. & RAUSER-CHERNOUSSOVA, D.M., 1978.— Stratigraphical and facial significance of the Asselian and Sakmarian Calcareous Algae (on materials of Shakh-Tau reef, Bashkiria). *Problems of Micropalaeontology, Moscow*, **21**: 216-233 (in Russian).

KUZKOKOVA, N.N. & CHERMNYKH, V.A., 1987.— Asselian reefs of Timan-Pechora province. *In*: *Phanerozoic Stratigraphy and Palaeogeography of Northern Part of USSR: 10th Geological Conference of Komi Republic*. Komi Scientific Center of Academy Sciences of USSR, Syktyvkar: 88-91.

LAPKIN, I.YU. & MOVSHOVICH, E.V., 1978.— A Joint of the Eastern-European platform with burial Variscides. *Izvestya of Academy Sciences of USSR, Geological Series*, **6**: 73-85.

LAPKIN, I.YU. & MOVSHOVICH, E.V., 1994.— A History of Permian system study of southern part of Eastern-European platform. Paper 3th. Recent researches. *Bulletin of Moscovian Society of Ispytateley Prirody*, **69** (5): 77-95.

LATSKOVA, V.E., 1976.— Criticism of the concepts uncompensated development of the Precaspian Depression. *In*: *Reef Formations of Oil and Gas-Bearing Areas of Russian Platform*. Volume 1. VNIGNI, Moscow: 100-106 (in Russian).

LEVEN, E.YA., 1998.— Stratigraphy and fusulinids of the Moscovian Stage (Middle Carboniferous) in the Southwestern Darvaz (Pamir). *Rivista Italiana di Palaeontologia e Stratigrafia, Milano*, **104** (1): 3-42.

LEVEN, E.YA., BOGOSLOVSKAYA, M.F., GANELIN, V.G., GRUNT, T.A., LEONOVA, T.B. & REIMERS, A.N., 1996.— Reorganization of Marine Biota during the Mid-Early Permian epoch. *Stratigraphy and Geological Correlation*, **4** (1): 61-70.

LEVEN, E.YA. & TSCHERBOVICH, S.F., 1978.— *The Asselian Fusulinids and Stratigraphy of Darvaz*. Nauka, Moscow: 1-164 (in Russian).

LEVINA, V.I., NIKOLSKAYA, A.V. & CHERNOVA, N.I., 1991.— Early Permian of the Precaspian Depression. *In*: B. CHUVASHOV (ed.), *International Congress: Permian System of the World. Abstract volume*. Uralian Branch of Academy Sciences of USSR, Sverdlovsk: 54-55 (in Russian).

MAKHLINA, M.KH., 1978.— A Borehole No 7 on left side of Kirzhakh River, 35 km to northeast Noginsk Town. *In*: D.E. AISENVERG, V.V. LAGUTINA, M.L. LEVENSTEIN & V.S. POPOV, *Field Excursion Guidebook for the Donets Basin: compte rendu du 8ème Congrès international sur la stratigraphie du Carbonifère, Moscow, 1975*. Nauka, Moscow: 70-72 (in Russian).

MAMET, B.L., ROUX, A. & NASSICHUK, W.W., 1987.— Algues carbonifères et permiennes de l'Arctique canadien. *Geological Survey of Canada, Ottawa*, **342**: 1-143.

MATVEEV, V.P., SOBOLEV, N.N., USTRITSKY, V.I. & CHERNYAK, G.E., 1989.— Carboniferous and Permien of Ledyanaya Gavan Area (Northern Island of Novaya Zemlya). *In*: V. BONDAREV (ed.), *Palaeozoic Stratigraphy and Palaeontology of Soviet Arctic*. Okeangeologia, Leningrad: 32-41 (in Russian).

MOVSHOVICH, E.V., 1977.— *Palaeogeography and Palaeotectonic of the Nizhnee Povolzhye Region during Permian and Triassic*. Saratov University, Saratov: 1-240.

NESTERENKO, L.P., 1978.— General information on the Donets Basin. Permian Stratigraphy. *In*: D.E. AISENVERG, V.V. LAGUTINA, M.L. LEVENSTEIN & V.S. POPOV, *Field Excursion Guidebook for the Donets Basin: compte rendu du 8ème Congrès international sur la stratigraphie du Carbonifère, Moscow, 1975*. Nauka, Moscow: 167-169.

Source : MNHN, Paris

NGUEN VAN LIEM 1982.— *Fusulinid Biostratigraphy of Carboniferous-Permian of Vietnam: Abstract of Doctor's Thesis.* Moscow Prospecting Geological Institute, Moscow: 1-35 (in Russian).

PAK, Z.V., 1988.— Southern Prearalie is potential for oil and gas region. *Petroleum and Gas Geology*, **2**: 17-21 (in Russian).

PAKHOMOV, V.I. & DOZORTZEV, R.N., 1966.— The Palaeogeography and sedimentation of Moscovian sediments on Western slope of the Middle Urals and Prekamie. *In*: O. BOGATYREVA, I. PAKHOMOV, H. STEPANAITYS & E. LUSHNIKOV (eds), *Problems of Carboniferous Palaeogeography*. Permian Politekhnical Institute, Perm: 196-206 (in Russian).

PILIPENKO, A.I., 1990.— Upper Palaeozoic of the Aral Sea region according to seismic data. *Petroleum and Gas Geology*, **4**: 23-25 (in Russian).

PLATONOV, E.G., POVYSHEVA, K.G. & USTRITSKY, V.I., 1992.— About origin of the Carbonate-Manganese ores of the Pay-Khoy and Novaya Zemlya region. *Litologya and Poleznye iscopaemye*, **4**: 76-89 (in Russian).

PREOBRAZHENSKAYA, E.N., USTRITSKY, V.I. & CHUVASHOV, B.I., 1993.— Late Palaeozoic organic buildups of Kolguev Island. *Doklady of Russian Academy Sciences*, **329** (1): 71-74 (in Russian).

RA'CZ, L., 1966.— Carboniferous calcareous algae and their associations in the San Emiliano and Lois-Ciquera formations. *Leidse Geologische Mededelingen, Leiden*: 1-112.

RAUSER-CHERNOUSSOVA, D.M., 1961a.— Middle Carboniferous of the Vozhgaly Region. *In*: S. SHATSKY (ed.), *Regional Stratigraphy of USSR*. Volume 5. Academy Sciences of USSR, Moscow: 55-79 (in Russian).

RAUSER-CHERNOUSSOVA, D.M., 1961b.— Middle Carboniferous Stratigraphy of Permian Prikamie. *In*: S. SHATSKY (ed.), *Regional Stratigraphy of USSR*. Volume 5. Academy Sciences of USSR, Moscow: 80-148 (in Russian).

RAUSER-CHERNOUSSOVA, D.M. & KOROLUK, I.K., 1981.— About morphology and taxonomy of the Late Palaeozoic Siphonales (Calcareous Algae) and their rock-building significance. *Problems of Micropalaeontology*, **24**: 157-177 (in Russian).

RAUSER-CHERNOUSSOVA, D.M. & KOROLUK, I.K., 1993.— Sterlitamakian Shikhan-Early Permian Reefs. *In*: B.I. CHUVASHOV & A.E.M. NAIRN (eds), Permian system: guide to geological excursions in the uralian type localities. *Occasional Publications ESRI, New Series*, **10**: 72-85.

ROGOV, V.S., GALITSKAYA, E.I., DAVYDOV, V.I. & POPOV, A.V., 1988.— New data about stratigraphy of manganese-bearing sediments of Pay-Khoy Mts. *Sovetskaya Geologia*, **6**: 59-68 (in Russian).

SEMINA, S.A., 1961.— *Stratigraphy and Forams (fusulinids) of the Oka-Zna Uplift*. Academy Sciences of USSR, Moscow: 1-73 (in Russian).

SEMIKHATOVA, E.N., 1961.— Significance of forams to study of Middle Carboniferous of Don-Medveditsa uplift. *In*: S. SHATSKY (ed.), *Regional Stratigraphy of USSR*. Volume 5. Academy Sciences of USSR, Moscow: 297-356 (in Russian).

SHAMOV, D.F., 1957.— Sakmarian and Artinskian facies of Ishimbaisk Preuralie. *In*: A. BOLTYSHEV (ed.), *Problems of Oil's Extraction*. Gostoptekhisdat, Moscow: 3-77.

TEODOROVICH, G.I., 1949.— *Carbonate Facies of Lower Permian and Upper Carboniferous of the Volga-Ural Region*. Moscovian Society of Ispitateley Prirody, Moscow: 1-304 (in Russian).

TORIYAMA, R., HAMADA TAKASHI & IGO, H., 1975.— The Carboniferous and Permian system in Thailand and Malaysia. *In*: *Contribution to the Geology and Palaeontology of South-East Asia*. University of Tokyo Press, Tokyo, **149** (15): 39-76.

TSCHEKOTOVA, I.A., 1990.— *Carbonate Formations of Southern Preuralie*. Nauka, Moscow: 1-111 (in Russian).

TSCHERBAKOV, O.A. & TSCHERBAKOVA, M.V., 1966.— Stratigraphy of Middle and Upper Carboniferous of the Western slope of Middle Urals. *In*: N. STEPANAITYS & E. LUSHNIKOV (eds), *Problems of Carboniferous Stratigraphy*. Permian Politekhnical Institute, Perm: 173-187 (in Russian).

TSCHERBAKOVA, M.V., TSCHERBAKOV, O.A., CHUVASHOV, B.I. & KITAEV, P.M., 1979.— Carboniferous of reference section "Orel". *In*: G. PAPULOV & I. PAKHOMOV (eds), *Carboniferous Reference Sections of the Urals*. Uralian Scientific Centre of Academy Sciences of USSR, Sverdlovsk: 48-59 (in Russian).

TURKOV, O.S. & UMIRSHIN, S.K., 1980.— A Geological structure, oil and gas of Tortay Area. *Petroleum and Gas Geology*, **9**: 57-61 (in Russian).

USAKOV, KH., 1985.— Upper Palaeozoic lithology and biostratigraphy of Bukhara-Karsha region. *Uzbek Geological Journal*, **3**: 53-58 (in Russian).

VINOGRADOV, A.P. (ed.), 1961.— *Atlas of Lithologic-Palaeogeographic Maps of Russian Platform and its Geosinclinal Frames*. Nedra, Moscow; Leningrad: 38 maps (in Russian).

YAROSHENKO, A.V., 1985.— The Types of Late Palaeozoic organic buildups on the Northern Border of Precaspian Depression. *In*: A. YANSHIN (ed.), *Problems of Exogenic and Metamorphogenic Rocks: Ores Origin* Nauka, Moscow: 72-83 (in Russian).

YUFEREV, O.V. & SOKOLOV, A.D., 1976.— Bashkirian-Moscovian Sedimentation. *In*: V. DUBATOLOV (ed.), *Pre-Balkhash Region-Transitional Zone of Late Carboniferous Biogeographical Belts*. Nauka, Moscow: 26-32 (in Russian).

ZOLOTOVA, V.P., DEVINGTAL, V.V., KHURSIK, V.Z., EKHLAKOV, YU.A., SHIRINKINA, A.P. & GRAIFER, B.I., 1973.— Biostratigraphy of Permian of Permian Preduralie. *In*: A. OBORIN (ed.), *Lower Permian of Kamsk Preduralie*. VNIGNI, Perm: 49-135 (in Russian).

ZOLOTUKHINA, G.P., KETAT, O.B., DANSHINA, N.V. & ALESHIN, V.M., 1989.— Stratigraphy of Upper Palaeozoic of south-eastern area of Precaspian Depression (Tengiz oil field). *Doklady of Academy Sciences of USSR*, **304** (4): 933-936 (in Russian).

Source : MNHN, Paris

Source : MNHN, Paris

Palaeotectonic conditions of Cretaceous basin development in the southeastern segment of the Mid-Polish Trough

Jolanta SWIDROWSKA & Maciej HAKENBERG

Institute of Geological Sciences, Polish Academy of Sciences, Twarda 51/55, 00-818 Warszawa, Poland

ABSTRACT

The analysis of the deposit accumulation rates, treated as a reflection of subsidence rates, coupled with the recognition of sedimentary conditions, made possible to distinguish synsedimentary fault patterns for six time-spans of the Cretaceous. The zones of major subsidence gradients were interpreted as synsedimentary faults. They determined the location of palaeouplifts and depocentres. Two main fault zones were distinguished which separated the axial part of the trough from its marginal portions. Asymmetry of the basin, observed in its transversal section up to the Turonian (inclusive), resulted from these discontinuities. The axis of subsidence was shifted towards the NE boundary of the trough until the Cenomanian, during the Turonian it was shifted towards the SW boundary. Since the Coniacian, the role of the bounding faults decreased. Subsidence increased at the beginning of the late Albian transgression; however, the rate of sediment accumulation during the Albian did not reach high values. The significant increase of subsidence during the Turonian, combined with the synsedimentary activity of the southwestern zone of the bounding fault, shows the important role of a tectonic factor for the basin opening. We made an attempt to determine palaeotectonic conditions controlling basin development. The evolution of palaeostress fields has been proposed on the basis of the fault patterns. A clockwise rotation of a strike-slip stress field occurred, during Cretaceous times. It is expressed by a change of the WNW-ESE azimuth of σ_1 axis, deduced for the Early Cretaceous, to the NE-SW direction at the end of Cretaceous time. This rotation was followed by variation of character of strike-slip movement component along Teisseyre-Tornquist Zone: from sinistral component (till the middle Albian) to the dextral one (from the Turonian till inversion time). Basins developed in the transtensional regime till the end of the Turonian and later in the transpressional regime. The succession of palaeotectonic conditions of Cretaceous basins opening seems to be compatible with the relative movements between Africa and Eurasia plates during this time.

RÉSUMÉ

Conditions paléotectoniques de développement du bassin crétacé dans la partie sud-est du Bassin Polonais.

Le taux d'accumulation des sédiments est analysé et interprété comme le reflet du taux de subsidence. Il est couplé à l'identification des environnements sédimentaires dans le but de reconstituer le réseau des failles synsédimentaires. Le Crétacé est divisé en six périodes caractéristiques. Les zones de fort gradient de subsidence sont assimilées à des failles

SWIDROWSKA, J. & HAKENBERG, M., 2000.— Palaeotectonic conditions of Cretaceous basin development in the southeastern segment of the Mid-Polish Trough. *In*: S. CRASQUIN-SOLEAU & É. BARRIER (eds), Peri-Tethys Memoir 5: new data on Peri-Tethyan sedimentary basins. *Mém. Mus. natn. Hist. nat.*, **182** : 239-256. Paris ISBN : 2-85653-524-0.

Source : MNHN, Paris

synsédimentaires. Elles individualisent des domaines de soulèvement et de dépôt-centre. Deux zones faillées principales limitent la partie axiale du bassin. En coupe transversale, le bassin apparaît asymétrique en raison du jeu des deux zones faillées principales jusqu'au Turonien (inclus). Dès le début du Crétacé et jusqu'au Cénomanien, le dépôt-centre est situé sur la marge NE du bassin. Puis pendant le Turonien, le dépôt-centre bascule sur la marge SW. A partir du Coniacien, le rôle des failles bordant le bassin diminue. Lors de la transgression à l'Albien supérieur, le taux de subsidence augmente. Cependant, le taux d'accumulation des sédiments pendant l'Albien n'atteint pas de fortes valeurs. Au contraire, la hausse de la subsidence pendant le Turonien s'accompagne d'un taux élevé d'accumulation des sédiments. Cette période est de plus caractérisée par l'activité synsédimentaire de la zone faillée de la marge SW, confirmant le rôle majeur de la subsidence tectonique. Nous avons tenté de reconstituer les conditions paléo-tectoniques contrôlant le développement du bassin. Les réseaux de failles sont interprétés en termes de champs de contraintes. Pendant le Crétacé, le régime décrochant évolue en tournant dans le sens horaire. Il s'ensuit un changement de sens de la composante décrochante le long de la Zone Teisseyre-Tornquist. Jusqu'à l'Albien moyen, la composante décrochante est sénestre. Elle devient dextre à partir du Turonien et jusqu'à l'inversion tectonique du bassin. Le bassin se développe dans un régime tectonique transtensif jusqu'à la fin du Turonien, puis le régime tectonique devient transpressif. L'évolution du contexte paléo-tectonique contrôlant l'ouverture du bassin crétacé est compatible avec le déplacement relatif des plaques Afrique et Eurasie à cette époque.

INTRODUCTION

The Mid-Polish Trough (MPT) developed during Permian and Mesozoic times (DADLEZ, 1989; DADLEZ *et al.*, 1994, 1995) over the Trans European Suture Zone (TESZ) joining the Eastern European Platform of Precambrian and the Western European Platform formed by the Palaeozoic orogens. In Poland, the northeastern part of the TESZ coincides with the Teisseyre-Tornquist Zone (TTZ), a crustal weakness zone extending from Scania through Bornholm south-easterly to the Black Sea (GUTERCH *et al.*, 1994; DADLEZ, 1997; BERTHELSEN, 1998). At the turn of the Maastrichtian/Early Tertiary an inversion of the trough occurred and the Mid-Polish Swell has originated with two adjacent synclines (Fig. 1).

The investigated area is located around the Palaeozoic of the Holy Cross Mountains (HCM). From the palaeotectonic point of view, the studied area includes three distinct regions. The first was connected with the axial and near-axial parts of the Mid-Polish Trough extending southeastwards. The subsidence and the thickness of sediments in this region during the Permian and the Mesozoic were relatively of high values, and breaks in sedimentation and erosional episodes were rare and short. The second and third regions situated on both sides of the trough occupy the present areas of the Miechów Syncline and the Warsaw-Lublin Syncline. Reverse trends in sedimentary conditions as compared with those in the Mid-Polish Trough are the characteristic features of both zones (GLAZEK & KUTEK, 1970; DADLEZ, 1989; MORAWSKA, 1996; HAKENBERG & SWIDROWSKA, 1996, 1997).

We have tried to reconstruct the palaeotectonic conditions, which controlled basin development. An analysis of subsidence and tectonic factor for all MPT was carried out by STEPHENSON (1993) and DADLEZ *et al.* (1994, 1995). A restriction of studied area to southeastern part of MPT allowed to show similar problems in more detail and to focus our efforts on the identification of synsedimentary faults. We based our analysis on the relationships between sedimentation, basin subsidence and fault activity. Data were acquired from outcrops of the Cretaceous and from wells situated in the marginal synclines. Both archival and published descriptions of profiles were analysed (HAKENBERG & SWIDROWSKA, 1998). Abundant bibliography dealing with Cretaceous sediments in the Mid-Polish Trough is contained in the papers of CIESLINSKI & POZARYSKI (1970) and MAREK & PAJCHLOWA (1997).

METHODS

This study is based on the thickness and lithofacies patterns. The thickness maps for particular stages of the Cretaceous (HAKENBERG & SWIDROWSKA, 1998) provided a base for palaeotectonic analysis. Isopach maps compared with maps of regions of similar lithological successions made possible to distinguish regions of different palaeogeographical locations in the basin.

Presently, the basin analysis is based on high-quality seismic profiles. In this case no effort has been made so far in this area to carry out a new seismic survey or to reprocess and reinterpret available seismic sections. Synsedimentary breccias or poorly sorted conglomerates, as lithofacies that normally

Source : MNHN, Paris

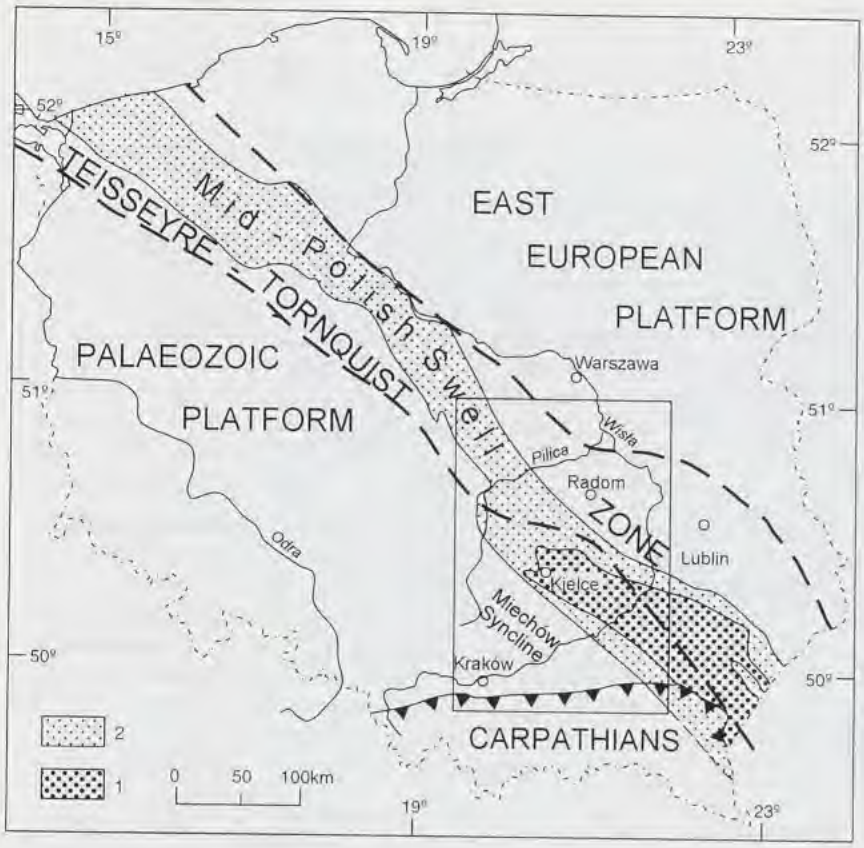

FIG. 1.— Location of investigated area. **1**, Palaeozoic; **2**, Triassic and Jurassic of the Polish Swell; dashed line, boundary of Teisseyre-Tornquist Zone; closed triangle line, boundary of Carpathian thrust.

*FIG. 1.— Localisation de la zone d'étude. **1**, Paléozoïque ; **2**, Trias et Jurassique du "Polish Swell" ; grands tirets, limite de la Zone de Teisseyre-Tornquist ; ligne à triangles noirs, limite des chevauchements des Carpates.*

are formed at the foot of underwater fault escarpments developing on the basin floor, could not be identified in any of the profiles.

Only an indirect way could be employed in an effort to identify synsedimentary faults when there is a lack of geophysical and lithological evidences. Zones of relatively fast changes in the basin subsidence have been considered as testifying the activity of synsedimentary faults. They are visible on the maps where isopachs or isolines of rates of persistent accumulation of sediments are dense and probably also document high gradients of subsidence rates. Synsedimentary faults delineated this way, may have acted in the basin basement without reaching its floor or producing a fault-scarp relief and high-energy, poorly sorted sediments. It is most likely that in upward direction they decreased, passing in flexures; their synsedimentary role resulted in a differentiation of subsidence rate of the basin floor (Fig. 2).

A comparison of facies and isopach patterns was also used in the analysis of tectonic subsidence and the identification of synsedimentary faults. Where the isopachs and lithofacies boundaries are parallel to each other it means that the subsidence was a decisive factor governing the sedimentary conditions in this part of the basin: the rate of subsidence was often higher that the rate of sedimentary infill. Recurrent coincidence of lithofacies boundaries with zones of increased thickness gradients was considered a strong argument for the identification of synsedimentary faulting.

Transverse faults can be inferred where rapid changes of isoline directions occur, though in this case a later origin of such faults cannot be excluded. Sometimes only local disturbances are visible in general isoline course which may indicate mechanical weakness zones, probably of fault origin. Such a situation can be reflected by a local increase in the accumulation of sediments.

The interpolation of facies boundaries and of isopachs was based on well data (black circles on Fig. 3). As some of these wells are situated at large distance one from another, faults shown on the Mesozoic map of this area were taken into consideration when the facies boundaries and the isopachs were plotted. An assumption was made that the faults manifested during inversion might have been active earlier as synsedimentary faults.

Source : MNHN, Paris

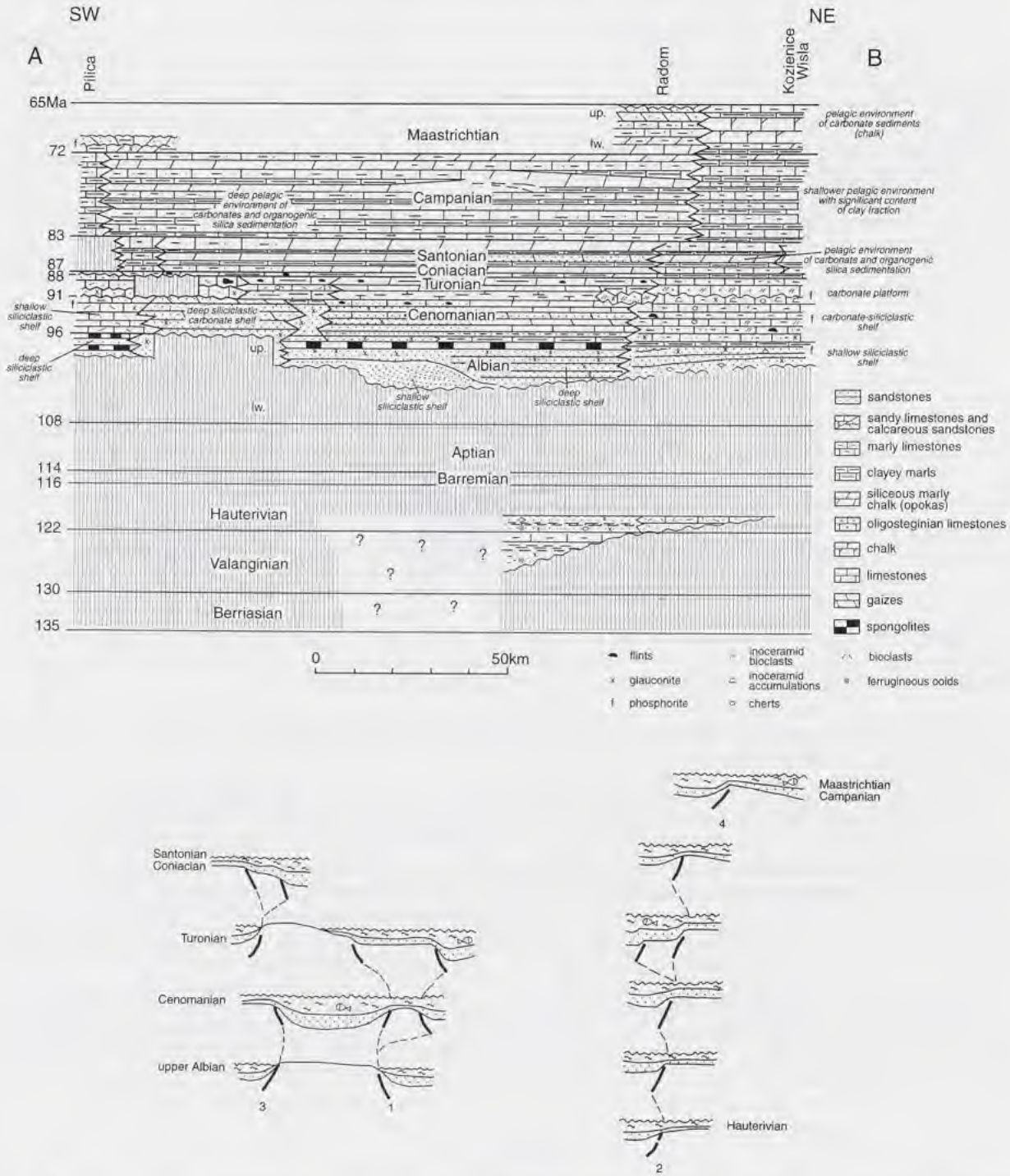

FIG. 2.— Chronostratigraphic diagram of lithofacies and sedimentary environments characteristic for Holy Cross segment of the Mid-Polish Trough (after HAKENBERG & SWIDROWSKA, 1998, modified). **1-4**, fault zones reflected in facies changes; main fault zones **1**, Przedbórz – Checiny – Mielec fault, **2**, Nowe Miasto – Ilza fault.

*FIG. 2.— Diagramme chronostratigraphique des lithofaciès et des environnements caractéristiques de la Montagne Sainte Croix, Bassin Polonais (d'après HAKENBERG & SWIDROWSKA, 1998, modifié). **1-4**, zones de failles marquées dans les changements de faciès ; principales zones de failles **1**, faille de Przedbórz – Checiny – Mielec, **2**, faille de Nowe Miasto – Ilza.*

Source : MNHN, Paris

GENERAL EVOLUTION OF DEPOSITIONAL CONDITIONS

The development of lithofacies and the sequence of sedimentary environments are shown, in a synthetic way, on the chronostratigraphic diagram (Fig. 2) based on a cross-section running from headwaters of the Pilica River through Radom to the line of the Wisla River (Fig. 3). Two sedimentary megacycles are visible. The first one is a regressive member of the Jurassic-Early Cretaceous megacycle (KUTEK, 1994), preserved in fragmentary way only and represented by sediments of the upper Valanginian and lower Hauterivian. The second, the main Cretaceous cycle, is composed in this section of sediments of the middle Albian to the Maastrichtian (CIESLINSKI & POZARYSKI, 1970). Sedimentary cycles of lower order, are recorded due to biostratigraphic documentation of stratigraphic gaps as well as a detailed recognition of lithology. They include cycles of the Albian, the Cenomanian, a early part of the lower Turonian, an upper part of the early to late Turonian, and the last, the Coniacian to the Maastrichtian (CIESLINSKI & POZARYSKI, 1970; WALASZCZYK, 1987, 1992; HAKENBERG, 1986; MARCINOWSKI & RADWANSKI, 1983). They could not be included in the diagram.

Sedimentation began (Fig. 2) in the environment of a shallow siliciclastic shelf (mostly during the Albian), then developed through the phase of the deepening siliciclastic shelf, with increasing content of silica derived from sponges (in Cenomanian depocentres). Then carbonate-siliciclastic shelf (in places, during the Cenomanian and the Turonian) occurred and a carbonate platform with organodetritic sedimentation (in the marginal zone of the Turonian basin) until pelagic environments developed. The latter are characterised by the inflow of finest terrigenous fractions (marls and siliceous marly chalk). They appeared in the central parts of the trough during the Turonian; later, they successively expanded towards NE and SW. A pure carbonate pelagic environment was the last member of this succession; it was deprived of the inflow of terrigenous material so chalk deposits could have developed. The tendency of the earlier appearance of open-sea members is observed in the northeastern flank of the trough by the way of a decrease of content of terrigenous material with an increased productivity of carbonates instead.

The deepening sedimentary environments, with decreasing share of terrigenous material, are contemporaneous with the disappearance of areas affected by erosion (also those without sedimentation) which reflects the advancement of transgression. It reached its maximum during the Campanian. Till the Campanian, the boundaries of inferred sedimentary environments were spreading, larger and larger area became covered with pelagic facies and the areas of shallow shelf disappeared. Maastrichtian sediments represent a regressive part of this megacycle, mainly in the axial and southwestern part of the trough.

SUBSIDENCE CHARACTERISTICS

In order to present changes in subsidence rates, a backstripping method is usually applied, so that quantitative data of real thicknesses (before compaction) could be referred to selected time intervals. These results for NW and central part of MPT were presented by DADLEZ *et al.* (1994, 1995). As such method was unavailable in our work, a set of 6 maps of preserved sediment accumulation rates was plotted (Fig. 3). Ratios of sediment thicknesses to respective time intervals were determined (the ODIN & ODIN (1990) time scale was used). In order to better compare carbonate sediments with clastic ones, an approximate factor was used to multiply the values of thicknesses of clastic sediments (affected by stronger compaction than carbonate ones). It should be noted that the time spans of gaps of various origin (such as non-deposition, submarine erosion or uplifting combined with sub-aerial erosion) were also used to select the stratigraphic time intervals (characterised on maps in Fig. 3). Rates of subsidence can be, to some extent, an "artificial" effect of opposite movements of the basin floor. An assumption can be made that, approximately, the range of subsidence is directly proportional to the rate of accumulation of sediments.

Source : MNHN, Paris

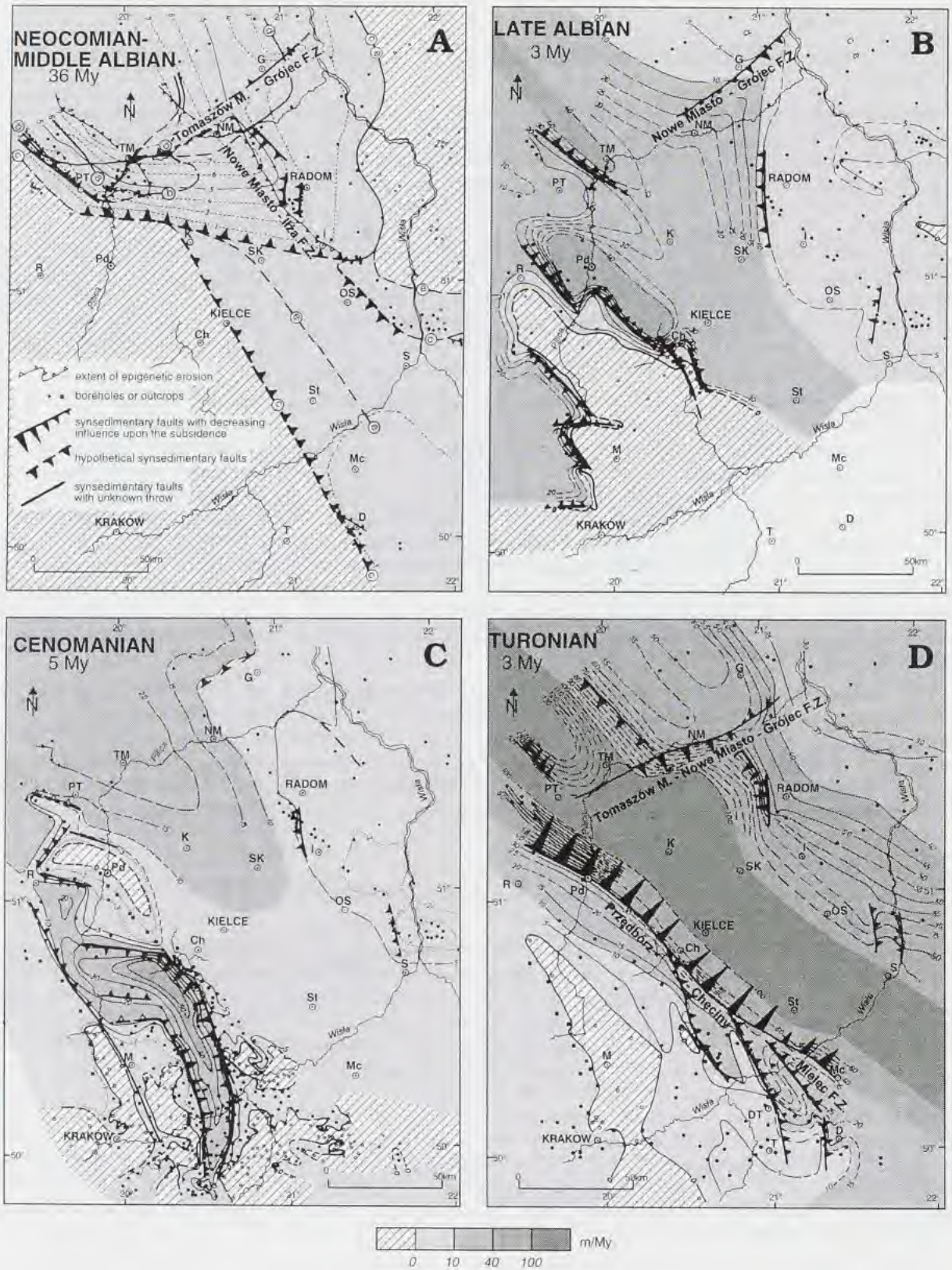

Source : MNHN, Paris

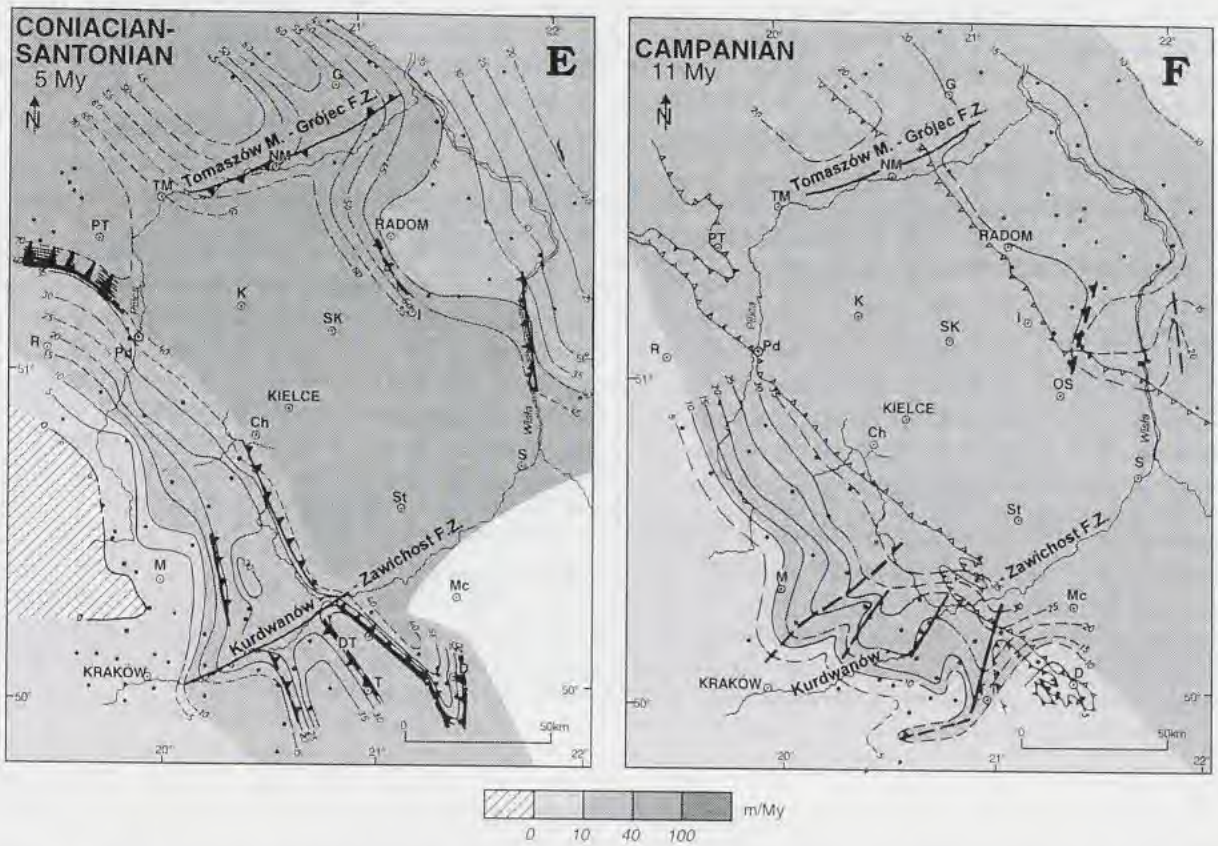

FIG. 3.— Maps of sediment accumulation rates for the particular Cretaceous time-intervals (**A-F**). Localities: **G**, Grójec; **NM**, Nowe Miasto; **TM**, Tomaszów Mazowiecki; **PT**, Piotrków Trybunalski; **Pd**, Przedbórz; **R**, Radomsko; **K**, Konskie; **I**, Ilza; **SK**, Skarzysko-Kamienna; **OS**, Ostrowiec Swietokrzyski; **S**, Sandomierz; **St**, Staszów; **Ch**, Checiny; **M**, Miechów; **Mc**, Mielec; **D**, Debica; **DT**, Dabrowa Tarnowska; **T**, Tarnów. On map **A** extents of: **a**, late Berriasian; **b**, early Valanginian; **c**, late Valanginian and early Hauterivian; **d**, Barremian and Aptian; **e**, middle Albian.

*FIG. 3.— Cartes du taux d'accumulation des sédiments pour des intervalles de temps particuliers du Crétacé (**A-F**). Localités : **G**, Grójec ; **NM**, Nowe Miasto ; **TM**, Tomaszów Mazowiecki ; **PT**, Piotrków Trybunalski ; **Pd**, Przedbórz ; **R**, Radomsko ; **K**, Konskie ; **I**, Ilza ; **SK**, Skarzysko-Kamienna ; **OS**, Ostrowiec Swietokrzyski ; **S**, Sandomierz ; **St**, Staszów ; **Ch**, Checiny ; **M**, Miechów ; **Mc**, Mielec ; **D**, Debica ; **DT**, Dabrowa Tarnowska ; **T**, Tarnów. Sur la figure 3A : **a**, extension du Berriasien ; **b**, extension du Valanginien inférieur ; **c**, extension du Valanginien supérieur et de l'Hauterivien inférieur ; **d**, extension du Barrémien et de l'Aptien ; **e**, extension de l'Albien moyen.*

NEOCOMIAN-MIDDLE ALBIAN

The character of subsidence from the Neocomian to the middle Albian (Fig. 3A) was complicated due to substantial differentiation of sedimentary processes and erosion with time, combined with the frequent lack of biostratigraphic record. There is a discontinuous stratigraphic record, with stratigraphic gaps noted on the contacts between: (1) middle Volgian-late Berriasian, (2) late Berriasian-early Valanginian (*Platylenticeras*), (3) early Valanginian (*Polyptychites*)-late Valanginian, (4) early Hauterivian-middle Albian (KUTEK *et al.*, 1989). Transgressive pulses of increasing extents appeared (*op. cit.*): (1) late Berriasian, (2) early Valanginian, (3) late Valanginian, and (4) middle Albian. Time of erosion that changed the lines of extents of the Berriasian and early Valanginian was relatively short, as it was limited by later transgressions (Fig. 3A). Only the extent of the late Valanginian and Hauterivian sediments in the area between Radom and the Wisla River is, in main part, erosional as undetermined (in respect of their age) sediments conventionally considered Barremian and Aptian (MAREK, 1983) are less extended and located north of the Pilica River.

Source : MNHN, Paris

The extents of sediments of the first two transgressions are closely connected with the axial part of the trough, two consecutive transgressions also comprise a part of its eastern margin. However, all of them were connected with the NW-SE direction. The transgressions that followed during the late Valanginian and the middle Albian were facilitated by the activation of the Nowe Miasto-Ilza fault of the same direction (Fig. 3A). This fault was synsedimentary active already in the Early and Middle Jurassic (HAKENBERG & SWIDROWSKA, 1997).

The two longest regressive events document the uplifting of the central part of the area, the axis of which extends accordingly to a line running WNW-ESE (Fig. 3A) through Radomsko-Kielce-Sandomierz (Vistula Swell: CIESLINSKI, 1976; Meta-Carpathian Arc: KUTEK *et al.*, 1989; KUTEK, 1994). The first was at the turn of the Jurassic/Cretaceous, and the second one, comprised the Barremian-early Albian. The Purbeckian facies of the early and middle Volgian are present north of the Piotrków Trybunalski-Radom line and sediments considered to be of Barremian-Aptian age occur exclusively north of the Pilica River (Fig. 3A). It is accepted that the expansion of Tethyan species of ammonites was connected with transgressions while periods of regressions showed domination of boreal forms (KUTEK & MARCINOWSKI, 1996). It is a question whether the appearance of tethyan/boreal fauna resulted only from sea level changes or from tectonically facilitated communication between Tethyan and boreal domains. The different structural directions observed in transgression and regression time spans can be admitted as contra-argument against the exclusive role of an eustatic control.

The first period of development of the Cretaceous basin (36 My; Fig. 3A) exhibits a very low rate of accumulation of sediments. A fault along the lower course of the Pilica River (the line running through Tomaszów Mazowiecki-Nowe Miasto-Grójec) was active. Transversal asymmetry of the middle Albian basin changed along its line, and the axis of depocentre became Z-shaped. Its action in earlier times (Berriasian-Aptian) resulted in more intensive subsidence in the N and NNE areas.

LATE ALBIAN

The trangression in the late Albian is a continuation of the transgression started in the middle Albian; however, its range is different qualitatively and quantitatively as this transgression covered a dominant part of the area and the sediment accumulation rate has considerably increased (Fig. 3B). The Nowe Miasto-Grójec fault was only a weakness zone, which caused an increased subsidence there. Tectonic activity during the late Albian affected mostly the western part of the area, where a set of short faults delineating elevations and depocentres of NW-SE direction has developed along the upper course of the Pilica River. In this zone of N-S to NNE-SSW direction, the Pilica fault was intensively active during the Permian till Middle Jurassic (MORAWSKA, 1996; HAKENBERG & SWIDROWSKA, 1996). The Pilica fault was inherited after the Late Palaeozoic structural setting. It was rejuvenated during the Albian and is manifested in this basin as a zone of several small oblique faults.

CENOMANIAN

The main axis of the trough remains in the place where it was previously (between Kielce and Radom, Fig. 3C). However, the location of a new subsidence depocentre shows that a rigid (so far) southwestern rim of the trough has lost its stability. This is a continuation of the process that started during the late Albian, although elevated and depressed areas are inversed. The Albian peninsula, shown in the SW part of the map (Fig. 3C), changed into a narrow through developed during the Cenomanian. It had a character of a graben where the sediment thickness is the highest in comparison with the whole Poland territory deposits. The graben is S-shaped which most likely results from the rejuvenation of E-W and N-S faults known in this area in the Palaeozoic structural stage (JURKIEWICZ, 1975; HAKENBERG, 1978, 1986; MORAWSKA, 1996; HAKENBERG & SWIDROWSKA, 1996).

Source : MNHN, Paris

TURONIAN

A substantial increase of sediment accumulation rate occurred in the Turonian; it is likely that subsidence was also much faster (Fig. 3D), especially so that deeper facies appeared at that time (compare with Fig. 2). A large zone of very rapid increase of sediment thickness appeared along present-day SW Mesozoic margin of the Holy Cross Mountains (compare Fig. 3D with Fig. 1). Thus, it is also the zone, along which the central part of the trough was inverted and uplifted together with the Palaeozoic of the HCM.

We identify a set of smaller feathering faults at the SW the Przedbórz-Checiny-Mielec main fault zone. They are genetically connected with it. The strikes of faults, against the main fault, suggest their tensional origin and also dextral slip component of the main fault zone. Tensional character of this set seems to be confirmed by pattern of sediment accumulation rate. These faults manifest themselves by the occurrence of tilted blocks (Fig. 3D) with upthrown western sides and downthrown eastern sides. These faults can explain also a facies differentiation of early Turonian sediments, which is observed in the NW-SE line of outcrops paralleling Palaeozoic/Mesozoic contact (HAKENBERG, 1978; WALASZCZYK, 1992; HAKENBERG & SWIDROWSKA, 1998). Three short approximately N-S faults are visible in the eastern part of the trough; they also can be considered as indicating a dextral slip movement along the Nowe Miasto-Ilza fault.

The considerable acceleration of sediment accumulation rate in the Turonian and the existence of good documented synsedimentary zone of Przedbórz-Checiny-Mielec fault testify that intensive tectonic subsidence was going on at that time.

CONIACIAN AND SANTONIAN

Two consecutive stages of the Cretaceous are considered jointly (Fig. 3E) due to serious discrepancies on their estimated duration (compare the time scales *in* GRADSTEIN *et al.*, 1995 and ODIN & ODIN, 1990). A more distinct differentiation in subsidence was pronounced in the area south of the line of the Wisla River. Small areas of faster and slower accumulation of sediments are elongated there consistently with the axis of the trough. The Kurdwanów-Zawichost fault strikes between Kraków and Sandomierz. It probably existed during the Coniacian and Santonian and acted as a transfer fault, as it was suggested for the Tomaszów Mazowiecki – Nowe Miasto – Grójec fault during Late Permian-Late Jurassic times (HAKENBERG & SWIDROWSKA, 1997).

CAMPANIAN

During the Campanian, the transgression of the Late Cretaceous reached its maximum (Fig. 3F). Regions that are devoid of sediments (either land or omission ones) do not exist within the limits of the studied area. Already since the Turonian, the subsidence rate was higher in the southwestern part of the trough; however, the synsedimentary faults had a very limited role. Subsidence during the Campanian could be compared with that in the Late Jurassic: sufficiently high rates but without great gradients (HAKENBERG & SWIDROWSKA, 1997).

It is likely that several faults existed in the south, along the Wisla line, that could indicate a sinistral slip component of the Kurdwanów-Zawichost fault. Isolines of sediment accumulation rates changed their directions in the south and became to be W-E in course.

Source : MNHN, Paris

MAASTRICHTIAN

As the complete thickness of sediments in this stage is preserved only in a narrow belt along the parallel course of the Wisla River, with overlying Danian sediments, no data were available to draw a map of the Maastrichtian. In this belt, the thickness of the Maastrichtian is more than 350 m. Most often the Maastrichtian is covered with the Quaternary only. The process of shallowing of the basin with effective increase of clastic material supply was observed in the Maastrichtian (HAKENBERG & SWIDROWSKA, 1998). This process was asymmetric, because it occurred earlier and was more intensive in the southwestern part of the basin. It is suggested also by the lack of upper Maastrichtian sediments in the Miechów Syncline and by the development of chalk facies in the northeastern limb. This last fact testifies to a decay of inflow of terrigenous material in this direction.

LONGITUDINAL ZONATION AND SYNSEDIMENTARY ACTIVITY OF BASIN FLOOR

The parallelism of facies zones with longitudinal basin axis is expressed (Figs 2 and 3) by the presence of axial parts subjected to the earliest sedimentation and the earliest appearance of deep siliciclastic shelf environments replaced later by pelagic sedimentation. Two marginal zones in the NE and the SW display symmetry in sediment development only during the Albian and (partly) the Turonian. Usually, the southwestern slope of the trough was different from the northeastern one due to: (1) the increased share of terrigenous material, (2) long-lasting existence of areas subjected to erosion or only omission ones, (3) diversity in sedimentary conditions, and (4) a higher energy of sedimentary environments. The two last points concern time span till the Turonian (inclusive). These differences decreased during the Campanian, but during the Maastrichtian they were effective again due to the regression.

When analysing the chronostratigraphic diagram (Fig. 2), it should be noted that the boundaries of various sedimentary environments manifest themselves in the same places at different periods of time. This suggests that the variable rate of the basin subsidence was connected with the presence of tectonic discontinuities, an important factor for the basin depth. Four fault zones can be distinguished out of which two main zones (Figs 2 and 3) delimit the axial part of the trough and its marginal limbs.

The first fault zone appears on the SW from Radom (Figs 2 and 3) where boundaries of different environments contacted in the Hauterivian and from the Albian to the Santonian, constituting a NE limit of the axial part of the trough. Effects of faster subsidence in this zone are evidenced by the facts that Valanginian sediments are preserved there and transgressive sediments of the middle Albian appear earlier at the beginning of the next sedimentary megacycle. Another argument is provided by the appearance – at the turn of the Albian and the Cenomanian – of deeper facies that spread not earlier than in the upper stages of the Cretaceous. Only bigger share of organic silica and the inflow of terrigenous material are decisive factors for specific sedimentary conditions in the axial part of the trough during the Coniacian and the Santonian. In this way the Nowe Miasto-Ilza fault displayed its synsedimentary activity during the Cretaceous. This fault was also the NE limit of the trough during Triassic and Early-Middle Jurassic times (HAKENBERG & SWIDROWSKA, 1997). Its role decreased during Cretaceous times as high thickness gradients did not appear there.

The second fault zone, being active from the late Albian to the Turonian (Fig. 2), runs in the vicinity of the southwestern contact of the Mesozoic with the Palaeozoic of the HCM. It is Przedbórz-Checiny-Mielec fault zone (Fig. 3), the fragment of bigger Poznan-Rzeszów fault zone. The considerable thickness gradients are also linked with this zone during the Turonian. An assumption can be made that a great synsedimentary fault bounding the trough in the SW acted here. Its maximum activity occurred during the Turonian. It could be consistent with the zone of intensive deformation of the Mesozoic, which was manifested during the inversion of the trough (STUPNICKA, 1971; POZARYSKI, 1971).

The transversal asymmetry of the basin can be suggested accordingly to the activity of the bounding faults. At the beginning of the Cretaceous and until the Cenomanian the axis of deposition would be shifted towards the NE boundary of the trough, and later – during the Turonian – towards the SW

Source : MNHN, Paris

boundary. From the Coniacian the role of bounding faults has decreased. When drawing conclusions on the subsidence during the Maastrichtian, one should consider not only the thickness of sediments but also a probable increase in depth of the basin, with this trend advancing to NE where pelagic lithofacies of siliceous marly chalk (opokas) and chalk appeared.

RATE OF SUBSIDENCE

In order to compare the rate of subsidence (or more precisely, the sediment accumulation rate, probably proportional to the rate of subsidence), average thicknesses of sediments were calculated for the consecutive stages (Fig. 4). The simplified method used here does not allow to quantify rates of subsidence or to distinguish tectonic factor of an external strength from an isostasy induced by sediment and water column loading. A full backstripping procedure was applied for the central and NW parts of the MPT by DADLEZ *et al.* (1994, 1995). We could only relatively compare sediment accumulation rates and interpret them in relation to the fault patterns.

After several long-lasting repeatable episodes of the uplift at the turn of Jurassic/Cretaceous time (CIESLINSKI, 1976; KUTEK, 1994; KUTEK *et al.*, 1989), subsidence increased at the beginning of the late Albian transgression. However, the sediment accumulation rate did not reach important values. During the Cenomanian, subsidence decreased. It is illustrated by the flat segment of "subsidence" curve (Fig. 4) and by the light grey-tones of the Cenomanian map (Fig. 3C). The next stage, the Turonian, is characterised by the significant acceleration of subsidence. The rate values reached over 100 m/My (i.e. more than during Late Jurassic time) in aerial restricted elongated axial belt. During Coniacian, Santonian and Campanian times the average sediment accumulation rate decreased a little. The different style of subsidence consists in the lack of deep depocentres, nevertheless an intensive subsidence embraced almost the all area.

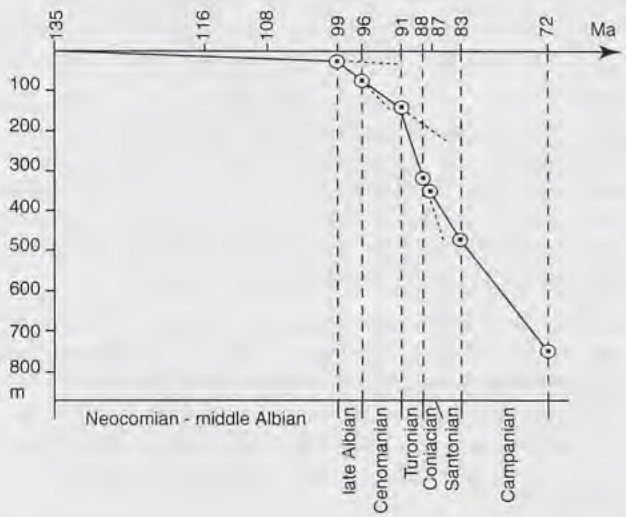

FIG. 4.— Curve of medium rate of sediments accumulation (time scale according to ODIN & ODIN, 1990).

FIG. 4.— Courbe du taux moyen d'accumulation des sédiments (échelle des temps géologiques d'après ODIN & ODIN, 1990).

Our views concerning the evolution of the Mid-Polish Trough during the Cretaceous agree with those of STEPHENSON (1993) and DADLEZ *et al.* (1994, 1995) only in part. One event of subsidence acceleration was stated by all the authors in the Cretaceous basin. We found an acceleration of subsidence in the southeastern part of the trough during the Turonian and STEPHENSON (1993) and DADLEZ *et al.* (1994, 1995) during the Cenomanian in the entire Mid-Polish Trough. The difference may result from the fact that in the first case the Cenomanian was compared with the whole Albian whereas in the second one it was compared with the late Albian only. In the first case, the difference of subsidence was related to older Cretaceous stages whereas in the second one, the subsidence acceleration is to be observed but a clear contrast is noted with the late Albian. A comparison of thickness maps of the Cenomanian and Turonian in Poland (MAREK & PAJCHLOWA, 1997) allows to assume that such a subsidence acceleration had taken place during the Turonian (SWIDROWSKA & HAKENBERG, 1999).

Source : MNHN, Paris

HYPOTHETICAL PALAEOSTRESS FIELD EVOLUTION BASED ON SYNSEDIMENTARY FAULT PATTERNS

Based on the maps of sediment accumulation rates, some simplified maps were constructed showing the main palaeotectonic elements such as synsedimentary faults, axes of palaeoelevations and depocentres for the particular stages of the Cretaceous (Fig. 5). Geometric relationships between those elements made the basis for an attempt to define the evolution of hypothetical palaeostress fields during the Cretaceous.

The turn of the Jurassic/Cretaceous in broad understanding (from the beginning of the late Kimmeridgian to the middle Albian) was characterised by quite different palaeotectonic conditions than those ones in earlier time and those in stages to come. Two series of events can be distinguished in the alternating appearance of regressive and transgressive periods; both series seem to be joined together in a cause-and-effect interdependence. The first one is: regression, limitation of influence of the Tethyan Ocean (decline of connections), an uplift of the area (in the central part) with its axis running WNW-ES-E, remaining of sedimentary basins only in the northern part of the area. The conclusion could be that geodynamic conditions resulted from the course of the border of the Eurasia plate. The second series is: transgression, facilitated contact with the Tethys (opening of connections), origin of tectonic depressions of graben type, with their NW-SE axes consistent with the extent of the trough. It suggests that geodynamic factors have activated the Teisseyre-Tornquist Zone (Fig. 5).

At that time, development of tectonic structures of NW-SE trend was not confined to the Mid-Polish Trough only. On its northeastern flank, already in the East European Platform, narrow grabens were formed (BAC-MOSZASZWILI & MORAWSKA, 1975; MAREK, 1983). This testifies that stresses expanded northwards. The grabens are long and very narrow; this suggests that their tensional origin is "restricted". Instead, their development can be connected with the presence in the basement of steep strike-slip faults that were split upward in a flower-like manner and made that way the structures of grabens with slip component of transtension.

Repetitive erosional and depositional periods could have been connected with the permutation of principal stress axes σ_1 and σ_2. Extensive regime: σ_1 vertical, σ_2 horizontal trending WNW-ESE – regression. Strike-slip regime: σ_2 vertical, σ_1 horizontal trending WNW-ESE – transgression. In both cases principal minimum stress axis σ_3 was similarly oriented (NNE-SSW) (Fig. 5). A phase of intensified rifting process with slip component during the Early Cretaceous is known from various areas of Central and Western Europe as the so-called "Late Cimmerian" rifting pulse (ZIEGLER, 1990).

Tectonic activity during the Albian was noted within the southwestern limb of the trough. A set of *en échelon* faults developed above the Pilica fault existing in Palaeozoic basement (Fig. 5). They can be defined as tensional fractures that caused a number of elevations and depocentres of short axes. This arrangement suggests a strike-slip regime of stresses with the principal maximum stress axis σ_1 close to NW-SE, thus parallel to the trough axis. As compared with the former stage, a dextral rotation happened by approximately 22°; this was probably followed by an increase of the difference between σ_1 and σ_3. This resulted in a sinistral-slip component along the Pilica fault.

A graben that developed over the Albian peninsula during the Cenomanian was a dominant and clearly identified structure (Fig. 3C, B). So, the process of disruption of the SW frame of the trough continued, and only a permutation of stress axes σ_1 and σ_2 happened (Fig. 5) due to relaxation of principal maximum stress. Extensional regime became decisive and the position of the axis σ_3 could be defined from the S-shaped graben: only the axis σ_3 of principal minimum stress of NE-SW direction could ensure opening of the graben in all its segments (Fig. 5). The Cenomanian fault pattern in this area does not allow to interpret tectonic conditions as "a response of the lithosphere to compression" suggested for the central and NW parts of the MPT by STEPHENSON (1993) and DADLEZ *et al.* (1994, 1995).

Consequences of an intensive basin opening had taken place during the Turonian. A long fault zone (the Przedbórz-Checiny-Mielec fault) developed southwest of Kielce. This fault is expressed by very high thickness gradients (Fig. 5). It means that the process of pulling of the southwestern region into the

Source : MNHN, Paris

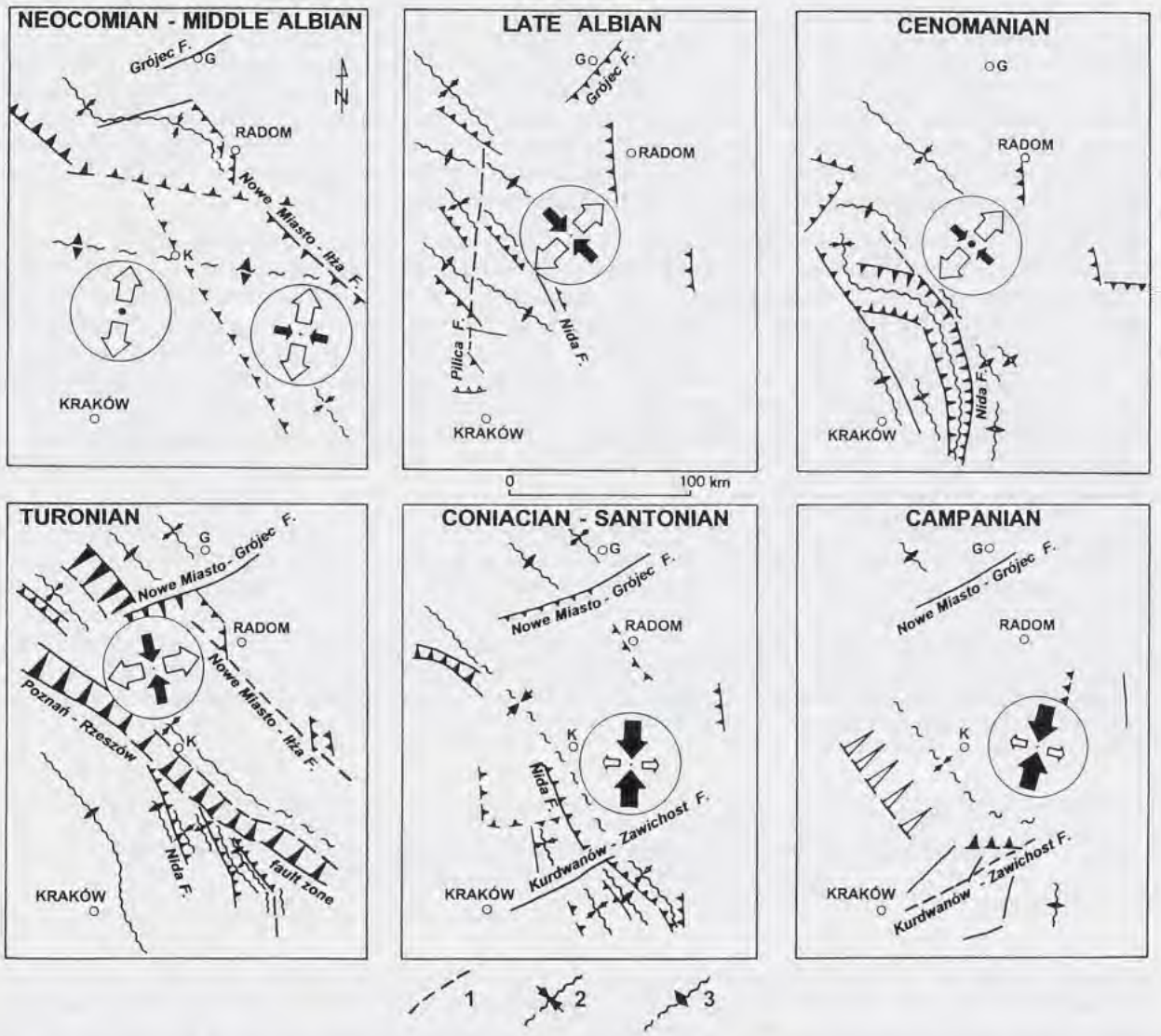

FIG. 5.— Hypothetical palaeostress field evolution based on synsedimentary fault patterns. **1**, active basement faults; **2**, axes of depocentres; **3**, axes of uplifted areas; other explanations see Fig. 3. Stress regimes: extensive or transtensive: stress pattern with σ_1 marked with a solid circle in the centre; pure strike-slip or transpressive: stress pattern with σ_2 marked with a dot in the centre. Horizontal stress axes: black inward arrows: compressional stress axes σ_1, white outward arrows: extensional stress axes σ_3.

*FIG. 5.— Évolution hypothétique du champ des paléocontraintes basées sur le réseau de failles synsédimentaires. **1**, failles actives dans le substratum ; **2**, axe de dépôt-centre ; **3**, axe des zones soulevées ; autres figurés voir Fig. 3. Régime des contraintes : extensif ou transtensif : σ_1 figuré par un gros point noir au centre ; décrochant pur ou transpressif : σ_2 figuré par un petit point noir au centre. Axes des contraintes horizontales : compression σ_1 figurée par des flèches noires centripètes ; extension σ_3 figurée par des flèches blanches centrifuges.*

trough was restrained. It should be noted here that during the Turonian this region was left on the southwestern limb of the trough. A set of T-fractures turned into normal faults in the SW sector of the main fault zone, definitely points to a dextral-slip component during opening of the Turonian basin in transtensional regime. Similar dextral-slip component along the Nowe Miasto-Ilza fault could be suggested by three faults running northwestwards as well as southeastwards of Radom. The stress pattern was most likely affected by further clockwise rotation, which resulted in the change of axis orientation σ_1 into NNW-SSE and of σ_3 into WSW-ENE (Fig. 5).

Source : MNHN, Paris

The style of subsidence during Coniacian-Campanian times has changed. An overall decrease of fault activity is observed (Fig. 5). Relatively intensive subsidence concerned a significant part of the studied area but it was not related to fault zones. The southern part of area was tectonically activated and separated from the central part of the basin by the Kurdwanów-Zawichost transfer fault (Fig. 5). Though subsidence was intensive especially during the Campanian and the eroded areas disappeared, the closing of the basin is visible in its south-western part. It is evidenced by the isolines of subsidence rate turning E-W in the area south of the Wisla line. Several faults situated along the upper course of this river may point to a sinistral-slip component along the Kurdwanów-Zawichost fault (Fig. 5).

It seems likely that the development of the basin during the Coniacian, Santonian and Campanian occurred in different tectonic conditions than previously. Observations noted in other basins (STEPHENSON *et al.*, 1990, 1992) suggested the interpretation of the compressional origin of tectonic control of the MPT development during the time prior to inversion; in this case it was dated as Cenomanian-Maastrichtian time span (STEPHENSON, 1993; DADLEZ *et al.*, 1994, 1995). According to our results, an increase of the compression seems very probable, but in a shorter time (Coniacian-Maastrichtian). A different interpretation presented here (for the SE part of MPT) consists also in understanding the effects of compression as a deflection of the axial part of the basin till the end of Campanian times. An inversion in the axial part of the entire MPT since Coniacian was suggested (DADLEZ *et al.*, 1994, 1995).

As a consequence of the increase of compression, the method of fault identification applied here fails because faults did not manifest in form of upthrown and downthrown sides which obviously did not control accumulation rate. The increase of compression in the NNE-SSW direction (suggested by sinistral component along Kurdwanów – Zawichost fault zone) may explain considerable subsidence of the trough during Coniacian-Campanian times. Simultaneous uplift of SW limb of the Mid-Polish Trough (the Sudetes and Fore-Sudetic Monocline areas; MILEWICZ, 1973) seems to confirm the deduced flexural mechanism (compare with CLOETINGH & KOOI, 1992) of effective subsidence during Coniacian-Campanian times.

STRIKE-SLIP COMPONENT ALONG THE TEISSEYRE-TORNQUIST ZONE IN RELATION TO PLATE KINEMATICS

During the Mesozoic, the Mid-Polish Trough developed on the Eurasia plate, over the contact of the Precambrian and Palaeozoic Platforms (TESZ) the basement structure of which is similar to the East European Craton (BERTHELSEN, 1998). The basement is weakened there by the deep-seated zone of the crustal discontinuity (TTZ). Stresses from collisional plate edges can be transferred over thousands of kilometres toward the plates (CLOETINGH, 1988; ZIEGLER, 1990; ZOBACK *et al.*, 1993). The movement of Africa relative to Eurasia has been determined (LE PICHON *et al.*, 1988). A question arises: what relation exists between hypothetical intraplate stress fields in the TTZ, which was deduced in the previous section of this paper, and the theoretical strike-slip component that could occur along the TTZ due to relative movement of the both plates?

Tracks of two points (Tunisian Bay and Suez) situated in the Africa plate were taken into consideration (Fig. 6A); among other points analysed in the reference work both are at shortest distance to Poland. From the Early Jurassic (190 Ma) to the Santonian (80 Ma) the relative movement path of Africa towards Eurasia was more or less parallel to the TTZ. Africa shifted relatively to the left (Fig. 6A) thus there was a relative sinistral motion between the plates (ZIEGLER, 1990). The parallelism of relative movement path of Africa against Eurasia to the crust weakness zone of TTZ theoretically suggests that sinistral component along the TTZ could be very probable during that time. Conclusions drawn from the distribution of palaeotectonic elements since the Early Cretaceous to the Middle Albian (Fig. 5) seem to be in line with the sinistral drift resulting from plate kinematics. Also, the distribution of synsedimentary fault pattern in the Early Jurassic induced the authors (HAKENBERG & SWIDROWSKA, 1997) to assume that the sinistral component of strike-slip stress field was common during that epoch and that the axis σ_3 of the principal minimum stress was oriented NNW-SSE.

Source : MNHN, Paris

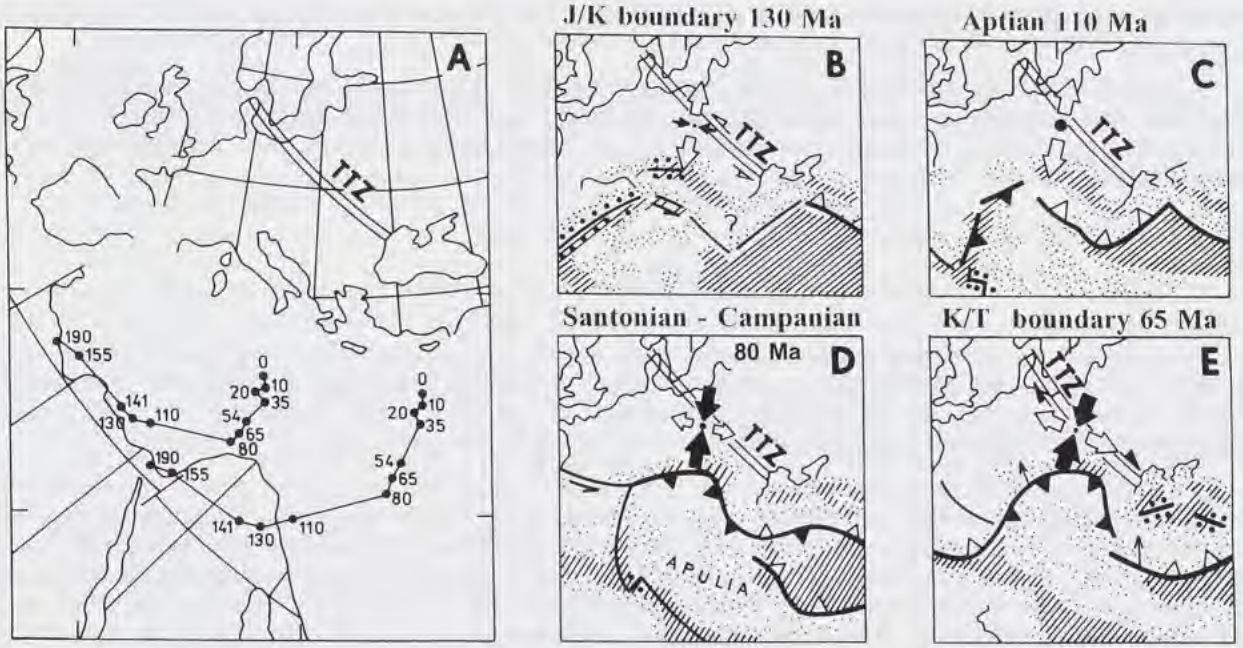

FIG. 6.— Strike-slip component along the Teisseyre-Tornquist Zone (TTZ) during Cretaceous time shown in relation to plate kinematics presented by LE PICHON *et al.* (1988, fragments of Figs 1 and 2). **A**, relative motion history of Africa with respect to Eurasia from Early Jurassic (190 Ma) to Present time; **B-E**, simplified plate tectonic schemes along northern boundary of Tethys. Schematic plate boundaries: continuous line, transform; open triangles, oceanic subduction; closed triangles, continental collision; double dotted line, oceanic accretion; hachured pattern, oceanic crust; dotted pattern, thinned continental crust.

FIG. 6.— Composante décrochante le long de la Zone de Teisseyre-Tornquist (TTZ) pendant le Crétacé en relation avec la cinématique des plaques (LE PICHON et al., *1988). **A**, reconstruction du mouvement relatif de l'Afrique par rapport à l'Eurasie du Jurassique inférieur (190 Ma) à l'Actuel. **B-E**, schémas simplifiés de la tectonique des plaques le long de la bordure nord de la Téthys. Limites de plaques : ligne continue, transformantes ; ligne à triangles blancs, subduction ; ligne à triangles noirs, collision ; ligne pointillée double, accrétion océanique ; hachures, croûte océanique ; pointillés, croûte continentale amincie.*

During the Turonian the dextral-slip component along the NW-SE direction of TTZ came into evidence in transtensional regime. It may be a reflection of overthrusting in the Western Inner Carpathians (MATEJKA & ANDRUSOV, 1931).

A rapid break in the track of relative motion occurred at the point characterising the Santonian (80 Ma): Africa started to move towards Eurasia (Fig. 6A); this motion was decisively northwards (LE PICHON *et al.*, 1988). GUIRAUD & BOSWORTH (1997) presented a comprehensive compilation of tectonic processes going on in intracratonic sedimentary basins over the Africa, Arabia and India plates. Their compilation is intended to prove that a close relation exists between the Senonian inversion of many basins and the change in direction of relative movement of the southern plates toward Eurasia.

A comparison of the stress field, supposed here for the Santonian-Campanian (Fig. 5) with the GIRAUD & BOTHWORTH (1997) and LE PICHON *et al.* (1988) findings, allows to conclude about the coherence of these data. The compression nearly N-S ought to create dextral-slip component along the trend of the TTZ. The analysis of brittle deformation observed in the Mesozoic rocks of the investigated area carried out by LAMARCHE *et al.* (1998) show a N-S compression, which is suspected to occur before the main stage of the Laramide tectonic inversion (compression NE-SW; JAROSZEWSKI, 1972; SWIDROWSKA, 1980; LAMARCHE *et. al.*, 1998). It could be dated as the Santonian-Campanian compression.

Another comparison of evolution of stress conditions proposed here (Fig. 5) with tectonic events occurring in the northern border of Tethys (Fig. 6 B-E) is necessary. It leads to the conclusion that continuous change in the stress regime from sinistral transtensional to dextral transpressive is not

Source : MNHN, Paris

contradictory to the distribution of zones of spreading, subduction and overthrusts already identified in the northern Tethyan area (LE PICHON *et al.*, 1988).

It should be stressed that strike-slip movements along TTZ, which could result from the suggested transtensional to transpressional stress regimes, were of small scale, and did not exceed few tens of kilometres. It pertains both to the movements leading to basin opening and to those ones acting during inversion.

CONCLUSION

The analysis of the deposits accumulation rates, treated as a reflection of subsidence rates, was coupled with the recognition of basin sedimentary conditions. It made possible to distinguish synsedimentary fault patterns for six time-spans of the Cretaceous. The fault patterns gave a base for the reconstruction of the palaeostress field evolution controlling basins development.

The extensional regime came into evidence twice in the history of Cretaceous basin: at the beginning of the Cretaceous but during regressions only, and then during the Cenomanian. These episodes were connected with a decrease of subsidence rates. Strike-slip stress field characterised the remaining time-periods of the Cretaceous basin development from the beginning of the Cretaceous but during transgressions only till the Campanian (the Cenomanian excluded). The main episode of accelerated subsidence during the Turonian was controlled by accentuated activity of SW bounding fault.

The evolution of tectonic regime can be characterised by the clockwise rotation of the strike-slip stress field in transtensional regime from the beginning of Cretaceous (σ_1 WNW-ESE) till the end of Turonian (σ_1 NNW-SSE), and later on, from the Coniacian-Santonian, in transpressional regime (σ_1 N-S to NNE-SSW) till the inversion time (σ_1 NE-SW) at the turn of Cretaceous/Tertiary. This rotation was followed by change of character of a strike-slip component along the Teisseyre-Tornquist Zone: from the sinistral component (till the middle Albian) to the dextral one (from the Turonian till inversion time). The beginning of increase of compression during the Turonian, resulted in basin opening in well expressed strike-slip stress field, but still in transtensional regime. The succession of palaeotectonic conditions of Cretaceous basins opening seems to be compatible with the relative movements between Africa and Eurasia plates during this time. The extensional stress field manifested at the transition from the Jurassic to the Cretaceous during regressions times could be interpreted as a reaction of southern edge of Eurasia plate to spreading in the northern Tethys.

ACKNOWLEDGEMENTS

We are indebted to Dr F. BERGERAT for discussion and comments on earlier version of the manuscript. Critical comments and constructive suggestions made by Dr R.A. STEPHENSON and an anonymous reviewer contributed to improve the manuscript. Their efforts are highly appreciated. The manuscript benefited also from Prof. J. LEFELD helpful remarks. Dr J. LAMARCHE is thanked for the translation of the abstract into French.

The study has been performed within the framework of the statute problem in the Geological Institute of Polish Academy of Sciences titled "Palaeotectonics of the Holy Cross Mountains area during the Cretaceous".

REFERENCES

BAC-MOSZASZWILI, M. & MORAWSKA, A., 1975.— Tectonic structures in the Cretaceous formations of the Warsaw Basin and their relation to the substratum dislocations. *Acta Geologica Polonica*, **25** (4): 577-586 (in Polish with English summary).

BERTHELSEN, A., 1998.— The Tornquist Zone northwest of the Carpathians: an intraplate pseudosuture. *Geologiska Foreningens i Stockholm Forhandlingar*, **120**: 223-230.

Source : MNHN, Paris

CIESLINSKI, S., 1976.— Development of the Danish-Polish Furrow in the Góry Swietokrzyskie Region in the Albian, Cenomanian and Lower Turonian. *Biuletyn Panstwowego Instytutu Geologicznego*, **295**: 249-269 (in Polish with English summary).

CIESLINSKI, S. & POZARYSKI, W., 1970.— Kreda. *In*: W. POZARYSKI (ed.), The Stratigraphy of the Mesozoic in the margin of the Góry Swietokrzyskie. *Prace Panstwowego Instytutu Geologicznego, Warszawa*, **56**:185-231 (in Polish with English summary).

CLOETINGH, S., 1988.— Intraplate stresses: a new element in basin analysis. *In*: K.L. KLEISPEHN & C. PAOLA (eds), *Frontiers in Sedimentary Geology: New Perspectives in Basin Analysis*. Springer, New York: 205-230.

CLOETINGH, S. & KOOI, H., 1992.— Tectonic stress and dynamic aspects of rifted sedimentary basins. *Tectonophysics*, **215**: 167-185.

DADLEZ, R., 1989.— Epicontinental Permian and Mesozoic basins in Poland. *Kwartalnik Geologiczny*, **33** (2): 175-198.

DADLEZ, R., 1997.— Seismic profile LT-7 (northwest Poland): geological implications. *Geological Magazine*, **134** (5): 653-659.

DADLEZ, R., NARKIEWICZ, M., STEPHENSON, R.A. & VISSER, M.T.M., 1994.— Subsydencja bruzdy sródpolskiej w permie i mezozoiku. *Przeglad Geologiczny*, **42** (9): 715-720 (in Polish with English summary).

DADLEZ, R., NARKIEWICZ, M., STEPHENSON, R.A. & VISSER, M.T.M. & VAN WEES, J.D., 1995.— Tectonic evolution of the Mid-Polish Trough: modelling implications and significance for central European geology. *Tectonophysics*, **252**: 179-195.

GLAZEK, J. & KUTEK, J., 1970.— The Holy Cross Mts area in the Alpine diastrophic cycle. *Bulletin de l'Académie polonaise des Sciences, Série des Sciences géologiques et géographiques*, **18** (4): 227-235.

GRADSTEIN, F., AGTERBERG, F., OGG, J., HARDENBOL, J., VAN VEEN, P., THIERRY, J. & HUANG, Z., 1995.— Geochronology time scales and global stratigraphic correlation. *SEPM Special Publications*, **54**: 95-121.

GUIRAUD, R. & BOSWORTH, W., 1997.— Senonian basin inversion and rejuvenation of rifting in Africa and Arabia: synthesis and implications to plate-scale tectonics. *Tectonophysics*, **282**: 39-82.

GUTERCH , A., GRAD, M., JANIK, T., MATERZOK, R., LUOSTO, U., YLINIEMI, J., LUCK, E., SCHULZE, A. & FORSTE, K., 1994.— Crustal structure of the transition zone between Precambrian and Variscan Europe from new seismic data along LT-7 profile (NW Poland and eastern Germany). *Comptes Rendus de l'Académie des Sciences, Paris*, **319** (II): 1489-1496.

HAKENBERG, M., 1978.— Albian-Cenomanian palaeotectonics and palaeogeography of the Miechów Depression, northern part. *Studia Geologica Polonica*, **58**: 5-104 (in Polish with English summary).

HAKENBERG, M., 1986.— Albian and Cenomanian in the Miechów Basin (Central Poland). *Studia Geologica Polonica*, **86**: 57-85 (in Polish with English summary).

HAKENBERG, M. & SWIDROWSKA, J., 1996.— Palaeogeographic evolution of the Miechów Syncline area and its structural control from the Late Triassic till the Middle Jurassic. *Prace Instytutu Geografii WSP w Kielcach*, **1**: 77-92 (in Polish with English summary).

HAKENBERG, M. & SWIDROWSKA, J., 1997.— Propagation of the southeastern segment of the Polish Trough connected with bounding fault zones (from Permian to Late Jurassic). *Comptes Rendus de l'Académie des Sciences, Paris*, **324** (II): 793-803.

HAKENBERG, M. & SWIDROWSKA, J., 1998.— Evolution of the Holy Cross segment of the Mid-Polish Trough during Cretaceous time. *Geological Quarterly*, **42** (3): 239-262.

JAROSZEWSKI, W., 1972.— Mesoscopic structural criteria of tectonics of non-orogenic areas: an example from north-eastern Mesozoic margin of the Swietokrzyskie Mountains. *Studia Geologica Polonica*, **38**: 9-215 (in Polish with English summary).

JURKIEWICZ, H., 1975.— The geological structure of the basement of the Mesozoic in the central part of the Miechów Trough. *Kwartalnik Geologiczny*, **18** (1): 90-109 (in Polish with English summary).

KUTEK, J., 1994.— Jurassic tectonic events in south-eastern cratonic Poland. *Acta Geologica Polonica*, **44** (3-4): 167-221.

KUTEK, J. & MARCINOWSKI, R., 1996.— Faunal changes in the Valanginian of Poland: tectonic or eustatic control?. *Mitteilungen aus dem Geologisch Paläontologischen Institut der Universität in Hamburg*, **77**: 83-88.

KUTEK, J., MARCINOWSKI, R. & WIEDMANN, J., 1989.— The Wawal Section, Central Poland: an important link between Boreal and Tethyan Valanginian. *In*: J. WIEDMANN (ed.), *Cretaceous of the Western Tethys: Proceedings 3rd International Cretaceous Symposium, Tubingen, 1987*. E. Schweizerbart'sche Verlagsbuchhandlung, Stuttgart: 755-770.

LAMARCHE, J., SWIDROWSKA, J., BERGERAT, F., HAKENBERG, M., MANSY, J.-L., WIECZOREK, J., STUPNICKA, E. & DUMONT, T., 1998.— Development and deformation of a Mesozoic basin adjacent to the Teisseyre-Tornquist Zone: The Holy Cross Mountains (Poland). *In:* S. CRASQUIN-SOLEAU & É. BARRIER (eds), Peri-Tethys Memoir 4: Epicratonic basins of Peri-Tethyan platforms. *Mémoires du Muséum national d'Histoire naturelle*, **179**: 75-92.

LE PICHON, X., BERGERAT, F. & ROULET, M.-J., 1988.— Plate kinematics and tectonics leading to the Alpine belt formation; a new analysis. *Geological Society of America, Special Paper*, **218**: 111-131.

MARCINOWSKI, R. & RADWANSKI, A., 1983.— The Mid-Cretaceous transgression onto the Central Polish Uplands (marginal part of the Central European Basin). *Zitteliana*, **10**: 65-95.

MAREK, S., 1983.— Kreda dolna. *In*: The geological structure of the Warsaw (Plock) Trough and its basement. *Prace Panstwowego Instytutu Geologicznego*, **103**: 161-177 (in Polish with English summary).

Source : MNHN, Paris

MAREK, S. & PAJCHLOWA, M. (eds), 1997.— The epicontinental Permian and Mesozoic in Poland. *Prace Panstwowego Instytutu Geologicznego*, **153**: 1-452 (in Polish with English summary).

MATEJKA, A. & ANDRUSOV, D., 1931.— Aperçu de la géologie des Carpates occidentales de la Slovaquie centrale et des régions avoisinantes. *In*: Guide des excursions dans les Carpates occidentales. *Knihovna Statniho Geologickeho Ustavu C.S.R, Praha*, **13** (A): 19-165.

MILEWICZ, J., 1973.— Kreda górna. Sudety. *In*: *Budowa Geologiczna Polski. Stratygrafia. Mezozoik*. Wydawnictwa Geologiczne, Warszawa (in Polish): 619-627.

MORAWSKA, A., 1996.— Structural control of Permian-Early Triassic sedimentation in the Miechów Trough. *Prace Instytutu Geografii WSP w Kielcach*, **1**: 69-75 (in Polish with English summary).

ODIN, G.S. & ODIN, C., 1990.— Échelle numérique des temps géologiques, mise à jour. *Géochronique*, **35**: 12-21.

POZARYSKI, W., 1971.— The tectonics of the Radomsko elevation. *Rocznik Polskiego Towarzystwa Geologicznego*, **41** (1): 169-179 (in Polish with English summary).

STEPHENSON, R.A., 1993.— Continental rift development in Precambrian and Phanerozoic Europe: Europrobe and the Dnieper-Donets rift and Polish trough basins. *Sedimentary Geology*, **86**: 159-175.

STEPHENSON, R.A., RICKETTS, B.D., CLOETINGH, S.A. & BEEKMAN, F., 1990.— Lithosphere folds in the Eurekan orogen. Arctic Canada. *Geology*, **18**: 603-608.

STEPHENSON, R.A., VAN BERKEL, J. & CLOETINGH, S.A., 1992.— Relationship between salt diapirism and the tectonic history of the Sverdrup basin. Arctic Canada. *Canadian Journal of Earth-Sciences*, **29**: 2695-2705.

STUPNICKA, E., 1971.— Tectonics of the Mesozoic rocks of the southern border of the Holy Cross Mts. *Rocznik Polskiego Towarzystwa Geologicznego*, **40** (3-4): 393-409 (in Polish with English summary).

SWIDROWSKA, J., 1980.— Tectonic stylolites as a tectogenetic index in the area of SW margin of the Holy Cross Mts. *Przeglad Geologiczny*, **28** (3): 159-164 (in Polish with English summary).

SWIDROWSKA, J. & HAKENBERG, M., 1999.— Subsydencja i poczatki inwersji bruzdy srödpolskiej na podstawie map miazszosci i litofacji osadów górnokredowych. *Przeglad Geologiczny*, **47** (1): 61-68 (in Polish with English summary).

WALASZCZYK, I., 1987.— Mid-Cretaceous events at the marginal part of the Central European Basin (Annopol-on-Vistula section, Central Poland). *Acta Geologica Polonica*, **37** (1-2): 61-73.

WALASZCZYK, I., 1992.— Turonian through Santonian deposits of the Central Polish Uplands; their facies development, inoceramid paleontology and stratigraphy. *Acta Geologica Polonica*, **42** (1-2): 1-122.

ZIEGLER, P.A., 1990.— *Geological Atlas of Western and Central Europe*. Shell Internationale Petroleum Maatschappij, B.V., The Hague: 1-239.

ZOBACK, M.D., STEPHENSON, R.A., CLOETINGH, S., LARSEN, B.T., VAN HOORN, B., ROBINSON, A., HORVATH, F., PUIGDEFABREGAS, C. & BEN-AVRAHAM, Z., 1993.— Stresses in the lithosphere and sedimentary basin formation. *Tectonophysics*, **226**: 1-14.

Source : MNHN, Paris

INDEX

A

Aalenian 62; 65; 71; 72; 74; 83; 84; 85; 87; 111; 124; 162
Aaliji 185; 186; 187; 188; 189
Abba 162; 173
Abd Al Aziz 178; 199; 201
Adoumaz 45
Africa 12; 34; 94; 96; 101; 102; 103; 123; 124; 125; 130; 131; 150; 239; 252; 253
Aganane 41; 47; 51
Ahmer Akhdar 113
Ain el Morra 59
Aïn Hamra 143; 150
Ain Nokra 99
Ait Attab 99
Aït Bougemmez 41; 45
Ait Oufella 101
Aktyubinsk 211
Al Furat 180; 182; 183; 184; 185; 186; 187; 188; 191; 192
Al Kharrata 190; 198
Albian 148; 155; 169; 177; 178; 183; 185; 189; 192; 198; 239; 243; 245; 246; 248; 249; 250; 252
Aleppo 159; 161; 165; 166
algae 41; 59; 214; 216; 219; 222; 224; 225; 226; 228; 230
Algeria 34; 68; 80; 87; 102; 148; 153
Alibek-Mola 211; 212
Alljutovella 216
Alps 75; 80; 226
Alveosepta (Iberina) prealusitanica 165
Alveosepta jaccardi 164; 165
Amanos 165
America 29; 94; 123; 130
Amezraï 41; 45
Amijiella amiji 162; 163
ammonite 41; 45; 57; 58; 62; 63; 64; 65; 68; 69; 71; 81; 82; 84; 87; 111; 112; 163; 164; 233; 246
ammonoid 213; 214; 216; 222; 223; 228; 230; 231; 232
Amsitten 131
Amu-Darya 216
Anah 170; 173
Anceps Zone 68; 72
Anchicodium 219; 226
Anergui 45
Annaplophora littica 105
annelid 63
Anoplophora lettica 26
Antakia 165
Anti-Atlas 94; 146
Anti-Lebanon 160; 161; 164; 165; 166
Appalachian Basin 152
Aptian 129; 136; 139; 148; 159; 172; 245; 246
Aqaba 171
Arabian platform 169; 170; 171
Aral Sea 215; 216; 225; 228
Arctic 207; 217; 219; 226; 228
Argana 25; 26; 28; 32; 33; 34
Argovian 152
Arkhangelsk 203; 204
Artinskian 203; 204; 213; 225; 226; 228; 230; 231; 232; 233; 234
As Sirra 186; 188; 190
Asia 218; 232
Asphinctites patrulii 68
Asphinctites replictus 67
Aspidoceras circumspinosum 71
Aspidoceratidae 70
Asselian 203; 204; 213; 216; 219; 223; 224; 225; 226; 231; 232; 233
Astrakhan 213; 225; 231
Atalla 180; 184; 185; 188; 191; 192
Athleta Zone 69; 74
Atlantic 23; 25; 28; 32; 33; 34; 94; 95; 96; 97; 99; 100; 102; 107; 123; 124; 125; 130; 143; 145; 147; 148; 154; 156
Atlas 21; 23; 24; 25; 26; 28; 29; 30; 32; 33; 39; 40; 45; 47; 51; 59; 68; 93; 94; 95; 96; 97; 98; 99; 100; 101; 102; 103; 138; 147; 148; 155; 156
Aulotortus sinuosus 161
Aurigera Zone 68
Aurigerus Zone 71; 72; 74
Autunian 28
Ay 213; 228
Azilal 45; 47
Azira 112
Azizia 79
Azores 29; 94

B

Bajocian 62; 63; 65; 66; 69; 71; 73; 74; 76; 79; 81; 83; 84; 85; 86; 87; 97; 111; 124; 136; 148
Balanocidaris glandifera 164
Balkhash Lake 216
Barents Sea 223
Barremian 159; 245
Bathonian 40; 62; 63; 67; 68; 69; 71; 72; 73; 74; 76; 79; 81; 83; 84; 85; 86; 87; 96; 111; 124; 159; 163; 166
Batroun 164

Source : MNHN, Paris

Bechar 12
belemnite 62; 63; 64; 67; 69; 75; 81
Beni Bou Yahi 109
Beni Snassen 108; 111; 112; 113; 116; 123; 124; 125
Beni-Mellal 99
Béni-Mellal 40; 41; 45
Beresella 219
Beresellid 219
Berrechid 25; 32; 34
Berriasian 72; 113; 136; 245
Bifrons Zone 65; 72
Bihenithyris sp. 164
Bihenithyris weiri 164
Bimammatum Zone 71
Bishri 177; 180; 182; 185; 199
Bitlis 169; 170; 199
bivalve 41; 214; 215; 216; 222; 223; 228; 230
Black Sea 240
Bornholm 240
Bou Beker 112
Bou Draa 143
Bou Fekrane 25
Bou Garnine 79; 83
Bou Hedma 72
Bou Kornine 76
Bou Rhennja 113; 124
Boudenib 147
Boudoufoud 109
Boufekrane 34
Boulemane 97; 99
Bourdine 109; 123
Bou-Regreg river 15
Bqassem 163
brachiopod 41; 62; 63; 163; 164; 214; 216; 218; 219; 222; 223; 224; 225; 226; 228; 230; 232
Brachithyrina subcarnica 218
Bremeri Zone 68; 69; 72; 74
bryozoan219; 222; 224; 225; 226; 228; 230; 232
Bukhara-Karsha 216
Bullatimorphites (Bullatimorphites) gr. *bullatimorphus* 68
Bullatimorphites (Bullatimorphites) sp. 68
Bullatimorphites (Bullatimorphites) sp. juv. 68
Bullatimorphites (Sphaeroptychius) marginatus 68
Busachi Peninsula 216; 225

C

Cadomites (Cadomites) bremeri 68
Cadomites (Cadomites) cf. *bremeri* 68
Cadomites (Cadomites) orbignyi 68
Cadomites sp. 67
Cainozoic 40; 93; 94; 130; 150; 173; 190
Calamites 14
Caledonian 94
Callovian 63; 64; 67; 68; 69; 72; 74; 76; 79; 81; 83; 84; 86; 87; 88; 111; 112; 124; 136; 147; 148; 163; 164
calpionnelid 76
Cambrian 146
Campanian 169; 173; 181; 182; 183; 185; 189; 194; 195; 199; 243; 247; 248; 249; 252; 253; 254
Campos 156
Campylites 70; 87
Campylites (Campylites) cf. *delmontanus* 70
Campylites (Campylites) cf. *delmontanus helveticus* 70
*Campylites (Campylites) delmontanus*69; 70
Campylites (Campylites) delmontanus helveticus 69; 70
Campylites (Campylites) gr. *delmontanus* 70
Campylites (Campylites) taeniolatus 69
Canada 226
Cap Juby 143; 152
Carboniferous 11; 12; 18; 94; 146; 147; 153; 154; 172; 173; 175; 189; 192; 203; 204; 207; 212; 213; 216; 219; 224
Cardiocarpus 14
cardioceratids 70; 87
Carixian 41; 45; 47; 51; 59; 71; 72; 75; 79; 81; 84; 85; 86
Carnian 23; 26; 28; 29; 30; 32; 33; 34; 95
Casablanca 154
Caspian Sea 233
Celtic basin 138
Cenoceras sp. 67; 68; 69
Cenomanian 99; 175; 178; 179; 185; 191; 239; 243; 246; 248; 249; 250; 252; 254
cephalopod 96; 216
Châabet el Attaris 58; 59; 62; 63; 65; 67; 68; 69; 71; 72; 74; 75; 79
Chaoiella gruenewaldti 218
Checiny 247; 248; 250
Chibli 184; 188
Chichaoua 131
Chilou 188; 189; 198
China 232
Choffatia (Subgrossouvria) sp. 68
Choffatia sp. indet. 69
Choffatia sp. juv. 69
Chondrites 63
Chondroceras 67; 71
Chondroceras cf. *gervillei* 67
Chondroceras cf. *orbignyanum* 67
Choristites fritchi 216
Choristites priscus 218
Choristites sowerby 218
Chott 75; 76; 79; 83; 86; 87
Chussovaya 213; 224
Cimmerian 250
Claromontanus Zone 70
Clypeina jurassica 164
Coenoceras sp. 71
Collotia 69; 87
Collotia sp. 69
Concavum Zone 65; 71; 72; 74
Coniacian 169; 173; 179; 239; 243; 247; 248; 249; 252; 254
conodont 213; 214; 222; 223; 225; 226; 228; 230
coral 79; 164; 214; 216; 222; 223; 224; 225; 228; 230
Cordaites 14

Source : MNHN, Paris

Cordatum Zone 70
Cretaceous 59; 79; 86; 93; 97; 98; 102; 103; 107; 109; 116; 123; 124; 125; 129; 130; 131; 132; 134; 136; 137; 138; 139; 143; 148; 150; 135; 154; 156; 159; 163; 169; 170; 172; 173; 175; 177; 178; 181; 183; 186; 189; 192; 194; 196; 201; 239; 240; 243; 246; 247; 248; 249; 250; 252; 254
crinoid 63; 34; 76; 214; 222; 224; 225; 228
Cyclotosaur 26

D

Dactylioceras sp. 65
Daghanirhynchia subversabilis 163
Daixina bosbytauensis - Daixina robusta zone 219
Dakhla 148; 154
Danian 248
Darvaz 218; 232
Darwinula 26
Dasycladacea 163
Davoei zone 45
Dead Sea 165
Debdou 109; 123
Deir Ez Zor 175; 177; 191
Demet 62; 67; 71; 72; 73
Demnat 45
Derro 170; 176; 179; 180; 181; 185; 189; 194
Devonian 11; 12; 18; 19; 20; 21; 146; 150; 173
Dikfaya 164
Dinantian 94
Discites zone 67; 71; 74
Discus zone 68; 69
Distichoceras sp. 69
Dogger 57; 86; 96; 107; 116; 125; 147; 162; 166
Dolaa 161; 166
Dolikephalites gr. *gracilis* 68
Domerian 41; 45; 47; 51; 72; 84; 85; 96; 111; 150
Donetsk 203; 204; 207; 214; 218; 219; 225; 226
Dorsetensia 67
Dorsetensia (Nannina) sp. 67
Doukkala 25; 26; 28; 32; 34; 153
Dutkevichia 226
Dutkevichites 226
Dvinella 219

E

Eastern European Basin 203; 204; 206; 217; 218; 219; 232; 233
Eastern European Platform 240
Eastern Uralian Gulf 203; 204; 210; 214; 218
Ebrayiceras 67; 87
Ebrayiceras sp. 67
Ebrayiceras sulcatum 67
echinoderm 62; 63; 64
echinoid 63; 164
Egypt 162
El Aïoun 123; 124
El Gamgouma 79
El Gara 32; 34
el Guefaïet 79
El Hajeb 26; 28; 33
El Hamra 180; 183; 185; 186
El Haoureb 77; 79
El Jadida 130
El Liel 180; 186; 188; 192
El Ward 180; 182; 184; 185; 186; 188; 193
Elatmites sp. 68
Emba 212
Emileia 57; 65; 66; 71; 87
Emileia gr. *polyschides* 66
Endersonella palastiniensis 163
Enteletes lamarcki 218
Eocene 99; 100; 103; 107; 113; 123; 125; 132; 143; 148; 154; 169; 172; 188; 189; 198
Eofusulina 217
Epalxites sp. 67
Epimastopora 219; 226
Epistrenoceras 68; 69
Epistrenoceras sp. 68; 69
Erek 182; 183; 184
Ermoceras 87
Ermoceras gr. *coronatoides* 87
Errachidia 147
Erymnoceras 164
Essaouira 25; 26; 28; 34; 129; 130; 131; 132; 134; 137; 138; 139; 143; 147; 148; 150; 152; 155
Euaspidoceras cf. *douvillei* 69
Euaspidoceras cf. *knechti* 69
Euaspidoceras gr. *williamsoni* 70
Euaspidoceras sp. 70
euaspidoceratids 87
Eugonophyllum 2269
Euhoploceras 67
Euphrates169; 170; 171; 172; 173; 175; 176; 178; 180; 181; 183; 185; 187; 188; 189; 191; 192; 194; 198; 201
Eurasia 94; 125; 148; 201; 252; 253
Europe 58; 62; 65; 66; 76; 84; 94; 101; 102; 103; 130; 131; 240
Euxinus Zone 72
Ez-Zehiliga 19

F

Faïd 79
Falcifer zone 65
Feddane Lebtam 15; 21
Fès 26
fish 75; 81; 213; 214; 222; 223; 228; 230
foraminifera 41; 161; 162; 163; 164; 183; 213; 214; 216; 218; 222; 223; 224; 225; 226; 228; 230
Foraminifers 26; 63; 64
fusulinids 211; 214; 217; 218; 219; 222; 224; 225; 226; 228; 230; 231; 233

Source : MNHN, Paris

G

Galeanelia aff. *laticarinata* 161
Galilee 159; 162; 163; 164; 165; 166
Garantiana sp. 69
Gareb 123
gastropod 41; 62; 163; 216
Gemmanella 26
Germany 67
Gibraltar 29; 32; 94
Globifusulina 226
Globifusulina caudata 226
Globifusulina krotowi 226
Globifusulina nux 226
Globuliferoporella 226
Gondwana 165
Gracilis Zone 69; 74
Graphoceras (G.) cf. *limitatum* 65
Graphoceras (G.) sp. 65
Gregoryceras riazi 71
Grójec 246; 247
Grossouvria sp. 69
Grou river 15; 20
Gsollbergella spiriloculiformis 161
Guefaïet 59; 68; 71; 72; 73; 76; 79
Guefait 123
Guercif 25; 33; 109; 123; 124; 154
Gulf of Lions 138
Gulf of Suez 173
Gyroporella 219; 226

H

Hadar 164
Hadid 21; 131
Haifa 163; 164
Hamad 159; 161; 165; 170; 172; 176; 178
Hammam Lif 76; 79
Haricha 143
Harpoceras cf. *falcifer* 65
Hassi-Messaoud 153
Haurania deserta 163
Haute Moulouya 33; 99
Hauterivian 129; 136; 139; 243; 245; 248
Hauts Plateaux 25; 33
Hecticoceras (Prohecticoceras) cf. *blanazense* 68
Hecticoceras (Prohecticoceras) crassum 68
Hecticoceras (Prohecticoceras) ochraceum 68
Hecticoceras (Prohecticoceras) sp. 68
Hemifusulina 217
Hercynian 13; 21; 23; 29; 30; 34; 88; 93; 94
Hesperithyris 96
Hettangian 39; 41; 45; 59; 75; 84
High Atlas 21; 23; 24; 25; 26; 28; 30; 32; 33; 39; 40; 45; 47; 51; 93; 95; 96; 97; 99; 101; 102; 103; 147
High Plateaux 111; 112; 123; 124; 147; 154
Hildaites gr. *serpentiniformis* 65
Hildaites sp. 65
Hildoceras cf. *sublevisoni* 65
Holcophylloceras gr. *mediterraneum* 69
Holcophylloceras mediterraneum 69
Holcophylloceras sp. 68; 69; 70
Holcophylloceras sp. juv. 68
Holy Cross Mountains 240; 247; 254
Homoeoplanulites (H.) gr. *furculus* 68
Humphriesianum Zone 67; 71

I

Iberia 34; 125
Ibex zone 45
Idrissides 99
Ilek River 211
Ilza 246; 247; 248; 251
Iran 161; 171
Iraq 161; 163; 165; 170; 173
Ishimbay 224

J

Jabal Akraa 165
Jaddala 187; 188; 189; 198
Jbel Taguendouft 45; 47
Jeanneticeras cf. *meridionale* 68
Jebel Bishri 177
Jebel Châabet el Attaris 58; 59; 62; 65; 67; 68; 69
Jebel el Guemgouma 65
Jebel el Haouareb 59; 63; 67; 68; 69; 71; 72; 74
Jebel Hadid 21
Jebel Krechem el Kelb 58; 62; 63; 65; 67; 68; 69; 71; 72; 74; 79
Jebel Nara 72
Jebel Nefzaoua 79
Jebel Rheouis 59; 67; 69; 70; 74; 86
Jebel Sidi Kralif 72
Jeffara 58
Jerada 12; 154
Jeribe 189
Jibal As-Sahilyeh 160; 161; 165
Jido 180; 182; 183; 184; 186
Jordan 162; 163; 165; 178
Joura 177; 178; 179; 180; 182; 183; 185; 186; 188; 190; 196; 199
Judea 175; 178; 179; 189
Jurassic 23; 24; 26; 29; 33; 34; 40; 45; 51; 57; 58; 59; 62; 64; 65; 71; 75; 76; 77; 79; 81; 83; 84; 85; 86; 87; 88; 97; 98; 102; 103; 107; 110; 112; 116; 125; 129; 131; 132; 134; 136; 137; 139; 143; 147; 148; 150; 152; 153; 154; 155; 156; 159; 160; 161; 162; 164; 165; 166; 175; 216; 243; 246; 247; 248; 249; 250; 252; 254
Jurusan 228

Source : MNHN, Paris

K

Kama 203; 204; 206; 211; 213; 218; 219; 224; 226; 230; 231; 234
Karachaganak 213; 231
Karpinsky Kryazh 231; 232; 233
Karsk 211
Kasserine 79
Kechoula 131
Kef el Hassine 62; 63; 65; 66; 67; 69; 71; 72; 74; 76; 79; 87
Kef el Khouadja 65; 67; 68; 71; 72; 73; 74
Kerrouchen 25; 30; 33
Khabour 180; 182; 183; 184; 185; 186; 187; 188; 191; 192
Khémisset 25; 28; 32; 33; 34
Khouribga 12
Kielce 246; 250
Kilianina blancheti 163
Kimmeridgian 72; 76; 79; 83; 84; 88; 107; 112; 112; 124; 159; 164; 166; 250
Kisyl-Kum 216; 218
Kolguev Island 223
Kolva 213; 224
Komia 219
kosmoceratids 87
Ksour 97
Ktab Lahmar 19; 20
Kumubia palastiniensis 164; 165
Kurd Dagh 160; 161; 163
Kurdwanów 247; 252
Kutchirhynchia indica 164

L

Laayoune 154
Laâyoun 32; 33; 34
Ladinian 23; 24; 26; 28; 34; 95; 109
Laevaptychus sp. 71
Laeviuscula Zone 67; 71
Lamberti Zone 74
Lebanon 161; 163; 164; 165; 166
Lemoineiceras sp. 68
lenticulines 67
Levant 159; 165
Levantinella egyptiensis 164; 165
Levantinella egyptiensis biozone 164
Liassic 23; 24; 33; 34; 39; 40; 41; 42; 45; 47; 51; 75; 77; 79; 83; 93; 95; 96; 103; 107; 110; 116; 123; 124; 125; 129; 131; 132; 136; 137; 139; 143; 147; 150; 154; 161; 162
Libya 79
Likharevites 226
Limnocythere keuperea 26
Linoproductus simensis 218
Liospiriferina undulata 161
Lissoceratoides sp. 70
Lithotis sp. 161
Lobosphinctes sp. 67
Loridga 58; 59; 62; 63; 65; 68; 71; 72; 74; 76; 77; 79; 86
Lublin 240
Lunuloceras aff. *pseudopunctatum* 69
Lunuloceras gr. *paulowi* 68
Lunuloceras romani 68
Lutkevichinella 26
Lutkevichinella kristanae 26
Lutkevichinella lata 26
Lytoceras 69; 87
Lytoceras aff. *eudesianum* 69
Lytoceras cf. *eudesianum* 69

M

Maastrichtian 154; 169; 173; 179; 182; 183; 185; 189; 190; 191; 192; 195; 196; 199; 240; 243; 248; 249; 252
Macrocephalites sp. 69
Macrocephalites sp. juv. 68
Macrocephalitids 69
Macrocephalus Zone 68
Macroporella 219
Maezalieh 180; 186
Maj dal Chains 164
Majora 86
Malagasy 87
Mardin 159; 161; 165; 172
Margaritatus zone 45
Mariae zone 70; 72; 74
Marrakech 24; 94; 96
Mayncina termieri 161
Medenine 79; 81; 83
Meekella eximia 218
Megalodontidae 111
Meseta 11; 12; 13; 17; 21; 28; 32; 94; 96; 99; 147
Meskala 131; 136; 150
Mesopotamian 172
Mesozoic 40; 57; 58; 75; 80; 93; 94; 98; 101; 120; 103; 109; 112; 130; 131; 132; 147; 150; 169; 171; 172; 175; 189; 196; 201; 207; 215; 240; 241; 247; 248; 253
Metoposaurids 26
Metoposaurus lyazidi 26
Metoposaurus ouazzoui 26
Metroh 123
Microcanthum Zone 72
Microderoceras sp. 72
Micromphalites sp. 68
Middle Atlas 24; 26; 28; 30; 32; 68; 93; 95; 96; 97; 99; 101; 102; 103; 147
Midelt 26; 96
Mid-Polish Trough 239; 240; 249; 250; 252
Miechów 240; 248
Mielec 247; 248; 250
Miocene 101; 116; 125; 143; 148; 150; 171; 189
miospore 213; 214; 215; 225; 226; 231; 232
Mirus Zone 70
Mixoneura 14

Source : MNHN, Paris

Morocco 11; 12; 21; 23; 24; 26; 28; 29; 30; 32; 34; 39; 68; 79; 87; 93; 94; 95; 97; 99; 102; 107; 108; 113; 123; 124; 125; 129; 143; 144; 145; 146; 147; 148; 149; 150; 153; 156
Morphoceras 67; 87
Morphoceras aff. *jactatum* 67
Morphoceras egrediens 67
Morphoceras sp. 67
Morphoceras sp. cf. *M. macrescens* 67
Morphoceras sp. juv. 67
Morphoceras sp. juv. cf. *jactatum* 67
Morrisi zone 68
Moscovian 203; 204; 207; 211; 212; 213; 214; 216; 217; 218; 219; 224; 231; 232; 233
Moscow 207; 214; 219; 224; 228
Moulay Idriss 124
Moulouya 25; 33; 96
Mount Hermon 159; 161; 162; 163; 164; 166
Moyenne Moulouya 25
M'rhilla 79
Mugodzhary Mountains 211; 219
Mugodzhary Peninsula 215; 232
Mulussa 170; 175; 189

N

Naïma 123; 124
Namurian 146
Nannolytoceras tripartitum 67
Nara Loridga79
nautiloids 222; 223; 228; 230
Neknafa 152
Neoanchicodium 219; 226
Neocomian 165; 245
Neogene 93; 101; 102; 103; 125; 143; 150; 155; 171; 175
Neospirifer postriatus 218
Neostreptognathodus pnevi 226
Newfoundland 29
Niortense Zone 67
Norian 23; 26; 28; 32; 33; 95; 161; 189
Normannites sp. 67
North America 29; 94; 130
North Sea 138; 173
Nova Scotia 29
Novaya Zemlya 211; 213; 222
Nowe Miasto 246; 247; 248; 251
Nura-Tau Mountains 216

O

Obtusum zone 45
Odontoperis 14
Oka-Zna 224
Oligocene 100; 101; 148; 152; 169; 188; 189; 198; 201
Oman 199
oppeliids 87
Oranesan meseta 108
Oranese Meseta 96
Oraniceras 57; 67; 68; 87
Oraniceras cf. *hamyanense* 68
Oraniceras hamyanense 67
Ordovician 11; 12; 146; 150; 153
Orenburg 224
Orenburgian 225
Orthosphinctes (Orthosphinctes) sp. 71
ostracod 26; 28; 29; 30; 33; 94; 96; 102; 103; 109; 111; 112; 113; 116; 124; 125
Ouaouizart 99
Ouarzazate 101
Oued Abiod 79
Oued Himmer 123
Oujda 23; 26; 28; 29; 30; 33; 94; 96; 102; 103; 109; 111; 112; 113; 116; 123; 124; 125
Oulmes 12
Ouriak 26
Oxfordian 63; 64; 65; 69; 70; 71; 72; 73; 74; 76; 79; 83; 84; 86; 87; 88; 112; 124; 136; 143; 148; 150; 152; 164
Oxycerites cf. *yeovilensis* 67
Oxycerites gr. *yeovilensis* 67
Oxycerites seebachi 67
Oxycerites sp. 68
Oxycerites yeovilensis 67

P

Pachyerymoceras 87; 164
Palaeoaplysina 219; 224
Palaeocene 99; 148; 169; 185; 186; 187; 188; 189; 192; 198
Palaeogene 169; 175
Palaeo-Tethys 12
Palaeozoic 24; 29; 58; 79; 80; 94; 96; 102; 109; 134; 143; 146; 150; 153; 154; 173; 190; 207; 211; 216; 240; 246; 248; 250; 252
Paleopfenderina salernitana 163
Paleopfenderina trochoidea 163
Palmyra 170; 199
Palmyrides 160; 161; 163; 165; 169; 170; 171; 172; 177; 178; 187
Paltarpites sp. 65
Pamir 207; 218; 225; 228; 232
Pangea 29; 107; 125
Paracypris 26
Parafusulina solidissima zone 226
Parapatoceras sp. 70
Paraschwagerina 226
Parkinsonia sp. juv. 67
Passendorferia (Enayites) cf. *birmensdorfensis* 70
Passendorferia (Enayites) czentochovensis 70
Pay-Khoy Mountains 211; 212
Pechora 213; 224; 228
Pechoria 219
Pelagian Sea 58

Source : MNHN, Paris

pelecypod 62; 63; 64
Pelecypoda 161
Peltoceras (Metapeltoceras) sp. 69
Peltoceras (Peltoceras) sp. 69
Peltoceras cf. *diversiforme* 69
Peltoceratidae 70
peltoceratids 87
Peltoceratoides 70; 87
Peltoceratoides cf. *stephanovi* 70
Peltoceratoides cf. *williamsoni* 69; 70
Peltoceratoides gr. *williamsoni* 69
Peltoceratoides sp. 70
Perisphinctes (?Arisphinctes) cf. *gyrus* 69
Perisphinctes (?Dichotomosphinctes) cf. *episcopalis* 70
Perisphinctes (?Dichotomosphinctes) cf. *laisinensis* 69
Perisphinctes (Kranaosphinctes) cf. *promiscuus* 69; 70
Perisphinctes (Otosphinctes) sp. 69
Perisphinctidae 70; 71; 87
perisphinctid 70
Peri-Tethyan domain 27
Peri-Tethyan Platform 27; 83
Permian 11; 21; 24; 27; 79; 83; 94; 175; 203; 204; 211; 213; 215; 216; 223; 233; 234; 240; 246; 247
Phylloceras 67; 68; 69; 70; 87
Phylloceras gr. *plicatum* 69
Phylloceras plicatum 68
Phylloceras sp. 67; 68; 69; 70
Pilica 343; 345; 346; 250
Piotrków Trybunalski 246
Planisphinctes 67
Platylenticeras 245
Pleistocene 101
Pliensbachian 39; 41; 42; 45; 47; 51; 79; 88; 161
Pliocene 150
Podolsk 214
Poitou 67
Poland 240; 246
pollen 15; 26
Polymorphum Zone 65
Polyplectus sp. 65
Polyptychites 246
Polysphinctites polysphinctus 67
Portlandian 113; 124
Posidonomya 97
Poznan 248
Praekurnubia crusei 163
Precambrian 146; 240; 252
Precaspian Basin/Depression 203; 204; 206; 211; 213; 214; 219; 222; 223; 224; 225; 228; 231; 232
Pre-Rif 143; 147; 148; 150; 154; 155
Procerites gr. *tmetolobus* 68
Procerites sp. 67; 68
Procerites sp. juv. 67
Profusulinella rhomboides 216
Progracilis Zone 68; 71; 74
Properisphinctes cf. *bernensis* 70
Properisphinctes gr. *bernensis* 69
Properisphinctes sp. 70
Propinquans Zone 66
Prososphinctes cf. *mairei* 70
Prososphinctes cf. *mazuricus* 69
Prososphinctes sequeirosi 70
Proterozoic 171; 172
Proto-Atlantic 23; 28; 32; 33; 34
protoglobigerines 63
Protophites christoli 71
Przedbórz 247; 248; 250
Pseudocyclammina liasica 161
Pseudoepimastoipora 226
Pseudofusulina concavutas - P. pedissequa zone 226
Pseudofusulina juresanensis zone 226
Pseudofusulinella 217; 226
Ptychophylloceras sp. 69
Pulchrella 217
Purbeckian 125; 246
Putealiceras arkelli 68
Putealiceras sp. cf. *P. rossiense* 69
Putrella 217; 218
Pyguropsis noetlingi 164
Pyrenees 219

Q

Quaternary 102; 103; 125; 131; 171; 175; 190; 193; 196; 248

R

radiolaria 63; 76; 79; 213; 222; 223; 228; 230; 231
Radom 243; 245; 246; 248; 251
Radomsko 246
Raqqa 162
Rawda 164
Read Sea 171
Redmondoides lugeoni 163
Rehamna massif 21
Rehmannia 68; 87
Rehmannia (Loczyceras) cf. *richei* 68
Reineckeid 69
Rekame 123
Retrocostatum Zone 68; 69; 74
Rhaetian 28; 59; 161
Rhar Roubane 109; 123
Rharb 25; 34; 143; 150; 155
Rheouis 58; 67; 69; 70; 71; 72; 74; 77; 79; 86
Rhynchonella absoleta 163
Rhynchonella hopkinsi 163
Rif 25; 28; 93; 94; 101; 102; 108; 124; 143; 147; 148; 150; 154; 155; 156
Rif-Tell 108; 124
Rugosofusulina 226

Source : MNHN, Paris

Russian Platform 204; 206; 207; 213; 219; 222; 224
Rutbah 161; 165; 170; 175; 189
Rzeszów 248

S

Saccocoma 63; 34; 76; 83
Sahara 156
Saharan Platform 58
Sakmara 211; 222
Salpingoporella annulata 163
Samara 211; 214
Sandomierz 246; 247
Santonian 169; 181; 189; 192; 194; 247; 248; 249; 252; 253; 254
Scania 240
schizosphere 79
Schwema 184
Sehoul 94
Senonian 100; 154; 253
Serpentinum zone 65
Sherifeh 163; 165; 166
Shiranish 184; 185; 189; 196
Shwema 184; 186; 193
Sidi Aïch 86
Sidi Amara 131
Sidi El Abid 123
Sidi Khalif 64; 72
Sidi Mohammed ben Hammou 14; 16
Sidi Rhalem 152
Sidi-Kassem 12; 14; 15; 17; 18; 21
Siemiradzkia cf. *pseudorjasanensis* 68
Siemiradzkia sp. 67
Silurian 18; 21; 143; 146; 150; 153; 154; 173; 190
Sinai 162
Sinemurian 24; 26; 39; 40; 41; 51; 59; 75; 79; 81; 88
Sinjar 172; 178; 199
Siroua 102
Slovenia 226
Somalirhynchia africana 164
Sonninia 66; 71
Sonninia (Euhoploceras) polyacantha 66
Sonninia (Euhoploceras) simplex 66
Souss 29; 101; 131
Sowerbyceras cf. *subtortisulcatum* 69
Sowerbyceras cf. *tortisulcatum* 70
Sowerbyceras sp. juv. 68
Sowerbyceras tortisulcatum 70
Speluncella n. sp. 26
Sphaeroceras gr. *brongniarti* 67
Sphaeroschwagerina fusiformis zone 219; 225
Sphaeroschwagerina moelleri - Pseudofusulina fecunda zone 219; 225
Sphaeroschwagerina sphaerica - Pseudofusulina firma zone 219; 225
Spinatum zone 45
spirillines 64
Spiroceras sp. 67
Spiroceras sp. cf. *S. bifurcati* 67
sponge 79; 213; 222; 223; 224; 228; 230; 243
spore 26
Staroutkinsk 214
Steinekella crusei 163; 164
Steinekella steinekei 163; 134
Stephanian 21
Stephanoceras 67; 71
Stephanoceras (S.) cf. *tenuicostatum* 67
Stephanoceras (S.) gr. *humphriesianum* 67
Sterlitamak 224
Strigoceras sp. 67
stromatopora 164
Subcontractus zone 68
Subgrossouvria sp. 69
Sublunuloceras aff. *nodosulcatum* 68
Suez 173; 252
Sulcocythere hajbensis 26
Syria 159; 160; 161; 162; 163; 164; 165; 169; 170; 171; 173; 175; 178; 188

T

Tadla 146; 153; 154
Tafouralt 123; 124
Tamadout 42; 47
Tamazert 100; 103
Tamdafet 25
Tanak 180; 183
Tanouralt 109; 123
Taourirt 100; 103; 108; 109; 111; 113; 116; 123; 124
Taramelliceras 69; 70; 71; 87
Taramelliceras aff. *T. argoviense* 70
Taramelliceras aff. *T. callicerum* 70
Taramelliceras argoviense 70
Taramelliceras cf. *baccatum* 70
Taramelliceras cf. *costatum* 71
Taramelliceras cf. *pseudoculatum* 69
Taramelliceras pseudoculatum 69; 70
Tarfaya 25; 32; 34; 143; 148; 152; 154; 155
Tataouine Remada 79
Taurus 190
Tazekka 26; 28; 33
Tebaga 79; 83
Teisseyre-Tornquist Zone 239; 240; 250; 254
Teloceras 67
Teloceras blagdeni 67
Telouet 41; 47; 51
Terebratula marucchensis 41
Terebratula moreti 41
Terebratula quillyensis 163
Terebratula subsella 164
Terebratula superstes 163
Terni Masgout 116

Source : MNHN, Paris

Tertiary 130; 147; 148; 150; 165; 173; 189; 240; 254
Tethyan 23; 28; 34; 57; 58; 68; 76; 79; 86; 87; 94; 107; 116; 123; 124; 147; 159; 165; 166; 169; 199; 204; 206; 217; 218; 226; 232; 233; 234; 250; 254
Tethys 23; 29; 30; 58; 86; 88; 93; 99; 102; 103; 107; 123; 124; 148; 203; 204; 228; 232; 250; 253; 254
Thailand 218
Thaumatoporella parvovesiculifera 163
Thayyem 180; 186; 188
Thouarsense Zone 65
Tidsi 131
Tighboula-Oudiksou 99
Tilougguit 39; 41; 45; 47
Timidonella sarda 162; 163
Tindouf 12; 94; 147
Tiouli 33; 109; 123
Titeft 109
Tithonian 64; 72; 76; 84; 88; 136; 165; 166
Tizi n'Test 29; 95
Tizi-N-Targhist 147
Tizi-N-Test 45
Tlemcen 109
Toarcian 41; 45; 59; 65; 71; 72; 73; 75; 76; 79; 81; 82; 83; 84; 85; 86; 96; 111; 136; 161
Tobol 214
Tokhtinikhtau Mountains 216
Tomaszów Mazowiecki 246; 247
Tortay 212
Tortonian 101; 148
Touila 79
Touissit 109; 110; 111; 123
Triassic 11; 21; 23; 24; 26; 28; 29; 30; 33; 34; 41; 59; 75; 93; 94; 95; 96; 98; 102; 103; 107; 109; 113; 116; 123; 125; 129; 131; 132; 136; 138; 139; 143; 147; 1550; 153; 154; 161; 165; 166; 170; 172; 175; 178; 216; 248
trilobites 222; 223; 228; 230
Trimarginites arolicus 71
Trimarginites sp. 70
Trimarginites stenorhynchus 71
Tschugor River 228
Tubiphytes 224; 226; 230
Tunisia57; 58; 59; 62; 74; 75; 76; 79; 80; 81; 82; 83; 84; 85; 86; 87; 88; 102; 252
Turansk 203; 206; 219
Turkey 87; 162; 171; 188
Turonian 99; 100; 148; 154; 169; 175; 179; 183; 189; 191; 194; 198; 199; 239; 243; 247; 248; 249; 250; 253; 254
Tyan Shan 207; 225; 232; 234

U

Ufa 211; 224
Ultradaixina 226
Ultradaixina bosbytauensis-Daixana robusta zone 225
Ungdarella 219
Ural (river) 211; 222
Uraloporella 219
Urals (mountains) 203; 204; 206; 207; 213; 214; 218; 219; 224; 226; 230; 231; 234

V

Vaigach Island 212; 228
Valanginian 243; 245; 246; 248
Valvulinella jurasica 163
Variabilis Zone 65
Variscan 11; 12; 18; 21; 94
vertebrate 26
Vietnam 218
Visean 146
Vishera 213; 224; 228
Volga 203; 204; 206; 207; 213; 214; 218; 219; 224; 226; 230; 231; 234
Volgian 245
Volgograd 214
Voronezh 203; 225

W

Wadi Al-Karn 164
Wadi Nahr Az-Zarqua 162
Wadi Nahr Ibrahim 161
wadi Souyah 70
Warsaw 240
Wedekindellina 217
Westphalian 11; 12; 13; 14; 15; 17; 18; 19; 20; 21; 146
Wisla 243; 245; 247; 248; 252
worm trails 222; 223

Y

Yuzhno-Embensk 213; 232

Z

Zagros 169; 171; 190; 199
Zawiat Ahançal 47
Zawichost 247; 252
Zebdani 164
Zeilleria arethusa 41
Zekkara 154
Zelten 131; 136; 150
Zem Zem 131
Zemmour 33
Zhanazhol 211
Zigzag Zone 68; 71; 72
Ziz-Guir 25
Zmilet el Ghar 79
Zoophycos 62; 63; 67; 68; 71; 72; 74; 76; 83; 111

BIBL. DU MUSÉUM PARIS
Source : MNHN, Paris

REMERCIEMENTS AUX RAPPORTEURS / *ACKNOWLEDGEMENTS TO REFEREES*

La Rédaction tient à remercier les experts extérieurs au Muséum national d'Histoire naturelle dont les noms suivent, d'avoir bien voulu contribuer, avec les rapporteurs de l'Établissement, à l'évaluation des manuscrits (1997/2000) :
The Editorial Board acknowledges with thanks the following referees who, with Muséum referees, have reviewed papers submitted to the Mémoires du Muséum (1997/2000):

ADKISON D. L.	Macon	USA
AKAM M.	Cambridge	Grande-Bretagne
ANDERSEN N.	Copenhague	Danemark
AUGELLI I.	Milan	Italie
BABA K.	Kumamoto	Japon
BANKS T.	Egham	Grande-Bretagne
BARRIER E.	Paris	France
BAUD A.	Lausanne	France
BERNET-ROLLANDE M.C.	Paris	France
BESSE J.	Paris	France
BEST M.	Leiden	Pays-Bas
BIJU-DUVAL B.	Rueil-Malmaison	France
BONAVIA F.	Paris	France
BOURDON R.	Roscoff	France
BOURSEAU J.P.	Villeurbanne	France
BRUCE J.	Helensvale	Australie
BRUCE N.	Copenhague	Danemark
BRUNTON H.	Londres	Grande-Bretagne
CARPENTER J.	New York	USA
CASSAGNEAU P.	Toulouse	France
CASTLE P.H.J.	Wellington	Nouvelle-Zélande
CHACE F. A.	Washington	USA
CHILD C. A.	Washington	USA
CHERIX D.	Lausanne	Suisse
CLOBERT J.	Paris	France
COHEN D.	Los Angeles	USA
COOK P. L.	Victoria	Australie
CORDEY F.	Lyon	France
DARLU P.	Paris	France
DANCHIN E.	Paris	France
DEJEAN A.	Villetaneuse	France
DELEPORTE P.	Paimpont	France
DIETRICH C.	Champaign	USA
DUFFELS J. P.	Amsterdam	Pays-Bas
ELLOUZ N.	Rueil-Malmaison	France
FAHAY M.	Highlands	USA
FELDER D.L.	Los Angeles	USA
FLOQUET M.	Marseille	France
FODOR L.	Budapest	Hongrie
GAGNÉ R.	Washington	USA
GALTIER J.	Montpellier	France
GRANATH J.	Houston	USA
GULLAN P.	Canberra	Australie
HAMAYON R.	Paris	France
HANCOCK P.	Bristol	Grande-Bretagne
HARVEY A.W.	New York	USA
HARMELIN J.G.	Marseille	France
HAYWARD P.J.	Swansea	Grande-Bretagne
HEEMSTRA P.	Grahamstown	Afrique du Sud
HODGSON C.	Ashford	Grande-Bretagne
HOLTHUIS L. B.	Leiden	Pays-Bas
HUC A.Y.	Rueil-Malmaison	France
HUMPHREY C.	Cambridge	Grande-Bretagne
INGRISCH S.	Frankfurt	Allemagne
KABAT A.	Washington	USA
KERP H.	Munster	Allemagne
KOMAI T.	Chiba	Japon
KRAPP F.	Bonn	Allemagne
KRISTENSEN N.	Copenhague	Danemark
LEDOUARAN S.	Paris	France
LEMAITRE R.	Washington	USA
LOVELOCK P. E. R.	La Haye	Pays-Bas
LOWRIE J.	Zürich	Suisse
MACHIDA Y.	Kochi	Japon
MACKINNON D.	Christchurch	Nouvelle-Zélande
MACPHERSON E.	Barcelona	Espagne
MADDISON D.	Tucson	USA
MANNING R.	Washington	USA
MARKLE D.	Oregon	USA
MARSHALL B.	Wellington	Nouvelle-Zélande
MASAKI S.	Hirosaki	Japon
MASSE P.	Paris	France
MCLAUGHLIN P.	Washington	USA
MCLENNAN D.	Toronto	Canada
MESSING C.	Dania	USA
MEULENKAMP J.	Utrecht	Pays-Bas
MORAND S.	Perpignan	France
MORETTI I.	Rueil-Malmaison	France
MOUTY M.	Damas	Syrie
MUGNIER J.L.	Grenoble	France
NAKAMURA I.	Kyoto	Japon
NAUMANN C.	Bonn	Allemagne
NEWMAN W. A.	San Diego	USA
NG P.	Singapore	Singapour
OOSTEN J.G.	Leiden	Pays-Bas
OROUSSET J.	Paris	France
PACKER L.	York	Canada
PLATEAUX C.	Nancy	France
PROUST J. N.	Lille	France
RAVENNE C.	Rueil-Malmaison	France
RENTZ D. C. R.	Canberra	Australie
REYMANE J.	Neuchâtel	Suisse
RICHARDS W.	Miami	USA
RICHTER S.	Berlin	Allemagne
ROBERTS C.	Wellington	Nouvelle-Zélande
SALDANHA L.	Cascais	Portugal
SALOMON M.	Marseille	France
SAZONOV Y.	Moscou	Russie
SCHAER J.P.	Neuchâtel	Suisse
SCHOLTZ C.	Pretoria	Afrique du Sud
STAMPFLI G.	Lausanne	Suisse
STEPHENSON R.A.	Amsterdam	Pays-Bas
STEWART A.	Wellington	Nouvelle-Zélande
THIERRY J.	Dijon	France
THORNE B.	Maryland	USA
TRIBOVILLARD N.	Paris	France
VAN BAAREN J.	Rennes	France
VERNON P.	Paimpont	France
VIALLY R.	Rueil-Malmaison	France
VICKERY VERNON R.	Ste-Anne / Bellevue	Canada
WÄGELE J. W.	Bielefeld	Allemagne
WARÉN A.	Stockholm	Suède
WENZEL J.	Colombus	USA
WICKSTEN M.K.	College Station	USA
WIEGMANN B.	Maryland	USA
WILSON M.	Cardiff	Grande-Bretagne
WILSON S.	Warrensburg	USA
YEATES D.	Brisbane	Australie
YOUNG P.S.	Rio de Janeiro	Brésil
ZAPPATERA E.	Londres	Grande-Bretagne
ZEZINA O.	Moscou	Russie
ZIBROWIUS H.	Marseille	France
ZIEGLER P. A.	Binningen	Suisse

Source : MNHN, Paris

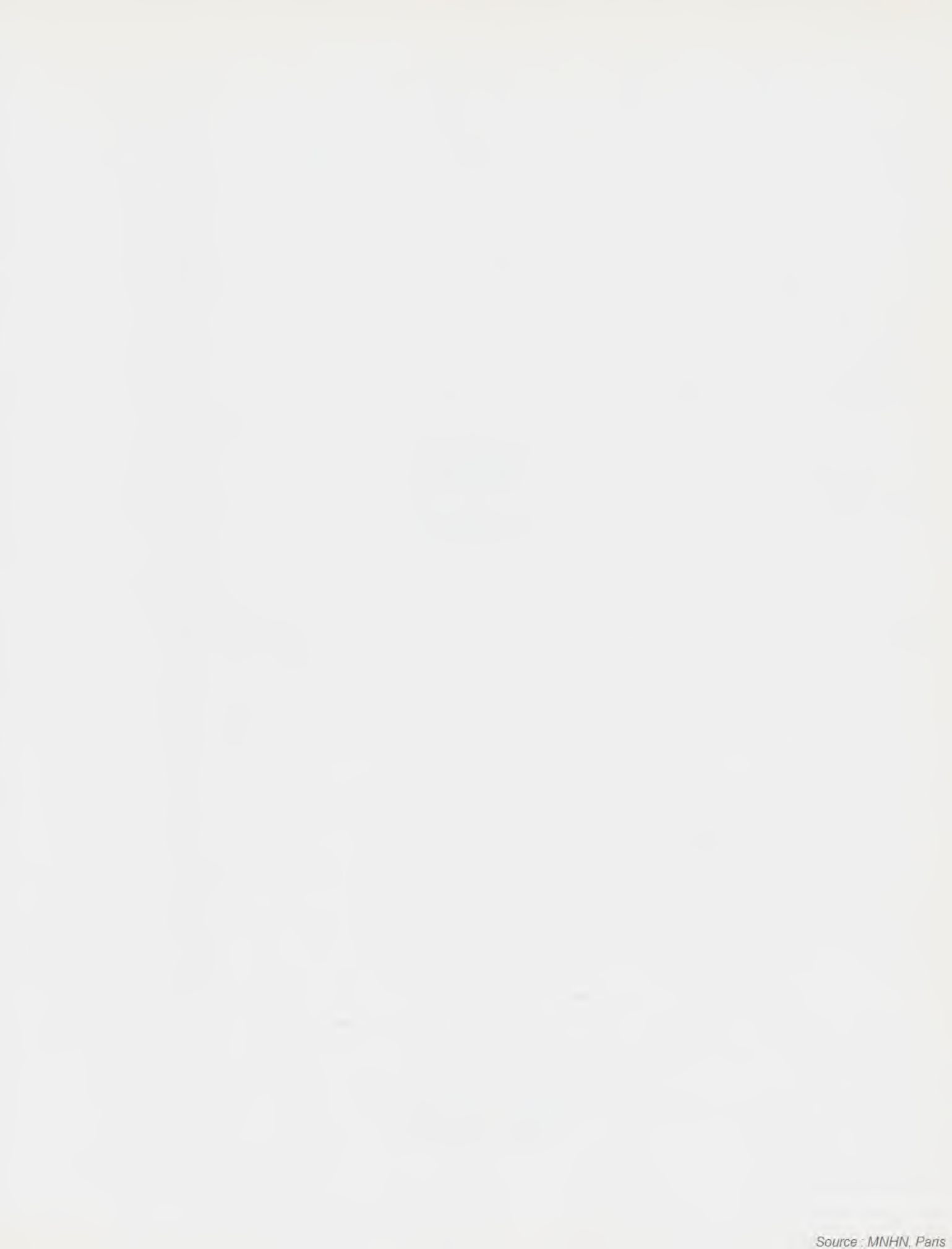

Source : MNHN, Paris

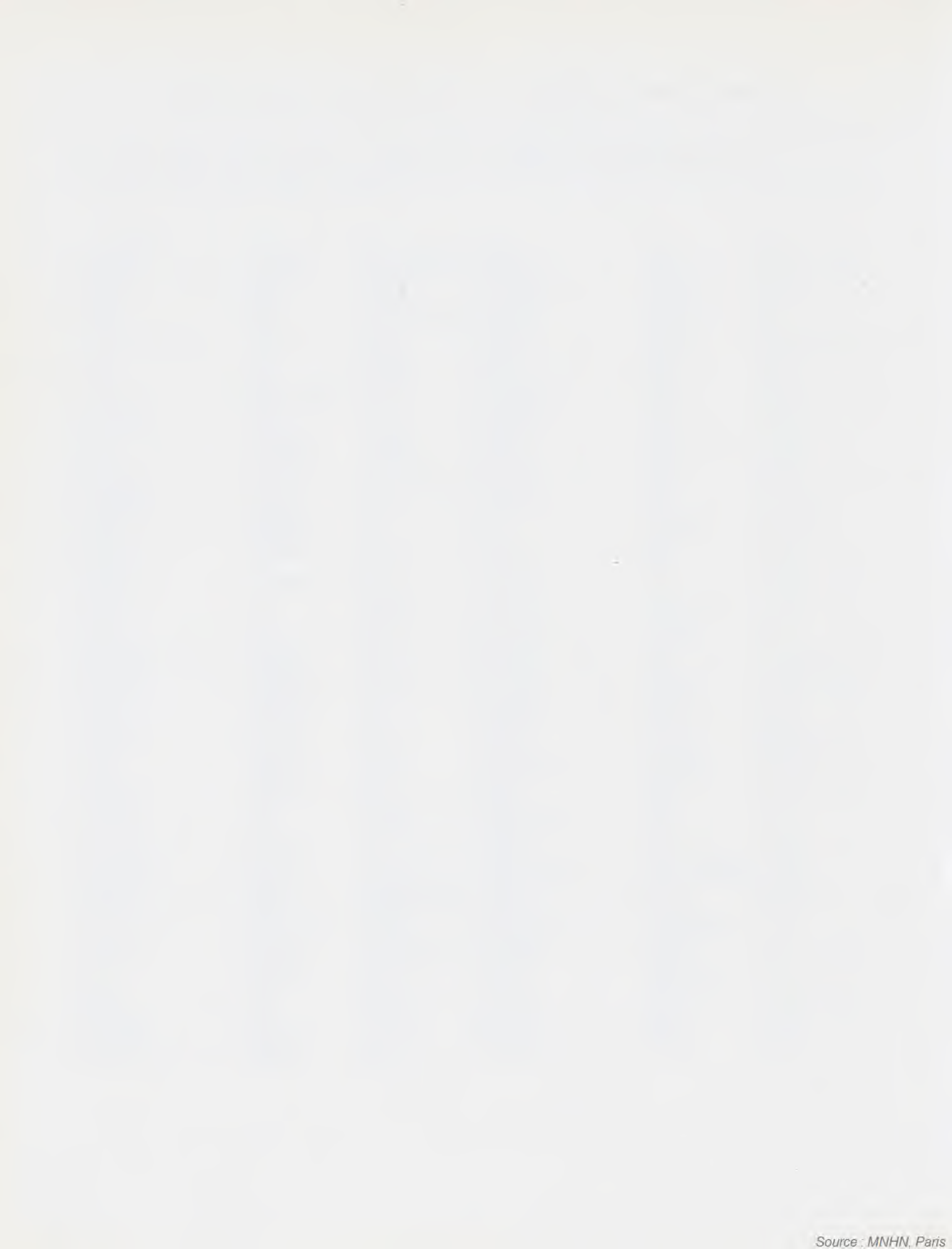

Source : MNHN, Paris

ACHEVÉ D'IMPRIMER
EN MARS 2000
SUR LES PRESSES
DE
L'IMPRIMERIE F. PAILLART
À ABBEVILLE

Date de distribution : 17 mars 2000.
Dépôt légal : Mars 2000
N° d'impression : 10841

Source : MNHN, Paris

2 1 MARS 2000

Source : MNHN, Paris

DERNIERS TITRES PARUS

RECENTLY PUBLISHED MEMOIRS

Tome 181 : Marie-Lise BEFFA & Laurence DELABY, 1999.— Festins d'âmes et robes d'esprits : les objets chamaniques sibériens du Musée de l'Homme. 241 pp. (ISBN : 2-85653-513-5) 350 FF.

Tome 180 : Alain CROSNIER (ed.), 1999.— Résultats des Campagnes MUSORSTOM. Volume 20. 588 pp. (ISBN : 2-85653-520-8) 600 FF.

Tome 179 : Sylvie CRASQUIN-SOLEAU & Éric BARRIER (eds), 1998.— Peri-Tethys Memoir 4: Epicratonic Basins of Peri-Tethyan Platforms. 294 pp. (ISBN : 2-85653-518-4) 300 FF.

Tome 178 : Alan G. BEU, 1998.— Indo-West Pacific Ranellidae, Bursidae and Personidae (Mollusca: Gastropoda). A monograph of the New Caledonian fauna and revisions of related taxa. Résultats des Campagnes MUSORSTOM. Volume 19. 256 pp. (ISBN : 2-85653-517-8) 350 FF.

Tome 177 : Sylvie CRASQUIN-SOLEAU & Éric BARRIER (eds), 1998.— Peri-Tethys Memoir 3: Stratigraphy and Evolution of Peri-Tethyan Platforms. 262 pp. (ISBN : 2-85653-512-7) 260 FF.

Tome 176 : Alain CROSNIER (ed.), 1997.— Résultats des Campagnes MUSORSTOM. Volume 18. 570 pp. (ISBN : 2-85653-511-9) 600 FF.

Tome 175 : Isabel PÉREZ FARFANTE & Brian KENSLEY, 1997.— Penaeoid and Sergestoid Shrimps and Prawns of the World: Keys and Diagnoses for the Families and Genera. 233 pp. (ISBN : 2-85653-510-0) 350 FF.

Tome 174 : Bernard SÉRET (ed.), 1997.— Résultats des Campagnes MUSORSTOM. Volume 17. 213 pp. (ISBN : 2-85653-500-3) 245,04 FF.

Tome 173 : Philippe GRANDCOLAS (ed.), 1997.— The Origin of Biodiversity in Insects: Phylogenetic Tests of Evolutionary Scenarios. 356 pp. (ISBN: 2-85653-508-9) 490 FF.

Tome 172 : Alain CROSNIER & Philippe BOUCHET (eds), 1997.— Résultats des Campagnes MUSORSTOM. Volume 16. 667 pp. (ISBN : 2-85653-506-2) 612,60 FF.

Informations sur les Publications Scientifiques du Muséum national d'Histoire naturelle :
Informations about the Scientific Publications of the Muséum national d'Histoire naturelle:
Look at the Mémoires server on World Wide Web
http://www.mnhn.fr/publication/memoire/memoire.html

Prix TTC, frais de port en sus.
Prices in French Francs, postage not included.

Source : MNHN, Paris

The Peri-Tethys Programme, started in 1993, examines the influence of the Tethyan evolution on the bordering cratons since the break-up of the Pangea through the accretion of oceanic domains and finally the collision between the major bordering plates which led to inversions within the epicratonic basins.

The Peri-Tethys Memoir 5 is the issue of the International Meeting held in Rabat (1997). This volume like the two previous ones (Peri-Tethys Memoirs 3 and 4) deals with the two great geographic domains involved in the Programme: the Southern and the Northern Platforms. It differs from the other volumes by the fact it is mainly devoted to the Southern Platform (ten papers) and particularly to Morocco (seven papers). Only two papers concern the Northern Platform.

In the first part, the first paper analyses the Late Carboniferous of Morocco, the second and the third papers are devoted respectively to the Triassic and Liassic of Morocco. The fourth one presents the Jurassic global events and their records in Tunisia. The paper 5 presents the Mesozoic and Cainozoic evolution of the Moroccan Atlasic domain. The two next papers deal with the tectonic evolution and the subsidence history of Morocco. The eighth paper presents the hydrocarbon system of Morocco. The next one is an overview of the Syrian Jurassic. The last paper of this first part concerns the basin development and the tectonic history of the Euphrates grabens using subsurface data.

In the short second part, one paper presents the palaeogeographic evolution of the Eastern European basin during the Late Palaeozoic. The last paper focuses on the palaeotectonic evolution of the Polish Trough Cretaceous basins.

Sylvie Crasquin-Soleau and Éric Barrier (CNRS - Université Pierre et Marie Curie, Paris) coordinated this volume which follows the International Peri-Tethys Meeting held in Rabat (Morocco in June 1997).

PERI-TETHYS PROGRAMME

PUBLICATIONS
SCIENTIFIQUES
DU MUSÉUM
57, RUE CUVIER
75005 PARIS

ISBN 2-85653-524-0
ISSN 1243-4442

280 FF TTC 42,69 Euros TTC

Source MNHN, Paris